

LEVEL

AGARD-AR-175

AGARD-AR-175

ADA109292

AGARD

ADVISORY GROUP FOR AEROSPACE RESEARCH & DEVELOPMENT

7 RUE ANCELLE 92200 NEUILLY SUR SEINE FRANCE

AGARD ADVISORY REPORT No. 175

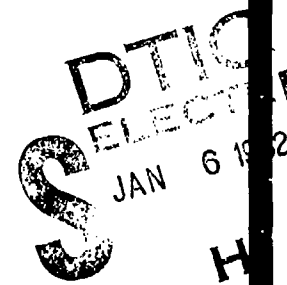
Propulsion and Energetics Panel Working Group 12

on

Through Flow Calculations in Axial Turbomachines

DISTRIBUTION STATEMENT A

Approved for public release;
Distribution Unlimited



DTIC FILE COPY

NORTH ATLANTIC TREATY ORGANIZATION



DISTRIBUTION AND AVAILABILITY
ON BACK COVER

82 01 04 004

NORTH ATLANTIC TREATY ORGANIZATION
ADVISORY GROUP FOR AEROSPACE RESEARCH AND DEVELOPMENT
(ORGANISATION DU TRAITE DE L'ATLANTIQUE NORD)

AGARD Advisory Report No.175
PROPELLION AND ENERGETICS PANEL
WORKING GROUP 12

on

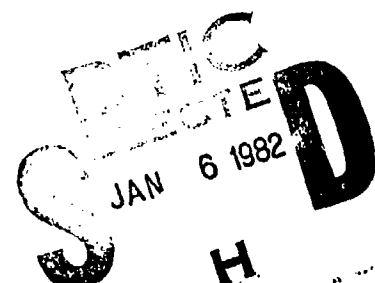
THROUGH FLOW CALCULATIONS IN AXIAL TURBOMACHINES

Edited by

Ch.Hirsch
Vrije Universiteit Brussel
Dienst Stromingsmechanica
Pleinlaan 2
1050 Brussel, Belgium

and

J.D.Denton
Science Research Council
Whittle Laboratory
University Engineering Department
Madinley Road
Cambridge CB3 OEL, UK



DISTRIBUTION STATEMENT A
Approved for public release;
Distribution Unlimited

This Advisory Report was prepared at the request of the Propulsion and Energetics Panel of AGARD.

THE MISSION OF AGARD

The mission of AGARD is to bring together the leading personalities of the NATO nations in the fields of science and technology relating to aerospace for the following purposes:

- Exchanging of scientific and technical information;
- Continuously stimulating advances in the aerospace sciences relevant to strengthening the common defence posture;
- Improving the co-operation among member nations in aerospace research and development;
- Providing scientific and technical advice and assistance to the North Atlantic Military Committee in the field of aerospace research and development;
- Rendering scientific and technical assistance, as requested, to other NATO bodies and to member nations in connection with research and development problems in the aerospace field;
- Providing assistance to member nations for the purpose of increasing their scientific and technical potential;
- Recommending effective ways for the member nations to use their research and development capabilities for the common benefit of the NATO community.

The highest authority within AGARD is the National Delegates Board consisting of officially appointed senior representatives from each member nation. The mission of AGARD is carried out through the Panels which are composed of experts appointed by the National Delegates, the Consultant and Exchange Programme and the Aerospace Applications Studies Programme. The results of AGARD work are reported to the member nations and the NATO Authorities through the AGARD series of publications of which this is one.

Participation in AGARD activities is by invitation only and is normally limited to citizens of the NATO nations.

Parts II, III and IV of this publication have been reproduced
directly from material supplied by AGARD or the authors.
Part I has been set by Technical Editing and Reproduction Ltd.

Published October 1981

Copyright © AGARD 1981
All Rights Reserved

ISBN 92-835-1400-9



Printed by Technical Editing and Reproduction Ltd
Harford House, 7-9 Charlotte St, London, W1P 1HD

CONTENTS

	Page
GENERAL INTRODUCTION	v
PART I – AXIAL TURBINE PERFORMANCE PREDICTION	
Notation for Part I	3
I.1 Introduction	5
I.2 Review of Performance Prediction Methods	13
I.3 Influence of Correlation and Computational Methods on the Prediction of Overall Efficiency	29
I.4 Influence of Correlations and Computational Procedures on Flow Field Predictions	33
I.5 Discussion and Conclusions	57
APPENDICES	
A.I.1 Cambridge Turbine. Geometry, Test Data and Sample Calculation	59
A.I.2 The Two Stage Aero Engine Turbine	69
A.I.3 Ansaldo Steam Turbine. Geometry, Test Data and Sample Calculation	85
A.I.4 Hannover Turbine. Geometry, Test Data and Sample Calculation	99
PART II – AXIAL COMPRESSOR PERFORMANCE PREDICTIONS	
II.1 Introduction	111
II.2 Review of Loss and Deviation Prediction Methods	115
II.2.1 Survey on Diffusion Factors and Profile Losses	116
II.2.2 Survey of Models for Shock and Shock/Boundary Layer Interaction Loss Prediction	127
II.2.3 End Wall Boundary Layer Calculation Methods	137
II.2.4 Correlation for Secondary Flows and Clearance Effects	151
II.2.5 Effects of Reynolds Number and Turbulence Level on Axial Cascade Performance	164
II.2.6 Survey on the Effect of Blade Surface Roughness on Compressor Performance	171
II.2.7 Part Span Damper Loss Prediction for Transonic Axial Fan Rotors	181
II.2.8 Deviation/Turning Angle Correlations	184
II.2.9 Axial Compressor Stall and Surge	212
II.2.10 Summary of Answers to the Questionnaire	214
II.3 Presentation of Test Cases	219
APPENDICES	
A.II.3.1 Single-Stage Transonic Compressor and Equivalent Plane Cascade	221
A.II.3.2 BBC/Sulzer. 4-Stage Transonic Compressor	229
II.4 Results of Calculations	245
II.4.1 The Through Flow Calculations	247
II.4.2 Evaluation of Profile Loss Predictions Based on Diffusion Factors	269
II.5 Conclusions	281
PART III – REVIEW OF CALCULATION METHODS	
III.1 Axial-Flow Turbomachine Through-Flow Calculation Methods	285
III.2 Blade-to-Blade Computations and Boundary Layer Corrections in Axial Compressors and Turbines	307
PART IV – GENERAL CONCLUSIONS AND RECOMMENDATIONS	329
WORKING GROUP MEMBERSHIP LIST	331
LIST OF CONTRIBUTORS	333
LIST OF CONTRIBUTIONS	335

Accession For
NTIS QUART
DTIC TIB []
Unnumbered []
Justification
for file
By _____
Distribution/
Availability Codes
A - Regular or
Dist - Special
A [] []

GENERAL INTRODUCTION

The specialist meeting on "Through Flow Calculations in Axial Turbomachinery" organized by the Propulsion and Energetics Panel in 1977 showed that, although the basic calculation methods could be considered as satisfactory, large difference appeared in the performance predicted for some test cases by different authors (AGARD CP 195).

This was observed even with results emanating from authors using the same mathematical calculation method and obviously the central problem in through flow prediction is connected to the various loss and deviation correlations used.

Following the conclusions reached after this meeting, the Propulsion and Energetics Panel of AGARD recommended the creation of a Working Group on "Through Flow Calculations in Turbomachinery".

The terms of reference were defined as follows :

1. A critical review was to be made of blade element and end-wall correlations available in the literature or from sources not subject to military or commercial restrictions. Emphasis was to be put on off design performance prediction and on transonic range of operation.
This critical review was to be backed by comparisons between duct and through flow calculations using various correlation combinations and selected well-documented experimental data on single and if possible, multistage reference machines (compressor and turbine).
This phase was to be concluded by a precise inventory of the shortcomings of the existing information and recommendations on the most suitable correlation system.
2. Determination of the trends of the effect of variables such as streamtube thickness and streamline change of radius in rotors, chordwise losses and turning variation and other parameters detected through the study under 1, through advanced blade-to-blade calculations. Tentative incorporation of additional correlations in design systems and check on reference machines.
This phase was to be concluded by the assessment of the validity of the "computer experiment" versus test for the improvement of machine performance prediction and hopefully lead to improved correlations.
The Working Group activity was to be limited to steady state operation of machines.

The activities started in January 1978, under the chairmanship of Prof. J. Chauvin who initiated this Working Group and kept on contributing to and stimulating the activities even after having, for professional reasons, left the Propulsion Panel and hence, the chairmanship of the Working Group.

The structure of the present report reflects the history of the activities and its organisation. From the start, two separate Subgroups were formed to analyze the turbine and the compressor fields with their own specific problems, but both Subgroups considered similar strategies in order to fulfill the objectives.

The objectives were soon recognized to represent an enormous task due to the large number of existing correlations, the need to define their limitations and degree of validity, separate the various effects at design and at off-design conditions and finally try to synthetize and to bring improvements.

If obviously all the initial objectives were not met, it is felt that a considerable amount of work has been accomplished. This is due essentially to the voluntary contributions from many people, not only from the members of the Working Group, representing all sectors in the field of turbomachinery, industry, research organisations and Universities with representations from nearly all NATO countries, but also from organizations which were not represented in the Working Group, and from individuals. More specifically, we acknowledge the efforts of all the organizations who answered the questionnaire of the Compressor Subgroup, the Brown Boveri Company, which proposed a four stage compressor test case, Dr. Groschup and Prof. Bammert of Hannover University, Germany for a single stage turbine data, the Ansaldo Company (Italy) for providing a multistage turbine test case, Dr. W.B. Roberts who produced two short reviews of his work on Re-number effects and partspan damper losses and others who made calculations which they submitted to the Working Group.

The first task of the two Subgroups were to collect representative and reliable test cases of single and multistage machines. This appeared as a difficult task, due to the lack of publicly available and well documented multistage data.

Nevertheless, each Subgroup succeeded in collecting and presenting in this report several test cases : Three single stage machines (two turbines and one compressor), two 2-stage machines (one turbine and one compressor), a four stage compressor and a six stage low pressure steam turbine. These data are fully documented in this report when they are not available elsewhere in the open literature. Also, because of the importance of blade-to-blade calculations to sustain the correlations approach, some detailed compressor blade-to-blade data are included in this report.

The second task was to review and attempt to summarize the existing correlations. If this task could be handled more easily in the turbine field, the large number of components entering a compressor correlation required a stronger division of the work.

Five main turbine correlations for turning and loss predictions based on loss component analysis, including secondary and clearance losses were discussed. The complete and comprehensive correlations which are reviewed and considered in the turbine calculations are those developed by the following authors : Ainley and Mathieson (with correction by Dunham and Came), Traupel, Balje and Binsley, Dejc and Trojanovsky and Craig and Cox, the latter two providing only the design point conditions. Of course predictions for the outlet angle are also discussed and reviewed. None of these correlations appeared to have a sufficiently strong and adequate physical basis in the light of our present knowledge. This is especially true for high Mach number effects on turning and losses, shock-boundary layer interactions, and the secondary flow phenomena.

Within the compressor Subgroup, an initial (unpublished) general review of existing correlations was established by Ch. Hirsch as a starting working document. It appeared quite clearly that if many correlations have common points, such as the concept of a diffusion factor to characterize the loading level of a compressor blading, important differences exist when more detailed effects have to be estimated. This is a consequence of the severe conditions with respect to the adverse pressure gradient as well as the complexity of the flow behaviour in a compressor and of our present limited knowledge of it.

In an attempt to answer some of the many questions and problems raised by this preliminary review, it was considered necessary to have some more detailed surveys of various topics and also some more information about the way the compressor correlations are used in the practice of the design work.

Therefore, detailed surveys were produced on the following topics : diffusion factor predictions and profile losses; shock and shock-boundary layer interaction loss prediction; end-wall boundary layer calculation methods; correlations for secondary flows and clearance effects; Reynolds number effects and influence of blade surface roughness; part span damper losses; deviation angle correlations. A note was also prepared on stall and surge. As the reader will notice some of these surveys are extensive reviews of the subject, while others reflect more the authors' experience. This is the case for the topics on which little information is existing or available in the literature and the Working Group was fortunate enough to benefit from the participation or collaboration of some well known experts in the corresponding fields and willing to present and summarize their knowledge and experience.

On the other hand, a questionnaire, reproduced in section II.2.10 was distributed to various industries and organisations involved in design work in order to gain some information on how some of the questions raised by the reviews are answered by the people designing the actual compressors. The answers from 14 industrial and non-industrial organisations from six different countries were very stimulating and instructive and their contribution is gratefully acknowledged.

These answers are summarized in II.2.10 by J. Chauvin, and the shortcomings noted by the designers should provide guidelines for future work and directions for improvements.

Both Subgroups attempted a series of through flow calculations with different correlations on the various test cases. The calculations within the turbine subgroup were quite systematic. Different outlet angle prediction methods as well as various loss distribution schemes were compared with the data. As a general conclusion it can be said that detailed flow predictions are generally poor mainly due to the lack of prediction methods for secondary flow deviations, although overall performance is fairly well predicted.

Similar conclusions were reached in the compressor calculations, although the secondary flow effects are less important. Detailed radial distributions of loss and deviation are, due to the lack of sufficiently valid physical inputs in the correlations, poorly predicted. Some important conclusions arose however, such as the need to distribute secondary losses and deviations along the span in turbines and the importance of introducing end-wall boundary layer calculations in the through flow in order to handle in a coherent way the secondary and tip clearance losses.

Due to the importance of the through-flow and blade-to-blade calculation techniques in the performance prediction method, two additional reviews have been included in the present report on these two topics, as part III.

The organization of this report reflects the organization of the activities. The first part contains the turbine group report while the second part is devoted to the compressor subgroups' activities. Both parts contain their own conclusions and these are summarized by some general considerations and recommandations in the last part of this report.

The key to the improvement of the loss and turning correlations lies clearly in the simultaneous development of the physical understanding of the phenomena through basic experiments and the use of two and three-dimensional viscous calculations.

It is the Working Groups' opinion that from a coherent use of fundamental experiments with the systematic use and analysis of viscous flow calculations a more rigorous basis would be given to the necessary correlations.

1

PART I

AXIAL TURBINE PERFORMANCE PREDICTION

NOTATION FOR PART I

a	Throat width
b	Back bone length
c	Blade chord
d	Blade channel inlet width
e	Blade rear suction surface curvature
g	Blade pitch (gap)
h	Blade height, static enthalpy
H	Total enthalpy
i	Incidence angle
M	Mach number
m	Mass flow rate
n	Rotational speed (RPM)
p	Static pressure
P ₀	Stagnation pressure
R	Radius
Re	Reynolds number
s	Entropy
T	Static temperature
T ₀	Stagnation temperature
te	Trailing edge thickness
U	Rotation velocity
v, V	Absolute velocity
w, W	Relative velocity
Y	Stagnation pressure loss coefficient
z	Ainley's blade loading parameter
α	Absolute flow angle (from tangential)
β	Relative flow angle (from tangential)
α', β'	Blade angles
γ	Stagger angle, specific heat ratio
δ	Deviation angle, tip clearance
δ*	Boundary layer displacement thickness
ε	Meridional pitch angle ($\tan^{-1} V_r/V_x$)
ρ	Fluid density
η	Turbine efficiency
θ	Blade camber angle, boundary layer momentum thickness
λ	Ainley's secondary loss parameter
Φ	Turbine flow coefficient, V_x/U
ψ	Stage loading coefficient $2\Delta H/U^2$
ψ̄	Stage loading coefficient $2\Delta h_{is}/U^2$
ξ	Kinetic energy loss coefficient, $(V_{is}^2 - V^2)/V^2$

Subscripts

a	At throat
is	Isentropic
m	meridional
M	Mid blade height
opt	Optimal
s	Static

t	Total
tt	Total to total (efficiency)
ts	Total to static (efficiency)
x	Axial
r	Radial
θ	Circumferential
o	Stator inlet
1	Stator exit, rotor inlet
2	Rotor exit

The term 'through flow calculation' as used throughout this report refers to an axisymmetric computation of the flow through a turbine annulus, wherein the flow may be described by a series of concentric stream surfaces across which no mass or momentum is exchanged. Flow parameters are circumferentially invariant (or represent circumferential averages if you prefer).

Chapter I.1

INTRODUCTION

1.1 OBJECTIVES OF THROUGHFLOW CALCULATIONS

Throughflow calculation programs are probably the most important tool of the turbine aerodynamic designer. At the initial design stage a one-dimensional mean-line calculation might be used to obtain estimates of blade height and so to lay out a first approximation to the annulus line. Such mean-line calculations usually include estimates of blade loss and deviation, so that predictions of turbine performance can be obtained, but these must be based only on the blade geometry at mid-height so high accuracy cannot be expected. Although spanwise variations in flow are small for very high radius ratio turbines these variations become significant at radius ratios below about 0.9. It is well known that most turbine blades are remarkably tolerant to off-design incidences (compared to compressor blades), but even so optimum performance, particularly at off-design conditions, cannot be expected unless the blades are matched to the spanwise variation in flow. The main objective of a throughflow calculation is, therefore, to provide a prediction of this spanwise variation so that suitable blade profiles can be selected to cope with the variations in inlet angle, turning, Mach number; etc.

Throughflow programs may be either of the analysis or design type. In the former the blade geometry is specified and solutions are sought for the resulting flow pattern. The design type of program is less commonly used and is provided with the required enthalpy variations (and hence indirectly with swirl velocity) and obtains solutions for the meridional velocity and hence flow angles. In either type of calculation accurate solutions cannot be expected unless the entropy gradients resulting from viscous effects are reasonably well predicted. Similarly the solution obtained from an analysis program is very dependent upon the values of blade exit flow angle specified. In a design program the flow angle is calculated but it is not possible to lay out blade sections to produce this angle without first estimating the deviation. A further problem associated with design programs is that the viscous effects have to be estimated at the stage before blade angles become available.

Once loss and deviation models have been incorporated into a program it can be used to predict overall machine performance, i.e. the pressure ratio : mass flow and efficiency : mass flow characteristics at off-design conditions. The inclusion of spanwise variations in flow should enable better estimates of these characteristics to be obtained than are possible from mean-line calculations. However, the accuracy of the results is entirely dependent on the methods used to predict loss and deviation and in particular their variation with incidence.

Experience suggests that the weakest links in this design procedure are the empirical correlations used to provide estimates of loss and deviation. It was this realisation which led to the formation of the Turbine Sub-Group.

1.2 REVIEW OF THROUGHFLOW CALCULATION METHODS

It is not the purpose of this report to discuss in detail methods of performing the basic inviscid calculation on which all throughflow solutions are based. These are well covered in the papers presented in AGARD CP 195 and in more recent publications by Denton (1978), Doria et al. (1979), Hirsch (1978) and Spurr (1980). It should, however, be mentioned that the theoretical basis of all such methods rests on the concept of performing the calculation on a mean hub to tip stream surface, as originally advocated by Wu (1951). Within a blade row the flow properties on the mean stream surface are not the same as those of the passage averaged flow, as they are when the flow is circumferentially uniform far upstream and far downstream of the blade row. Many methods (so called duct flow methods) only place calculating stations at the leading edge and trailing edge of blade rows and so do not need to distinguish between the flow on the mean stream surface and the passage average flow. Methods which do include stations within the blade rows also usually ignore this distinction. There is no evidence that this approximation has a significant effect on the resulting solution. In fact the solution outside the blades seems to be remarkably insensitive to the form of the mean stream surface within the blades. It is, however, highly dependent on the prescribed blade exit flow angles. The main information required from the solution within the blades is the relative thickness of the blade to blade stream surface. Since the whole concept of axisymmetric blade to blade stream surfaces within blade rows is a major approximation some error in the prediction of their thickness is probably acceptable.

The main problem encountered when developing through flow calculations for turbines, as opposed to compressors, arises from the need to be able to calculate the flow through stages with high-pressure ratio and in particular with regions of transonic relative flow. The latter is much more easily handled by streamline curvature methods than by stream

function methods although severe difficulties arise even for the former type of method. Time-marching methods are much better suited to calculating transonic flow but are not yet highly developed for use in throughflow calculations (see Spurr (1980)). Problems with calculating transonic flow are currently much more severe in steam turbines than in gas turbines.

With the streamline curvature method difficulties occur whenever the flow through any blade row approaches the choking condition (see Novak & Hearsay (1976)). Denton (1978) shows how these problems can be overcome by calculating a supersonic deviation at the trailing edge whenever the local exit Mach number exceeds unity but his model does not permit calculating stations to be placed between the throat and trailing edge. This method enables calculations to be continued to the point where the relative exit flow is supersonic over almost the whole blade height but as this condition is approached further problems occur due to the extreme sensitivity of the solution to the mass flow rate specified. Most throughflow methods work with prescribed inlet flow stagnation conditions and mass flow rate but at choking it is not possible to specify these arbitrarily. For fixed inlet stagnation pressure and temperature there is only one mass flow rate for which realistic choked solutions can be obtained. It is then necessary to prescribe the turbine pressure ratio and to obtain the mass flow rate as part of the solution. This approach is also necessary for multi-stage high-pressure ratio (but unchoked) turbines because of the steepness ($\text{large } dP_2/dm$) of their pressure ratio: mass flow characteristic. Denton (1978) also shows how it is possible to change the structure of throughflow calculations to work in terms of a prescribed pressure ratio and a similar approach is used by Doria et al. (1979). This prescribed pressure ratio approach is strongly recommended to anyone developing a program which might be used for high-pressure ratio turbines.

Apart from these problems arising from transonic flow and high-stage pressure ratios there are thought to be no difficulties peculiar to turbine applications of the basic throughflow methods.

1.3 PHYSICS OF LOSS AND DEVIATION

Methods of estimating loss and deviation will be reviewed in the next chapter but before studying these it is worth first reviewing the physical processes involved so as to obtain a feel for the degree of understanding available. When reading Chapter 2 it should be noted how little of this Physics is embodied in the correlations currently available.

Entropy increases in turbines occur due to viscous effects, shock waves and flow mixing (heat transfer is usually considered negligible). Viscous effects are invariably assumed to be confined to the blade and annulus boundary layers and dissipation in the mainstream is assumed negligible. The resulting loss on the blade surfaces and in the wake is referred to as profile loss whilst that on the annulus walls is usually (and misleadingly) called secondary loss.

Boundary-layer growth on the blade surfaces is influenced by Reynolds number, surface roughness, surface curvature, turbulence level and, above all, by surface pressure distribution. In 2D flow it is believed that the effects of all these are understood and boundary-layer growth can be computed with fair accuracy (of the order $\pm 10\%$ on trailing-edge momentum thickness). However, a correlation method of estimating the loss is unable to take into account many of these factors (in particular it cannot know the surface pressure distribution) and a great deal of accuracy is lost. Denton (1973) compared several correlations with a large body of cascade data and found that the best of them had a standard deviation of the order 30% in the ratio of predicted to measured loss coefficient. In a turbine the surface boundary layers are subject to 3D, centrifugal and coriolis effects and to unsteadiness in addition to those found in cascade tests and the predictions of correlations can be expected to be significantly worse. In particular it is not really known whether or not it is possible to maintain a laminar boundary layer on a blade in a real turbine environment.

The additional loss due to finite trailing-edge thickness is believed to be comparatively small in most cases but current methods of estimating it are very unsatisfactory (see Herbert (1972)). In particular estimates of the base pressure acting at the trailing edge vary wildly. This is a particularly important parameter for blades with supersonic outflow when trailing-edge losses become much more significant.

In duct flow annulus wall boundary layers can be predicted with similar accuracy to blade surface boundary layers. However, within blade rows very complex secondary flows are set up by the influence of the circumferential pressure gradient on the low momentum boundary-layer fluid. In most turbines it seems that the annulus boundary layers entering the blade rows are swept completely off the end walls and end up in a passage vortex displaced typically half a blade chord from the end walls. As a result mainstream fluid is brought into contact with the wall to form a new annulus boundary layer. Initially this new boundary layer is very thin and highly skewed and hence is a source of high loss. Details of this complex process are described for cascade flow by Langston et al. (1976) and Marchal & Sieverding (1977). In a turbine the process is further complicated by skewing of the inlet boundary layer. The resultant loss per unit surface area is several times greater than on the blade surfaces but the complete mechanism of loss generation is not yet fully understood.

The secondary loss is dependent on all the factors influencing profile loss and in addition on the inlet boundary-layer thickness and profile. When expressed as a loss coefficient averaged over the whole span the coefficient will clearly vary inversely as the blade height.

Methods of correlating this secondary loss were reviewed by Dunham (1970) who found a disturbing lack of agreement between them with predictions differing by up to an order of magnitude. There is also considerable evidence that the magnitude of the loss may be different in turbines from that in cascades (see Dunham & Came (1970)).

Tip leakage flows are the other main source of entropy in turbines. The mechanism of loss generation differs considerably for shrouded and unshrouded blades. For shrouded blades it is necessary to predict the leakage flow rate as well as the loss because this flow does no work on the blades. Detailed measurements of the flow over shrouded blade tips have been made by Denton & Johnson (1976) who show that the leakage flow behaves very much like that through an orifice. The flow contracts to a jet just downstream of the tip seal and the flow rate can be closely estimated from the ratio of leakage area to blade throat area multiplied by a contraction coefficient. The loss can be estimated from the mixing loss of this leakage jet. It was found that the leakage flow suffered little change in angular momentum.

The flow over an unshrouded blade tip is much more complex. Fluid will flow over the tip from pressure surface to suction surface forming a leakage jet whose subsequent mixing produces loss in a manner similar to that of a shrouded blade. However, the pressure difference driving this leakage jet is not readily predictable in this case because it depends on the blade surface pressure distribution which in turn is influenced by the leakage. An important point is that this pressure difference does not decrease for low-reaction blading as does that over a shrouded tip seal. In addition to the loss it produces the clearance flow will reduce the blade loading towards the tip thereby causing undeturning, but no loss, of the mainstream flow. This undeturning results in reduced work and hence increased meridional velocities of the flow leaving the tip region. A complete correlation of the effects of leakage over unshrouded blade tips should include predictions of the undeturning as well as of the loss.

Profile loss, secondary loss and tip leakage loss are the major sources of entropy in turbines. Their relative magnitude depends on the details of the design but for many machines all three are similar. At low aspect ratios (less than 1) secondary loss tends to dominate whilst at very high aspect ratios profile loss may be the major component.

The exit flow angle from turbine blades is usually expressed as a deviation from the angle given by $\sin^{-1}(a/g)$ (note: In this report all angles are taken to be measured from the circumferential direction). This is because the well known sine rule provides a very good approximation to the exit angle in 2D flow. The rule may be derived theoretically by applying the continuity equation between the blade throat and the downstream flow at the condition when the blade is choked with an exit Mach number of unity. If losses downstream of the throat are neglected and if the specific mass flow is assumed constant, at the sonic value, across the throat the relationship

$$\sin \alpha_1 = a/g$$

results immediately. The same method can be used to predict the supersonic deviation which occurs when the exit Mach number exceeds unity.

In practice there will be some degree of non-uniformity in the flow across the throat and this will reduce the choking mass flow and hence increase the turning at a downstream Mach number of unity. Similarly the inevitable increase in loss between throat and downstream will reduce the turning and produce a positive deviation.

Similar considerations (i.e. continuity equation) show that in incompressible flow the deviation increases (undeturning) with the ratio of suction surface peak velocity to downstream velocity. Hence blades with a high suction surface diffusion will tend to have a high deviation at low Mach numbers whilst blades with a "flat topped" suction surface velocity distribution should show little deviation over the whole subsonic range.

These considerations show that the deviation is dependent upon the blade profile and is not solely a function of the opening:pitch ratio and Mach number. It is also affected by radius change, rotation and stream surface thickness. These factors are included in Traupel's method (1973) of prediction exit angles but are neglected by most other methods.

The 2D deviations discussed above are usually of the order of a few degrees. Much larger deviations can occur as a result of the secondary flows near the annulus walls. It will be shown in Chapter 4 that the latter are often the main source of discrepancy between calculated and measured flows in turbines. These secondary deviations result from the streamwise vorticity generated by the turning of the endwall boundary layers. A passage vortex is formed with its centre just off the end wall and its sense of rotation such that fluid very close to the wall is overturned whilst fluid just outside the inlet boundary layer is undeturned.

Methods of predicting this secondary flow have been the subject of a great deal of theoretical research, however, despite drastic approximations the methods are still too complex to include directly in throughflow calculations. A severe limitation is that they require a knowledge of the thickness and profile of the annulus boundary layers entering the blade rows and in practice this is seldom available. Since secondary flow is inherently non-axisymmetric it cannot be included directly in throughflow calculations. The best hope of including some allowance for it is via correlations of the magnitude and spanwise distribution of the deviation. The only known correlation of this type is by Bardon et al. (1975).

1.4 INCORPORATION OF LOSS AND DEVIATION RULES INTO THROUGHFLOW CALCULATIONS

As far as is known there are no loss or deviation prediction methods which have been developed specifically for use in throughflow calculations. All the overall performance prediction methods reviewed in Chapter 2 (e.g. Ainley and Mathieson, Craig and Cox, Traupel) were developed as mean line methods and were not originally intended to be used to predict spanwise variations of loss or deviation. Despite this limitation such methods are not universally used to predict the loss and deviation on each streamline of a throughflow calculation and this extrapolation beyond their original intended application must be the cause of some of the errors found when using throughflow calculations for overall performance prediction.

Loss correlations in general provide a value of loss coefficient, ξ or Y , whilst the equations used for throughflow calculations require a value of entropy at each grid node. If there is no loss entropy is conserved along streamlines whilst loss generation will cause it to increase along streamlines from upstream to downstream grid points. Given the loss coefficient ξ based on relative velocity at the downstream point the entropy increase is easily obtained from

$$\Delta s = \frac{1}{2} W^2 \xi / \Gamma .$$

Note that it is more convenient to use the loss coefficient ξ which is based on the actual relative velocity than the alternative definition which is based on the isentropic exit velocity. The use of a stagnation pressure loss coefficient, Y , is even less convenient as the stagnation pressure is not directly available to the calculation.

It would be realistic to include profile and secondary losses between any two calculating stations which lie within a blade row. In order to do this the distribution of loss along the axial chord of the blade would have to be specified. In practice this distribution is not known and the loss is usually only added at the trailing-edge station. It is, however, important that the entropy increase is included in the radial equilibrium and continuity equations at the trailing-edge station, otherwise the effect of the loss on the blade exit velocity is not correctly modelled.

It is arguable that a more realistic way of including profile and secondary losses would be to introduce a blockage factor within and at the trailing edge of blade rows to simulate the displacement thickness of the boundary layers. An entropy increase would then only occur downstream of the trailing edge to simulate mixing of the boundary layers with the mainstream. As far as is known this model has not been used.

It is clear from the above that a value of loss coefficient must be available to the calculation at each grid point along the trailing-edge station. In the simplest approach this coefficient may be estimated outside the program and read in as data. It is, however, more usual to build correlations into the calculation so that the coefficient can be obtained from the current values of incidence, Reynolds number; etc.

In addition to its effect on the entropy gradient it is shown by Horlock (1971) that the loss enters into the throughflow equations via a frictional force, T_{ds}/dm , acting along the streamlines. Only the component of this force acting along the lines along which the momentum equation is being solved (i.e. the quasi-orthogonal lines) enters into the equations and if these lines are truly nearly orthogonal to the streamlines this component will be very small. Since the frictional force is anyhow small and not accurately calculable it is not usually included in the equations.

The treatment of tip leakage flow and loss is rather more complicated than that of the other loss components. For shrouded blades the leakage flow may be assumed to do no work and so must be subtracted from the blade flow for all calculating stations between (and including) the leading and trailing edge. The leakage flow suffers an entropy increase but may be assumed to do no work and to undergo no change in angular momentum (rV_θ), it must be mixed with the blade flow downstream of the trailing edge in such a way that these quantities are globally conserved. Although in reality this mixing is confined to the tip region and affects only a small part of the main flow it is probably more usual to assume uniform mixing over the whole span. The latter model completely washes out the tip leakage jets which are often found in practice.

For unshrouded blades it is much more difficult to formulate a realistic model because the leakage flow and blade flow are not readily distinguishable. It is probably preferable not to try to distinguish between them but to increase the entropy and reduce the turning of the tip streamline to simulate loss and tip unloading respectively. Because it is difficult to predict how much of the span will be affected by the leakage it is again more usual to distribute the loss and deviation uniformly over the whole span.

As with tip leakage loss, it is clearly more realistic to concentrate secondary loss near to the end walls so that it only affects part of the span (of order half a blade chord in length at each wall). Such concentrations of loss near the endwalls can give reasonable results on a single-stage machine as shown in Chapter 4. However, on a multistage turbine the accumulation of entropy near the walls can lead to very steep entropy gradients which may cause the solution to predict reverse flow and hence possibly to break down completely. In practice such loss accumulations are prevented by turbulent mixing of endwall and mainstream flow. This mixing is easily simulated in throughflow calculations by allowing transfer of enthalpy, entropy and angular momentum between streamlines. For example the entropy on streamline J at the lth calculating station can be obtained from

$$S_{I,J} = (1 - \alpha) S_{I-1,J} + \frac{1}{2}\alpha(S_{I-1,J-1} + S_{I-1,J+1}) + \Delta S$$

where α is a mixing factor dependent on the rate of diffusion. Instead of from the usual

$$S_{I,J} = S_{I-1,J} + \Delta S.$$

The most realistic value of the mixing factor α is not known but values of about 0.5 cure any problems of entropy buildup and have little effect on single-stage calculations.

It was stated in Section 1.2 that the shape of the mean stream surface within blade rows has little effect on the calculated results outside blade rows. Hence it is only really worth including the deviation in the flow angle at the trailing-edge station. This deviation must be predicted using the local value of opening: pitch ratio and current values of incidence, stream surface divergence, radius change, etc. available to the program. Correct allowance for the latter two effects is very difficult to obtain in correlation form and it is common to use 2D data, in the absence of better information, even in highly flared steam turbine stages.

Inclusion of secondary deviation near the end walls is important if full details of the velocity profiles are to be predicted (see Chapter 4). However, prediction of these deviations demands a knowledge of the annulus boundary-layer thickness which is seldom available. As a result secondary deviation is not usually included separately in the calculation.

Calculations of annulus wall boundary-layer growth and blockage are common in compressor calculations but are not usually included in turbine throughflow methods, the reason being that in a turbine an annulus boundary layer does not really exist within the blade rows. As described in 1.3 any annulus boundary layer at inlet is swept off the end wall and a new, highly skewed, layer starts within the blade passage. When large regions of duct flow need to be calculated the blockage due to annulus boundary-layer displacement thickness may become significant. In such cases the thickness may be calculated using the methods reviewed by Hirsch and de Ruyck in the compressor sub-group's report.

1.5 COMPARISON OF CALCULATIONS WITH TEST DATA

The results from throughflow calculations must be compared with as much test data as possible in order to establish confidence in their predictions. The comparison may be made on the basis of overall performance (i.e. mass flow : pressure ratio, efficient : pressure ratio characteristics) or may include comparisons of measured and predicted velocity profiles. The latter type of comparison requires much more detailed test data and so is less common than the former.

The predicted efficiency is dependent mainly on the accuracy of the loss correlations and as will be clear from Section 1.3 high accuracy cannot be expected. Nevertheless many claims to high accuracy are made for efficiency predictions, the reason being that it is common practice to scale loss predictions based on cascade data in order to obtain the best possible agreement with turbine tests. For example Dunham (1970) developed a correlation for secondary loss in cascades but when used by Dunham & Came (1970) in a turbine performance prediction method the loss level was considerably increased. If all the many loss components are scaled in this way it is possible to get good agreement with the turbine data used to determine the scaling factors. For example Dunham & Came claim an accuracy of $\pm 2\%$ on efficiency whilst Craig & Cox claim $\pm 1\frac{1}{4}\%$. Clearly such comparisons of a prediction method with the test data on which it is based are not really valid and the only valid comparisons are with data not embodied in the correlations. Few such comparisons have been published but some are included in Chapter 3 of this report.

The mass flow : pressure ratio characteristic is mainly influenced by the deviation rule used. At low Mach numbers the flow rate obtained at a given pressure ratio will be almost directly proportional to blade exit area, i.e. to $\sin \alpha_1$. Hence, at $\alpha_1 = 20^\circ$, at 1° error in deviation will cause about 5% error in mass flow. For multistage high-pressure ratio machines changes in pressure drop across the first stage are greatly amplified by the downstream stages so the mass flow obtained at a prescribed pressure ratio is determined mainly by the throat areas of the first stage. In particular, if the first nozzle is choked, the mass flow is directly proportional to its throat area for fixed inlet conditions. Hence it is important that the program is able to distinguish between throat area and blade exit area once the choking point is reached.

Comparisons of predicted velocity profiles, blade losses and exit angles are often limited by the accuracy of the test data. It must be remembered that the flow in a turbine is unsteady and non-axisymmetric (see Hunter (1979)) whilst probe measurements are usually of the time average flow at one circumferential position. A useful check on the accuracy of traverse data can often be obtained by comparing the integrated mass flow with that measured elsewhere in the system. It is the author's experience that agreement to better than $\pm 5\%$ is hard to obtain, this error being the combined result of non-axisymmetric flow and effects of unsteadiness and shear flow on the probe calibration.

It is particularly difficult to measure blade losses accurately, except for those in the first nozzle row, and losses must usually be inferred from the local stage temperature drop. This leaves the detailed breakdown of loss between nozzle and rotor indeterminate.

A further source of discrepancy arises if measurements and calculations are not compared at exactly the same point. Traverses must inevitably be made some distance behind a trailing edge and may be compared with predictions at the trailing edge. The relative flow angle in particular can change very rapidly between the trailing edge and a traverse line just downstream of it due to changes in stream surface thickness. If this is disregarded a completely false picture of the deviation can be obtained.

1.6 OBJECTIVES OF THE TURBINE SUB-GROUP

The objectives of the turbine sub-group can now be explained in the light of the review of its field of activity which has been presented in the earlier sections of this Chapter.

It was realised early in the work that there were insufficient reliable test cases for which data were publicly available, to support any attempt to produce new correlations. It was therefore decided to concentrate on reviewing existing methods of predicting loss and deviation and on applying them to those test cases which were available. The limitations of the methods could then be assessed and areas where improvements were necessary could be pointed out. It was not considered that the turbine sub-group would have the time or the data available to implement improvements themselves.

In view of the extreme shortage of turbine test data it was felt that an important contribution would be to fully document the test cases used by the turbine sub-group and this is done in the Appendices to this report.

REFERENCES

1. Denton, J.D. *Throughflow Calculations for Transonic Axial Flow Turbines*. ASME, J. Eng. Power, April 1978.
2. Doria, G. Troillo, M. *Throughflow Calculation of Large Steam Turbines*. Conference on Steam Turbines for Nuclear Power Stations, Plzen, Czechoslovakia, May 1979.
3. Hirsch, Ch. Warzee, G. *An Integrated Quasi-3D Finite Element Program for Turbomachinery Flows*. ASME Paper 78-GT-56, 1978.
4. Spurr, A. *Prediction of 3D Transonic Flow in Turbomachines Using a Combined Throughflow and Blade-to-Blade Time Marching Method*. I. Mech. E. J. Heat and Fluid Flow, December 1980.
5. Wu, C.H. *A General Throughflow Theory of Flow with Subsonic or Supersonic Velocity in Turbomachines of Arbitrary Hub and Casing Shapes*. NACN TN 2302, 1951.
6. Novak, R.A. Hearsay, R.M. *A Nearly 3D Intrablade Computing System for Turbomachinery*. Parts I and II. ASME Papers 76-FE-19 & 20, 1976.
7. Denton, J.D. *A Survey and Comparison of Methods of Predicting the Profile Loss of Turbine Blade*. I. Mech. E. Paper C76/73, 1973.
8. Herbert, M.V. *Some Notes on Loss Coefficients Relating to Turbine Blades with Finite Trailing-Edge Thickness*. UK Aero Research Council paper 34755, 1972.
9. Langston, L.S. Nice, M.L. Hooper, R.M. *Three-Dimensional Flow within a Turbine Cascade Passage*. ASME Paper 76-GT-50, 1976.
10. Marchal, Ph. Sieverding, C.H. *Secondary Flow within Turbomachinery Bladings*. AGARD CP 214, 1977.
11. Dunham, J. *A Review of Cascade Data and Secondary Losses in Turbines*. J. Mech. Eng. Sci., January 1970.
12. Dunham, J. Came, P.M. *Improvements to the Ainley-Mathieson Method of Turbine Performance Prediction*. ASME, J. Eng. Pow., July 1970.
13. Denton, J.D. Johnson, C.G. *An Experimental Study of the Tip Leakage Flow Around Shrouded Turbine Blades*. CEGB Report R/M/N848, 1976.

14. Traupel, W. *Prediction of Flow Outlet Angle in Blade Rows with Conical Stream Surfaces.* ASME Paper 73-GT-32, 1973.
15. Bardon, M.F.
Moffatt, W.C.
Randall, J.L. *Secondary Flow Effects on Gas Exit Angles in Rectilinear Cascades.* ASME, J. Eng. Pow., January 1975.
16. Horlock, J.H. *On Entropy Production in Adiabatic Flow in Turbomachines.* ASME Paper 71-FE-3, 1971.
17. Hunter, I.H. *Endwall Boundary-Layer Flows and Losses in Axial Turbomachines.* Ph.D. Thesis, Cambridge University, 1979.

Chapter I.2

REVIEW OF PERFORMANCE PREDICTION METHODS

2.1 INTRODUCTION

Turbine performance prediction methods can basically be split into two major categories: The first category groups together the so-called overall stage methods. The use of such methods does not in general require any details of the blading and the complex flow patterns in the turbine are deliberately ignored. Turbines are treated more or less as black boxes. These methods are in general derived from overall performance measurements of a large number of turbines with similar characteristics. Their use is justified in the initial design phase for the selection of the turbine design parameters.

The optimization of a turbine for a given duty requires, however, a deep understanding of the flow and only very refined performance prediction methods, which take into account details of the blading and of the meridional flow channel can be of real help. This is attempted by the second category of performance estimation methods which evaluate the total losses as the sum of a great number of individual loss components each of which is influenced by a large number of geometric and aerodynamic parameters. The problem consists in defining clearly the important parameters and in making certain that the influence of each parameter can be studied separately. Such systematic variations of the parameters can in general only be done on simplified models. There are, however, limitations to the degree of simplification beyond which model tests become meaningless. A constant effort has therefore to be made to simulate the real flow conditions as closely as possible. The magnitude of the differences remaining between the real turbine flow and the model flow determines whether the model test results can be applied to the turbine without any corrections or whether the model test results indicate only the correct trends whilst the absolute loss level needs significant correction factors. The need to adjust one or more loss components in order to match the total losses to measured turbine efficiencies presents a great problem in cases where one wishes to replace one loss component correlation by another better one in a given performance prediction method. Such a change is in fact only meaningful if the overall losses can again be calibrated against a large number of reference turbine cases. Such test results only exist, however, in large turbine manufacturing companies and are not accessible to the individual researcher and designer. This situation is dramatically demonstrated by the efforts of the present turbine sub-group. Only three fully described turbine test cases could be found in the literature.

2.2 OVERALL STAGE PERFORMANCE METHODS

2.2.1 Design Point Performance

As mentioned before overall stage methods are in general developed for families of similar turbines. Hence their use is limited to turbines being designed with similar characteristics e.g. same range of degree of reaction, same aspect ratio, same family of blade profiles. Latimer¹ has given a number of such correlations which have been used in the past by Rolls Royce. The most widely known turbine efficiency correlation of Rolls Royce is the correlation of Smith².

The Smith correlation is based on data of some 70 HP and LP cold flow model turbine stages. All stages have the following features in common:

- axial velocity ratio of unity,
- design point incidence equal to zero,
- degree of reaction: for the HP-stages down to 20%, for LP-stages up to 60%. The degree of reaction is always chosen to be sufficiently high to avoid losses associated with recompression at the blade roots.

The turbine efficiencies are presented as a function of the stage loading ψ and the flow coefficient ϕ , taken at the mean radius. The measured efficiencies were corrected to zero clearance. The Re-number effect on the turbine efficiency was found to be negligible in the range $10^5 < Re < 3 \cdot 10^5$. Smith claims an accuracy of $\pm 2\%$ for his correlation.

*Latimer*¹ produced the following design point correlation which allows a very rapid estimation of the effects of such parameters as: trailing-edge thickness, aspect ratio and blade clearance.

Note: The angle definitions used in this review are always those of the original papers.

$$100 - \eta = \frac{42}{(h/0)_s + (h/0)_r} + 16 \left(\frac{\psi^2 + (\phi + 1)^2}{\phi} \right) \left[2 \left(\frac{te}{0} \right)_s + \left(\frac{te}{0} \right)_r \right] - 8.5\lambda + 100B \cdot k/h + 6.8$$

where:

- $h/0$ -- blade height to throat ratio,
- $te/0$ -- trailing-edge thickness to throat ratio,
- λ -- Ainley's secondary loss parameter (derived from experimental data),
- k -- clearance,
- B -- clearance constant,
- subscripts s and r indicate stator or rotor.

Soderberg's correlation³ also seems to be based on high-speed turbine data. All losses, except the clearance losses are calculated from the simple relation.

$$\xi = \left(\frac{10^5}{R_H} \right)^{1/4} [(1 + \xi')(0.975 + 0.075b/h) - 1]$$

where:

- R_H -- hydraulic mean diameter at throat section ($= 2 \cdot h \cdot g \cdot \cos \alpha_2 / (g \cdot \cos \alpha_2 + h)$),
- b/h -- axial chord to height ratio,
- ξ' -- depends on the overall turning and the maximum blade thickness.

It should be noted that the above relation is only valid for optimum pitch to chord ratio and zero incidence angle. The tip clearance effect can be accounted for by simply multiplying the blading efficiency by the ratio of the blade area to the total annulus area (including the tip clearance).

The oversimplified relation $\xi' = f$ (flow turning) illustrates the lack of a physically sound concept for the loss evaluation. It is unrealistic to assume that the degree of reaction for a given flow turning angle does not matter.

Presentation of Soderberg's correlation in the form of efficiency curves on the $\psi - \phi$ diagram shows very similar general tendencies to the Smith diagram. For the case of $R_H = 10^5$ and $b/h = 3$ it was found that Soderberg's efficiencies were low by 0.5 to 2 points compared with Smith's efficiencies. This difference might at least partially be explained by the progress in turbine design between the date of Soderberg's correlation (1949) and Smith's correlation (1965).

2.2.2 Off-Design Performance

Based on the experience that turbines tended to show a unique variation of efficiency with stage loading Latimer¹ attempted to produce a simplified model of turbine off design behaviour. The best consistency was found when using a logarithmic presentation of the efficiency-stage load relation.

As pointed out by Latimer himself care has to be taken when using his off-design curve because the turbine performance curves depend strongly on whether the turbines are designed for zero incidence or for the incidence resulting in lowest absolute losses. At zero incidence design the peak efficiency will occur at design load while for optimum incidence angle designs the turbine efficiency will peak at part load. This difference has to be taken into account when using Latimer's curve.

2.3 LOSS COMPONENT ANALYSIS METHODS

Authors who use this approach distinguish in general between two categories of loss:

- (a) losses used to evaluate the blading efficiency: profile losses, secondary loss and annular losses which are calculated separately for the stator and rotor blades;
- (b) losses which are introduced only between the stages: clearance losses, disc windage losses, losses due to partial admission lacing wire losses, balance hole losses and guide gland clearance losses:
these losses are taken together as a deficiency term $\Delta\eta$ when calculating the overall turbine efficiency as

$$\eta = \eta_{blading} - \Delta\eta$$

Although the various loss components are evaluated individually, their final value is adjusted in order to fit the maximum possible number of turbine efficiency data points available to the authors. The difficulty lies not only in the quantitative adjustment but in the correct selection of the main parameters influencing the prediction.

The number of complete comprehensive loss correlations for estimating axial turbine performance is rather limited as shown by the following list:

- Ainley and Mathieson⁴ (with correction by Dunham and Came⁵),
- Traupel⁶,
- Baljé and Binsley⁷,
- Dejc and Trojanovski⁸,
- Craig and Cox⁹.

Ainley-Mathieson, Traupel and Craig-Cox provide means of predicting both design and off-design performances while Baljé-Binsley and Dejc-Trojanovski provide only the design point calculation.

Since all methods require a knowledge of the outlet flow angle let us discuss first the various methods of predicting this most important parameter.

2.3.1 Outlet Flow Angle

There are basically 3 approaches to the determination of the outlet flow angle:

- (1) Single airfoil approach using the flow deviation angle δ . This approach is widely used for compressor cascades. The correlations are based on experimental data.
- (2) Channel flow approach calculating α_2 , basically via the throat to pitch ratio. The original empirical relation $\alpha_1 = f(a/g)$ has later been substantiated through theoretical derivations by Traupel and other authors.
- (3) Calculation of outlet flow angle using a potential flow theory with a suitable closure condition at the trailing edge.

Deviation Angle

Carter and Hughes¹⁰ suggest that the unstalled low-speed deviation for turbine cascades may be calculated by:

$$\delta = m \cdot \theta \cdot \sqrt{g/c}$$

with $m = f$ (stagger angle and camberline shape),
 θ camber angle,
 g/c — pitch to chord ratio.

Dunavant and Erwin¹¹ provide a limited amount of data of $\delta = f(\theta, \alpha_1)$ for some NACA turbine blades tested in the range from impulse conditions to axial inlet conditions.

Mukherjee¹² seems to be the most recent author providing information on the deviation angle. His experimental results are presented in the form:

$$\delta = (\delta_{10} + A)m - A$$

where $\delta_{10} = \delta$ for blade with 10% thickness,
 $\delta = f(\alpha'_2, \theta, g/c)$,
 $m = f$ (blade thickness),
 $A = f$ (blade camber).

Sine-rule

The sine-rule was in use a long time before a well-founded theoretical explanation could be given for the particular suitability of this rule in the transonic range.

Ainley⁴ proposes the following empirical expression for the Mach number range $M_2 < 0.5$:

$$\alpha_2 = \alpha_2^* - 4g/e$$

where $\alpha_2^* = f(a/g)$ is a linear variation valid for blades with a straight suction surface while the term $4g/e$ (e = radius of rear suction side curvature) presents the influence of the rear suction side curvature. At $M_2 = 1$ Ainley considers the sine-rule to be valid. For the range $0.5 < M_2 < 1.0$, Ainley proposes either a linear variation of α_2 between the angle calculated at $M_2 = 0.5$ and at $M_2 = 1.0$ or a smooth curve with an inflection point at $M_2 = 0.75$. Ainley also suggests that the effect of a positive incidence angle on the outlet angle can be expressed by a linear relationship with a decrease of α_2 by 2° between zero incidence and positive stall incidence.

Bammert and Sonnenschein¹³ carried out low-speed tests on 4-blade profile with evenly thickened and thinned blade contours. On the basis of these experimental results they arrived at a modified sine rule taking into account the effect of the trailing-edge thickness.

$$\sin \alpha_2 = K_1 \left(\frac{a}{g} + K_2 \cdot \frac{te}{2g} \right)$$

where $K_2 = 0.8$ and $K_1 = f \left(\frac{a}{g} + 0.8 \frac{te}{2g} \right)$.

Traupel⁶ has derived a simple equation for outlet prediction including the Mach number effect on α_2 by applying the continuity and momentum equations to the space between the throat and far downstream plane. With the two assumptions that

- (a) the resultant pressure force in the tangential direction is negligible, and
- (b) the flow is isentropic

he arrives at the following expression:

$$\tan \alpha_2 = \frac{a}{g} \cdot \frac{h_a}{h_2} \cdot \frac{1}{\cos \alpha_a} \left[1 + \frac{\gamma + 1}{2} M_2^2 \left(1 - \left(\frac{\cos \alpha_2}{\cos \alpha_a} \right)^2 \right) \right]^{\frac{1}{\gamma-1}}$$

where h_a, h_2 = blade height in throat and downstream,

α_a, α_2 = throat angle (direction normal to throat) and downstream angle.

The equation takes the effect of the suction side curvature into account via the throat angle. It has been verified that the assumption of a negligible pressure force in the tangential direction is reasonable for blades with thin trailing edges and little curvature on the rear suction surface.

In the latest edition of his book "Thermische Turbomaschinen"¹⁴ Traupel shows a simple way of evaluating the effect of stream tube divergence, radius change and rotational speed on the outlet flow angle.

Potential Flow Theory

The successful use of potential flow theory for outlet flow angle prediction depends entirely on the judicious choice of the closure condition at the trailing edge. At VKI practically all subsonic blade to blade calculations are made with a compressible form of the Martensen method¹⁵. It seems that the Wilkinson condition (i.e. equal velocities on opposite points on the blade contour near the trailing edge) at present provides the best closure condition. This closure condition has, however, some shortcomings. It is the experience of K.Sieverding that if the location of the points in which the Wilkinson condition is imposed is kept constant then the outlet flow angle (referred to tangential direction) increases slightly with Mach number instead of decreasing as would be indicated by Traupel's equation. Cascade data confirm the tendency given by Traupel's equation. Furthermore cascade tests at VKI have shown that the point of equal velocity on pressure and suction side depends on the trailing-edge wedge angle and/or the rear suction side curvature. The isentropic outlet flow angle can of course be corrected for the effects of boundary-layer thickness and base pressure.

It seems that in modern turbomachinery practice turbine designers give preference to some sort of modified sine rule or to outlet flow angle calculations from blade to blade potential flow calculation methods. Deviation angle rules are nowadays practically out of use. The prediction capability of both modified sine-rule methods and blade to blade potential flow methods is of the same order of accuracy. From comparison with experimental data on some 25 cascades it appears that one can expect, at best, an accuracy of $\pm 1^\circ$. Tests at transonic outlet Mach numbers confirm that the simple sine rule is very well suited to predict the outlet flow angle for well shaped conventional blades. It is also our experience that outlet flow angles at transonic outlet Mach numbers calculated with time marching methods agree very closely with the simple sine rule. It should be noted that the above related experiences refer strictly to two-dimensional flows.

The turbine sub-group carried out a limited number of calculations for the prediction of the outlet flow angle of a gas turbine rotor blade ($\alpha_1 = 60^\circ$, $\arcsin a/g = 18^\circ$). The following methods were used: singularity method, finite element method and three different versions of time marching methods. Both the singularity method and the finite element method predicted an increase of α_2 with increasing Mach number. The curves differ, however, by as much as 2.5° . The time marching methods predicted, in agreement with the experiments, a decrease of α_2 up to sonic outlet flow conditions and an increase of α_2 for $M_2 > 1.0$. The results of the time marching methods lie between those of the singularity method and the finite element method. Compared with the experimental data their angles are too low by 0.5 to 2° .

2.3.2 Profile Losses

In contrast to compressor loss correlations there exist very few turbine loss correlations which do not refer to a specific blade family designed with one particular design concept. The reason lies in the fact that with some practice

anyone can draw up, not optimal, but reasonable turbine blade profiles. The need for a systematic blade design optimization is therefore less obvious. Nevertheless, we can distinguish 4 typical steps in turbine blade design practice:

- (a) profiles with contours composed only from circular arcs and straight lines,
- (b) NACA blade series and British blade profile series,
- (c) blades with continuous blade curvature and small deceleration rates,
- (d) hodograph methods and prescribed velocity distributions.

At present loss correlations distinguish, at the best, only between "old" profiles and "modern" profiles.

The table below indicates the main parameters considered explicitly by the correlations in Section 3 for the evaluation of profile losses:

Correlation	α_1	α_2	g/c	Profile	te	M_2	Re	Off-design
Ainley-Mathieson	X	X	X	t/c	X	X	X	X
Traupel	X	X	X		X	X	X	X
Baljé-Binsley	X	X	X				X	
Dejc-Trojanovski	X	X	X					
Craig-Cox	X	X	g/b	CR	X	X	X	X

Ainley-Mathieson (with corrections due to Dunham & Came) rely on cascade tests as well as on losses derived from overall tests on a variety of turbine stages.

α_1 : limited to a range extending from nozzle to impulse blades.

Profile: blades belonging to group a and b (above) with limits of blade thickness $0.15 < \frac{t}{c} < 0.25$ (outside of these limits take limit values).

M_2 : originally limited to $M_2 < 1.0$. Extension to $M_2 > 1$ by Dunham and Came¹¹.

te: correction factors for trailing-edge thicknesses $\left(\frac{te}{c} \neq 0.02 \right)$ are based on theoretical work.

Re: based on chord length and outlet velocity.

Ainley and Mathieson give Re-corrections for both profile losses and overall stage efficiency. For $Re > 1.0 \times 10^5$ the correction is the same for both.

Off-design: the losses are evaluated as a function of the ratio i/i_s where the stalling incidence i_s is a function of α_1 , α_2 and g/c. Note: Zero incidence is the incidence giving lowest losses for a given blade.

*Traupel*¹⁴: Traupel evaluates the basic profile losses for zero trailing-edge thickness, $\xi_{p,0}$, on the basis of an analytical expression for the dissipated energy using a dissipation coefficient of $c_d = 0.03$. The solution involves a reasonable choice of the mean blade velocity. The basic profile losses are given as a function of the inlet flow angle (zero incidence) and outlet flow angle.

te: the evaluation of the trailing-edge losses includes both the losses due to the finite trailing-edge thickness (Carnot-shock) and due to the difference between base pressure and the pressure in the trailing-edge plane between the blades. The base pressure is based on the work of Hörner¹⁶.

Profile: the correlation does not refer to a particular blade family. In general Traupel's profiles should be representative of group C above.

M_2 : based on data from various sources Traupel concludes that the Mach number influence depends strongly on the cascade geometry. For $M > 1$ Traupel recommends the calculation of shock losses on the basis of the supersonic deflection model.

Re: based on chord length and outlet velocity; Re correction in the range $10^4 < Re < 10^7$. (For a sandgrain roughness of $k_s/c = 2 \times 10^{-4}$ there will be no Re-influence for $Re > 3 \times 10^5$.)

g/c: the cascades are supposed to work at optimum pitch to chord ratios. The values of $(g/c)_{opt}$ are given by Traupel as a function of inlet and outlet angle (theoretical derivation with adaptation to experimental data).

$$\text{Off-design: } \xi_{p,\text{off}} = \xi_{p,0} + z \left(\frac{V_1}{V_2} \right)^2$$

where $\xi_{p,0}$ presents the losses the blade would have if it was designed for the off-design angle α_1 . Hence, $\xi_{p,0}$ is not a fixed value, it changes with α_1 . The factor z is a function of $(\alpha_1 - \alpha_1^*)$ with α_1^* as design inlet angle. Traupel recognises that there is a strong influence of the blade and cascade geometry on z but is unable to find well-defined trends. He therefore suggests a bandwidth with an uncertainty factor of approximately 2 for z .

Note: Traupel points out that cascades, which are designed with zero-incidence at a given design inlet flow angle α_1^* , might indeed have their optimum at α_1^* . However, for inlet flow angles $\alpha_1^* < 60^\circ$ other cascades can be designed which have their optimum profile losses at angles $\alpha_1 > \alpha_1^*$ but which at α_1^* still perform better than a cascade designed with zero incidence at α_1^* . Example: for $\alpha_1^* = 30^\circ$ lowest absolute losses will be obtained with a cascade designed with zero incidence at $\alpha_1 = 40^\circ$.

Baljé & Binsley⁷: The profile losses are calculated by assuming a linear variation of the velocity with camber-line length from the leading edge to the trailing edge. The momentum thickness along the blade surfaces is calculated using Truckenbrodt's equation for turbulent boundary layers. It turns out that the referred momentum thickness θ/l (l – camberline length) depends only on the acceleration ratio $\sin \alpha_2 / \sin \alpha_1$ and a constant k which is needed to match the theoretical predictions to available experimental data. The losses (referred to the isentropic downstream velocity) are presented as functions of the inlet and outlet blade angle.

- Te : it might be assumed that Baljé's final loss diagram is calculated for zero trailing-edge thickness. The equation for the losses includes, however, an allowance for non-zero trailing-edge thickness. The base pressure effect is not included; it could nevertheless easily be added (see Traupel).
- Profile: no reference is made to particular blade families. However, use is made of particular functions, relating both the stagger angle and the camberline length to chord ratio to the inlet and outlet flow angle.
- M_2 : there are no indications with respect to the Mach number level and the possible Mach number influence on ξ_p . However, Baljé points out in another paper¹⁷ that the losses will decrease with increasing Mach number since the acceleration ratio will increase. The fact that Baljé and Binsley use the ratio $\sin \alpha_1 / \sin \alpha_2$ for the acceleration rate rather than the velocity ratio suggests that the profile losses are given for incompressible flow.
- Re : the effect of Reynolds number is based on data by Gersten¹⁸. The Reynolds number (based on outlet velocity and camberline length) affects the losses up to $Re = 10^7$. Since no information on the effect of surface roughness is given, care has to be taken when using the curve at high Re-numbers.
- g/c : the loss diagram is given for optimum pitch to chord ratios (based on Zweifel coefficient $\psi_2 = 0.9$). No provision is made to calculate the losses at pitch chord ratios away from the optimum value.
- Off-design: no provision is made for off-design calculations.

Dejc & Trojanovski⁸: This loss correlation is based on experimental data gathered at various Russian institutes. The basic friction losses ξ_{RO} are given as functions of inlet and outlet flow angles for optimum pitch to chord ratios at an outlet Mach number $M_2 = 0.8$ and zero trailing-edge thickness. The optimum pitch to chord ratios are also given for $M_2 = 0.8$ and $te = 0$.

- M_2 : due to the fact that the $(g/c)_{opt}$ is a function of M_2 , the effect of a Mach number variation on the losses can be associated with a (g/c) effect resulting from the difference between $(g/c)_{opt, M_2=0.8}$ and $(g/c)_{opt, M_2 \neq 0.8}$.

- g/c : the effect of $g/c \neq (g/c)_{opt}$ is calculated from the equation

$$\xi_R = \xi_{RO}(1 + \Delta\xi_R)$$

where $\Delta\xi_R$ is given as function of

$$\Delta g' = \frac{g - g_{opt}}{g_{opt}} \quad \text{and} \quad (g/c)_{opt}$$

$(g/c)_{opt}$ was calculated in the preceding step as a function of the Mach number.

- te : the profile losses including the trailing-edge losses are calculated from

$$\xi_p = \xi_R + \xi_{te=0} + k \cdot \left(\frac{te}{a} \right)$$

with $\xi_{te=0} \approx 0.08$ and $k = f(M_2 \text{ and } Re)$.

- Re : based on chord length and isentropic outlet velocity. The basic friction losses are representative of the Re-range $0.4 \times 10^6 < Re < 1.2 \times 10^6$.

- Profile: these investigations refer to blades presented in the Russian profile atlas¹⁹. The blades belong to the groups c mentioned above.

- Off-design: no information is given.

It should be noted that Dejc and Trojanovski are the only authors to make a distinction between profile losses in straight cascades and in turbines. The correction factor depends on the axial distance between stator and rotor.

*Craig & Cox*⁹ present a correlation based on experimental data from straight cascades. The main parameters are: inlet and outlet flow angles, expressed in terms of a lift parameter, the ratio of pitch to backbone length g/b and the contraction ratio of the internal cascade passage. These parameters result in a basic profile loss term for zero trailing-edge thickness which is subsequently modified by correction terms for the influence of t_e , Re , M , etc.

- g/c : the authors are the only ones who use the ratio of the pitch with respect to the backbone length g/b rather than the chord length g/c . The use of the backbone length has the advantage of being closer related to the boundary-layer development, however, it is more difficult to handle.
- Profile:** the effect of the profile shape is to a certain extent indirectly implied by the passage contraction ratio. The correlation also includes the effect of the rear suction side curvature at high outlet Mach numbers, $M_2 > 0.8$.
- t_e : the trailing-edge losses are evaluated theoretically in a similar manner to Traupel.
- M_2 : shock losses are evaluated for $M_2 > 1.0$.
- Re : based on throat and outlet velocity. The Re number effect is predicted for the range $10^4 < Re < 10^7$.
- Off-design:** Craig & Cox evaluate the positive and negative stall incidence as well as the optimum incidence. The correction factor for off-design is calculated as a function of the incidence parameter: $(i - i_{\min}) / (i_{\text{stall}} - i_{\min})$.

Denton²⁰ compared four of the preceding loss correlations (the method of Dejc used by Denton is different from the method presented in this paper) plus his own method²¹ (which is based on theoretical calculations of a large number of cascades) with experimental data from some 80 cascades. The comparison was made for near optimum (g/c -values, zero-incidence, high Re -numbers and low Mach numbers. It appears from this study that the method of Baljé & Binsley, followed very closely by Denton's method, shows the best agreement with experimental data. In spite of this favourable result for Baljé & Binsley there seem to remain some inconsistencies in this correlation since the losses for nozzle blades with 20° outlet angle are predicted to be higher than for a blade with the same outlet angle but 45° inlet flow angle.

VKI data confirm that the Craig & Cox method systematically overpredicts two-dimensional profile losses. An important question is whether two-dimensional profile losses can be applied to turbines without any correction. It could well be that Craig & Cox have assessed the general level of profile losses for the benefit of a better accuracy of the final overall performance estimation for which the authors claim an accuracy of $\sim \pm 1.25\%$ based on the analysis of more than fifty turbines.

It seems that any progress in the reliability of profile loss correlations must be along Denton's approach i.e. establishment of correlations on a theoretical basis for certain blade families where all blades have similar characteristics. This implies in particular efforts to predict more accurately the boundary-layer transition point and transition length and the effects of blade roughness and turbulence on both and finally to develop methods to predict locally and fully separated boundary layers. As a back-up for the theoretical methods some well-defined and well documented special purpose tests are needed. Such an experimental program could only be carried out with the collaboration of several research institutes.

2.3.3 Secondary Losses

The number of correlations available bears no relation to the number of comprehensive data sets published in the literature. There seem to be only two organizations which have provided any systematic data in this domain i.e. members of the group of Schlichting and members of the University of Dresden (in particular Wolf). Apart from these data there exists a number of published data of very limited value due to the fact that they are concerned in general only with one particular aspect of the problem and investigated only a small number of cascade configurations, making an eventual extrapolation very dangerous.

Most of the data were obtained on straight cascades. The effect of radial migration of losses in real stages is acknowledged and demonstrated in some cases (i.e., Ref.22) but no systematic investigations are made. The secondary loss correlations naturally suffer greatly from this lack of understanding of the real flow phenomenon: all correlations provide an additional loss coefficient to be added to the two-dimensional or mid-span loss for non-twisted blades and usually for unit axial velocity ratio. Information on the spanwise loss distribution is practically non-existent in the literature.

It is in particular discouraging and frustrating that the most recent investigations into the effect of inlet boundary-layer thickness cannot usually be applied to turbine stages because of the difficulty of defining an equivalent endwall boundary-layer profile. Present investigations in this domain are therefore only justified to the extent in which they serve as guideline for a better understanding of the physical phenomena. This effort needs to be extended both experimentally and theoretically to flows in annular cascades and finally to turbine stages where only full three-dimensional treatment can provide real progress.

There exist several review papers (e.g. References 13 and 24) which discuss the numerous secondary flow correlations in detail. As in the case of profile loss we shall only consider those correlations which are integral parts of more or less

complete turbine performance prediction methods. Table 2.1 presents the main parameters used in the correlations. The background of the various correlations as well as their limitations and peculiarities will be briefly discussed.

Ainley & Mathieson (corrected by Dunham & Came⁵): The basic equation for secondary losses on nozzle blades was mainly derived from test data on bent metal sheet blades. The secondary losses in rotor blades were derived from performance measurements on turbines with conventional blading (i.e. belonging to groups a and b on page 17) using the correlation already established for profile losses in stator and rotor, for secondary losses in the nozzle and clearance loss in the rotor. Ainley showed that the secondary losses for both nozzle and rotor could be expressed by the equation

$$Y_s = \lambda \cdot z$$

where $z = \frac{C_l^2}{(g/c)} \cdot \frac{\cos^2 \beta_2}{\cos^3 \beta_{\infty}}$ is known as Ainley's loading parameter.

TABLE 2.1

Secondary Loss Correlations

Correlation	Turning angle	Velocity or Angle ratio	Aspect ratio	g/c	Profile	Inlet B.L.	M ₂	Re	Extension of second. reg.	Off-design
Ainley-Mathieson (Dunham-Came)	X	V	A	id/od	X					
Traupel	X	V	A	g/h	X	negl.	ind		X	X
Balje				h/c		X				
Dejc-Trojanovski	X	V	A	h/c	X	X		X		
Craig-Cox	X	V		h/b				ind		limited

Note: authors using loading parameters rather than explicitly turning angle and velocity (or angle) ratio are also listed in columns 1 and 2.

Aspect ratio: λ is a function of the inlet and outlet flow area of the blade passage and the inner to outer diameter ratio of the blade row. For two-dimensional cascades the relation becomes

$$\lambda = f\left(\frac{1}{2} \cdot \frac{\cos \beta_2^2}{\cos \beta_1'^2}\right).$$

(Note: angles with respect to axial direction.)

McDonald¹ shows that λ correlates the loss data much better than the original Ainley parameter if expressed as a function of $\cos \beta_2 / \cos \beta_1$. This means that the original Ainley method does not properly account for the aspect ratio effect. Dunham²³ modifies Ainley's equation as follows:

$$Y_s = \frac{c}{h} \cdot z \cdot \frac{\cos \beta_2}{\cos \beta_1'} \cdot f\left(\frac{\delta^*}{c}\right)$$

where $f(\delta^*/c)$ presents the inlet endwall boundary-layer effect. Using Wolf's data²⁵ plus data from other less systematic investigations, Dunham concludes that the secondary losses increase constantly with δ^*/h following the relation

$$f(\delta^*/h) = 0.0055 + 0.078\sqrt{\delta^*/h}.$$

This is contrary to the conclusion of Wolf who finds that the loss very rapidly reaches an asymptotic value.

In a later paper by Dunham and Came⁵ it is proposed to replace $f(\delta^*/h)$ by a single constant $f(\delta^*/h) = 0.0334$. This modification appears to improve the prediction for low-aspect ratio turbines but it appears that secondary losses for LP turbines are overestimated.

Re : Dunham & Came suggest that secondary losses are affected by Reynolds number in the same way as profile losses: i.e. in proportion to

$$\left(\frac{Re}{2 \times 10^5}\right)^{-0.2}$$

Off-design: the use of the flow angle β_1 , in the loading parameter z instead of the blade angle β_1' implies *a-priori* that situations in which β_1 differs from β_1' can be handled. However, this can scarcely be looked upon as a method of calculating off-design conditions. Incidence angle effects not only influence the overall load but also change the chordwise load distribution.

Traupel: the structure of Traupel's secondary loss correlation is derived from Wolf's presentation of secondary loss data obtained on straight cascades. The quantitative values are, however, obtained by comparison with unpublished results on turbine stages. Traupel's secondary losses are twice as high as those of Wolf. The secondary losses are expressed as:

$$\xi_s = \frac{\xi_p}{\xi_{p_0}} \cdot F \frac{g}{h} \quad \text{with} \quad F = f\left(\frac{V_1}{V_2}, \Delta\beta\right)$$

the factor ξ_p/ξ_{p_0} indicates that the secondary losses should be increased in the same ratio as that by which the profile losses exceed the basic profile losses ξ_{p_0} .

V_1/V_2 : the use of the ratio V_1/V_2 instead of $\cos \alpha_1/\cos \alpha_2$ implies that the correlation does account for compressibility effects. Using the ratio V_1/V_2 without limitation of V_2 must certainly lead to an excessive compressibility effect (due to the rapid change of V_1/V_2) in the high subsonic range at nearly constant β_2/β_1 .

g/h : in contrast to other authors Traupel uses g/h instead of c/h or similar expressions.

inlet boundary layer: Traupel refers to the results of Wolf indicating that the influence of a variation of the inlet boundary-layer thickness is limited to a zone $\delta^*/h < 0.03$ which according to Traupel is of no interest in real turbines.

extension of secondary flow zone: the critical height to pitch ratio at which the secondary zones grow together is given as

$$\left(\frac{h}{g}\right)_{cr} = 6 + 10\sqrt{\xi_p}.$$

The values of ξ_p should be limited to the subsonic range. Traupel also proposes the calculation of a total blade loss coefficient in cases where the blade height is below the critical height using the equation

$$\xi_s = \frac{\xi_p}{\xi_{p_0}} \cdot \frac{F}{(h/g)_{cr}} + (0.02 \rightarrow 0.035) \left(c/h - \frac{c/g}{(h/g)_{cr}} \right).$$

The secondary losses at off-design conditions are calculated in the same way as the profile losses at off-design, i.e. by

$$\xi_s = \xi_{s,0} + z \left(\frac{V_1}{V_2} \right)^2.$$

Baljé & Binsley⁷: the authors believe that Wolf's data²⁵ are the most comprehensive set of experimental data available at present. The authors present Wolf's data in the form of a minimum referred endwall loss coefficient for zero initial endwall boundary-layer thickness as a function of inlet and outlet blade angle.

inlet boundary-layer thickness: the authors use Wolf's curve

$$k = \frac{\xi_{s,\delta^*=0}}{\xi_{s,\delta^*=0}} = f\left(\frac{\delta^*}{h}\right)$$

with a limiting value of $k = 3$ for $\delta^*/h = 0.03$.

In contrast to Traupel, who argues that the range of $\delta^*/h < 0.03$ is of no interest for turbines, Baljé and Binsley try to take advantage of the variation of ξ_s with δ^*/h and suggest applying different coefficients 'k' for nozzle and rotor.

Re: the authors rely on Wolf whose data do not show evidence of a Reynolds number influence.

extension of secondary flow region: again based on the work of Wolf, Baljé suggests evaluating the critical blade height for which the secondary flow zones start to grow together through the equation.

$$\frac{h_{cr}}{h} = \frac{\Delta\beta \left(1 + \frac{\sin \beta'_2}{\sin \beta'_1} \right) 0.022}{(\delta^*/h) \cdot (h/g)} \cdot \frac{\delta^*}{h}.$$

(Note: angles with respect to tangential direction.)

Dejc & Trojanovski⁸ present a correlation based on Russian experimental data as in the case of profile losses

$$\xi_s = \frac{AK_1}{(c/h)Re^m} \left[1 + B \left(1 + \frac{\rho_2}{\rho_1} \frac{\operatorname{ctg} \beta_1}{\operatorname{ctg} \beta_2} \right)^2 \frac{g}{c} \cos^2 \beta_2 \right].$$

(Note: angles with respect to tangential direction.)

The coefficients A, K₁, m and B depend on whether one is dealing with impulse or reaction cascades with laminar or turbulent boundary layers.

*Craig & Cox*⁹: the correlation is based on experimental data from straight cascades. The main variables are the lift factor already used for the evaluation of the profile losses and the square of the ratio of inlet to outlet velocity:

$$X_s = X_{s,b} \times N_R \times N_{h/b}$$

with $X_{s,b}$ — basic secondary loss factor,
 N_R — influence of Re ,
 $N_{h/b}$ — influence of aspect ratio.

The authors draw attention to the fact that a distinction must be made between shrouded and unshrouded blade rows. The correlation proposed here refers to shrouded blades.

$(V_1/V_2)^2$: the authors maintain that the correlation holds approximately over a range of incidences (not specified by the authors) provided that the correct velocities are used in evaluating the basic loss coefficient.

h/b : for high values of h/b the losses vary linearly with h/b . For small aspect ratios the tip and root loss concentrations tend to merge together and the rate of increase is less than would be expected from a simple inverse law.

Re : the Re number effect is supposed to be the same as for the profile losses.

A comparison of the preceding secondary flow correlations plus five other correlations was carried out by Chauvin²⁴ for both nozzle and impulse blades with the following conditions: $h/c = 1$, optimum g/c , low M_2 and $Re = 2 \times 10^5$. The result is discouraging. The losses of the five correlations reported herein vary not only by a factor of up to five but their slopes and shapes are completely different. Similar levels of disagreement were found by Dunham²⁵.

Considering the amount of research work which has been carried out in previous years and, keeping in mind how few reliable, systematic and well documented data are available one must conclude that much of the work has contributed very little to progress in this field.

Isolated research projects are of little use. What is needed for a better understanding of the generation of losses, and as back-up for theoretical investigations, are systematic investigations with very well-defined test conditions on a large number of carefully selected blade profiles (possibly carried out in collaboration by several research groups) coupled with a limited number of very detailed investigations of the whole three-dimensional flow field in stationary and moving blade rows. The second type of tests are so time and money consuming that their number is severely limited. Hence a general consensus between the various research groups should be reached as to the choice of the particular configurations. Furthermore better collaboration is needed between theoreticians and experimentalists for analysis of the test data. It often happens that valuable information gets lost because the experimentalist cannot take full advantage of the mass of recorded data which, if presented differently, could be helpful to the theoretician in the development of a new approach to the understanding of complex three-dimensional boundary layers.

2.3.4 Annulus Losses

This group of losses is dealt with separately only by Traupel and Craig and Cox.

Traupel: considers in particular the losses occurring in stages with shrouded blades, where the flow has to traverse axial spaces with free shear layers at the ends of the blading. The main influence parameters are:

- the outlet angle from stator or rotor,
- the ratio of the axial spacing to the blade height,
- the overlapping between two successive blade rows (i.e. step changes in annulus height).

(A positive overlapping might result in an "ejector effect" which causes additional losses.)

Craig and Cox: base their annulus loss factor on the sum of 3 individual loss components:

- (a) annulus loss factor due to controlled or uncontrolled expansion in the annulus area between two blade rows (between stator and rotor in general small),
- (b) cavity loss factor (i.e. cavities for internal water separation),
- (c) cavity loss due to sudden expansion (e.g. positive overlapping between two blade rows).

Ainley: considers the annulus losses as part of the secondary losses which of course excludes a detailed analysis of effects such as overlapping and wall cavities.

2.3.5 Clearance Flows

The treatment of clearance flows must include both the evaluation of the clearance losses and the effect of the clearance flow on the mass flow. Due to a lack of data on straight and annular cascades the clearance losses are in general evaluated from turbine tests. This source of information is in general, however, only available to turbine manufacturers. It appears that the only systematic investigation in straight and annular cascades was done by Hubert²⁷. His data are used by both Traupel and Balje for their clearance loss correlations. Dejc and Trojanovski argue that a direct application of Hubert's results to turbine stages is not possible because of the influence of rotation which is particularly strong in the case of small clearances.

Detailed measurements of the tip leakage flow rates and losses in both a cascade and in a model turbine are also reported by Denton and Johnson²⁷.

Ainley & Mathieson (Dunham & Came): the authors present the clearance loss as a function of the same load parameter as the secondary loss. The only difference is that the aspect ratio parameter is replaced by the clearance to blade height ratio:

$$Y_{cl} = B \cdot \frac{\delta_r}{h} \left(\frac{C_l^2}{\frac{g}{c}} \right) \underbrace{\frac{\cos^2 \alpha_2}{\cos^3 \beta_\infty}}_Z$$

The difference between unshrouded and shrouded blading is taken into account by the factor B ($B = 0.5$ for unshrouded, $B = 0.25$ for shrouded blades).

An obvious criticism is that the totally different flow mechanism in the two cases is not reflected in this approach.

Dunham & Came have introduced a modification based on Hubert's data which suggest that the usual linear dependence of losses on tip clearance should be replaced by a power law. The final expression is:

$$y_{cl} = B \cdot \frac{c}{h} \left(\frac{\delta_r}{c} \right)^{0.78} \cdot Z$$

where $B = 0.47$ for unshrouded blades and

$B = 0.37$ for shrouded blades.

In case of multiple seals, δ_r is to be replaced by

$$\delta_r^* = \delta_r \times (\text{number of seals})^{-0.42}$$

The effect of the clearance on the mean outlet flow angle is evaluated by assuming that the mass flow through the clearance is undeflected:

$$\beta_{2,cl} = \tan^{-1} \left[\left(1 - X \left(\frac{\delta_r}{h} \right) \left(\frac{\cos \beta_1}{\cos \beta_2} \right) \right) \tan \beta_2 - X \left(\frac{\delta_r}{h} \right) \left(\frac{\cos \beta_1}{\cos \beta_2} \right) \tan \beta_1 \right]$$

*Traupel*⁶: this author takes completely different approaches for unshrouded and shrouded blades. For unshrouded blades he proposes the equation

$$\xi_c = 4 \cdot K \cdot G \cdot \frac{V_x}{u} \frac{\delta_r - 0.002C}{\left(1 - \left(\frac{D_H}{D_T} \right)^2 \right) D_T}$$

for the rotor and a similar expression for the stator

where $K = f \left(\frac{\delta_r}{C} \right)$ and

$G = f$ (inlet angle and outlet angle).

The structure of the functions K and G are based on Hubert's experimental data. The quantitative values have been adjusted by experiments on turbine stages.

The effect on the mass flow is expressed by the mass flow coefficient k :

$$\dot{m} = k \cdot \rho \cdot V_x \cdot A$$

with

$$k = B + C \frac{\delta_r}{\left(1 - \left(\frac{D_H}{D_T}\right)^2\right) D_H} \cdot \frac{g}{c} \cdot H$$

for the rotor and a similar expression for the stator

$$\begin{aligned} B &= f \text{ (endwall displacement thickness)} = 0.98 \rightarrow 1.0, \\ C &= 1.5 \text{ to } 2.5, \\ H &= f \text{ (inlet and outlet angle).} \end{aligned}$$

The approach taken by Traupel for shrouded blades follows the evaluation of flows through seals. Hence, the clearance mass flow is calculated as:

$$\dot{m}_{cl} = \mu A_{cl} \sqrt{\frac{1}{z} \frac{\rho_1}{p_1} (p_1^2 - p_2^2)}$$

with μ -- mass flow coefficient,

A_{cl} -- clearance area,

z -- number of seals,

p_1, p_2 -- upstream and downstream pressure taken at the blade extremity near the seal.

Having determined \dot{m}_{cl} the flow coefficient k in the equation

$$\dot{m} = k \cdot \rho \cdot V_x \cdot A$$

is calculated as

$$k = B + \frac{\dot{m}_{cl}}{\dot{m}_{bl} - \dot{m}_{cl}}$$

where \dot{m}_{bl} = total mass flow through blade row,

$B = 0.98 \rightarrow 1.0$ as in the case of unshrouded blades.

A graph presenting $\xi_{cl} = f\left(\frac{\dot{m}_{cl}}{\dot{m}_{bl} - \dot{m}_{cl}}\right)$ is used for calculation of the clearance losses.

Baljé¹⁷ bases his expression for clearance losses on the data by Hubert on straight cascades:

$$\sqrt{\frac{h}{\delta r}} \frac{h}{c} \xi_{cl} = f(\delta u, \beta_{\infty}).$$

For the angle deviation due to the clearance flow Baljé refers again to Hubert, who found that $\Delta\beta_{cl}$ varied linearly with the relative clearance and that all experimental points fall on one single straight curve when relating Δ_{cl} to an appropriate expression for the blade loading:

$$\Delta\beta_{cl}^* = \Delta\beta_{cl} \cdot \frac{c}{g} \cdot \frac{1}{\delta_{\mu,e}} \cdot \frac{\sin_{\infty,e}}{\sin_{2,e}^2} = K \cdot \frac{\delta}{c}$$

where $\delta_{\mu,e} = Ag\beta_{2,e} - Ag\beta_1$,

$\beta_{\infty,e}$ -- mean vector angle for zero clearance flow,

$\beta_{2,e}$ -- outlet flow angle for zero clearance flow,

$\beta_{2,cl}$ -- outlet flow angle in presence of tip clearance flow,

$$\Delta\beta_{cl} = \frac{h}{2c} (\beta_{2,cl} - \beta_{2,e}) \text{ referred outlet angle.}$$

Dejc & Trojanovski⁸ base their correlation on data from actual tests performed by various Russian organizations. For unshrouded blades the deterioration of the stage efficiency is mainly attributed to a significant distortion of the meridional streamlines and a redistribution of the mass flow along the radius:

$$\xi_{cl} = a \cdot \frac{\pi \cdot D_T \cdot \delta_r}{A_1} \sqrt{\frac{R_T}{1 - R_m}} \cdot \eta_u \left(1 + R_m^{\frac{1-\pi}{\pi}}\right)$$

where R_T, R_m — degree of reaction at tip and mean radius,
 π — pressure ratio across blading,
 A_1 — annulus area between stator and rotor,
 η_u — stage blading efficiency (including profile, secondary and annular losses).
 $a = 0.45 \rightarrow 0.65$.

For shrouded blades

$$\xi_{cl} = k_r \cdot \frac{\pi \cdot D_T \cdot \delta_{equ}}{A_1} \sqrt{\frac{R_T}{1 - R_m}} \left(1 + \frac{1-\pi}{\pi} \right)$$

where $\delta_{equ} = \frac{1}{\sqrt{\frac{4}{\delta_a^2} + \frac{1+5+z}{\delta_r^2}}}$,

δ_a — axial clearance,

δ_r — radial clearance,

z — number of seals,

$$k_r = A \left(0.2 + \frac{\sin \beta_2}{\sin \beta_{1,H}} \right)$$

(angles with respect to tangential direction),

$A = 1$ for blades with constant profile,

= 1.2 for blades with variable profile.

The authors also give a second equation which is easier to use:

$$\xi_{cl} = k_r \cdot \frac{\delta_{equ}}{h_1 \cdot \sin \alpha_1} \cdot \eta_u \cdot \chi_{cl}$$

where h_1 and α_1 refer to the stator exit,

η_u — stage blading efficiency (including profile, secondary and annular losses),

χ_{cl} — f (degree of reaction at mid-span and mean diameter to blade height ratio).

Craig & Cox: For unshrouded blades the authors consider the data of Ainley as fairly representative "provided that axial velocity remains approximately constant across the blade row and provided that the relative velocities are well below the sonic value". For shrouded blades they calculate an efficiency debit

$$\Delta \eta_{cl} = F_{cl} \cdot \frac{A_{cl}}{A_{bl}} \cdot \eta \text{ (zero clearance)}$$

where A_{cl} — clearance annulus area,

A_{bl} — blade annulus area,

$$F_{cl} = f \left(\frac{\Delta h}{h}, \frac{W_2^2 - W_1^2}{W} \right)_{tip},$$

Δh — amount of overlap.

The approach is similar to the one expressed by the second equation for ξ_{cl} given by Dejc and Trojanovski.

2.3.6 Miscellaneous Losses

2.3.6.1 Disc Windage Losses

The disc friction moment for a disc rotating in a housing is given by

$$M = 2 \cdot \rho \cdot u^2 \cdot D^3 \cdot C_f$$

where C_f is an empirical friction coefficient.

Baljé, Dejc & Trojanovski as well as Cox refer to the work of Daily and Nece²⁹ for the evaluation of the coefficient C_f . Ainley refers to much older work and Traupel refers to Schlichting.

2.3.6.2 Partial Admission Loss

Ainley: no indication is given.

Traupel: this author refers to experimental work by *Suter* and *Traupel*³⁰. They distinguish between two loss components:

- (a) ventilation loss,
- (b) filling and emptying loss at the ends of the admission sectors

$$\xi_{p.a.} = C \frac{1 - \epsilon}{\epsilon \cdot \phi \cdot \psi} + \frac{0.30 \cdot z \cdot b}{\epsilon \sqrt{\psi} \cdot D_m}$$

ventilation sector end
loss losses

where C – coefficient dependent on whether non-admitted part of rotor turns in open or closed space and is further dependent on mean diameter to blade height ratio,

ϵ – partial admission,

z – number of sectors,

b – axial width of rotor,

$\phi = V_x/u$,

$\psi = \Delta h_{is}/(u_2^2/2)$ (stage loading coefficient).

The tip clearance loss does not need special treatment except that for shrouded blades where the partial admission coefficient ϵ has to be introduced.

*Balje & Binsley*⁷: consider the following loss components:

- (a) filling and emptying losses,
- (b) scavenging losses,
- (c) blade pumping losses,
- (d) leakage losses.

The authors refer to work of *Stenning*³¹ for loss component (a) and (b), to *Mann* and *Marston*³² for loss (c) and to *Linhardt* and *Silvern*³³ for loss (d).

*Dejc & Trojanovski*⁸: Consider only ventilation losses and sector end losses (as in Traupel's method). Referring to *Suter* and *Traupel*, they state that their equation in general leads to too low an estimate of the loss.

Dejc & Trojanovski propose for the case of the uncovered rotor with one single admission segment and $\epsilon = 0.3$ to 0.9:

$$\xi_v = 0.35 \left(\frac{0.3 \cdot x_f}{D \cdot \sin \alpha_1} + \frac{1 - \epsilon}{\epsilon} \right) x_f^2 - \eta_b l$$

where

$$x_f = \frac{u}{\sqrt{2(\Delta h_{stage} + V_0^2)}}$$

$$D = D/D_0 \text{ and } D_0 = 1 \text{ m.}$$

In the case of several admission sectors the additional losses are evaluated as

$$\xi_z = 0.25 \cdot \frac{b \cdot h_2}{A_1} x_f \cdot \eta_b / (z - 1)$$

where b – axial width,

h_2 – rotor blade height at outlet,

A_1 – annular area at rotor inlet.

*Craig & Cox*⁹ refer to the work of *Suter & Traupel*.

2.4 RADIAL LOSS AND ANGLE DISTRIBUTION

The only suggestion with respect to the radial distribution of loss is made by Traupel:

$$\eta(r) = \underbrace{1 - \xi_p}_{\text{outside}} - \Delta\eta \left(\frac{x}{\Delta l} \right)^2$$

where η includes only profile and secondary losses. Δl presents the extension of the secondary flow region:

$$\Delta l = (3 \rightarrow 5) \cdot g \cdot \sqrt{\xi_p}$$

The $\Delta\eta$ values have to be chosen such that the integration over r correctly represents the mean value of profile and secondary losses.

The only known method proposed for radial distribution of the deviation angle is that of Bardon et al.³⁴ who base their correlation on the results of secondary flow theory. Use of the correlation requires knowledge of the annulus boundary-layer thicknesses at entry to the blades. Further discussion of means of distributing the secondary deviation is included in Chapter 4.

REFERENCES

1. Latimer, R.J. *Axial Turbine Performance Prediction*. VKI, LS 1978-2.
2. Smith, S.F. *A Simple Correlation of Turbine Efficiency*. Journal of Royal Aeronautical Science, Vol.69, p.467, 1965.
3. Soderberg, C.R. Unpublished notes. Gas turbine Laboratory, MIT (1949) (see "Axial Flow Turbines", Horlock, London Butterworths 1966).
4. Ainley, D.G. Mathieson, G.C.R. *An Examination of the Flow and Pressure Losses in Blade Rows of Axial Flow Turbines*. ARC R & M, 1951.
5. Dunham, J. Came, P.M. *Improvements to the Ainley-Mathieson Method of Turbine Performance Prediction*. Trans. ASME(A), Vol.92, No.3, p.252, July 1970.
6. Traupel, W. *Thermische Turbomaschinen*, Bd. I, Springer Verlag, 1966.
7. Balje, O.E. Binsley, R.L. *Axial Turbine Performance Evaluation. Part A: Loss-Geometry Relationship*. ASME Transactions, Series A, J. Engrg for Power, Vol.90, October 1968.
8. Dejc & Trojanovski *Untersuchung und Berechnung axiauer Turbinenstufen*. VEB Verlag Technik, Berlin, 1973.
9. Craig, H.R.M. Cox, H.J.A. *Performance Estimation of Axial Flow Turbines*. Proc. Inst. Mech. Engrs, Vol.185, 32/71, 1970-71.
10. Carter, A.D.S. Hughes, H.P. *A Theoretical Investigation into the Effect of Profile Shape on the Performance of Airfoils in Cascades*. ARC R & M 2384, 1950.
11. Dunavant, J.C. Erwin, J.R. *Investigation of a Related Series of Turbine Blade Profiles in Cascades*. NACA TN 3802, 1956.
12. Triebnigg, H. Mukherjee, D.F. *Ueber Verluste in Axialturbinenstufen und die Möglichkeiten einer optimalen Auslegung*. VDI Zeitschrift, Reihe 6, Nr. 7, 1966.
13. Bammert, K. Sonnenschein, H. *Der Einfluss von verdickten und verdünnten Turbinenschaufeln auf die Gittereigenschaften*. Archiv für Eisenhüttenwesen, Heft 4, 1967.
14. Traupel, W. *Thermische Turbomaschinen*, Bd. I, Springer Verlag, 1978.
15. Van den Braembussche, R.A. *Calculation of Compressible Subsonic Flow in Cascades with Varying Blade Height*. Journal of Eng. for Power.

16. Hoerner, S.F. *Base Drag and Thick Trailing Edges.* J. Aeronautical Sci., Vol.17, pp.622-628, 1950.
17. Baljé, O.E. *Axial Cascade Technology and Application to Flow Path Designs. Part I: Axial Cascade Technology.* J. of Engrg for Power, Vol.90, October 1968.
18. Gersten, K. *The Influence of Reynolds Number on the Flow Losses in a Plane Cascade (in German).* Proc. of the Braunschweig Scientific Society, Vol.11, 1959.
19. Dejc, M.E. *Atlas of Axial Turbine Characteristics.* Mashinostroenie Publishing House, Moscow, 1965.
Filippov, G.A.
Lazarev, L.Ya.
20. Denton, J.D. *A Survey and Comparison of Methods for Predicting the Profile Loss of Turbine Blades.* Proc. Inst. Mech. Engrgs, Warwick, Paper C76/73, 1973.
21. Denton, J.D. *A Method of Predicting the Profile Loss of Turbine Cascades.* Aeronaut. Res. Council, 33222 Turbo. 176, 1971 (unpublished).
22. Allen, H. *Experimental Investigation of Losses in Annular Cascade of Turbine Nozzle Blades of Free Vortex Design.* NACA TN 2871, 1953.
Kofskey, M.G.
Chamness, R.E.
23. Dunham, J. *A Review of Cascade Data on Secondary Losses in Turbines.* J. Mech. Engrg Science, Vol.12, No.1, p.48, 1970.
24. Chauvin, J. *Turbine Cascade Endwall Losses. A review.* VKI LS 72, January 1972.
25. Wolf, H. *Die Randverluste in geraden Schaufelgittern.* Wissenschaftl. Z. der TH Dresden, 10, Heft 2, 1961.
26. Hubert, G. *Untersuchung über die Sekundärverluste in axialen Turbomaschinen.* VDI Forschungsheft 496.
27. Denton, J.D. *An Experimental Study of the Tip Leakage Flow Around Shrouded Turbine Blades.* CEGB Report R/M/N848, 1976.
Johnson, C.J.
28. Utz, C. *Experimentelle Untersuchung der Strömungsverluste in einer mehrstufigen Axialturbine.* Mittl. Inst. Term. Turbomasch., ETH Zurich, Nr. 19, 1972.
29. Daily, J.W. *Chamber Dimensions Effects on Induced Flow and Frictional Resistance of Enclosed Rotating Discs.* ASME Transct., Series D, J. Basic Engrg, Vol.82, No.1, 1960.
Nece, R.E.
30. Suter, P. *Untersuchungen über den Ventilations-verlust von Turbinenradern.* Mittl. Inst. Therm. Turbomasch., ETH Zurich, Nr. 4, 1959.
Traupel, W.
31. Stenning, A.A. *Design of Turbines for High-Energy-Fuel-Low-Power Output Applications.* MIT, Dynamic Analysis and Control Lab., Report 79, 1953.
32. Mann, R.W. *Friction Drag on Bladed Discs in Housings as a Function of Reynolds Number, Axial and Radial Clearance and Blade Aspect Ratio and Solidity.* ASME Transact., Series D, J. Basic Engrg, Vol.83, No.4, 1961.
Marston, C.A.
33. Linhardt, H.D. *Analysis of Partial Admission Axial Impulse Turbines.* J. American Rocket Soc., March 1961.
Silvern, D.H.
34. Bardon, M.F. *Secondary Flow Effects on Gas Exit Angles in Rectilinear Cascades.* ASME J. Eng. Power 97A, 1975.
Moffat, W.C.
Randall, J.L.

Chapter I.3

INFLUENCE OF CORRELATION AND COMPUTATIONAL METHODS ON THE PREDICTION OF OVERALL EFFICIENCY

The process of designing a gas turbine or a steam turbine begins with an evaluation of the influence of component design parameters on the overall operating cost. For both the steam turbine and the gas turbine, energy costs are rapidly increasing and component efficiency is therefore a primary design objective. For the aircraft gas turbine the weight of the component influences the fuel consumption and is therefore also an important energy cost consideration. The prediction of turbine efficiency is a critical part of the design optimization process for both steam turbines and gas turbines.

Turbine efficiency predictions, together with information which influence the weight and cost, are obtained from flow field calculations which define the thermodynamic properties and velocity triangles throughout the turbine. These computational methods may be full span through flow calculations which predict the fluid properties from the hub to the tip between each blade row or they may be mean-line calculations. In either case they are dependent upon loss and deviation models for their effectiveness in the efficiency optimization stage of the design process. The loss and deviation correlations which are in common use by steam turbine and gas turbine manufacturers are frequently developed internally and are maintained as proprietary information. The overall efficiency predictions which will be discussed are therefore limited to results obtained using the correlations built into the methods which are described in the Appendices. For this reason the quality of the results described in this chapter may not be a valid indication of the capability of today's existing turbine efficiency prediction methods. In addition to being limited to published correlations, this study has also been constrained by a very limited number of available test cases for which complete data are available. The test case geometries and operating conditions are described in detail in the Appendices together with test data and sample calculations. The influence of these correlations and computational methods on the prediction of overall efficiency is presented in the following sections.

3.1 THE PREDICTION OF DESIGN POINT EFFICIENCY

3.1.1 The Influence of the Computational Method on Efficiency Prediction

It is generally accepted that the quality of any turbine efficiency prediction system is primarily dependent upon the loss correlations which are used in support of the basic aerodynamic model. As a means of evaluating the importance of the other factors which influence the efficiency prediction, four individuals using different computational methods have each predicted the efficiency of the Cambridge Turbine using the Craig & Cox loss correlations.

Cambridge Turbine – Craig and Cox Correlations

Computational Method	Predicted η	Pred. η – Test η
Streamline curv. (by Denton)	91.47	-2.33
Streamline curv. (by Macchi)	91.9	-1.8
NISRE (by Sieverding)	92.2	-1.6
Finite Element (by Ucer)	90.4	-3.4

The Cambridge Turbine has a test efficiency (total-total) of approximately 93.8% although this is subject to a good deal of uncertainty, possibly $\pm 3\%$. All of these efficiency predictions are substantially below the test result. This may have been caused by extensive regions of laminar flow in the Cambridge Turbine which are not accounted for in the loss correlations. A significant finding in this comparison is the 1.8% variation in the efficiency predictions with the same loss correlation. This is thought to be a result of different interpretations of the published correlation rather than the effect of the same correlation on different calculation methods. In support of this interpretation is the finding that the same loss subroutine gives very similar predictions of overall efficiency when applied in a mean-line analysis and in a full throughflow calculation.

3.1.2 The Influence of the Loss Correlation on the Efficiency Prediction

Because of the possible significance of other factors on the efficiency predictions, the influence of the loss correlation can be best evaluated when comparison predictions are made consistently using a single computational method. This has been done for the Cambridge Turbine by Denton using the streamline curvature method with four different loss correlations.

Cambridge Turbine – Streamline Curvature Method (Denton)

<i>Correlations by</i>	<i>Predicted η</i>	<i>Pred. η – Test η</i>
Dunham & Came	89.87	-3.93
Craig & Cox	91.47	-2.33
Traupel	91.4	-2.4
Denton	94.3	+0.5

It is apparent from the Cambridge Turbine comparisons that only the correlations used by Denton respond properly to the low-speed, high-efficiency turbine test case. The Craig & Cox and Traupel correlations result in almost the same efficiency prediction for this test case.

Comparisons of efficiency predictions with the Craig & Cox and Traupel loss correlations have also been made by Sieverding using the NISRE method for the Hannover Turbine test case. The Hannover Turbine has a total-total efficiency of 90.5 at its design point.

Hannover Turbine – NISRE Method (Sieverding)

<i>Correlations by</i>	<i>Predicted η</i>	<i>Pred. η – Test η</i>
Craig & Cox	92.2	+1.7
Traupel	93.9	+3.4

For the Cambridge Turbine these two loss correlations produced consistent results but for the Hannover turbine the efficiency predictions vary by 1.7%. Both predictions are significantly higher than the test result. It is clear from these comparisons that the selection of turbine loss correlations can have an important influence on both the level of the efficiency prediction and on the prediction of the efficiency variation between turbines.

3.1.3 The Efficiency Prediction Model

It has been established in the previous sections that both the correlations and a consistent computational method are important aspects of a turbine efficiency prediction model. Unfortunately there are not enough calculations or turbine test cases available to give a fair evaluation of most of the correlations and computer methods.

However, it should be recognized that the most important quality of an efficiency prediction model is not its ability to predict the absolute level of turbine efficiency. It is more important that the model be able to predict the efficiency variation between turbines. This is the characteristic of the prediction model which is used in the design optimization process. The streamline curvature model with the Denton Correlation was used to predict the efficiency of the four test case turbines and two additional turbines with the following results.

Streamline Curvature Method (Denton) with Denton Correlation

<i>Turbine</i>	<i>Predicted η</i>	<i>Test η</i>	<i>Pred. η – Test η</i>
Cambridge	94.3	93.8	+0.5
Gas Turbine (2 stage)	92.0	88.4	+3.6
Hannover	91.4	90.5	+0.9
Ansaldo	89.7	90.0	-0.3
NGTE (Ref.1)	91.5	92.2	-0.7
NASA (Ref.2)	91.5	93.0	-1.5

In four of the six cases the efficiency prediction is within one percent of the test level. It should be remembered that variations in test procedures and experimental error can contribute to an apparent prediction error. The two cases where the efficiency is not well predicted represent turbines with unusually high and unusually low efficiency levels.

3.2 THE PREDICTION OF OFF-DESIGN EFFICIENCY

The capability of predicting the off-design performance of a gas turbine is used primarily in defining the engine characteristics over its operating range. In addition the examination of off-design prediction capability is useful in evaluating the quality of the efficiency prediction system. Five different operating points are available for the Hannover Turbine. The off-design performance has been predicted (a) using the streamline curvature method (Denton) with the Denton correlations and (b) using the NISRE Method (Sieverding) with both the Craig & Cox and Traupel correlations. As seen in Figure 3.1 the streamline curvature method with the Denton correlation predicts the peak efficiency level within 1% but is less successful in predicting the shape of the efficiency characteristic. The efficiency prediction is too high at low loading and too low at high loading. The NISRE calculation with both the Craig & Cox and the Traupel correlations predicts the shape of the efficiency characteristic reasonably well over the moderate and low loading range of the data. The predicted efficiency fall off at high loading is too steep with the Traupel correlation

and much too steep with the Craig & Cox correlation. At peak efficiency the level predicted with the Craig & Cox correlation is 1.7% higher than the test efficiency and the level predicted with the Traupel correlation is 3.4% higher than the data. In general Denton's correlation is more successful in predicting the level while the others provide a more accurate shape for the efficiency characteristic.

REFERENCES

1. Smith, D.J.L.
Johnson, I.H.
Investigations on a Single Stage Turbine of Conservative Design. ARC R & M 3541, 1967.
2. Kofskey, M.G.
Nusbaum, W.J.
Design and Cold Air Investigation of a Turbine for a Small Low Cost Turbofan Engine. NASA TN D-6967, 1972.

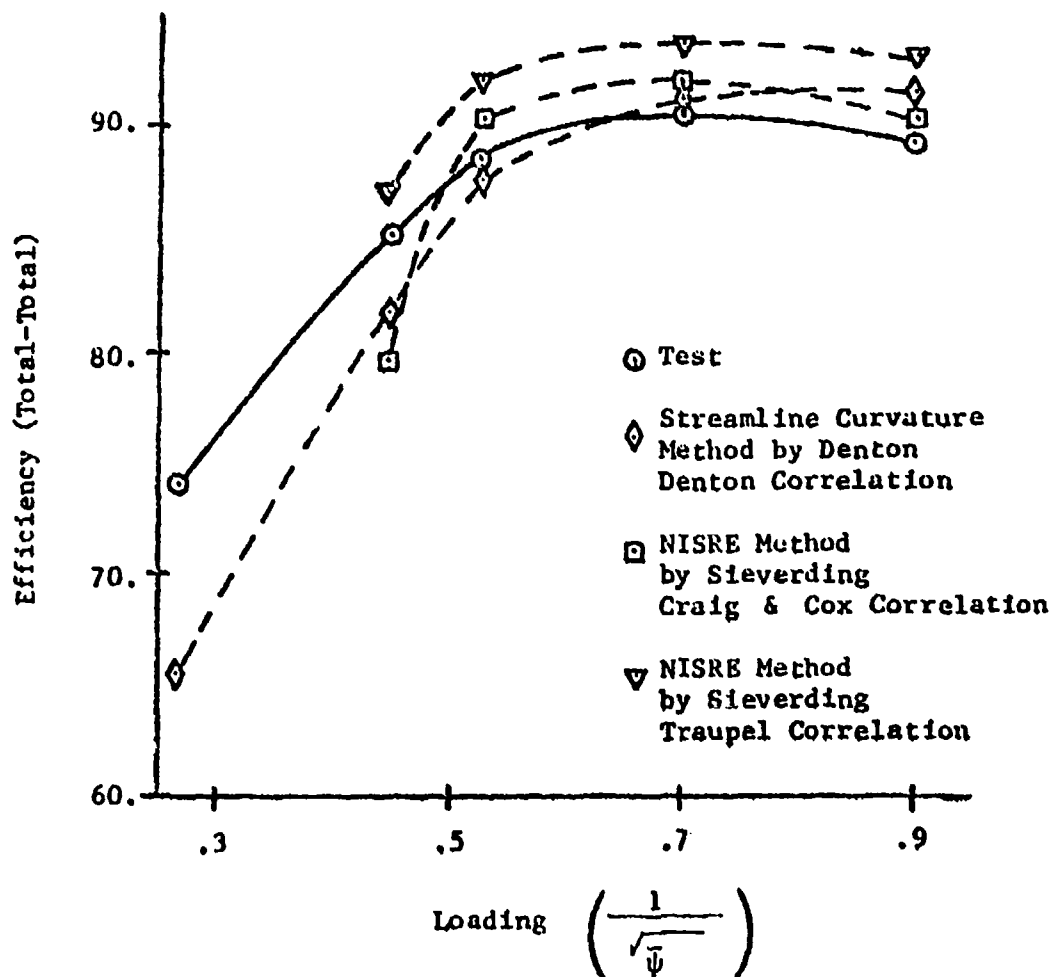


Fig.3.1 Off-design efficiency prediction

Chapter 1.4

INFLUENCE OF CORRELATIONS AND COMPUTATIONAL PROCEDURES ON FLOW FIELD PREDICTIONS

4.1 THE RADIAL EQUILIBRIUM EQUATION

In order to understand the influence of the empirical input on the results of throughflow calculations it is necessary to examine the relative magnitudes of the terms in the radial equilibrium equation. This equation is effectively the momentum equation applied along quasi-orthogonal lines which are roughly perpendicular to the streamlines through the machine. For the simplest case of a radial line it becomes:

$$\frac{d}{dr} \left(\frac{1}{2} V_m^2 \right) = \frac{dH}{dr} - T \frac{ds}{dr} - \frac{1}{2r^2} \frac{d}{dr} (r^2 V_\theta^2) + \frac{V_m^2}{r_c} \cos\epsilon + V_m \frac{dV_m}{dm} \sin\epsilon + F_r. \quad 4.1$$

The last two terms, arising from the convective acceleration along streamlines and from the radial component of blade force respectively, are usually small and will be neglected.

Within or at the trailing edge of a blade row V_θ is completely determined by V_m and by the geometry of the prescribed stream surface and we may write

$$V_\theta = \Omega r - V_m \cos\alpha \quad 4.2$$

where α is the angle imposed by the stream surface and would equal the blade angle in 2D flow. Equation 4.1 (with the last 2 terms neglected) can then be re-written as

$$\frac{d}{dr} \left(\frac{1}{2} V_m^2 \operatorname{cosec}^2 \alpha \right) = \frac{d}{dr} (H - \Omega r V_\theta) - T \frac{ds}{dr} - \frac{V_m^2}{r} \cot^2 \alpha + 2\Omega V_m \cot\alpha + \frac{V_m^2}{r_c} \cos\epsilon. \quad 4.3$$

It is clear by comparing 4.1 and 4.3 that the effect of the enthalpy and entropy gradients, and of the streamline curvature term, on the gradient of meridional velocity is considerably reduced when α is small, as it is at the trailing edge of a turbine blade. Hence at exit from a blade row the velocity distribution is determined mainly by the variation of exit angle, α , along the span and is only slightly influenced by loss, streamline curvature or inlet stagnation enthalpy and entropy gradients. This may be illustrated by considering the order of magnitude of the terms on the RHS of 4.3 for the case of a fixed blade row with no enthalpy or entropy gradients (i.e. a uniform flow) at entry; these are:

$$\begin{aligned} \frac{d}{dr} (H - \Omega r V_\theta) &= 0 \quad (\Omega = 0) \\ T \frac{ds}{dr} &\sim \xi V_m^2 \operatorname{cosec}^2 \alpha / \Delta r \\ \frac{V_m^2}{r} \cot^2 \alpha &\sim V_m^2 \cot^2 \alpha / \Delta r \\ 2\Omega V_m \cot\alpha &= 0 \quad (\Omega = 0) \\ \frac{V_m^2}{r_c} \cos\epsilon &\sim V_m^2 / \Delta r \end{aligned}$$

where Δr is the annulus height. Remembering that ξ is likely to be of order 0.1 and α of order 20° it is seen that the 3rd term is almost an order of magnitude greater than the other terms. Hence it can be concluded that the velocity profile at exit from a turbine blade is very largely determined by the prescribed distribution of exit flow angle and is relatively insensitive to the estimates of loss and streamline curvature. Since the exit angle includes the deviation it is clear that the method used to estimate this will have an important influence on the solution. Exactly the same argument can be applied at the trailing edge of a moving blade row.

Within a duct region or at the leading edge of a blade row the flow is not confined to a prescribed stream surface and equation 4.1 must be used. If we consider only changes in velocity profile between the closest upstream trailing edge and the duct station in question, enthalpy, entropy and angular momentum will be conserved along streamlines and changes in their gradients will only occur through changes in streamline radius. If the shift of the mid streamline is of order δ then the changes produced in these gradients will be of order $2 \delta/h$ and will be of opposite signs in the

inner and outer parts of the annulus. It may also be shown from actuator disc theory (e.g. Horlock (1978)) that the change in streamline curvature between a trailing edge and downstream is of order $\pi^2 \delta/h$ and that this is of the same sign in both halves of the annulus. Hence changes in velocity gradient between a trailing edge and downstream occur mainly as a result of changes in streamline curvature and the velocity profiles calculated in duct regions are much more dependent on the estimate of streamline curvature than are those at the trailing edge.

It is important to note that the estimate of streamline curvature at a trailing edge has a significant effect on the downstream velocity profiles even though it has little effect at the trailing edge itself. This is easily seen by applying equation 4.3 to a 2D flow with all terms on the RHS equal zero except the last (streamline curvature) term which = a constant, K. If α is also taken as constant we get, at a trailing edge,

$$V_m^2 = 2 \sin^2 \alpha (A + Kr) \quad 4.4$$

where A is a constant of integration to be determined by the continuity equation. Hence, at the trailing edge we have

$$V_\theta^2 = V_m^2 \cot^2 \alpha = 2 \cos^2 \alpha (A + Kr). \quad 4.5$$

Now applying 4.1 downstream of the trailing edge at a point where the streamline curvature is zero we get

$$\frac{d}{dr} \left(\frac{1}{2} V_m^2 \right) = -\cos^2 \alpha \left(\frac{2A}{r} + 3K \right) \quad 4.6$$

Since r has been assumed very large (i.e. 2D flow) we see that the radial gradient of V_m^2 which was $2K \sin^2 \alpha$ at the trailing edge has become $-6K \cos^2 \alpha$ at the downstream station; i.e. the effect of the curvature at the trailing edge is multiplied by $-3 \cot^2 \alpha$ at the downstream station. This is likely to represent an order of magnitude amplification.

These results obtained by simple consideration of the radial equilibrium equation will be illustrated by practical examples in the subsequent sections of this chapter.

4.2 INFLUENCE OF STREAMLINE SLOPE AND CURVATURE

A complete investigation of the effects of streamline slope and curvature on the solution would involve using different methods of calculating these terms in a program which was otherwise unchanged and then applying it to the same test data. Because of the effort involved in inserting different streamline slope and curvature routines into already complex programs this has not been attempted. However, Novak and Hearsay (1976) report that they found little difference between solutions obtained using spline fits and quadratic fits to obtain slope and curvature and that the quadratic method was more stable. This result is in agreement with the findings of Wilkinson (1970) who investigated the accuracy and stability of a large number of curve fits on a sinusoidal streamline. He concluded that polynomial fits, using the same curve to obtain both slope and curvature, were the most accurate and stable whilst the use of splines and of 'double differentiation' were undesirable.

A simple method of investigating the influence of the streamline slope and curvature on the solution, without the need for any re-programming, is to vary the number of calculating stations used between the limits of a very coarse and a very fine grid. This was done on a simple test case consisting of the single fixed blade row shown in Figure 4.1. The casing was made up of circular arcs and straight lines so that the discontinuities in curvature at the leading and trailing edges and at mid chord would provide a severe test of the method. The inlet flow was taken to be uniform and axial and the stream surface angle ($\tan^{-1} V_t/V_x$) varied linearly with axial distance from zero at inlet to 65° at the trailing edge. The blades were taken to have no thickness and, initially, zero loss.

Solutions were obtained using a quadratic curve fit (i.e. 3 points) to obtain both slope and curvature, initially with a coarse grid having no stations internal to the blade row and then with progressively finer grids having 1, 3 and 5 internal stations in addition to those at the leading and trailing edges. Although there is no analytical solution for this case the latter, fine grid, solution is expected to be almost exact.

Figure 4.2 illustrates the results at leading edge, trailing edge and far downstream (at $x = 0.4$). At the leading edge, Figure 4.2a, the velocity profile would be uniform were it not for the effects of streamline curvature. As expected the use of no internal calculating stations leads to an underestimate of the streamline curvature and hence velocity gradients. Using one central internal point causes the parabola to overestimate the curvature at the leading edge but the maximum error in V_x is less than 3%. This is roughly halved by using 3 internal points. The surprisingly accurate results obtained with coarse grids are due to the fact that the curvature only varies rapidly on the casing. At mid span changes in streamline slope are much more gradual and reasonable results can be obtained with few points.

At the blade trailing edge the results, Figure 4.2b, confirm the conclusions of the last section that the solution is very insensitive to the value of streamline curvature as varied by the number of internal calculating points. The steep velocity gradient is almost entirely due to the radial equilibrium terms in equation 4.3.

The changes between the trailing edge and far downstream shown in Figure 4.2c are exactly as predicted at the end of section 4.1. The effect of curvature is to slightly steepen the velocity gradient at the trailing edge. When the curvature is relaxed downstream the gradient is reduced to considerably below the value it would have had if there had been no curvature at the trailing edge. The overshoot is greatest at the tip where the curvature was largest.

It should be emphasised that this is a severe test case with higher curvatures and pitch angles than are likely to occur in most gas turbines. In most cases the use of a coarse grid with no internal calculating stations is likely to lead to even less error than was found here.

4.3 INFLUENCE OF BLADE EXIT ANGLE

The effect of the blade exit angle on the solution was investigated using the same simple test case described in the previous section. All results described in this section used 5 internal calculating points with the flow angle varied only at the trailing edge station.

Figure 4.3 shows the result of increasing the turning by 2° (i.e. -2° deviation) over the whole span. The mass flow was held fixed (at 150 Kg/s) and so the 7.5% reduction in blade exit area required a higher exit Mach number and consequently lower back pressure. The main effect on the solution is the increase in velocity level resulting from the lower density but there is no significant change in velocity gradient either at the trailing edge or far downstream. This result is predictable from equation 4.3 which shows that changes in the gradient of exit angle are more significant than changes which are uniform across the span.

Figure 4.3 also shows the result of a parabolic variation in exit angle with 2° of overturning at root and tip. As expected the effects on the velocity gradient are much greater than previously but because the change of exit area is less there is much less change in velocity level. The result confirms that small changes in the spanwise gradient of exit angle have a large effect upon the predicted velocity profiles.

To illustrate the sort of discrepancies between measured and predicted exit angles which can occur in practice Figures 4.4 and 4.5 show comparisons for the Hannover turbine and Figure 4.6 for the nozzles of the Cambridge turbine. At mid span most of the deviation rules appear to be accurate to about $\pm 2^\circ$ but Traupel's method appears to consistently overestimate the deviation. The large differences between measurement and prediction which occur near the end walls (particularly at the rotor root) are typical of the effects of secondary flow. They result in large discrepancies between calculated and measured velocity profiles as illustrated by Figures A1.2 and A4.3.

It is clear that accurate predictions of turbine velocity profiles cannot be obtained unless some attempt is made to model the secondary deviation. The results of such attempts are described in section 4.5. The errors of a few degrees in deviation at mid-span have comparatively little effect on the predicted velocity profiles but are very significant as regards the prediction of the mass flow:pressure ratio characteristic.

4.4 EFFECT OF LOSS ESTIMATES

The effect of loss on the flow field predictions will again be illustrated using the simple test case of Figure 4.1. Figure 4.7 compares solutions with no loss and with a constant value of $\xi = 0.1$ over the whole span. The increased loss causes an increased pressure drop at constant mass flow and hence an increase in velocity level. However, it can be seen that there is also a reduction in the velocity gradient at the trailing edge. This arises because, although the loss coefficient does not vary across the span, the entropy produced ($\Delta S = \frac{1}{2} V^2 \xi / T$) varies as the square of the relative velocity being greatest at the hub where the velocity is higher. The resulting negative entropy gradient can be seen from Equation 4.1 to produce a more positive velocity gradient. Physically the frictional forces acting along the streamlines are greatest at the hub where they produce a greater reduction in velocity.

The same explanation applies to the results with a parabolic variation in loss coefficient which are also shown in Figure 4.7. The loss coefficient has been taken as zero at mid span increasing parabolically to 0.2 at the end walls. The result is a significant reduction in velocity near the walls but no change in velocity gradient at mid span. This is a result of a comparatively large variation in ξ . In many situations the spanwise variation of loss coefficient and the consequent effect on the velocity distributions will be less than shown in Figure 4.7. In particular, for high aspect ratio blading, the low levels of loss (of order a few percent) over most of the span will cause most of the effect to be concentrated near the end walls. In this region the effects of loss gradients may well be dwarfed by those of angle variation. This is well illustrated by Figure 4.9 which shows the result of distributing the loss in the rotor of the Hannover turbine in the manner shown in Figure 4.8. It is clear that only a very small part of the disturbance near the end walls is due to loss gradients. Similar results were obtained for the Cambridge turbine.

The spanwise extent of the region of increased loss near the end walls depends greatly on the inlet boundary layer thickness, being typically about twice the overall thickness at entry to the blade row. However, there are no correlations available to predict its extent and the boundary layer thickness is not usually known. Hence any prediction must be based on some aspect of blade geometry which is known. It may be argued that the diameter of the secondary vortex

is limited to the dimension of the blade opening. Hence, in the absence of any alternative, it is suggested that this should be used as a measure of the extent of the region of increased loss. It must be emphasised that this suggestion is not based on any experimental evidence but is presented as a hypothesis to be tested against whatever evidence becomes available.

4.5 DISTRIBUTION OF SECONDARY DEVIATION

It was concluded in section 4.1 that the spanwise variation of blade exit angle was the most important factor influencing the predicted velocity profiles. In view of the large and rapidly varying deviation angles caused by secondary flows it is therefore important to try to include some measure of these in the throughflow calculation.

Secondary flows in turbine blades can only accurately be predicted by fully 3D methods and some results from such a method are presented in the next section. The classical approach to the calculation of secondary flows is based on analytical theory and involves assumptions (such as small disturbances and no distortion of stream surfaces) which are not at all valid in turbine blades. Nevertheless these theories appear to give reasonable predictions of the spanwise variation in pitchwise average exit angle. Unfortunately such methods are still too complex to include directly in throughflow calculations, even if the necessary data in the form of detailed inlet boundary layer profiles were available. The only possibility therefore remains the use of correlations to predict the magnitude and extent of secondary flow.

Such a correlation has been proposed by Bardon et al. (1975) based on the application of secondary flow theory to a range of cascades. Although its authors only compare its predictions with a small amount of cascade data, this correlation remains the only method available for estimating and distributing the secondary deviation.

The deviation is distributed over two inlet boundary layer thicknesses in the simple manner shown in Figure 4.10. The magnitude of the maximum overturning and undeturning are the same and are obtained from the equation

$$\Delta\alpha/\epsilon = 0.068 + 0.03 \log_{10} P \quad 4.7$$

where ϵ is the blade turning and the parameter P is given by

$$P = \frac{g'^3}{(g' + h/2)\delta^2} \quad 4.8$$

The parameter g' is a corrected pitch given by

$$g' = \frac{\cos^2 \gamma_2}{\cos^2 \gamma_1} \cdot g \quad 4.9$$

where γ is the flow angle measured from the normal to the stagger line.

The only parameter required which is not readily available to a throughflow calculation is the inlet boundary layer thickness δ . As described in the last section it is reasonable to assume that the diameter of the secondary vortex is limited to the blade opening and hence that the maximum undeturning occurs at this distance from the end wall. On this basis, it is suggested that in the absence of any other information the inlet boundary layer thickness δ should be set equal to the blade opening a .

It should be noted that the correlation breaks down at very low values of δ when very high deviations are predicted and also at very large values of δ/g' when the deviation can become negative. In practice the secondary flows occupy a significant spanwise distance, and the deviations remain finite, even when the inlet boundary layer thickness is zero. They should tend to zero for very closely pitched blades. It is also not realistic to expect the blade height to affect the deviation when the secondary flow regions do not interact as in the case of high aspect ratio blades.

Despite these limitations the correlation of Bardon et al remains the only one available and so was built into the throughflow calculation method of Denton (1978) which is described in Appendix 1. At the same time the secondary loss correlation was replaced by that of Morris and Hoare (1975) and the secondary loss was distributed linearly over two inlet boundary layer thicknesses at each end wall. In order to obtain meaningful results from this distribution of loss and deviation it is clearly necessary to have several streamlines within two boundary layer thicknesses of the end wall. For normal calculations adequate accuracy can be obtained with only 9 streamlines but for the calculations reported in this section 21 streamlines were used. This decrease of streamline spacing caused no instability problems when running the program.

The method was first applied to the single nozzle blade (Figure 4.1) used as a test case earlier in this chapter. Figure 4.11 shows the predictions with two different estimates of inlet boundary layer thickness. With $\delta = 0.1 h$ the predictions look realistic for a nozzle with thin inlet boundary layers. With $\delta = a$ the secondary flow region at the tip appears unreasonably large in extent for a nozzle with this aspect ratio.

The Cambridge turbine provides an ideal test case because the inlet boundary layer profiles are known accurately and detailed measurements of the secondary flow were obtained. Figure 4.12 shows very good agreement of measured and predicted exit angles from the nozzles and this is reflected in improved predictions of the axial velocity profile as shown in Figure 4.13. The agreement is less good behind the rotor, as shown in the same Figures, but is still a significant improvement on the prediction without concentration of loss and deviation at the end walls (Figures A1.2 and A1.4).

The annular cascade tested by Goldman and McLallin (1975) would also provide a good test case for this method but the reference was not discovered until the calculations had been completed.

The inlet boundary layer thickness is not so well defined for the Hannover turbine but from the inlet velocity profiles it was estimated to be 15 mm at the hub and 10 mm at the tip; these values were used for both blade rows. In this case the correlation appeared to considerably overestimate the deviation at nozzle exit, Figure 4.14, particularly at the hub where the exit angle is low (close to tangential). Figure 4.14 also shows the exit angles predicted by Sieverding using a simple form of classical secondary flow theory.

The deviation is again overestimated at the hub but the underturning is in better agreement than the predictions of Bardon's correlation. The exit angle from the rotor blade varies in a complex manner and as shown by Figure 4.14 the correlation fails to predict its details adequately. The increased deviation measured very close to the end walls is an unusual feature, not included in the prediction, which was also found to a lesser extent behind the rotor of the Cambridge turbine. (Figure A1.4).

The inlet boundary layer thickness to the 2 stage gas turbine is not known and so the assumption that $\delta = a$ was applied to this case. The test results show that the flow in this machine is considerably influenced by secondary flows particularly at exit from the rotor blades. Figures 4.15 and 4.16 compare the measured and predicted relative flow angles at exit from each blade row. It is clear that putting $\delta = a$ considerably overestimates the extent of the secondary flow region for the nozzles but underestimates it for the rotors. However, the magnitudes of the deviations are, if anything, overestimated for the nozzles and reducing the estimate of boundary layer thickness would cause even larger deviations to be predicted.

It is also noteworthy that at the tip of the LP rotor the secondary deviation predicted appears to be of the wrong sign (i.e. underturning at the wall). This was traced to a negative deviation being predicted by Bardon's correlations as a result of equation 4.9 producing a very low value of corrected pitch. The use of the corrected pitch is clearly suspect for low camber tip sections where there is little difference between the stagger angle and flow exit angle (i.e. γ_2 in equation 4.9 becomes small).

These studies of the effects of distributing the deviation have concentrated on comparisons of relative blade exit angles. However, the trends of the velocity distributions can be inferred from these using the observation that the magnitude of the relative blade exit velocity is not greatly changed by the deviation. Hence a region of underturning will correspond to a region of high axial velocity and vice-versa.

In summary the results of distributing the secondary deviation are disappointing. Although encouraging results were obtained in the Cambridge turbine neither the magnitude nor the extent of the secondary deviation were well predicted for the other two machines. It seems likely that the secondary flows are greatly influenced by blade profile and so cannot be at all well predicted by correlation methods.

4.6 FULLY THREE DIMENSIONAL CALCULATIONS

If the conclusions of the previous section are accepted it seems likely that the full complexity of turbine secondary flows can only be predicted by fully 3D methods. Such methods are now becoming available but are not yet widely used because of the cost of the long computer runs needed. Viscous effects may also be included (e.g. Dodge (1976), Moore & Moore (1979)) but these greatly increase the complexity and cost. The only 3D method available to the Turbine Sub-Group was the inviscid method of Denton (1975) the latest form of which is described by Denton & Singh (1979). This method has the ability to calculate shear flows although the amount of detail obtainable is limited by the number of grid points which can be used. It was used on the Cambridge turbine and on the 2 stage gas turbine test cases. In order to obtain sufficient detail in the secondary flow region separate calculations were performed for the inner and outer halves of each blade row; the mid stream surface, as obtained from a throughflow calculation, being input as a solid boundary with no shear layer on it.

Results for the nozzles of the Cambridge turbine are shown in Figure 4.17 and are very encouraging despite the fact that only 3 streamwise grid surfaces could be placed in the secondary flow region. Both the measured velocity profile and flow angles after the nozzles were input to the calculation for the rotor blade. The results shown in Figure 4.18 are not as good as those after the nozzles but are still better than were obtained from throughflow calculations. Clearly the complex angle distribution near the rotor root could not possibly be resolved with so few grid points.

3D calculations on the 2 stage gas turbine were reported by Denton & Singh (1979). These were for the whole HP stage (in one calculation) and did not include any shear flows. However, it is noteworthy that good agreement was

obtained for the relative exit Mach number distribution from each blade row despite the fact that the calculation was inviscid and made use of no loss or deviation correlations, only geometric data being input.

The calculations with shear flow were confined to the HP turbine and each blade row was treated in two parts as previously described. The thickness and shape of the inlet boundary layers are not known for this machine and so were guessed, the thickness being guessed at 20% of blade height on each end wall. As shown in Figure 4.19 this was clearly an overestimate for the nozzle blades, the calculated secondary flows are much too extensive and the amount of overturning is too small. However, it was not thought to be worth attempting calculations with thinner boundary layers because of the limitations on the number of grid points previously mentioned.

The predictions at rotor exit show some signs of the large region of overturning near the hub but it is thought likely that this is largely due to viscous effects (i.e. a flow separation) within the blade row. However, the blade surface pressure distributions, which are obtained as an integral part of the 3D calculation, showed no cause to expect such a separation. The spanwise variations of relative Mach number obtained from the 3D calculations were in excellent agreement with the experimental data when the blade exit pressure (which is input to the calculation) was adjusted to give the correct value on the hub.

On the basis of these limited comparisons it seems that fully 3D calculations show promise of being able to predict secondary flows in turbines but that fine grids and hence expensive computer runs will be needed to obtain accurate results with thin boundary layers. The calculations described each took about 8 minutes CPU time on an IBM 370-165.

ACKNOWLEDGEMENT

The 3D calculations described were carried out by Dr S.Uzui of Nippon Kokan K.K., Technical Research Centre, whilst he was studying at the Whittle Laboratory, Cambridge.

REFERENCES

- Horlock, J.H. *Actuator Disk Theory*. McGraw Hill, 1978.
- Novak, R.A.
Hearsay, R.M. *A Nearly Three-Dimensional Intrablade Computing System for Turbomachinery*, Parts I and II. ASME Papers 76-FE-19 and 76-FE-20, 1976.
- Wilkinson, D.H. *Stability, Convergence and Accuracy of Two-Dimensional Streamline Curvature Methods using Quasi-Orthogonals*, I. Mech. E. Thermodynamics and Fluid Dynamics Convention, Paper 35, 1970.
- Bardon, M.F.
Moffatt, W.C.
Randall, J.L. *Secondary Flow Effects on Gas Exit Angles in Rectilinear Cascades*. ASME J. Eng. Power, Jan. 1975.
- Denton, J.D. *Throughflow Calculations for Axial Flow Turbines*. ASME J. Eng. Power, April, 1978.
- Morris, A.W.H.
Hoare, R.G. *Secondary Loss Measurements in a Cascade of Turbine Blades with Meridional Wall Profiling*. ASME J. Eng. Power April, 1978.
- Goldman, L.J.
McLellan, K.L. *Cold Air Annular Cascade Investigation of Aerodynamic Performance of Core Engine Cooled Turbine Vanes*. NASA TM-X 3224, 1975.
- Dodge, P.R. *Numerical Method for 2D and 3D Viscous Flow*. AIAA paper 76-425, 1976.
- Moore, J.
Moore, J.G. *A Calculation Procedure for 3D Viscous, Compressible Duct Flow*, Pts. I and II. ASME, J. Fluid Eng., Vol.101, Dec. 1979.
- Denton, J.D. *A Time Marching Method for 2 and 3 Dimensional Blade to Blade Flows*. ARC R. & M. 3775, 1975.
- Denton, J.D.
Singh, U.K. *Time Marching Methods for Turbomachinery Flow Calculation*. V.K.I. Lecture Series 7, 1979.

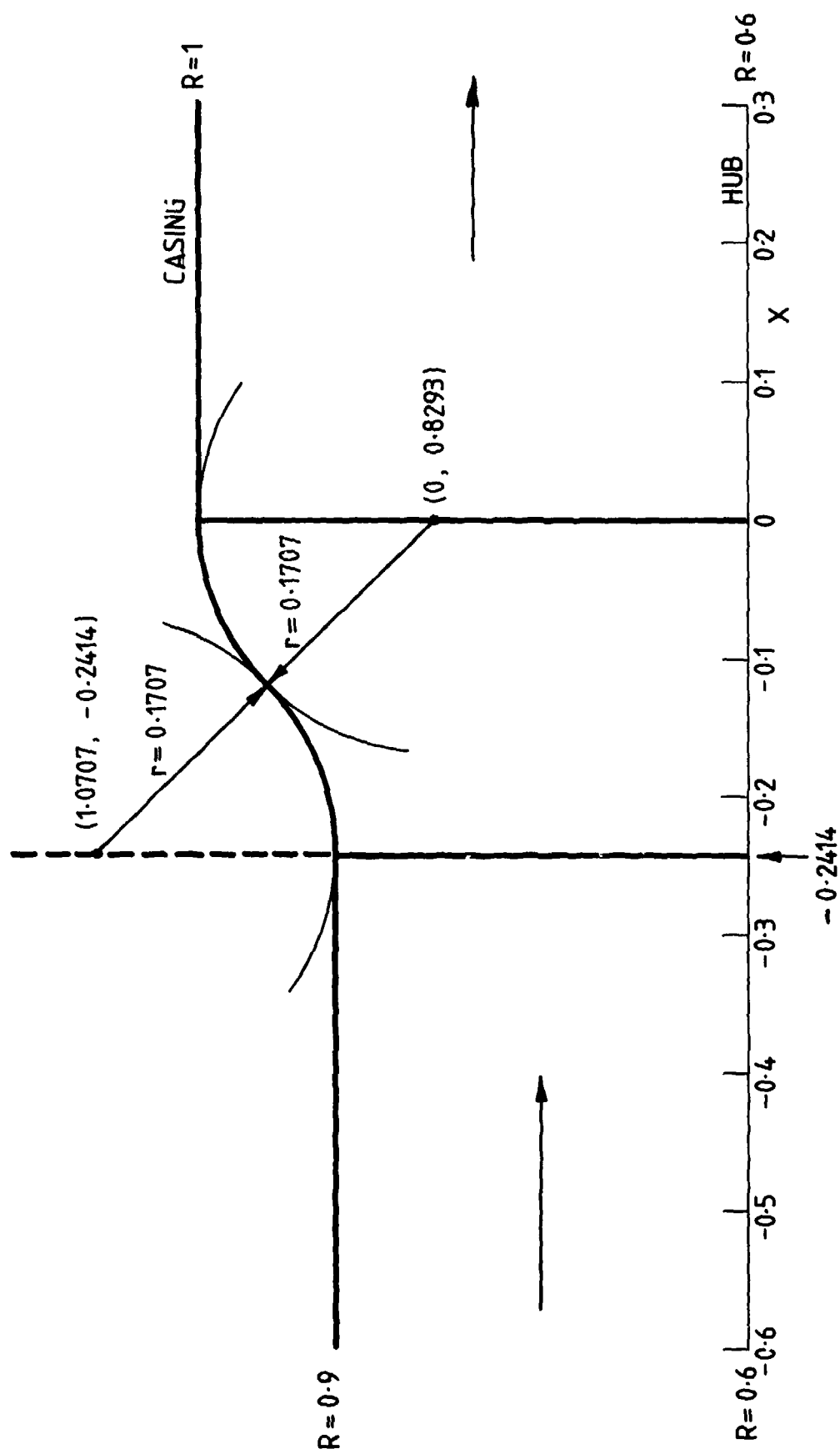


Fig.4.1 Geometry of test nozzle

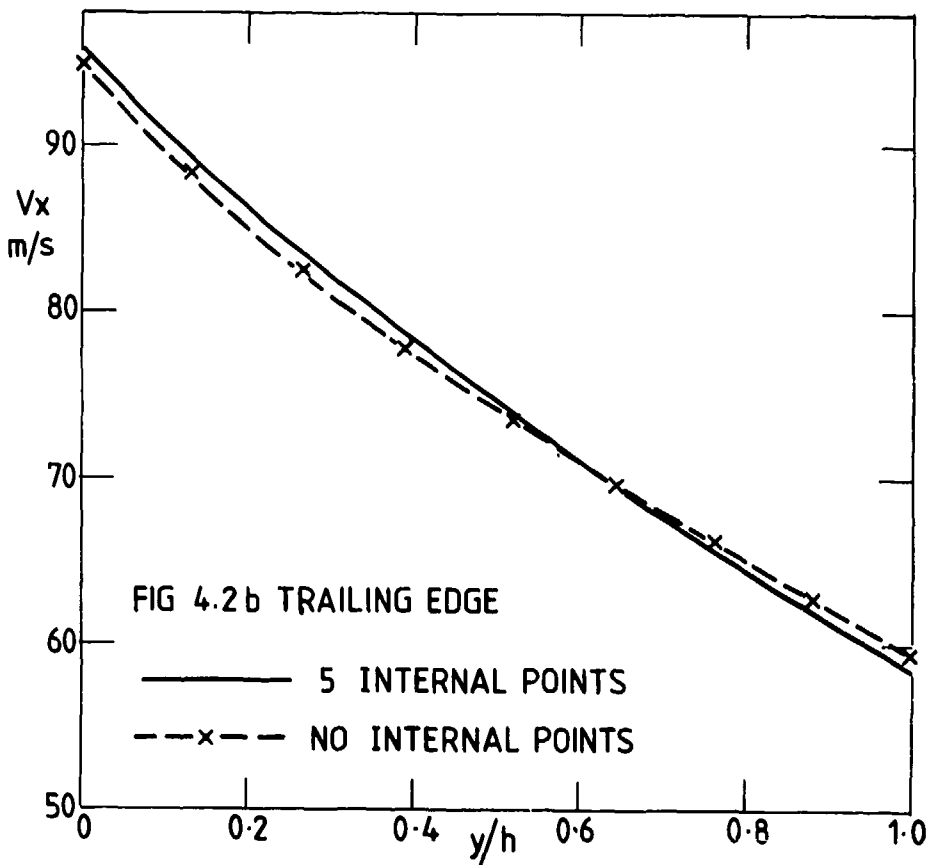
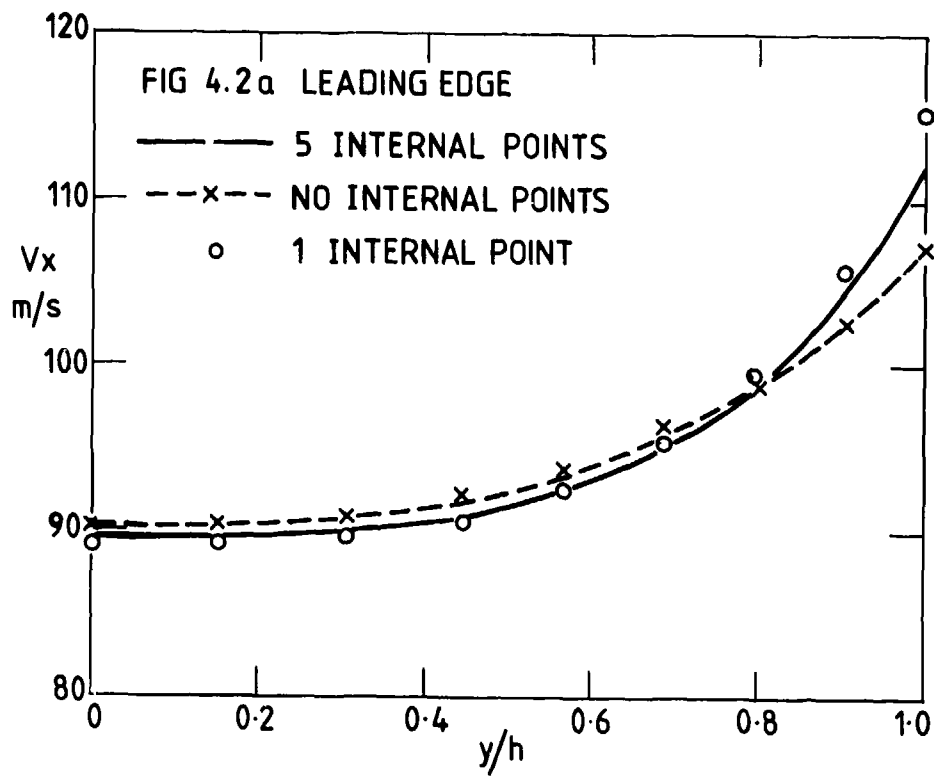


Fig.4.2 Effect of number of internal calculating stations

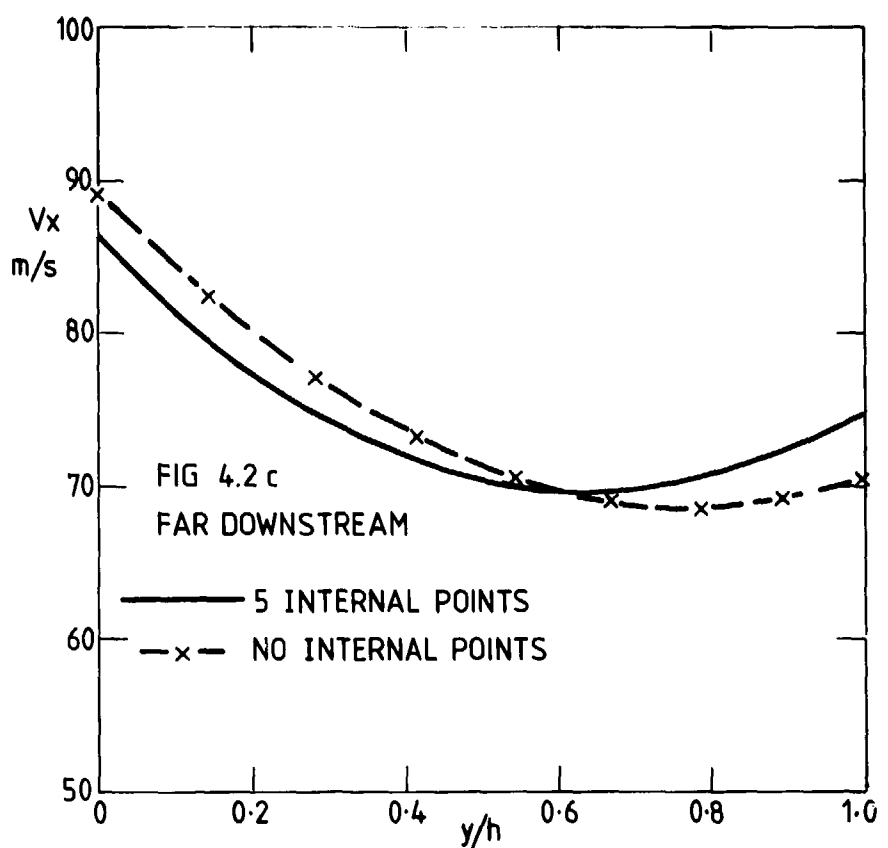


Fig.4.2 (concluded)

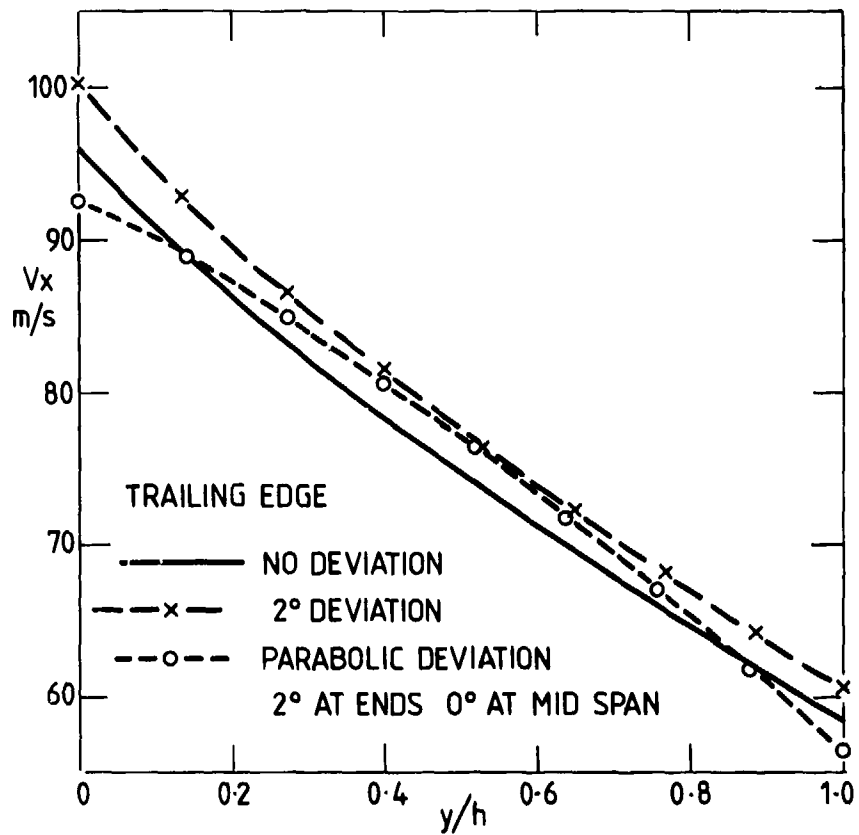


Fig.4.3 Effect of deviation

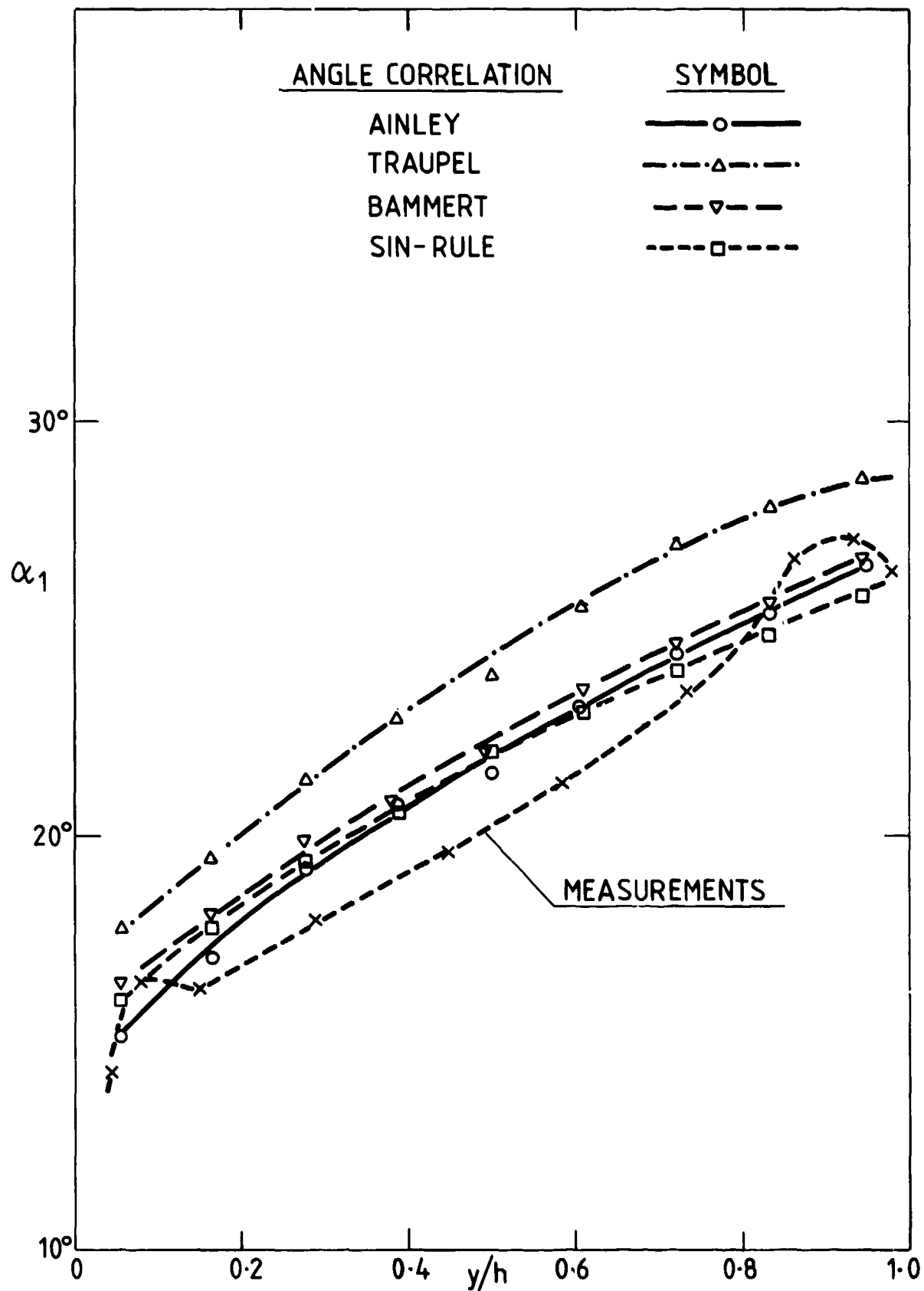


Fig.4.4 Hannover turbine nozzle exit angles

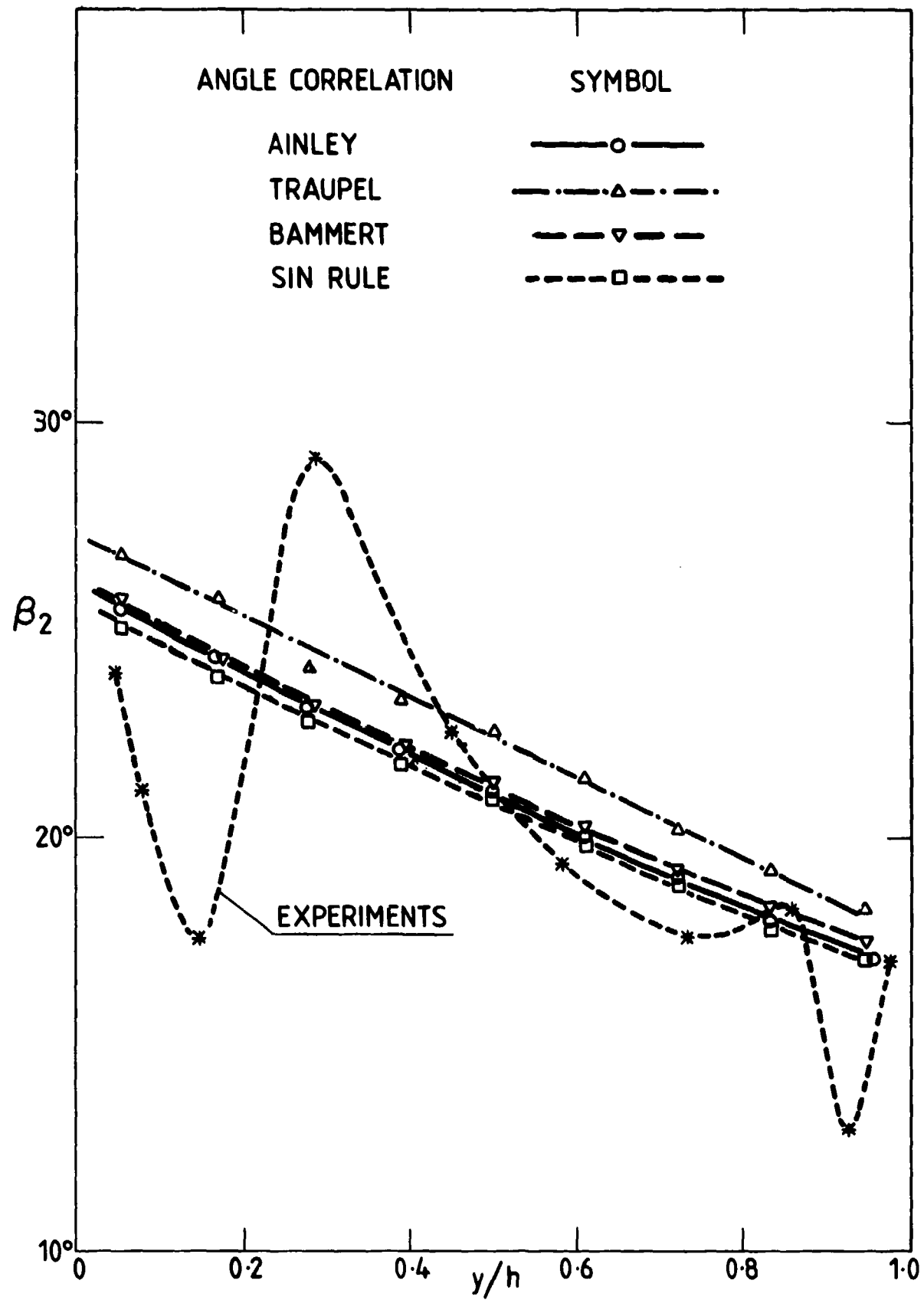


Fig.4.5 Hannover turbine rotor exit angles

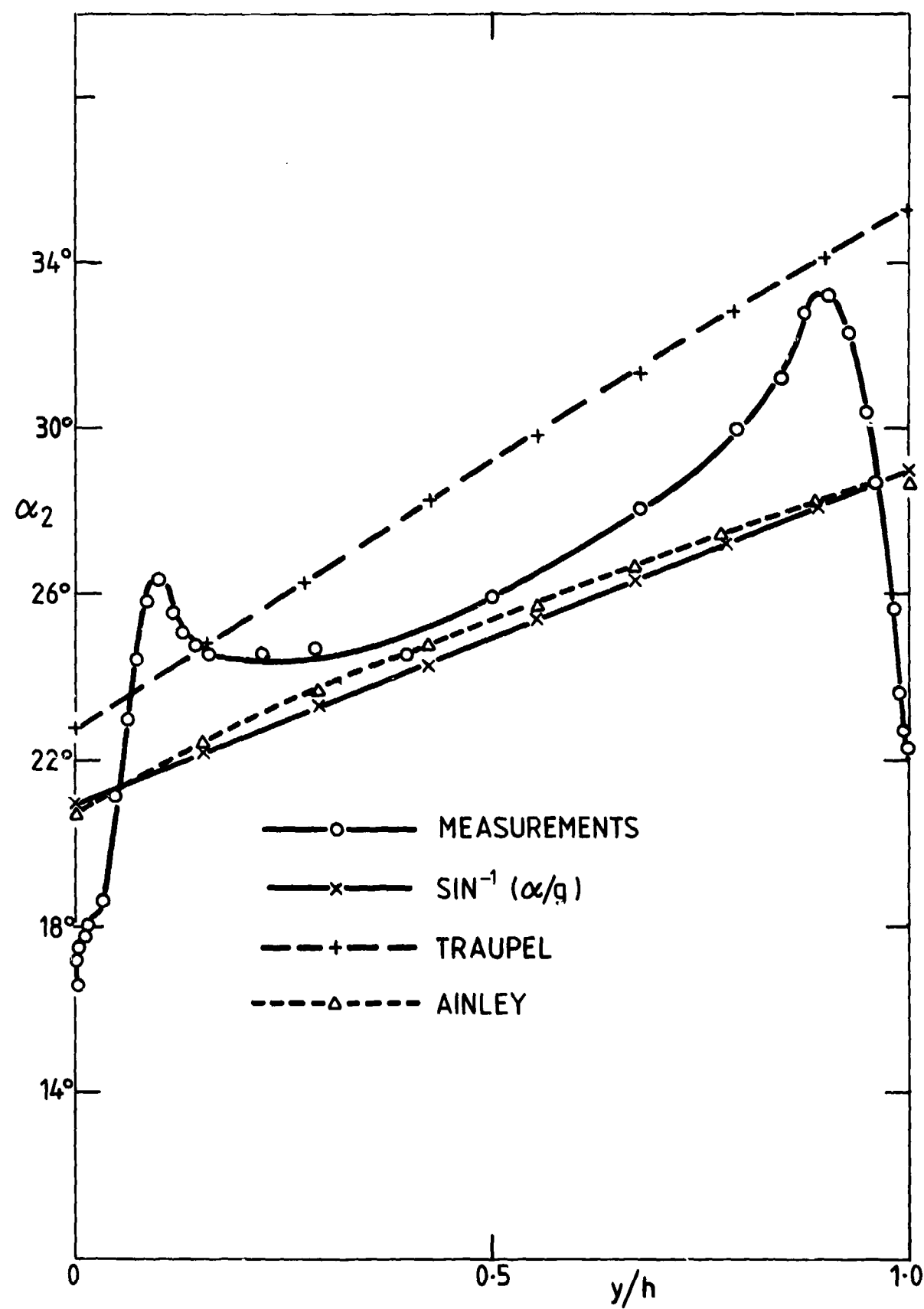


Fig.4.6 Cambridge turbine nozzle exit angles

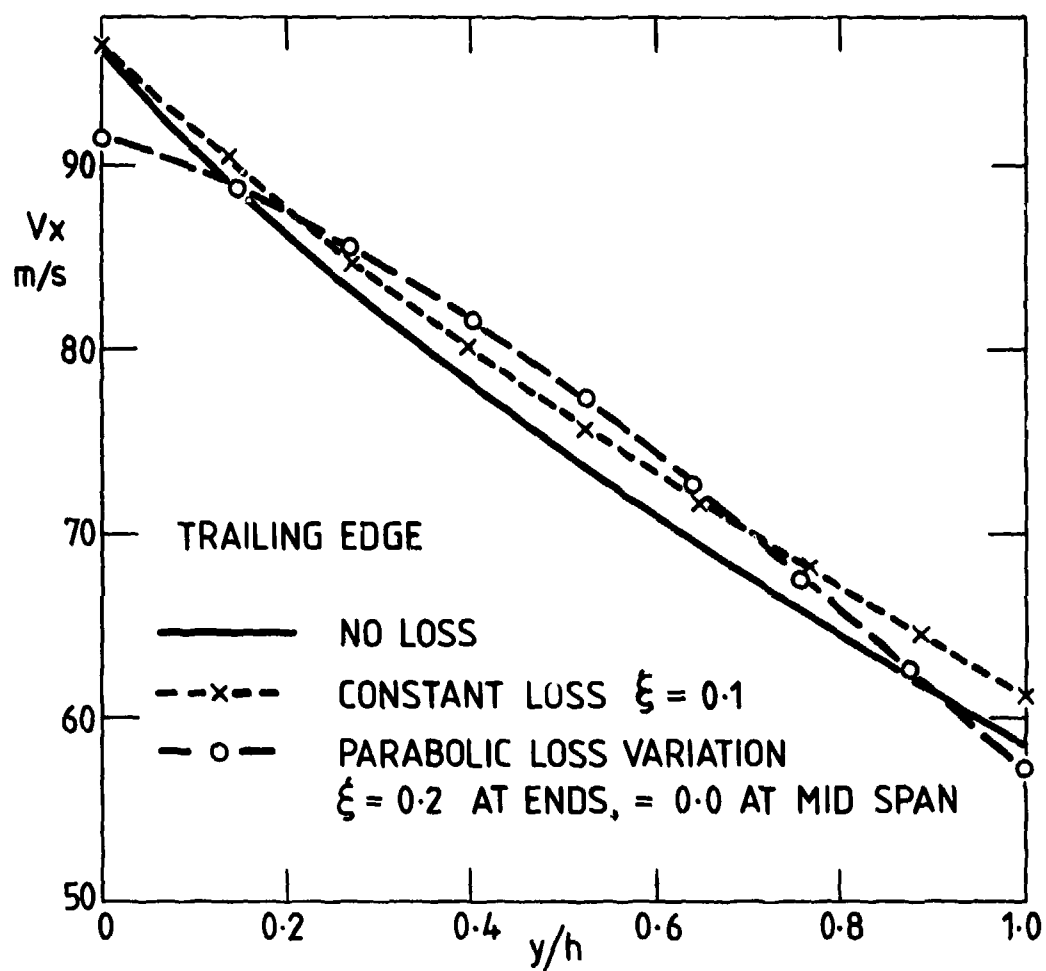


Fig.4.7 Effect of loss

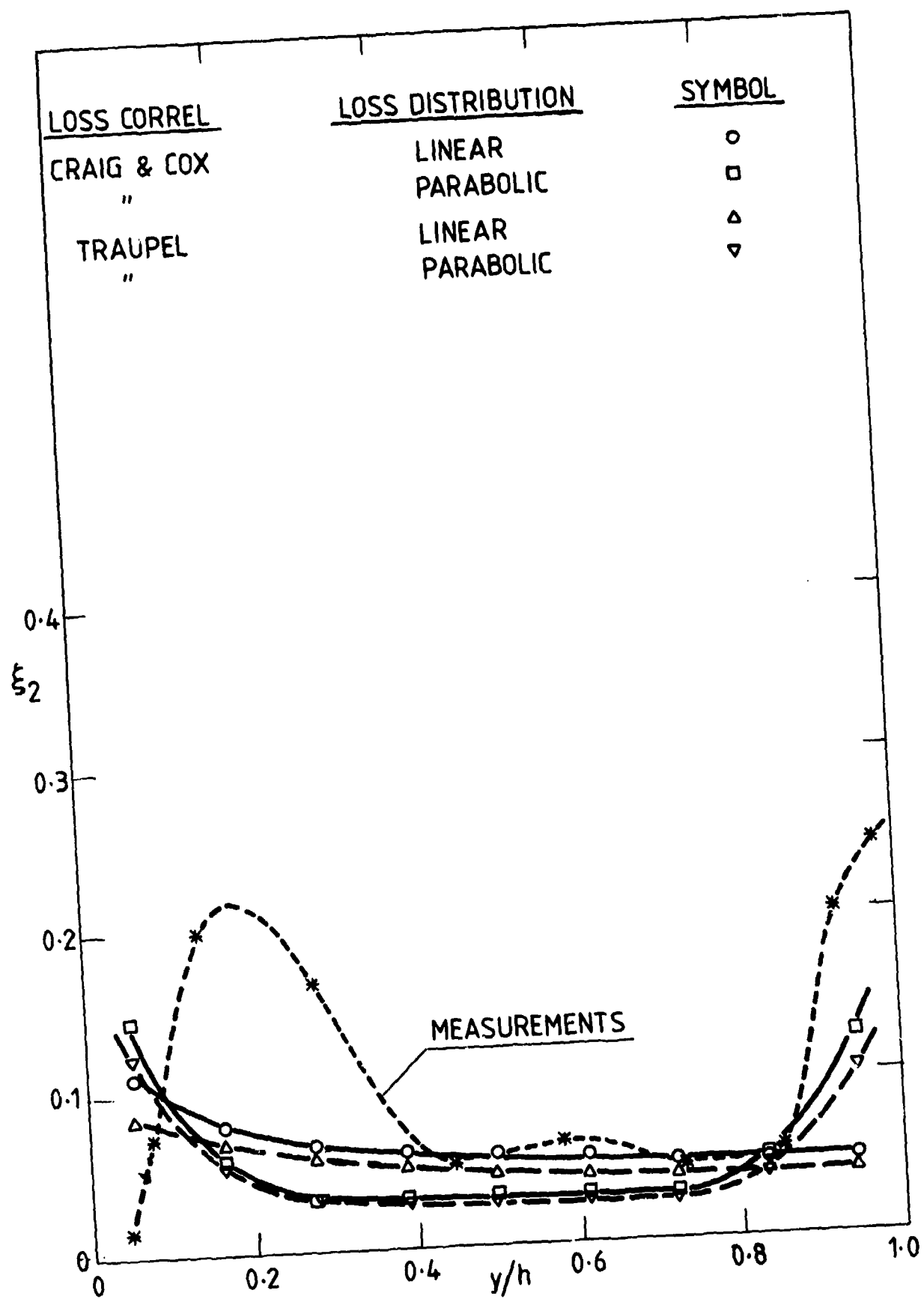


Fig.4.8 Hannover turbine loss distribution at rotor exit

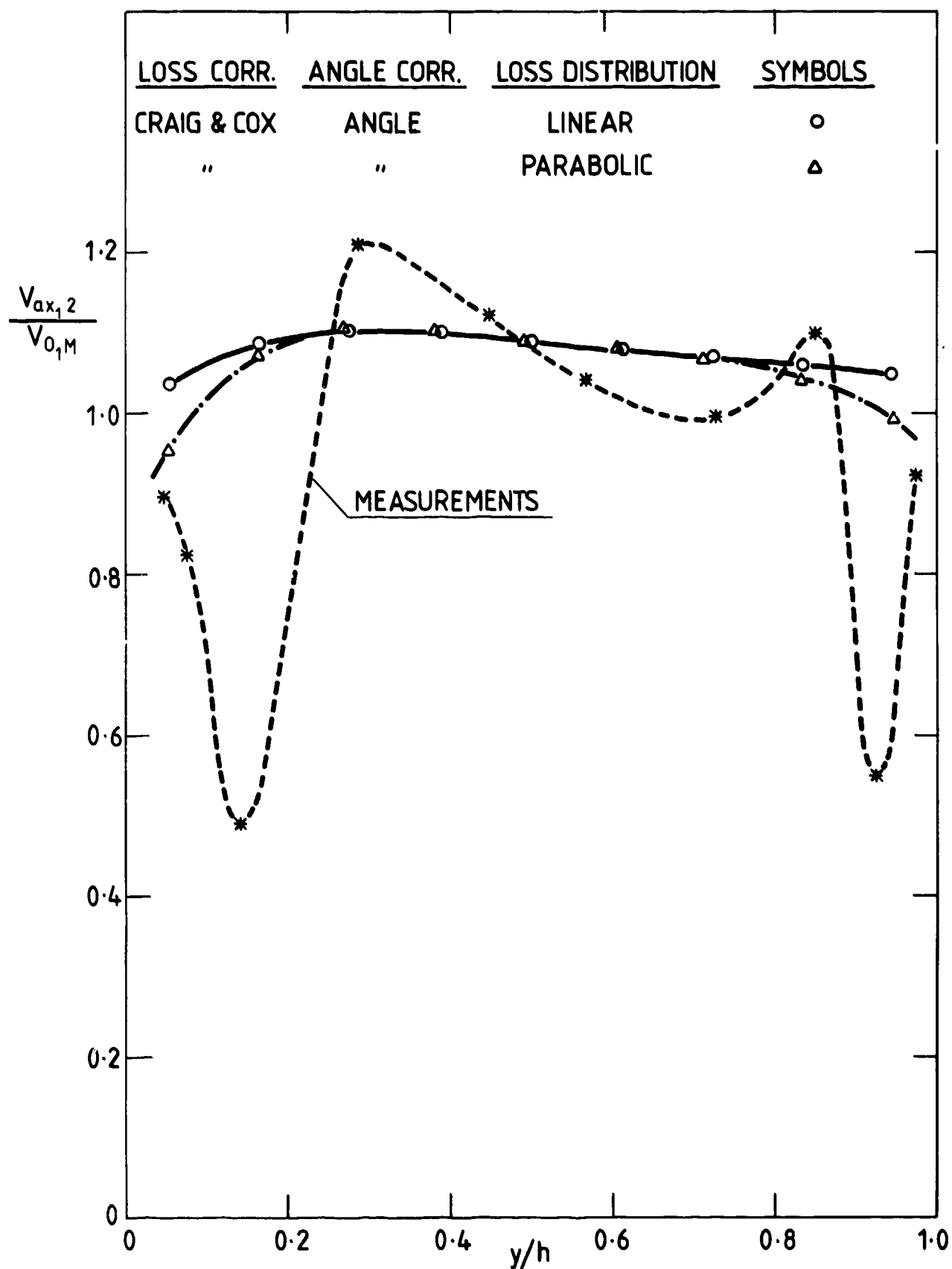


Fig.4.9 Hannover turbine effect of loss distribution at rotor exit

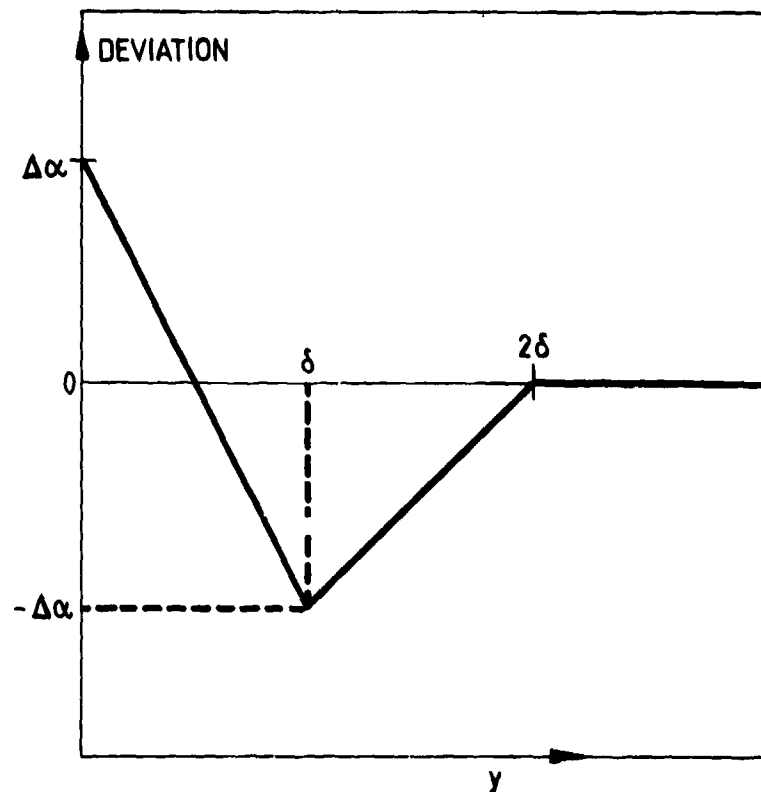


Fig.4.10 Bardon's distribution of deviation

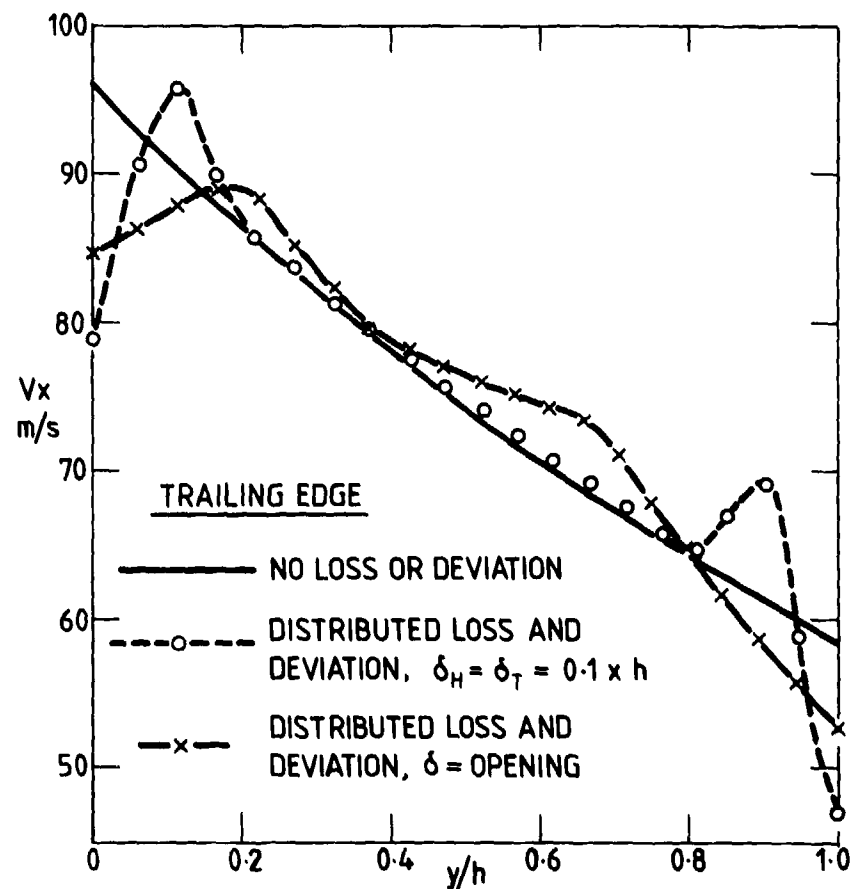


Fig.4.11 Test nozzle with distributed loss and deviation

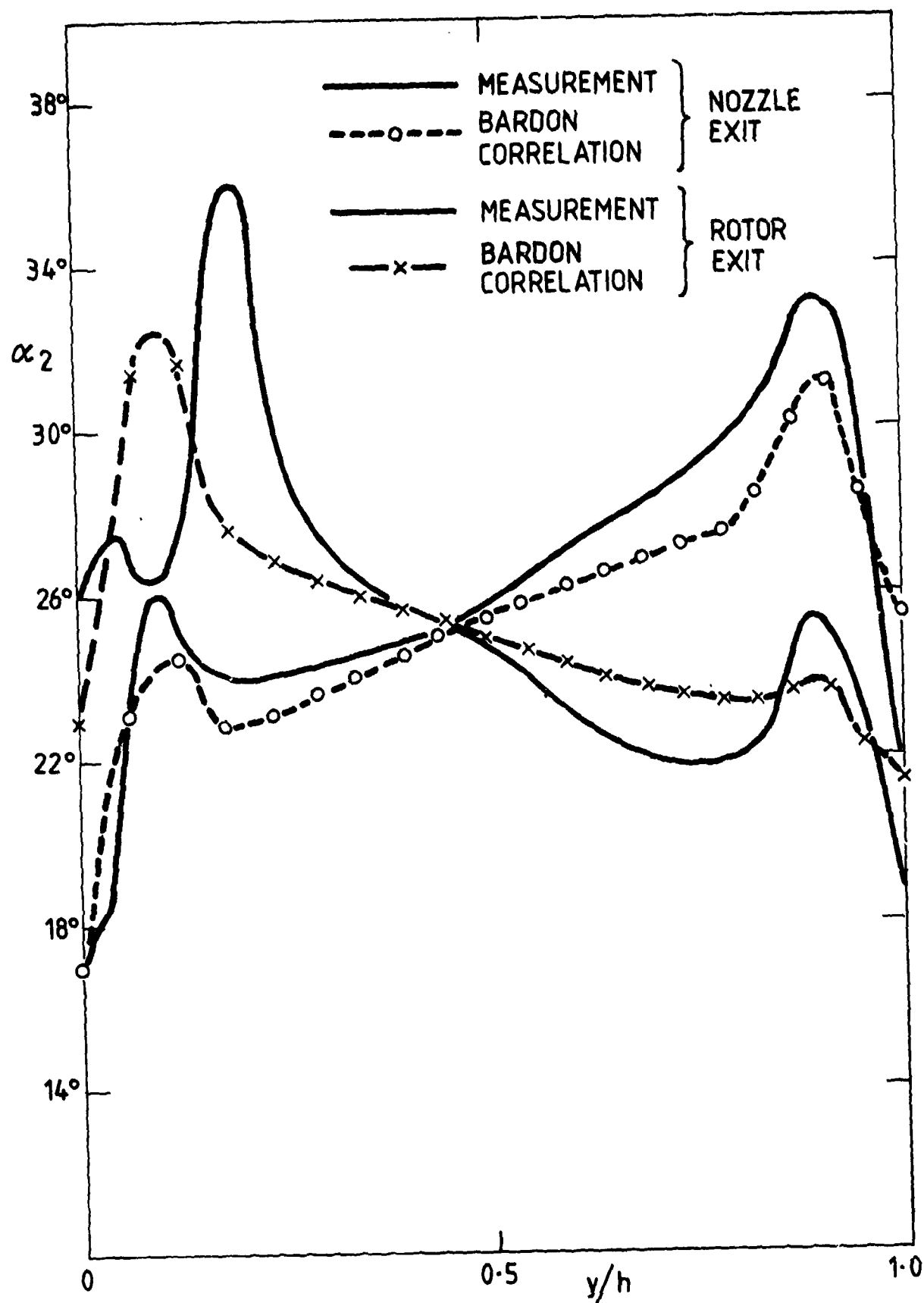
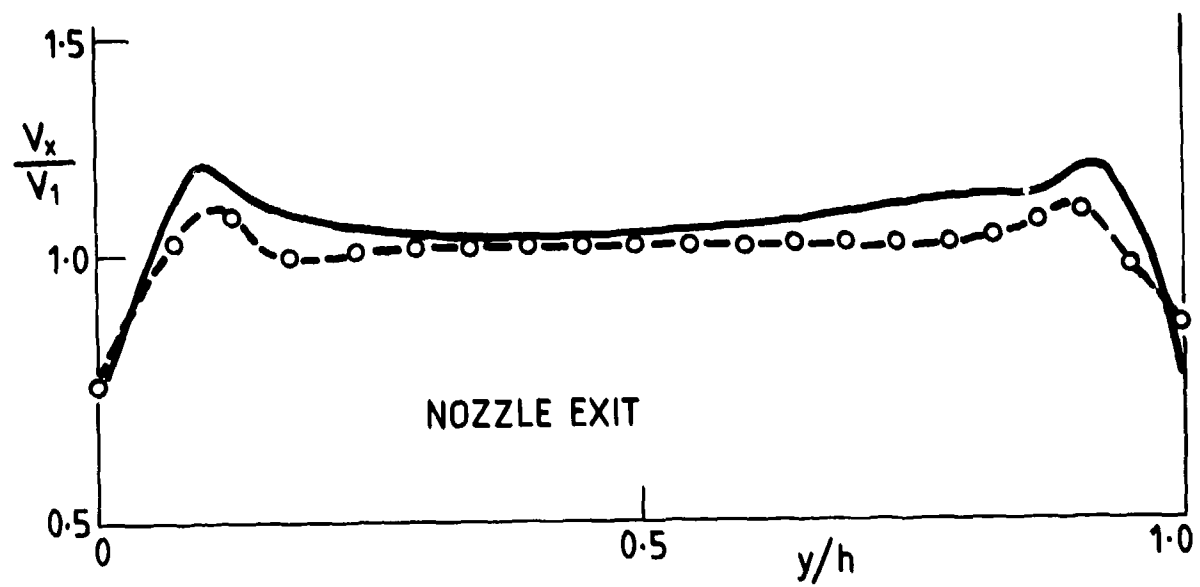
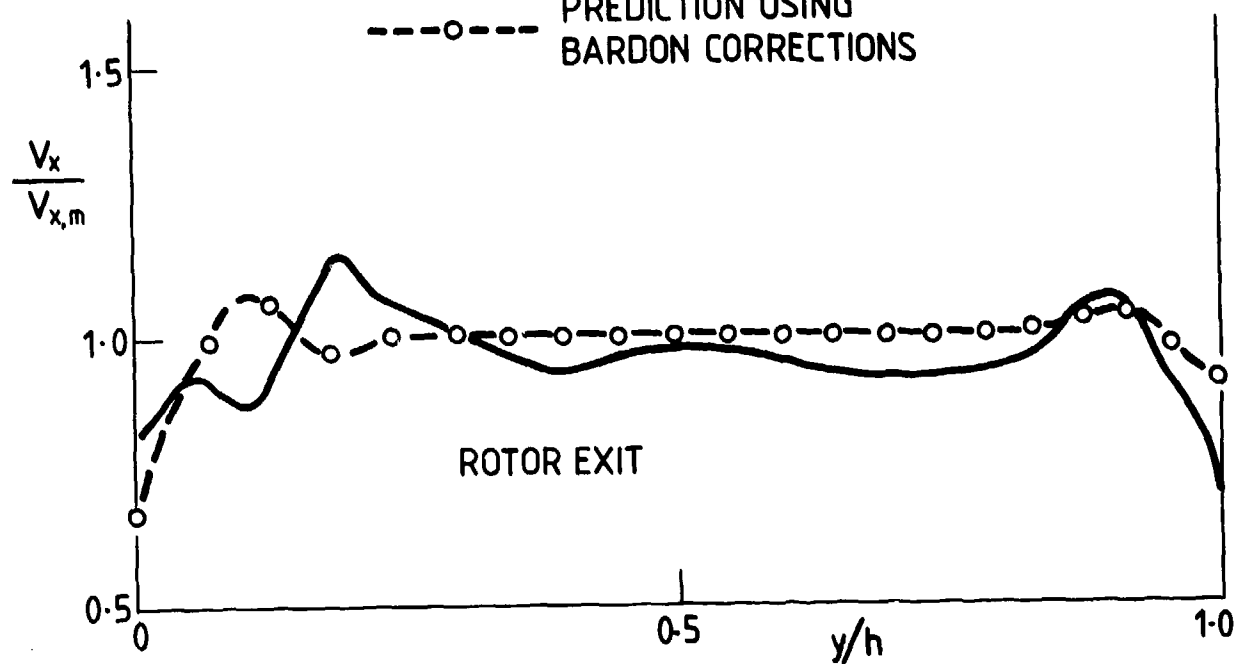


Fig.4.12 Cambridge turbine exit angle predictions



NOZZLE EXIT

MEASUREMENT

PREDICTION USING
BARDON CORRECTIONS

ROTOR EXIT

Fig.4.13 Cambridge turbine axial velocities

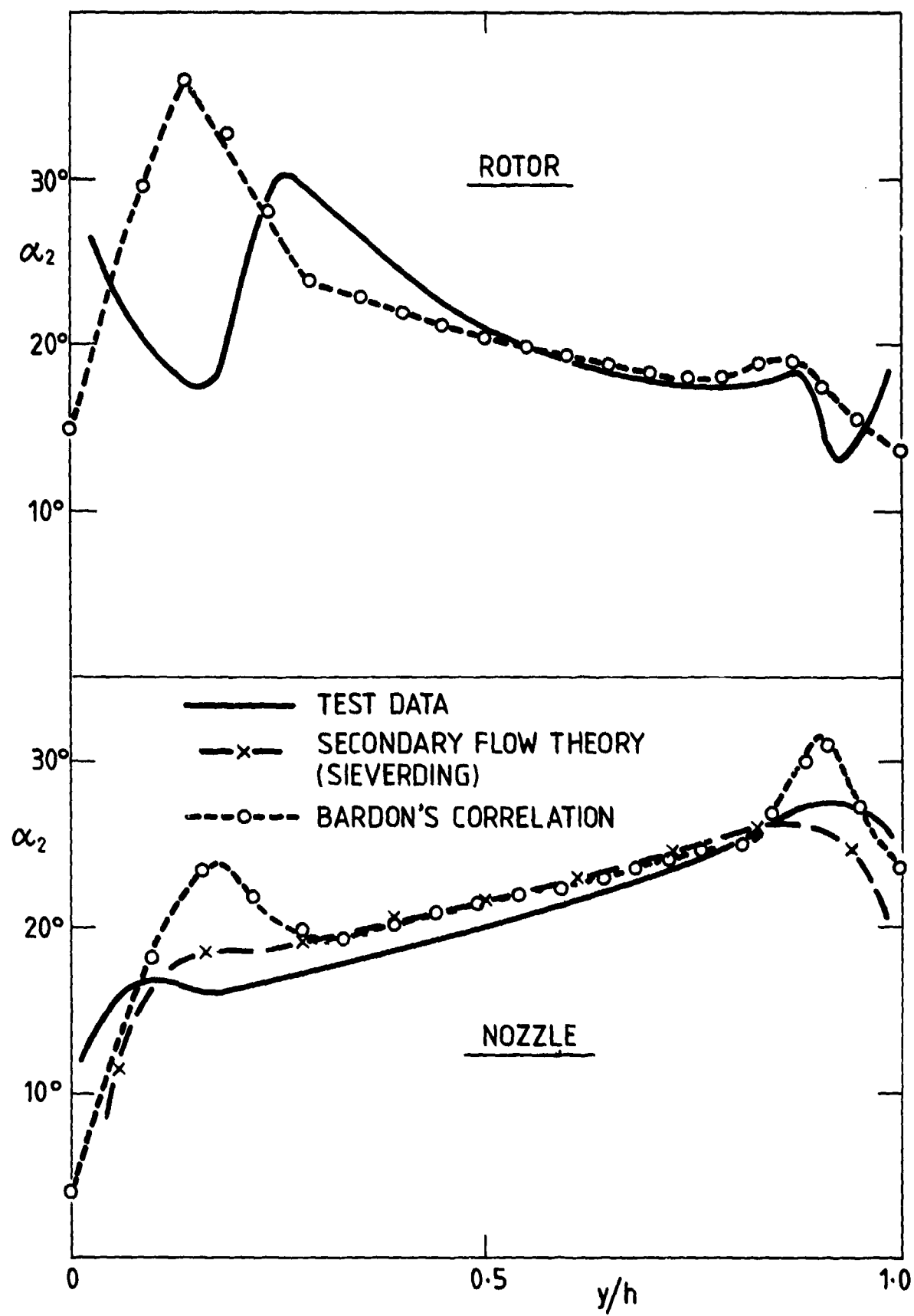


Fig.4.14 Hannover turbine relative flow angles

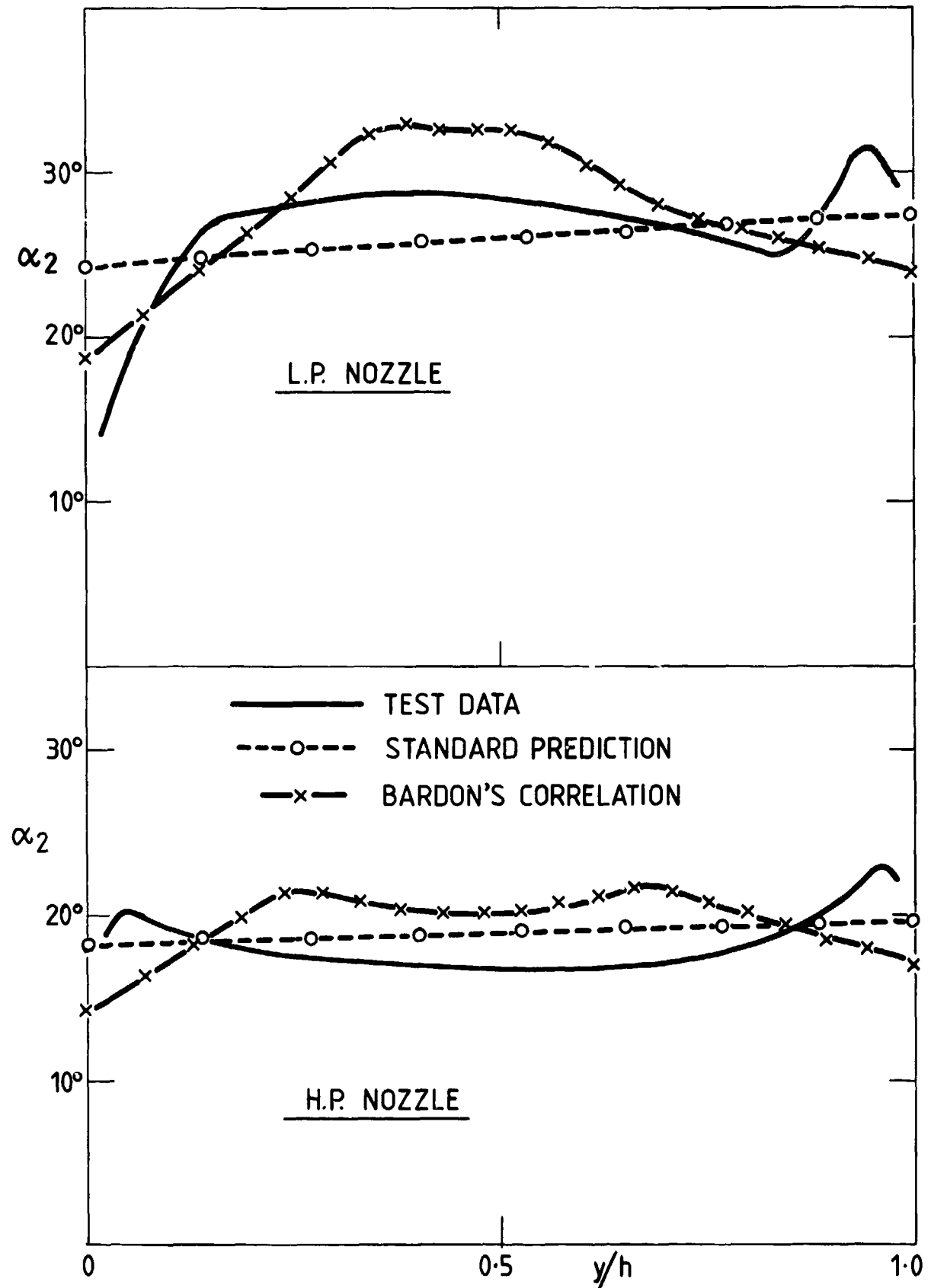


Fig.4.15 2 stage gas nozzle exit angles

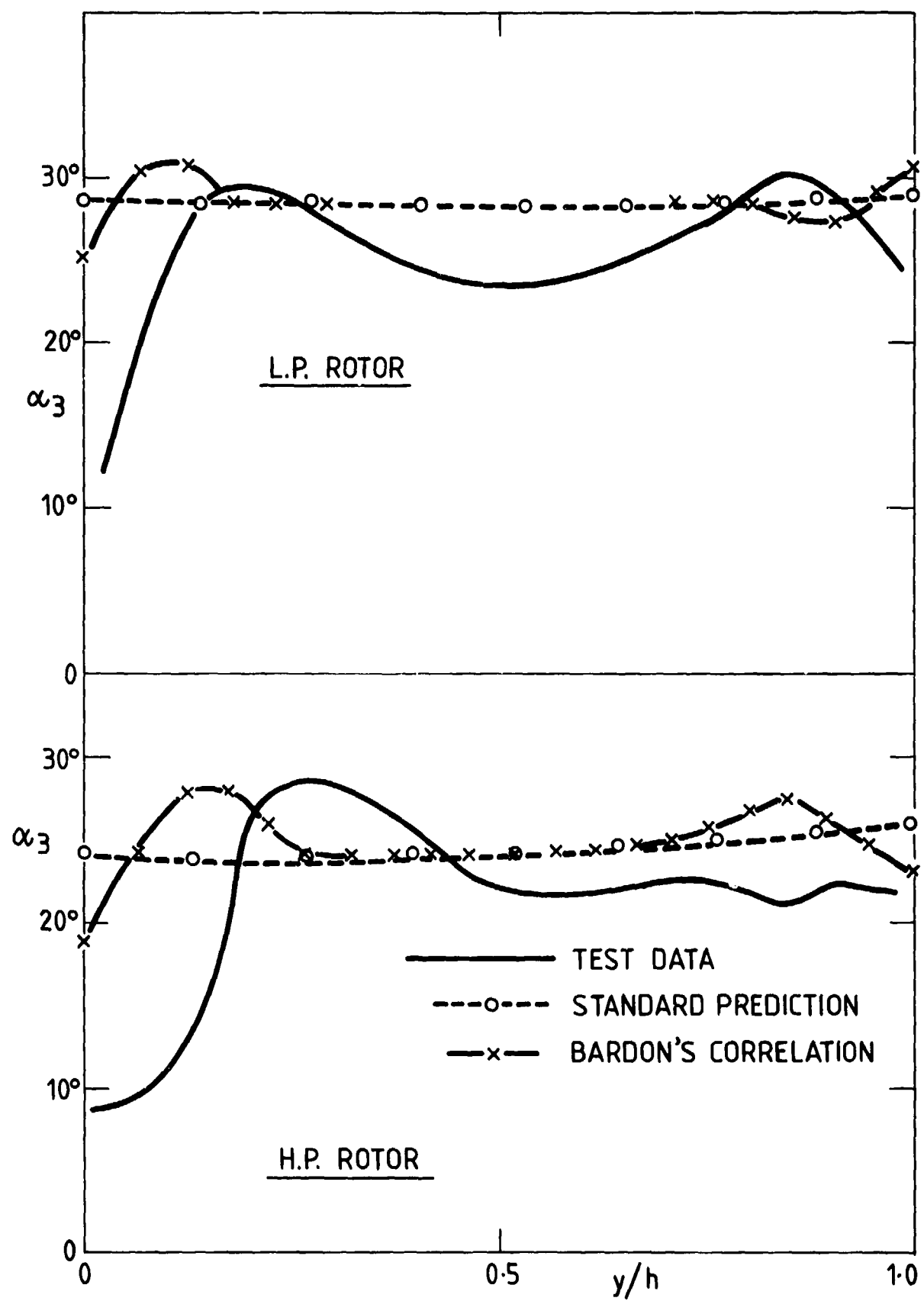


Fig.4.16 2 stage gas turbine rotor exit angles

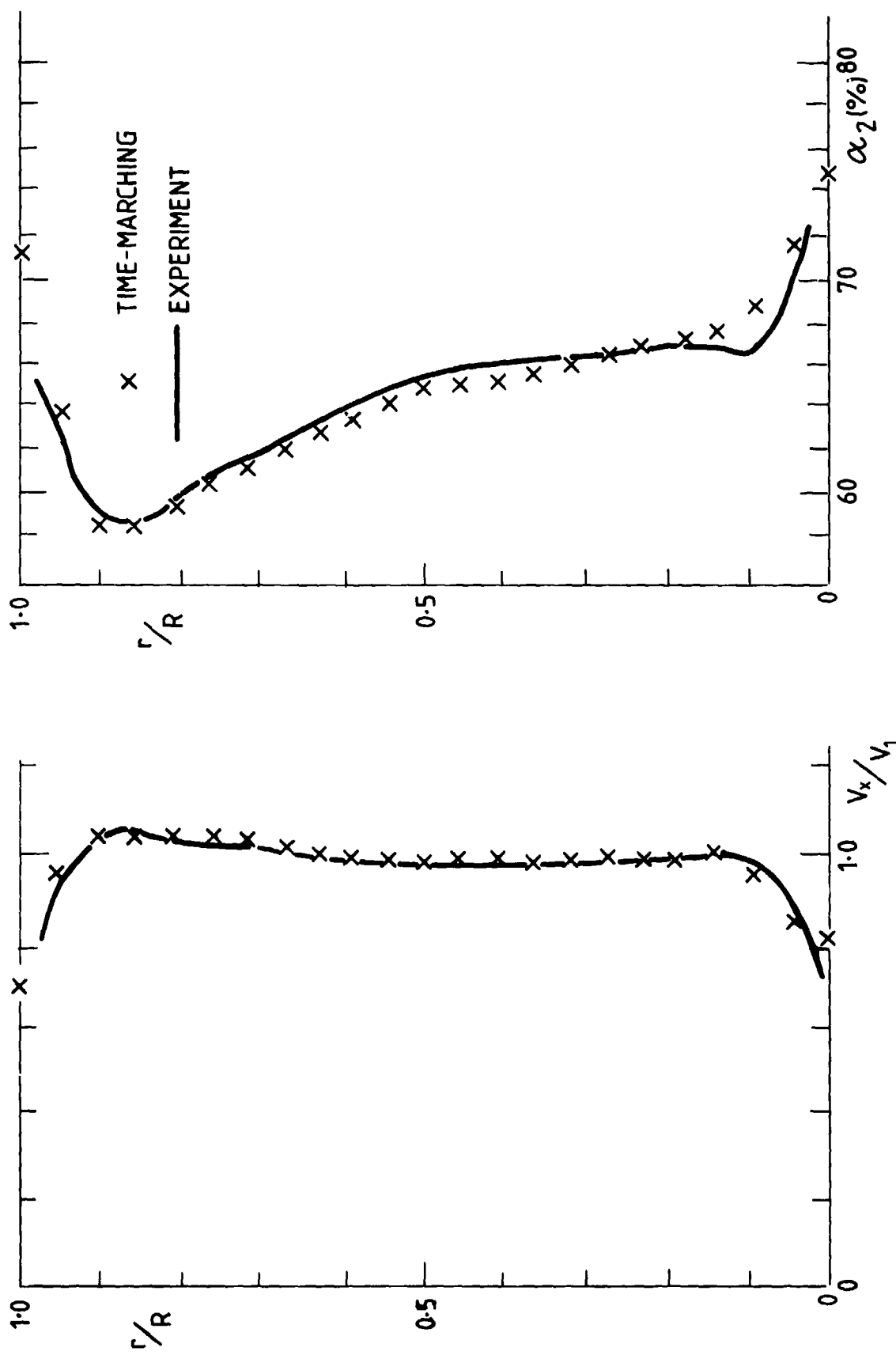


Fig.4.17 Downstream of nozzle blades — Cambridge turbine

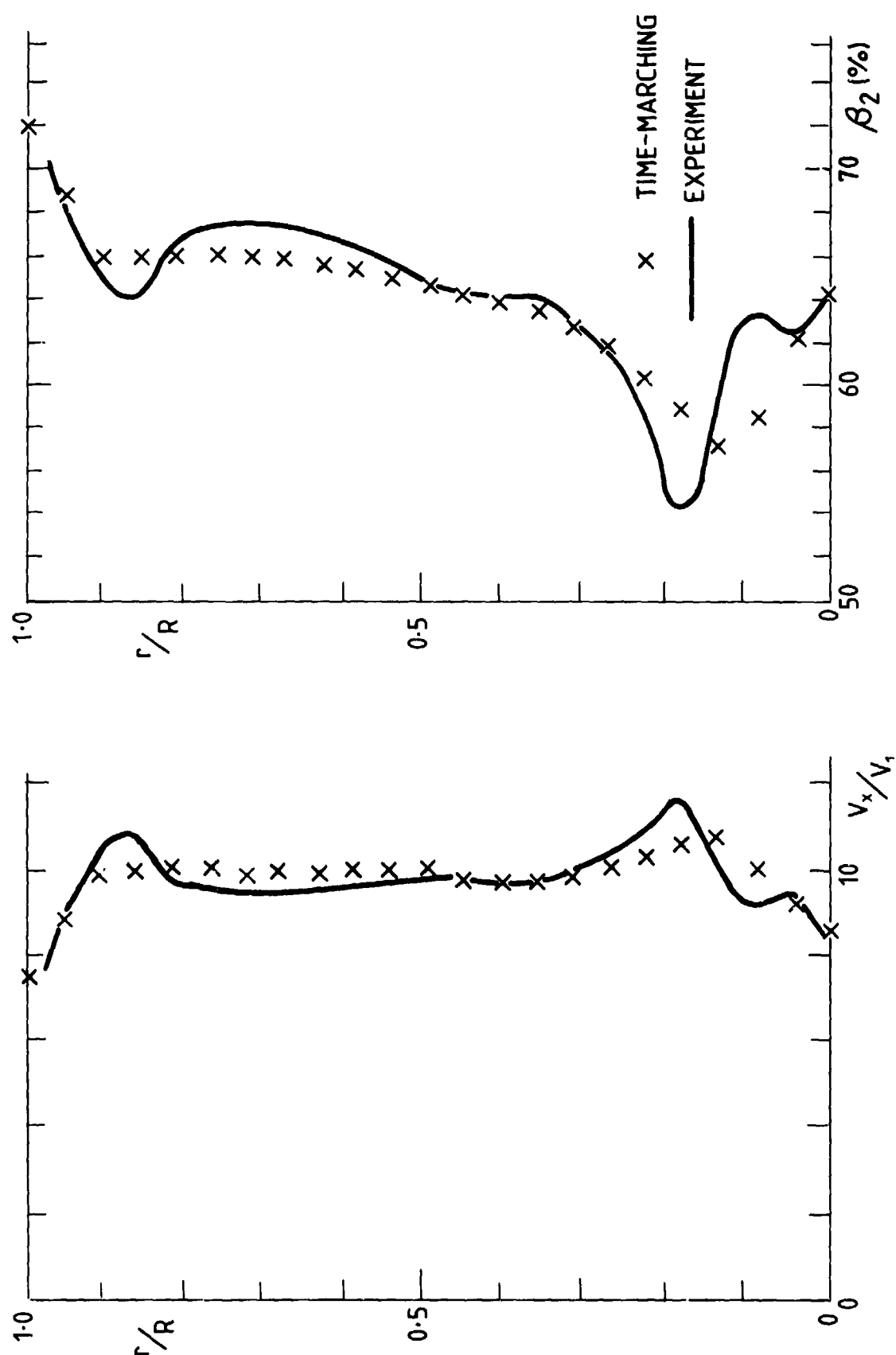


Fig.4.18 Downstream of rotor blades - Cambridge turbine

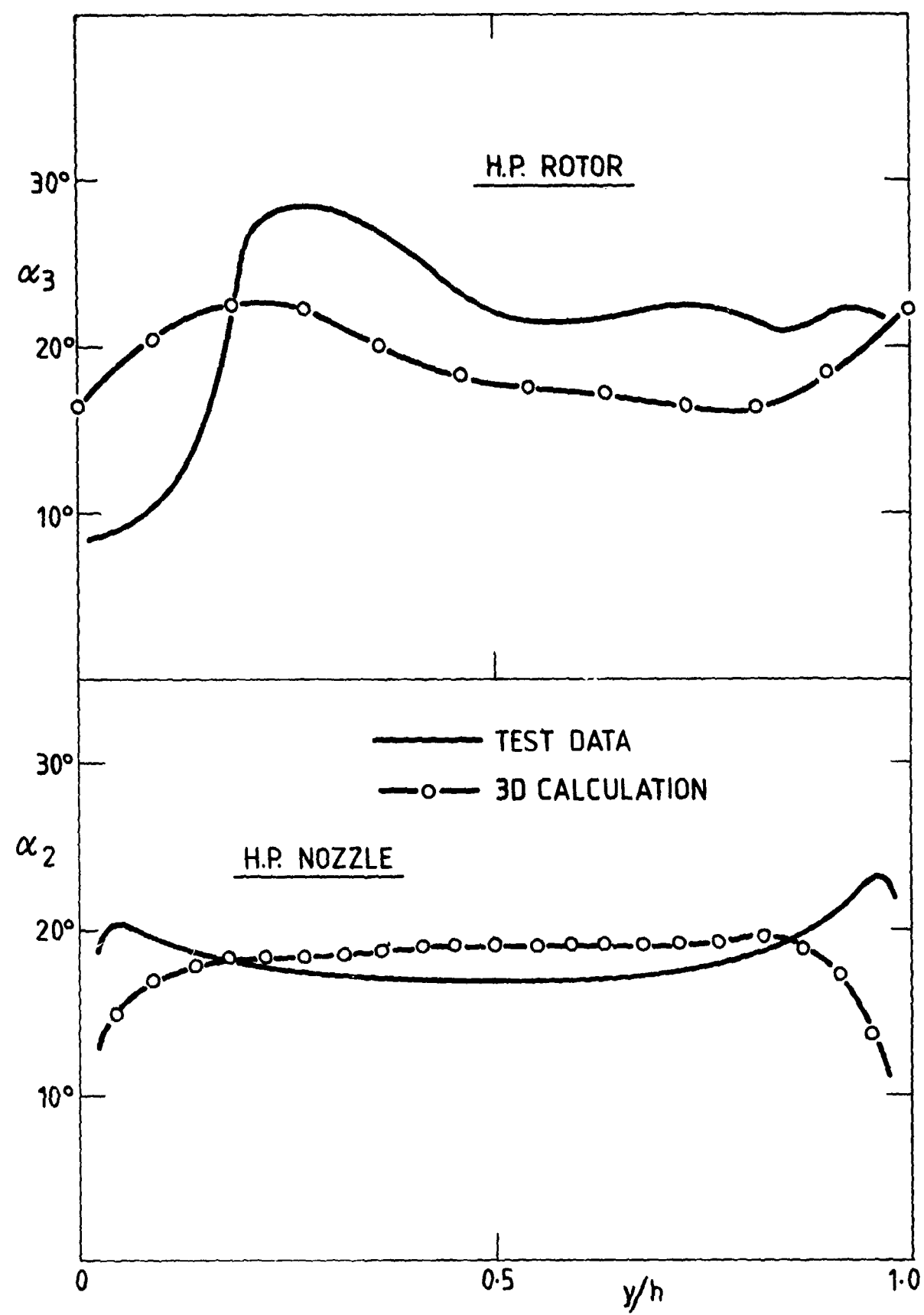


Fig.4.19 2 stage gas turbine H.P. stage exit angles

Chapter I.S
DISCUSSION AND CONCLUSIONS

5.1 OVERALL PERSPECTIVE

The most striking finding of the Turbine Sub-Group was the lack of good, publicly available, test data on turbines. There is certainly a large amount of proprietary data held by turbine manufacturers. Although unable to quote directly from such data, the conclusions of the Turbine Sub-Group draw heavily upon its members' experience with data other than that published in this report.

The Turbine Sub-Group agrees with the view current at the start of this work that the accuracy of throughflow calculations is mainly limited by the empirical correlations used to predict loss and deviation. This view is supported by the experience that when measured losses and angles are input to a calculation the measured flow field can be recreated almost exactly.

The state-of-the-art of turbine throughflow calculations must be considered separately as regards overall performance and detailed flow field prediction.

The situation as regards overall performance is reasonably satisfactory. It seems that several methods are available which are able to predict turbine efficiency to better than $\pm 2\%$. Even remembering that this represents an error of the order $\pm 20\%$ in loss prediction the result is considered surprisingly good. In fact when the complexity of the physical situation is considered, together with how little we understand of the effects of factors such as unsteady flow, stream tube divergence, centrifugal forces, boundary-layer skew, and many others, on the loss production processes the accuracy obtainable seems scarcely credible. There can be no doubt that it is achieved only by ad-hoc adjustments of the many loss parameters so as to obtain agreement with as large a body of test data as is available. It would be highly instructive to compare all methods against a large collection of publicly available test data which had not been used in their development. Unfortunately such a body of data does not exist at present.

The situation regarding flow field predictions is less satisfactory. The calculated velocity profiles are determined mainly by the prescribed relative flow angles at exit from the blade rows. These angles are predictable to better than $\pm 2^\circ$ in 2D flow but in a turbine they are influenced by stream tube divergence, coriolis forces and, above all, by secondary flows. The secondary deviations near to the end walls dominate the flow at aspect ratios of less than about 2.0 and at present they are not accurately predictable. The problem of predicting them within a throughflow calculation appears formidable since annulus boundary-layer growth would also need to be calculated. In the near future fully 3D calculations offer the prospect of improved calculation of secondary flows. However, if these are ever to replace throughflow calculations they will have to include viscous effects and to calculate through several blade rows and such developments must be regarded as long term.

In summary it may be said that throughflow calculations for turbines have almost reached the limit of their possible development. Future improvements in the prediction of loss and deviation are likely to be small until such time as fully 3D viscous methods become available.

5.2 CONCLUSIONS

1. There is an acute shortage of publicly available test data on turbines, particularly on high-speed machines.
2. The physics of loss generation in turbines, as opposed to in cascades, has not been widely studied and is poorly understood.
3. Reasonably good predictions of turbine overall efficiency can be obtained at the design point. Agreement is less good off-design.
4. In order to obtain good predictions of the flow field within turbines it is necessary to distribute both the loss and the deviation along the span. However, variations in deviation are likely to have a much more significant effect than are those in loss.
5. Current throughflow methods can only give good predictions of the flow field for high aspect ratio machines. Low aspect ratio machines are dominated by the effects of secondary flow which are not yet predictable.
6. Fully 3D methods appear promising for calculating secondary flows but they are only likely to replace conventional throughflow calculations in the very long term.

Appendix A1.1

CAMBRIDGE TURBINE – GEOMETRY, TEST DATA AND SAMPLE CALCULATION

The Cambridge turbine is a large, low-speed research facility operated at the Whittle Laboratory of Cambridge University Engineering Department. Full details of the turbine design and of the measurement made on it are given by Hunter (1979) and the Turbine Sub-Group are greatly indebted to Dr Hunter for his help and cooperation in making these results available.

The turbine is a free vortex design with hub:tip ratio 0.7 and with incompressible flow. Hence in the absence of viscous and secondary flow effects the axial velocity profiles would be everywhere uniform and constant. At design conditions there should be no absolute swirl at exit from the rotor and the experimental flow rate was set to satisfy this condition at mid-height. The turbine was tested with various values of rotor-stator spacing but only results for Build 1 (Fig.A1.1) were used for comparison with calculations. This build has a larger stator-rotor gap than is usual in axial turbine design practice.

Details of the machine and blading are given in Tables A1.1, A1.2 and A1.3. All geometrical details are based on design rather than on measured data.

Flow measurements downstream of the nozzles were made with a 5 hole spherical head probe which was traversed circumferentially over two blade pitches. Great detail of the complex secondary flow regions near the end walls was obtained. Flow visualisation on the nozzles showed them to have largely laminar boundary layers which partly accounts for their remarkably low loss coefficient, about 1.4% at mid-span.

The flow behind the rotor was studied both with the five hole probe and with hot wire probes. The latter were used in conjunction with a computer based data acquisition system to obtain ensemble averaged flow patterns. These were obtained at different circumferential positions of the probe so as to study the variation of rotor exit flow pattern with rotor position relative to the stator wakes. The resulting picture of the rotor exit flow was very complex making comparison with throughflow predictions difficult. The results shown in Figures A1.2 and A1.3 were obtained from the averaged hot wire signals at what was thought to be a mean circumferential position. However, it should be emphasized that circumferential variations in the average signal were significant and no attempt was made to obtain a true circumferential average.

The stator loss coefficients were easily obtained from the 5 hole probe measurements but the rotor loss was not measured directly. Instead, the overall efficiency and rotor loss were estimated by applying the Euler equation along streamlines computed from the measured velocities. This process is subject to accumulation of experimental errors and the final estimate of total to total efficiency (93.8%) is thought to be only accurate to $\pm 3\%$. Similarly the accuracy of the rotor loss coefficient does not justify comparison with predictions although the large spanwise variations found in it are probably significant.

In general the detailed experimental results available from this machine emphasize the complexity of the flow in even the simplest of turbine geometries and in particular show that the flow behind a rotor is highly unsteady and non-axisymmetric in an absolute frame.

The throughflow method used to illustrate the results for this test case is that of Denton (1978). This is a streamline curvature method with stations included inside the blade rows. The profile loss is obtained from the method of Baljé and Binsley multiplied by a constant factor of 1.135 (see Denton (1973)), secondary loss from Dunham and Came's (1970) prediction factored by 0.375 and tip leakage loss and flow from the method of Denton and Johnson (1976). The factors multiplying the loss components have been adjusted to obtain good agreement with a large number of measured turbine efficiencies but were not changed from previously optimised values for any of the calculations reported here.

The method takes the blade exit flow angles as \cos^{-1} (opening/pitch) for all subsonic exit flows and adds a supersonic deviation based on continuity for supersonic exit flows.

Profile loss and exit angle are evaluated separately on each streamline and 9 streamlines were used for the present calculations. Secondary loss is evaluated separately at root and tip and then assumed to vary linearly with streamline number (i.e. with mass flow). Tip leakage loss and flow are evaluated at the tip and then added uniformly to each streamline.

The results shown in Figures A1.1—A1.3 were obtained using the measured mass flow (20.1 kg/s) in the calculations. However, with this flow the calculation predicted about 12° of swirl behind the rotor whilst the experimental flow was set to have no exit swirl. In order to predict zero exit swirl the mass flow used had to be reduced by 10% to 18 kg/s. It is significant that the mass flow rate which Hunter obtained from traverse measurements behind the rotor was also 8% higher than the measured inlet mass flow. These two results (computational and experimental) suggest that there may be an error of about +10% in the measured inlet mass flow at which the tests were performed.

As might be expected the computed velocity profiles for this free vortex turbine (Fig.A1.2) are almost uniform and show none of the measured effects of secondary flow. The computed total-total efficiency was 94.3% which is in good agreement with the measured value of 93.8%; however, considering the degree of uncertainty in the latter this agreement is probably fortuitous.

It is clear from this comparison that better agreement between measured and computed velocity profiles can only be obtained if some means of predicting the secondary flows and losses is included in the calculation.

REFERENCES

References to this Appendix are the same as in Part 1.

TABLE A1.1
Cambridge Low-Speed Turbine
Geometrical and Flow Data

	<i>Stator</i>	<i>Rotor</i>
Number of blades	36	51
Blade chord (mm)	152.4	114.3
Axial chord root (mm)	106.3	106.1
" " mid "	108.7	81.6
" " tip "	111.5	62.7
Hub diameter (mm)	533.4	533.4
Tip diameter (mm)	762.0	762.0
Tip clearance (mm)	0.0	0.63

<i>Inlet Boundary Layer (natural)</i>	<i>Hub</i>	<i>Tip</i>
Overall thickness (mm)	21.3	22.1
Displacement thickness (mm)	1.90	2.87

Rotational Speed	525 rpm
Inlet Stagnation Pressure	101.3 kN/m ²
Inlet Stagnation Temperature	293 K
Air Flow Rate	20.1 Kg/s

TABLE A1.2
Cambridge Turbine
Geometry of the Rotor

	<i>Radius*</i>	<i>Chord**</i>	<i>Pitch</i>	<i>Throat***</i>	<i>Throat Angle</i>	<i>Rear S.S. Curvature</i>	<i>Inlet** Angle</i>	<i>Backbone*** Length</i>	<i>T.E.** Thickness</i>
STRL 1	0.55626	0.11601	0.06853	0.03228		0.21510	54	0.0598	0.1360
2	0.57912	0.11574	0.07135	0.03287		0.22220	63	0.0642	0.1320
3	0.60198	0.11548	0.07417	0.03334		0.22930	72	0.0685	0.1280
4	0.62484	0.11521	0.07698	0.03372		0.23640	81	0.0729	0.1240
5	0.64770	0.11494	0.07980	0.03399		0.23435	90	0.0773	0.1200
6	0.67056	0.11488	0.08262	0.03410		0.25060	97	0.0793	0.1190
7	0.69342	0.11482	0.08543	0.03469		0.25770	104	0.0813	0.1180
8	0.71628	0.11477	0.08825	0.03459		0.26480	111	0.0832	0.1170
9	0.73914	0.11471	0.09107	0.03552		0.27190	118	0.0852	0.1160
HUB	0.53340	0.11628	0.06571	0.03154		0.20800	125	0.0554	0.1400
TIP	0.76200	0.11465	0.09388	0.03652		0.22190	45	0.0872	0.1150

* equally spaced
** linearly interpolated from hub and tip to the mean line
*** from provided graph of opening/pitch ratio

Note: all dimensions in [m]

TABLE A1.3
Cambridge Turbine
Geometry of the Stator

	<i>Radius*</i>	<i>Chord**</i>	<i>Pitch</i>	<i>Throat***</i>	<i>Throat Angle</i>	<i>Rear S.S.** Curvature</i>	<i>Inlet Angle</i>	<i>Inlet** Width</i>	<i>Backbone** Length</i>	<i>T.E.**** Thickness</i>
STRL 1	0.55626	0.1531	0.09709	0.03900		0.31428	90	0.0878	0.16160	0.00310
2	0.57912	0.1531	0.10108	0.04191		0.30656	90	0.0916	0.16120	0.00305
3	0.60108	0.1531	0.10507	0.04406		0.29884	90	0.0954	0.16080	0.00300
4	0.62484	0.1532	0.10906	0.04615		0.29112	90	0.0992	0.16040	0.00290
5	0.64770	0.1532	0.11305	0.04822		0.28340	90	0.1030	0.16000	0.00290
6	0.67056	0.1532	0.11704	0.05042		0.27568	90	0.1068	0.15960	0.00295
7	0.69342	0.1532	0.12103	0.05265		0.26796	90	0.1106	0.15920	0.00300
8	0.71628	0.1533	0.12502	0.05522		0.26024	90	0.1144	0.15880	0.00305
9	0.73914	0.1533	0.12900	0.05880		0.25252	90	0.1182	0.15840	0.00310
HUB	0.53340	0.1533	0.09310	0.03344		0.32290	90	0.0840	0.16200	0.00310
TIP	0.76200	0.1533	0.13299	0.06564		0.24480	90	0.1220	0.15800	0.00310

* equally spaced

** linearly interpolated from hub to tip

*** from provided graph of opening/pitch ratio

**** linearly interpolated from hub and tip to the mean line

Note: all dimensions in [m]

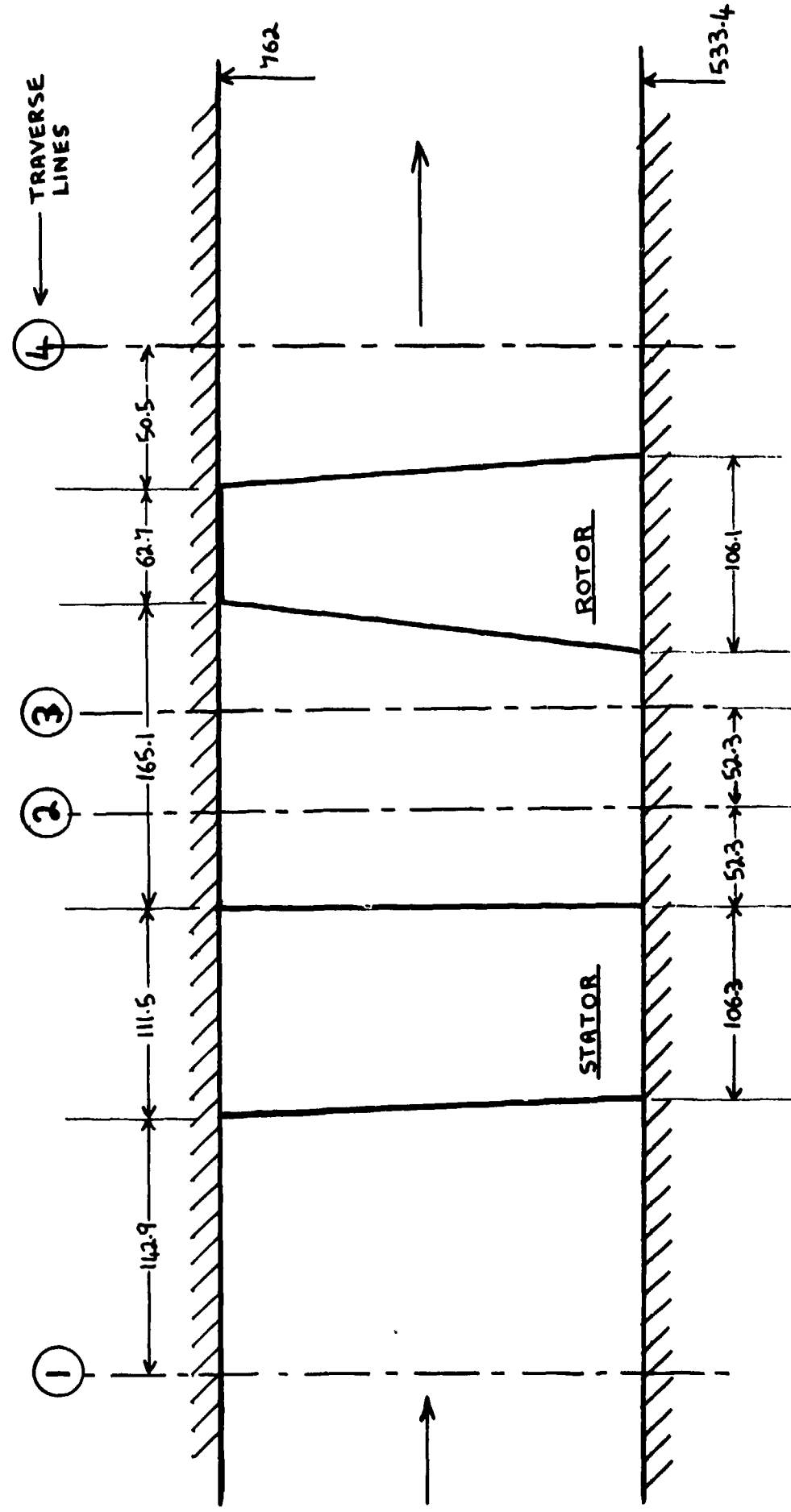
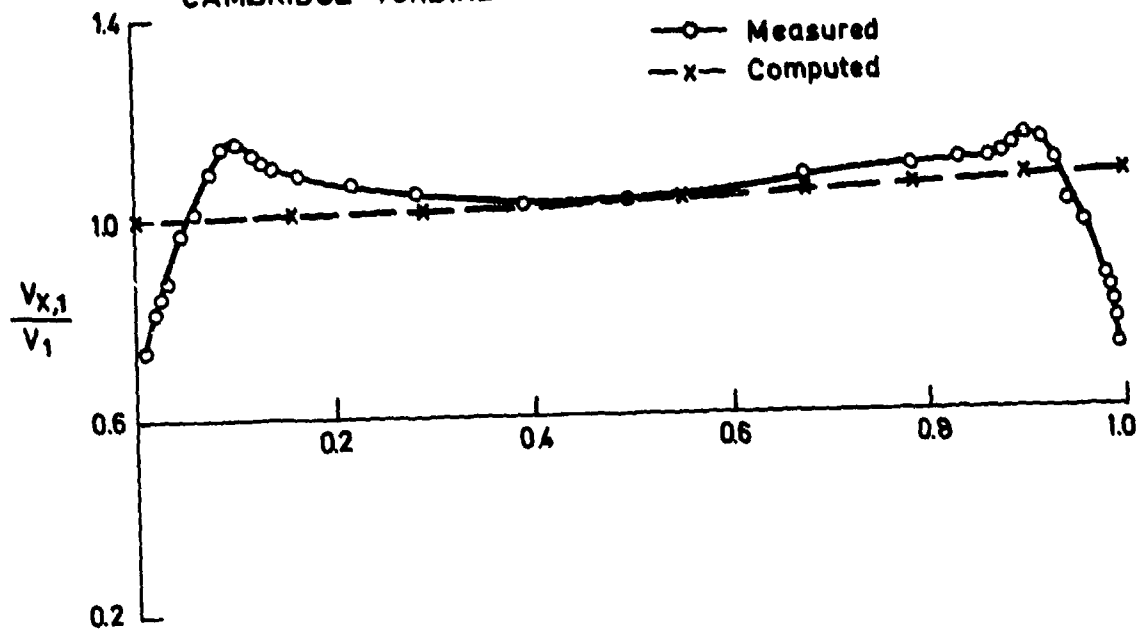


Fig.A1.1 Layout of turbine

CAMBRIDGE TURBINE



CAMBRIDGE TURBINE

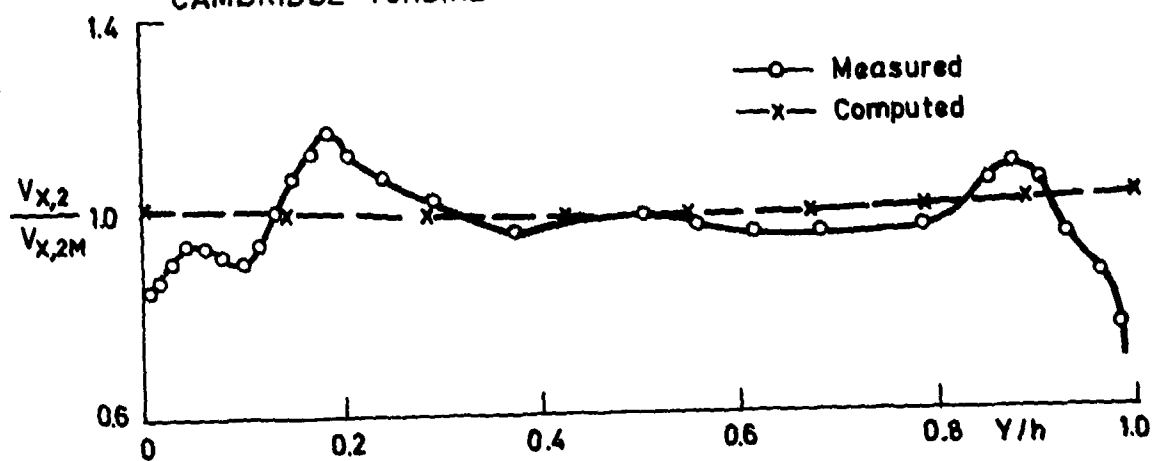


Fig.A1.2 Axial velocity profiles after rotor and stator

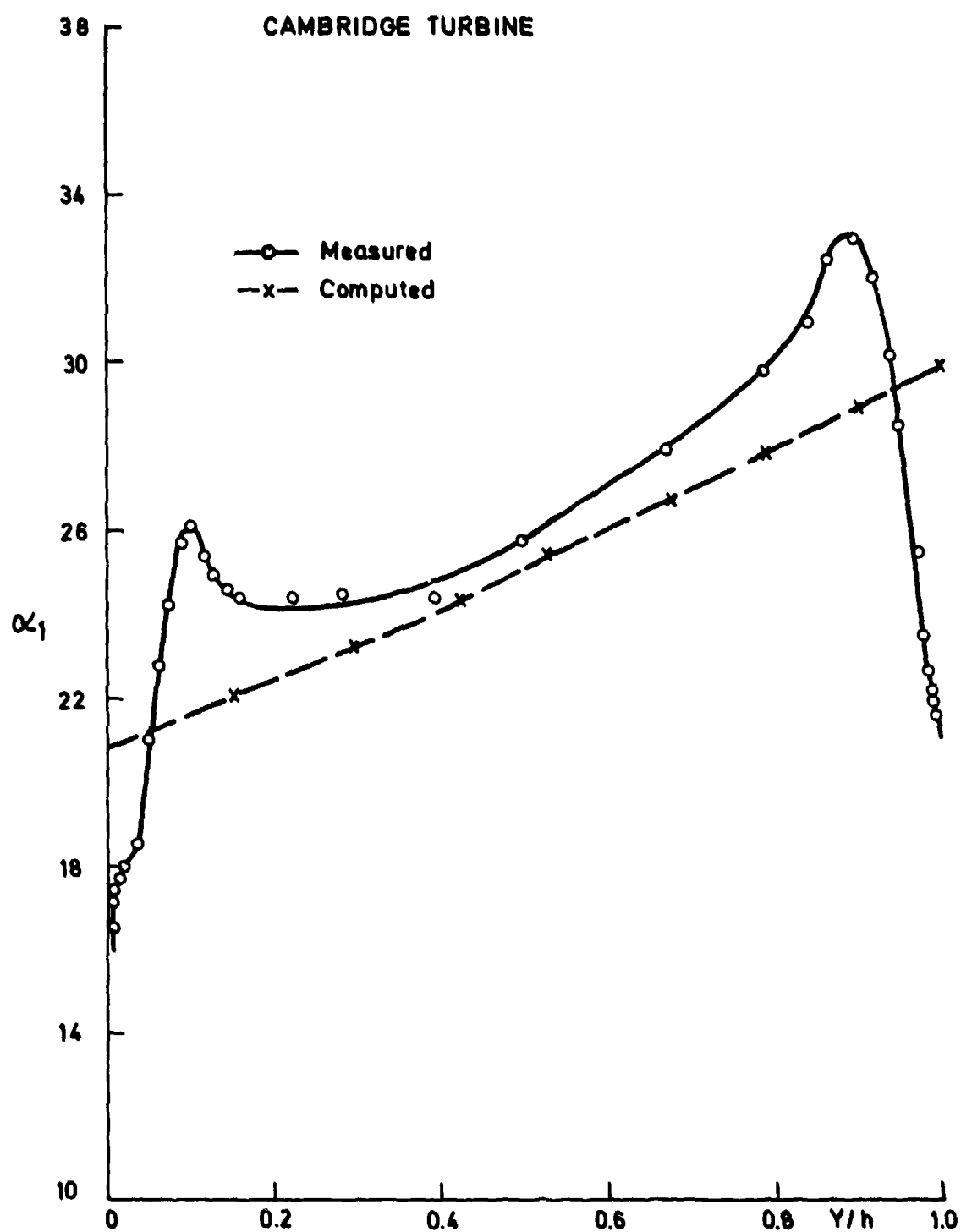


Fig.A1.3 Stator exit angles

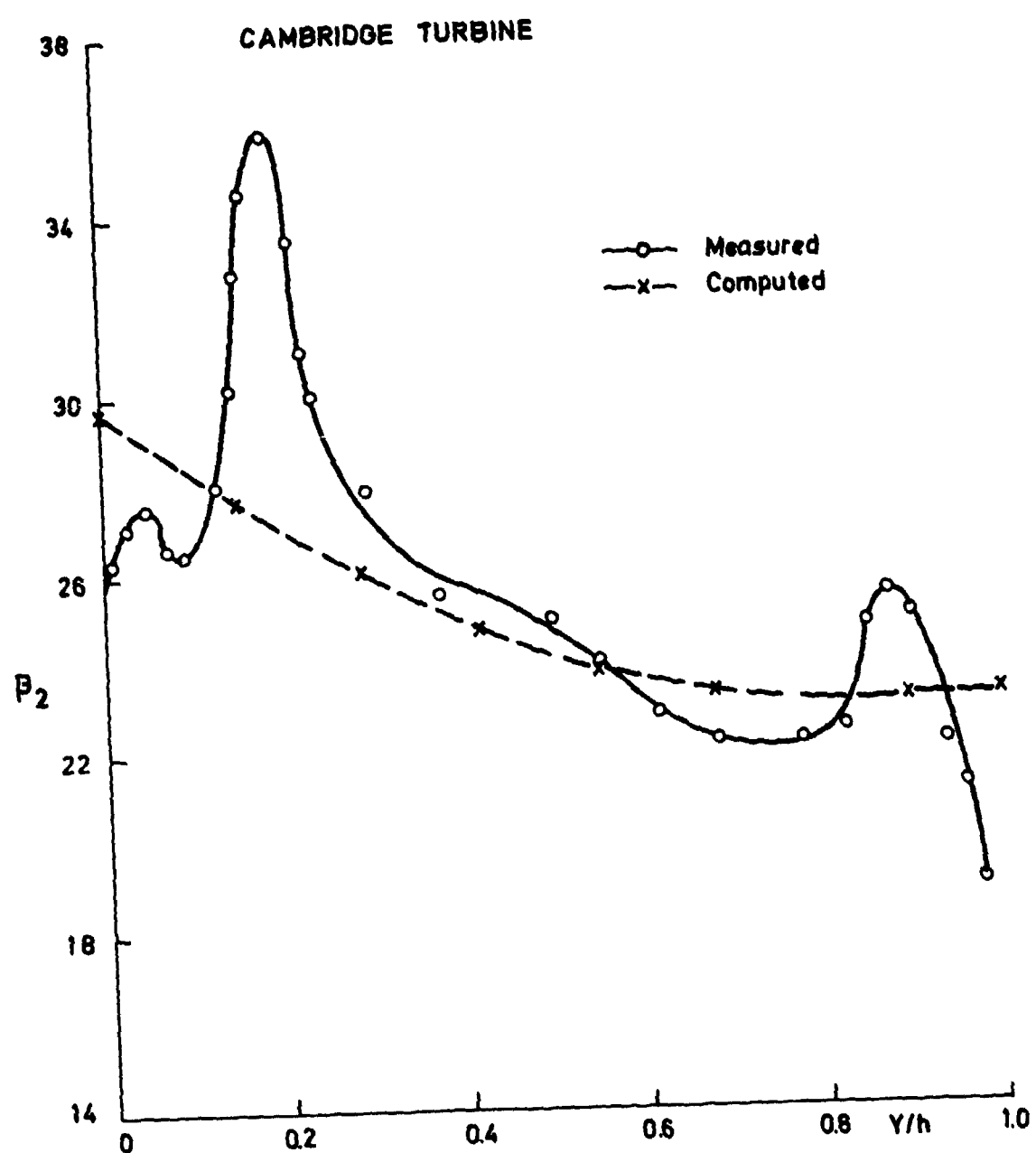


Fig.A1.4 Rotor exit angles

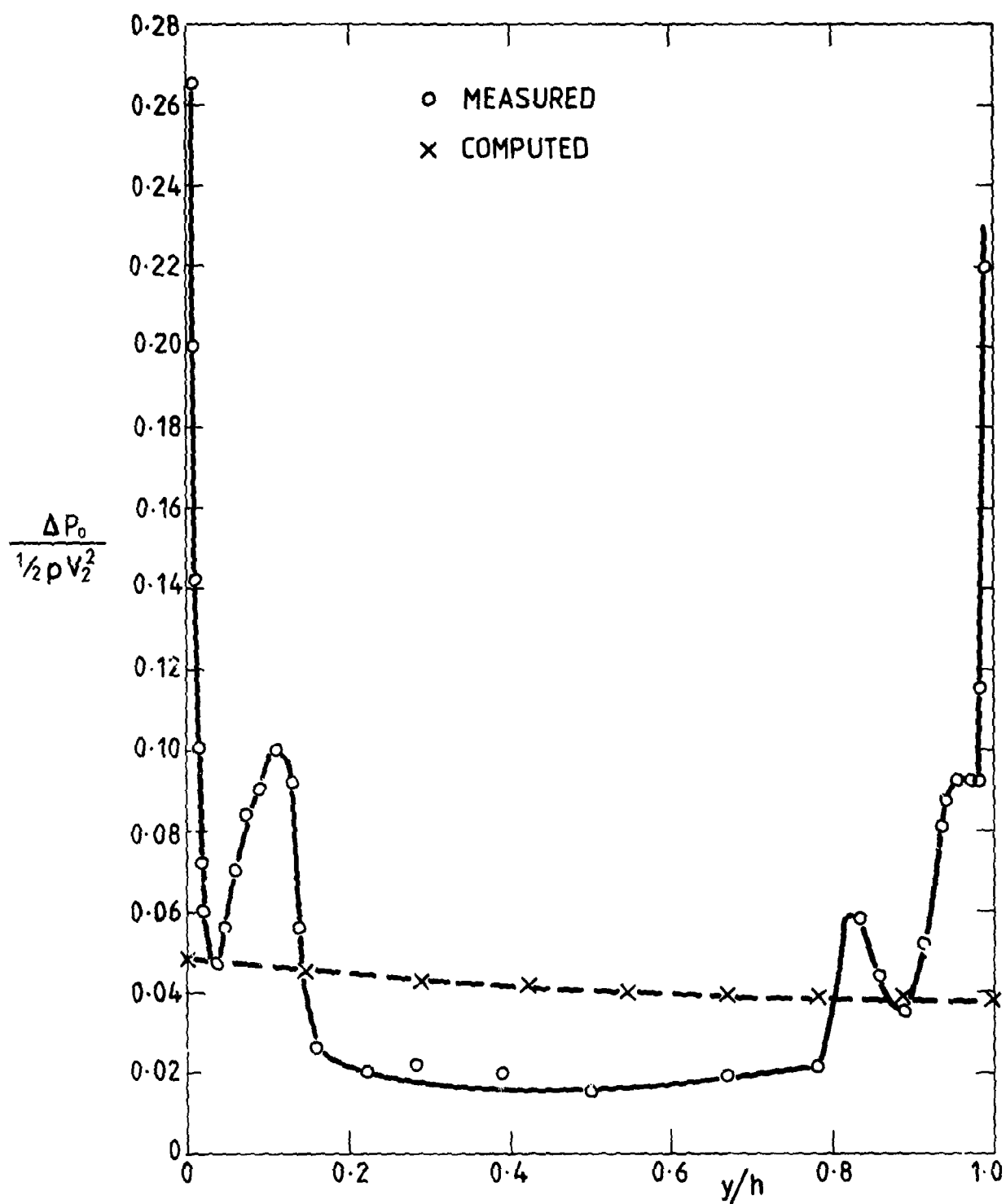


Fig.A1.5 Stator loss coefficients

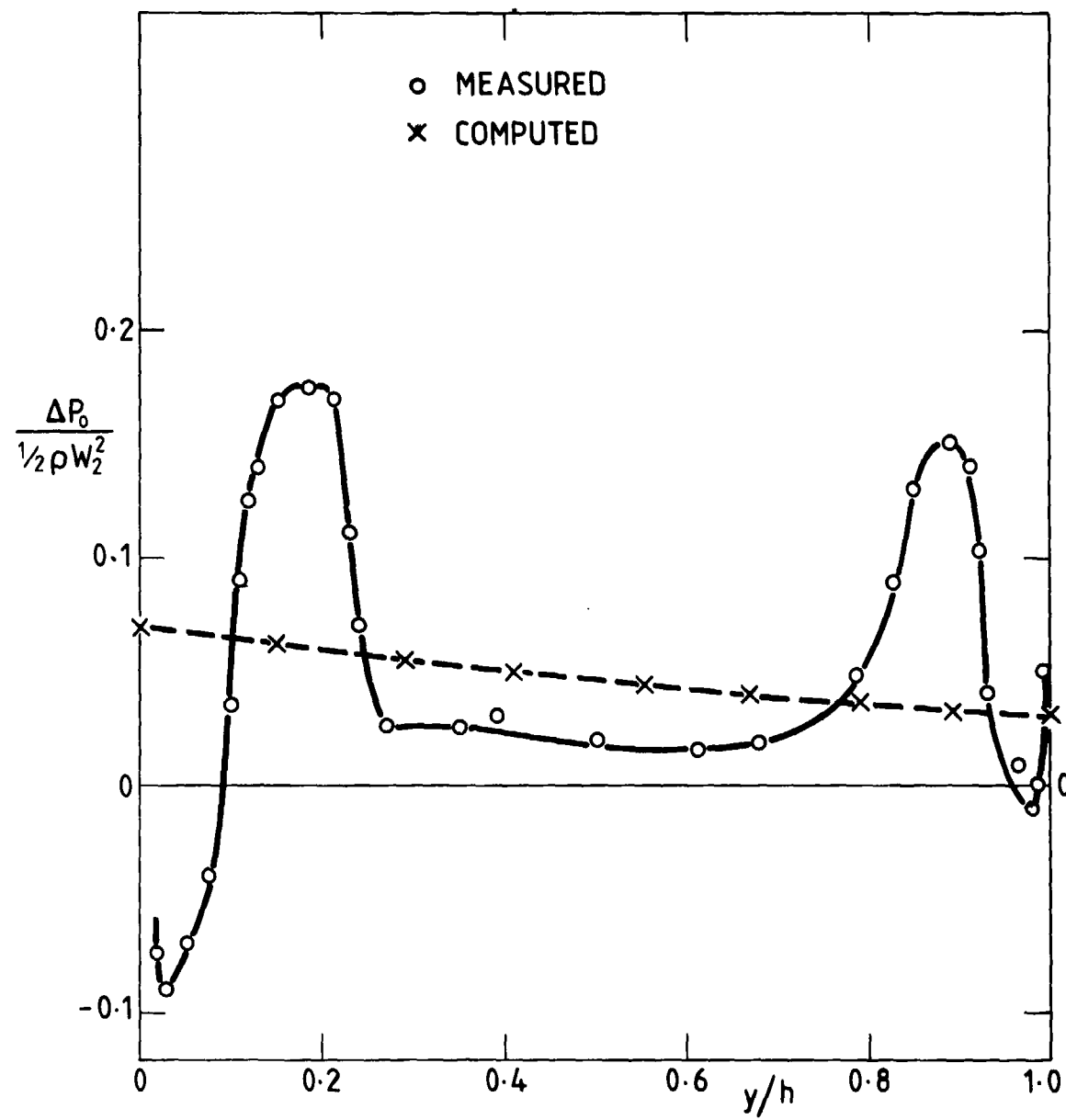


Fig.A1.6 Rotor loss coefficients

Appendix A1.2

THE TWO STAGE AERO ENGINE TURBINE

This turbine was tested by Rolls-Royce Ltd., and was used as a test case for the 1976 AGARD meeting on throughflow calculations. The geometric details and test results are published in AGARD CP 195 and are reproduced here, Tables A2.1 - A2.5, with no additional information being included. Drawings of the blade sections are available in AGARD CP 195.

Few details of the turbine and test procedure are available. The turbine was a model of the H.P. and I.P. stages of an aircraft gas turbine with the two rotors running at different speeds. It was 'cold flow' tested using air at 420 K and 2.95 bar. Both hot wire and pressure probe instrumentation was used with radial and circumferential traverses after each blade row. Only the circumferentially averaged flow properties are available to the Turbine Sub-Group and the degree of confidence in the results cannot be established without more details of the experimental techniques. However, it is considered likely that the measured loss coefficients of all but the first blade row are subjected to a great deal of uncertainty as a result of the non-uniform total pressure field at inlet to these blades.

The design is unusual because of the very low aspect ratio of the I.P. nozzle row and the measurements indicate very high losses for this row which are consistent with a flow separation within it. There are also signs of a possible flow separation at the root of the first rotor. Because of this the overall efficiency is expected to be lower than might be obtained for a well designed machine with this geometry.

Apart from the difficulties of estimating the losses correctly this machine provides a severe test of any throughflow calculation procedure because both blade rows of the H.P. stage are very nearly choked (some calculations predicted the nozzle to be choked). Hence the pressure ratio:mass flow characteristic is very steep and it is necessary to work to a prescribed pressure ratio rather than a prescribed mass flow.

The throughflow program used to provide sample results was developed by E.Macchi and is based on Vavra's (1960) method of solution for axisymmetric and steady flow in axial turbomachines; it solves the complete radial equilibrium equation — accounting for enthalpy and entropy gradients and streamline curvature effects — in a specified number of stations ahead of and after the blade rows. An orthogonal curvilinear system of coordinates, having the meridional co-ordinates coincident with the generatrices of the flow stream surfaces, is used in the solution.

It makes use of iterative methods for the numerical solution of the radial equilibrium and continuity equation at each considered station. An iterative procedure is also applied for the location of the streamlines over the whole machine. Streamlines curvature and slope are numerically derived from the radial positions of three adjacent stations. Entropy gradients are assumed to occur only between stations ahead and after a blade row, and are computed from blade loss coefficients. The Craig & Cox loss correlation is used: the profile losses are computed along each streamline, as a function of the local blade geometry and flow condition; the secondary losses are evaluated at mid radius and uniformly distributed. No other losses are considered.

In the continuity equation, leakage flow rate is accounted for by means of the following relation:

$$\dot{m}_{CL} = \frac{A_{CL}}{K_{CL}} \frac{P_T}{\sqrt{R T_T}} \Phi \cos \epsilon$$

where:

A_{CL} = clearance area

K_{CL} = coefficient, assumed equal to 2 in the present calculations

P_T, T_T = total conditions ahead of the leakage region

Φ = flow coefficient, given by:

$$\Phi = \sqrt{\frac{2\gamma}{\gamma-1} \left[\left(\frac{P}{P_T}\right)^{2/\gamma} - \left(\frac{P}{P_T}\right)^{(\gamma+1)/\gamma} \right]}$$

Flow angles in the stations after the blade rows are computed by the following relation, derived by applying the continuity equation between the blade throat section and the station after the blade where the equilibrium equation is solved:

$$\alpha = \sin^{-1} \left(\frac{a}{g} \frac{h}{h_a} \frac{\sin \epsilon}{\sin \epsilon_a} - \frac{1}{1 + \frac{H}{K} \xi^*} \frac{1 + \xi \left[\left(\frac{P_T}{P} \right)^{(\gamma-1)/\gamma} - 1 \right]}{\sqrt{1-\xi}} X \right)$$

where

- a = blade throat
 - g = spacing
 - h_a = stream tube height at throat
 - h = stream tube height at considered station
 - H/K = boundary layer form factor (assumed 0.9 in calculations)
 - ξ^* = loss coefficient at throat
 - ξ = overall loss coefficient
 - ϵ_a = elevation angle at throat
 - ϵ = elevation angle at considered station
 - X = 1 for unchoked throat
 - X = Φ_{cr}/Φ for choked throat, with the flow coefficient to be calculated for isentropic flow.
- In the calculations, it was assumed $\xi^* = \xi_{PROFILE} + \frac{1}{2}\xi_{sec}$.

Comparisons of measured and computed flow distributions are shown in Figures A2.1 to A2.12. For the H.P. stage the relative Mach numbers at blade exit agree well but the very large secondary deviations at rotor exit (Fig.A2.5) completely distort the measured axial Mach number profiles. (Fig.A2.4). The mean level of loss is reasonably well predicted for both H.P. blade rows but the concentration of loss near the walls is not included in the calculation.

The relative exit Mach numbers are again reasonably well predicted for the I.P. stage although the computed stage reaction seems to be higher than measured (relative Mach number low for nozzle high for rotor). The levels of loss are underpredicted for both I.P. blade rows, particularly the rotor, and the complex variations in blade exit angle (Figs A2.8, A2.11) are not reproduced by the calculation.

The overall efficiency of the machine is well predicted 89.1% (c.f 88.4% or 89.1 measured) but this agreement may be misleading because significant tip leakage losses were included in the calculation whilst they are expected to be negligible in the turbine (rubbing seals). If no tip leakage loss had been included in the calculation the low losses predicted for the I.P. turbine would have caused the overall efficiency to be overpredicted.

The comparisons on this machine show that relative blade exit velocities profiles can be predicted much better than can axial or meridional velocity profiles. The latter are greatly distorted by the effects of secondary flow which are possibly greater than usual in this machine as a result of flow separations in the H.P. rotor and I.P. nozzle. For the same reason the efficiency of the turbine might be expected to be rather lower than predicted by standard correlations.

REFERENCES

Vavra, M.H.

Aerothermodynamics and Flow in Turbomachines, pp.439-470, Wiley, 1960.

TWO STAGE AERO ENGINE GAS TURBINE TEST CONDITIONS

Mass flow	= 11.5 Kg/s
Inlet total pressure	= 2.94 bar
Inlet total temperature	= 423 K
Rotational speed	= HP turbine 8250 rpm IP turbine 4693 rpm
Overall total:total pressure ratio	5.8359
Inlet total pressure distribution	= not available
Inlet total temperature distribution	= not available
Inlet velocity distribution (at station z = -68.6)	

<i>Radius</i>	<i>Axial Mach Number</i>	<i>Angle</i>
0.25943	0.1019	90
0.26055	0.1524	90
0.26168	0.1502	90
0.26280	0.1468	90
0.26505	0.1429	90
0.26955	0.1393	90
0.28080	0.1446	90
0.29205	0.1561	90
0.29655	0.1566	90
0.29880	0.1545	90
0.29993	0.1529	90
0.30105	0.1496	90
0.30218	0.1434	90

Radial clearance = Effectively zero (shrouded blades with rubbing seal)

Number of blades =	first stator	54
	first rotor	102
	second stator	36
	second rotor	148

Measured Efficiencies

(1) Total-total based on brake work and total pressures from wall statics and continuity.

Overall:	88.4%
H.P.:	85.7%
I.P.:	89.6%

(2) Total-total based on total temperatures and total pressures from traverse data

Overall:	89.1%
H.P.:	89.8%
I.P.:	89.5%

TABLE A.1
Geometry of the First Stator

Geometry of the Cowl Section									T.E. Thickness
	Radius*	Chord**	Pitch	Throat**	Rear S.S.** Curvature	Inlet Angle	Inlet ** Width	Backbone** Length	
STRL	1	0.26911	0.04740	0.03131	0.00949	0.20960	90	0.02510	0.04966
	2	0.27728	0.04744	0.03174	0.00979	0.20386	90	0.02594	0.04970
	3	0.27653	0.04748	0.03217	0.01008	0.19828	90	0.02671	0.04974
	4	0.28024	0.04752	0.03260	0.01036	0.19286	90	0.02745	0.04978
	5	0.28395	0.04756	0.03304	0.01063	0.18769	90	0.02817	0.04982
	6	0.28766	0.04759	0.03347	0.01089	0.18253	90	0.02886	0.04986
	7	0.29137	0.04763	0.03389	0.01116	0.17749	90	0.02957	0.04990
	8	0.29508	0.04766	0.03433	0.01140	0.17267	90	0.03021	0.04994
	9	0.29879	0.04770	0.03477	0.01165	0.16785	90	0.03087	0.04997

$$(R_{TIP})^{LE} = 0.30250$$

$$(R_{HUB})^{L.E.} \equiv 0.23830$$

* equally spaced

* equally spaced λ and given values at $R = 0.27173$ and $R = 0.29703$

Note: all dimensions in [m]

TABLE A2.2
Geometry of the First Rotor

	<i>Radius*</i>	<i>Chord**</i>	<i>Pitch</i>	<i>Throat***</i>	<i>Throat Angle</i>	<i>Rear S.S. Curvature</i>	<i>Inlet*** Angle</i>	<i>Inlet*** Width</i>	<i>Backbone** Length</i>	<i>T.E.** Thickness</i>
STRL	1	0.27610	0.22002	0.01701	0.00677		0.08076	40.0	0.01198	0.02523
	2	0.28090	0.22414	0.01730	0.00682		0.08134	41.2	0.01222	0.02592
	3	0.28570	0.22827	0.01760	0.00688		0.08192	42.4	0.01245	0.02661
	4	0.29050	0.22340	0.01789	0.00693		0.08249	43.7	0.01269	0.02730
	5	0.29530	0.23653	0.01819	0.00698		0.08307	44.4	0.01293	0.02799
	6	0.30010	0.24065	0.01849	0.00703		0.08364	48.2	0.01316	0.02868
	7	0.30490	0.24478	0.01878	0.00709		0.08422	52.0	0.01340	0.02937
	8	0.30970	0.24891	0.01908	0.00714		0.08480	55.8	0.01363	0.03006
	9	0.31450	0.25303	0.01937	0.00719		0.08537	59.6	0.01387	0.03075
$(R_{HUB})_{LE.} = 0.26800$		$(R_{TIP})_{LE.} = 0.30860$		$(R_{HUB})_{TE.} = 0.27130$		$(R_{TIP})_{TE.} = 0.31930$				

* equally spaced

** linearly interpolated from given values at $R = 0.27387$ and $R = 0.30504$

*** linearly interpolated from given values at $R = 0.27387$, $R = 0.29150$ and $R = 0.30500$

Note: all dimensions in [m]

TABLE A2.3

Geometry of the Second Stator

	<i>Radius*</i>	<i>Chord**</i>	<i>Pitch</i>	<i>Throat**</i>	<i>Throat Angle</i>	<i>Rear S.S.** Curvature</i>	<i>Inlet** Angle</i>	<i>Inlet** Width</i>	<i>Backbone** Length</i>	<i>T.E.** Thickness</i>
STR1	0.31218	0.07703	0.05449	0.02247		0.19500	55.20	0.04202	0.08243	0.00168
2	0.31836	0.07721	0.05556	0.02329		0.20271	55.00	0.04294	0.08151	0.00153
3	0.32454	0.07738	0.05664	0.02411		0.21043	54.80	0.04386	0.08059	0.00137
4	0.33072	0.07755	0.05772	0.02493		0.21814	54.60	0.04478	0.07967	0.00122
5	0.33690	0.07773	0.05880	0.02575		0.22586	54.40	0.04570	0.07876	0.00106
6	0.34308	0.07791	0.05988	0.02658		0.23357	54.20	0.04661	0.07784	0.00091
7	0.34926	0.07808	0.06096	0.02740		0.24129	54.00	0.04753	0.07692	0.00075
8	0.35544	0.07826	0.06204	0.02822		0.24900	53.80	0.04845	0.07600	0.00060
9	0.36162	0.07844	0.06311	0.02904		0.25671	53.60	0.04937	0.07598	0.00045
$(R_{HUB})_{L.E.} = 0.27510$		$(R_{TIP})_{L.E.} = 0.33040$		$(R_{HUB})_{T.E.} = 0.30600$		$(R_{TIP})_{T.E.} = 0.36780$				

* equally spaced

** linearly interpolated, from given values at $R = 0.31237$ and $R = 0.35307$

Note: all dimensions in [m]

TABLE A2.4
Geometry of the Second Rotor

	<i>Radius*</i>	<i>Chord**</i>	<i>Pitch</i>	<i>Throat**</i>	<i>Throat Angle</i>	<i>Rear S.S.** Curvature</i>	<i>Inlet** Angle</i>	<i>Inlet*** Width</i>	<i>Backbone** Length</i>	<i>T.E. Thickness</i>
STRL 1	0.322274	0.19700	0.01370	0.00652		0.05700	51.60	0.01984	0.22163	0.00046
2	0.33079	0.20100	0.01404	0.00662		0.05850	55.20	0.02098	0.22282	0.00046
3	0.33883	0.20400	0.01438	0.00672		0.06000	58.40	0.02211	0.22400	0.00046
4	0.34688	0.20000	0.01473	0.00682		0.05980	62.65	0.02325	0.22996	0.00046
5	0.35492	0.19600	0.01507	0.00692		0.05950	66.90	0.02439	0.23591	0.00046
6	0.36297	0.19200	0.01541	0.00702		0.05900	71.15	0.02552	0.24187	0.00046
7	0.37101	0.18800	0.01575	0.00712		0.05850	75.40	0.02662	0.24782	0.00046
8	0.37906	0.18400	0.01609	0.00722		0.05800	79.65	0.02779	0.25378	0.00046
9	0.38710	0.18000	0.01644	0.00732		0.05750	83.90	0.02893	0.18590	0.00046
$(R_{HUB})_{L.E.} = 0.31130$										
$(R_{HUB})_{T.E.} = 0.31470$										
$(R_{TIP})_{L.E.} = 0.37630$										
$(R_{TIP})_{T.E.} = 0.38710$										

* equally spaced

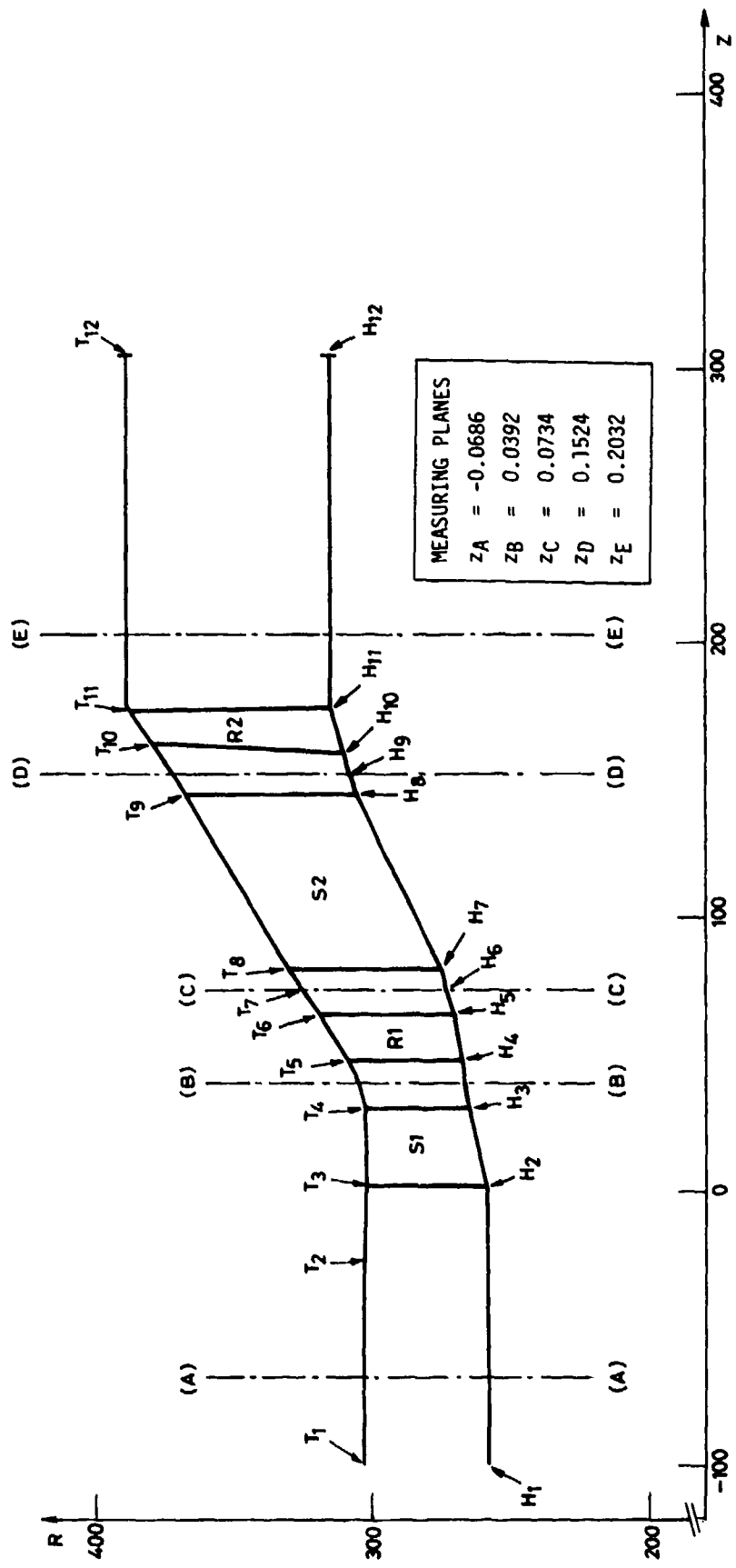
** linearly interpolated from given values at $R = 0.30873$, $R = 0.33930$ and $R = 0.36995$

*** linearly interpolated from given values at $R = 0.30873$ and $R = 0.36995$

Note: all dimensions in [m]

TABLE A2.5

POINT	H_1	H_2	H_3	H_4	H_5	H_6	H_7	H_8	H_9	H_{10}	H_{11}	H_{12}
Z	-0.1016	0.0018	0.0321	0.0473	0.0649	0.0734	0.0819	0.1448	0.1524	0.1600	0.1722	0.3048
R	0.2583	0.2583	0.2659	0.2680	0.2713	0.2372	0.2751	0.3060	0.3087	0.3113	0.3147	0.3147
POINT	T_1	T_2	T_3	T_4	T_5	T_6	T_7	T_8	T_9	T_{10}	T_{11}	T_{12}
Z	-0.1016	-0.254	0.0018	0.0321	0.0473	0.0649	0.0734	0.0819	0.1448	0.1600	0.1772	0.3048
R	0.3033	0.3033	0.3025	0.3029	0.3086	0.3193	0.3248	0.3304	0.3678	0.3763	0.3871	0.3891



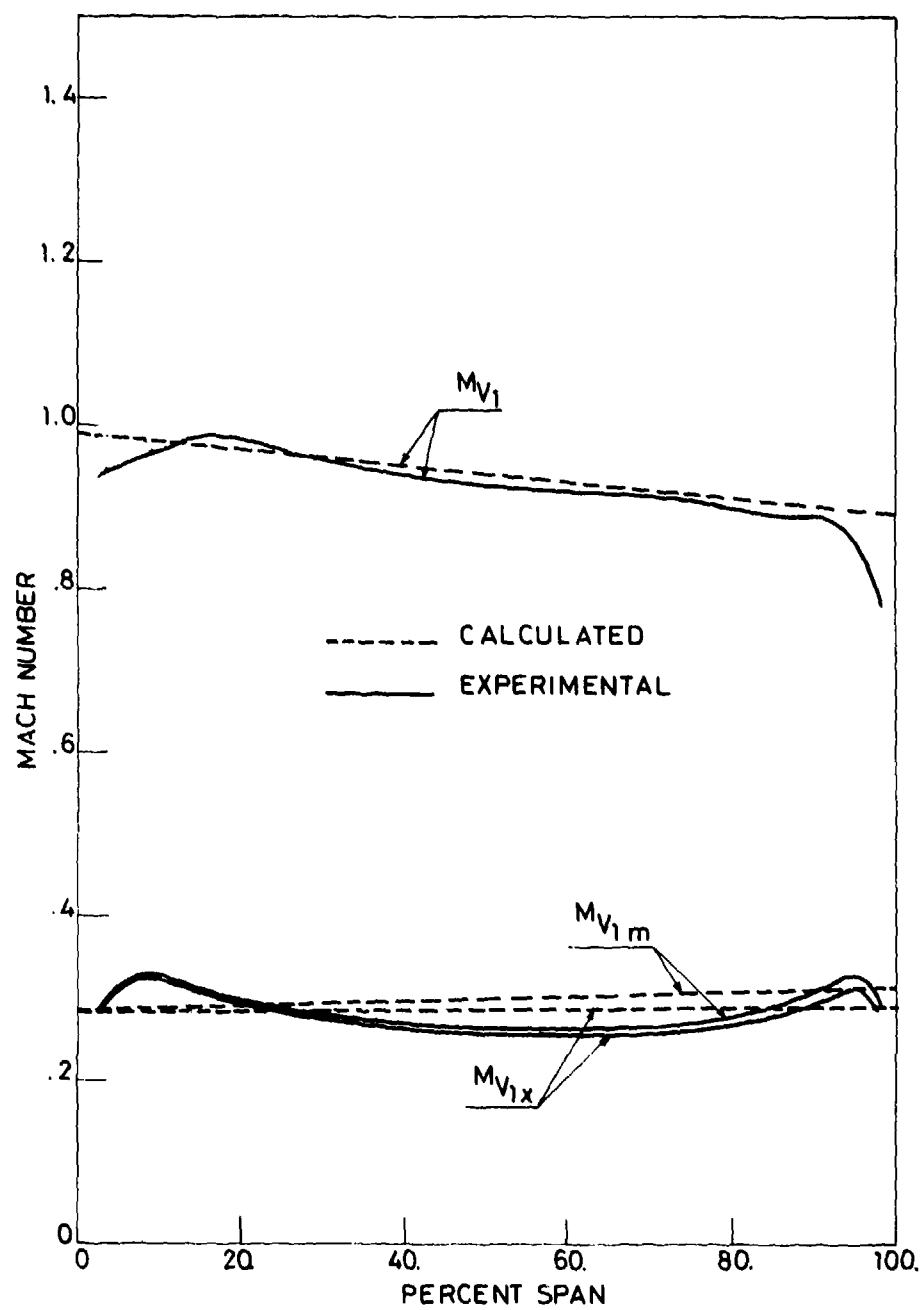


Fig.A2.1 Comparison between experimental and calculated Mach numbers at H.P. stator exit

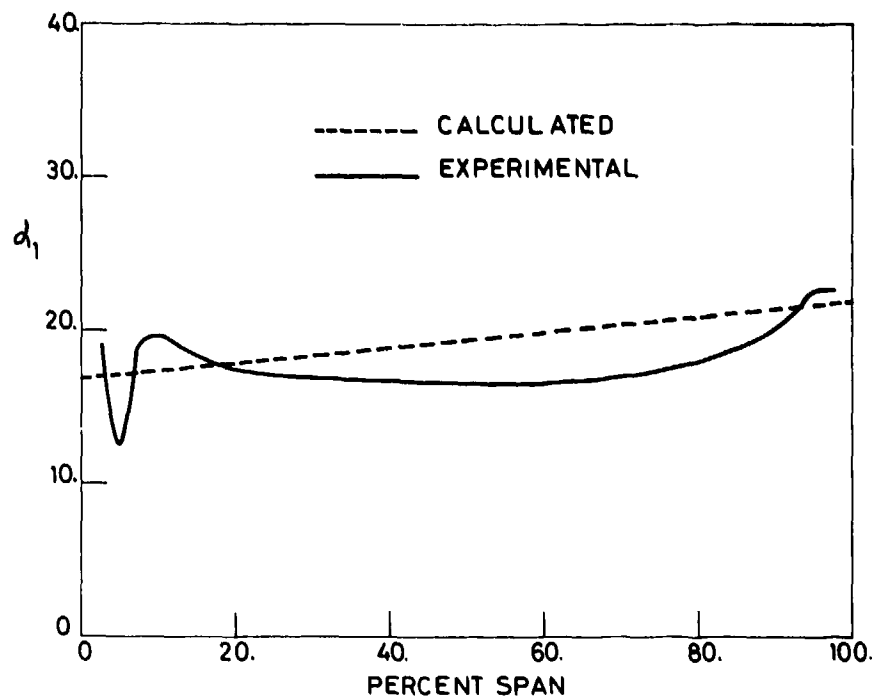


Fig.A2.2 Comparison between experimental and calculated absolute exit flow angles at H.P. stator exit

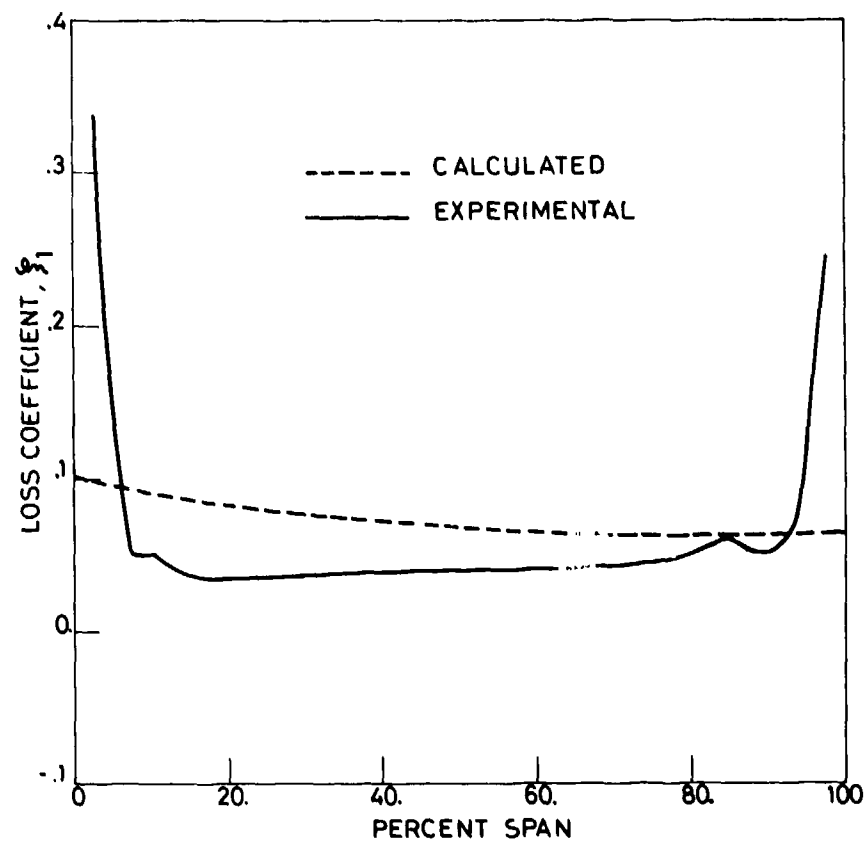


Fig.A2.3 Comparison between experimental and calculated loss coefficients at H.P. stator exit

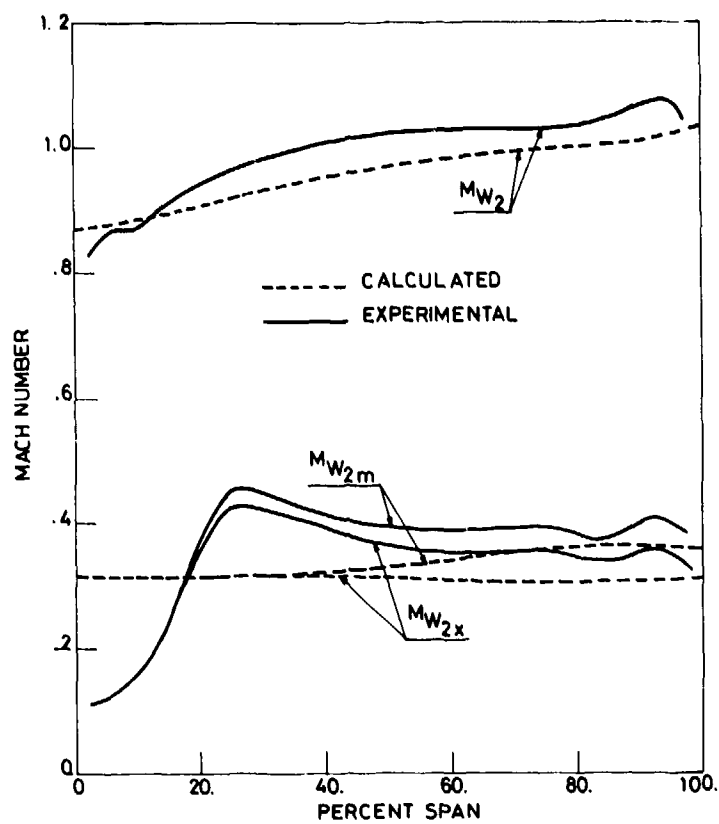


Fig.A2.4 Comparison between experimental and calculated Mach numbers at H.P. rotor exit

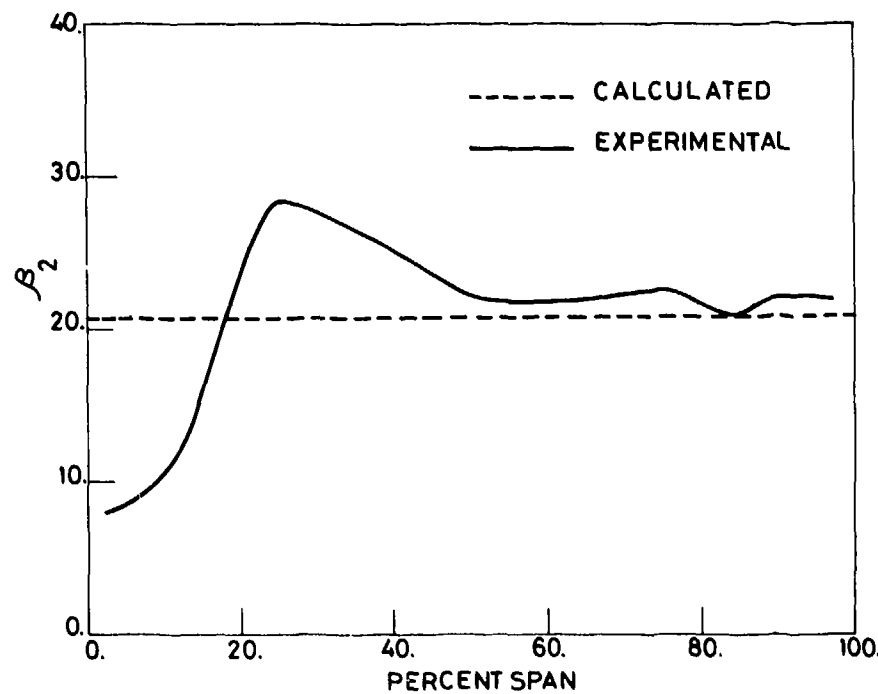


Fig.A2.5 Comparison between experimental and calculated relative exit flow angles at H.P. rotor exit

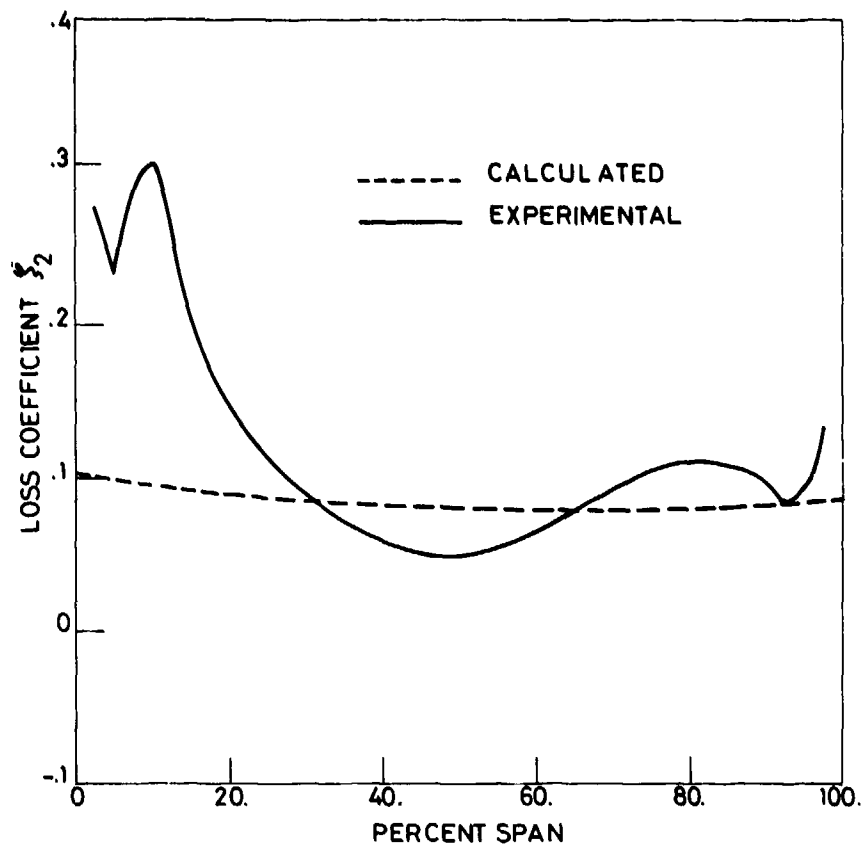


Fig.A2.6 Comparison between experimental and calculated loss coefficients at H.P. rotor exit

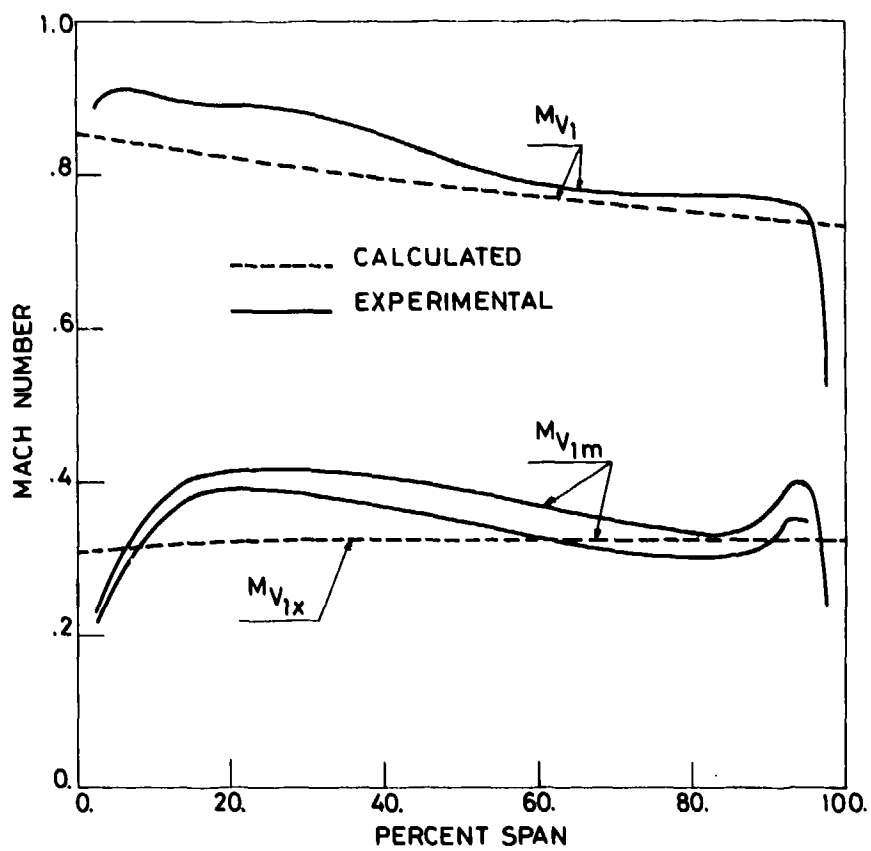


Fig.A2.7 Comparison between experimental and calculated Mach numbers at L.P. stator exit

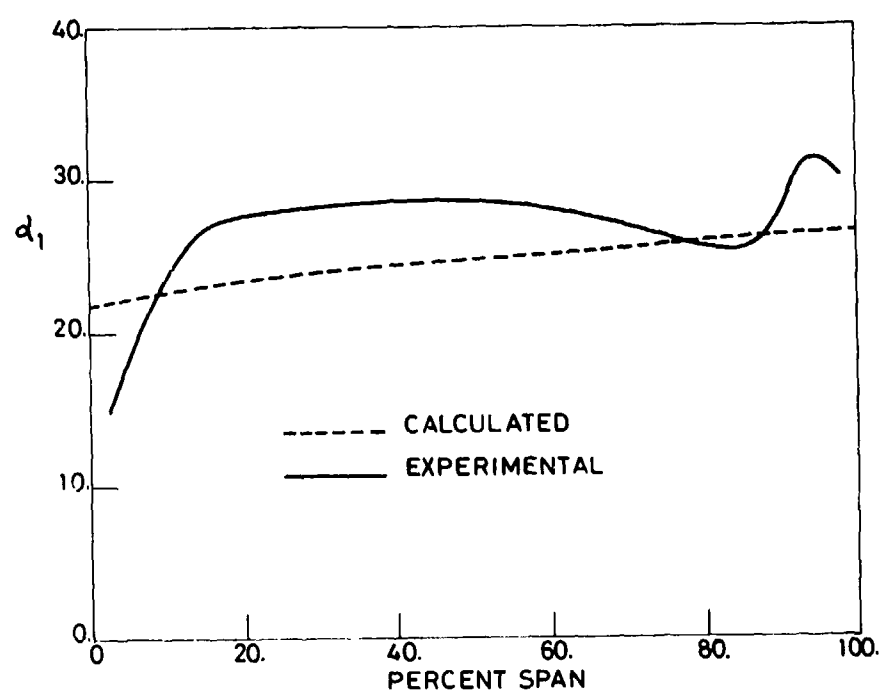


Fig.A2.8 Comparison between experimental and calculated absolute exit flow angles at L.P. stator exit

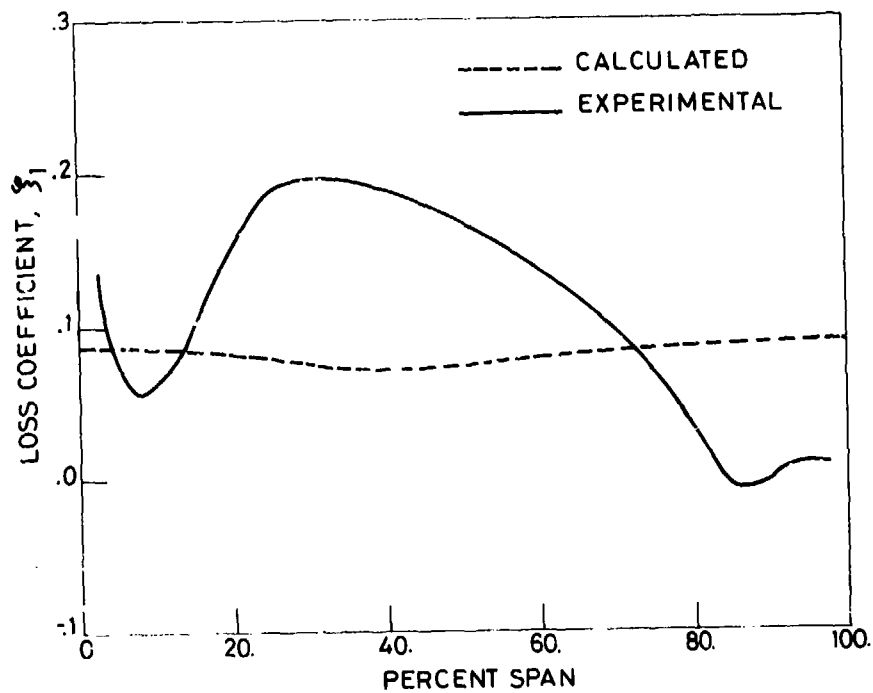


Fig.A2.9 Comparison between experimental and calculated loss coefficients at L.P. stator exit

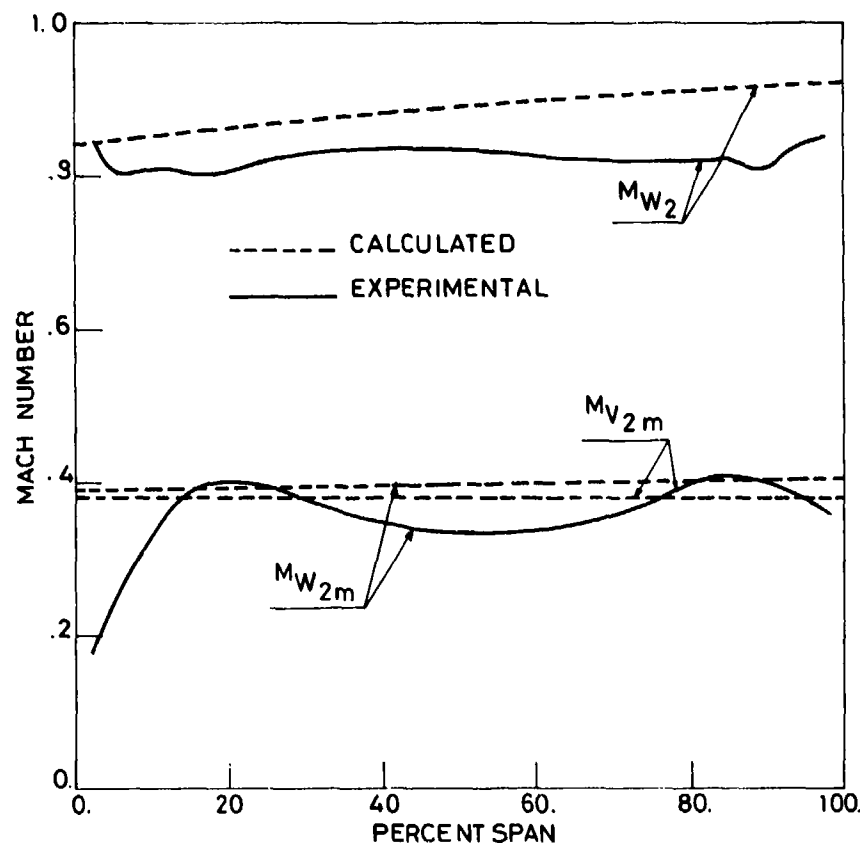


Fig.A2.10 Comparison between experimental and calculated Mach numbers at L.P. rotor exit

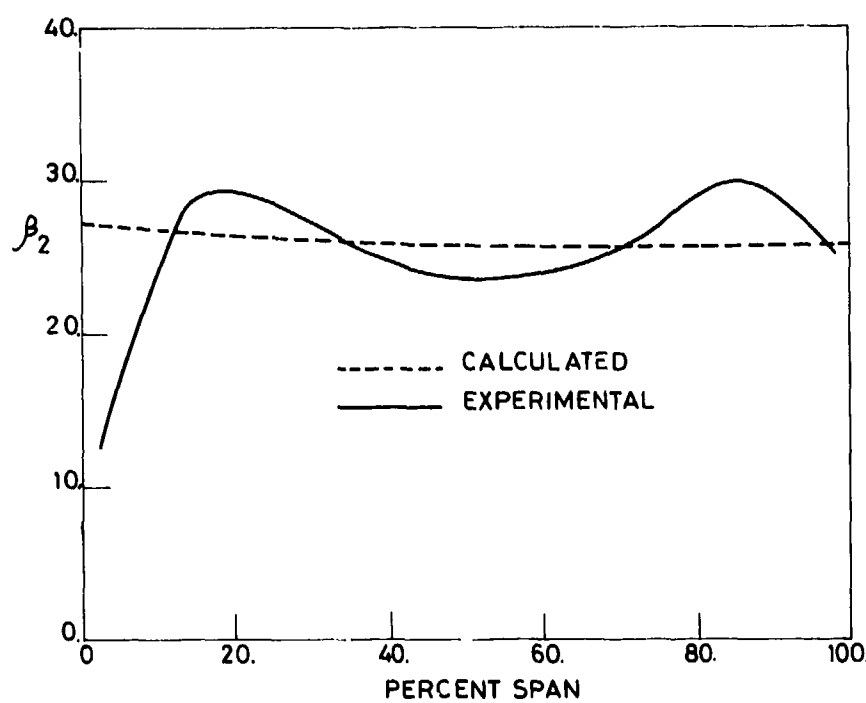


Fig.A2.11 Comparison between experimental and calculated relative exit flow angles at L.P. rotor exit

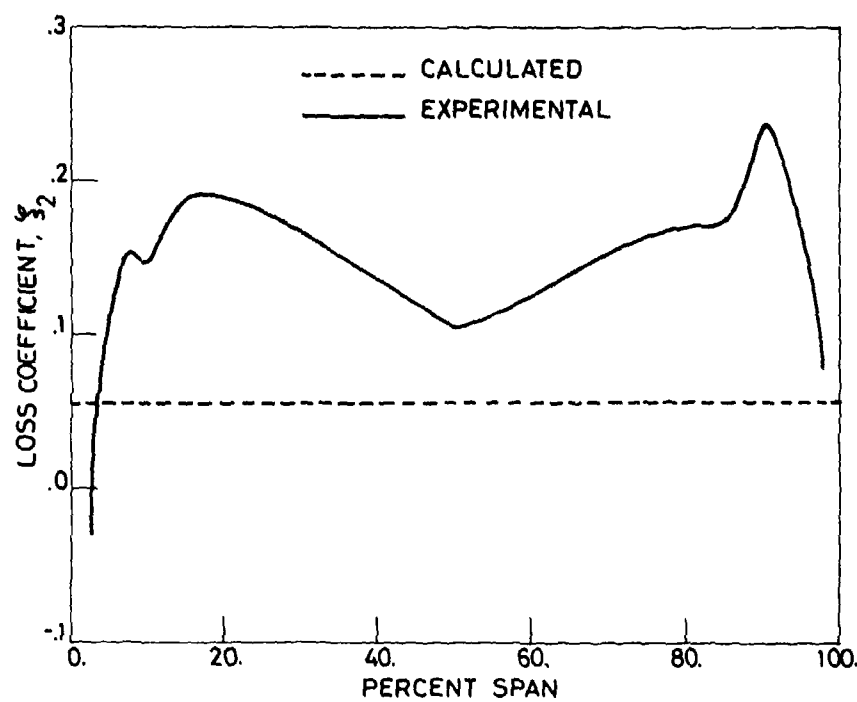


Fig.A2.12 Comparison between experimental and calculated loss coefficients at L.P. rotor exit

Appendix A1.3

ANSALDO STEAM TURBINE – GEOMETRY, TEST DATA AND SAMPLE CALCULATION

As a result of the difficulty encountered by the Turbine Sub-Group in finding suitable test cases Dr Zunino offered to make available data obtained by his company (Ansaldo) on a large low pressure steam turbine. Although the main interest of AGARD is in gas turbines these steam turbine data were considered an equally valid test of loss and deviation correlations and so the offer was gratefully accepted by the Turbine Sub-Group, several of whom had the ability to calculate steam as well as gas flows.

The turbine geometry is fairly typical of large low pressure 3000 RPM machines, having 6 stages with a very high casing flare to accommodate the large increase of volume flow. This results in very high blade speeds and pressure ratios for the last stage. The Ansaldo machine has a last stage pressure ratio of over 6:1 which, coupled with a low hub:tip radius ratio, results in very high relative Mach numbers (≈ 1.7) at nozzle root and rotor tip.

The layout of the turbine is shown in Figure A3.1 and full geometric details of stages 3–6 are given in Tables A3.1–A3.9 (all dimensions in mm). Details of steam conditions, bleed flow rates and blade clearances are given in Table A3.10.

A complete set of all measurements necessary to obtain a heat balance for the turbine were performed in parallel with the traverse measurements. These consisted of 42 pressure, 67 temperature and 6 mass flow measuring devices. The overall electrical output was also monitored and the LP cylinder output was measured by means of a shaft torque-meter and telemetry. These measurements enabled the LP cylinder efficiency to be evaluated separately from that of the whole turbine.

The probe used for aerodynamic measurements was a 5 hole spherical head probe with a thermocouple incorporated into its stem. This probe was calibrated in air up to a Mach number of 0.9. Traverses were made with the turbine at full power and after allowing sufficient time for conditions to stabilise.

At each traverse point the probe was nulled in yaw and a complete set of readings taken at least 5 times before moving on to the next point. As a result the measurements at each traverse point required from 2–10 minutes and a complete radial traverse from 6–8 hours. The use of an average of 5 or more sets of readings at each position should ensure that random errors are negligible. Further details of the experimental technique are given by Accornero et al. (1980).

On the whole the measurements seem to have been very carefully performed and, although measurements in steam are inevitably less accurate than in air, they should be considered reliable.

The throughflow calculation used to provide sample results is that described by Doria et al. (1979). This is a streamline curvature type of method developed specifically to calculate the flow in low pressure steam turbines. It includes allowances for: profile and secondary losses; lacing wire and windage loss; blade tip, gland and balance hole leakage losses; flow extraction (bleed) for feed heaters and spanwise distribution of secondary deviation. The program works with a prescribed mass flow rate and exit steam conditions (pressure and enthalpy) and the inlet steam conditions are allowed to vary during the calculation.

The loss and deviation rules used for the calculation are not generally available. The losses are based on cascade data for the nozzles and on Craig and Cox for the rotors. Blade exit angles are obtained from a modified sine rule with an additional deviation based on continuity applied for supersonic exit flow. The method of Bardon et al. (Chapter 4) was used to estimate and distribute secondary flow deviation.

Comparisons of measured and computed results are shown in Figures A3.2–A3.13. On the whole the agreement is remarkably good and similar results were obtained from other calculation methods on this machine.

The large distortions of the velocity profiles caused by secondary flow, which are present in the other test cases, are not evident in this machine.

This is possibly because the high turbulence levels which must be present in a multi-stage turbine mix out the secondary flows both within the blade rows and between trailing edge and traverse plane. The good agreement of measured and calculated velocity profiles after the last stage is particularly gratifying since such a high pressure ratio, low hub tip/ratio stages provides the most difficult test of a throughflow program.

REFERENCES

1. Doria, G.
Troilo, M.
Throughflow Calculation of Large Steam Turbine. Proc. 6th Conf. on Large Steam Turbines, Plzen, Czechoslovakia, May 1979.
2. Accornero, A.
et al.
Flow in a 320 MW Low Pressure Section. Theoretical and Experimental Evaluation. VKI Lecture Series, Steam Turbines for Large Output, April 1980.

TABLE A3.1
Annulus Geometry (Coordinates of Points in Figure A3.1)

<i>Point</i>	H_1	H_2	H_3	H_4	H_5	H_6	H_7	H_8	H_9	H_{10}	H_{11}	H_{12}
Z	518.5	590.5	662.82	804.0	870.0	966.65	1150.5	1215.5	1324.38	1560.5	1715.0	1962.8
R	840.75	840.75	838.2	840.75	840.75	838.2	840.75	840.75	838.2	880.5	850.72	838.2
<i>Point</i>	T_1	T_2	T_3	T_4	T_5	T_6	T_7	T_8	T_9	T_{10}	T_{11}	T_{12}
Z	519.5	590.5	658.7	781.0	870.0	952.0	1137.0	1239.0	1299.2	1534.5	1781.5	1890.7
R	973.05	995.05	1020.7	1070.0	1114.25	1158.51	1240.0	1293.75	1330.45	1517.5	1672.6	1681.0

Measuring Planes

$Z_A = 706.0$
$Z_B = 1010.0$
$Z_C = 1368.0$
$Z_{D'} = 2004.0$
$Z_{D''} = 1946.7$

ANSALDO TURBINE

TABLE A3.2
Geometry of the Third Stage

STATOR

<i>Radius</i>	<i>Inlet angle</i>	<i>Throat</i>	<i>Chord</i>	<i>Pitch</i>	<i>T.E. thickness</i>	<i>Backbone length</i>	<i>Inlet width</i>
840.75	89.61	10.058	90.484	44.02	1.5	105.25	35.09
860.75	89.10	10.763	90.484	45.07	1.5	105.25	36.04
900.75	88.42	11.989	90.484	47.163	1.5	105.25	37.97
940.75	88.07	13.043	90.484	49.257	1.5	105.25	39.95
970.75	87.99	13.724	90.484	50.828	1.5	105.25	41.47

TABLE A3.3
Geometry of the Third Stage

ROTOR

<i>Radius</i>	<i>Inlet angle</i>	<i>Throat</i>	<i>Chord</i>	<i>Pitch</i>	<i>T.E. thickness</i>	<i>Backbone length</i>	<i>Inlet width</i>
838.2	28.66	12.59	57.37	32.11	0.59	79.24	13.41
898.2	33.42	13.11	56.93	34.41	0.69	78.42	16.65
934.72	37.65	13.32	56.97	35.81	0.66	77.72	19.31
988.2	44.09	13.39	57.17	37.86	0.67	76.03	22.09
1018.2	48.61	13.36	57.47	39.01	0.66	74.89	24.05

TABLE A3.4
Geometry of the Fourth Stage

STATOR

<i>Radius</i>	<i>Inlet angle</i>	<i>Throat</i>	<i>Chord</i>	<i>Pitch</i>	<i>T.E. thickness</i>	<i>Backbone length</i>	<i>Inlet width</i>
840.75	88.38	14.117	99.309	66.032	0.8	111.374	56.99
900.75	86.99	16.766	105.937	70.745	0.8	118.820	60.71
980.75	85.78	19.727	115.736	77.028	0.8	129.831	65.71
1040.75	85.49	21.301	122.927	74	0.8	137.910	69.62
1068.75	85.6	21.698	126.170	83.940	0.8	141.554	71.54

ANSALDO TURBINE continued

TABLE A3.5

Geometry of the Fourth Stage

ROTOR

<i>Radius</i>	<i>Inlet angle</i>	<i>Throat</i>	<i>Chord</i>	<i>Pitch</i>	<i>T.E. thickness</i>	<i>Backbone length</i>	<i>Inlet width</i>
838.2	27.22	17.20	81.28	45.01	1.64	113.23	19.44
918.51	38.18	17.94	77.99	49.33	1.32	104.83	26.19
958.2	40.75	18.31	76.54	51.45	1.57	101.87	28.71
998.85	41.74	18.63	75.50	53.64	1.53	100.115	31.71
1079.17	69.92	17.90	79.10	57.95	1.57	97.44	44.21

TABLE A3.6

Geometry of the Fifth Stage

STATOR

<i>Radius</i>	<i>Inlet angle</i>	<i>Throat</i>	<i>Chord</i>	<i>Pitch</i>	<i>T.E. thickness</i>	<i>Backbone length</i>	<i>Inlet width</i>
840.75	87.69	14.857	99.31	66.032	0.8	111.374	56.83
940.75	85.99	18.693	110.87	73.886	0.8	124.365	63.11
1040.75	84.92	22.07	122.86	81.740	0.8	137.831	69.43
1140.75	84.79	24.387	134.49	89.594	0.8	150.90	76.06
1230.75	85.28	25.519	145.42	96.663	0.8	163.178	82.22

TABLE A3.7

Geometry of the Fifth Stage

ROTOR

<i>Radius</i>	<i>Inlet angle</i>	<i>Throat</i>	<i>Chord</i>	<i>Pitch</i>	<i>T.E. thickness</i>	<i>Backbone length</i>	<i>Inlet width</i>
838.2	28.09	19.11	86.52	45.8	1.49	118.35	21.02
914.4	34.35	20.32	81.51	49.96	1.47	109.85	26.41
1022.78	48.99	21.91	75.97	55.88	1.46	95.87	37.90
1133.55	76.06	22.25	77.14	61.93	1.48	86.72	53.17
1268.93	136.04	21.84	86.28	69.33	1.48	86.88	67.92

ANSALDO TURBINE continued

TABLE A3.8
Geometry of the Sixth Stage

STATOR

<i>Radius</i>	<i>Inlet angle</i>	<i>Throat</i>	<i>Chord</i>	<i>Pitch</i>	<i>T.E. thickness</i>	<i>Backbone length</i>	<i>Inlet width</i>
850.72	91.286	17.82	183.48	89.087	2.0	213.77	71.44
950.72	89.89	22.15	207.19	99.56	2.0	241.48	79.16
1050.72	88.82	26.41	230.06	110.03	2.0	268.2	86.97
1150.72	88.19	30.49	242.77	120.5	2.0	283.04	95.77
1250.72	88.02	34.16	249.54	130.97	2.0	290.96	105.28
1350.72	88.07	37.20	262.25	141.45	2.0	305.80	114.35
1450.72	88.29	39.65	277.49	151.92	2.0	323.62	123.31

TABLE A3.9
Geometry of the Sixth Stage

ROTOR

<i>Radius</i>	<i>Inlet angle</i>	<i>Throat</i>	<i>Chord</i>	<i>Pitch</i>	<i>T.E. thickness</i>	<i>Backbone length</i>	<i>Inlet width</i>
838.2	33.39	28.67	194.80	56.03	2.02	238.59	28.67
965.84	41.67	33.54	172.23	64.56	3.04	205.33	41.25
1093.47	56.99	36.55	151.67	73.09	2.18	176.80	56.65
1427.48	128.37	37.25	132.10	95.42	1.52	133.73	94.61
1604.01	150.70	32.76	132.96	107.21	1.01	133.09	106.14

TABLE A3.10

1. Inlet Steam Conditions to the Last 4 Stages																					
Static Pressure = 3.176 bar																					
Static Enthalpy = 2895 kJ/kg																					
2. Inlet Mass Flow to these 4 Stages 99.826 Kg/s																					
3. Exhaust Pressure 0.0671 bar																					
4. Tip Clearance and Number of Seals for Each Blade Row																					
<table> <thead> <tr> <th><i>Stage N.</i></th> <th><i>Tip Clearance (mm)</i></th> <th><i>Actual Number of Seals in Operation</i></th> </tr> </thead> <tbody> <tr> <td>1</td> <td>1.8</td> <td>4</td> </tr> <tr> <td>2</td> <td>1.6</td> <td>3</td> </tr> <tr> <td>3</td> <td>1.8</td> <td>3</td> </tr> <tr> <td>4</td> <td>2.0</td> <td>5</td> </tr> <tr> <td>5</td> <td>2.3</td> <td>7</td> </tr> <tr> <td>6</td> <td>7.3</td> <td>19</td> </tr> </tbody> </table>	<i>Stage N.</i>	<i>Tip Clearance (mm)</i>	<i>Actual Number of Seals in Operation</i>	1	1.8	4	2	1.6	3	3	1.8	3	4	2.0	5	5	2.3	7	6	7.3	19
<i>Stage N.</i>	<i>Tip Clearance (mm)</i>	<i>Actual Number of Seals in Operation</i>																			
1	1.8	4																			
2	1.6	3																			
3	1.8	3																			
4	2.0	5																			
5	2.3	7																			
6	7.3	19																			
5. Efficiency of Last 4 Stages = 0.890%																					
6. Bleed Flow Rates																					
<table> <thead> <tr> <th><i>Bleed N.</i></th> <th><i>Flow (Kg/s)</i></th> <th></th> </tr> </thead> <tbody> <tr> <td>1</td> <td>3.582</td> <td>Between first and second stage</td> </tr> <tr> <td>2</td> <td>7.578</td> <td>Between second and third stage</td> </tr> <tr> <td>3</td> <td>8.13</td> <td>Between fourth and fifth stage</td> </tr> </tbody> </table>	<i>Bleed N.</i>	<i>Flow (Kg/s)</i>		1	3.582	Between first and second stage	2	7.578	Between second and third stage	3	8.13	Between fourth and fifth stage									
<i>Bleed N.</i>	<i>Flow (Kg/s)</i>																				
1	3.582	Between first and second stage																			
2	7.578	Between second and third stage																			
3	8.13	Between fourth and fifth stage																			
7. Exhaust Geometry - Downstream of D'D'' (Fig.A3.1)																					
<table> <thead> <tr> <th><i>Point</i></th> <th>D'</th> <th>D''</th> <th>E'</th> <th>E''</th> <th>F'</th> <th>F''</th> </tr> </thead> <tbody> <tr> <td>Z (mm)</td> <td>2004.0</td> <td>1946.7</td> <td>2081.55</td> <td>1971.95</td> <td>2217.3</td> <td>1998.2</td> </tr> <tr> <td>R (mm)</td> <td>838.2</td> <td>1697.25</td> <td>838.2</td> <td>1702.25</td> <td>874.45</td> <td>1708.5</td> </tr> </tbody> </table>	<i>Point</i>	D'	D''	E'	E''	F'	F''	Z (mm)	2004.0	1946.7	2081.55	1971.95	2217.3	1998.2	R (mm)	838.2	1697.25	838.2	1702.25	874.45	1708.5
<i>Point</i>	D'	D''	E'	E''	F'	F''															
Z (mm)	2004.0	1946.7	2081.55	1971.95	2217.3	1998.2															
R (mm)	838.2	1697.25	838.2	1702.25	874.45	1708.5															

ANSALDO TURBINE

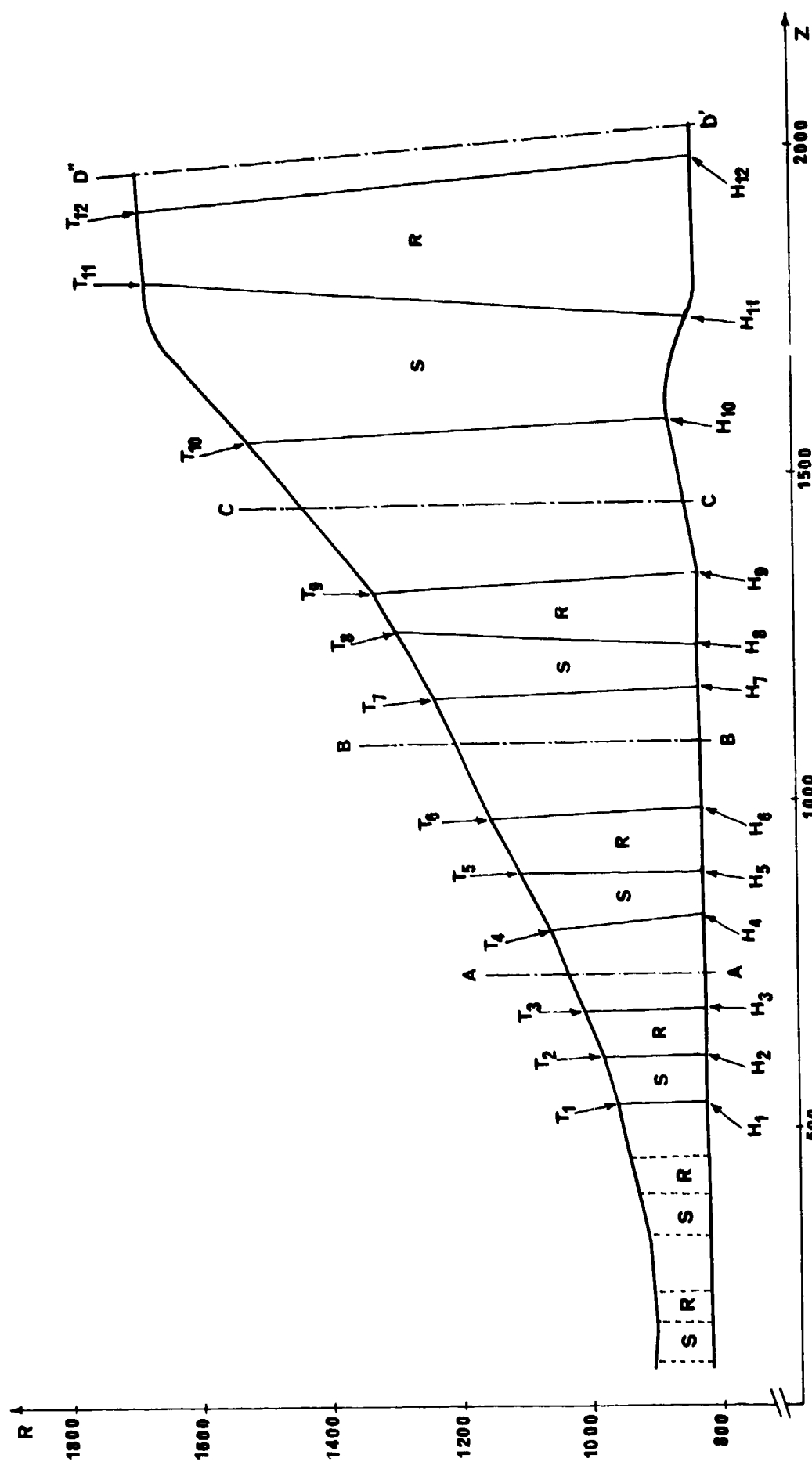


Fig.A3.1 Meridional section of Ansaldo turbine

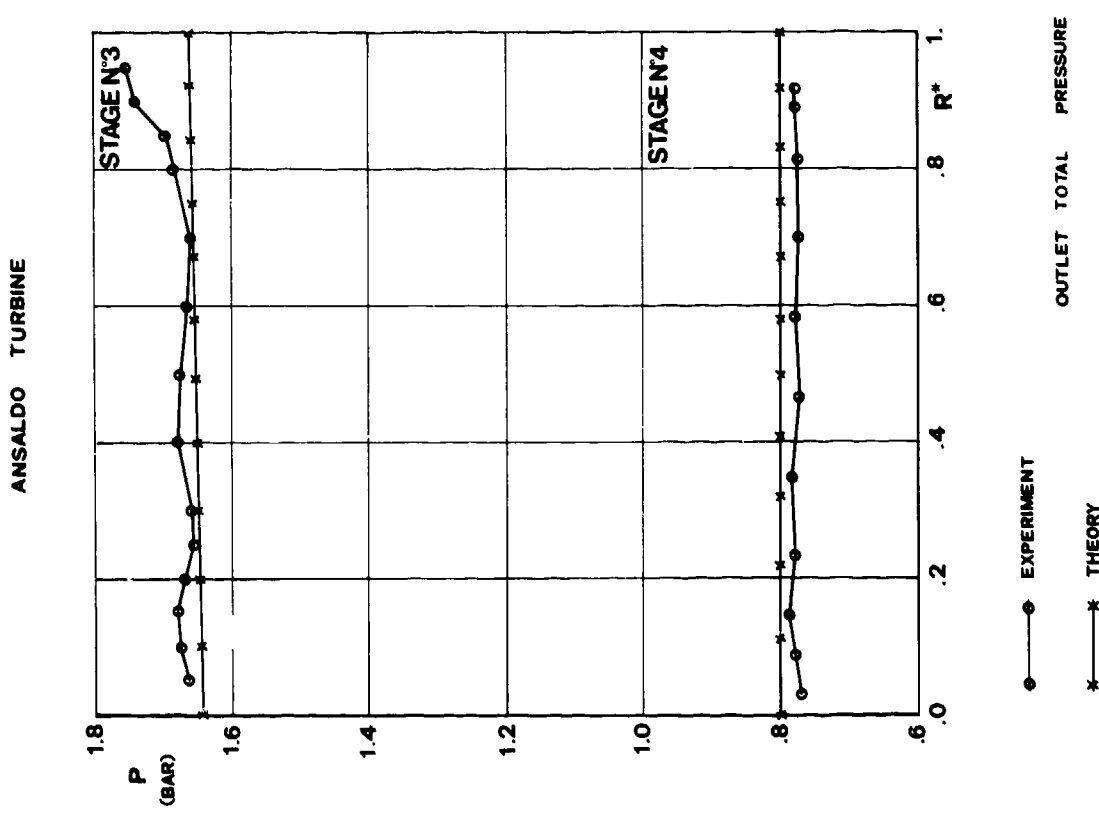


Fig.A3.2 Total pressures, stages 3 and 4

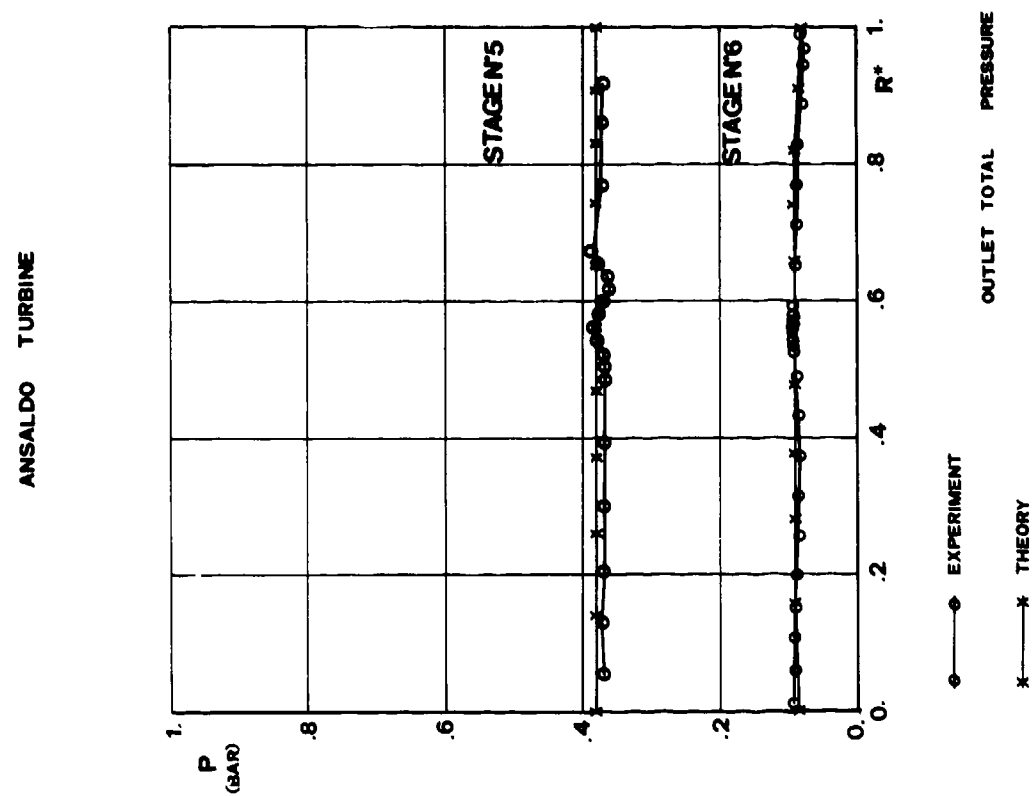
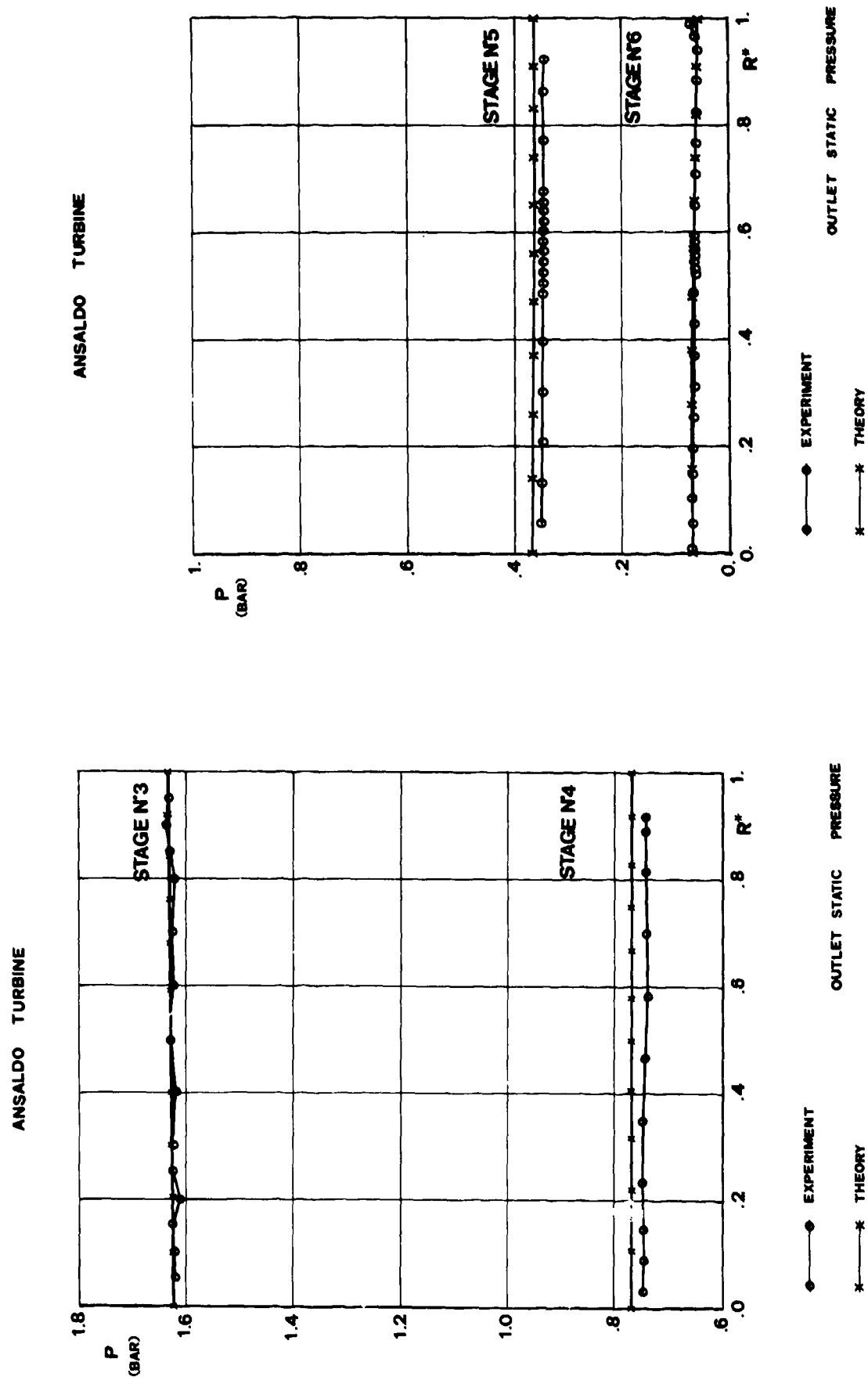


Fig.A3.3 Total pressures, stages 5 and 6



ANSALDO TURBINE

AXIAL MACH NUMBER

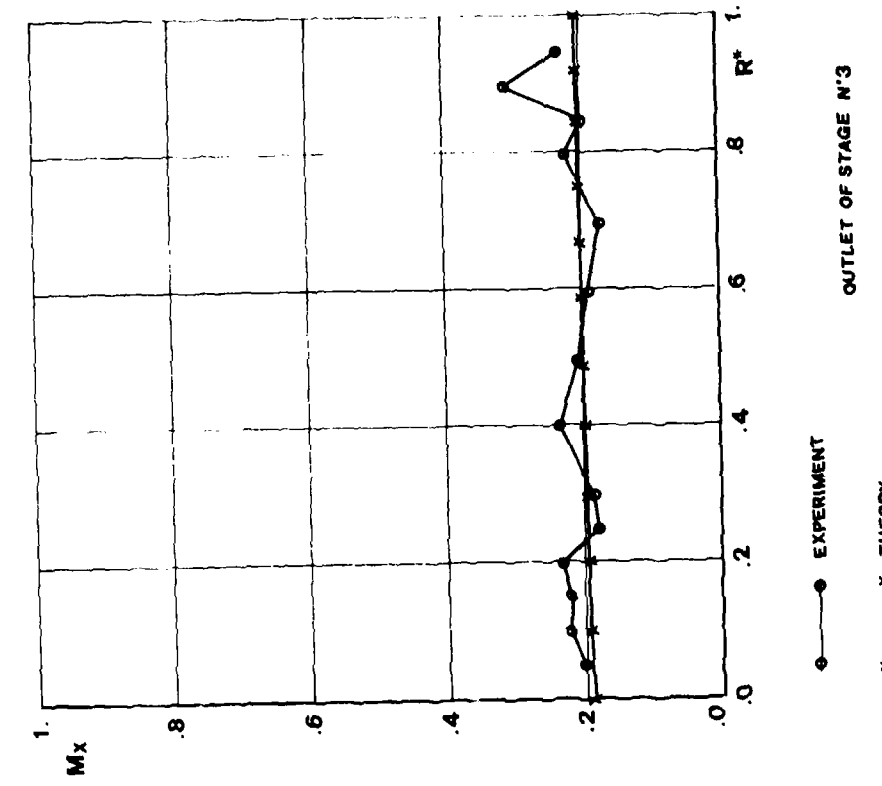


Fig.A3.6 Axial Mach number, stage 3

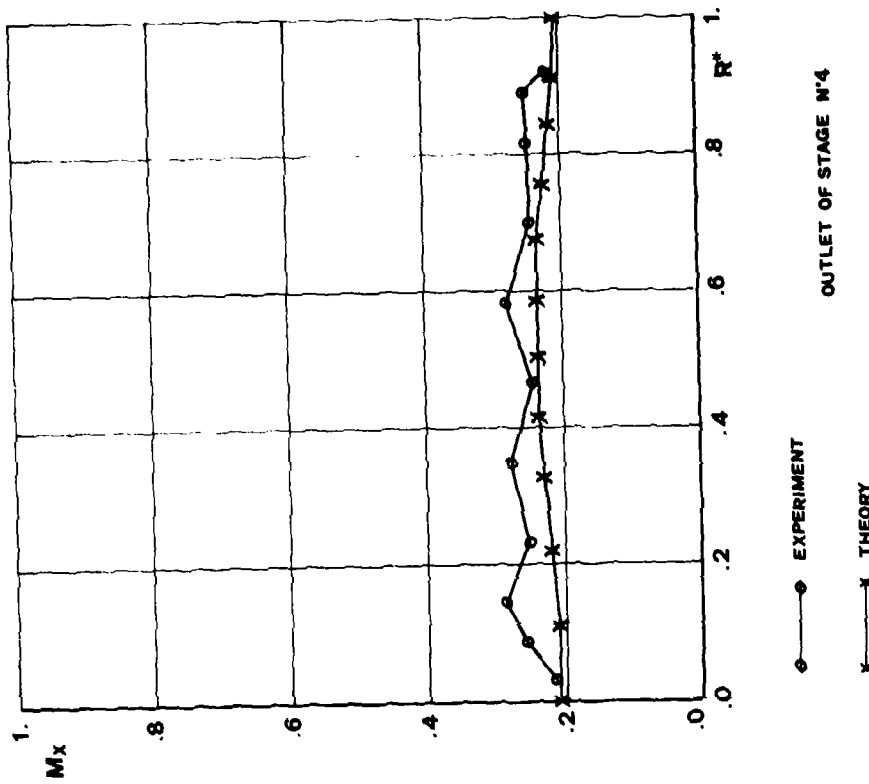


Fig.A3.7 Axial Mach number, stage 4

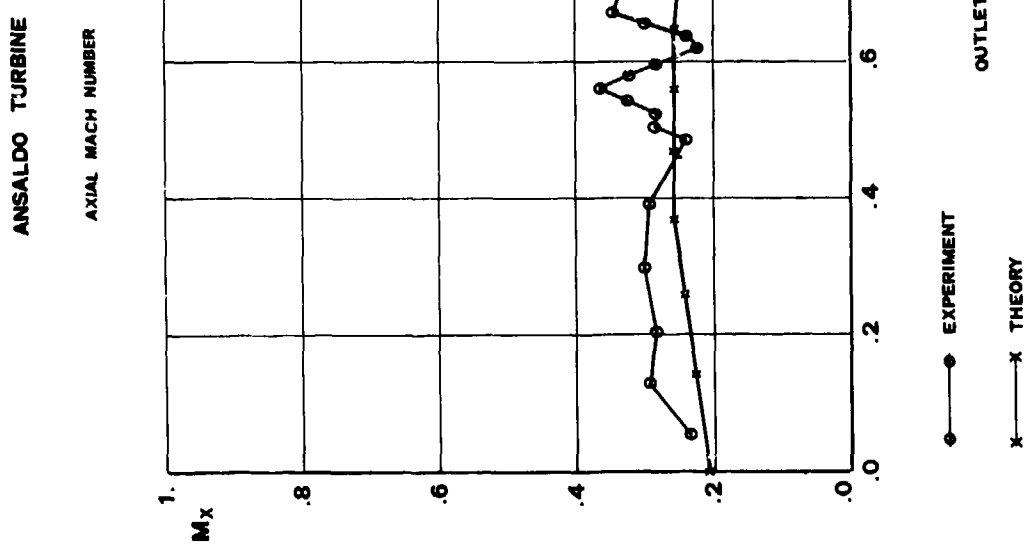


Fig. A3.8 Axial Mach number, stage 5

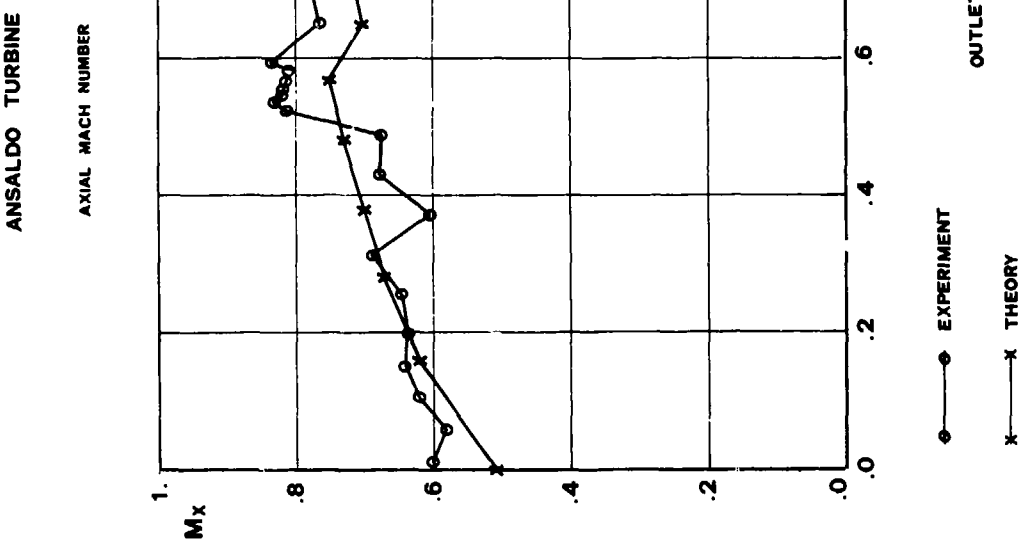


Fig. A3.9 Axial Mach number, stage 6

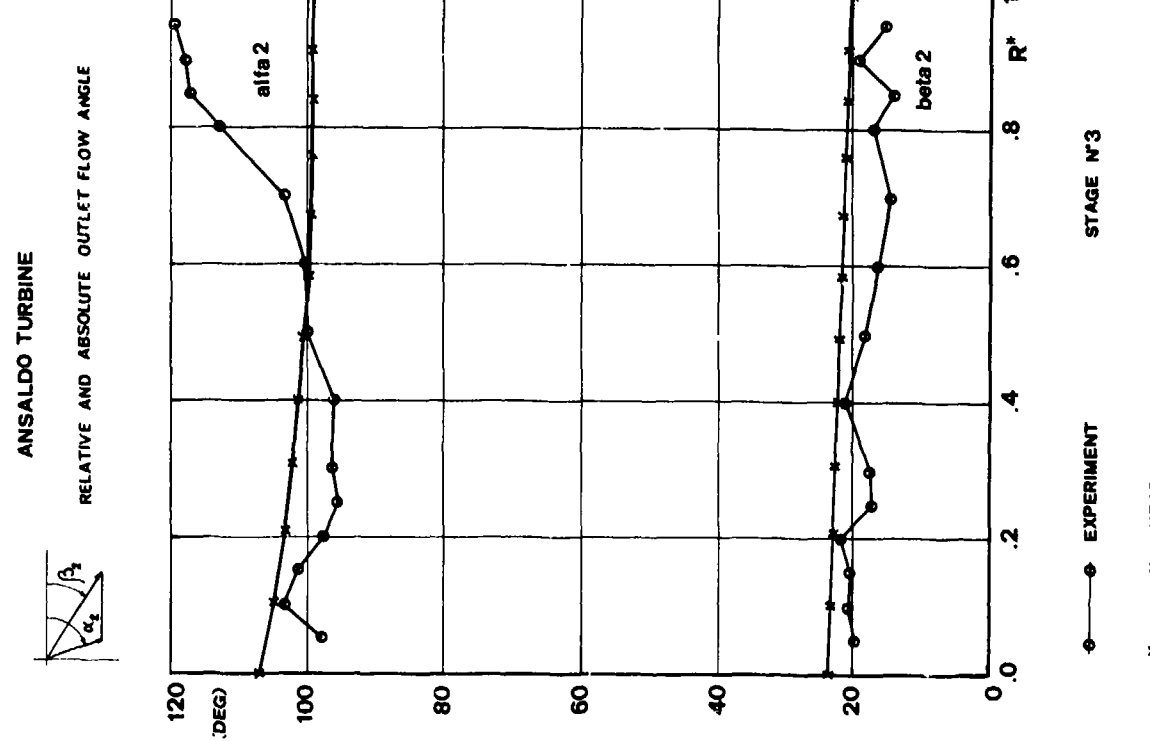


Fig.A3.10 Flow angles, stage 3

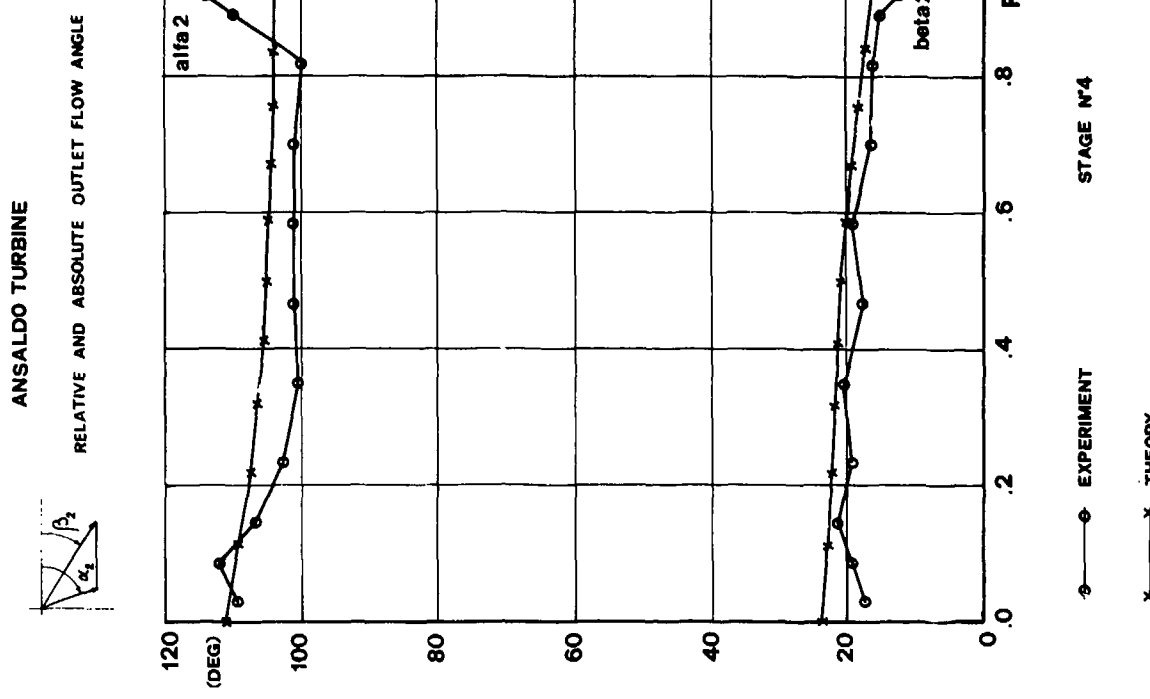


Fig.A3.11 Flow angles, stage 4

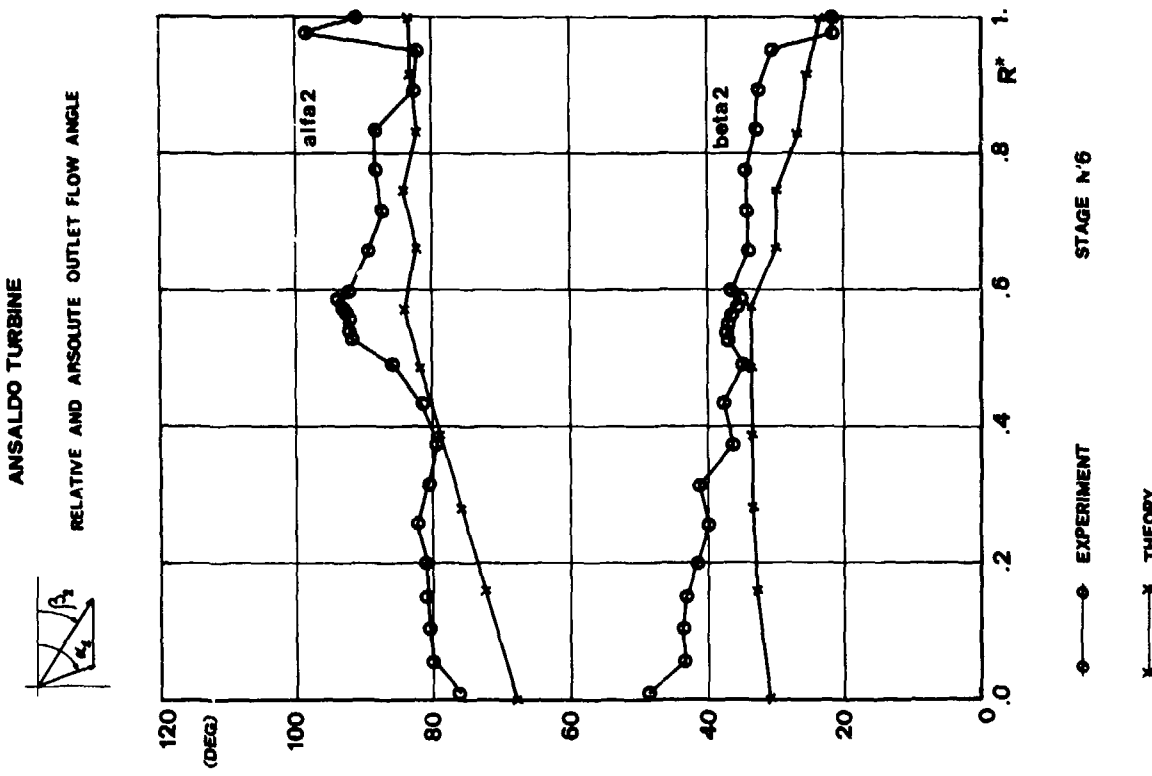


Fig.A3.13 Flow angles, stage 6

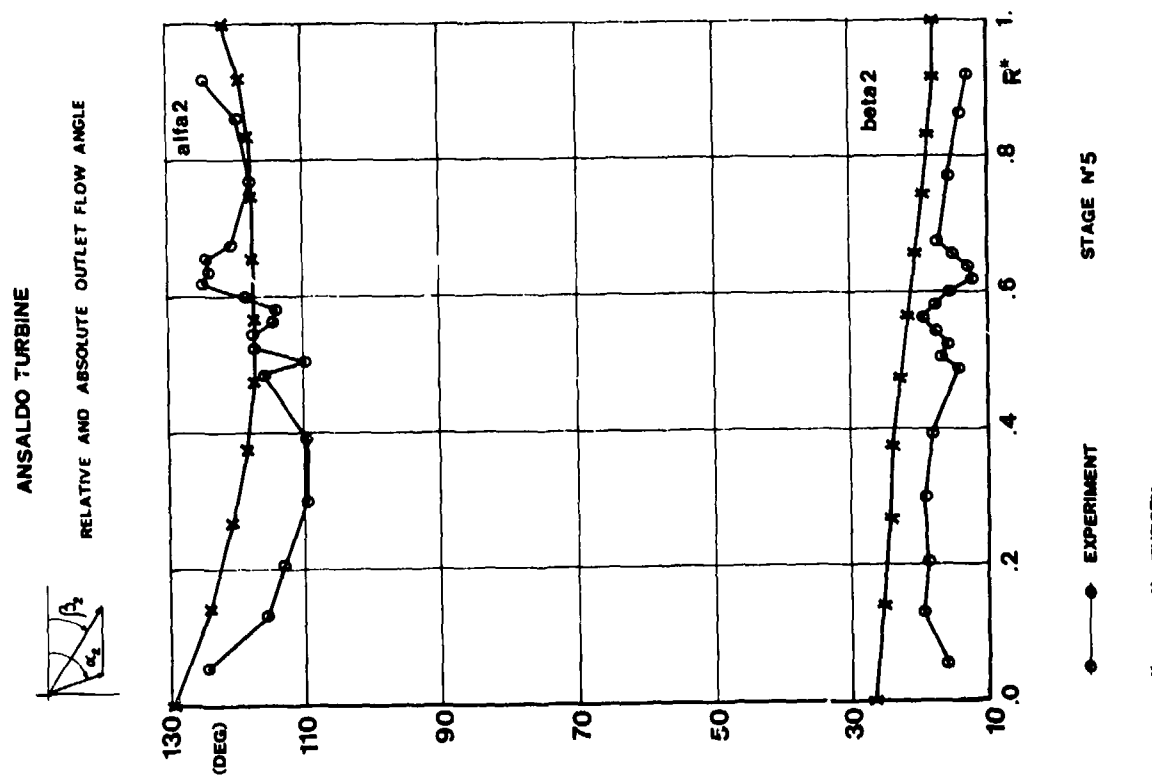


Fig.A3.12 Flow angles, stage 5

Appendix A1.4

HANNOVER-TURBINE – GEOMETRY, TEST DATA AND SAMPLE CALCULATION

This turbine was investigated by G.Groschup at the Institut für Strömungsmaschinen of the Technical University of Hannover, Germany. The tests were part of the doctoral thesis of Groschup in 1977 (Ref.1). We are very grateful to Dr Groschup for his assistance in compiling the full data of this turbine. Our thanks go also to Professor Bammert, former head of the same Institute, for permission to publish these data in the present report.

TEST FACILITY

The turbine facility is an open loop configuration with exhaust to atmosphere. The air is supplied by three parallel screw compressors with a maximum volume flow of $11 \text{ m}^3/\text{s}$ at maximum pressure of 4 bar. The compressed air passes through a cooler which maintains a constant inlet turbine temperature. A turbulence grid placed at 1 m upstream of the turbine flange produces a turbulence level of about 2% just ahead of the turbine stage. The power of the turbine is absorbed by an eddy-current-brake.

TURBINE

The facility was basically laid out for a four-stage turbine which was designed to have the same blade sections in all stages at a given radius. The blading is of the free vortex type and the nominal mass flow of the turbine is $\dot{m} = 7.8 \text{ kg/s}$ and the nominal rotational speed is 7500 RPM.

The set up allows each stage of the four-stage turbine to be tested separately. The tests referred to in this paper are concerned only with stage No. 4 which was tested in the single-stage mode. Details of the meridional flow path are shown in Figure A4.1. The turbine has a constant hub diameter of $D_H = 270 \text{ mm}$. The outer casing is cylindrical except across the blading where it is conical. The rotor has extremely small radial clearances: $S = 0.24 \text{ mm}$ at nominal RPM. The stator is shrouded and the leakage flow across the stator hub is minimized by multiple seals.

BLADE AND CASCADE GEOMETRY

The blade sections are stacked radially along their centre of gravity as shown in Figure A4.2, the same figure also defines all other relevant blade parameters. The values of these parameters on 9 equally spaced "streamlines" are given in Table 1.

MEASUREMENT TECHNIQUE

Overall Performance

The mass flow is measured with a standard nozzle (DIN 1952) in the inlet duct ($\phi 500 \text{ mm}$) far upstream of the turbine flange. The mass flow is determined with a precision of 0.2%. The torque is measured with the eddy-current-brake with a precision of 0.5% of the full scale of the balance (range: $0 \rightarrow 60 \text{ bar}$ or $0 \rightarrow 120 \text{ bar}$).

Survey of Turbine Stage Flow

The measurement stations are indicated in Figure 1 and are located as follows:

- Plane 0: 20 mm upstream of guide vane.
- Plane 1: Between stator and rotor. The axial distance between the blade rows is about 0.6 to 0.8 × axial chord length of the stator. The distance between probe tip and stator trailing edge varies from 6 mm at the tip to 17 mm at the hub.
- Plane 2: Close to rotor trailing edge. The distance between probe tip and rotor trailing edge varies from 15 mm at the tip to 6 mm at hub.
- Plane 3: 290 mm downstream of plane 2.

Reference 1 quotes only data taken in planes 0, 1 and 2. All the data presented are taken with a combined wedge probe. This probe measures total and static pressure, flow angle and total temperature. The meridional flow angle was not measured but checks were made to ensure that the probe was not sensitive to meridional flow angles of the order of the ones existing in the turbine. The survey of the flow behind the stator was made by slowly rotating the stator.

The problem of measuring behind the rotor in an unsteady flow field is discussed by Groschup in Reference 1. Groschup comes to the conclusion that the error on the total pressure measurement is of the order of 0.25%.

TESTS RESULTS

Traverse and overall performance measurements were made at 5 different operating conditions. The inlet flow conditions for these are given in Table 2 as traverses of inlet total pressure and temperature together with the ratios of actual to design speeds and mass flow rates. Test point 4 is taken as being closest to design conditions.

The variation of efficiency with blade loading parameter is given in Chapter 3 in comparison with computed results. Traverse results are given for test point 4 only in Figures A4.3 to A4.7. Traverse results at the other 4 test points are given in Groschup's thesis.

COMPARISONS WITH SAMPLE CALCULATION

The throughflow method used to provide sample results for this test case is that of Denton which has already been described in Appendix 1. The comparisons with test results at test point 4 are shown in Figures A4.3 to A4.7. This machine is of free vortex design and since the Mach numbers are low all axial velocity profiles should be uniform in the absence of viscous effects, streamline curvature and secondary flows.

Figure A4.3 shows that the measured velocity profile after the stator is very uniform except near the end walls. The calculated profile shows a positive slope near the tip due to the effects of streamline curvature and a negative one near the root due to overestimation of the turning. The velocity profile after the rotor is highly distorted by the effects of secondary flow whilst the computed profile is very uniform.

The large spanwise variation of exit angle from the stators, Figure A4.4, is reasonably well predicted apart from the secondary flow effects which are confined to small areas near the end walls. However, these effects dominate the flow behind the rotor, Figure A4.5, where the large and complex secondary flows at the root extend to mid-span.

The average level of loss is well predicted for both blade rows but once again the complex distribution of secondary loss is missed by the calculation. The predicted efficiency of 91.4% (total to total) is in reasonable agreement with the measured value of 90.5%. Further comparisons at off-design conditions are given in Chapter 3.

It is instructive to compare the results from this turbine with those from the Cambridge turbine. Both are free vortex designs with similar values of aspect ratio. However, the lower flow coefficient of the Hannover turbine results in greater turning in each blade row and consequently much stronger secondary flows at the rotor root. These in turn are the probable cause of the lower efficiency. Whilst calculation methods do reasonably well in predicting the efficiency of both machines the large discrepancies between measured and computed velocity profiles after a single stage of simple design are discouraging as regards the use of throughflow methods to predict velocity profiles in multi-stage turbines.

REFERENCES

1. Groschup, G. *Strömungstechnische Untersuchung einer Axialturbinenstufe im Vergleich zum Verhalten der ebenen Gitter ihrer Beschaufelung*. Doktor Ingenieur Dissertation Technical University of Hannover, 1977.

Hannover Turbine – Stage Geometries

Radius	Chord	Pitch	Throat		Rear SS curvature	Inlet	Inlet width	Backbone length	<i>T.E.</i> thickness
			α_0	σ					
STRL 1	0.14039	0.05100	0.03041	0.0083	32.20	0.08460	80.0	0.02240	0.00038
2	0.15117	0.05265	0.03275	0.00995	32.20	0.10100	80.0	0.02422	0.00038
3	0.16195	0.05440	0.03508	0.0115	32.35	0.11140	80.0	0.02650	0.00038
4	0.17272	0.05610	0.03742	0.0131	33.15	0.10900	80.0	0.0274	0.00048
5	0.18350	0.05780	0.03975	0.01502	34.50	0.10900	80.0	0.02960	0.00210
6	0.19428	0.05960	0.04209	0.01635	35.63	0.11580	80.0	0.03158	0.06380
7	0.20506	0.06120	0.04442	0.01790	37.39	0.12870	80.0	0.03338	0.06539
8	0.21583	0.06288	0.04676	0.01950	37.74	0.14130	80.0	0.03513	0.06690
9	0.22661	0.06460	0.04909	0.02115	37.27	0.15280	80.0	0.03692	0.06855

$$R_T = 0.232$$

MOTOR Exit:	
RH =	0.135
0.14072	0.04618
0.15217	0.04770
0.16361	0.04973
0.17506	0.05217
0.18650	0.05490
0.19794	0.05770
0.20939	0.06070
0.22083	0.06372
0.23228	0.06720
0.14072	0.04618
0.15217	0.04770
0.16361	0.04973
0.17506	0.05217
0.18650	0.05490
0.19794	0.05770
0.20939	0.06070
0.22083	0.06372
0.23228	0.06720
0.14072	0.04618
0.15217	0.04770
0.16361	0.04973
0.17506	0.05217
0.18650	0.05490
0.19794	0.05770
0.20939	0.06070
0.22083	0.06372
0.23228	0.06720
0.14072	0.04618
0.15217	0.04770
0.16361	0.04973
0.17506	0.05217
0.18650	0.05490
0.19794	0.05770
0.20939	0.06070
0.22083	0.06372
0.23228	0.06720

$$B\pi = 0.2380$$

NOTE: All dimensions in metres

Nominal mass flow, $\dot{m}_0 = 7.80 \text{ kg/s}$
 Nominal rotational speed, $n_0 = 7500 \text{ RPM}$

Test Points	TP 1		TP 2		TP 3		TP 4		TP 5		Radius (m)
	PTOT0 bar	TTOT0 K									
1	1.423	361.9	1.150	348.3	1.470	368.4	1.222	360.8	1.155	350.4	0.135
2	1.428	363.0	1.151	347.2	1.465	367.1	1.237	360.0	1.156	349.4	0.14014
3	1.431	363.7	1.151	346.6	1.462	366.4	1.246	359.6	1.156	348.9	0.14258
4	1.432	363.6	1.151	345.9	1.483	366.2	1.249	359.3	1.157	348.5	0.14854
5	1.433	364.0	1.151	345.5	1.479	366.1	1.248	359.2	1.157	348.7	0.16099
6	1.433	363.6	1.150	345.5	1.474	365.9	1.248	358.7	1.156	348.6	0.17425
7	1.431	363.5	1.151	346.0	1.490	365.2	1.250	358.9	1.157	348.4	0.18711
8	1.430	363.9	1.151	345.4	1.492	364.7	1.253	359.2	1.159	348.0	0.19927
9	1.432	363.8	1.152	344.9	1.494	364.6	1.252	359.0	1.159	347.3	0.21080
10	1.431	363.2	1.149	345.0	1.491	364.5	1.252	358.7	1.162	346.6	0.21730
11	1.427	362.3	1.146	345.0	1.485	364.5	1.250	358.1	1.161	346.5	0.22149
12	1.424	361.7	1.144	344.9	1.482	364.4	1.248	357.8	1.160	346.4	0.2242
\dot{m}/\dot{m}_0	1.18	0.71			1.21		0.87		0.67		
n/n_0	0.50	0.50			0.96		0.96		0.92		

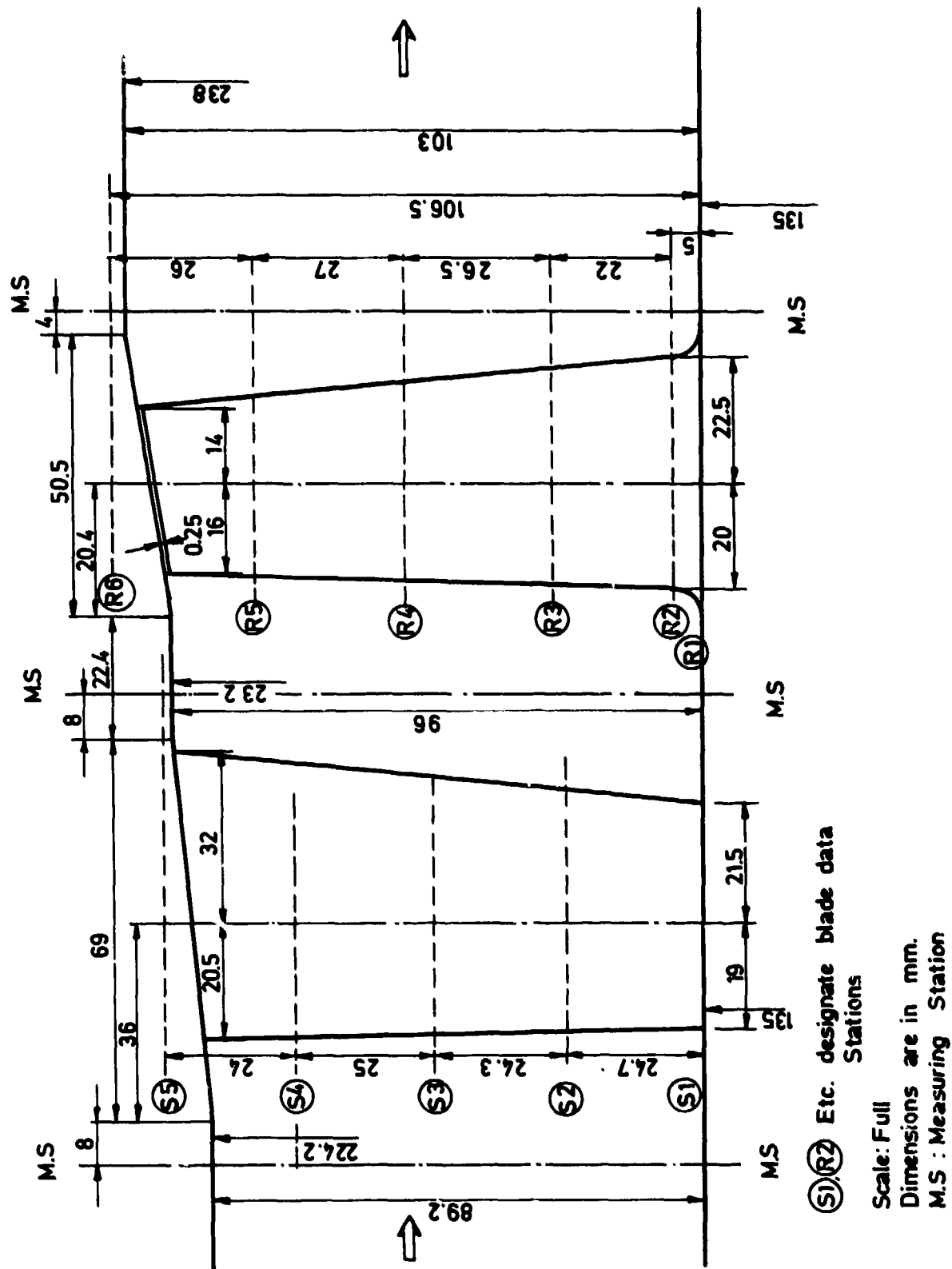


Fig.A4.1 Meridional view of Hannover turbine

(S),(R2) Etc. designate blade data
Stations

Scale: Full
Dimensions are in mm.
M.S : Measuring Station

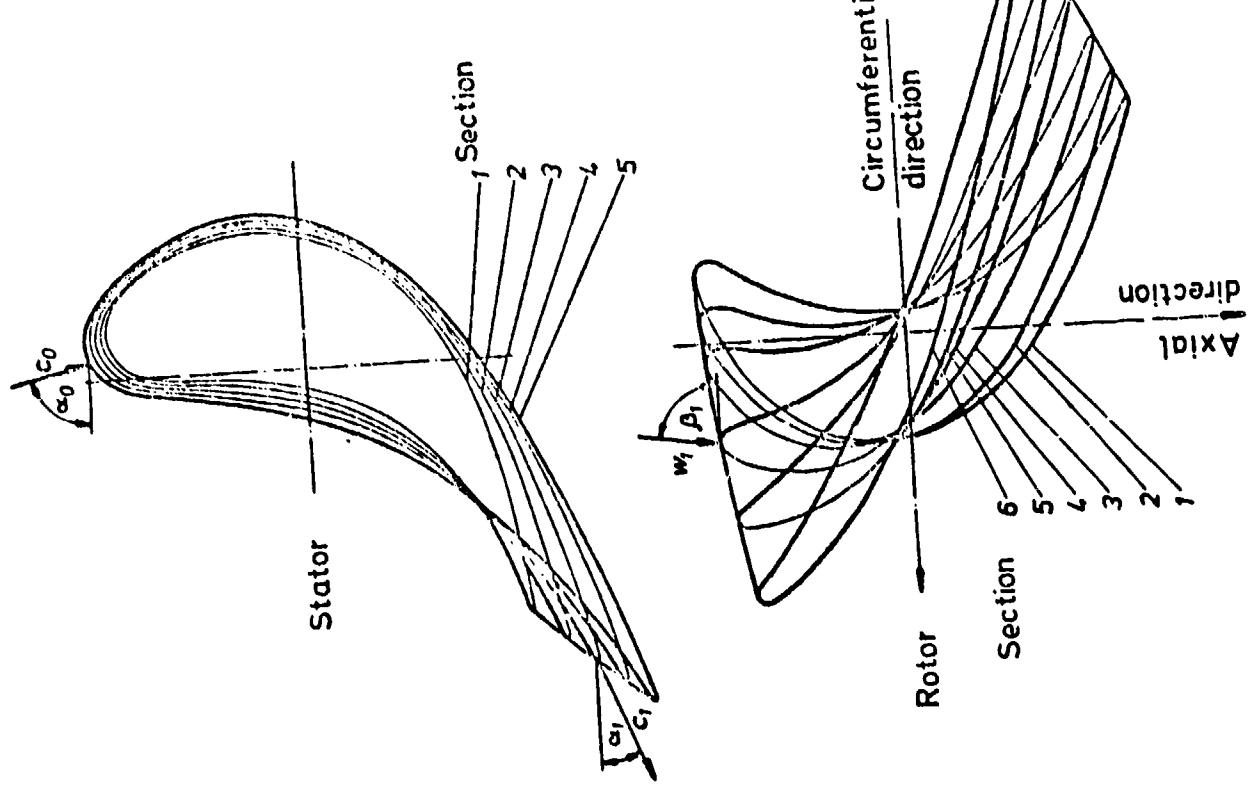
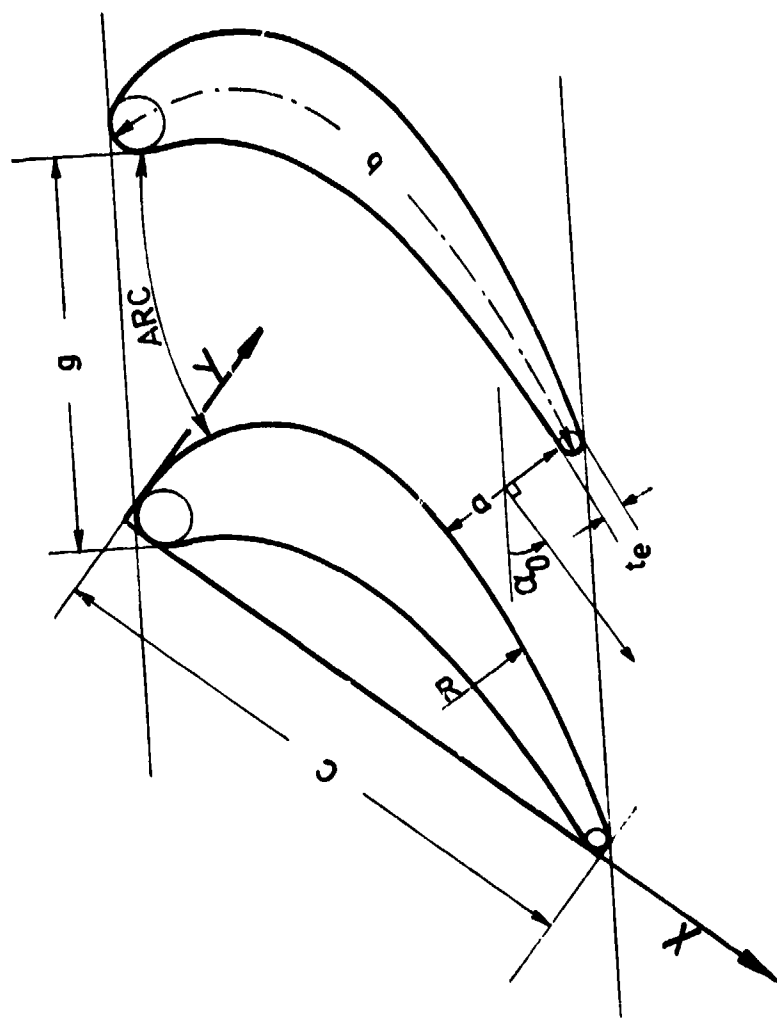


Fig.A4.2 Blade stacking and notation for Table A4.1

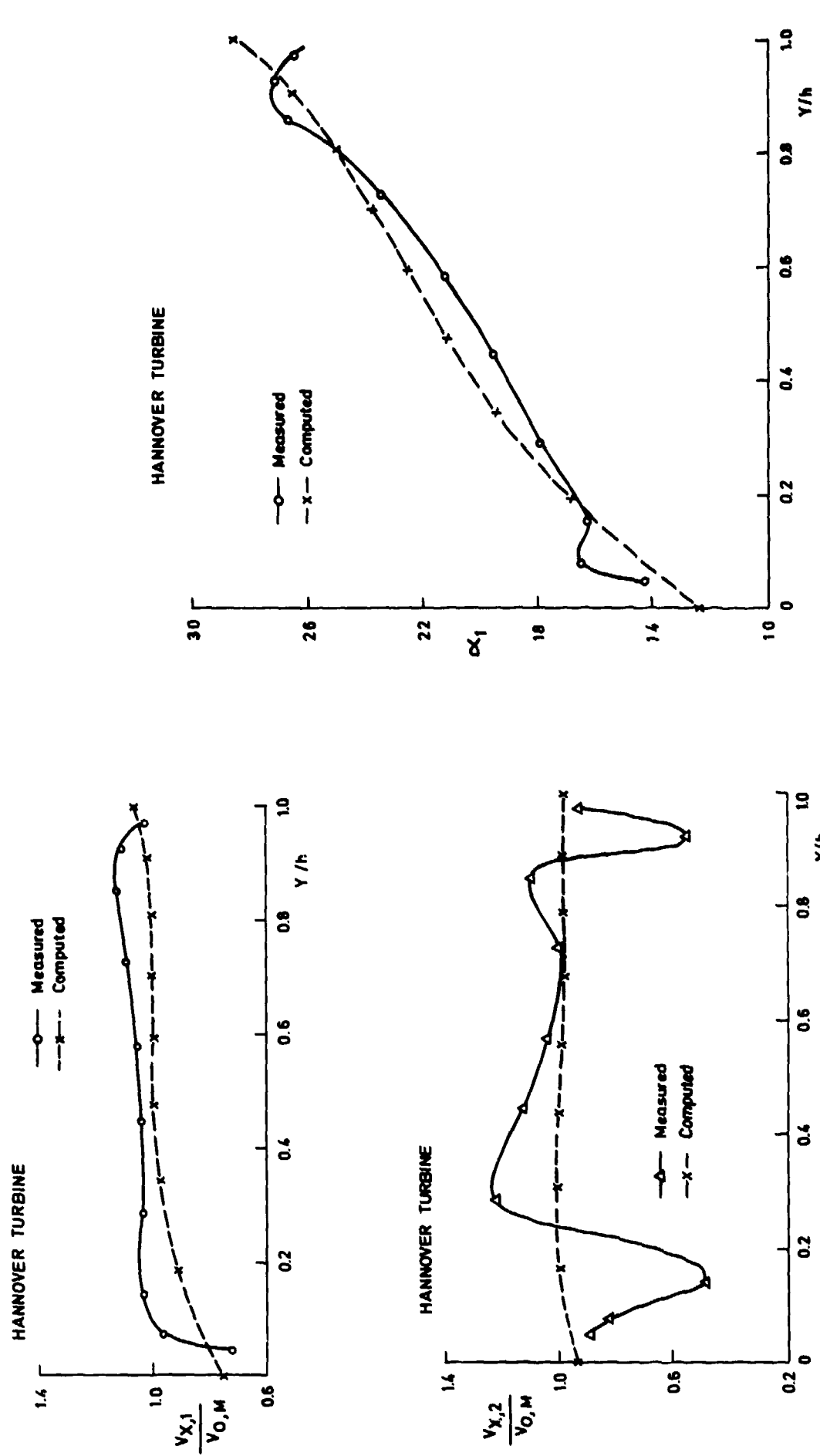


Fig.A4.4 Nozzle exit angles

Fig.A4.3 Axial velocity profiles

HANNOVER TURBINE

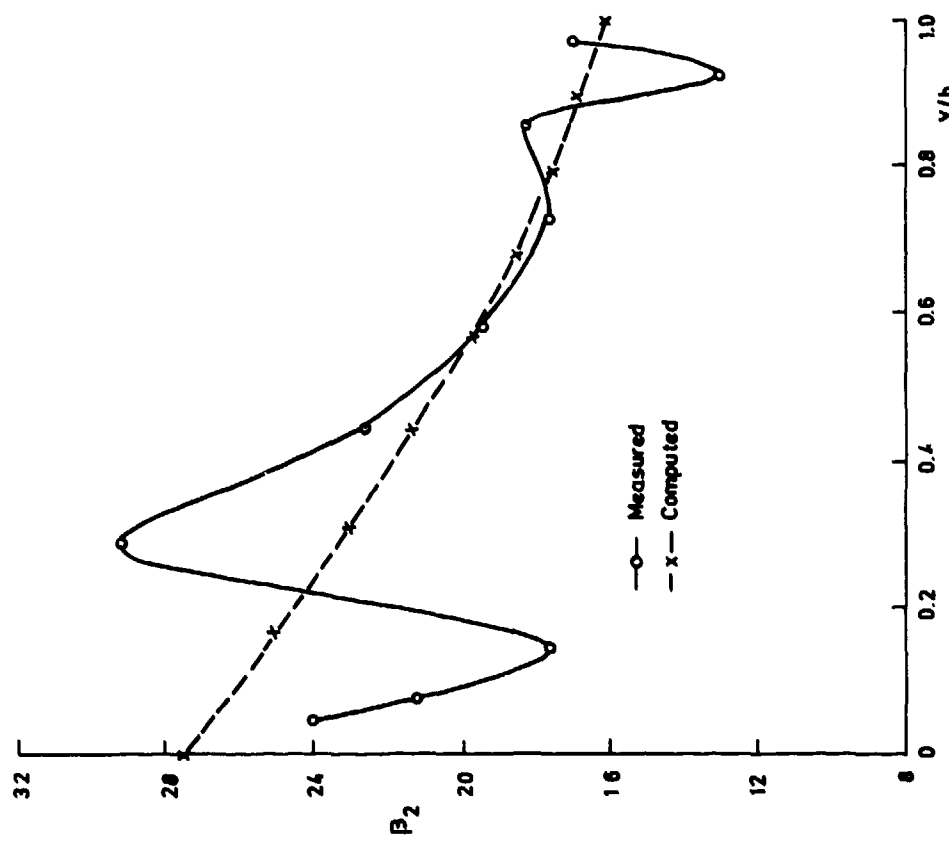


Fig.A4.5 Rotor exit angles

HANNOVER TURBINE

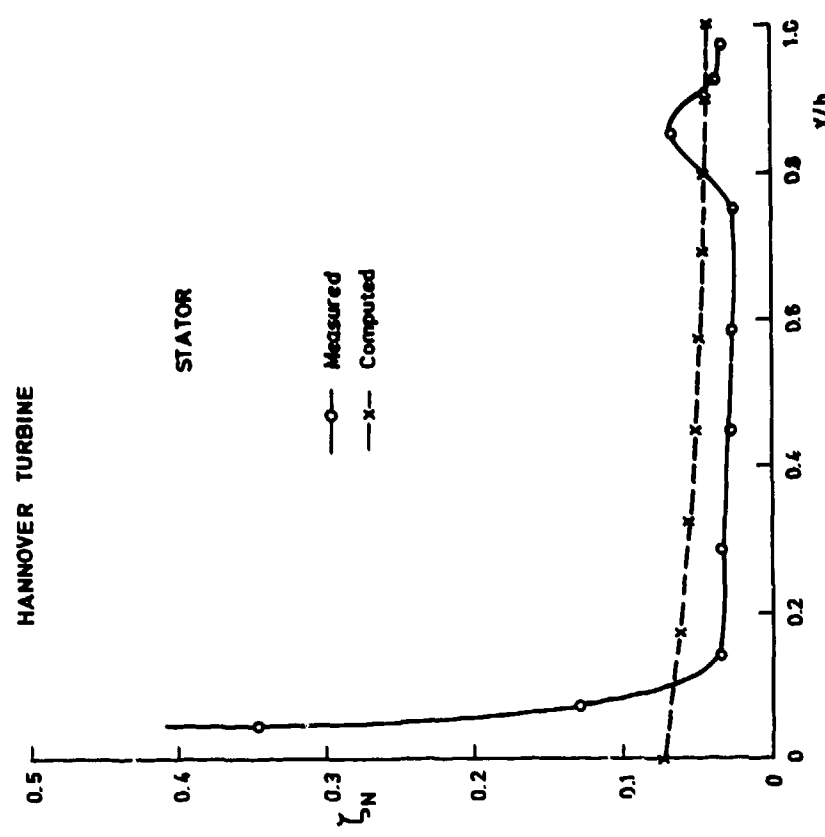


Fig.A4.6 Nozzle loss coefficients

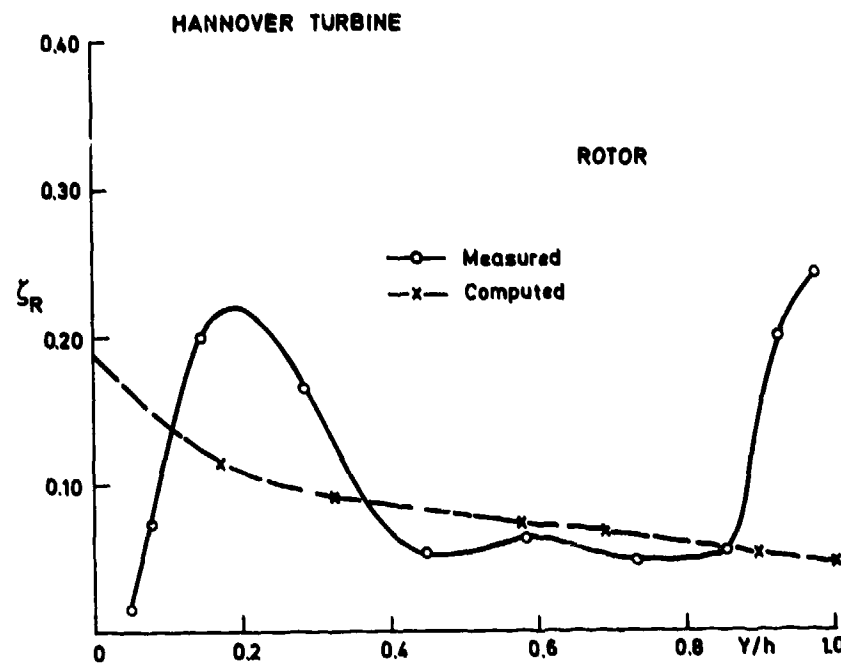


Fig.A4.7 Rotor loss coefficients

PART II
AXIAL COMPRESSOR PERFORMANCE PREDICTIONS

PRECEDING PAGE BLANK-NOT FILMED

II.1. Introduction

In the field of axial compressors a very large number of correlations and correlation formulas can be found in the literature and in the design groups of engine and industrial turbomachinery manufacturers.

Although many, if not all, of the correlations have common points, as for instance the use of a diffusion factor in estimating the minimum profile losses, large differences appear when it comes to estimating the effects of the various geometrical or physical variables on overall losses and deviations. This is obviously a consequence of the strong complexity of the flow structure and of our present poor understanding of detailed flow mechanism in an axial compressor.

Bearing this in mind, it was considered necessary to summarize the state of the art in the field of the existing methods in an attempt to put forward the main influences and the most sensitive parameters, as well as to provide some trends or general concensus, at least with respect to some components of the complex system of correlation formula's.

Therefore, a double action was initiated by the Compressor Subgroup : detailed surveys on some particular topics were written by various members of the subgroup, in particular on diffusion factors and profile losses, deviation angle correlations, models for shock losses and shock-boundary layer interaction, part-span damper losses, Reynolds number and roughness effects, secondary flow and clearance effects on losses and turning, and end-wall boundary layer calculation methods. Moreover a review on blade-to-blade calculations and a discussion of the through flow calculation methods were produced.

On the other hand it was felt important to have some information or feedback from industry and research organizations on the various topics and questions raised by the review of the existing correlations and a questionnaire was prepared and distributed in that sense.

Roughly 15 answers and comments were received from six different countries covering a representative cross-section of the aeronautical and non-aeronautical industrial and research organisations. This allowed the Working Group to draw some guidelines and the answers provided also a reasonably clear picture of the deficiencies and shortcomings of the present-day situation as they are felt in industry. Also, indications about some important loopholes and directions where improvement is needed came forward.

In order to clear some of the questions raised by the review of the present state of the art, test cases were selected for calculations with various correlations and with inclusion of end-wall boundary layer effects. Three compressor test cases, a single stage, a two stage and a four stage compressor were selected as well as two compressor cascades for additional blade-to-blade calculations in order to provide a criterion for distinguishing among the various expressions for the diffusion factor and its relation to wake momentum thickness found in the literature.

Several organisations contributed to the calculations on a voluntary basis and their contribution and effort is gratefully acknowledged. Without their active support, the work and activity of the Working Group would have lost much of its significance.

For obvious practical reasons of time and cost limitations, the amount of extensive and systematic comparative calculations had to be limited. Therefore the analysis of the influence of a systematic variation of certain parameters on the overall performance prediction and (or) the internal flow distribution could not be extended as far as necessary. However, very useful trends came forward from the calculation results.

This report summarizes and presents the various contributions, comments, results and conclusions obtained by the Compressor Sub-group. The first chapter contains the reviews of the state of the art as written by the participants in the Working Group as well as a summary and discussion of the answers to the questionnaire. The test cases are presented and partly documented in the second chapter. Chapter three discusses the results of the calculations.

Finally, the last chapter contains the overall conclusions which have been reached after several discussions between the participants and puts also forward trends and recommendations for future research and improvements.

The objective in all correlations is the determination of deviation angles and losses from a reduced set of parameters related to the blade row geometry and to the flow properties. This set of parameters should be as small as possible but sufficiently representative in order to describe all of the main effects and influences. It is obvious that this always will require a certain amount of empiricism but the actual trend and the ways for improvements certainly lie in a better understanding of the basic flow phenomena, through clean and fundamental experimental data as well as through systematic 2-D or 3-D blade-to-blade calculations.

Nearly all correlations define firstly basic two-dimensional low speed design (or reference) incidences, deviations and losses. Corrections are then introduced for Mach number effects, Reynolds number and non two-dimensional effects such as axial velocity density ratio and secondary flows. Based on the design values, off-design contributions to the design values of losses and deviations are then estimated in function of incidence.

Three different families of parameters enter as variables in all correlations : the cascade parameters, the blade parameters and the aerodynamic variables.

The cascade factors are the blade spacing, the blade height and chord, the stagger angle and the tip clearance. They are generally expressed in non-dimensional form through solidity, aspect ratio (defined as height over chord ratio) and a clearance parameter (clearance to chord or to height ratio).

The main blade parameters are, for a given family of profiles, the blade inlet and outlet angles or the camber angle, the value and position of maximum thickness, the leading edge and trailing edge radii and the blade roughness height. The two most influencing variables are the thickness over chord ratio and the camber. The trailing edge radius is not often considered explicitly as a parameter, although it influences the blade profile losses due to the wake mixing process and some indications do exist that its influence has perhaps been underestimated. The leading edge radius affects directly the leading edge bluntness losses at supersonic incidence Mach numbers. The blade roughness, expressed as a roughness Reynolds number has a non-negligible effect on losses above a certain critical value, where they become independent of Reynolds number.

The aerodynamic variables entering correlations are inlet Mach number, Reynolds number generally based on chord and inlet velocity, axial velocity density ratio and a parameter or a set of parameters measuring blade loading.

The measure of blade loading is a central point in every system of correlations and since Lieblein's work it is a general practice to use the diffusion factor as the most representative loading parameter.

Actually, the diffusion factor is a measure of the ratio of suction surface peak velocity to trailing edge velocity and many different chordwise distributions of loading could be obtained on different blade profiles with the same value of diffusion factor. Hence, a certain "regularity" in the velocity distributions is implicit in the use of this velocity ratio to represent the loading, and therefore its use at off-design can be questioned. However, at design the correlations between D-factor and trailing-edge momentum thickness are very strong. The discussion of the various formulas available in the literature and connecting D-factor with inlet and outlet flow conditions are discussed in the review paper by R. Dunker and H. Weyer.

These relations contain empirical constants which have been correlated through the relation between D-factor and trailing edge momentum thickness on one hand and the relation between momentum thickness and loss coefficients on the other hand. For instance, Swan's and Fottner's correlations are based on eq. (8); Montsarrat's correlation is based on eq. (9) while Koch and Smith's correlation is based on a wake mixing calculation. Therefore, extreme caution should be given to use a consistent set of correlations, in particular since the various relations between momentum thickness and loss coefficient have very different behaviours with regard to the effects of some variables like Mach numbers, Reynolds number and axial velocity ratio. Also special attention should be given to avoid duplication of influences of parameters.

The losses are generally separated into three contributions : Profile losses, including shock losses, secondary losses including clearance effects and part-span damper losses.

The profile losses are expressed as design losses and off-design corrections with various expressions for the influence of Mach number, axial velocity ratio, Reynolds number, and so on. At high Mach numbers, shock losses, influenced by shock boundary layer interaction effects, become very important. Due to the complexity of these phenomena and their extreme sensitivity to detailed blade geometry, the available correlations are based on very simplified assumptions and it is considered that this is one of the most important topics deserving extensive further research. This opinion is also fully substantiated by the answers to the questionnaire and most of the existing correlations are reviewed in L. Fottner's contribution on shock losses and shock boundary layer interactions.

Mach number influence on design losses is very difficult to summarize in a consistent way, since the compressibility effects are introduced in the various correlations at very different levels. Koch and Smith's approach is perhaps one of the most consistent in that sense. Predictions of choking and critical Mach numbers still require much research effort in order to achieve a satisfactory state.

Reynolds numbers effects are considered to be important and a contribution by W. Roberts for the low Reynolds number range is included in the present report as well as a contribution by A. Schäffler and L. Fottner on the effects of blade surface roughness.

With regard to off-design profile losses, empirical relations can be found relating the loss increase to the variations of D-factor from its design value as in Swan's correlation. However, a more reliable approach, very empirical in nature, is to connect the off-design losses to the incidence variations referred to the choking or stalling incidence range. This approach is advocated by Jansen and Moffat as well as by Novak (see AGARD LS83). The difficulties are displaced towards the prediction of the stalling and choking incidences and the available expressions are indeed very rough and uncertain particularly in the range of high Mach numbers (transonic and supersonic) and especially for the blading used in modern designs.

Finally, two controversial contributions on part-span damper losses by W. Roberts and by

R. Novak (summarizing Koch and Smith approach) are included in the present report.

With regard to secondary losses, two ways can be followed. The more classical way in which additional losses are calculated separately and added to the profile losses, being distributed or not along the blade span. A large number of formulas can be found in the literature and most of them are discussed in J. Chauvin and J. Salvage's contribution on secondary flow and clearance effects. Another approach consists in defining an overall efficiency drop due to the end-wall boundary layers and to calculate their evolution in a coherent way following Mellor and Wood's original approach. This approach is discussed in De Ruyck and Hirsch's contribution on End Wall Boundary Layer Calculations. It appears, from the results of the test cases performed within the Working Group activities, as well as from other sources that this is a right way to follow and it can be considered as one of the recommendations of the Working Group.

The various problems, connected with the turning prediction are summarized in G. Serovsky's paper. Most important is the correct assessment of the interaction between the various parameters, Mach number, axial velocity ratio and geometrical factors on design and off-design deviation rules.

A note on axial compressor stall and surge by J. Chauvin has been included for completeness in the present review.

It had been considered from the start, that the analysis of the basic computational aspects of through-flow and blade-to-blade flows was outside the scope of the Working Group. However, since the interaction between the computational method and the correlations can have a large influence on the produced results it was decided to include a summary of both the through-flow methods and of the blade-to-blade methods. A contribution by G. Serovsky on the first topic and by G. Meauze and R. Van de Braembussche on the second topic complete therefore the review of existing methods.

As already mentioned, three test cases representative of modern design techniques were selected for through-flow calculations. They are described partly in the second chapter and more extensive data and results can be obtained from PEP at AGARD headquarters. It undoubtedly appears that most of the available data have limited accuracy and that very well controlled experiments, especially on multistage machines, are urgently needed.

The calculations performed by several participants to the Working Group, although limited in scope, gave some interesting information. Notwithstanding the fact that the results of a through-flow calculation are depending not only on the correlation but also on the computational aspects of the method, some trends could be defined.

The through-flow results as well as blade-to-blade results indicate that the systematic use of numerical calculations is able to provide information which come closer to experimental data than the methods of more empirical character.

It appears that the time has come when a drastic improvement of the methods for performance predictions, most of them originating in the 60's or even earlier, can be obtained with a more extended and carefully defined use of computational tools. This should allow a deeper understanding of the phenomenon and a reduction in the amount of empiricism by an equivalent increase in the physical insight of the complex flow behaviour in modern turbomachines.

II.2. Review of Loss and Deviation Precision Methods

Introduction to the "Review Papers" and "Answers to the questionnaire"

The first review paper of Hirsch, written at an early stage of the Working Group activities, raised several problems on the state of the art and indicated tentatively areas where short-comings were evident. Two actions were set forth in parallel : a questionnaire on the state of the art was sent to industries and research organizations, and Working Group Members were asked to produce review papers on specific items, i.e. :

- . Diffusion factor
- . Shock losses and shock boundary layer interaction
- . Secondary flow and clearance effects (correlations)
- . End-wall boundary layers
- . Deviation/Turning angle correlations
- . Blade-to-Blade calculation methods

to which were added, as a result of the questionnaires and of the WG Work, two papers :

- . Reynolds number effect
- . Part span damper losses (2 contributors)

This part of the final WG report contains the review papers, a summary and comments on the answer to the questionnaire, and conclusions derived from the information contained in this section.

It was also deemed necessary, although this was not included in the original task, to include a short discussion on surge line prediction.

II.2.1 Survey on Diffusion Factors and Profile Losses

List of Symbols

A _a	Annulus Area
C	Chord Length
D	Diffusion Factor
D _{eq}	Equivalent Diffusion Factor
i	Incidence Angle
H ₂	Boundary Layer Shape Factor
M	Mach Number
r	Radius
t	Blade Thickness
U	Rotor Speed
V	Relative Velocity to Blade Element
β	Relative Flow Angle to Blade Element
Δ	Difference in Magnitude
σ	Solidity
θ	Boundary Layer Momentum Thickness at Blade Trailing Edge
W̄	Profile Loss Coefficient

Subscripts

c	Choke Condition
ink	Incompressible Flow
kom	Compressible Flow
max	Maximum Value
m	Meridional Component
s	Surge Condition
θ	Circumferential Component
1	Blade Inlet (LE)
2	Blade Outlet (TE)

Superscripts

*	Optimum Flow Condition
"	Corrected Values (Jansen/Moffat)

Introduction

This section summarizes the various attempts published in the open literature to correlate compressor profile loss with blade loading. The correlation techniques described here are already briefly reviewed by Ch. Hirsch in (1).

The following subjects are discussed in some detail:

- diffusion factor and its development since Lieblein (2,3,4)
- profile loss correlation of:
W.C. Swan (5), N.T. Monsarrat (6), W. Jansen, W.C. Moffat (7), L. Fottner (8,9), P. Strinning (10), L.H. Smith (11).

This calculation procedures used for compressor design and analysis are based more or less on empirical correlations for flow losses and flow turning. For two-dimensional incompressible cascade flow the profile loss is related to the boundary layer parameters at blade trailing edge as follows:

$$\bar{w} = \frac{2 \sigma}{\cos \theta_2} \left(\frac{\theta}{C} \right) \left(\frac{\cos \theta_1}{\cos \theta_2} \right)^2 \left\{ \left[1 - \left(\frac{\theta}{C} \right) \frac{\sigma H_2}{\cos \theta_2} \right]^{-3} \left(\frac{3H_2 - 1}{2H_2} \right)^{-1} \right\} \quad (1)$$

The boundary parameters themselves depend primarily on the blade loading, involving the maximum blade suction surface velocity as well as the cascade inlet and outlet flow conditions.

Diffusion Factor

In 1953 Lieblein (2) made his first attempt, based on Buri's separation criterion, to establish a relevant loading parameter that appeared to describe satisfactorily the low speed relation between blade loading and losses at optimum flow condition (s. Fig.1). Lieblein defined the so-called diffusion factor D as a worthwhile loading parameter:

$$D = \frac{V_{max} - V_2}{V_1} \quad \text{with} \quad \frac{V_{max}}{V_1} = 1 - \frac{1}{2} \frac{14 V_0}{6 V_1} \quad (2)$$

The model is based on low speed measurements of NACA 65-blades of 10 % thickness and is thus limited to the prediction of blade element losses caused by surface friction, boundary layer separation, and wake mixing.

Lieblein's later work (3,4) on blade losses led to a refined parameter called the equivalent diffusion factor and expressed as the ratio of maximum suction surface velocity to outlet velocity:

$$D_{eq} = \frac{V_{max}}{V_2} \quad (3)$$

This factor derived from Schlichting's boundary layer work offers a more general correlation of blade wake momentum thickness i.e. profile loss with blade loading.

As far as cascade measurements are available all flow data including maximum surface velocity and wake flow distribution are known. As an example Fig.2 and 3 demonstrate the wake momentum thickness as a function of D_{eq} for minimum loss and off-design respectively. Data for NACA 65 (C_{10A10}) 10 and C. 4 8° circular arc blades are shown.

For design purposes and off-design analysis the maximum surface velocity and the wake parameters are generally unknown. Only the inlet and outlet flow data are prescribed for design or otherwise evaluated for off-design analysis. Thus, Lieblein formulated the following correlation between D_{eq} and cascade inlet and outlet flow conditions:

$$D_{eq}^* = \frac{\cos \beta_2^*}{\cos \beta_1^*} \left[1.12 + 0.61 \frac{\cos^2 \beta_1^*}{\sigma} (\tan \beta_1^* - \tan \beta_2^*) \right] \quad (4)$$

This equation was proved by the cascade tests mentioned before; it is therefore limited to these types of cascades. Furthermore, it is only valid for the minimum loss situation in incompressible flow.

Lieblein's method is still used for compressor design. There have been some successful attempts to enlarge the range of applicability to high subsonic Mach numbers and arbitrary blade shapes. Furthermore, some modifications were implemented concerning streamline shift and streamtube convergence in actual compressors (12). The details are described in the succeeding chapter on profile loss correlations.

Profile Loss Correlations

The relations today used for predicting profile losses are simplifications of Eq.(1). Approximately all correlations, valid for design as well as off-design, start with defining the minimum (design) profile loss for a 2d-blade element in incompressible flow. Then corrections for Mach and Reynolds number effects as well as for non-2-dimensional geometry are provided. The profile losses at off-design are estimated as a function of incidence angle and blade loading variations based on the design values previously calculated.

Swan's Correlation (5)

For design Swan first determines the equivalent diffusion factor with the well-known inlet and outlet flow conditions. When using the following equation for D_{eq} , streamline radial shift and blade thickness distribution are incorporated:

$$D_{eq}^* = \frac{V_{m1}}{V_{m2}} \frac{\cos \beta_2^*}{\cos \beta_1^*} \left(1.12 + 0.61 K \right) \quad (5)$$

$$\text{where } K = \frac{\cos^2 \beta_1^*}{\sigma} \left[\tan \beta_1^* - \frac{r_2 V_{m2}}{r_1 V_{m1}} \tan \beta_2^* - \frac{U_2}{V_{m1}} \cdot \left(1 - \frac{r_2^2}{r_1^2} \right) \right]$$

Swan established correlations of trailing edge momentum thickness with diffusion factor D_{eq}^* (Eq.(5)) separately for rotors and stators based on experimental compressor element data. Blade height effects as streamline shift, boundary-layer centrifugation are included as shown e.g. in Fig.4. The actual profile loss is estimated using the simplified equation:

$$\left(\frac{\theta}{c}\right)^* \approx \frac{\bar{w}^* \cos \beta_2^*}{2 \alpha} \left(\frac{\cos \beta_2^*}{\cos \beta_1^*} \right)^2 \quad (6)$$

At off-design the analysis of the compressor element data showed that spanwise location of the element has little effect, however inlet relative Mach number does influence the loss-loading compilations. Fig.5 presents a typical curve fit ($\theta/c - \theta/c^*$ versus $D_{EQ} - D_{EQ^*}$) obtained for double-circular arc rotor blade elements demonstrating the independency of blade height:

$$\frac{\theta}{c} - \frac{\theta^*}{c} = (.827 M_1 - 2.692 M_1^2 + 2.675 M_1^3) (D_{EQ} - D_{EQ^*})^2$$

For $D_{EQ} > D_{EQ^*}$

$$\frac{\theta}{c} - \frac{\theta^*}{c} = (2.80 M_1 - 8.71 M_1^2 + 9.36 M_1^3) (D_{EQ} - D_{EQ^*})^2$$

For $D_{EQ} < D_{EQ^*}$

The off-design diffusion factor D_{eq} is defined as:

$$D_{eq} = \frac{V_{m1}}{V_{m2}} \frac{\cos \beta_2}{\cos \beta_1} \left[1.13 + a(i - i^*)^{1.43} + 0.61 K \right] \quad (7)$$

$$K = \frac{\cos^2 \beta_1}{r_1 V_{m1}} \left[\tan \beta_1 - \frac{r_2 V_{m2}}{r_1 V_{m1}} \tan \beta_2 - \frac{U_2}{V_{m1}} \cdot \left(1 - \frac{r_2^2}{r_1^2} \right) \right]$$

$a = 0.0117$ for NACA 65-; $a = 0.007$ for C-Series-, DCA-blades

The off-design losses can be calculated by means of Eq.(6) incorporating the actual flow angles. Some worthwhile modifications of this off-design techniques are given by Davis in (13).

Monsarrat Correlation (6)

For design purposes Monsarrat presents curves of wake momentum thickness versus diffusion factor D (s. Eq.(2)) separately for rotors and stators based on experimental compressor element data. The minimum losses occur at mid span. The losses increase when approaching hub and tip as shown in Fig.6 and 7. Thus, tip clearance, secondary, and end wall boundary layer losses are at least partly included.

Allowing for streamline radial shift and axial velocity changes the following expression for D is derived from Eq.(2):

$$D = 1 - \frac{V_2}{V_1} + \frac{r_1 V_{\theta_1} - r_2 V_{\theta_2}}{(r_1 + r_2) V_1 \alpha} \quad (8)$$

The design profile loss is defined as function of wake momentum thickness θ/c using the following simplification of Eq.(1):

$$\bar{w}^* = \frac{2 \alpha}{\cos \beta_2^*} \left(\frac{\theta}{c} \right)^* \quad (9)$$

There is no off-design loss correlation available.

Jansen/Moffat Correlation (7)

This correlation is based on cascade as well as on compressor blade element data. The basic parameter used for design loss determination is the design diffusion factor D as defined in Eq.(8). The relation between the design loss coefficient w^* is determined by Eq.(6) using the following equation for $(\theta/c)^*$ given in polynominal form:

$$\left(\frac{\theta}{c} \right)^* = (0.003 + 0.02375 D - 0.05 D^2 + 0.125 D^3) \quad (10)$$

Mach number effects and incidence effects at off-design are accounted for using the method of Wiggins (14) which proceeds as follows:

1. If the inlet Mach number exceeds 0.7, the inlet flow angles for design, choke and surge condition will be corrected by means of the following equations:

$$\begin{aligned}\beta''_{1s} &= \beta_{1s} \\ \beta''_{1c} &= \beta_{1c} + 1.5\Delta\beta \\ \beta''_1 &= \beta_1 + \Delta\beta\end{aligned}$$

s = surge
c = choke
" = corrected values,

where

$$\Delta\beta = 10 M_1 - 7.$$

2. The design loss coefficient w^* will be corrected in a similar way if the inlet Mach number exceeds its critical value. This correction is of the form:

$$\bar{w}'' = \bar{w}^* (2 (M_1 - M_{1cr}) + 1) \quad \text{cr = critical}$$

where again the double prime denotes the corrected value.

3. For off-design operation a parabolic variation of loss with incidence is assumed with choke or surge being achieved if the loss is twice its minimum value. The loss coefficient therefore is given by the relation

$$\bar{w} = \bar{w}'' (0.8333 \bar{S}^2 + 0.1667 \bar{S} + 1.0) \quad (12)$$

where \bar{S} is defined as

$$\begin{aligned}\bar{S} &= \frac{\beta_1 - \beta_1^*}{\beta_{1c} - \beta_1^*} \quad \text{for } \beta_1 < \beta_1^* \\ \text{and} \\ \bar{S} &= \frac{\beta_1 - \beta_1^*}{\beta_{1s} - \beta_1^*} \quad \text{for } \beta_1 > \beta_1^*\end{aligned}$$

Fottner Correlation (8, 9)

For incompressible flow and design purpose Fottner extended the relation of wake momentum thickness versus diffusion factor D^* to arbitrary blade thicknesses t . The following equations based on cascade data are proposed:

$$u_{ink}^* = 2 \frac{\theta^*}{c} \left(\frac{\cos \beta_1^*}{\cos \beta_2^*} \right)^2 \frac{\sigma}{\cos \beta_2^*} \quad (13)$$

$$\left(\frac{\theta}{c} \right)^* = (6.6 \frac{t}{c} + 0.34) (0.0088 + 0.0107 D - 0.052 D^2 + 0.116 D^3) \quad (14)$$

$$D = \frac{v_{max} - v_2}{v_1} \quad (15)$$

$$\frac{v_{max}}{v_1} = 1.03 + (0.4 + \frac{t}{c}) - \frac{\Delta v_\theta}{v_1} + 0.7 \frac{t}{c} \quad (16)$$

Eq.(13) is again a simplification of Eq.(1). Fig.8 illustrates the comparison of results calculated with Eq.(15) for different blade thicknesses t to corresponding experimental data.

In order to allow for higher inlet Mach numbers and to perform off-design analysis Fottner uses the same procedure as described by Jansen-Moffat, however, proposing a factor of 1.8 instead of 2 in Eq.(11) for Mach number correction.

Strinning Correlation (10)

This correlation technique valid only for design is based on cascade data and covers the inlet Mach number range up to 1.4. At first the losses in incompressible flow are determined using the equations of Fottner. For compressible flow the following diffusion factor is defined:

$$D_{kom} = \left(\frac{v_{max}}{v_1} \right)_{kom} - \frac{v_2}{v_1} \quad (17)$$

where

$$\frac{v_{max}}{v_1}_{kom} = \frac{1}{M_1} \sqrt{\frac{k+1}{k-1}} \left\{ 1 - \left[1 - \left(\frac{v_{max}}{v_1} \right)^2_{ink} \right] \right. \\ \left. \cdot \left(1 - \left(1 - \frac{k-1}{k+1} M_1^2 \right)^{\frac{k}{k-1}} \right)^{\frac{k-1}{k}} \right\}$$

(The inlet Mach number is related to sonic condition)

$$\left(\frac{v_{max}}{v_1} \right)_{ink} = 1.03 + (0.4 + \frac{t}{c}) - \frac{1}{c} \frac{\Delta v_\theta}{v_1} + 0.7 \frac{t}{c}$$

At supersonic inlet flow the diffusion factor is calculated assuming an equivalent subsonic flow ahead of the shock that leads to the same Mach number at the position just downstream of the shock. The equivalent subsonic inlet velocity v_1'' is determined by the normal shock equation:

$$v_1'' = \frac{v_1}{M_1^2}$$

The deceleration from v_1 to v_1'' assuming constant flow direction changes the tangential velocity component:

$$\left(\frac{\Delta v_\theta}{v_1} \right)'' = \frac{v_{\theta 1} - v_{\theta 2}''}{v_1''} \quad (19)$$

Eq.(19) is written with the actual flow velocity components, the term $(\Delta v_\theta/v_1)$ is then used to calculate $(v_{max}/v_1)_{ink}$ and the same procedure is followed to determine the diffusion factor:

$$D_{kom} = \left(\frac{v_{max}}{v_1} \right)_{kom} - \frac{v_2}{v_1''} \quad (20)$$

Smith Correlation (11)

This correlation technique only valid for design loss prediction is based on boundary-layer calculations along blade surfaces with normalized root top velocity distributions as shown in Fig.9. Compressible turbulent boundary-layer theory has been employed to relate profile loss to suction surface diffusion ratio, streamtube contraction, Mach number, Reynolds number, and specific geometric blade parameters.

These investigations led to a more general definition of diffusion factor - including compressibility effects, streamtube contraction, and arbitrary thickness/chord ratios:

$$D_{eq}^* = \frac{v_1}{v_2} \left[(\sin \beta_1 - K_1 \sigma r^*)^2 + \left(\frac{\cos \beta_1}{A_p^* \sigma^*} \right)^2 \right]^{\frac{1}{2}} \left(1 + K_3 \frac{t}{c} + K_4 r^* \right) \quad (21)$$

The various terms in Eq.(21) may be written:

$$r^* = \frac{r_1 v_{\theta 1} - r_2 v_{\theta 2}}{\bar{r} \sigma v_1}$$

$$\bar{r} = \frac{(r_1 + r_2)}{2}$$

$$A_p^* = \left(1 - \frac{K_2 \sigma \frac{t}{c}}{\cos \beta} \right) \left(1 - \frac{A_{a1} - A_{a2}}{3A_{a1}} \right)$$

$$\bar{\theta} = \frac{(\theta_1 + \theta_2)}{2}$$

$$\rho^* = 1 - \frac{M_1^2}{1 - M_1^2} (1 - A_p^* - K_1 \frac{\tan \theta_1}{\cos \theta_1} \text{ or } r^*)$$

with:

$$\begin{aligned} K_1 &= 0.2445 \\ K_2 &= 0.4458 \\ K_3 &= 0.7688 \\ K_4 &= 0.6024. \end{aligned}$$

In (11) Koch and Smith discuss in more detail the effects of Mach number, Reynolds number etc., however the general relation of losses, trailing edge momentum thickness, and diffusion factor are not presented in detail.

Conclusion

World wide great emphasis is placed upon the development of new and sophisticated stage and blade design procedures that finally will replace the simple loss prediction techniques today in use. Momentarily however these new techniques are still difficult to apply to real machine design because extensive iterative hub-to-tip, blade-to-blade, and boundary-layer flow calculation is needed. Great and long term efforts are still necessary to improve the physical basis and the handling of these programs. Thus in the near future actual machine design and off-design performance prediction will utilize current empirical loss correlations that however must be refined towards more general validity and reliability without giving up their simplicity.

Parametric studies with blade-to-blade flow and boundary-layer calculation codes are progressively attempted to refine the diffusion factor concept and loss correlation at design as well as off-design compressor operation. The codes begin to demonstrate how the flow parameters (incl. Mach- and Re-number) and the details of blade geometry interact to produce performance characteristics, as was stated in a very encouraging paper on the relation of measured losses to calculated blade-surface velocities which has been recently published by T.F. Gelder et al. (15).

List of References

- (1) Hirsch, Ch., Survey of Deviation and Loss Correlations, ACARD-PEP Working Group 12, Axial Compressor Performance Prediction.
- (2) Lieblein, S., et al., Diffusion Factor for Estimating Losses and Limiting Blade Loadings in Axial-Flow-Compressor Blade Elements, NACA RM E53D01, 1953.
- (3) Lieblein, S. Loss and Stall Analysis of Compressor Cascades. Trans. ASME, Series D, J. of Basic Eng., Vol.81, 1959, p. 387.
- (4) Lieblein, S., Johnson, I.; Resume of Transonic-Compressor Research at NACA-Lewis Laboratory. Trans. ASME, J. of Eng. for Power, 1961, p.219.
- (5) Swan, W.C. A Practical Method of Predicting Transonic Compressor Performance. Trans. ASME, J. of Eng. for Power, July 1961, p. 322.
- (6) Monsarrat, N.T., et al., Design Report Single Stage Evaluation of Highly Loaded High-Mach-Number Compressor Stages, NASA N69-30869, 1969.
- (7) Jansen, W., Moffat, W.C. The Off-Design Analysis of Axial-Flow Compressors, Trans. ASME, J. of Eng. for Power, Oct. 1967, p.453.
- (8) Fottner, L. Kennfeldrechnung für Axialverdichter, MTU, Technischer Bericht 72/008, 1972.
- (9) Fottner, L. Answer to Questionnaire on Compressor Loss and Deviation Angle Correlations., AGARD-PEP, Working-Group 12, 1979.
- (10) Strinning, P., Dunker, R. Grundlagen des Auslegungsverfahrens und Vergleich Messung/Rechnung, Forschungsberichte Verbrennungskraftmaschinen, Heft 235, 1977.
- (11) Koch, C.C. Smith, L.H. Loss Sources and Magnitudes in Axial-Flow Compressors. Trans. ASME, J. of Eng. for Power, July 1976, pp. 411-424.
- (12) NASA Aerodynamic Design of Axial-Flow Compressors. NASA-SP 36, 1965.
- (13) Davis, W.R. Axial Flow Compressor Analysis using a Matrix Method, Carleton Univ. Report ME/A 73/1, 1973.
- (14) Wiggins, J.O. A Procedure for Determining the Off-Design Characteristics of Multistage Axial Flow Compressors. MS dissertation, Univ. of Cincinnati, Cincinnati, Ohio, 1963.
- (15) Gelder, T.F., Schmidt, J.F., Esgar, G.M. Aerodynamic Performances of Three Fan Stator Designs Operating With Rotor Having Tip Speed of 337 Meters Per Second and Pressure Ratio of 1.5⁴; NASA-TP 1614, 1980.

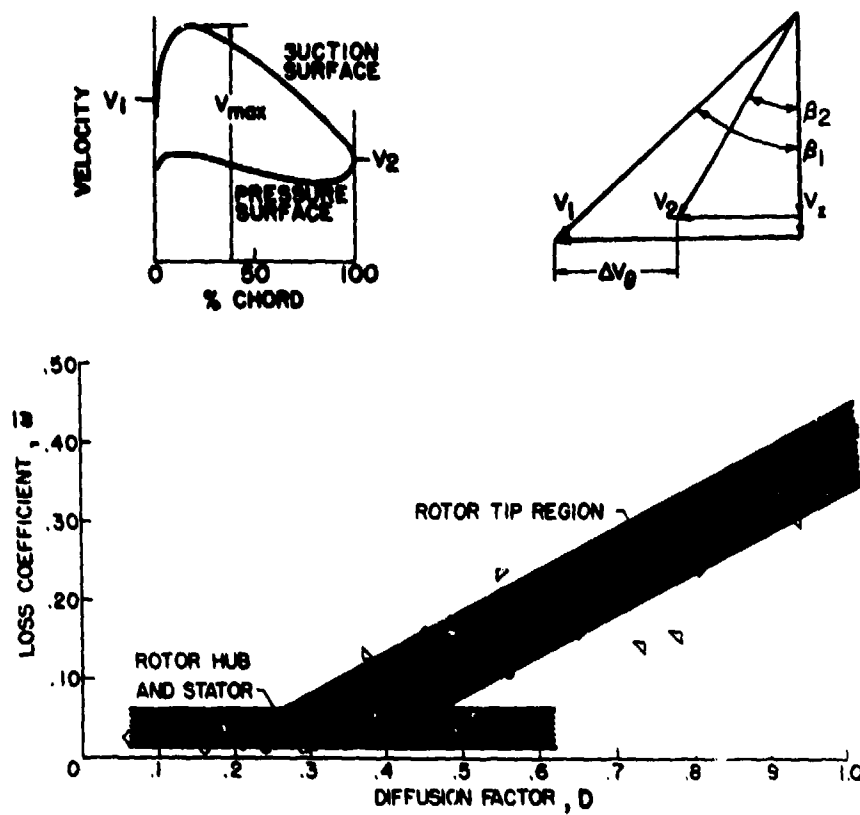


Fig.1 Loss correlation with diffusion-factor for compressor inlet stages.

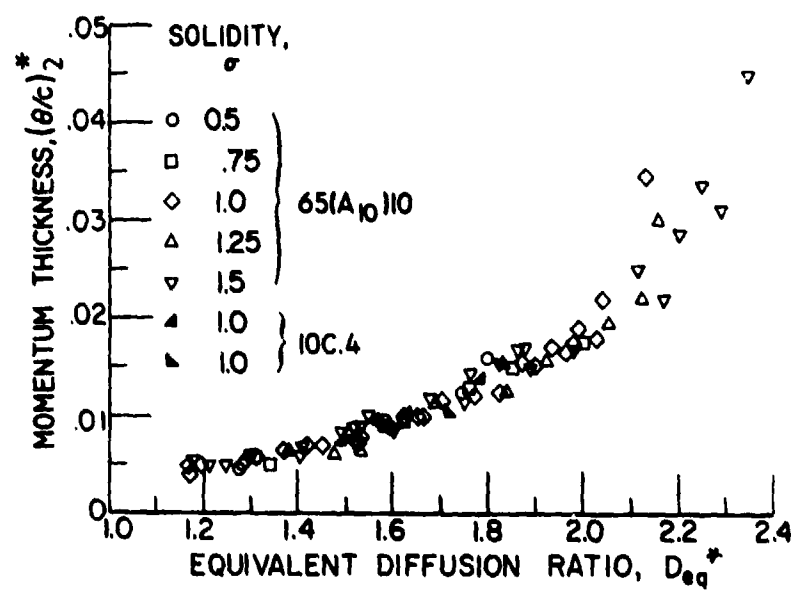


Fig.2 Correlations of wake momentum thickness with equivalent diffusion ratio at minimum loss incidence angle.

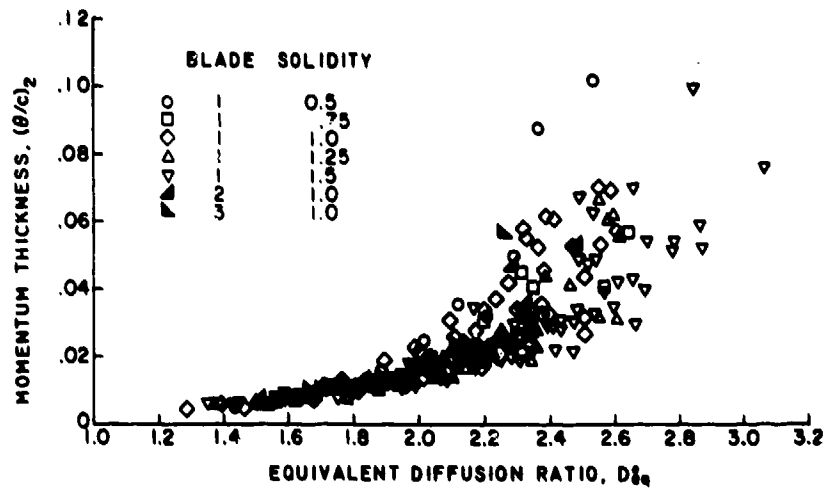


Fig.3 Correlation of wake momentum thickness with equivalent diffusion ratio at incidence angles larger than minimum loss incidence.

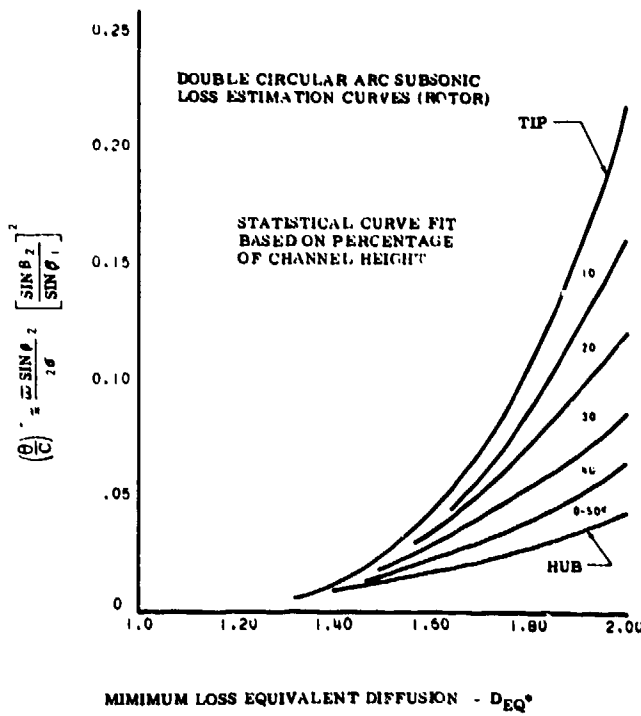


Fig.4 Estimated variation of wake momentum thickness with minimum loss equivalent diffusion.

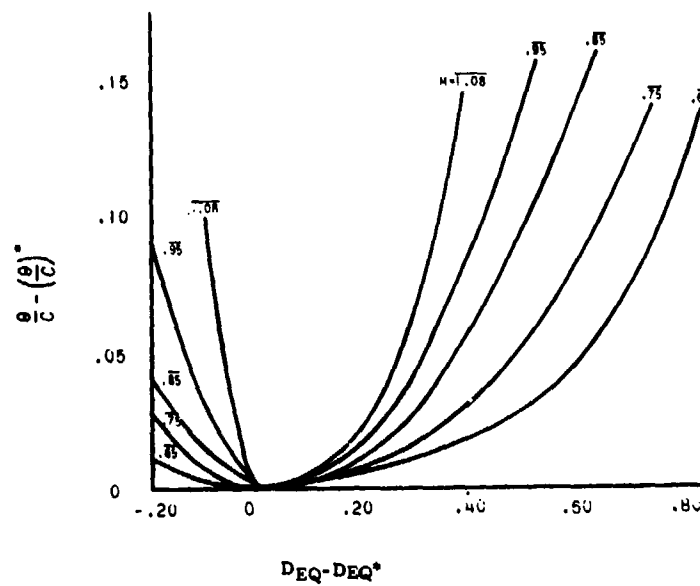


Fig.5 Estimated off-minimum loss variation of wake momentum thickness with equivalent diffusion.

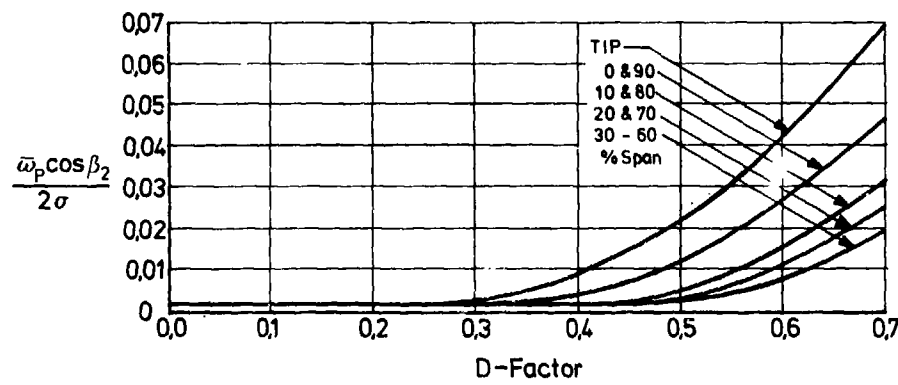


Fig.6 Rotor profile loss parameter vs diffusion factor D

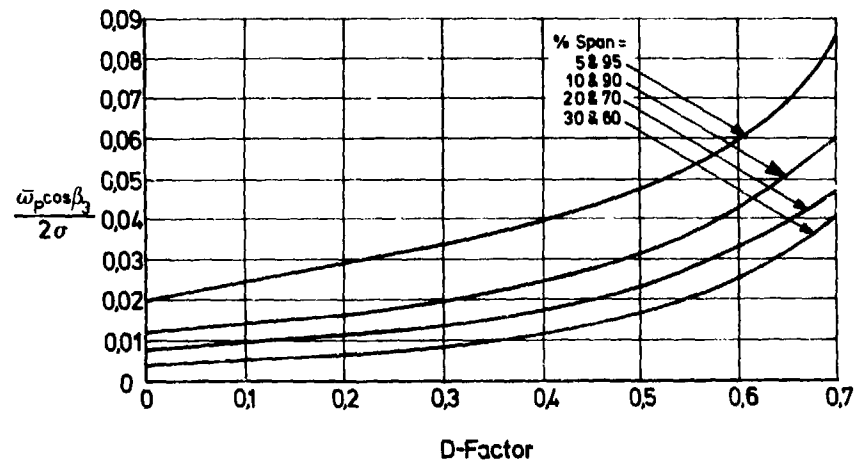


Fig.7 Stator profile loss parameter vs diffusion factor D

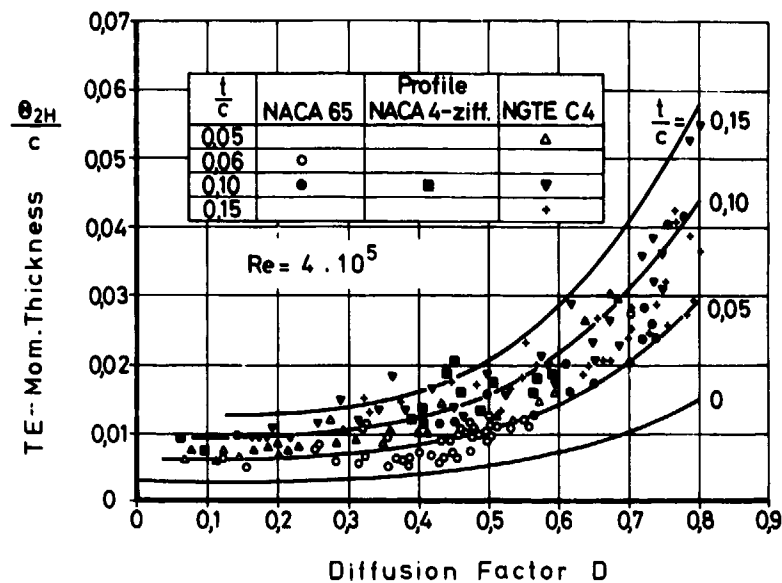


Fig.8 Blade trailing edge momentum thickness as function of diffusion factor D

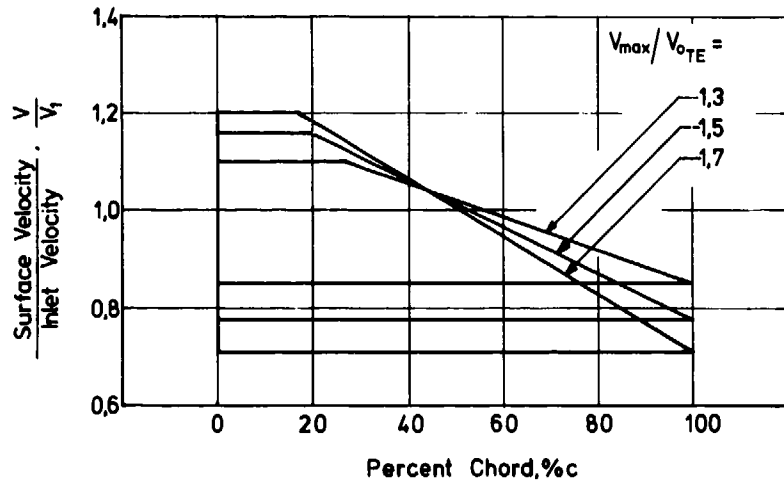


Fig.9 Blade surface velocity distributions employed to determine Mach and Reynolds number effects on blade profile loss using compressible boundary-layer theory.

II. 2.2 Survey of Models for Shock and Shock/Boundary Layer Interaction Loss Prediction

List of Symbols

		<u>Indices</u>
b	axial chord length	c Carnot loss
c_p	static pressure coefficient	crit critical
d	blade thickness	D pressure surface
F	area	g circumferential
l	chord length	ik incompressible
La	Laval number, based on critical sonic velocity	max maximal
m	mass flow	min minimal
Ma	Mach number, based on local sonic velocity	N leading edge
p	static pressure	S shock position
r	radius	t stagnation condition
s	entropy	thr throat
t	pitch	1 inlet
T	temperature	2 exit
w	velocity	- average value
Δw	change of velocity	\perp normal shock
γ	specific heat ratio	\wedge downstream of shock
ΔV	supersonic expansion	
W	loss coefficient	

1. Introduction

Increasing the inlet Mach number leads to a condition for which locally on the suction surface the peak velocity is equal to sonic velocity. This inlet Mach number is called the critical Mach number. Above this value a local supersonic field terminated by a normal shock is built up (see Fig. 1a). For the so called choking Mach number this shock limits the mass flow, because for this flow condition the throat velocity reaches sonic conditions. For further increase of the inlet Mach number to supersonic inlet conditions, there is a shock system (see Fig. 1b) consisting of an oblique shock which influences the region upstream of the cascade (for subsonic axial velocity) and a normal shock within the blade passage. It has been experienced that the oblique shock in front of the cascade produces very low losses, whereas the normal shock within the blade passage produces high losses for high shock Mach numbers (Fig. 2). The strong increase of losses in transonic compressor cascades at high inlet Mach numbers is not only attributed to the shock losses according to shock correlations, but primarily to the shock/boundary layer interaction which leads to boundary layer separation due to the strong pressure gradient of the shock.

These very complicated flow conditions have made it impossible up to now to accurately calculate the shock losses with analytical methods. Therefore most of the published methods are derived using very simple shock models and empirical shock loss correlations.

2. Empirical Shock Loss Correlations

The evaluation of cascade measurements shows that for low inlet Mach numbers (see Fig. 3) the losses are independent of the inlet Mach number. Above the critical Mach number the losses are increased due to local shocks and shock/boundary layer interaction. For supersonic inlet flow conditions the gradient of the losses becomes more steep because of the boundary layer separation downstream of the shock. The Mach number dependency can be divided into three regions (see Fig. 4):

- in the region up to the critical Mach number the losses are independent of the Mach number and are equal to the incompressible value (this case is treated separately)
- the region between the critical Mach number and the sonic inlet condition with supercritical inlet Mach numbers
- the region for supersonic inlet velocity

2.1 Critical Inlet Mach Number

The critical inlet Mach number is by definition the inlet Mach number for which the peak velocity on the profile suction surface reaches the sonic condition. By applying the gasdynamic functions for this flow condition, the following equation is obtained:

$$La_{1\text{crit}} = \sqrt{\frac{x+1}{x-1}} \left\{ 1 - \left[\frac{\left(\frac{2}{x+1}\right)^{\frac{x}{x-1}} (c_{p1})_{\min}}{1 - (c_{p1})_{\min}} \right]^{\frac{x-1}{x}} \right\} \quad (1)$$

and

$$Ma_{1\text{crit}} = \frac{La_{1\text{crit}}}{\sqrt{0.5 [1 + x - (x-1) La_{1\text{crit}}^2]}} \quad (2)$$

The local static pressure coefficient

$$c_{p1} = \frac{P - P_1}{P_{t1} - P_1}$$

is assumed to be constant in the region up to $Ma_{1\text{crit}}$, this yielding:

$$(c_{p1})_{\min} = (c_{p1})_{\min ik} = 1 - \left(\frac{W_{\max}}{W_1} \right)_{ik} \quad (3)$$

Applying one of the known modern pressure distribution calculation methods it is possible to calculate the peak velocity very accurately. But for fast loss estimation it is convenient to use approximations. Ref. 1 contains, similar to Ref. 2 and 3, an empirical correlation for NACA 65 profile series:

$$\left(\frac{W_{\max}}{W_1} \right)_{ik} = 1.03 + (0.4 + d/l) \cdot t/l \cdot \frac{\Delta W_g}{W_1} + 0.7 d/l \quad (4)$$

A similar expression for the peak velocity, which must also be used for calculating the diffusion factor is given in Ref. 4:

$$\frac{W_{\max}}{W_1} \approx \frac{W_{\max}}{W_{\text{thr}}} = 1 + 0.7688 d/l + 0.6024 t/l \cdot \frac{\Delta W_g}{W_1} \quad (5)$$

2.2 Correlations for Supercritical Subsonic Inlet Condition

Ref. 1 contains a very rough empirical correlation taking into account the compressibility effect on the profile losses as well as the losses due to local shocks:

$$W_1 = \frac{P_{t1} - P_{t2}}{P_{t1} - P_1} = W_{1ik} [A (Ma_1 - Ma_{1\text{crit}}) + 1] \quad (6)$$

for $Ma_1 > Ma_{1\text{crit}}$.

The coefficient A is set to A = 2.0 in Ref. 1 but our evaluations of cascade measurements suggest to set it A = 1.8. Practical application has shown sufficient agreement with measurements, if the inlet Mach number does not exceed $Ma_1 = 1.2$. An empirical correlation very similar to equation (6) is given in Ref. 5. For compressor cascades with double circular arc profiles an evaluation of numerous cascade and stage measurements gives:

$$W_1 = W_{1ik} \left\{ 14 \left[Ma_1 - (Ma_{1\text{crit}} - 0.4)^3 \right] + 1 \right\} \quad (7)$$

While these two correlations give corrections for the compressibility effects, Ref. 6 tries to calculate the shock losses by calculating the viscous pressure distribution on the profile surfaces taking into account empirical corrections for the supersonic field and the terminating compression shock. This shock is extended from the shock position on the suction surface into the blade passage with a suction surface Mach number immediately upstream of the shock corresponding to the supersonic expansion on the profile decreasing to sonic condition at the sonic line. In the subsonic region the Mach number is further decreased to the value on the pressure surface. The shock loss is calculated for a mean shock Mach number

$$\bar{Ma}_s = \frac{1}{2} (Ma_s + 1.0) \quad (8)$$

using the normal shock equation

$$\omega_1 = \bar{L}_{as} \left[\frac{\frac{x-1}{x+1} \bar{L}_{as}^2}{1 - \frac{x-1}{x+1} \cdot \frac{1}{\bar{L}_{as}^2}} \right]^{\frac{1}{x-1}} \quad (9)$$

This loss has to be distributed in the blade passage between two blades to get a pitch averaged total pressure at the exit of the cascade, yielding:

$$\frac{\hat{P}_t}{P_{t1}} = 1 - \frac{M_{as} - 1}{M_{as} - M_{a0}} \left(1 - \frac{\hat{P}_t}{P_{t1}} \right) \quad (10)$$

If the local Mach number on the pressure side is not known, it should be replaced by the inlet Mach number.

2.3 Correlations for Supersonic Inlet Conditions

The first published correlation for shock loss prediction is given in Ref. 7. The method is based on a very simplified shock model, with an oblique shock in front of the cascade with negligible losses, and a normal shock in the blade passage which is assumed to be normal to the mean streamline. The Mach number immediately upstream of the shock on the suction surface is calculated as a function of the supersonic expansion from the inlet direction to the profile tangent at the shock position. The Mach number immediately upstream of the shock at the leading edge of the adjacent profile is equal to the inlet Mach number. In Ref. 7 the Mach number to be taken for shock loss prediction is calculated as a mean value:

$$\bar{M}_{as} = \frac{1}{2} (M_{as} + M_{a1}) \quad (11)$$

M_{as} is a function of the inlet Mach number and the supersonic expansion

$$M_{as} = f(M_{a1}, \Delta V) \quad (12)$$

Ref. 7 contains some analytical expressions for this function applied to circular arc profile parts.

If further details of the blading are known, i.e. if the blading design is available and the cascade losses are to be recalculated (contrary to the design task, for which the blading is to be designed), Ref. 8 presents a method for detailed taking into account the blade properties for calculations of the shock Mach number. The advantage of this method is that it is also applicable to the off-design case.

Since the finite leading edge thickness leads to a detached shock ahead of the profiles, Ref. 9 proposes a further method for shock loss prediction on the basis of Ref. 10 and 11. The shock model consists of a detached shock immediately upstream of the profile and a normal shock in the blade passage. By use of the method of characteristics (Ref. 12) the Mach number distribution upstream of the shock at each position across the blade passage can be calculated. Thus, also the local shock loss is known. The total loss of the compression shock system is calculated by a mass averaged integration across the blade passage.

Apart from the losses due to shocks, there are additional losses caused by the shock/boundary layer interaction, which can be even higher because of possible boundary layer separation induced by the shock. Ref. 13 contains a method for estimating shock losses near the design point. The shock model consists of a λ -shock in the entrance region of the cascade causing boundary layer separation. In the region outside of the boundary layer the suction surface velocity remains supersonic and is decelerated to subsonic condition by a normal shock emanating from the pressure surface. Downstream of the shock there is a mixing of the main stream with the separated boundary layer.

In Ref. 14 a method is developed taking into account a pseudo-shock-system in the separated region downstream of the normal shock. Due to the separated region the flow is reaccelerated to sonic conditions. The following deceleration to subsonic exit conditions is accomplished by a Carnot deceleration, the losses of this mixing process to be calculated using the laws of momentum and continuity:

$$\left(\frac{P_{t2}}{\hat{P}_{ts}} \right) = \frac{m \sqrt{T_{t1}} / \hat{P}_{ts} F_s}{\frac{m \sqrt{T_{t2}}}{P_{t2}} \frac{F_2}{F_s}} \quad (13)$$

with

$$\frac{F_2}{F_s} = 1 + \frac{\hat{L}_{as} (\bar{L}_{as}^2 + 1) - \bar{L}_{a2} (\bar{L}_{as}^2 + 1)}{\bar{L}_{a2} (1 - \frac{x-1}{x+1} \hat{L}_{as}^2)} \quad (14)$$

According to the just mentioned condition of sonic velocity due to reacceleration in the separated region λ_a has to be set to $\lambda_a = 1.0$. It is clear that the boundary layer does not separate for weak shocks, i.e. low shock Mach numbers. Therefore a correction has to be done for the Caihnon loss coefficient of equation (13):

$$\frac{P_{t2}}{P_{ts}} = 1 - \beta_D \left[1 - \left(\frac{P_{t2}}{P_{ts}} \right) \right] \quad (15)$$

where $\beta_D = f(\hat{p}/p)$ is a function of the static pressure rise of the normal shock. Experience has shown that $\hat{p}/p > 1.35$ leads to separation of the boundary layer downstream of the shock, i.e.

$$\beta_D = 1.0 \text{ for } \hat{p}/p = 1.35$$

Ref. 4 presents a shock loss model which determines the losses of the two shock parts separately. For supersonic inlet conditions an additional supersonic expansion around the leading edge has to be taken into account resulting in an additional loss. This loss is determined in Ref. 4 in terms of an entropy increase:

$$\frac{\Delta s}{r} = - \ln \left\{ 1 - \frac{r_N}{b \sin \beta_1} \left[1.28 (\text{Ma}_1 - 1) + 0.96 (\text{Ma}_1 - 1)^2 \right] \right\} \quad (16)$$

The entropy increase of the passage shock is calculated for an oblique shock, decelerating to sonic velocity.

Within the scope of MTU investigations on shock loss predictions methods, some of the above described correlations have been applied to relevant cascade measurements, done at DFVLR on specially MTU designed supersonic profiles for transonic compressors. Fig. 5 shows the results of the correlations compared with the measurements. At first an extrapolation of equation (6) had been done for high supersonic inlet Mach numbers, only to show the limits of this correlation. As had been mentioned in chapter 2.2 this correlation gives good agreement for Mach numbers lower than 1.2, but for higher Mach numbers the correlation underestimates the losses. Therefore, for supersonic inlet Mach numbers an additional normal shock loss had been calculated for a shock Mach number equal to the inlet Mach number. This could be done because the investigated profiles had been designed with a wedge profile in the supersonic part of the profile in order to reduce the shock Mach number. Quite good agreement can be seen between calculation and measurement. Finally in addition to the normal shock losses calculated for the inlet Mach number, equation (13) has been applied to take into account the shock boundary layer interaction downstream of the shock, also showing good agreement with measurements.

Summing up, it had been shown that a very simple correlation, consisting of the normal shock relation for the inlet Mach number and the compressibility correction term of Ref. 1, gives good agreement with measurements for the investigated supersonic profile types.

3. Analytical Methods

The losses due to shocks in a cascade with transonic flow can be calculated (with the exception of shock/boundary layer interaction), if the flow field in the cascade is known. This information comes from semi-empirical methods, or methods of characteristics in the entrance region or in recent years from very sophisticated analytical methods taking into account the mixed subsonic/supersonic type of the transonic cascade flow. Due to the effort necessary for application these methods are not considered within this survey.

4. Conclusions

The calculation of the shock losses has to take into account the losses due to normal shocks as well as the additional losses caused by the shock/boundary layer interaction. Due to the very complex flow behaviour, at present this is only possible by empirical correlations for very simplified assumptions. Therefore, additional effort has to be directed to the practical application of analytical methods and to better understanding of the shock/boundary layer interaction.

Basically, transonic cascades have to be designed in such a way that the shocks are not present or occur at minimum shock Mach number. It seems to be possible that for high subsonic inlet Mach numbers the use of new blading design concepts (i.e. supercritical profiles) can meet the first condition, whereas the second condition of minimal shock Mach numbers has been successfully verified by the use of wedge type profiles.

5. List of References

- Ref. 1 Jansen, W.
Moffat, W.C.
- Ref. 2 Lieblein, S.
- Ref. 3 Members of the
Compr. and Turbine
Res. Div.
- Ref. 4 Koch, C.C.
Smith, L.H.Jr.
- Ref. 5 Dettmering, W.
- Ref. 6 Fottner, L.
- Ref. 7 Miller, G.R.
Lewis, G.W.
Hartmann, M.J.
- Ref. 8 Balzer, R.L.
- Ref. 9 Starken, H.
- Ref. 10 Levine, P.
- Ref. 11 Möckel, W.E.
- Ref. 12 Lichtfuss, H.J.
- Ref. 13 Gustafson, B.A.
- Ref. 14 Volkmann, H.
Fottner, L.
Scholz, N.
- The Off-Design Analysis of Axial-Flow Compressors
Trans. ASME, J. of Engng. for Power, Oct. 1967, 453 - 462
- Loss and Stall Analysis of Compressor Cascades
Trans. ASME, J. of Basic Engng., Sept. 1959, 387 - 400
- Aerodynamic Design of Axial-Flow Compressors (Revised)
NASA-SP 36, 1965
- Loss Sources and Magnitudes in Axial Flow Compressors
J. Eng. for Power, July 1976, 411 - 424
- Machzahleinfluß auf die Verdichtercharakteristik
Z. Flugwiss. 19 (1971), 145 - 150
- Ein halbempirisches Verfahren zur Bestimmung der reibungsbehafteten transsonischen Schaufelgitterströmung
mit Einschluß von Überschallfeldern und Verdichtungs-
stößen
Dissertation TH München (1970)
- Shock Losses in Transonic Compressor Blade Rows
Trans. ASME, J. of Engng. for Power, Jul. 1961, 235 - 242
- A Method for Predicting Compressor Cascade Total
Pressure Losses, when the Inlet Relative Mach Number
is greater than Unity
ASME Paper No. 70-GT-57, 1970
- Untersuchung der Strömung in ebenen Überschallver-
zögerungsgittern
DLR FB 71-99 (1971)
- Two-Dimensional Inflow Conditions for a Supersonic
Compressor with Curved Blades
J. of Appl. Mech. 24 (1957) No. 2, S. 165
- Experimental Investigation of Supersonic Flow with
Detached Shock Waves for Mach Numbers between 1.8
and 2.9
NACA RM E50D05 (1950)
- Berechnung der ebenen Überschallgitterströmung mit
Hilfe des analytischen Charakteristikenverfahrens
DLR FB 73-34 (1973)
- A Simple Method for Supersonic Compressor Cascading
Performance Prediction Cascad
ASME-Paper No. 76-GT-64 (1976)
- Aerodynamische Entwicklung eines dreistufigen Trans-
sonik-Frontgebläses
ZfW 22 (1974) 4, 135 - 144

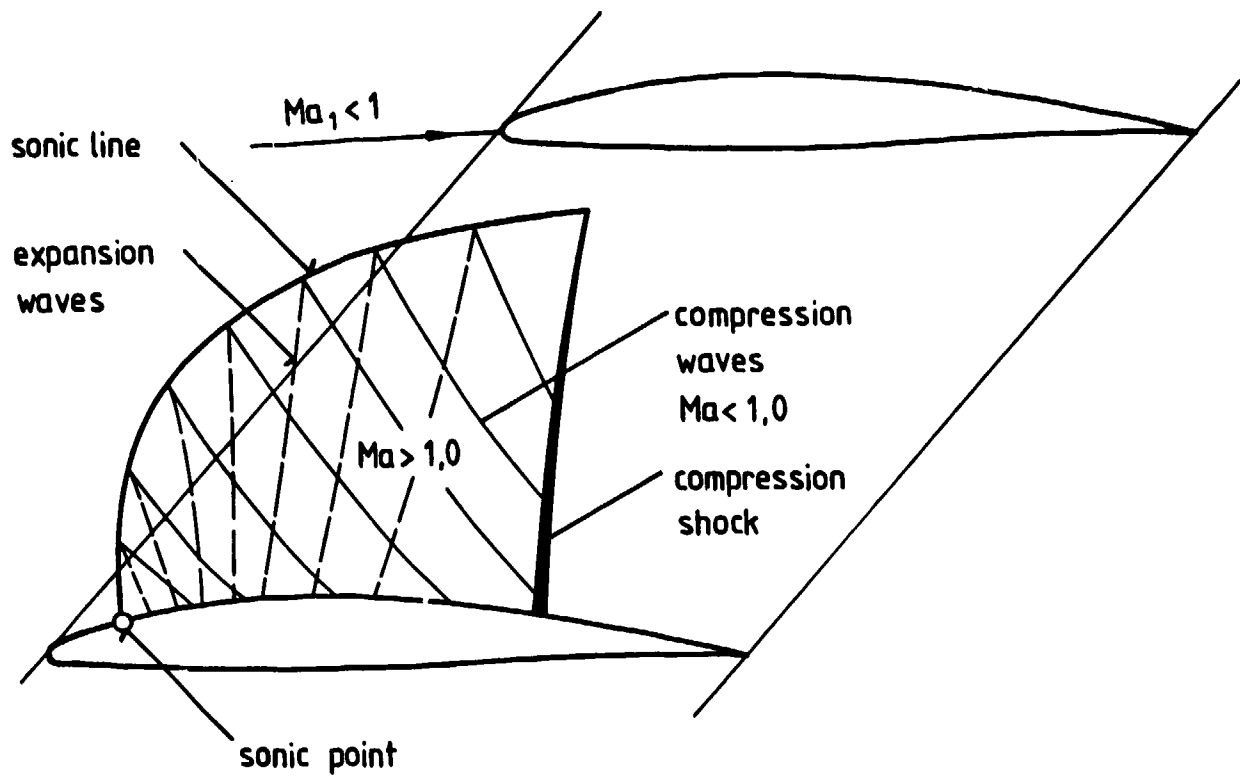


Fig. 1a: Mixed flow field for supercritical inlet condition

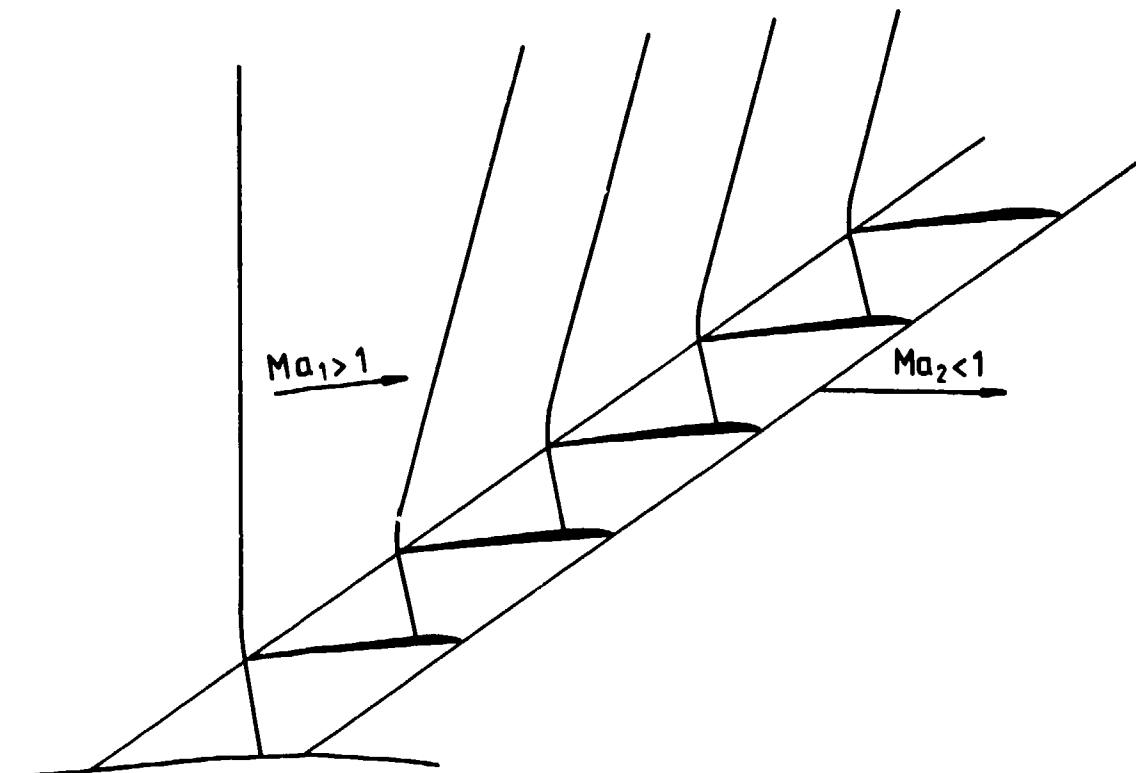


Fig. 1b: Shock system for supersonic inlet condition

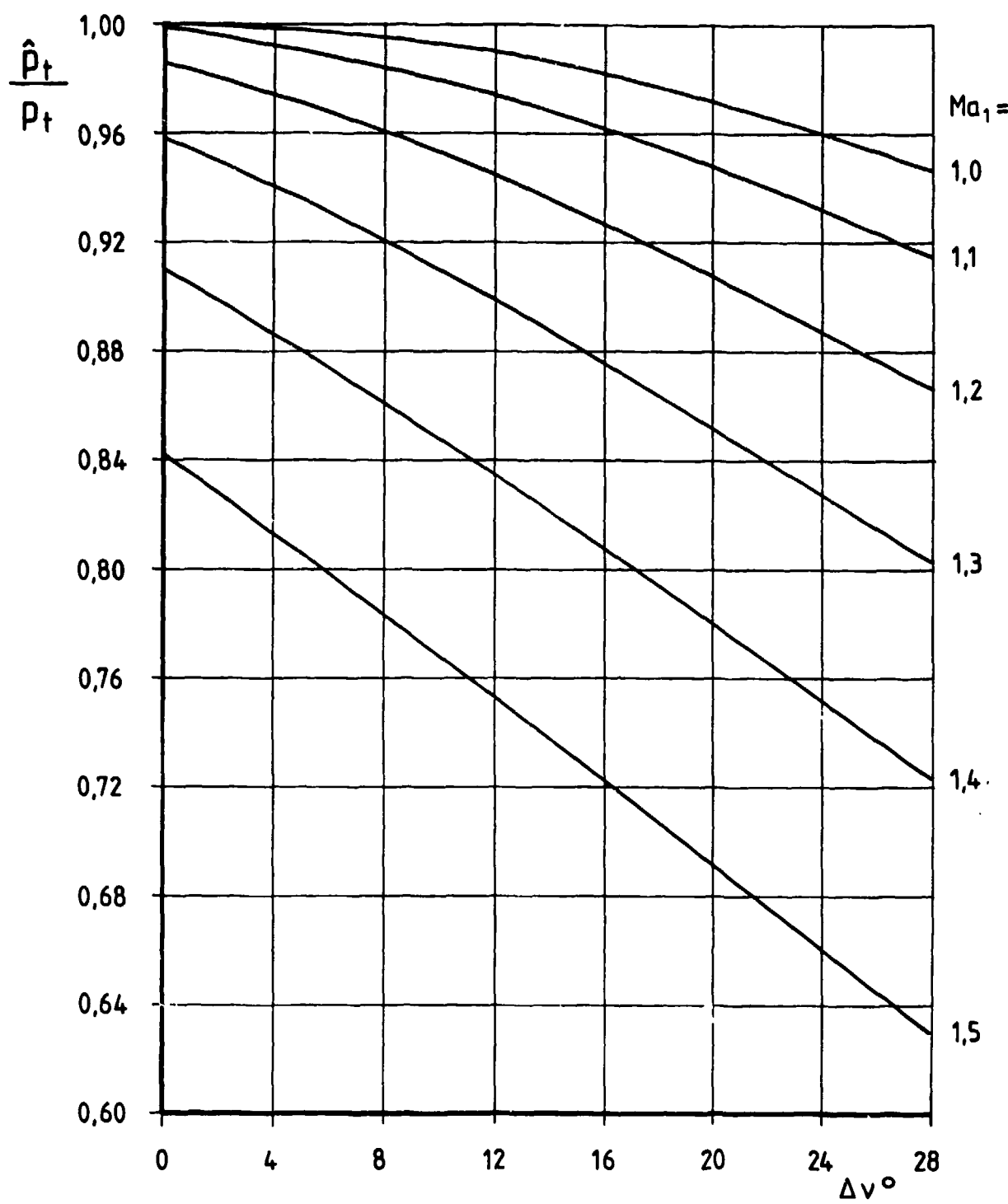


Fig. 2: Shock losses as function of inlet Mach number and supersonic expansion

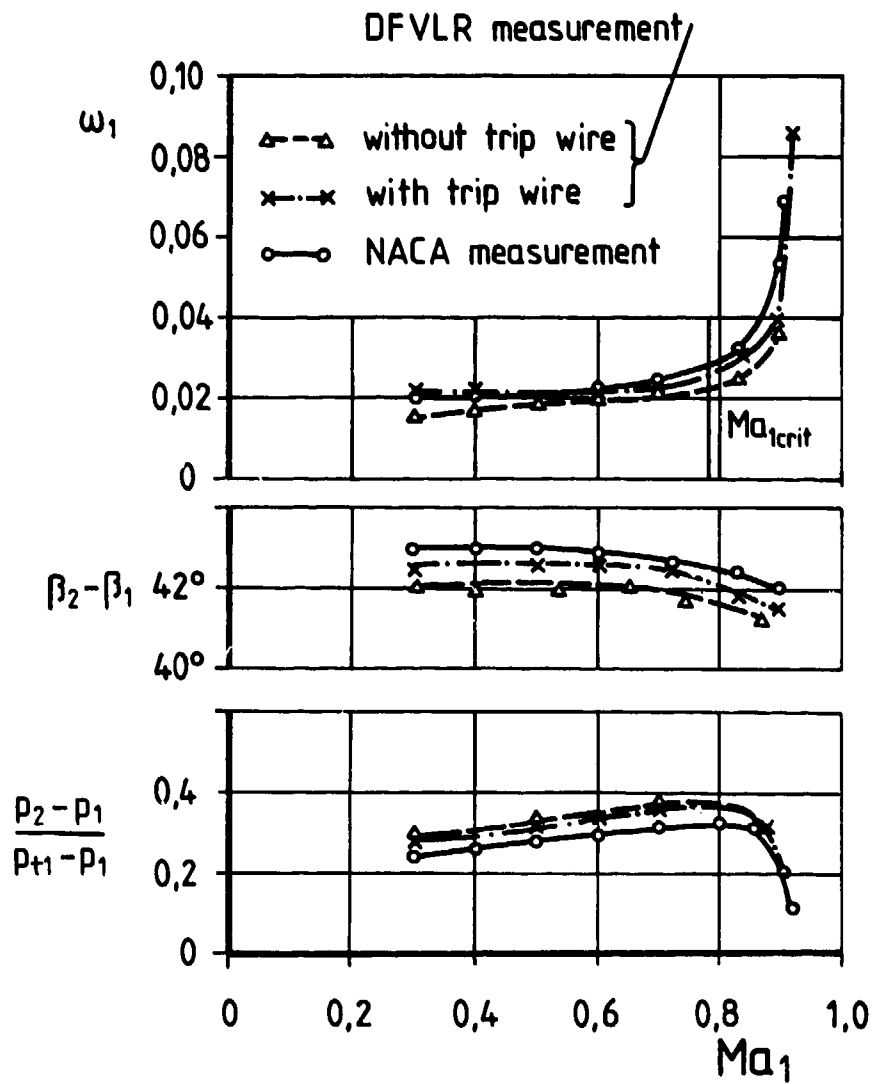


Fig. 3: Results of cascade measurements as a function of inlet Mach number

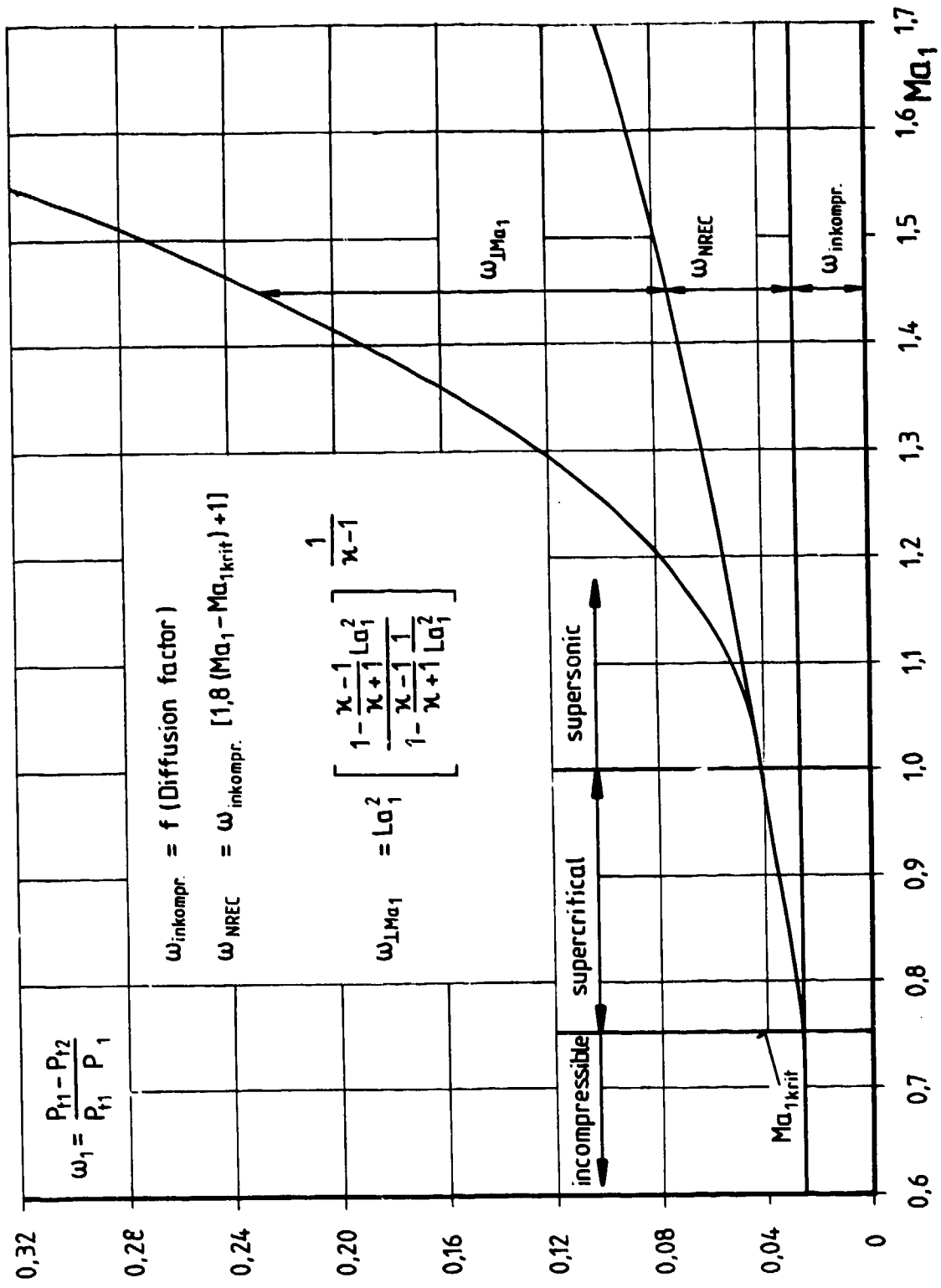


Fig. 4: Loss model including shocks and shock/boundary layer interaction

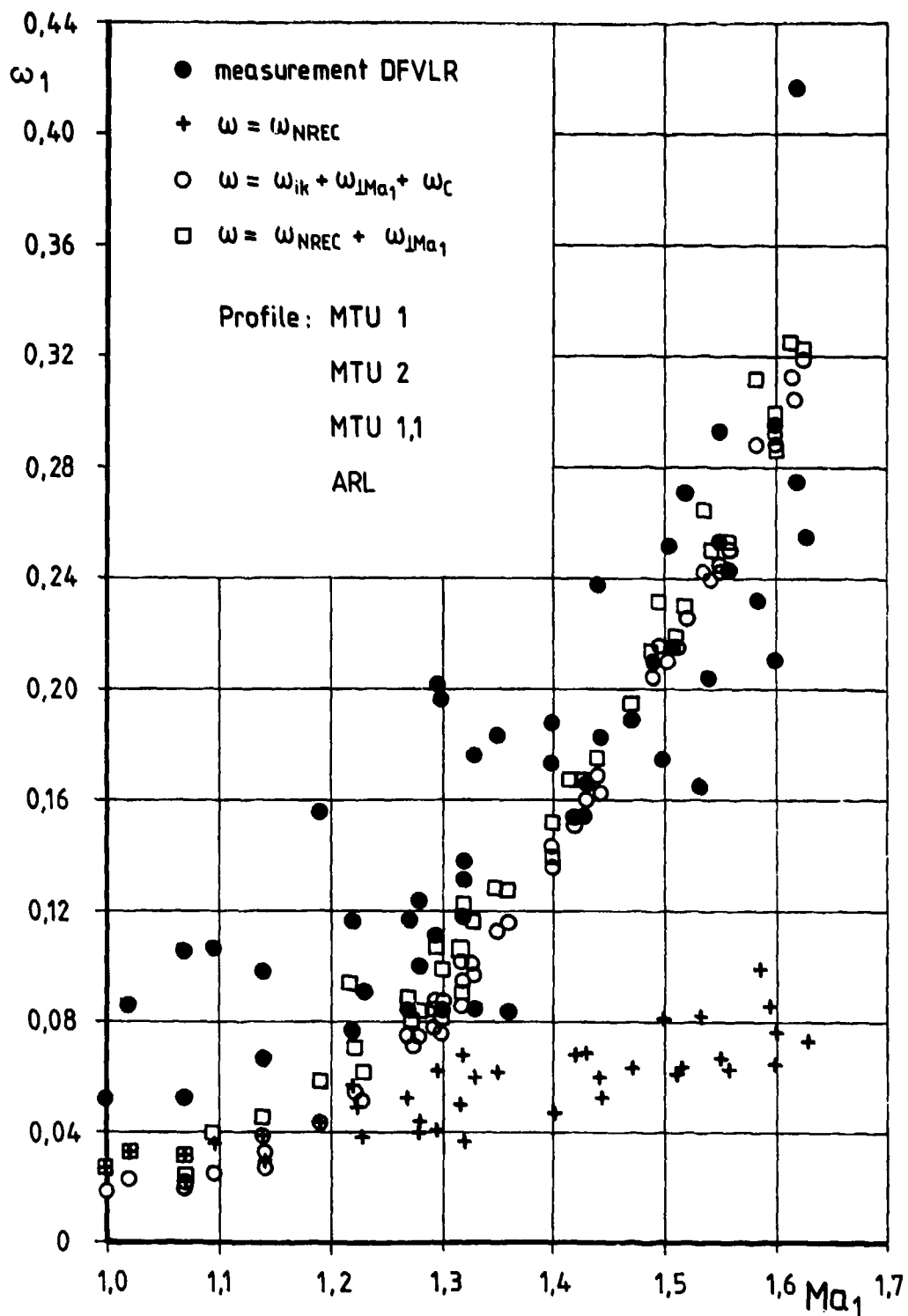


Fig. 5: Comparison of measured and calculated losses for different loss models

II.2.3. End-Wall Boundary Layer Calculation Methods

NOMENCLATURE

c velocity component
 C_f wall friction coefficient
 C_L lift coefficient
 F force defect
f blade force
h annular height
H total enthalpy
m mainstream coordinate
m mass flow
p static pressure
 p_t total pressure
r radius
s pitch
t transverse coordinate
t tip clearance
 T^o total temperature
u mainstream velocity component
v radial velocity component
U rotational speed
C absolute velocity
w transverse velocity component
W relative velocity
x axial coordinate
y coordinate normal to the wall
z tangential coordinate
 α flow angle
 β blade angle
 δ displacement thickness
 ϵ wall skewing angle
n efficiency
 θ momentum thickness
 ρ static density
 τ shear stress
 ψ pressure coefficient
 $\bar{\omega}$ pressure loss coefficient, rotor angular velocity
c solidity

Subscripts

m, y, t in streamline coordinates
 x, y, z in cartesian coordinates
e at the edge of the boundary layer
w at the wall

Superscripts

' fluctuation term
~ pitch averaged value

INTRODUCTION

Two ways can be defined to take into account the secondary flow effects on the performance of an axial compressor. The more classical way consists in defining correlations for the secondary losses as well as for the angle corrections and to distribute them in a certain way along the span. These losses are added to the profile and tip clearance losses and affect the overall efficiency. Although it is the most widely used method, correlations for secondary losses are subject to a large uncertainty and a large variety of formulas for the secondary loss coefficient can be found in the literature [1].

Another way, which will be discussed in this note, is based on a totally different approach. The starting point lies in the consideration that all secondary flow effects originate in the end-wall boundary layers along hub and shroud walls of the machine. Indeed, the existence of secondary flows is directly connected to the existence of an inlet boundary layer along the end wall and tied to its three-dimensional character. Therefore an estimation of the end-wall boundary layers and their development through the machine will provide information about the secondary flow effects, and define the efficiency drop due to the end-wall boundary layer losses.

When using end-wall boundary layer calculation methods, the basic flow equations are integrated in the pitchwise direction (pitch averaging) and over the boundary layer thickness, simplifying considerably the amount of information which is to be analysed. While detailed information is lost by integrating the equations, the method is able to take into account various aspects of secondary flow phenomena in pitch-averaged form.

The important properties of the end-wall boundary layers and their influence on the overall efficiency are based on the following considerations. One can, generally, distinguish three sources of effects on the end-wall boundary layer :

- i) The deviation of the main flow between two adjacent blades
- ii) The relative motion between blades and walls
- iii) The clearances at rotor tip and stator hub.

These three factors will not necessarily act in the same sense with the consequence that parameters such as geometrical details of the blading, initial boundary layer thickness, twisting of the blade, rotor-stator distance, e.a. could play an important role too.

The basic idea behind the calculation of the efficiency drop due to end-wall boundary layers lies in the fact that the blade sections in the boundary layer work under high incidences and hence do not perform any useful work, while the energy input per unit mass

flow is increased in these regions. Hence, there is a loss of efficiency compared to a situation without end-wall boundary layers. An elaborated end-wall boundary layer calculation procedure is able to deliver :

- i) A blockage factor which includes secondary flow effects, and which also affects the overall efficiency of the machine.
- ii) Terms defined as "force defect" which represent the blade force variations inside the boundary layers, and which on their turn affect the overall efficiency. The importance of these force defects is fully recognized in recent years and their non-zero value is responsible for possible equilibrium stage situations in multi-stage compressors where the boundary layer can reach an approximately constant thickness after a few stages.
- iii) With the introduction of families of velocity profiles in the boundary layers, radial variations of incidences and turning in the wall regions can be obtained. Also, with an extra assumption on the static pressure variation inside the boundary layer, full profiles of total pressures and hence of losses can be deduced (this would form a "local" alternative to the global approach consisting of defining an overall EWBBL efficiency loss). It therefore appears that the end-wall boundary layer method, with some adequate information for the force defect terms, provides a coherent and general approach for the through flow, including the influence on the overall efficiency.

SEVERAL PROPERTIES OF END-WALL BOUNDARY LAYERS

1. The three-dimensional character of the end-wall boundary layer

The turning of the flow through the blades gives rise to a transverse (pitchwise) pressure gradient which holds the centrifugal force, arising from the turning, in equilibrium. This pressure gradient is impressed on the wall boundary layer on account of the usual boundary layer properties, but centrifugal force is reduced inside the wall region due to velocity decrease. Hence, the dominating transverse pressure forces will act on the boundary layer flow and deflect the streamlines more strongly than outside the wall region. This simple fact can also be understood by considering that in order to maintain the same centrifugal force, and to satisfy the equilibrium equation

$$\frac{\partial p}{\partial t} = \frac{c_t^2}{r} \quad (1)$$

where t indicates transverse direction, the decrease in velocity has to be compensated by a decrease in curvature radius r .

Since this transverse pressure gradient acts from pressure side to suction side, the boundary layer streamlines will be deflected towards the suction surface. This implies the existence of transverse velocity components in the end-wall boundary layer and, through continuity, the existence of a secondary flow pattern (Fig. II.2.3.1), which is not confined exclusively to the boundary layer region. It should be noticed, however, that the existence of a secondary flow in the outlet plane of a blade row can, at least partly, be considered as an inviscid effect although one has to assume the existence of a wall boundary layer in the inlet plane of the blading.

In the language of inviscid fluids, this means the existence of a non-zero vorticity component in the transverse direction at inlet, which through turning round a spanwise direction, will give rise to a longitudinal component of vorticity, much in the same way as a gyroscopic effect. The intensity of the induced streamwise vorticity is proportional to the velocity gradient at inlet (the transverse vorticity of the inlet boundary layer) and the turning of the main stream.

This effect leads to an increase of flow deflection in the boundary layer compared with the deflection of the main stream, that is, an increase of circulation and hence of loading in the wall region. Also, as seen from Fig. II.2.3.1, the outlet angle, measured with respect to the axial direction, decreases in the wall region (Fig. II.2.3.2). One often speaks of overturning at the wall. It is clear then, supposing a two-dimensional wall boundary layer at inlet of the cascade, or what is also called a collateral boundary layer, that the boundary layer at outlet will no longer remain two-dimensional or collateral. One has a three-dimensional boundary layer where the velocity vectors are not all in the same plane. Projecting the velocities on the mainstream direction, one has profiles of the form indicated in Fig. II.2.3.3. An important parameter of these three-dimensional profiles is the angle of the streamline at the wall, or the limiting streamline, ϵ_w defined by

$$\operatorname{tg} \epsilon_w = \lim_{y \rightarrow 0} \frac{w}{u} = \lim_{y \rightarrow 0} \frac{\frac{\partial w}{\partial y}}{\frac{\partial u}{\partial y}} = \frac{(\tau_w)_t}{(\tau_w)_m} \quad (2)$$

where $(\tau_w)_t$ and $(\tau_w)_m$ are the wall shear stresses respectively in the transverse and the main direction. The angle ϵ_w is then also the angle of the resultant wall shear stress with the mainstream direction, u being the mainstream and w the cross-flow velocity component.

Various experimental and theoretical works have been carried out in order to make clear the properties of a turbulent three dimensional boundary layer (3DTBL). Most of the

efforts have been devoted to the analysis of the mean velocity profiles with the hope of putting forward a general form in the spirit of the law of the wall and wake profiles for two-dimensional turbulent boundary layers. This will not be discussed in this note.

2. The relative motion

The relative motion between a rotor and the shroud wall and between the stator and the hub wall exerts a profound influence on the nature of the boundary layer entering the blade row. In the following, we will concentrate on the rotor tip region.

2.1. Wall boundary layer entering the rotor

Supposing the wall boundary layer to be collateral before entering the rotor, the law of velocity composition $C=W+U$ allows to verify that the incoming boundary layer will not remain collateral relative to the rotor.

Moreover, Fig. II.2.3.4 shows that the absolute value of the entering velocity will not tend to zero when approaching the wall. On the contrary, the magnitude of the relative velocity will remain nearly constant. Fig. II.2.3.5 shows an isometric view of the boundary layer profile effectively entering the rotor as well as its resolution into the external relative streamline direction and the orthogonal transverse direction. It clearly appears that one has a highly skewed three-dimensional boundary layer entering the rotor, where the cross-flow components are oriented in a direction opposite to the blade velocity U , hence are directed from suction side to pressure side for a compressor.

From the energetic point of view one can say that the boundary layer receives a kinetic energy contribution from the relative motion and enters the rotor in a reenergized situation. One can also notice that the flow enters with high angles of attack in the boundary layer region.

2.2. Wall boundary layer deviation in the rotor

The secondary flow originating in the passage between two successive blades will act on the relative velocity profile entering the rotor. Whatever this profile may be, the action of the transverse pressure gradient is always directed towards the suction side of the blades, so that the transverse component at outlet will tend to be directed towards the suction side, that is in the direction opposite to the entering cross-flow component if the turning in the blades is sufficiently high.

In any case (\bar{W}_{out})_{b.l.} will be very near to the direction of \bar{W}_{out} if the turning is small, and to the left of \bar{W}_{out} with moderate to high turning blades (Fig. II.2.3.6). This indicates that the deflection will be much higher in the boundary layer than in the external flow, and also (Fig. II.2.3.6) that the absolute outlet angle α_{out} will be much higher in the boundary layer.

Consequently, one can expect the following behaviour at rotor outlet :

- i) The absolute outlet angle α_{out} increases when approaching the wall, and so does the deflection through the blade.
- ii) The tangential velocity variation Δc_z is distinctly higher in the boundary layer than in the external flow, with as consequence that the circulation for the whole blade row $\Gamma = 2\pi r \Delta c_z$ increases with decreasing distance from the wall.
- iii) The input energy for unit mass (or the input power for unit mass flow as measured by Euler's formula, $E = U \Delta c_z$, has the same behaviour as Γ and will also increase in the boundary layer.
- iv) Since the angles of attack in the boundary layer are large, they are generally not well matched to the blade geometry and the blade sections in this region will work under high incidences, leading to increased danger of local profile boundary layer separation with the subsequent increase in local profile losses. Added to the end-wall boundary layer losses, one can expect large total pressure drops or increased energy losses in these regions and therefore the blade sections in the end-wall region will operate under unfavorable conditions.

2.3. Wall boundary layer leaving the rotor

As shown in Fig. II.2.3.7 through an isometric view of the outgoing wall boundary layer, the composition of velocities when going over from the relative system to the absolute system leads here again to an absolute velocity profile whose magnitude is nearly constant and which does not go to zero at the wall. This is the situation inverse to the incoming profiles, where the role of absolute and relative velocities are interchanged. Fig. II.2.3.7 also shows a representative sketch of the axial and tangential profiles where the energizing effect of the relative motion on the wall boundary layer is seen and compared to the profiles of a "normal" boundary layer. It should however be observed here that these profile shapes, in particular the non-zero velocity at the wall, will soon be attenuated with axial distance due to the non-slip condition at the wall, and the skin-friction losses, indicating the importance of the axial clearance between rotor and stator, or the importance of axial distance of a measuring plane behind a rotor.

Clearly, the boundary layer flow is reenergized when leaving the rotor and the displacement thickness will be reduced, even if it was large at inlet. One does therefore not necessarily have an increase in boundary layer thickness with axial distance of the same amount as in ordinary boundary layers developing normally on a wall.

Summarizing, one can say that the regions near the wall receive an important amount of energy, since the flow is nearly tangential. This amount is larger than outside the boundary layer since $(\Delta c_z)_{b.l.}$ is larger than $(\Delta c_z)_e$. However this energy cannot be normally converted into useful work since the blades are operating under unfavorable conditions. The total pressure increase - or the useful work - does not follow the input energy increase, and the greatest part of the latter will be dissipated into heat, while part of it will also serve to reenergize the axial velocity profiles as shown in [2].

One can also expect then that in a multistage machine after a few identical stages, an equilibrium will be established between the energy supply and the dissipation in the boundary layer, so that the thickness of the wall boundary layer will remain nearly constant instead of increasing. This prediction as well as the energy supply in the wall region measured through the total temperature profiles according to

$$c_x \Delta c_z = c_p \Delta T_t \quad (3)$$

for a perfect gas, are well substantiated by experiments, as shown for instance by L.H. Smith [3] (Fig. II.2.3.8 and 9).

2.4. Implications on the forces acting on the fluid

The energy exchange takes place through the action of the tangential forces F_z , following

$$\frac{dP}{dm} = U \frac{dF_z}{dr} \quad (4)$$

where P is the shaft power, and dm the mass flow of a streamtube of width dr at radius r

$$dm = \rho c_x ds = \rho c_x 2\pi r dr \quad (5)$$

The total power at the shaft is given by

$$P = \int_{r_h}^{r_t} U dF_z = \int_{r_h}^{r_t} U f_z ds = \int_{r_h}^{r_t} 2\pi r U f_z dr \quad (6)$$

where the force f_z for unit surface $ds = 2\pi r dr$ of the axisymmetric streamtube is introduced. Outside the boundary layer, where the tangential shear stresses may be neglected, one has

$$\frac{dF_z}{dm} = \Delta c_{z_e} \quad \text{and} \quad f_{z_e} = \rho c_x \Delta c_{z_e} \quad (7)$$

Considering this expression as valid also in the boundary layer - as a first approximation - one sees that f_{z_e} will vary in the boundary layer as the product of two conflicting variable quantities. The increase of Δc_{z_e} will compensate in a certain way the decrease of axial velocity. Thus it is not impossible that f_{z_e} is larger than the tangential force outside the wall layer f_{z_e} in certain regions of the wall boundary layer.

It is however important to notice that the differences between f_z and f_{z_e} could be large and consequently it is not certain that one could neglect this difference with respect to the shear stresses in the boundary layer. Indeed, these differences are to be kept in the equations in order to arrive at a consistent picture.

3. Tip clearance effects

In the tip region of a rotor the wall relative motion is directed from suction side to pressure side of the next blade, for an observer moving with the rotor. Due to the wall shear stresses, fluid will be swept along by this wall motion in a sense opposite to the secondary flow deflection. Moreover, the pressure difference in the clearance region, from pressure side to suction side of the same blade will also induce a leakage flow opposite to the secondary flow. This clearance effects will therefore act against the influence of the relative motion on the wall boundary layer region. Since these effects increase when approaching the wall, one will observe a decrease of absolute outlet angle, tangential velocity variation, circulation and hence input energy (Fig. II.2.3.12) when approaching the wall. On the other hand, the total pressure increase in the clearance region will be reduced again with respect to the total pressure variation one would have without clearance, due to the leakage flow.

One has therefore a conflicting influence. On one hand, a small leakage flow will act against the negative influence of the skewed wall boundary layer, improving the flow conditions in this region. On the other hand clearance always reduces the useful work done on the fluid in the leakage flow region. Besides, a large clearance will strongly disturb the whole boundary layer flow but also will badly influence a large flow region outside the boundary layer. One understands then that an optimal clearance could exist, even if any clearance decreases the overall efficiency of a machine. This is indeed substantiated by cascade experiments [4] but it seems that optimum clearance would be too small to be realized in a machine.

Up to now, nothing has been said about the corner flows. This is indeed a complicated flow pattern where several concentrated vortices act in opposite senses, see e.g. [5]. Without clearance, one has a passage vortex, originating from the secondary flow which localizes in the corner between wall and suction side, where low energy boundary layer fluid accumulates and rolls up into a vortex, the passage vortex. With clearance, the leakage flow also produces a localized vortex, the tip clearance vortex, in the suction side corner, rolling up in opposite sense to the passage vortex and remaining next to it.

Moreover the motion of the blade relative to the wall in the clearance region has a "scraping effect" on the fluid which will accumulate in the pressure side corner of the blade (for a compressor, the pressure side is the leading side) and also finally roll up into a vortex with the same sense as the tip leakage vortex, the scraping vortex. The optimum clearance in cascades is explained by the conflicting action of the vortices in the suction side corner where, for small clearances, the tip clearance vortex attenuates the corner stall danger produced by the passage vortex.

In a real machine a given stage receives in fact a time averaged or equivalently the pitch averaged flow from the preceding stages and so does also a standing measuring instrument behind a blade row. Therefore it is not unreasonable to assume that little of the corner vortices will be noticeable in the pitch averaged flows. This is confirmed by the experiments of [2], where the transverse velocity component, as seen by a standing instrument behind the rotor, obeys a simple distribution law, the so called Mager profile law.

With regard to stall, one can expect that it will be conditioned by and arise in the regions where the flow is in the most unfavorable situation, that is in the end-wall regions. It is therefore possible to consider that stall will appear as soon as the end-wall boundary layers become too important, which is indeed an established experimental fact.

The quantitative influence of the clearance on the pitch averaged end-wall boundary layers and the effect on the efficiency will have to be introduced through some semi-empirical law connecting the force defect terms with the tip clearance.

REVIEW OF THE END-WALL BOUNDARY LAYER CALCULATION PROCEDURES

1. Basic equations

All the existing theories of wall boundary layer calculations in compressors involve solving the same basic boundary layer equations, mentioned here in their most general form. Each theory consists practically of making assumptions about two parameters, the direction of the force deficit and its magnitude.

Integrating the Navier-Stokes equations over pitch and boundary layer, the following general equation is obtained [6], all variables denoting pitch averaged values

$$\frac{d}{dx} c_{xe}^2 \bar{\theta} + c_{xe} \delta_x^* \frac{dw}{dx} = \frac{\tau_w}{\rho} + \bar{F} \quad (8)$$

where

$$c_{xe}^2 \bar{\theta} = \int_0^\delta (\bar{C}_e - \bar{C}) c_x dy = \int_0^\delta (\bar{W}_e - \bar{W}) c_x dy \quad (9)$$

$$c_{xe} \delta_x^* = \int_0^\delta (c_{xe} - c_x) dy \quad (10)$$

$$\bar{F} = \bar{F}_1 + \bar{F}_2 + \bar{F}_3 \quad (11)$$

$$\bar{F}_1 = \bar{l}_t \frac{1}{g} \int_0^\delta (\Delta p_e - \Delta p) dy \quad (12)$$

$$\bar{F}_2 = -\bar{l}_x \int_0^\delta \frac{d}{dx} (p_e - p) dy \quad (13)$$

$$\bar{F}_3 = -\rho \frac{d}{dx} \int_0^\delta (\widetilde{C}' c'_x - \widetilde{C}' c'_x) dy \quad (14)$$

or

$$\bar{F}_3 = -\rho \frac{d}{dx} \int_0^\delta (\widetilde{C}' c'_{xe} - \widetilde{C}' c'_{xe}) dy \quad (15)$$

The difference between (14) and (15) for \bar{F}_3 which contains the fluctuation terms is due to different approximations when averaging over the pitch, (14) being obtained by first integrating over the boundary layer thickness and (15) by first averaging the Navier-Stokes equations. From F_1 , F_2 and F_3 it follows that the direction of the total force deficit term is by no means obvious.

Equation (8) differs from standard integral momentum equations for three dimensional turbulent boundary layers by the presence of F in its r.h.s. These different defect forces play a fundamental role and represent the integrated difference in blade force over the boundary layer with respect to the blade force outside the end-wall boundary layer, including the "secondary stresses" $C' c'$ where C', c' are the deviations of the velocity components from axisymmetry, and are due partly to secondary flows. In order to close the system, additional assumptions are to be made with regard to the force deficit terms F .

2. Calculation of overall efficiency

According to section 1 and after solving the end-wall boundary layer equations, the corrected overall efficiency of the machine can be obtained through the definition of two "boundary layer" overall efficiencies which will be denoted as η_1 and η_2 . η_1 represents the overall efficiency drop only due to the boundary layer pressure losses and is a measure of the loss in output energy due to the presence of the end-wall boundary layers, while η_2 represents efficiency variations due to blade force variations inside the end-wall boundary layers and rotor shaft friction losses, and is a measure of the variations in rotor work due to the presence of the end-wall boundary layers. If $\hat{\eta}$ denotes the adiabatic efficiency of the machine which would be the total efficiency in absence of end-wall boundary layers, then the total efficiency is given by

$$\eta = \hat{\eta} \cdot \eta_1 \cdot \eta_2 \quad (16)$$

$$\eta = \frac{\Delta \int_{\text{hub}}^{\text{tip}} H^s dm}{\Delta \int_{\text{hub}}^{\text{tip}} \hat{H} dm} \quad (17)$$

and

$$\hat{\eta} = \frac{\Delta \int_{\text{hub}}^{\text{tip}} \hat{H}^s dm}{\Delta \int_{\text{hub}}^{\text{tip}} \hat{H} dm} \quad (18)$$

The efficiencies η_1 and η_2 are defined by

$$\eta_1 = \frac{\Delta \int_{\text{hub}}^{\text{tip}} H^s dm}{\Delta \int_{\text{hub}}^{\text{tip}} \hat{H}^s dm} \quad (19.a)$$

$$\eta_2 = \frac{\Delta \int_{\text{hub}}^{\text{tip}} \hat{H} dm}{\Delta \int_{\text{hub}}^{\text{tip}} H dm} \quad (19.b)$$

The head $\hat{\cdot}$ denotes values as they would be calculated in absence of end-wall boundary layers.

Both numerators and denominators of η_1 and η_2 can be related by the following equations.

$$\Delta \int_{\text{hub}}^{\text{tip}} H^s dm = \Delta \int_{\text{hub}}^{\text{tip}} \hat{H}^s dm - 2\pi \sum_{h,t} \Delta [\rho c_{xe}^2 (c_{xe} \theta_x + c_{ze} \theta_z)] \quad (20)$$

where the second term in the r-h-s is an approximation for the energy thickness

$$\rho \frac{C_e^2}{2} c_{xe} \delta^{**} = \int_{\text{hub}}^{\text{tip}} \rho c_{xe} \left(\frac{C_e^2}{2} - \frac{C^2}{2} \right) dr \approx \rho (c_{xe} \theta_x + c_{ze} \theta_z) c_{xe}^2 \quad (21.a)$$

and

$$\Delta \int_{\text{hub}}^{\text{tip}} H dm = \Delta \int_{\text{hub}}^{\text{tip}} \hat{H} dm - 2\pi \sum_{h,t} \int_{in}^{out} [r_w U_{blade} F_z - |r_w U_{wall} \tau_{zw}| - \rho c_{xe} \delta_x^* \frac{d}{dm} \hat{H}_w] dm \quad (21.b)$$

where the subscript w denotes wall values.

The total efficiency can be approximated in a one dimensional approach by [3]

$$\eta = \hat{\eta} \frac{1 - \sum_{h,t} \frac{\delta^*}{h}}{1 - \sum_{h,t} \frac{F_z}{h f_{ze}}} \quad (22)$$

It is to be noted that the displacement thickness δ^* can strongly be influenced by an axial force deficit F_z through equation (8). In general the axial defect force seems to affect the total efficiency through the displacement thickness in a more important way than the transverse component F_z .

3. Review of different assumptions

Starting from the basic equations, written here for convenience in cartesian coordinates

$$\frac{d}{dx} c_{xe}^2 \theta_x + c_{xe} \delta_x^* \frac{dc_{xe}}{dx} = \frac{\tau_x}{\rho} + \frac{F_x}{\rho} \quad (23)$$

$$\frac{d}{dx} c_{xe}^2 \theta_z + c_{xe} \delta_x^* \frac{dc_{ze}}{dx} = \frac{\tau_z}{\rho} + \frac{F_z}{\rho} \quad (24)$$

or in streamline coordinates [7]

$$\frac{d}{dm} u_e^2 \theta_1 + u_e \delta_x^* \frac{du_e}{dm} - u_e^2 (\theta_1 \operatorname{tga} + \theta_2) \frac{da}{dm} = \frac{\tau_m}{\rho} + \frac{F_m}{\rho} \quad (25)$$

$$\frac{d}{dm} u_e^2 \theta_2 + u_e^2 (\delta_x^* + \theta_1 - \theta_2 \operatorname{tga}) \frac{da}{dm} = \frac{\tau_t}{\rho} + \frac{F_t}{\rho} \quad (26)$$

where

$$\theta_1 = \bar{\theta}_1 m \cos a \quad (27)$$

$$\theta_2 = \bar{\theta}_1 t \cos a \quad (28)$$

and

$$\tau_t = \tau_m \operatorname{tga}_w \quad (29)$$

the following review can be made concerning the different theories.

- Railly and Howard [8] (1962)

Railly and Howard solved eq. (8) with $\bar{F} = 0$. They considered an "unbounded" axisymmetric boundary layer and didn't consider the interaction blade - boundary layer represented by F . The shear stress terms were evaluated using a shear stress coefficient related to the Reynolds number based on the boundary layer thickness. This method allows for the existence of a cross flow through eq. (26) which can be rewritten as, with $F=0$

$$\frac{d}{dx} u_e^2 \theta_2 = -c_{xe}^2 (\theta_x + \delta_x^*) \frac{dtga}{dx} + \frac{\tau_t}{\rho \cos a} \quad (30)$$

θ_2 being a direct measure for the cross flow. The first term of the r.h.s. of eq. (30) represents the pressure gradient which always tends to create an overturned flow, the second term is the cross shear stress which always acts against the cross flow. No efficiency corrections were introduced by Railly and Howard.

- Cooke and Hall [9] (1967)

Cooke and Hall proposed principally the same equations as Railly and Howard, but written in streamline coordinates and using four impulse moment thicknesses.

- Stratford [10] (1967)

Stratford's main intention was to estimate the blockage factor due to the end-wall boundary layers without considering detailed secondary flow effects. Stratford assumed there is no variation of flow angle within the boundary layer, always giving a collateral flow. In this way, only one of the momentum equations is to be solved, namely eq. (23), the axial defect force F_x being zero. In this case the cross flow equation (26) reduces to

$$\frac{F_z}{\rho} = \frac{F_t^{\text{coll}}}{\rho \cos a} = c_{xe}^2 (\theta_x + \delta_x^*) \frac{dtga}{dx} \quad (31)$$

The transverse defect force denoted as F_t^{coll} vanishes with the pressure gradient term in eq. (26), eliminating the origin of the passage secondary flow. Physically, this means a decrease in blade force inside the boundary layer, giving an increase in efficiency through equation (22).

Thus the method implies the existence of a defect force directed in the transverse direction z and which should be taken into account when calculating the overall efficiency of the machine. The validity of this simplified method is questionable, since the assumption of collateral flow cannot be valid at inlet of a multi-stage compressor blade row, where a strong inlet cross flow is present due to relative motion (see Fig. II.2.3.5). However it should be repeated that Stratford developed this method only to compute the end-wall boundary layer blockage without introducing explicit efficiency correlations.

- L.H. Smith [3] (1969)

L.H. Smith presented an experimental analysis of the dependency of the end-wall boundary layer on aerodynamic loading, blade-to-blade passage width and tip clearance, in the case of a repeating stage configuration. He showed the experimental evidence of defect forces and analysed the repercussion of the end-wall boundary layer parameters on the overall stage efficiency. Moreover, some simple correlations based on test results for tip clearance effects and force defects are also given. L.H. Smith proposed to impose a growth in blockage due to the tip clearance t_c through

$$\delta^* = \delta^*_{t_c=0} + \frac{\psi}{\psi_{\max}} t_c \quad (32)$$

This correlation is illustrated in Fig. II.2.3.11. Extrapolating this correlation to the basic equations, it would imply an axial defect force component proportional to t_c/c . On Fig. II.2.3.12 an idea is given of experimental results for a non-dimensionalized tangential force defect defined as

$$\frac{v}{\delta^*} = \frac{F_z}{\delta^* f_{ze}} \quad (33)$$

where $v = \frac{1}{f_{ze}} \int_0^\delta (f_{ze} - f_z) dy$ and $f_z = \rho c_x \Delta c_z$ (34)

Tentatively a value of 0,65 was given for v/δ^* . It is to be noted that the force deficit defined by L.H. Smith does not include all the force deficit terms defined in eq. (11).

- Horlock [11] (1969)

Horlock considered a three dimensional bounded boundary layer by introducing distributed body forces representing the action of the blades. He used hypothetical axisymmetric equations written in streamline coordinates and found extra terms - absent in Cooke and Hall's equations - which are due to the presence of a non zero vorticity normal to the wall outside the boundary layer, while Cooke and Hall's hypothetical flow was irrotational. These equations are equivalent to the basic ones (8) with zero defect forces and were applied by Horlock and Hoadley [12]. They allowed for variations of the flow angle across the boundary layer and assumed Coles and Mager velocity profiles. They used an averaged entrainment equation. The force defect terms were not considered.

- Mellor and Wood [13] (1970)

Mellor and Wood considered the bounded boundary layer equations and averaged them in the cartesian coordinate system. All fluctuation terms, including blade profile shear stresses were grouped in generalized, effective blade forces. The basic equations were integrated over the blade length, connecting inlet and outlet thicknesses directly. They assumed the defect force nearly perpendicular to the blades (introducing a small parameter) and eliminated its magnitude by combining both momentum equations. A semi-empirical correlation for the cross flow thickness θ_2 at outlet of a blade row was introduced based on secondary flow considerations, this thickness being zero in absence of tip clearance. With present notations, this correlation can be written as

$$(u_e \theta_2)^{out} = K t_c u_e^{C^{1/2}} \sin \Delta c_{ze} \quad (35)$$

In this case, the cross momentum equation (26) becomes, assuming a linear variation of $u_e^2 \theta_2$

$$\frac{d}{dx} u_e^2 \theta_2 = \frac{(u_e \theta_2)^{out}}{x - x_{out}} \quad (36)$$

implying a defect force in the t direction

$$\frac{F_t}{\rho c \cos \alpha} = \frac{F_t^{\text{coll}}}{\rho c \cos \alpha} + \frac{(u_e \theta_2)^{out}}{x - x_{out}} - \frac{\tau_t}{\rho c \cos \alpha} \quad (37)$$

This concept allows for negative values of the axial defect forces, with as a consequence the possibility of a quasi-equilibrium of the boundary layer after a few stages, through the axial component of equation (8) or through eq. (23). In this way a complete repeating stage configuration can be predicted.

It is to be noted that Mellor & Wood's method was the first to deliver a complete useful method, including the main secondary flow effects and the corrected efficiencies discussed in section 2.2. Although both hypothesis of direction of defect forces and cross flow at outlet of a blade row have no direct confirmation, the method delivers good results [14] [15].

- Marsh and Horlock [16] (1971)

Marsh and Horlock made a detailed analysis of the different ways to obtain the momentum equations and presented a large part of the present review. They analysed the defect forces in the case of a "many bladed" cascade, assuming the cross flow as practically inexistant. They presented the defect force corresponding with a collateral flow as

$$\frac{F_z}{\rho} = c_{xe}^2 (\theta_x + \delta_x^*) \frac{dt \tan \alpha}{dx} \quad (38)$$

$$F_x = -F_z \tan \alpha \quad (39)$$

This corresponds to the value of F_t^{coll} in equation (31).

The concept of using these forces does not take into account the effects of a cross flow at inlet of a blade row, as is the case in a turbomachine. This difficulty can be solved

by using Mellor & Wood's method, which is equivalent with Marsh & Horlock's equations in the case of zero cross flow at inlet and in absence of tip clearance (eq. 37), or by adding an extra defect force, as done by Horlock & Perkins [17].

The always positive axial defect force predicts an increase in boundary layer thickness. However, the corresponding efficiency drop is compensated by positive values of F_z in eq. (22). Lindsay [18] proposed the use of F_z^{coll} and zero axial defect force, which principally corresponds to Stratford's method, giving principally lower values of blockage.

- Daneshyar [19] (1972)

Following Marsh & Horlock [16], Daneshyar presented the complete derivation of equation (8) in both cartesian and streamline coordinate systems where the different force defect terms are discerned. He also proposed the use of force defects which partly compensate the transverse pressure gradient terms in eq. (26) using an empirical factor giving

$$F_z = k F_z^{\text{coll}} \quad (40)$$

- Horlock and Perkins [17] (1974)

Besides an interesting review, Horlock & Perkins presented a detailed calculation method which is principally based on the calculation of the overall secondary losses. They separated completely the calculation of blockage, tangential defect force F_z and extra secondary losses. In order to estimate the blockage they started from Stratford's principle by integrating only the axial momentum boundary layer equation (23), but they added an axial defect force depending uniquely on the tip clearance.

$$F_x = K_f t_c f_x e \quad (41)$$

$f_x e$ being the axial blade force component outside the boundary layer and K_f being a correction factor for high clearances.

$$K_f = 1 - \frac{t_c}{2t_{\max}} \quad (42)$$

t_{\max} being the maximum thickness of the blade profile. This method corresponds principally with the tip clearance correlation presented by L.H. Smith [3] when $K_f=1$.

Horlock & Perkins used an entrainment relation and a simple skin friction relation borrowed from Stratford's method. They did not solve the transverse momentum equation (24), but only estimated the transverse force defect. This defect force is based on the "collateral" force defect discussed earlier, but they added two extra correction terms :

- i) The effect of a skewed inlet flow is included. Assuming this inlet skew to be only due to relative motion, the following force defect is necessary to remove the flow in the collateral direction, L being the length over which the collateral flow is restored

$$\frac{F_z}{p} = - \frac{1}{L} (U_c x_e \theta_x)_{\text{inlet}} \quad (43)$$

- ii) The tip clearance also leads to a tangential defect force since the blade force vanishes over the clearance gap. The corresponding force defect was proposed as

$$\frac{F_z}{p} = K_t t_c f_{ze} \quad (44)$$

where K_t is a correction factor proposed as 0,44.

The total tangential defect force used by Horlock & Perkins, taking all these effects into account was

$$\frac{F_z}{p} = 0,44 \delta_x^* + K_t t_c \quad (45)$$

Besides the end-wall boundary layer losses, extra secondary losses were finally taken into account in the estimation of the blade profile loss coefficients. Horlock & Perkins only considered the effect of the highly skewed inlet flows inside the boundary layers, which induce incidence losses. This loss was taken proportional to the averaged kinetic energy normal to the inlet reference flow, being a measure for the inlet skew, giving

$$\bar{w} = 2 \frac{k}{h} \sum_{h,t} \left(\frac{U_c^2 x_e \theta_x}{4 u_e^4} \right)_{\text{inlet}} \quad (46)$$

They suggested a value $k=0,2$. For turbines, they suggested extra secondary loss correlations for passage secondary flow and tip clearance losses.

Their equations were all written in a meridional coordinate system, taking radii variations into account.

- Hirsch [7] (1976)

Hirsch presented a method principally based on Mellor & Wood's method but with equations written in streamline coordinates. He introduced Power and Mager laws for the velocity profiles, which led to the use of passage averaged boundary layer equations written in

the streamline coordinate system. A modified version of the secondary flow equation (35) of Mellor & Wood was used allowing for non-zero cross flows at outlet of the blade rows by introducing an extra empirical parameter K_2 .

$$(u_e \theta_2)_{\text{out}} = (K_1 t_c - K_2 c) u_e C_L^{1/2} \text{sign} \Delta c_{ze} \quad (47)$$

- De Ruyck, Hirsch and Kooi [6] (1978), [20] (1979)

- De Ruyck and Hirsch [21] (1980)

In reference [6] the authors presented equation (8) and introduced mainstream and cross-flow boundary layer profile models in order to obtain a complete description and prediction of the radial flow distribution including the end wall boundary layer regions.

An analysis is made of the different force defect assumptions and the following expressions are finally proposed

$$\frac{F_t}{\rho} = -k u_e^2 \frac{\theta_2}{s} \quad k \approx 1 \quad (48)$$

for the transverse component of the force defect while it is shown theoretically that the axial force defect component has to be proportional to the end wall losses, namely secondary and clearance losses, leading to

$$\frac{F_x}{\rho} = C_D \frac{u_e^2}{2} \frac{h \sigma}{g} \quad (49)$$

where g is the axial chord.

The drag coefficient C_D is given by

$$C_D = C_{D_S} + C_{D_T}$$

where C_{D_S} is due to the secondary losses and taken to be

$$C_{D_S} = 0.01 C_L^2 \frac{c}{h} \quad (50)$$

and C_{D_T} is due to the leakage losses and is taken to be

$$C_{D_T} = K C_L^2 \frac{t_c}{h} \sigma \quad (51)$$

with $K=0.3$.

In Fig. II.2.3.13 a comparison is given between different assumptions for the blade force defect showing that assumption (48) predicts the correct behaviour for boundary layer flows with inlet skew.

RESULTS TO BE EXPECTED FROM A EWBL APPROACH

The introduction of an end-wall boundary layer approach in a performance prediction method allows accounting for the secondary flow effects in a consistent way, as well as the calculation of the end wall blockage.

The through-flow calculation coupled interactively with an end wall boundary layer calculation method leads to a prediction of the efficiency drop due to the secondary flow effects whereby the through flow calculation acts as a mainstream "potential" type flow for the boundary layer.

The interaction of the through flow and the wall layers is illustrated in Fig. II.2.3.10 and it should be noted that the losses in the through-flow calculation have to be restricted, within this approach, to the profile and shock losses, all secondary losses being considered as part of the EWBL efficiency drop.

From results obtained in [20] and [21] it appears that most of the known effects are correctly predicted by the end wall boundary layer calculation. For instance, Figure II.2.3.14 illustrates the calculated maximum efficiency in function of tip clearance for various aspect ratios.

The influence of aspect ratio and tip clearance, Fig. II.2.3.15 and 16 is seen also to be well predicted as well as the influence of the axial gap between rotor and stator, Fig. II.2.3.17. Moreover, the introduction of velocity profiles, as in the method of (20) and (21) allows the prediction of complete profiles over the whole span. Figures II.2.3.18 and 19 show velocity and angle variation in the mainstream and the wall regions compared to experimental data for two different compressors. Thus an estimation of the stall limit as an end wall boundary layer separation is obtained and figure II.2.3.15 to 17 show that this estimation is a valid approximation to the stall limit as function of mass flow rate.

CONCLUSIONS

The end-wall boundary layer approach to secondary losses is based on the integration of the pitch-averaged three-dimensional boundary layers along the hub and tip walls, with extra assumptions for the blade force defect terms. From there an efficiency drop is calculated including secondary flow effects, as well as blockage.

The method allows in principle for the influence of inlet blockage, clearance, axial gap, aspect ratio and other parameters to be included through their effect on the end-wall boundary layers.

From the knowledge of the velocity profiles inside the boundary layers, the full radial variations of incidence and turning can be predicted (Fig. II.2.3.19) by coupling a radial equilibrium calculation to the EWBL calculation.

Similarly, with an assumption on the static pressure variation within the boundary layer total pressure and hence local loss coefficients can be estimated in the boundary layer regions as function of radius. This could lead to an alternative to the present approach, by using the loss and turning predictions in the EWBL region to estimate local efficiencies instead of the global efficiency drop (see calculation of overall efficiency).

This alternative illustrates the generality of the EWBL approach, based on a consistent set of equations, radial equilibrium and boundary layer equations, and a limited set of semi-empirical data for the force defect terms.

Since this approach is based on the integration of two equations it was not possible within this short review to discuss all the implications. However, more experimental data should allow to gain more insight in the validity of the various assumptions with regard to the turbulent properties of the end-wall boundary layers as well as with regard to the force defect hypothesis.

REFERENCES

- [1] J.W. SALVAGE, "Investigation of Secondary Flow Behaviour and End-Wall Boundary Layer Development Through Compressor Cascades", VKI, technical Note 107, 1974
- [2] A. MAGER, J. MAHONEY, R.W. BUDINGER, "Discussion of Boundary Layer Characteristics near the Wall of an Axial Flow Compressor", NACA Report 1085, 1952
- [3] L.H. SMITH, "Casing Boundary Layers in Multistage Axial Flow Compressors", Flow Research on Blading, Brown Boveri Symposium, Elsevier, 1969
- [4] J.H. HORLOCK, J.F. LOUIS, P.M.E. PARCEVAL, B. LAKSHMINARAYANA, "Wall Stall in Compressor Cascades", Trans ASME, Series D, 88, 637, 1966
- [5] A.G. HANSEN, H.Z. HERZIG, "Secondary Flows and Three-Dimensional Boundary Layer Effects", NASA SP36, Aerodynamics Design of Axial Flow Compressors, Chapt. XV, 1965
- [6] J. DE RUYCK, Ch. HIRSCH, P. KOOL, "An Axial Compressor End-Wall Boundary Layer Calculation Method", ASME Journal of Eng. for Power, Vol. 101, n°2, 1979, 233-249
- [7] Ch. HIRSCH, "End-Wall Boundary Layers in Axial Compressors", ASME paper n° 74-GT-72
- [8] J.W. RAILLY, J.H.G. HOWARD, "Velocity Profile Development in Axial Flow Compressors" J. Mech. Eng. Sci. p. 166, Vol. 4, 1962
- [9] J.C. COOKE, M.G. HALL, "Boundary Layers in Three Dimensions", Ch 2 in Progress in Aeronautical Sciences, Vol 2, Boundary Layer Problems, Pergamon, 1962
- [10] B.S. STRATFORD, "The Use of Boundary Layer Techniques to Calculate the Blockage from the Annulus Boundary Layers in Compressors", ASME paper n° 67-WA/GT-7
- [11] J.H. HORLOCK, "Boundary Layer Problems in Axial Turbomachines", Flow Research on Blading, Brown Boveri Symposium, Elsevier 1969
- [12] J.H. HORLOCK, D. HOADLEY, "Calculation of the Annulus Wall Boundary Layers in Axial Flow Turbomachines", Aero Research Council n° 31, 955, 1970
- [13] G.L. MELLOR, G.M. WOOD, "An Axial Compressor End-Wall Boundary Layer Theory", Trans. ASME, Series D, Vol 93, p 300, 1971
- [14] T.F. BALSA, G.L. MELLOR, "The Simulation of Axial Compressor Performance Using an Annulus Wall Boundary Layer Theory", ASME J. Eng. Power 305-318, 1975
- [15] K.G. GRAHL, "Prediction of Compressor Aerodynamic Performance for Multistage Compressors", Dynalysis of Princeton, Report n°29
- [16] H. MARSH, J.H. HORLOCK, "Wall Boundary Layers in Turbomachines", Joun. of Mech. Eng. Vol. 14, 6, p 411, 1972
- [17] J.H. HORLOCK, H.J. PERKINS, "Annulus Wall Boundary Layers in Turbomachines", AGARD AG 185, 1974
- [18] W.L. LINDSAY, 'Tip Clearance Effects in the Growth of Annulus Wall Boundary Layers in Turbomachines", Ph.D. Thesis, Cambridge Univ. 1974
- [19] M. DANESHYAR, "Annulus Wall Boundary Layers in Turbomachines", Ph.D. Thesis Cambridge Univ. 1973

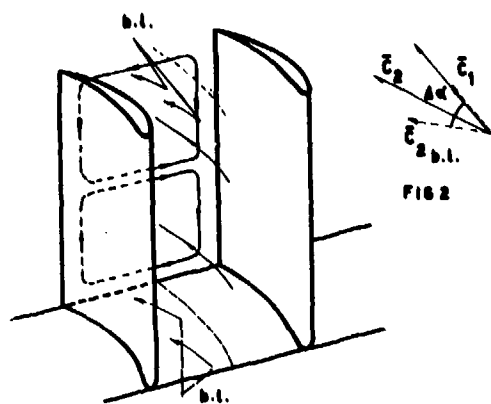


Figure II.2.3.1 : Secondary flow and boundary layer due to skewing

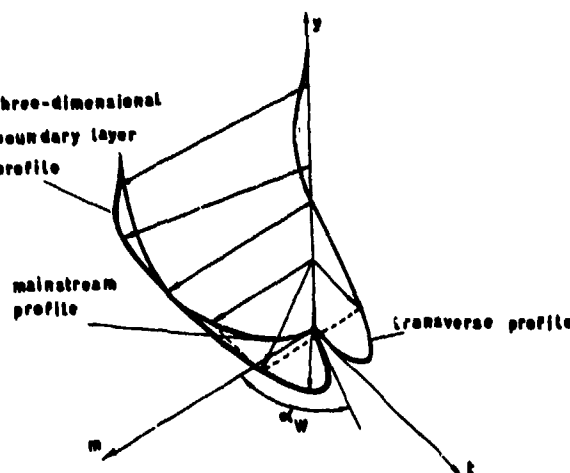


Figure II.2.3.3 : Velocity profiles

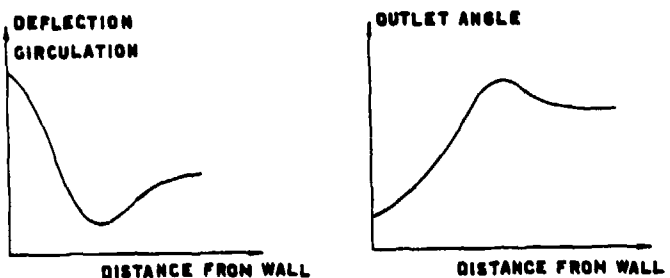


Figure II.2.3.2

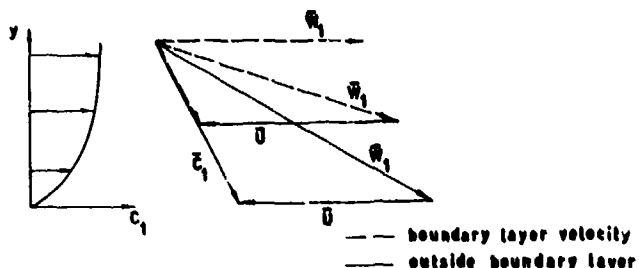


Figure II.2.3.4 : Skewing of relative profiles due to relative motion

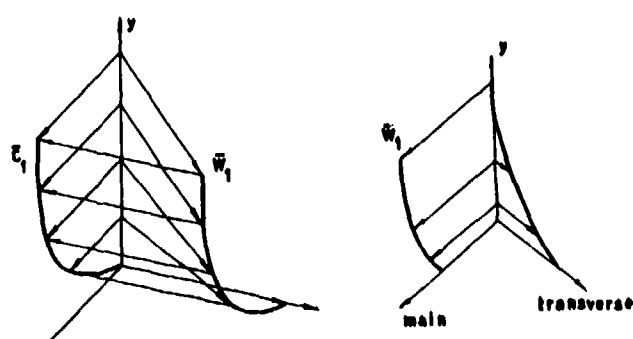
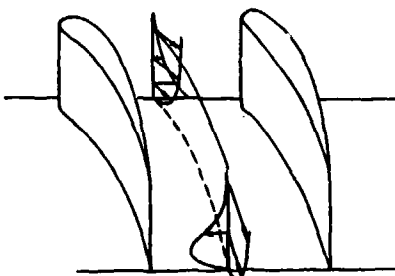


Figure II.2.3.5 : Skewing of relative velocity profile due to the relative motion between blades

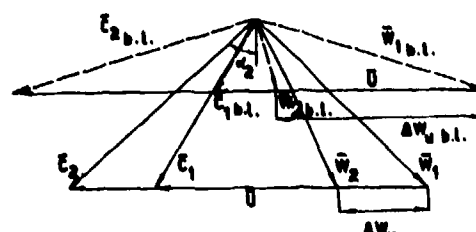


Figure II.2.3.6 : Wall boundary layer at outlet of rotor blade

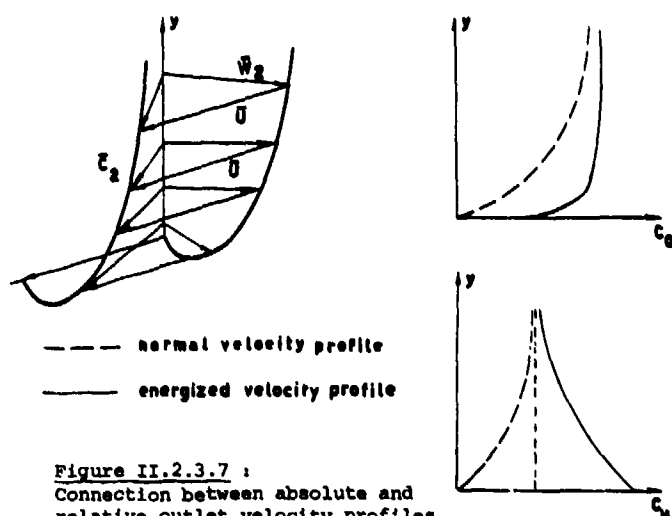


Figure II.2.3.7 :
Connection between absolute and
relative outlet velocity profiles

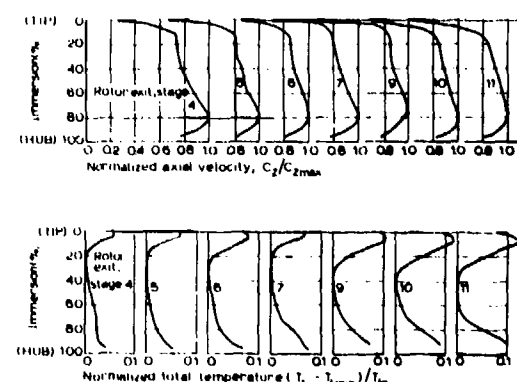


Figure II.2.3.8 and 9 :
Transverse measurements obtained from a twelve
stage compressor, from [3]

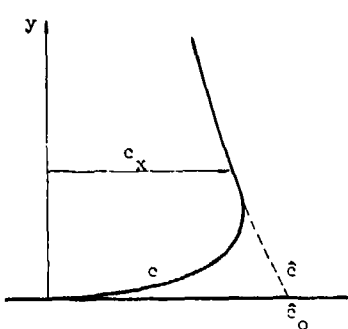


Figure II.2.3.10

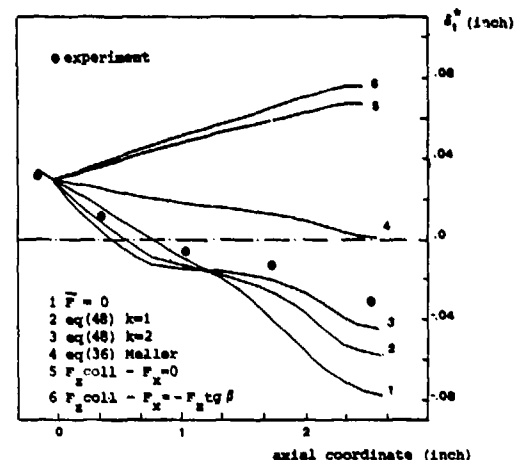


Figure II.2.3.13 :
Comparison of different assumptions for the force
defects with experimental data from
Moore and Richardson, from [6]

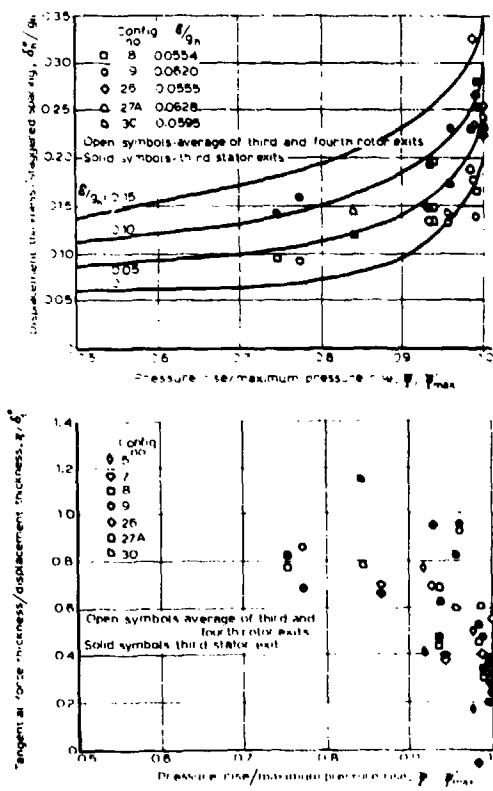


Figure II.2.3.11 and 12 :
GE 4 stage compressor
experimental boundary layer data, from [3]

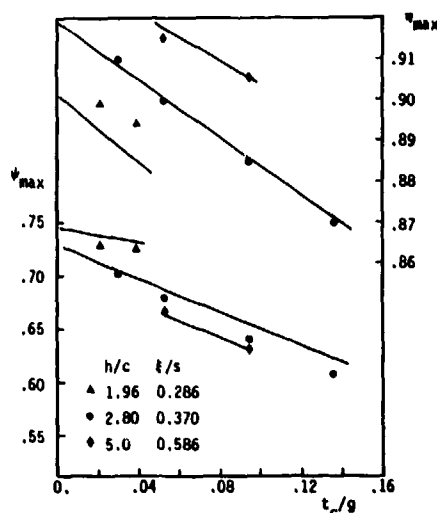


Figure II.2.3.14 :
GE 4 stage compressor
experimental and calculated data for
various aspect ratio and clearance [6]

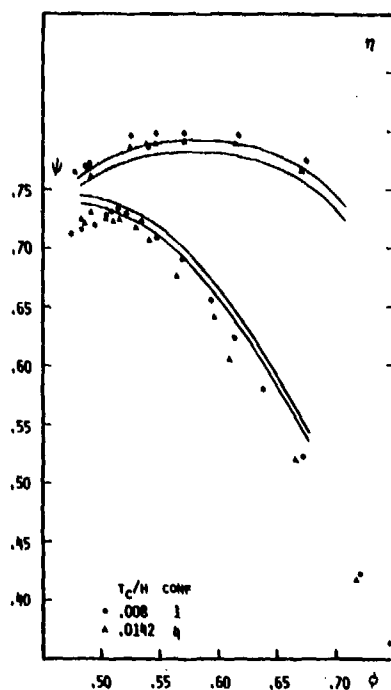


Figure II.2.3.15 : Low aspect ratio

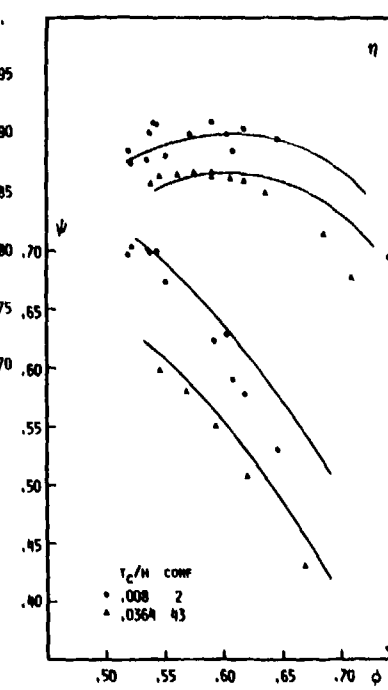


Figure II.2.3.16 : Mean aspect ratio

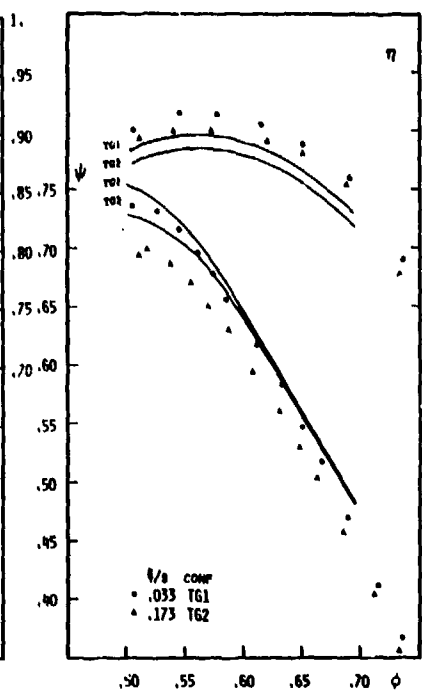


Figure II.2.3.17 : Two values of axial gap

General Electric Four Stage Compressor
Comparison between calculated and
measured characteristics, two values of
tip clearance, from [20]

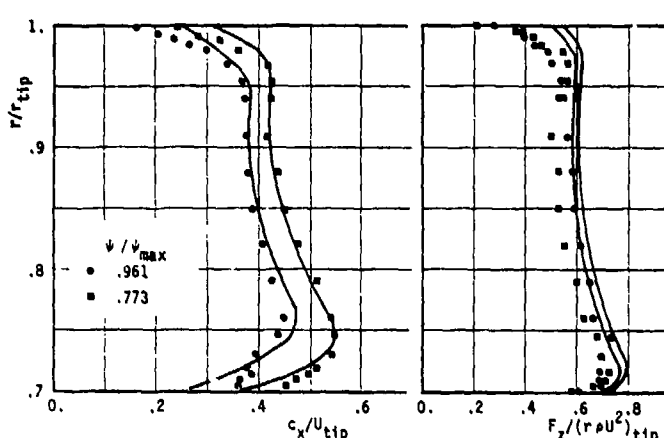


Figure II.2.3.18 : GE configuration 9
axial velocity and tangential
blade forces, solid line : calculated
from [20]

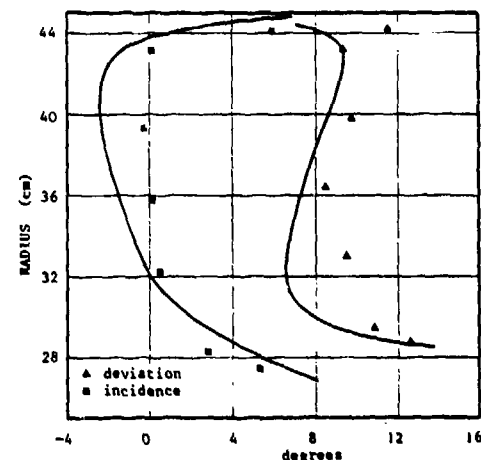


Figure II.2.3.19 : TASK II compressor
0°/0° schedule
Comparison between calculated and
measured stator incidence and deviation
angles near design point, from [21]

[20] J. DE RUYCK, Ch. HIRSCH, P. KOOL, "Investigation on Axial Compressor End-Wall Boundary Layer Calculations", Int. Joint Gas Turbine Congress, July 1979, HAIFA-ISRAEL

[21] J. DE RUYCK, Ch. HIRSCH, "Investigations on an Axial Compressor End-Wall Boundary Layer Prediction Method", 25th Annual Int. Gas Turbine Conference - New Orleans, March 1980, ASME Journal of Eng. for Power, Vol. 103, n°1, 1980, p. 20

II.2.4. CORRELATION FOR SECONDARY FLOWS AND CLEARANCE EFFECTS

INTRODUCTION

As indicated by Hirsch (1) in his review paper made for WG 12, in the field of secondary flow effects, to which belongs the influence of clearance, two approaches are possible when these effects are to be explicitly treated :

- Additional losses and modification of deviation can be calculated separately and added to the basic profile effects, for inclusion in the procedure for generalised radial equilibrium calculation, either as an average correction on blade height, or as a function of radius. For the clearance case, attempts can be made to introduce specific corrections, independent of the ones due to secondary flows with zero clearance.

- Calculation can be accomplished through a pseudo end wall boundary layer approach, leading either to a global correction on efficiency, and/or to a detailed description of the flow near the end walls, which is then matched to the "main flow" in the meridional plane, as calculated by the generalised radial equilibrium equation, in which only the profile and shock losses are introduced.

In the opinion of the author, this second approach is preferable as it is physically more sound, and leads to a coherent system for the prediction of blockage, force defect and additional losses due to secondary flow and clearance, taking into account, albeit in a synthetic way, the effect of relative motion between successive blade rows.

However, to provide a basis as complete as possible, the WG has decided to review some of the information available in the open literature on the explicit correlations for losses and turning due to secondary flows without clearance and to clearance effects, corresponding to the first approach. This is the sole object of this paper, the boundary layer approach being discussed elsewhere.

For the aspect of cascade secondary flow effects, without clearance the readers are referred to Salvage's comprehensive paper published by VKI(2). Conclusions on their use will be presented at the end of this paper.

For the clearance aspect correlations for losses and turning will be reviewed and compared for simple cases. As most of the data has been obtained from cascade tests, it will then be attempted to ascertain the validity of the application of cascade data to axial compressors.

Finally, the possible ways of utilizing the data for compressor performance prediction will be briefly discussed.

For both secondary flow and clearance effect, correlations specific to turbines were included, because their formulation covers basic factors relevant also for compressors.

It is clear however that the experimental calibration which has been made for the turbine case cannot be applied as such to compressors.

LIST OF REFERENCES FOR THE INTRODUCTION

1. HIRSCH, Ch. : "Axial compressor performance prediction survey of deviation and cross-correlation". WG12 Working Paper, March 1978.
2. SALVAGE, J.W. : "A review of the current concept of cascades secondary flow effects". VKI TN. 95, March 1974.

I. REVIEW OF EXISTING CORRELATIONS

A. Losses

There exists a large number of correlations or of theoretical expressions for the clearance loss calculation. Most of them are derived from a straight cascade model (cascade with constant blade profile, chord, stagger and pitch-chord ratio), some specifically for turbine application, others covering both compressor and turbines. Practically all the formulae have been derived for incompressible flows, with AVDR equal to unity and are meant to describe a pure clearance effect, the secondary flow influence being estimated separately and supposed independent of the clearance effect.

1. Parameters considered

- Loading effects

The formulae can be classified as follows :

- those which attribute the losses to a drag induced by the tip vortex created either by a lift reduction in the clearance space or by the rolling up of the clearance flow, considering only the effect of clearance from pressure to suction side and not from upstream to downstream. The induced drag is then proportional to C_{LM}^2 . Note that in the incompressible regime the lift coefficient is linked to both the upstream-downstream pressure difference (through the axial force) and to the pressure side suction side pressure difference (through the tangential force) as shown by a reasoning similar to the one used for establishing the diffusion factor formulae.
- those which attribute the loss to the dissipation of the kinetic energy contained in the clearance flow. The induced drag is then proportional to $C_{LM}^{3/2}$.
- those which consider the forces which create the clearance flow, i.e. the pressure difference between suction and pressure side and/or upstream and downstream, and express a relation between those pressure differences and the clearance loss.

The loading parameter used is that existing at mid-blade height, either ideally (infinite height) or in presence of the clearance effect.

. Effect of blade height

It is usually accepted that the clearance flow is independent of blade height, i.e. that the contribution of the clearance losses to the global losses is inversely proportional to the blade height. This is acceptable as long as the end-wall effect does not modify extensively the character of the cascade flow. Ref.(1) indicates that for the geometries considered the limit is reached for an aspect ratio of 1.3 for compressors and 1 for turbine cascade. For a clearance of the order of 3 % chord Ref. (15) gives a limit of the order of 1 and considers the loss as constant for lower values.

Salvage (8) has shown, for the case of secondary flows (without clearance), that the limit aspect ratio is a function of the non-dimensional upstream boundary layer displacement thickness based on blade height, of the loading, characterized by the turning, and of the aspect ratio. In presence of clearance, this limit should also be a function of the relative clearance based on blade height.

The effect of the blade height is sometimes expressed in function of aspect ratio, which leads to a non-dimensional expression of the clearance based on chord.

. Effect of clearance height

Physically, for constant blade chord and thickness, the cross section offered to the clearance flow is proportional to the effective clearance height, taking into account, if needed, the presence of labyrinth seals, the chord being the other characteristic length if the pressure-side/auction side pressure difference is predominant. The blade thickness is the other characteristic dimension if the upstream-downstream pressure difference is the major driving agent.

It appears (1), (5), (6), (9), that for unshrouded compressor blades, there is an optimal clearance, of the order of 1 to 5 % of the chord. This is explained physically by the fact that secondary and clearance vortices are of opposite direction of rotation. For clearances higher than the optimum, a quasi linear increase of losses with clearance is first noted, then, a progressive slope reduction, probably due to the effective relative height effect. This evolution is represented in Fig. 1 (VKI measurement on a highly loaded blade).

None of the formulae available in the literature considers the existence of an optimum clearance. Almost all of them consider that the losses vary linearly with a non-dimensional clearance based on blade height. When using aspect ratio based on chord, one obtains also a linear law in function of clearance based on chord. The appearance of chord as a reference parameter for clearance appears to be justified only if the upstream-downstream pressure difference is the dominating factor in the flow mechanism.

2. Selected formulae available in the literature

Group I - Induced drag approach

$$c_{Dm} = \frac{1}{2} C_{Lm}^2 \sigma \frac{j}{h} \frac{1}{\cos \beta_2} \quad (1) \quad \text{Mehdahl (M) (10)} \\ (\text{turbines})$$

$$c_{Dm} = \frac{1}{4} C_{Lm}^2 \sigma \frac{j}{h} \frac{1}{\cos \beta_2} \quad (2) \quad \text{Vavra I (correction Mehdahl) } V_1 \\ (\text{turbines}) (11)$$

$$\gamma = 0.5 \frac{j}{h} \left(\frac{C_{Lm}}{t/c} \right)^2 \frac{\cos^2 \beta_2}{\cos^3 \beta_m} \quad (3) \quad \text{Ainley} \\ (\text{turbines}) (12)$$

$$\gamma = 0.7 \frac{c}{h} (j/c)^{0.78} \left(\frac{C_{Lm}}{t/c} \right)^2 \frac{\cos^2 \beta_2}{\cos^3 \beta_m} \quad (4) \quad \text{Dunham-Came} \\ \text{D.C.} (13)$$

(correction of (4) on the basis of part of the results of (1) for turbines).

Group II - Kinetic energy approach

$$c_{Dm} = \frac{4/2}{5} K \lambda^3 \frac{j}{h} C_{Lm}^{3/2} = 0.29 j/h C_L^{3/2} \quad (5) \quad \text{Vavra II } V_2 (11)$$

K : contraction factor 0.5 (valid for both turbine and compressor cascades)

λ : characteristic factor of clearance resistance (≈ 0.8).

"Mixed" formulae Lakshminarayana - L (5)

$$\omega_1 = 0.7 C_L^2 j/h c/t \frac{\cos^2 \beta_1}{\cos^3 \beta_m} + 7 (C_L)^{3/2} \frac{c}{h} (j/t)^{3/2} \frac{\cos^2 \beta_1}{\cos^3 \beta_m} \quad (6)$$

$$\omega_1 = 0.7 C_L^2 j/h c/t \frac{\cos^2 \beta_1}{\cos^3 \beta_m} \left[1 + 10 \sqrt{\frac{j/t}{C_L}} \right] \quad (6')$$

The first term of the R.H.S. of (6) corresponds to an induced drag, the second to the kinetic energy lost by the spanwise motion of the blade boundary layer (valid for turbine and compressors).

All the preceding formulae indicate a continuous increase of the losses with clearance height.

Group III - Formulae based on pressure difference

$$\omega_a = Y_a = 0.0696 \tanh(13 j/c) \frac{c}{h} \frac{\Delta W_u}{W_a} \cos \beta_m \quad (7)$$

(formulae derived from the turbine cascade experimental data of Ref.(1)).

The pressure difference is expressed as $C_{Lm} \cdot \frac{c}{t}$. Balje B₁ identifies ω_a with Y , which comes to multiply the losses given in Ref.(1) by $1/\cos^2 \beta_2$.

$$\omega_a = f(j/c) \frac{c}{h} \frac{\Delta W_u}{V_A} \tan_m \quad (\text{Bauermeister(1)})$$

(formulae derived for compressors).

The pressure difference is expressed as

$$\frac{\Delta W_u}{V_A} \tan_m = \frac{1}{2} \frac{p_2 - p_1}{\rho V_a^2}$$

The function $f(j/c)$ is not explicitly defined. A particular shape is given in Fig. 1 :

high loss for zero clearance with a rapid decrease to a minimum corresponding to optimum clearance, then linear increase followed by a flatter part.

The available data do not allow a statistical evaluation. The optimal clearance, which, as said before, is of the order of 1 to 5 % chord in cascade seems to be much lower in actual machines.

Cross checking on the compressor cascade data in (1) and in view of the precision of measurement, and of the domain of practical interest ($0 \leq j/c \leq 5-6\%$) one can propose the following linear relation to be introduced in (8)

$$f(j/c) = 0.44 j/c$$

disregarding, like in all the other formulae, the existence of the optimum clearance, and the possible non linearity with clearance height.

An additional correlation, based on the concept of pseudo-end wall boundary layer derived from low speed multistage compressor data is presented in (15), allowing estimation of efficiency reduction due to secondary and clearance losses

$$n = \bar{n} \frac{1 - (\delta_h^* + \delta_t^*) / h}{1 - (v_h + v_t) / h} \quad (9)$$

with \bar{n} the efficiency without end wall effects, δ_i^* (+) and v_i the displacement and tangential force defect of the pseudo-end wall boundary layer at hub and tip. It is based partly on data, partly on general designing experience.

A correlation is given for the sums of δ_i^* , as function of a stage pressure rise coefficient, non dimensionalized by its maximum value, and mid-span axial gap (Fig. 2, 3, 4). Fig. 2 gives explicitly the normalized clearance effect (clearance normalized by mean diameter staggered tangential spacing).

This correlation provides an interesting global evaluation for clearance effects.

(+) Subscript i = h or t

3. Comparison between the various formulae

The correlation formulae, except the last one, have been compared for two types of compressor cascade, corresponding respectively to the tip condition of a first LP compressor rotor, and root condition for a rotor or a stator of an MP or HP compressor.

Cascade I : $\beta_1 = 65$ to 72.5° ; $\beta_2 = 55^\circ$; $t/c = 1$; $h/c = 3$

$\beta_1 = 45$ to 52.5° ; $\beta_2 = 0^\circ$; $t/c = 0.5$; $h/c = 1.5$

Comparison of the losses for constant clearance ($j/h = 0.01$) is given in Fig. 5 and 6. The lack of coherence of the data is evident.

Differences of an order of magnitude appear. Lakshminarayana and Dunham-Came formulae give the highest values. The empirical constants have been evaluated from machine data, essentially turbine for the latter and compressor for the former. Bauermeister's formulae gives average values. It is based on cascade test.

Fig. 7 and 8 give the clearance effect at constant load ($\beta_1 = 65^\circ$ or 45°), for Lakshminarayana, Came and Bauermeister. The slope for the first one is very high.

Conclusions on the respective value of the formulae could only be obtained by systematic evaluation with machine data. The dispersion of data can be attributed to the fact that the formulae do not really cover the real physical mechanism. The evaluation of the best formulae of this type of approach seems hardly warranted.

B. Angles

It is shown also that the clearance effect modifies the local and average flow outlet angle. Ref. (5) proposes an approximate method for the clearance induced angle correction, as function of blade height. Clearance effects appear to be more important than secondary effects. The pitch average correction is given by

$$\Delta \bar{\beta}_2 = \tan^{-1} [0.25 C_L \sigma (1 - \frac{y-j}{a})] \quad a+j \geq y \geq j$$

$$\Delta \bar{\beta}_2 = 0 \quad y > a+j$$

With a the radius of the clearance vortex supposed to be of the forced type ; j the centre of the vortex ; a and y must be calculated. The procedure is rather long but it can provide a spanwise evolution of the angle. More recently, in (17), in the scope of the development of pseudo end-wall boundary layer method, under the impetus of Prof. K. Papailiou, on the basis of Lakshminarayana's approach on the one hand, and of Yokohama's on the other, a method was developed for describing the pitch average angle correction from inlet to outlet of the blading.

Both these approaches could eventually be used to develop further simple correlations.

In Ref. (1) a pitch and spanwise averaged correction is given for turbine as :

$$(\Delta \beta_2)^0 = 2 K j/h t/c \left(\frac{w_{u2} - w_{u1}}{v_a} \right) \cos \beta_m \frac{\cos^2 \beta^2}{\cos \beta_m}$$

with $K = 1.5^\circ / \% j/c$

Fig. 9 and 10 show the evolution for the two cascades used in the loss comparison. The correction for the second one is small. The validity of a turbine correlation to compressor can be set in doubt.

II. VALIDITY OF THE CASCADE TESTS

Cascade flows can differ from machine flows on the following accounts :

- Reynolds number and turbulence level
- often, Mach number
- radial pressure gradient
- relative motion blade-end wall
- inlet boundary layer including effect of change of coordinate system from one blade row to the next.

A relatively systematic study of the first four effects was carried out by Prof. Schlichting's group in Braunschweig a number of years ago, and is summarized mainly in Ref. 1 and 2. Tests have been carried out on large aspect ratio cascade, thus avoiding direct contamination of the mid-span flow by the end-wall effects. The end wall blockage was thus small.

1. Reynolds number effect (1)

The cascade losses due to the clearance effect (as obtained by difference between secondary losses with and without clearance) and the average angle correction are independent of Reynolds number ($1.5 \sim 10^5 \leq Re \leq 8.5 \cdot 10^5$) even when the flow on the central part of the blading is affected by a laminar separation bubble. The losses and turning in the real machine, where the level of turbulence is usually much higher than that of the cascade tunnel should present all the more the same characteristic.

Note, however, that Sierverding and Marchal, VKI, (private communications) have noted differences in the extent of the laminar separation bubble on the central part of low aspect ratio turbine cascade blade, with the Reynolds number. This would imply a variation of the extent of the zone of influence of secondary flows with Re .

The Reynolds number effect is probably negligible for compressors. We will use this assumption, also accepted in (15).

2. Mach number effects (2)

Tests have been carried on turbine cascades in the high subsonic domain ($0.5 \leq M \leq 0.8$). In this range, no effect of Mach number or clearance loss is apparent, if the load variation due to compressibility is taken into account, for a given cascade.

Griepentrog (private communication) reaches the same conclusion for the secondary flow effects in highly cambered compressor cascades, operating with local supersonic pockets.

In a recent paper (16) Sieverding and Wilputte showed that there was some effect of Mach number for the turbine case, but which were not much outside of measurement accuracy if the inlet losses were taken into account.

At this stage we will consider that the Mach effect is negligible, if the blade loading is correctly taken into account, its change in function of M being due to density change, back-pressure in choked regime or incidence in the unchoked one. Mach number effect is also neglected in (15).

3. Effect of radial pressure gradient (1)

Test on fixed annular cascades of turbines (high and low camber) and compressor blades (NACA 8410 - Stagger 30° - inlet angle 45°, 20° turning) with no twist, but with variable pitch and variable hub-tip ratio from 0.5 to 0.8, for one of the turbine cases, show the same global losses than for the equivalent straight cascade tests. The loss and angle evolution in function of blade height can even be correctly calculated from the straight cascade data, if the pitch variation and the component of radial velocity due to the radial equilibrium are taken into account. The position of maximum loss only is slightly different.

For this type of conditions where the pressure difference between hub and casing is of the same order than the pressure difference between blade inlet and outlet, the mechanism of the clearance effect does not seem to be fundamentally altered.

Even for radial pressure gradients closer to the circumferential ones, the global effect in compressors seems small, the radial equilibrium effect being opposite on the clearance flow on the pressure and suction side (hindering or fostering). Secondary flows are more affected, and the same is true for centrifugation effects.

Further information based on detailed tests in machine or systematic application of end-wall boundary layer calculations (2 and 3 D) would be needed to ascertain exactly the effect of radial pressure gradients and of centrifugation. At this stage, we will accept that it does not seem to affect the clearance flow mechanism fundamentally and that it could eventually be taken into account by an increase of the thickness of the end-wall pseudo boundary layer.

4. Blade - end wall relative motion

This effect has been studied in an approximated way in (1) either by rotating the part of the hub immediately under the blade in a fixed annular cascade, or the whole hub, from the nose bullet to the cascade exit, for compressor and turbine cascades. Clearance has been varied from 0 to 10 % and non dimensional hub rotational velocity varied from ($0 \leq U_p/V_0 \leq 2$). The corresponding value of the velocity of rotation can be as high as 3 in actual machines. The scraping vortex can be expected to increase the clearance effect for decelerating cascade. However, if, as indicated by the visualisation of (3), taken in a straight cascade with a mobile end wall, the local phenomena are modified, the results of (1) show that for the compressor cascade the effect on the global loss and the average outlet angle are negligible (Fig.1). Figure 2 is the corresponding figure for turbine annular cascades. Although (1) does not give details on the clearance flow mechanism, it can be concluded that a system of calculation of global clearance losses and mean angle correction based on cascade data without rotation effect will yield results not too far from the truth when applied to compressor blading.

Rains (4) who studied in detail the clearance flow in multistage axial pumps suggests that the effect of rotation on the clearance flow is limited to a local lift increase, without modification of the fundamental flow mechanism.

Lakshminarayana (5) comparing his calculation results with the compressor data of (6) concludes that the effect of the scraping vortex is to reduce the optimal clearance from 2 to 5 % chord to - 1,5 %.

Grieb (7) proposes, on the basis of experimental compressor data, to weight differently the clearance effect of the rotor and stator, giving the latter half the contribution of the former in the efficiency reduction due to clearance. This difference could be attributed to the relative motion effect and/or to centrifugation, but might also be due to the energy exchange defect. The tests of (1) do not cover the effect of change of reference system from one blade row to the next. This has been shown to modify extensively the boundary layer state at blade inlet and outlet, and could tend to increase the clearance effect for the compressor case. Data is missing and only the pseudo-boundary layer approach could provide the needed information.

5. Inlet boundary layer effect

Apart from the skewing effect due to change of coordinate system referred to above, a wealth of information exists concerning the effect of boundary layer initial thickness on secondary flow. However, practically nothing is available with regard to the influence on clearance effects, except for the hub rotation effect in (1), as discussed above. Rains (4) estimates indirectly that the initial boundary layer effect is negligible. Lakshminarayana (5) attributed part of the clearance losses to the kinetic energy lost through the radial motion in the pressure and suction side boundary layer, in the vicinity of the clearance. The blade boundary layer thickness is certainly modified by the end wall boundary layer effect. Ref. (5) indicates that this part of the losses is proportional to boundary layer thickness based on the pitch.

The empirical values of the coefficients which have to be introduced in (5) to fit experimental results would lead to boundary layer seven times as thick as the pitch, indicating that the physical description given is probably not sound.

The main boundary layer effect is most probably that of the change of reference system.

For a global approximation of clearance influence, this effect could be neglected, assuming that it bears mainly on the secondary flow effects (i.e. as existing without clearance). This seems coherent with the compressor derived correlation of (15).

6. Conclusion

It can be concluded, guardedly, that correlations obtained from straight cascade data, will at least provide correct trends for the effect of clearance in compressors. As usual, with cascade data, the effect of variation of blade circulation with span is not known. This will cause problems if spanwise distributed correction for losses and angle are to be considered.

For turbine it is well known that for secondary flow effect the loss level as obtained from cascade data may differ of an order of magnitude from the machine losses. This is linked most probably to the effect of relative motion when passing from nozzle to rotor or vice-versa. In compressors this effect tends to bring back the end-wall boundary layer to a more collateral state, and the difference might be somewhat less.

III. POSSIBLE USE OF THE CORRELATIONS : Clearance effects.

Supposing that one of the formulae could be validated, the fact that they are derived for constant geometry constant circulation blading introduces further problems for their application

- if a global averaged correction is deemed sufficient, it could be applied to the mean diameter section (or to the section nearest to the clearance). For the angle correction, data corresponding to blade height averaging should be obtained, using the method presented in (5) and (17).
- if a local correction is needed, a distribution law must be found or assumed. An exercise similar to that carried out by the turbine group, on the effect of the loss distribution, could be carried, but this is worthwhile only if the pseudo and wall boundary layer approach is deemed unsatisfactory.
- as practically all formulae have to be more widely calibrated against machine data, it seems that a formulation of the type of (5) which is partly calibrated or, for the sake of simplicity and some analogy with the D factor approach, Bauermeister's formulae could be used for losses.

We cannot recommend the continuation of the use of the correlation type of approach on its present physical basis. The approach can only provide - at most - an indication of order of magnitude for a first rough evaluation for instance in a 1-D calculation.

The pseudo end-wall boundary layer should be further developed including the evaluation of its development inside the blade passage. The concept is very sound physically and its application very easy, requiring little additional computer time when coupled with a through flow calculation method.

LIST OF REFERENCES

- (1) Hubert G. and Bauermeister K.J. : Probleme der Sekundärströmung in axialen turbomaschinen
Teil I. Untersuchungen über die Sekundärverluste in axialen Turbomaschinen- Teil II.Uber den Einfluss
der Schaufelbelastung auf Verdichtergittern.VDI Forschungsheft 496 -Aufgab B - Band 19.
- (2) Hebbel H.H. : Untersuchungen über den Einfluss der Machzahl auf die Sekundärverluste eines geraden
Turbinen Schaufelgitters bei hohen Unterschallgeschwin - Z.F.W. Heft 9, Sept.1965, pp.324-333.
- (3) Hansen A.G. and Herzig Z. : Secondary flows and three-dimensional boundary layer effects.
Chap. XV of Aerodynamic Design of Axial Flow Compressors-NASA SP36, 1965.
- (4) Rains A. : Tip clearance flows in axial flow compressors and pumps.
Report no.5 Hydrodynamics and Mechanical Engineering Laboratories. Calif.Institute of Tech., June 1954.
- (5) Lakshminarayana B. : Methods of predicting the tip clearance effects in axial flow turbomachinery.
ASME Journal of Basic Engineering, Sept. 1970, pp. 467-481.
- (6) Horlock J.H. : Some recent research in turbomachinery.
Proc. Inst. of Mech. Eng. (London), Vol. 182, Part I. no.26, p.571.

- (7) Grieb H., Schaffer A., Laudenbergs H. : Entwicklungsprobleme an Axialverdichtern für Kleingasturbinen. MTU-12-11, 1974.
- (8) Salvage J.W. : Investigation of secondary flow behaviour and end wall boundary layer development through compressor cascades. VKI, TN-107, june 1974.
- (9) Raw H.G. : Turbomachinery tip clearance design considerations. VKI PR 72-300, 1972.
- (10) Mehdal A. : The end losses of turbine blades. Brown Boveri Review, Vol. 18, no.11, pp.356-361, november 1941.
- (11) Vavra M.H. : Aerothermodynamics and flows in turbomachinery. Wiley and Sons.
- (12) Ainley D.G. and Mathieson G.C. : A method of performance estimation for axial flow turbines. British ARC and M. 2974, 1951.
- (13) Dunham J. and Came P.M. : Improvements to the Ainley-Mathieson method of turbine performance prediction. ASME Paper GT-70-GT2.
- (14) Balje E., Binsley R.L. : Axial turbine performance evaluation. Part A. Loss geometry relationship. ASME Journal of Engineering for Power, October 1968, pp. 341-347.
- (15) Koch C.C., SMITH L.H. "Loss sources and magnitudes in axial-flow compressors" ASME Paper 75-WA-GT-6.
- (16) Sieverding, C.H. and Wilputte, Ph. : Influence of Mach number and end wall cooling on secondary flows in a straight nozzle cascade . V.K.I.
- (17) Ohayon G. : Contribution à l'étude des écoulements secondaires dans les compresseurs axiaux avec effets de jeu radial. Thèse de 3ème Cycle Université Claude Bernard, Laboratoire de Mécanique des Fluides, Ecole Centrale de Lyon, July 1979.
- (18) Stewart W.L., Whitney W.J., Wong R.Y. : A study of boundary layer characteristics of turbomachine blade rows and their relation to overall blade loss. ASME Transact. Series D : J. Basic Engineering , Vol. 82, 1960, pp. 588-592.

LIST OF SYMBOLS

A	Area
AR	Aspect ratio h/c
C	Chord
C_L	Lift coefficient
C_D	Drag coefficient
h	Blade height
j	Clearance height
K, k	Constants or proportionality factor
M	Mach number
m	Mass flow
N	Rpm
P	Pressure
Q	Volume flow
r	Degree of reaction
R	Radius
Re	Reynolds number
t	Pitch
T	Absolute temperature
U	Peripheric velocity
V	Absolute velocity
W	Relative velocity
Y	Ainley loss coefficient $Y = P_{01R} - P_{02R} / P_{01R} P_2$
α	Absolute angle (from axial direction)
β	Relative angle (from axial direction)
γ	Specific heat ratio or stagger angle (from axial direction)
n	Polytropic efficiency
ζ	Traupel's loss coefficient $\zeta = V_{2is}^2 - V_2^2 / V_{2is}^2$
ϕ	Flow coefficient
ψ	Pressure coefficient $\Delta w_u / U$
σ	Solidity c/t
ρ	Mass density
w_1	Loss coefficient $w_1 = P_{01R} - P_{02R} / P_{01R} - P_1$
w_A	Loss coefficient $w_A = P_{01R} - P_{02R} / 1/2 \rho V_a^2$

Subscripts

A Axial

1 Upstream of blade row (rotor)

2 i+1 Downstream of rotor blade row (upstream of stator for a stage)

3 i+2 Downstream of stator for a stage

m Average (based on mean velocity vector or at mean radius)

MS Mid Span

o Stagnation conditions

R Relative

S Secondary

id Ideal

- Averaged

LIST OF FIGURES

1. Losses in function of clearance for a compressor cascade
Blade 10C7-45-C50
2. Correlation of reference (15) for displacement thickness of end-wall boundary layers
3. Correlation of reference (15): effect of axial gap between blade row and end-wall boundary layer displacement thickness
4. Correlation of reference (15): correlation of tangential force thickness
5. Comparison of the different correlations formulae for a rotor tip section. Effect of clearance in function of loading
6. Comparison of the different correlations formulae for a rotor or stator hub section
7. Effect of clearance in function of clearance height. Same cascade as in figure 8
8. Effect of clearance in function of clearance height. Same cascade as in figure 9
9. Angle correction due to clearance for the cascade of figure 8
10. Angle correction due to clearance for the cascade of figure 9
11. Effect of relative motion clearance end-wall (annular compressor cascade)
12. Effect of relative motion clearance end-wall (annular turbine cascade).

List of Figures

Fig. 1a: Mixed flow field for supercritical inlet condition

Fig. 1b: Shock system for supersonic inlet condition

Fig. 2: Shock losses as function of inlet Mach number and supersonic expansion

Fig. 3: Results of cascade measurements as a function of inlet Mach number

Fig. 4: Loss model including shocks and shock/boundary layer interaction

Fig. 5: Comparison of measured and calculated losses for different loss models

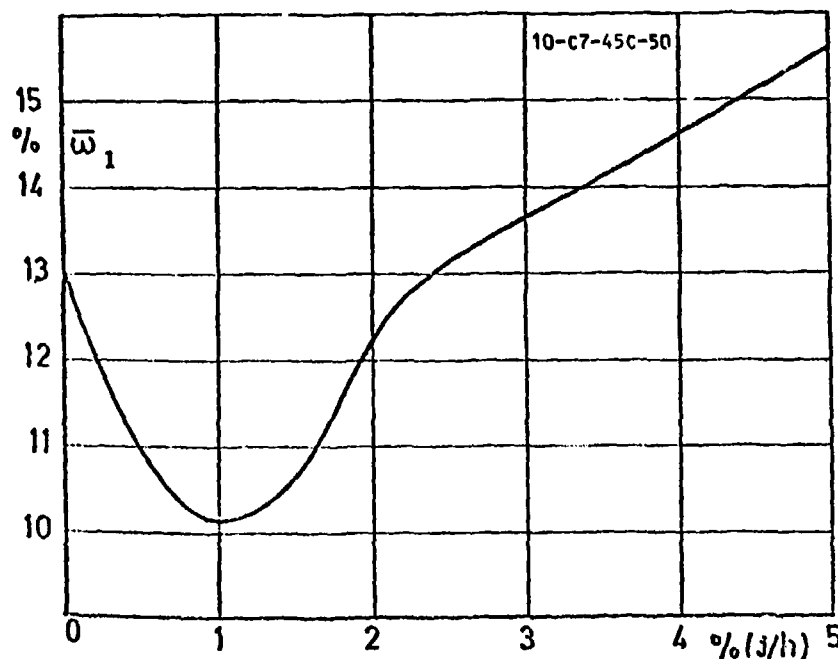


FIG. 1 - Losses in function of clearance for a compressor cascade. Blade 10.C7-45-C50
Courtesy VKI.

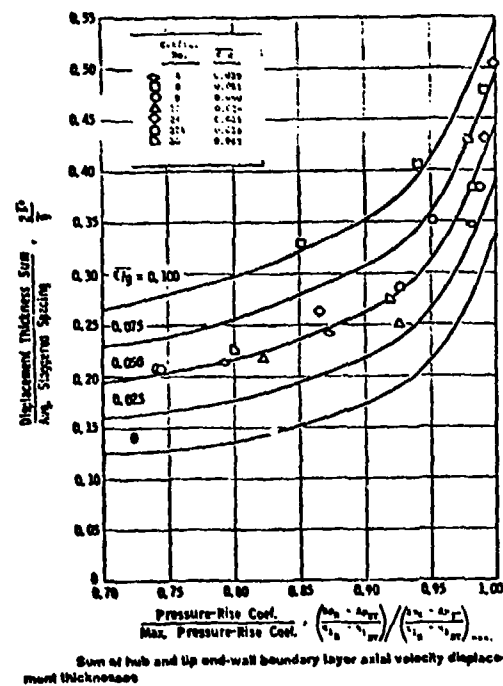


FIG. 2 - Correlation of reference (15) for displacement thickness of end-wall boundary layers.

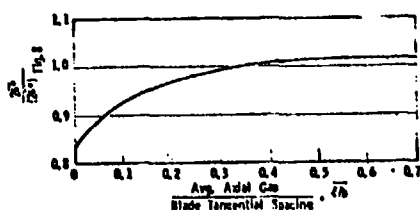


Fig. 6 Effect of axial gap between blade row edges on end-wall boundary layer displacement thickness.

FIG. 3 - Correlation of reference (15) : effect of axial gap between blade row and end-wall boundary-layer displacement thickness.

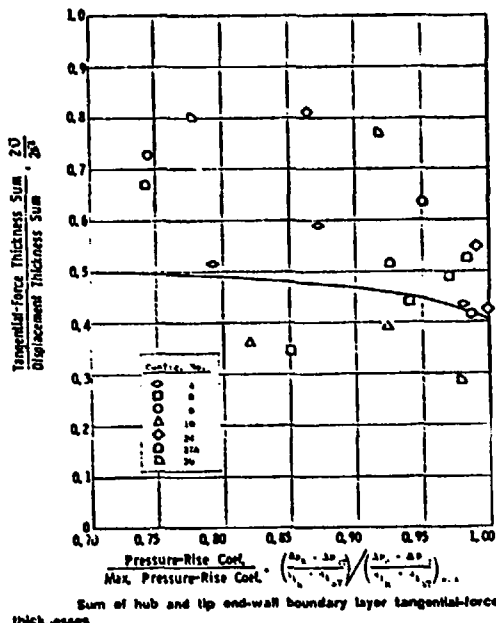


FIG. 4 - Correlation of reference (15) : correlation of tangential force thickness.

FIG. 5 - Comparison of the different correlations formulae for a rotor tip section. Effect of clearance in functions of loading. CASCADE I

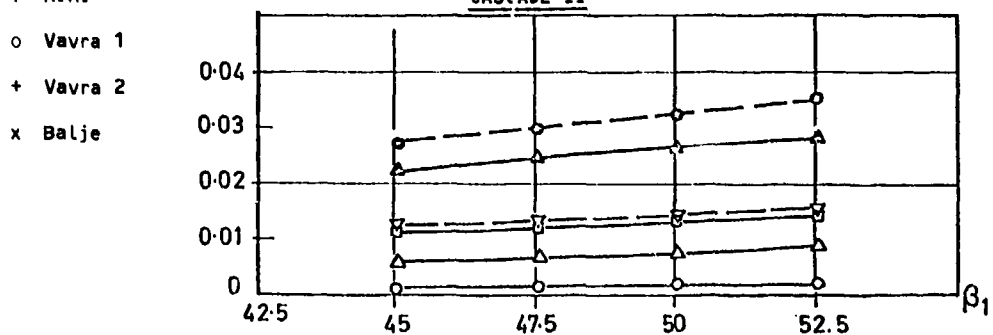
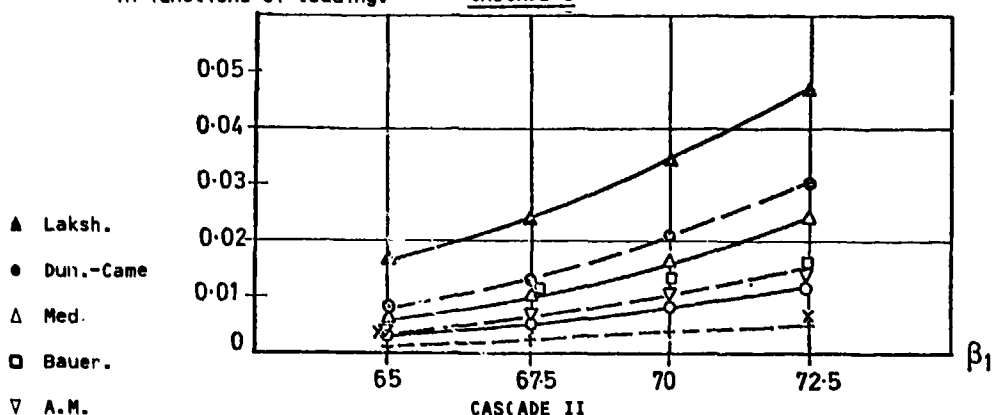


FIG. 6 - Comparison of the different correlations formulae for a rotor or stator hub section.

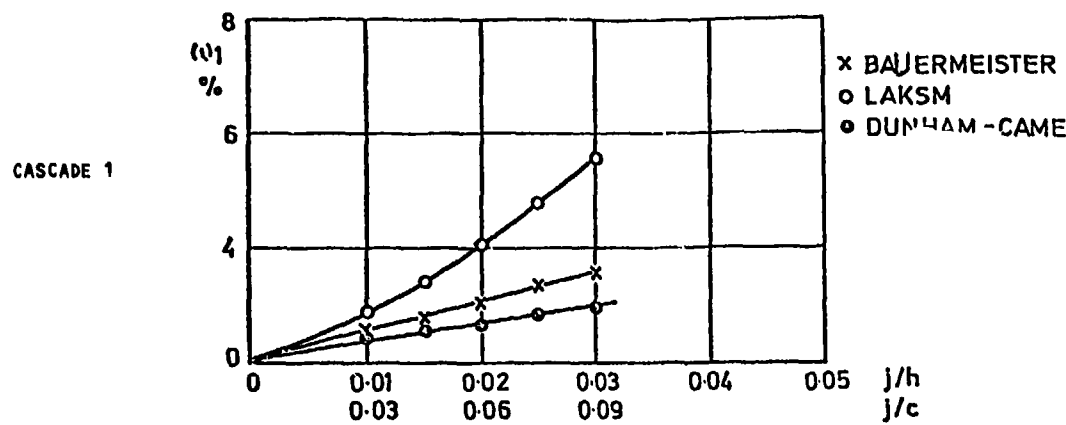


FIG. 7 - Effect of clearance in function of clearance height. Same cascade as in figure 5.

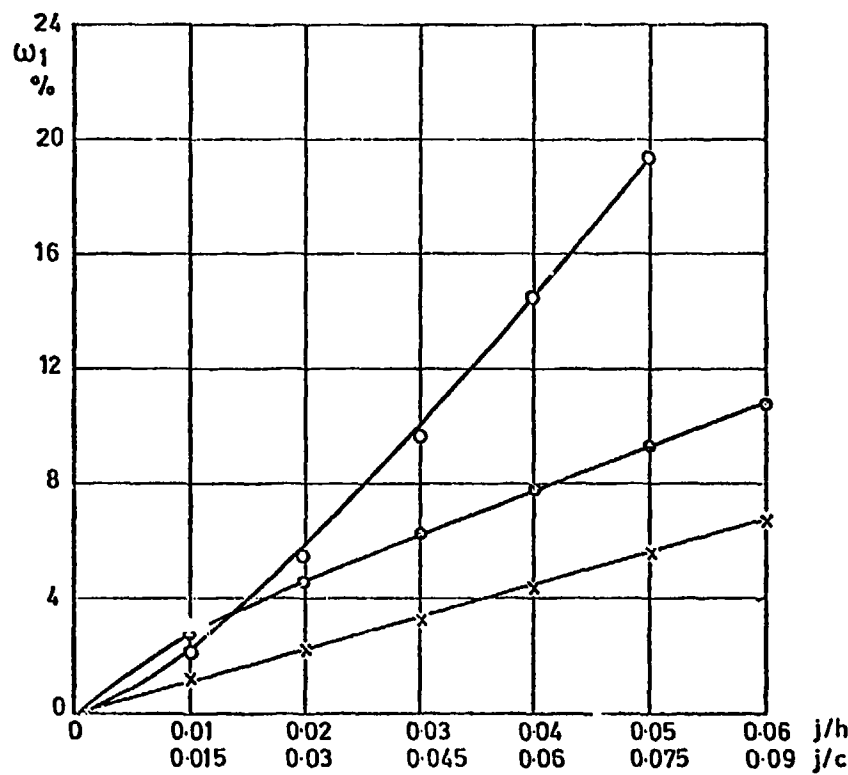


FIG. 8 - Effect of clearance in function of clearance height. Same cascade as in figure 6.

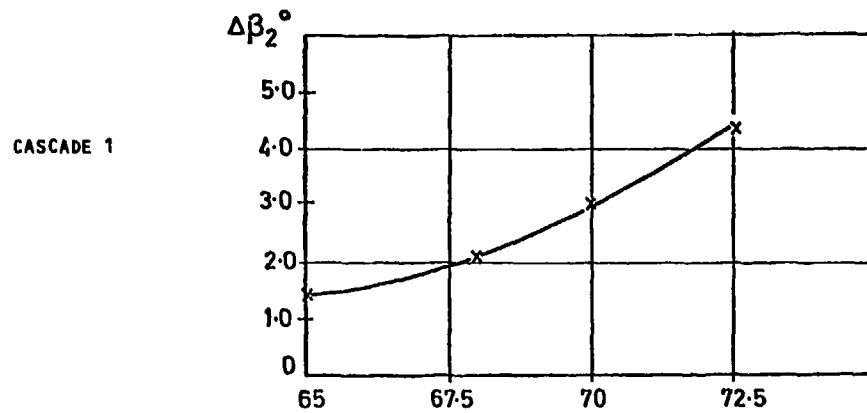


FIG. 9 - Angle correction due to clearance for the cascade of figure 7.

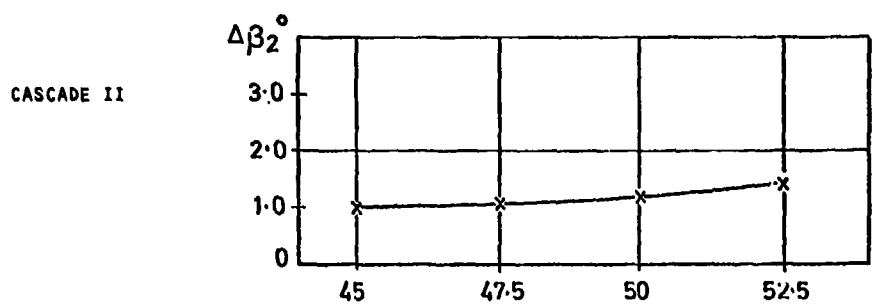
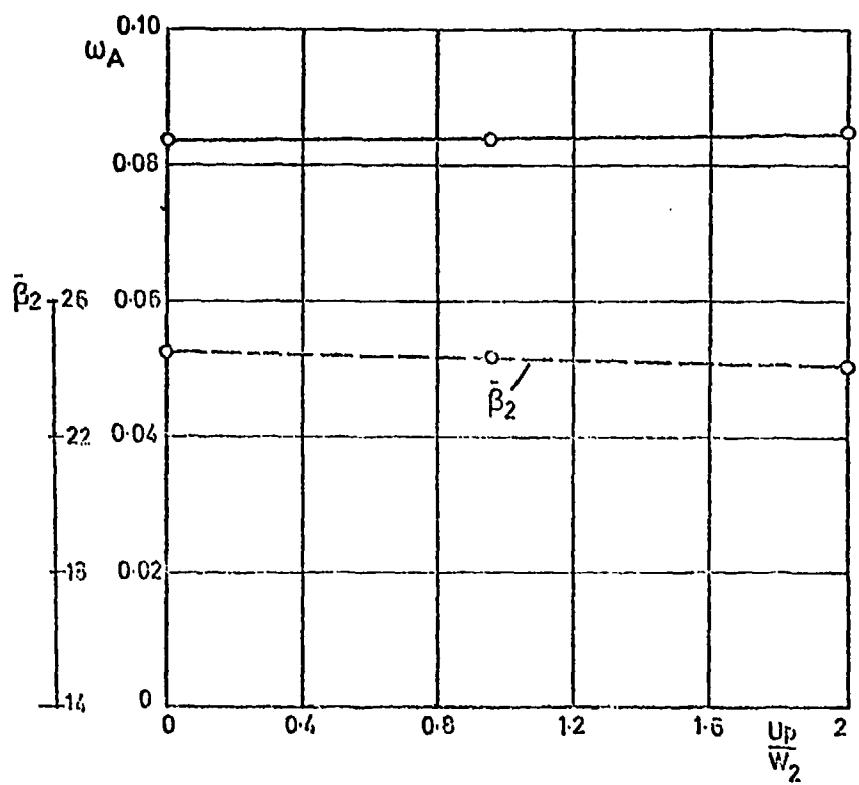


FIG. 10 - Angle correction due to clearance for the cascade of figure 8.

FIG. 11 - Effect of relative motion clearance end-wall (annular compressor cascade)
(from Ref.1).

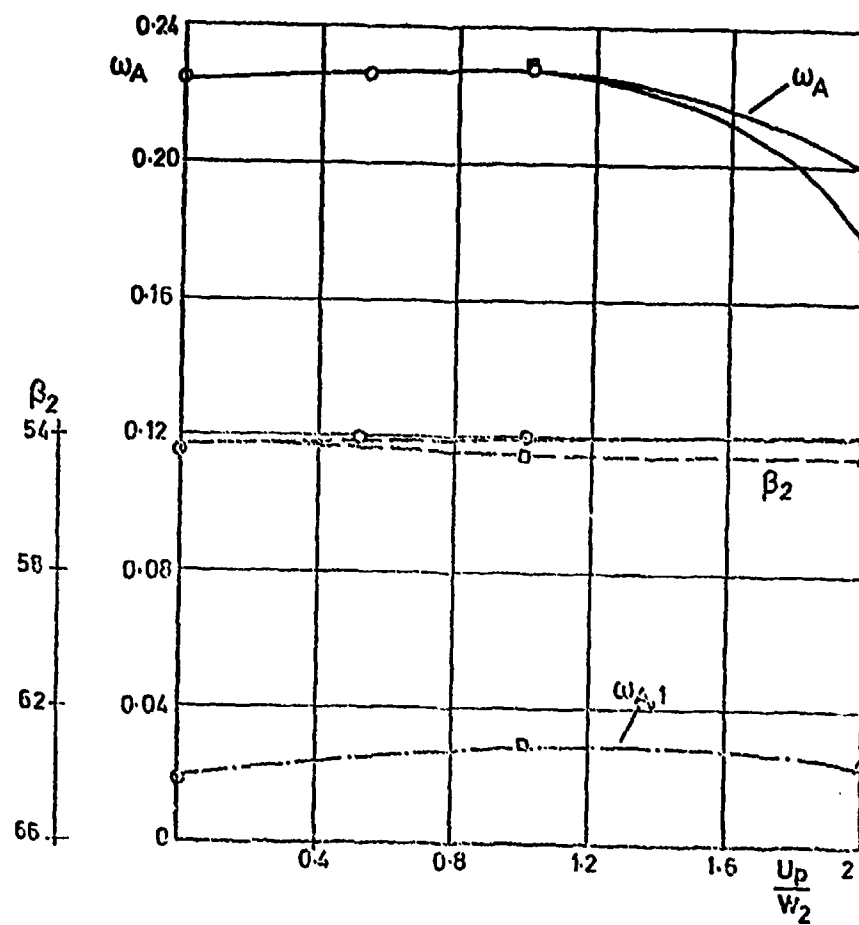


FIG. 12 - Effect of relative motion clearance end-wall (annular turbine cascade).

II.2.5 EFFECTS OF REYNOLDS NUMBER AND TURBULENCE LEVEL ON AXIAL CASCADE PERFORMANCE

A semiempirical theory is developed which will predict the behavior of the shear layer across a laminar separation bubble. The method is proposed for two-dimensional incompressible flow and is applicable down to short bubble bursting. The method can be used to predict the length of the laminar bubble, the bursting Reynolds number, and the development of the shear layer through the separated region. As such, it is a practical method for calculating the profile losses of axial compressor and turbine cascades in the presence of laminar separation bubbles. It can also be used to predict the abrupt leading edge stall associated with thin airfoil sections. The predictions made by the method are compared with the available experimental data. The agreement could be considered good.

NOMENCLATURE

AVR	= axial velocity ratio	S	= distance along a surface
C	= chord length	s	= the same as S
C_d	= dissipation coefficient, $\frac{2}{\rho U e^{\gamma f}} \tau \left(\frac{\partial u}{\partial z} \right) dz$	$T_{\bar{u}^2}$	= inlet turbulence intensity, $\sqrt{\frac{\bar{u}^2}{U_1}}$
$C_d(m)$	= mean dissipation coefficient	T.F. or TF	= Taylor's turbulence factor, $T_{\bar{u}^2} \left(\frac{C}{L_s} \right)^{1/5}$
C_f	= friction coefficient, $\tau w / (1/2) \rho U e^2$	U	= free stream velocity in the direction of the main flow, $U = \bar{U} + u'$
CC	= correlation coefficient, $\frac{u'_{11} u'_{22}}{\sqrt{u'_{11}^2} \sqrt{u'_{22}^2}}$	U	= time averaged component
D	= overall diffusion factor, $(1 - \frac{U_1}{U_2}) + \frac{\Delta U_0}{20 U_1}$	U_e	= local free stream velocity
g	= pitch or blade spacing	u'	= velocity in the boundary layer or free shear layer parallel to U_e
H	= δ^*/θ^*	u'	= randomly fluctuating com- ponent of velocity
H_e	= ϵ/θ^*	x	= distance along an x axis or chord line
i	= incidence	x_p	= probe separation
K_1	= a constant, 0.016	y	= distance normal to x
K_2	= a constant, 0.0011	z	= distance normal to s
L	= total length of a laminar separated bubble	a	= angle of attack
L_s	= macroscale of the inlet turbulence, $\int_{x_p}^{x_p} CC d(x_p)$	β_1	= cascade inlet flow angle
l_1	= distance between separation and transition in a laminar separation bubble	β_2	= cascade outlet flow angle
l_2	= distance between transition and reattachment in a laminar separation bubble	γ	= stagger angle
P_0	= total or stagnation pressure	δ^*	= displacement thickness
q	= dynamic head, $1/2 \rho U^2$	δ	= deviation angle
Rc	= Reynolds number based on chord	ϵ	= energy thickness
$R_{\theta}(s)^*$	= momentum thickness Reynolds number at separation	θ^*	= deflection angle, $\beta_1 - \beta_2$
$R_{l(1)}$	= Reynolds number based on l_1	v	= momentum thickness
\bar{w}_1	= loss coefficient, $\frac{P_0(1) - P_0(2)}{q_1}$	A_R	= kinematic viscosity
		p	= reattachment criterion
		σ	= density
		τ	= solidity, $1/(c_s)$
		ϕ	= turbulent shear stress
			= blade camber angle

NOMENCLATURE (Continued)Subscripts and Abbreviations

B	= bursting
M-M	= maximum loss, minimum turning
m	= mean value
R	= reattachment
S	= separation
SB	= sub-bursting
T	= transition
1	= upstream
2	= downstream
θ	= circumferential
VKI	= von Karman Institute

I. Discussion of the Flow Phenomenon

This discussion was developed from a thorough review of the pertinent literature. It is later confirmed by the author's experimental results.

If, for the time being, we postpone consideration of the factors that define whether a bubble is short or long, the conditions necessary for the formation of a laminar separation bubble are:

1. an adverse pressure gradient of sufficient magnitude to cause laminar separation, and
2. flow conditions over the blade surface such that the boundary layer will be laminar at the separation point.

Inherent in the second condition is that the blade surface be smooth, that the free stream turbulence level shall be relatively low, and that the distance between the stagnation and separation points be moderate (or more precisely, that the boundary layer Reynolds number at the laminar separation point, R_{θ^*} , be less than that required for transition).

The essential features of a laminar separation bubble are illustrated in Fig. 1.

The laminar boundary layer, starting at a stagnation point upstream of the separation point S, separates from the surface at S to reattach downstream at the point R. Between the points S and R, the flow may be divided into two main regions:

1. THE FREE SHEAR LAYER, contained between the outer edge S'T'R' of the viscous region and the mean dividing streamline ST'R.
2. THE RE-CIRCULATION BUBBLE contained between the mean dividing streamline and the blade surface STR.

These two regions may then be further subdivided into parts upstream and downstream of the transition point T. Upstream of T, the free shear layer is laminar and is incapable of doing any significant diffusion, because weak viscous shear stresses operate in this region. As shown in Fig. 1, the surface velocity is practically constant between separation and transition. This constant pressure "plateau" is a general feature of the laminar part of the separated flow.

So far, we have been discussing laminar separation bubbles in general, without making any distinction between short and long bubbles. Perhaps the most basic way of making this distinction was proposed by Tani (1)*. He has suggested that the difference between a short and long bubble lies in their effect upon the overall velocity and pressure distribution. The short separation bubble has only a slight effect upon the pressure distribution. Outside of the short bubble region, the pressure distribution is a close approximation to the inviscid distribution about the profile, apart from a slight reduction in the magnitude of the suction peak ahead of separation. On the other hand, a long bubble is one which interacts with the exterior flow to such an extent that the pressure distribution is appreciably modified from the inviscid model in a way that the velocity peak and circulation are decreased. This difference can be seen in Fig. 4 where Gaster's (2) Series II pressure distributions have been plotted.

*Numbers in parentheses denote reference at the end of the paper.

We can characterize laminar separation bubble behavior in the following way (for constant turbulence level):

When the overall blade chord Reynolds number gets low enough, the laminar boundary layer reaches the separation point before transition is achieved. After the laminar boundary layer separates, it forms a laminar free shear layer that eventually undergoes transition to turbulence. The turbulent free shear layer is able to do enough diffusion by entrainment of high energy free stream fluid to reattach to the surface as a turbulent boundary layer. This short bubble is seen as a small perturbation on the pressure distribution; its effect on the flow outside of the bubble region is minimal.

As R_c continues to decrease, the laminar free shear layer grows in length (the mechanism of this growth will be discussed in more detail in subsequent chapters). This growth causes the turbulent free shear layer to do more diffusion to reattach at a pressure near the inviscid pressure value (see Fig. 1). Finally, R_c becomes so low and the laminar shear layer so long that the turbulent entrainment process can no longer support the diffusion required for reattachment with a value close to the inviscid pressure level. This is when the bubble starts to significantly affect the flow outside the bubble region. The velocity peak and circulation decrease, thereby reducing the pressure gradient over the bubble. This allows the turbulent shear flow to reattach as a long bubble -- that is the short bubble has burst into a long bubble.

As R_c is further lowered, the velocity peak and circulation is further decreased. Finally, the bubble is so long that reattachment on the blade surface is no longer possible. The flow is then completely separated, and there is little change to the flow field around the profile with continued decrease of Reynolds number.

To summarize, within the incidence operating range of the cascade, there are four flow regimes possible across a large Reynolds number range (disregarding turbulent separation due to off-design conditions):

1. R_c sufficiently high for transition to occur before separation;
2. short bubble region (before bursting);
3. long bubble region (after bursting);
4. complete separation.

These four flow regimes are shown schematically in Fig. 2.

II. A Modified Semiempirical Theory For the Growth and Bursting of Laminar Separation Bubbles

Equations and Discussion. The method proposed here is a modification of Horton's (3) semiempirical theory. Using Horton's theory, calculations of cascade performance were compared with selected results of this author's research and that taken from the literature. It was found that, in general, Horton's method gave a delayed prediction of bursting and underestimated the losses. This was probably due to three factors:

1. Inadequate transition criterion;
2. possible error in the value of the reattachment criterion, Λ_R ; and
3. the low value of the mean dissipation coefficient, $C_d(m)$.

This author has done a thorough analysis (4) to correct these faults. The resulting modified theory is presented below:

1. THE LAMINAR PART

(a) Transition Length

$$\frac{l_1}{R_c} = T_1 = \frac{R_{l_1}}{R_{\theta_s}} = \frac{2.5 \times 10^4 \log_{10}(\coth((TF) \times 10))}{R_{\theta_s}}$$

where $TF = T_u \left(\frac{C}{L_s} \right)^{1/5}$ (1)

(If TF is not available, then $T(\bar{\mu})$ could be used in equation (1) as a first approximation.)

(b) Growth

$$\frac{d\theta^*}{ds} = 0,$$

$$\theta_s^* = \theta_T^*. \quad (2)$$

2. THE TURBULENT PART OF THE BUBBLE

(a) Reattachment Criterion

$$(\Lambda_R) = \left[\frac{\theta^* dU_e}{U_e dS} \right]_R = \left[\frac{-C_d}{H_e (H - I)} \right]_R ,$$

$$(\Lambda)_{\text{theory}} = -0.0059. \quad (3)$$

(b) Length Relations

$$\frac{l_2}{\theta_s^*} = \bar{I}_2 = \frac{B_1 \cdot (1-U_{eR})}{(U_{eR})^3 - C_1} , \quad \bar{L} = \bar{I}_2 + \bar{I}_1 , \quad (4)$$

$$B_1 = \frac{1}{C_d m} ,$$

$$(\frac{C_d m}{4H_{\epsilon_m}}) = \Lambda_R$$

$$C_1 = (\frac{C_d m}{4H_{\epsilon_m}}) \cdot B_1 .$$

(c) Growth

$$\frac{\theta_R^*}{\theta_s^*} = \frac{1}{(U_{eR})^3} + \frac{C_d m}{4H_{\epsilon_m}} \frac{\bar{I}_2 (1-U_{eR}^*)}{(U_{eR})^3 (1-U_{eR}^*)} , \quad (5)$$

$$\bar{I}_2 = l_2 / \theta_s^* ,$$

$$C_d m \approx 0.035 , \quad (6)$$

$$H_{\epsilon_m} \approx 1.5 .$$

A bar indicates normalization with respect to values at separation.

The equations in the foregoing follow from three approximations that are reasonable for a short bubble:

1. the perturbation to the inviscid velocity distribution is negligible, except over the length of the bubble itself.
2. the external velocity over the laminar part of the bubble is constant to a good approximation.
3. the external velocity falls linearly between the transition and reattachment points.

The modified method proposed in the foregoing has been successfully used to predict the bursting Reynolds number and bubble lengths for isolated airfoils, as well as for airfoils in cascade. Along with a reliable boundary layer method, it was also used to predict the losses of two-dimensional axial compressor and turbine cascades where separation bubbles were present (see Figures 3 and 4).

Note that Equation (1) denotes the effect of the turbulence on bubble behavior. For the same Reynolds number, the flow regime could be quite different for high and low turbulence levels.

REFERENCES

1. Tani, I., "Low Speed Flows Involving Bubble Separations," Progress in Aeronautical Science, Pergamon Press, 1964.
2. Gaster, M., "The Structure and Behavior of Laminar Separation Bubbles," NPL Aero Report, 1181, ARC 28.226, 1966.
3. Norton, H. P., "A Semi-Empirical Theory for the Growth and Bursting of Laminar Separation Bubbles," ARC, CP 1073, 1969.
4. Roberts, W. B., "The Effect of Reynolds Number and Laminar Separation on Axial Cascade Performance," ASME Transactions, Journal of Engineering for Power, Vol. 97, Series A, No. 2, April 1975.
5. LeFoll, J., "A Theory of the Representation of Boundary Layers on a Plane," Proc. Seminar on Advanced Problems in Turbomachinery, von Karman Institute, Oct. 1965.

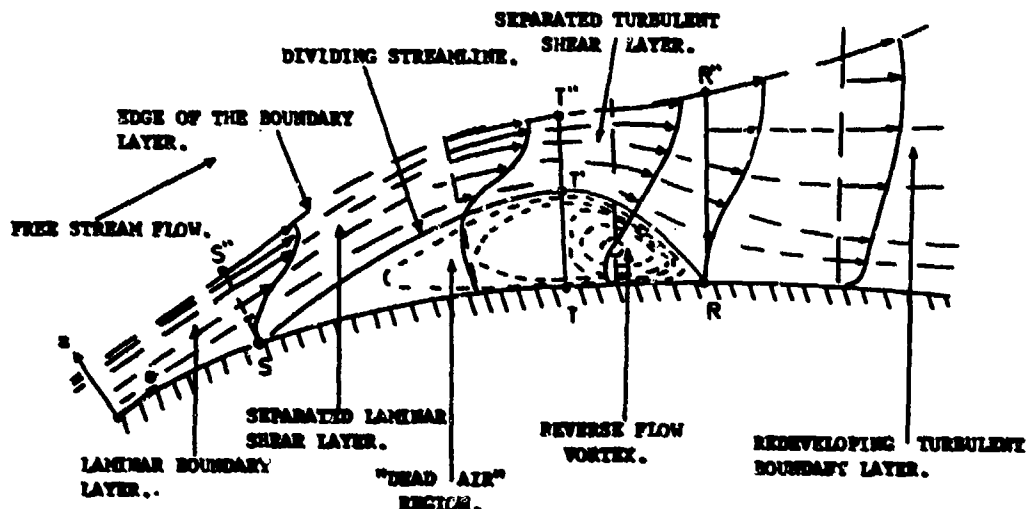


FIGURE 1a.
Sectional View of a Two-Dimensional Short Laminar Separation Bubble (z Scale Greatly Exaggerated)

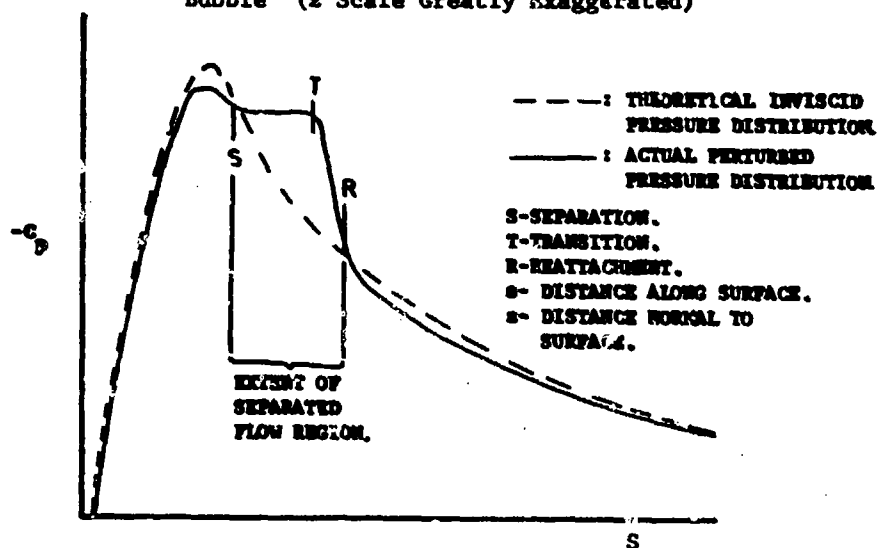


FIGURE 1b.
The Corresponding Surface Pressure Distribution

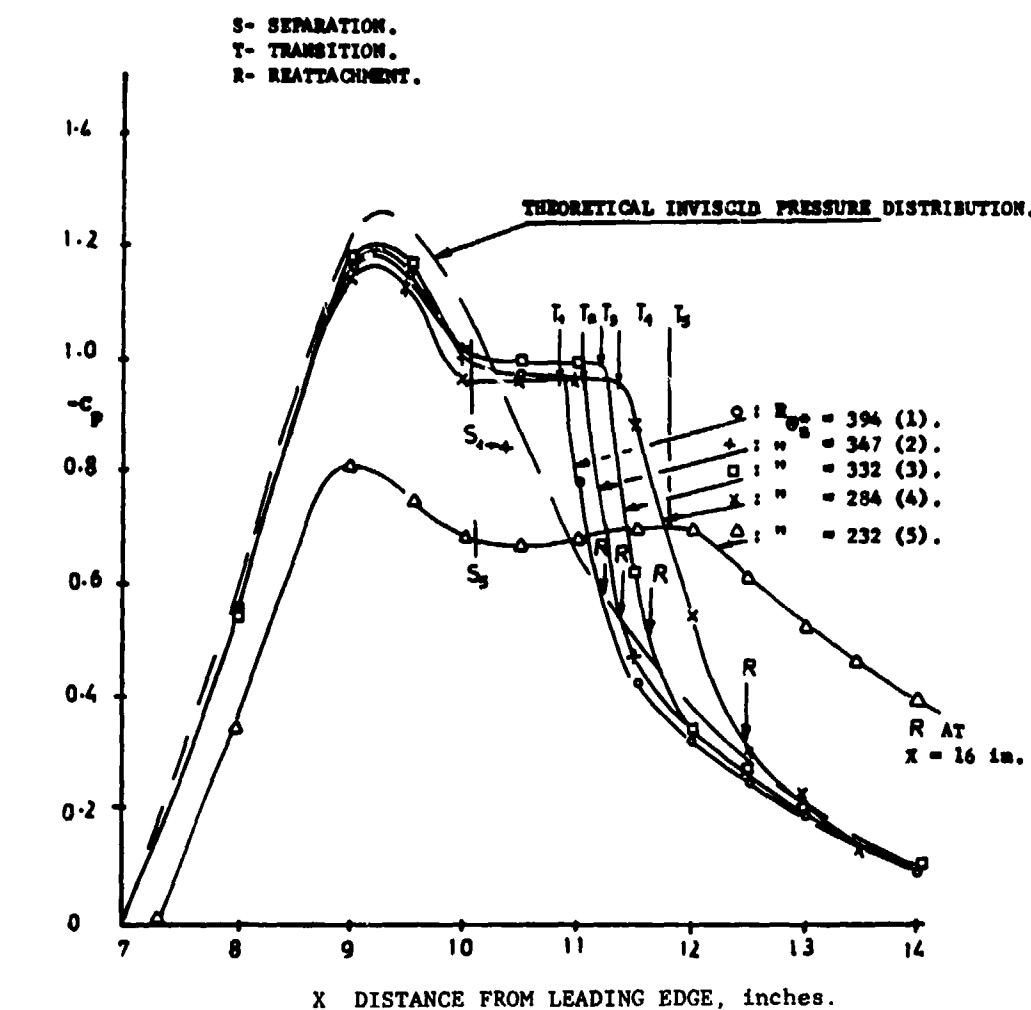


FIGURE 1c.
Pressure Distributions in the Vicinity of Separation Bubbles for the Series II Experiments of Gaster (2), Bubbles 1 to 4 are Short, 5 is a Long Bubble.

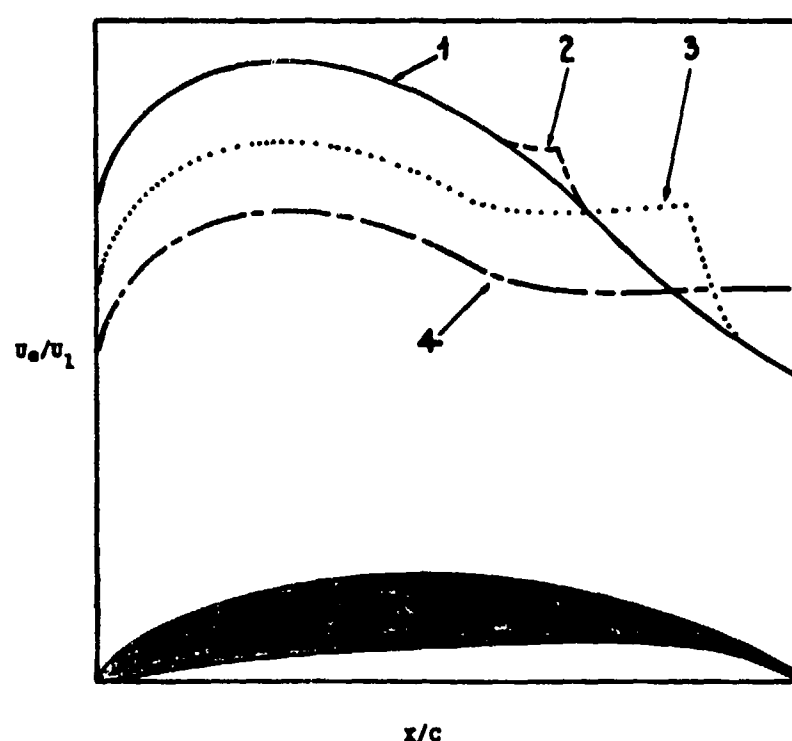
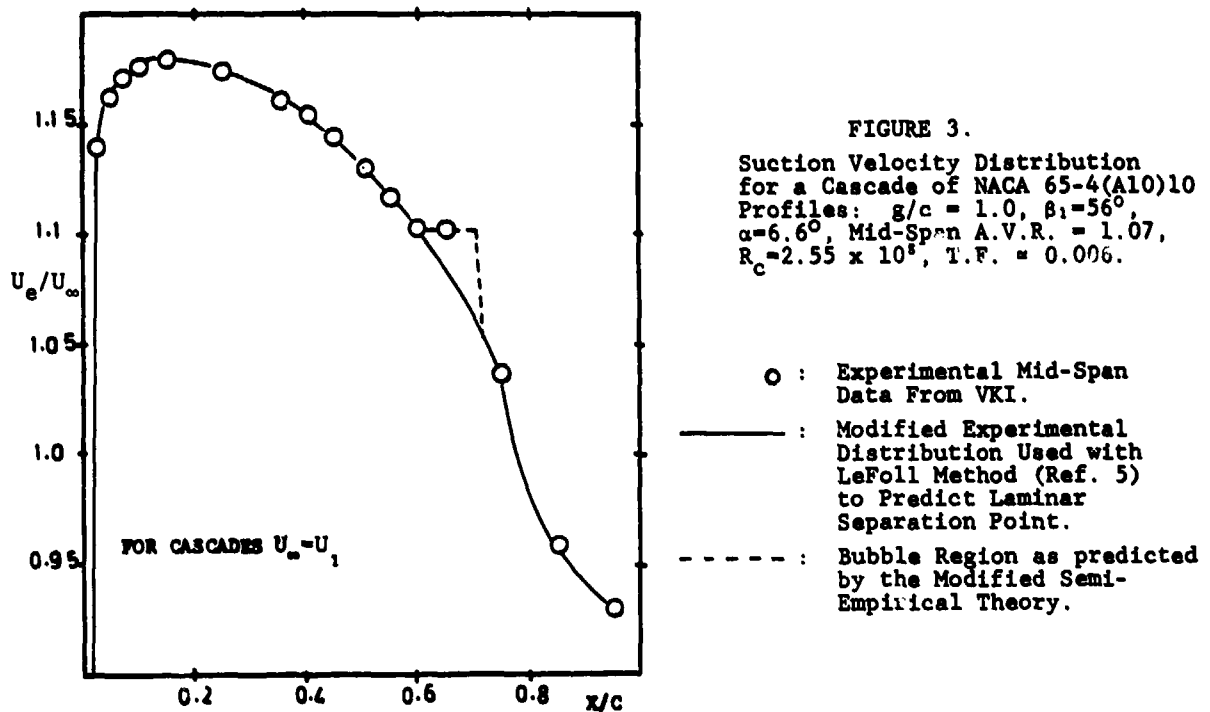


FIGURE 2.
Schematic of the Four Flow Regimes Possible with Varying Reynolds Number (10^4 - 10^5) Over the Suction Surface of a Compressor Profile.
(Low Speed Flow, $\alpha \ll$ Stall)

1. HIGH R_c : No separation, velocity distribution approximates inviscid distribution.
2. MEDIUM R_c : Short separation bubble, distribution approximately inviscid outside bubble region.
3. LOW R_c : Long bubble after bursting, distribution significantly affected.
4. LOWER R_c : Long bubble with complete separation.



NACA 65-4(A10)10: $g/c = 1.2$, $\beta_1 = 60^\circ$, $\alpha = 3.0^\circ$, T.F. ≈ 0.006 .

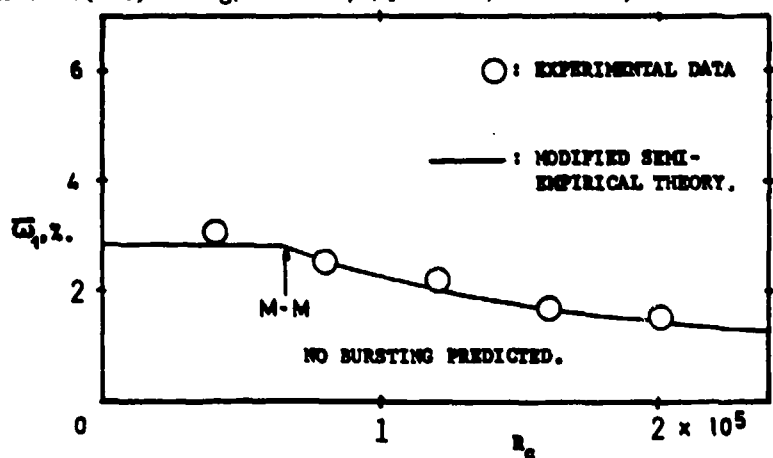


FIGURE 4
Loss Coefficient, $\bar{\omega}_1$, as a Function of Blade Chord Reynolds Number, R_c ,
for an Axial Compressor Cascade:
Modified Semi-Empirical Theory versus Experiment.

M-M: Point of Maximum Loss (and Minimum Deflection).

II.2.6 Survey on the Effect of Blade Surface Roughness on Compressor Performance

List of Symbols

			<u>Indices</u>
a	m	average distance between roughness peaks	a axial component
c	m	mid span chord length	f individual stage
k	μ m	roughness height, defin. Fig. 2	k technical roughness
ks	μ m	sand type roughness height	ks sand type roughness
lm	mm	roughness measuring length	crit. l "lower" critical Reynolds number
Ra	μ m	arithmetic average roughness, identical to AA or CLA	p maximum permissible roughness for hydrodynamically smooth boundary layer flow
Re		Reynolds number	pol polytropic
w	m/s	air velocity relative to cascade	crit. u "upper" critical Reynolds number
x	m	length coordinate	l entry to cascade
y	m	roughness height coordinate	ref reference condition
z		number of stages	- arithmetic average
Δ		change of parameter	
η		efficiency	
ν	m^2/s	kinematic viscosity	

1. Introduction

Blade surface roughness affects blade profile drag when the surface roughness elements protrude from the laminar or viscous sublayer of the turbulent boundary layer as known from the classic Nikuradse (Ref. 1) experiments. As long as the roughness elements are submerged within the viscous sublayer no further reduction of friction losses is achievable below the so called "hydrodynamically smooth" value. Friction drag in that regime depends exclusively on Reynolds number.

As soon as the roughness elements protrude from the viscous sublayer due to a thinner sublayer as the result of increased Reynolds number, the friction loss function turns toward independence of Reynolds number within a small Reynolds number interval. After that transition region friction drag is exclusively a function of the roughness height itself (Ref. 2).

The reaction of compressors to excessive blade surface roughness manifests itself in a distinct trend toward constant polytropic efficiency despite increasing Reynolds number (see Fig. 1). The Reynolds number where this "kink" occurs is called "upper critical Reynolds number" or "roughness boundary" and depends on the type of roughness and its height as well as the ratio of flow velocity over kinematic viscosity w/ν , or in other words Reynolds number per unit length Re/c .

The steadily increasing pressure ratios and flow velocities in modern gas turbine compressors increase the Reynolds number over chord length ratio in the back end of the compression system to an extent that even with the best presently available manufacturing methods noticeable losses of potentially achievable efficiency gains must be accepted. The latter applies primarily to all missions with high inlet pressures, i.e. low kinematic viscosity. The roughness problem occurs primarily in the higher Reynolds number regime where turbulent attached flow predominates.

2. Literature Survey

A number of experimental results are available in the literature on tests with sand type roughness, but little is published on technical roughness, especially for blades produced by modern manufacturing techniques. Basic information on the aerodynamic mechanisms of surface roughness can be taken from Ref. 3, 4, a very complete survey of roughness effects on compressor flow is given in Ref. 5 which includes a useful list of all relevant literature. New data from three high pressure compressors with blades produced by present day manufacturing techniques as grinding, forging/etching and electrochemical machining are described in Ref. 6. The latter will essentially be used in the present paper.

3. Criterion for Hydrodynamically Rough Boundary Layer Flow, Roughness Types and Definition of a Technical Roughness

3.1 Criterion for Hydrodynamically Rough Boundary Layer Flow

The classic Nikuradse (Ref. 1) experiments on sand type roughness show that the maximum permissible roughness up to which hydrodynamically smooth boundary layer flow can be expected is given by a simple relation, called critical roughness Reynolds number:

$$Re_{ks,p} = \frac{ks \cdot w}{\nu} = 100$$

The above mentioned equation does mean that the maximum permissible characteristic surface roughness height k for a certain roughness type depends exclusively on the velocity to kinematic viscosity ratio or Reynolds number per unit length $w/\gamma = Re/c$ and the average geometry of the roughness elements and not on a characteristic length as blade chord or compressor size.

For other roughness types large differences can be found in the literature for the critical roughness Reynolds number reaching from 50 - 260 (Ref. 2, 7).

3.2 Characteristics of Roughness Types Different from Sand Type Roughness

Investigations on rows of regularly spaced spheres, hemispheres, cones, sharp edged metal strips etc. (see Ref. 2) show a large variation of their effect on drag relative to sand type roughness. The distance to height ratio is of decisive importance, generally giving the impression that drag reduces linearly with the distance between peaks above a ratio of $a/k \geq 8$, which means every peak acts as a single body and hence the specific shape of each element matters. The technical surfaces produced by the typical blade manufacturing process as grinding, forging and electrochemical machining look like very flat hills in wide valleys with a slope hardly exceeding 10 degrees and typical distances to height ratios of $a/k = 50 - 200$ for the largest, aerodynamically effective peaks. It is a totally different type of roughness compared with sand type roughness.

3.3 Measurement and Definition of a Technical Roughness Height

The characterization of a technical roughness is very difficult due to various aspects as:

- individual shape of peaks
- density of essential roughness peaks per unit length
- spectrum of roughness height

Whereas sand type roughness described in text books is made up of sand grain of essentially constant diameter and quite small average distance between peaks, a technical roughness contains a whole spectrum of peak heights and possibly also large scale waviness. The multitude of shapes is the reason for the very limited data published on technical roughnesses. Roughness is usually described in industry by an arithmetic average value (R_a , AA , CLA) measured by a stylus which travels along a rough surface picking off roughness heights at constant distances. This arithmetic mean value alone is not too helpful in defining the hydrodynamic characteristic of the surface because a large portion of the smaller roughness elements is fully submerged in the laminar sublayer and therefore not at all felt by the turbulent flow, but are counted in the arithmetic mean value.

A more characteristic but still reasonably simple roughness height k is defined which describes the flow affecting peaks rather than the average.

Roughness k is arbitrarily defined as the difference between the arithmetic averages of the 10 highest peaks and the 10 deepest grooves which exist per millimetre length, i.e. in an average distance of $100 \mu\text{m}$. Measuring length is 5 mm in chord- and spanwise direction on the 20 % chord position of the suction surface, the forward 50 % of which are regarded as decisive for friction drag produced by surface roughness. In case that chordwise and spanwise measurement reveal different roughness levels, the higher value is chosen on the experimental evidence obtained in wind tunnel tests with a milled flat plate having considerable differences of roughness height in direction of milling and normal to it. The tests described in Ref. 8, show that only a 10 degrees incidence relative to the low roughness direction makes the high roughness fully effective.

Fig. 2 shows the definitions of the roughness parameters, where k yields essentially similar data as a more sophisticated definition used by Hürlimann, Ref. 9, for estimating roughness effects on steam turbine blades. A considerable number of blade surface roughness measurements done on forged and electrochemically machined blades with a roughness measurement device revealed a sensible correlation between k and the readily obtainable arithmetic average R_a (AA , CLA):

$$k = 8.9 R_a$$

The factor scattered from 7 - 12 with 80 % of the samples placed between 8 and 10. The measurements are done with a stylus of $5 \mu\text{m}$ tip radius, a cut off length (wave length) of 0.075 mm and a stylus contact force of 4.9 N .

4. Critical Roughness Reynolds Number for Technical Roughness and Permissible Roughness Height

4.1 Critical Roughness Reynolds Number

Critical roughness Reynolds numbers for blade surfaces produced by typical manufacturing methods were obtained from test results of three multistage high pressure compressors, which met the roughness boundary during variable Reynolds number tests (Ref. 6). From Figs. 3, 4 a mean Reynolds number was picked off at the crossing point of the elongations of the increasing efficiency slopes in the hydrodynamically smooth or intermediate regime with the constant η_{pol} line from the hydrodynamically rough regime. This "kink point" was used to calculate individual stage roughness Reynolds number from the measured blade roughnesses of the various stages. Roughness Reynolds number is based on relative cascade inlet velocity, roughness height k as defined on Fig. 2

and kinematic viscosity calculated from static pressure and temperature ahead of the respective cascade. A mean roughness Reynolds number was obtained by arithmetically averaging the individual stage data omitting atypically high values which were due to distinctly higher than average roughness levels. The analysis gave critical roughness Reynolds numbers of $Re_{k,p} = 88$ for forged and electrochemically machined blades and $Re_{k,p} = 137$ for ground blades as given on Tab. 1.

Tab. 1: Stage Roughness Reynolds Number at Roughness Boundary

Compressor	Res. HPC (5-stage)	HPC "A" (6-stage)	HPC "B" (6-stage)
Reynolds number at roughness boundary	$3.1 \cdot 10^5$	$6.0 \cdot 10^5$	$5.0 \cdot 10^5$
$Re_{k,p} = \frac{k_w}{\nu}$	stage 1 111 stage 2 119 stage 3 137 stage 4 153 stage 5 165 stage 6 -	83 91 70 97 173^+ 101 101	69 74 147^+ 105 101 166^+
$Re_{k,p} = \frac{k_w}{\nu}$	137	88	87
production method	grinding	ECM	ECM

⁺ omitted in averaging process

The significant difference between the ground blades and the forged or electrochemically machined blades may be connected with the definition of maximum roughness in case of the ground blades (see 3.3) which showed a 2:1 ratio of spanwise to chordwise roughness as opposed to forged and electrochemically machined blades which do have similar roughness in both directions. If average values of spanwise and chordwise roughness were used, which would be equally sensible on the argument that over at least 50 % of the blade height of a high hub/tip ratio compressor the flow is essentially chordwise, i.e. in direction of the lower roughness with flow angles certainly below 10 degrees relative to the minimum roughness direction and therefore unaffected by the increased spanwise roughness, the roughness Reynolds number would drop to $Re_{k,p} = 103$. This is very close to the critical roughness Reynolds number of sand type roughness and that of forged or ECM manufactured blades.

The values of $Re_{k,p} = 88$ however tie in extremely well with a value of 90 proposed by Koch and Smith in Ref. 10. Obviously more experimental evidence is needed for cases with significantly different roughness heights in chordwise and spanwise direction.

The average critical roughness Reynolds numbers given on Tab. 1 can be used to locate the Reynolds number where the individual stages enter the hydrodynamically rough boundary layer flow regime. These points are encircled for instance on Figs. 3 and 4. Limited experience shows that a distinct curl over of the efficiency/Re number function has to be expected if only about 2/3 of the decisive cascades enter the rough boundary layer flow regime. The reason for this behaviour is not really understood as one would expect a steady curl over as more and more stages enter the hydrodynamically rough boundary layer flow regime.

The observed effect of the technical roughness on the compressor behaviour is considerably more pronounced than could be expected from an extrapolation of data using hemispheres or cones (see Ref. 2) as a simulation of technical roughness elements. In fact the very similar critical roughness Reynolds numbers of sand type and technical roughness in spite of their totally different appearance, especially with respect to the distance/height ratio a/k , is surprising.

4.2 Permissible Blade Surface Roughness

The permissible blade roughness for hydrodynamically smooth flow is given on Tab. 2 for forged and electrochemically machined blades over a range of Reynolds numbers per unit length using the critical roughness Reynolds number of $Re_{k,p} = 88$.

Tab. 2: Permissible Roughness Height $Re_{k,p} = 88$ for Hydrodynamically Smooth Boundary Layer Flow Conditions

$Re_c 10^{-8} = \frac{w_1}{\nu} 10^{-8} m^{-1}$	0.10	0.25	0.50	0.75	1.00	1.25	1.50
$k_p \mu m$	8.8	3.5	1.75	1.2	0.9	0.7	0.6

Fig. 5 shows the permissible blade surface roughness height k_s against w_1/γ ratio for the roughness Reynolds numbers of 88 and 135 in Ref. 6-tests, showing the rapid reduction of surface roughness necessary in the back stages to keep the flow hydrodynamically smooth. An indication of which stages are running into problems at the various flight cases can be seen from the columns drawn at a surface roughness of $k = 2 \mu m$ which is about the best quality presently achievable with forging and electrochemical machining. The necessary surface roughness reduces as pressure increases from stage to stage.

As can be seen, all core engine compressor stages of high pressure ratio military engines operate in the hydrodynamically rough boundary layer flow regime at low level flight conditions; for civil engines the back end of the compression system is also limited in the potentially achievable efficiency gain due to increased Reynolds number by excessive surface roughness. The basis for the columns drawn is a compression system made up of present day average flow velocity according to Fig. 6.

5. Simple Method for Estimation of Roughness Effect on Efficiency

With the use of the obtained critical roughness Reynolds number the upper critical Reynolds number can be obtained for each stage and hence for the compressor by averaging:

$$\overline{Re}_{crit,u} = \frac{1}{z} \cdot \sum_{i=1}^z (Re_{k,p} \cdot \frac{c}{K})_f$$

Below this upper critical Reynolds number (hydrodynamically smooth region) polytropic efficiency follows a power function:

$$\frac{1 - \eta_{pol}}{1 - \eta_{pol, ref}} = \left(\frac{Re}{Re_{ref}} \right)^{-n}$$

Quite good agreement was found between the experimentally obtained exponent n and the Wessel prediction (Ref. 11). The exponent had a value of $n = 0.11$ for some multi-stage compressors and appeared to be valid also at part speed conditions.

If the exponent n is known for the hydrodynamically smooth regime from easily obtainable subatmospheric tests or a good correlation the potential efficiency vs Reynolds number relation can be drawn for hydrodynamically smooth flow. By making use of the experience that the bend over occurs within a small Reynolds number band the average upper critical Reynolds number $Re_{crit,u}$ can be marked on the η_{pol} -Re function as the bend over point towards constant η_{pol} efficiency for a certain roughness chosen. The potential efficiency losses can be picked off for various Reynolds numbers between the constant and the increasing efficiency line for hydrodynamically rough or smooth flow, respectively. If the picture is handled parametrically for various roughness heights it provides an easy and good insight into the potential efficiency losses due to roughness of blades involved in high Reynolds number operating points.

6. Conclusions

Analysis of limited experimental data reveals that critical roughness Reynolds numbers of compressor blades manufactured with typical present day methods as forging/etching and electrochemical machining are around 90 and therefore very close to sand type roughness if roughness height is based on the largest peaks.

Modern high pressure ratio engines suffer from blade surface roughness in the back stages of the compression system. Surface quality needed to keep the flow hydrodynamically smooth exceeds considerably the best present day quality achievable, thus limiting the potential efficiency gain at high Reynolds number flight conditions, i.e. essentially low level flight conditions.

7. References

- Ref. 1 Nikuradse, J. Gesetzmäßigkeit der turbulenten Strömung in glatten Rohren
Forschungsarbeit im Ingenieurwesen, H. 356, 1932
- Ref. 2 Schlichting, H. Grenzschicht-Theorie
Verlag Braun, Karlsruhe, 5. Auflag, Kapitel XX, XXI
- Ref. 3 Bammert, K.
Milsch, R. Boundary Layers on Rough Compressor Blades
ASME-Paper No. 72-GT-48, 1972
- Ref. 4 Bammert, K.
Woelk, G.V. The Influence of the Blading Surface Roughness on the
Aerodynamic Behaviour and Characteristics of an Axial
Compressor
ASME-Paper 79-GT-102, 1979
- Ref. 5 Bammert, K.
Woelk, G.V. Untersuchung des Rauigkeitseinflusses auf die Strömungs-
verluste im Axialverdichter
Sonderforschungsbereich 61, Bericht 18, Abschlußbericht
zum Teilprojekt C5 1977, Techn. Universität Hannover
- Ref. 6 Schäffler, A. Experimental and Analytical Investigation of the Effects of
Reynolds Number and Blade Surface Roughness on Multistage
Axial Flow Compressor
ASME-Paper No. 79-GT-2, 1979
- Ref. 7 Speidel, L. Einfluß der Oberflächenrauhigkeit auf die Strömungsverluste
in ebenen Schaufelgittern
Forschung im Ingenieurwesen 20, S. 124 - 140 (1954)
- Ref. 8 Scholz, N. Aerodynamik der Schaufelgitter, Band I
Verlag Braun, Karlsruhe, 1965
- Ref. 9 Hürlimann, R. Zum Einfluß der Oberflächenrauhheit, insbesondere der Fer-
tigungsgüte auf die Strömungsverluste von Dampfturbinen-
schaufeln
VDI-Berichte Nr. 193, 1973
- Ref. 10 Koch, C.C.
Smith, L.H. Jr. Loss Sources and Magnitudes in Axial-Flow Compressors
Trans. of the ASME, J. of Engng for Power, July 1976, 411-424
- Ref. 11 Wassel, A.B. Reynolds Number Effects in Axial Compressors
ASME Journ. of Engng. f. Power, April 1968

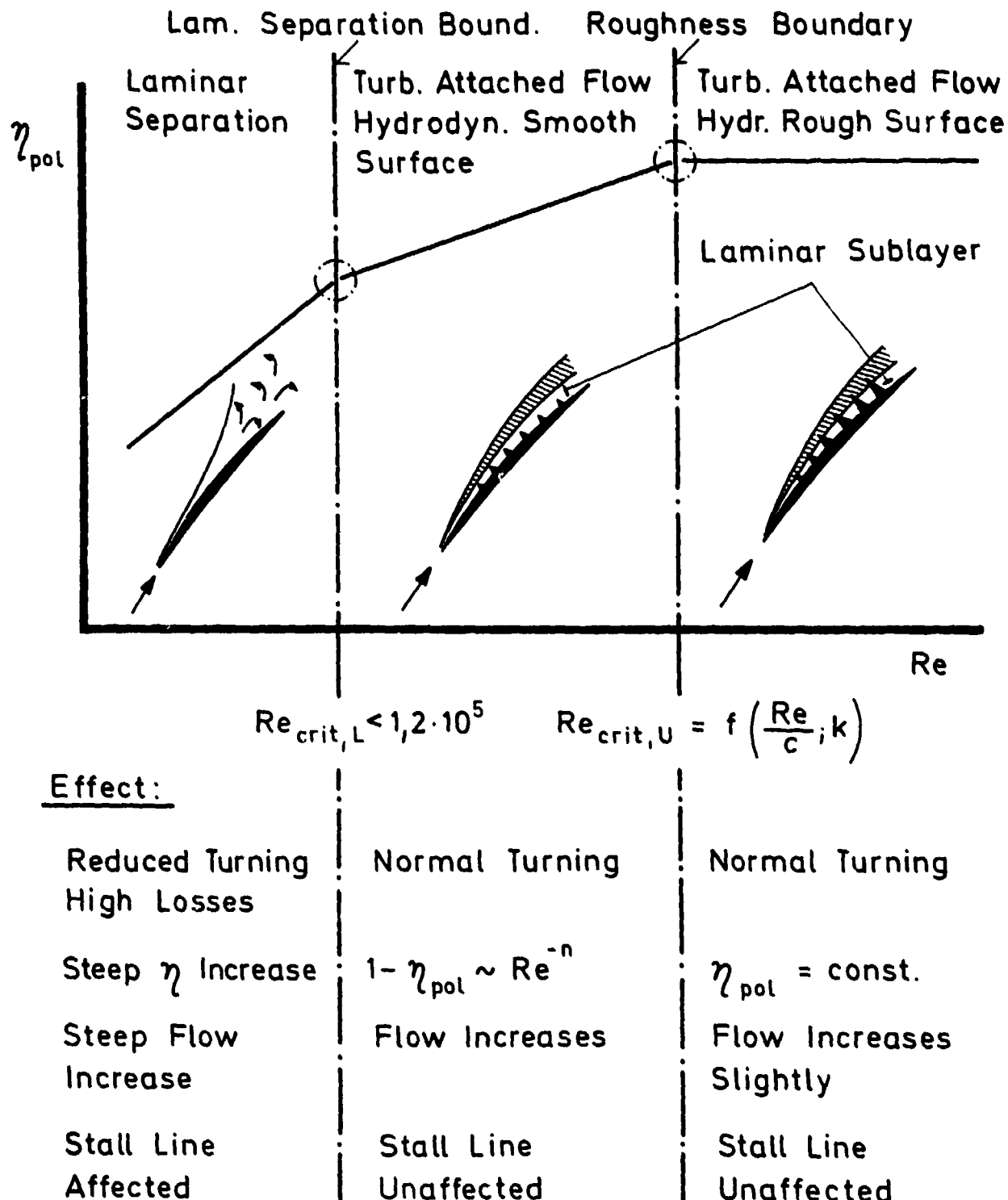
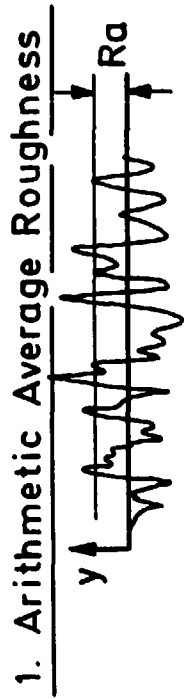
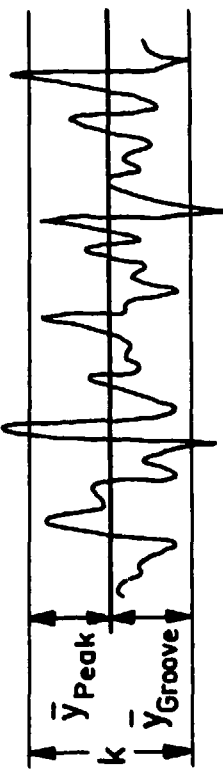


Fig.1 Effect of boundary layer conditions on compressor behaviour



$$R_a = AA = CLA = \frac{1}{l_m} \int_0^{l_m} |y| \cdot dx$$

2. Roughness Height k Used for Data Correlation



Roughness
Height
Defined to :

$$k = \bar{y}_{\text{Peak}} - \bar{y}_{\text{Groove}}$$

Arithmetic Mean of 10
Highest Peaks / Millimetre
Arithmetic Mean of 10
Deepest Grooves /
Millimetre

Average of 30 Roughness Samples Taken Over 5 mm
Length on Blades Produced by Forging / Etching
or Electrochemical Machining (ECM) :

$$k = 8,9 \cdot R_a$$

Fig.2 Definition of roughness parameters

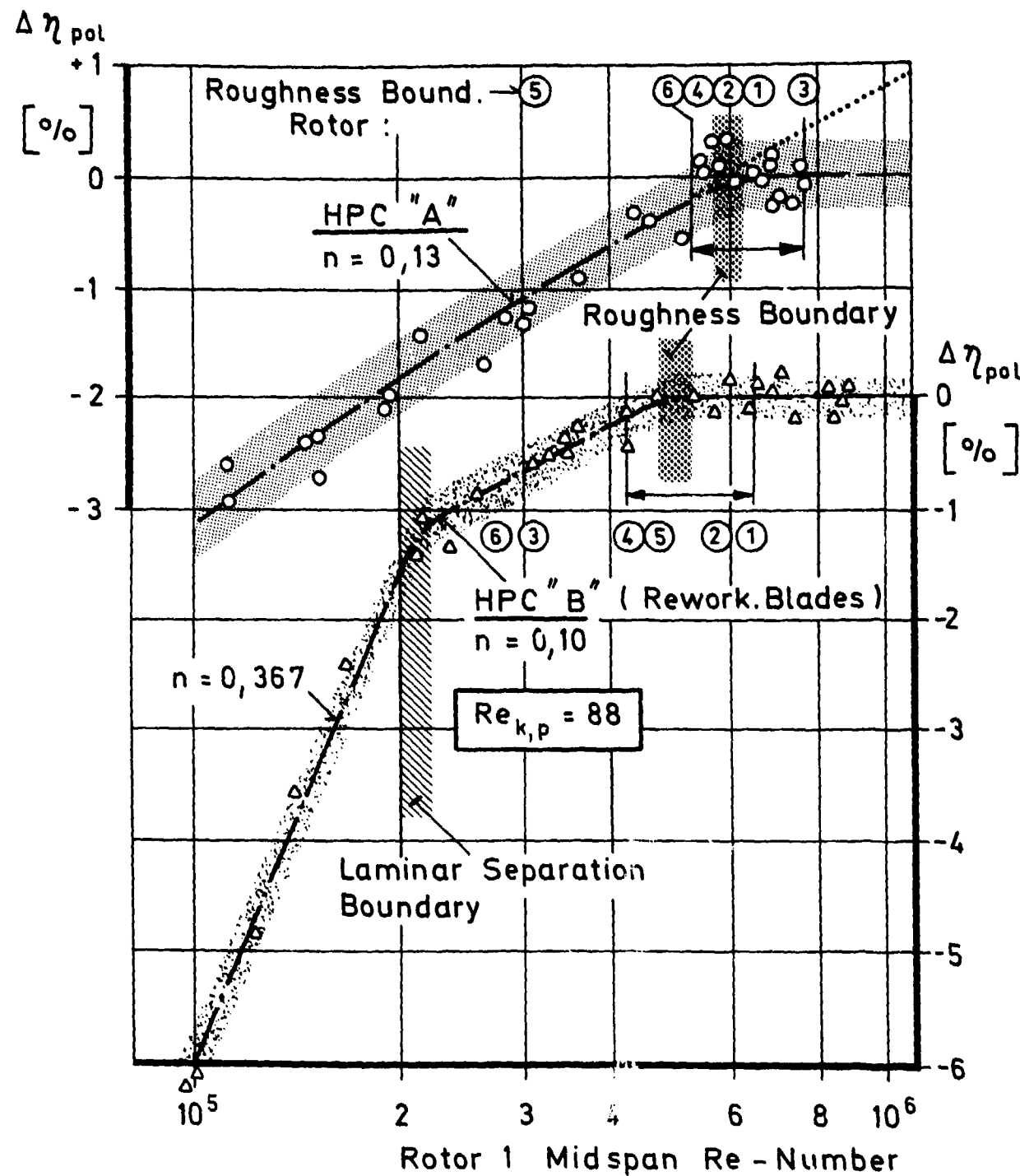


Fig.3 Effect of Reynolds-Number and surface roughness on polytropic efficiency
of two 6-stage high pressure compressors

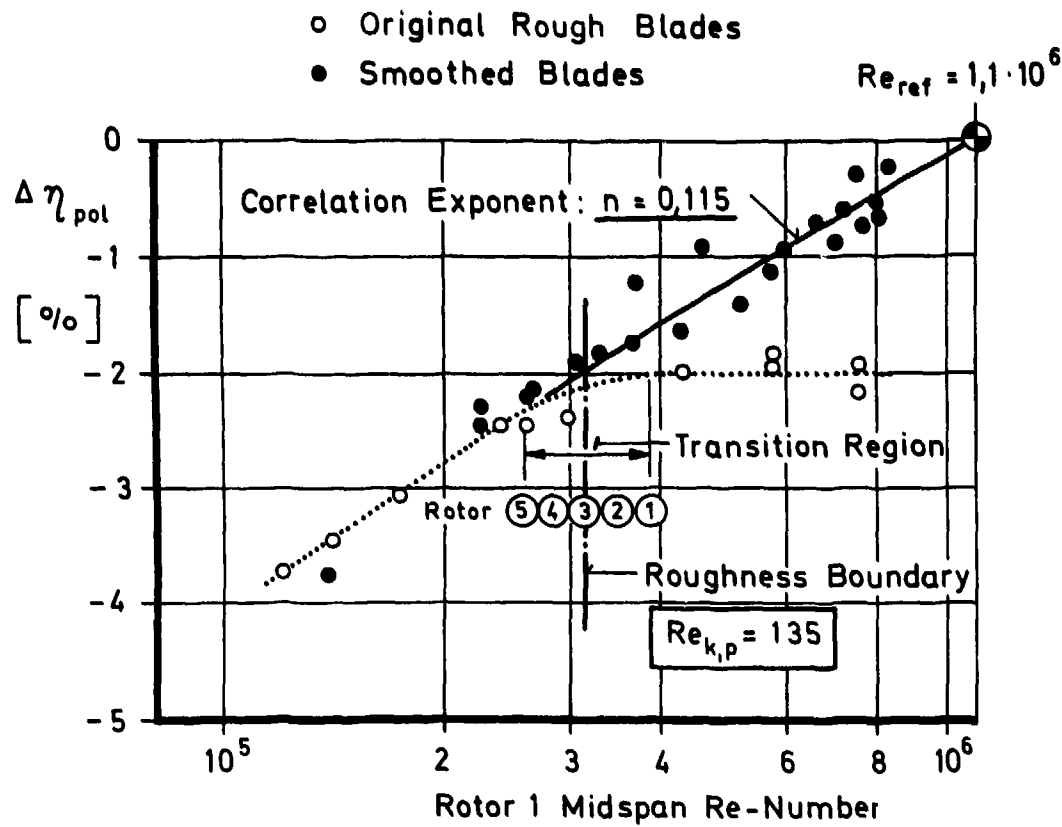


Fig.4 Effect of Reynolds-Number and surface roughness on polytropic efficiency of a 5-stage high pressure compressor

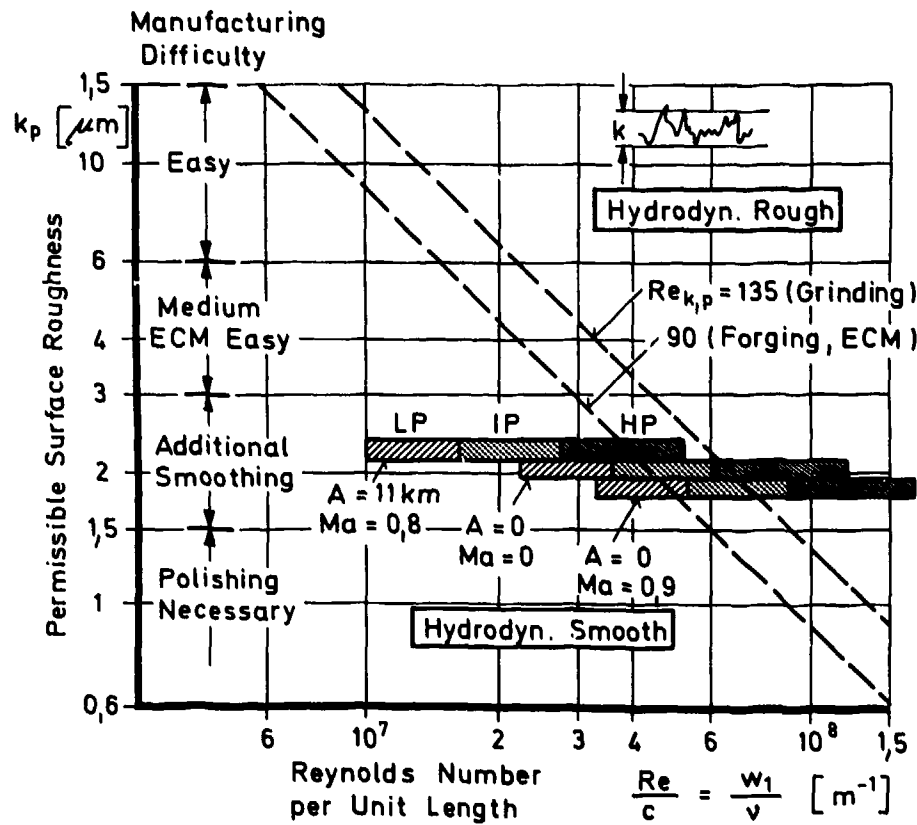


Fig.5 Permissible surface roughness for hydrodynamically smooth boundary layer flow

Assumption : $w_1 = 385 \text{ m/s} = \text{const.}$

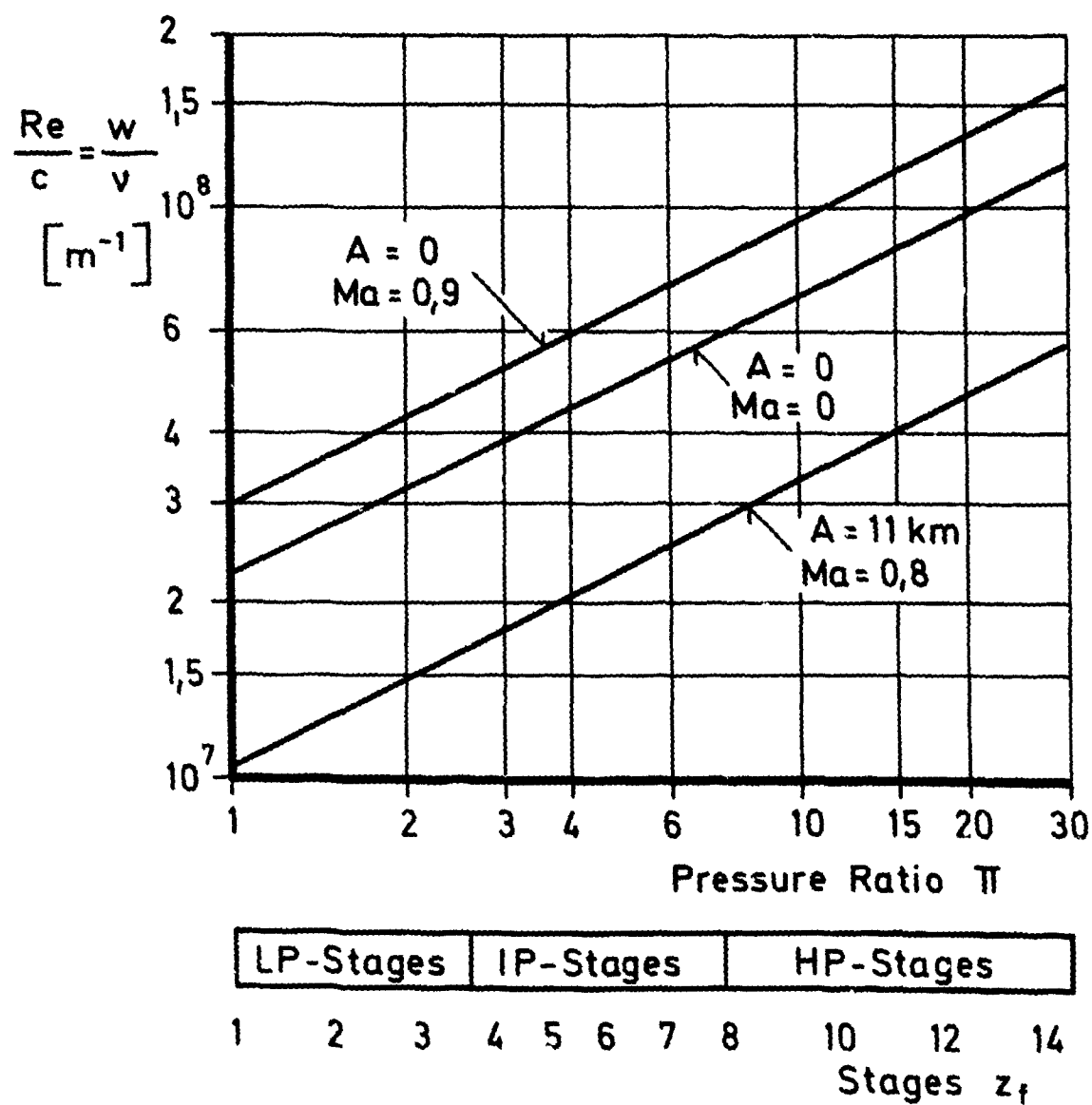
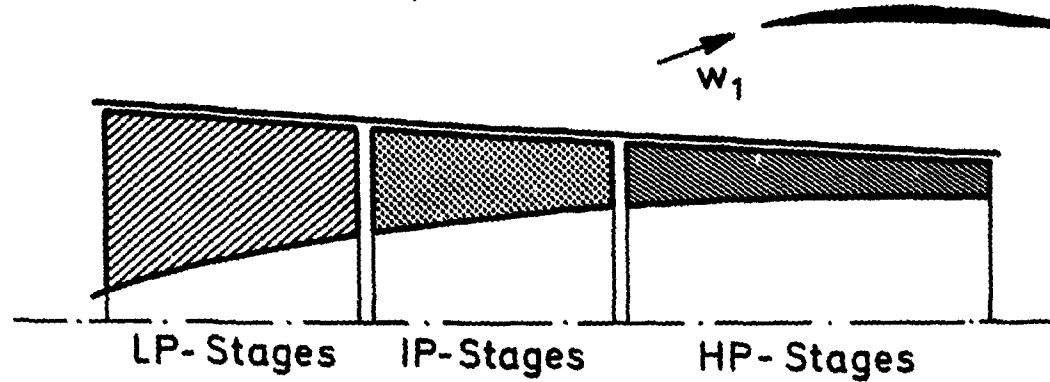


Fig.6 Reynolds-Number per unit length as a function of compressor pressure ratio and flight condition

II.2.7 Part Span Damper Loss Prediction For Transonic Axial Fan Rotors

There are only a limited number of references in the open literature on loss calculations for transonic axial fan rotors. Obviously the problem is quite arduous and many of the results are proprietary.

Evaluation of part span damper (PSD) losses is among the more difficult of these studies; two attempts have been documented in the open literature.

(i) Optimization of PSDs requires the knowledge of the minimum loss that can be achieved. This is the Koch & Smith (Reference 1) approach. They consider the situation to be divisible into two parts.

First one could identify a profile drag contributed by the series of PSDs that is equivalent to the drag of an annular shroud, not interrupted by the blades. This shroud is then treated as an infinite uncambered airfoil. Considered in this fashion, the significant Mach number is the meridional component of the relative Mach number. For all relevant cases this is always subsonic. Thus, even in the case of a transonic fan there is no PSD leading edge shock loss to be considered.

Second, one can define an interference drag coefficient, once again a function of the meridional Mach number.

These two drag coefficients are, of course, dependent also on the geometry of the PSD cross section. In most cases an equivalent elliptical section can be defined and the corresponding drag coefficient can be estimated. The pressure loss coefficient will then be related to the entropy increment that can be expressed in the following way

$$(1) \quad \frac{\Delta s}{R} = C_D \frac{1}{2} M_m^2 \frac{A_s}{A_a}$$

where C_D is the drag coefficient, Mach number M is based on the vector mean of the upstream and downstream velocities and on the average static temperature; A_s is the PSD ring area, A_a is the annulus area.

Examination of experimental data shows that to a theoretical shroud drag of the order of 0.3 there corresponds an effective drag coefficient that can be derived from experimental pressure losses using relation (1). This coefficient varies between 0.3 and 1.3.

In order to understand the reason for such scattering the experimental data should be examined in detail: total pressure, total temperature and flow angle traverse downstream of a transonic fan show that the effect of PSD is merely the increase of total temperature and a swing in absolute air angle due to damper wake. These effects increase with angle of attack and may be attributed to flow separation and interference effects with the blades.

From the theoretical approach a probable minimum value of PSD losses can be derived. The theoretical expression (1) has to be amended by means of an empirical coefficient of the order to 1.8 and the expression

$$(2) \quad \frac{\Delta s}{R} = 1.8 C_D \frac{1}{2} M_m^2 \frac{A_s}{A_a}$$

gives the minimum entropy increment that can be expected from PSDs on a transonic fan.

(ii) Correlation of experimental data was attempted by Roberts (References 2 and 3). A series of correlations has been formulated and proposed to predict the design and off-design aerodynamic performance of PSD on transonic rotors.

At the design point, the total pressure losses attributable to the damper were correlated with the following parameters:

1- The shroud loss coefficient, w_g , for the blade element containing the damper, which is the total pressure loss coefficient associated with a normal shock of strength M_1 . (M_1 is the relative Mach number at the rotor inlet.) Although it was shown by Koch and Smith that the flow relevant to the shroud is usually subsonic since it corresponds to the meridional Mach number, these authors did not take into account the interruption of the blade shock surfaces by the PSDs that generates this loss;

2- A blade aerodynamic loading parameter, such as the camber Φ divided by the solidity σ at the damper spanwise location;

3- The geometry of the damper itself, characterized by the leading edge and the trailing edge damper radius normalized by the mean span and damper chord respectively (as a usual order of magni-

tude one can take $r_{le}/h = 0.001$ and $r_{te}/C_{damp} = 0.005.$)

Correlation of experimental results obtained on more than twenty different fans leads to the following relation for the maximum pressure loss coefficient at the design point

$$(3) \quad \overline{w}_{PSD, M}^* = 500 \left(\frac{r_{le}}{h} \right) w_s + 8 \frac{r_{te}}{C_{damp}} \frac{\Delta}{\sigma}$$

The excess pressure loss due to the PSD can then be approximated by means of a normalized distribution, knowing that the spanwise region of influence can be taken as 12.5 times the damper thickness.

$$(4) \quad x = 12.5 t$$

For off-design conditions, the maximum loss due to the damper and region of influence at design point are calculated and these values are used as reference quantities for all off-design calculations. The point of intersection of a constant throttle or area operating line through the design point with a speed line defines the reference point where the PSD loss is minimum. From this point the suction surface incidence at the damper location is determined from experimental data or off-design analysis code. Then the damper maximum loss region of influence is calculated for any point on the speed line by taking the difference in suction surface incidence at that point and the reference incidence and using it in equations (5) and (6).

$$(5) \quad \overline{w}_{PSD, M} = \overline{w}_{PSD, M}^* + 0.02 \left(\frac{\Delta}{\sigma} \right) (\Delta i_{ss})^2$$

$$(6) \quad X/h = (X/h)^* + 0.06 \left(\frac{\Delta}{\sigma} \right) (\Delta i_{ss})^2$$

where $i_{ss} = i_{ss} - i_{ss}^*$

(iii) To minimize damper loss, several things should be taken into consideration. Both approaches agree on the following:

- 1- The damper should be as thin as possible so as to minimize the area influenced;
- 2- The damper should be located as near to the hub as possible;
- 3- Work input should be minimized at the PSD location.

Correlation of experimental results shows further that damper trailing and leading edge thickness should be as sharp as possible.

References

- (1) Koch, C.C. and Smith, L.H., Loss Sources and Magnitudes in Axial Flow Compressors - Journal of Engineering for Power, July 1976.
- (2) Roberts, W.B., A Design Point Correlation for Losses Due to Part-Span Dampers on Transonic Rotors, Journal of Engineering for Power, July 1979.
- (3) Roberts, W.B., Crouse, J.E., and Sandercock, D.M., An Off-Design Correlation of Part-Span Damper Losses Through Axial Fan Rotors, ASME Paper No. 79-GT-6.

Nomenclature

A_a	Annulus Area
A_s	Part-Span Damper Area
C_D	Drag Coefficient
C_{damp}	Part-Span Damper Chord
i_{ss}	Incidence Angle To Blade Suction Surface, Deg.
M_m	Meridional Mach Number
M_1	Mean Inlet Relative Mach Number
PSD	Part-Span Damper
R	Specific Gas Constant
r_{le}	Leading Edge Part-Span Damper Radius
r_{te}	Trailing Edge Part-Span Damper Radius
t	Part-Span Damper Maximum Thickness
X	Part-Span Damper Spanwise Region Of Influence
γ	Ratio Of Specific Heats
Δs	Entropy Increment
δ	Blade Camber Angle, Radians
ζ	Solidity, Ratio Of Blade Chord To Spacing
w	Total Pressure Loss Coefficient $(P_1 - P_2)/q_1$

Subscripts

PSD, M	Maximum Additional Loss Due To Part-Span Damper
*	Design Point Conditions

II.2.8. Deviation/Turning Angle Correlations

INTRODUCTION

In the past, and at present, compressor through-flow solutions have used substantial input from experimental measurements made in actual fan and compressor flow passages or in flows simulating real compressor conditions. For example, almost total reliance has been placed on experimentally supported methods for estimation of fluid turning angles in individual blade rows. Compressor design is, as a result, heavily dependent on the quality of the experiments and data correlations associated with these methods.

The three principal currently-used prediction methods for flow turning angle were developed during the period 1945 to 1960. One of these methods directly predicts fluid turning angles in terms of cascade geometry and aerodynamic parameters. The others predict the exit flow deviation angle, defined as the angle between the average exit flow direction and the direction of a line tangent to the blade section camber line at the trailing edge. There has been no substantial modernization of these deviation/turning angle procedures since 1960, while during this time the methods have been widely applied to airfoil section profiles and in aerodynamic regimes far outside the limits suggested by the original derivations and data correlations.

BLADE-TO-BLADE FLOW FIELD COMPUTATION

Most compressor aerodynamic design/analysis systems include blade-to-blade flow field computation to aid in optimizing blade section shapes and their orientation in the blade row, but it must be remembered that the optimization is carried out in an iterative procedure in which the hub-to-tip distribution of flow is used to set the upstream and downstream boundary conditions for the blade-to-blade solution. These boundary conditions include the upstream and downstream relative flow angles and stream tube areas. Even under these conditions a complete capability to compute the viscous and compressible blade-to-blade surface flow field in axial-flow compressor blade row geometries has not been demonstrated up to the present.

Many partial computation procedures do exist for blade-to-blade flows and these are the procedures used in optimization. Nearly all, for examples Refs. 1-5, begin computation by working with an inviscid flow, and viscous influences are introduced in an iterative sequence if at all. References 1, 6 and 7 represent some specific attempts to predict exit flow angles and/or losses for compressor blade rows by blade-to-blade flow field computation. These were constructive attempts but there is little evidence of regular use of these or other methods to replace experimental turning angle and loss correlations in the iterative hub-to-tip calculations of an overall design system. Increased utilization of high relative Mach numbers combined with high loading levels has made the task of prediction even more difficult (Refs. 8 and 9).

Since the current overall trend in blade-to-blade flow field computation appears to emphasize development of ability to control and optimize the flow patterns in the blade row rather than to predict the flow deflections and losses produced, the continuation of both qualitative and quantitative improvement of experimental correlations for turning angle and loss is essential, but the possibility of improvement exists only if a correct conceptual model of the blade-to-blade flow is established and understood. The following sections describe the most important turning angle correlation systems available to compressor designers in the published literature.

EXISTING DEVIATION/TURNING ANGLE PREDICTION EQUATIONS

Three principal correlation equations are used as the bases for prediction of changes in relative flow angle across compressor blade rows. The initial development of all of these correlations occurred before 1960, and there has been little substantive change in the base equations since that time. All of the equations are semi-empirical in nature, with an analytical background supported by the results of linear cascade experiments. As a consequence of the theoretical and experimental flow field conditions associated with all three deviation/turning angle correlations, certain real compressor blade row problems are not resolved by the basic procedures:

- 1) Stream surface radial location, radius change and shape are not linear cascade variables. The problem of effective blade section profile definition does not occur.
- 2) Changes in radius do not affect blade spacing or effective chord length determination. Problems of cascade geometry definition do not occur.
- 3) Stream tube effective area changes are not prediction equation variables. Axial velocity-density ratio (Ω) was assumed equal to 1.0 for analysis and experiments used to generate the correlations, or it was considered not to be a strong influence on the results.
- 4) The prediction methods are directed toward the selection of suitable cascade geometry combinations for design point operation in conservative, non-extreme compressor configuration. There is insufficient theoretical or experimental support in terms of marginal loading levels and setting angle-solidity combinations.

The conditions associated with the initial development of the three deviation/turning prediction methods are considered sufficiently important to justify a separate descriptive subsection and an Appendix devoted to each one. The Appendices also collect in one location material drawn from numerous sources which are sometimes difficult to locate. The Appendices are organized so that the restrictive conditions connected with each correlation are given in a standard format. Naturally in the application of the basic

correlations to the design or analysis problems for real compressor blade rows, strategies have been developed to adapt the definitions of equation variables to compressor geometry and to extend the ranges of geometric and aerodynamic variables outside the limits suggested by the base correlations. Each Appendix contains some examples illustrating these strategies.

It should be remembered that the objective in the case of each deviation/turning angle method was to permit estimation of the change in average relative flow direction across a cascade arrangement operating in a two-dimensional flow at specified entrance flow conditions including a defined entrance flow direction or incidence angle. The base incidence angle was different for each correlation, was not intended to represent a design incidence, and was indicative only of prevailing ideas concerning favorable aerodynamic operation.

1. NATIONAL GAS TURBINE ESTABLISHMENT (NGTE) CORRELATION

The overall development of axial-flow compressor design methods in the United Kingdom during the period 1939 to 1950 included research leading to the NGTE deviation angle prediction equation, commonly called Carter's rule. Figure 1 shows the primary pattern of development of the correlation by reference to supporting analysis and experiments.

The NGTE correlation was based on trends in deviation angle predicted by analysis of two-dimensional potential flow through cascades with sharp trailing-edge blade sections (to permit use of the Kutta-Joukowski circulation condition). This analysis was supported and the equation for deviation was adjusted by the results of plane cascade experiments. The correlation was initially proposed to give the deviation angle corresponding to a nominal flow turning angle, equal to 0.8 times the turning measured at cascade stall (maximum turning). In the theoretical studies the base incidence was either arbitrarily defined (Ref. 14, $i_c = 4$ deg) or set at the value for maximum lift/drag ratio (Ref. 15). In Appendix A the i_{opt} values of Ref. 15 were considered to be the base incidence. This Appendix summarizes the background and subsequent application of the NGTE deviation method.

In the recommended terminology of this report, the base equation of the NGTE correlation is

$$\delta = \frac{m_c \varphi}{\sqrt{\alpha}}$$

Reference 15 also included generalized performance curves to permit prediction of cascade turning angles for non-optimum incidence.

2. NATIONAL ADVISORY COMMITTEE FOR AERONAUTICS/NATIONAL AERONAUTICS AND SPACE ADMINISTRATION (NACA/NASA) CORRELATION

The NACA/NASA procedure for estimation of deviation angles for axial-flow compressor cascades was developed at the Lewis Flight Propulsion Laboratory of the NACA between 1952 and 1956 as a part of the preparation of a summary of NACA compressor design technology.

The NACA/NASA correlation used previous theoretical work (Refs. 16 and 17) as well as the NGTE correlation to suggest the form of the base equation, but specifically attempted to recognize and eliminate deficiencies noted in the NGTE method:

1. The NGTE correlation predicts zero deviation angle for zero camber blade section profiles. Both theoretical and experimental studies indicated a non-zero deviation angle for two-dimensional flow across staggered cascades with zero camber and non-zero thickness at zero incidence.
2. Both camber line shape and blade section thickness distribution were believed to significantly affect deviation angle.
3. Use of a constant exponent on the solidity parameter in the NGTE correlation was considered unsatisfactory.

In the recommended notation of this report the NACA/NASA correlation equation is (Ref. 23).

$$\delta_{ref} = \delta_0 + \frac{a - 1}{a^b} \varphi$$

To define the correlation, available plane cascade experimental data were evaluated to isolate a base of experiments which could be considered two-dimensional ($\Omega = 1.0$). This eliminated a substantial number of sources, including most potential variants in blade section profile. The final correlation was strongly influenced by NACA experiments (Refs. 18-20) carried out at low cascade inlet Mach numbers. Unfortunately these experiments also were sequences of data points at constant inlet flow angle β_1 with the variation in incidence obtained by changing stagger angle. This created difficulty in defining a base incidence angle related to the operation of real compressor cascade arrangements, where the stagger remains constant as inlet flow angle changes (Ref. 27).

The predicted deviation angle corresponds in the NACA/NASA correlation to a reference minimum loss incidence angle at low inlet Mach numbers. A procedure was derived for determining the effects of incidence changes. The equation is

$$\delta = \delta_{\text{ref}} + (i - i_{\text{ref}}) \left(\frac{d\delta}{di} \right)_{\text{ref}}$$

but it is limited to the relatively small range of incidence at low inlet Mach number in which the slope $\left(\frac{d\delta}{di} \right)_{\text{ref}}$ is constant.

Figure 1 shows the development pattern of the NACA/NASA correlation, and a more complete summary of its content is given in Appendix B.

3. USSR CORRELATION

This correlation is the product of extensive systematic plane cascade experiments performed in the Soviet Union between 1951 and 1956. Two independent sets of data are involved (Ref. 24 and 25), reporting results for cascade entrance Mach numbers up to 0.92 with Ω in the range 1.0 to 1.15 (not controlled).

The correlations developed (Ref. 26) are almost entirely empirical in nature, but they cover a wide range of cascade blade row geometry and substantial variations in blade section profile, unfortunately only including two camber line shapes with very limited movement of the position of the maximum camber location.

The principal prediction equation estimates the low-speed flow turning angle corresponding to two-dimensional flow across a cascade operating at an optimum incidence angle. In this case the optimum incidence is based on the minimum value in the loss-incidence curve at a specified high-subsonic Mach number level (Ref. 25). A relatively simple equation is suggested for the prediction of optimum incidence.

In the recommended notation of this report

$$\Delta\beta_o = \left[\frac{(\Delta\beta_o)_{d/c}}{(\Delta\beta_o)_{d/c} - 0.4} \right] \left[\frac{(\Delta\beta_o)_{t/c}}{(\Delta\beta_o)_{t/c} - 0.10} \right] \left[\frac{K\varphi}{1000} + B \right]$$

$$K = (5 - \frac{2}{\sigma}) \sqrt{(90 - \gamma)^2 - \frac{1000}{\sigma} + 100 (5.5 - \frac{2.6}{\sigma})}$$

$$B = 8 \left(\frac{1}{\sigma} \right)^2 - \frac{17}{\sigma} + 16$$

$$\frac{(\Delta\beta_o)_{d/c}}{(\Delta\beta_o)_{d/c} - 0.4} = 1 - 0.28 (d/c - 0.4) \text{ for } \frac{d}{c} = 0.3 \text{ to } 1.0$$

$$\frac{(\Delta\beta_o)_{t/c}}{(\Delta\beta_o)_{t/c} - 0.10} = 1 - 1.6 (0.10 - t/c) \text{ for } \frac{t}{c} = 0.0125 \text{ to } 0.125$$

Generalized curves are given in Ref. 25 for the influence of cascade entrance Mach number and incidence variation above and below optimum on cascade fluid turning angle $\Delta\beta_o$. Appendix C outlines the basis for the USSR correlation. Little is known about specific applications.

DEVIATION ANGLE CORRELATION FOR ADVANCED FAN AND COMPRESSOR DESIGN/ANALYSIS

1. EXPERIMENTAL DEVIATION/TURNING ANGLE DATA

a. Plane Cascade Data

Figure 1 shows that a very limited part of the linear cascade data available in the literature has been used in development of the principal existing deviation/fluid turning angle correlations. In the majority of linear cascade experiments carried out before 1950, the results were not suitable for correlation because of unsatisfactory control of aerodynamic variables in the test programs and because of inadequate measurement and data reduction methods (Refs. 23 and 28). However, after 1950 and up to the present, numerous linear cascade facilities have been used for experiments with both subsonic and supersonic inlet flow through compressor blade section profiles in cascade arrangement. Of the published results of experiments conducted during the past 25 years, some but not all might be satisfactory for extension or development of deviation/turning angle prediction methods. Certain preconditions should be considered in evaluation of the data:

- 1) Is the blade section profile and cascade geometry adequately described for definition of geometric variables?
- 2) Have the independent aerodynamic variables been satisfactorily controlled, so that the parameters influencing fluid turning angles can be considered numerically reliable?
- 3) Are the measurement and data reduction methods clearly described so that the basis of

numerical values of both deviation/turning angle and total-pressure loss parameters can be understood?

- 4) Is there sufficient data available to assist in extension of the range of applicability of existing correlation forms or to support the development of a new prediction method?

A large number of data sources were investigated during the present study and in the case of linear cascade results several sets of published data were considered suitable in terms of most of the above criteria. These includes Refs. 29,30,31,20 and 32-47. In addition, some unpublished data were obtained. In general both the published and unpublished results met all requirements except for number 4 above. While the data has been acquired in order to meet a limited research or development objective, it is not systematically planned so as to allow the generation of a new prediction method.

b. Fan and Compressor Cascade Configuration Data

Annular cascade results from flow passage surveys in rotor and stator rows of axial-flow fans and compressors are not available in significant quantities, especially where the data quality is adequate for possible correlation. A large number of reported and unpublished test data sets were considered as candidates, with the vast majority of these sets from rotor and stage experiments carried out by the NASA and by NASA contractors.

The principal question of data adequacy for deviation/turning angle and loss correlation exists as a result of the presence of part-span dampers or shrouds in the rotor blade rows involved. While the damper geometries do not reduce the value of the data for many purposes, the aerodynamic effects cover enough of the flow passage downstream from the shrouded row to confuse the data for angle and loss correlation (Ref. 48). Probable exceptions exist in the case of Refs. 49 and 50-53, and possible additional sets may be evaluated as satisfactory in the future (e.g. Refs. 54-59).

Some reservations must exist concerning the use of fan and compressor passage survey data measured with conventional pressure and temperature probes. The data-averaging characteristics of many probe types remain in question.

INFLUENCE ON DEVIATION/TURNING ANGLE OF AERODYNAMIC VARIABLES NOT INCLUDED IN PRINCIPAL EXPERIMENTAL CORRELATIONS

This section discusses several aerodynamic quantities known to have an effect on cascade deviation/turning angle, but not accounted for in the principal correlations of experimental data. These are quantities which in many typical axial-flow compressors will fall in a range of values outside the correlation boundaries. As a result some correction to correlation predictions should be made in design or performance prediction by through-flow methods.

Brief discussions of the principal variables follow, but the major relevant work is summarized in Table I to conserve space. Two kinds of references are called out for each variable. The first group consists of valid data sets indicating the quantitative order of the effect of each variable as a separate influence on turning angle. The second group includes methods for correction of two-dimensional, optimum incidence fluid turning angle/deviation predictions. It should be noted that many of the corrections account for the isolated effect of a single parameter, while in general the variables are highly-interrelated in the blade row of a compressor.

TABLE I. DATA BASE FOR EFFECT OF NON-CORRELATED CASCADE AERODYNAMIC VARIABLES ON TWO-DIMENSIONAL, OPTIMUM INCIDENCE FLUID TURNING ANGLE/DEVIATION

AERODYNAMIC VARIABLE	REFERENCE	DATA SOURCE	TURNING CORRECTION METHOD
Inlet Mach Number, M_1	Andrews 21 Todd 76 Dunavant, et al. 36 Briggs 39 Howell 11, 12 Robbins, et al. 77 Swan 78 Jansen, Moffatt 79 Novak 67 Davis, Millar 60, 80	X X X X X X X X X X	
Reynolds Number, Re_c	Howell 11, 12 Horlock, et al. 81 Hebbel 82 Roberts 83 Hoheisel, Klock 84 Davis, Millar 80	X X X X X	X
Free-Stream Turbulence	Barsun 85 Schlichting, Das 86 Klock 87, 88 Evans, B. 89	X X X X	X

AERODYNAMIC VARIABLE	REFERENCE	DATA SOURCE	TURNING CORRECTION METHOD
Free-Stream Turbulence (cont'd)	Evans, R. 90, 91	X	
Incidence Angle, i_c or i_{ss}	Howell 11, 12 Lieblein 23 Swan 78 Davis 60, 80 Novak 67		X X X X X
Axial Velocity-Density Ratio, Ω	Jansen, Moffatt 79 Heilmann 40, 41 Masek, Norbury 44 Ilyas, Norbury 45 Starken, et al. 42 Gustafson 92 Starke 93 Stark, Hoheisel 94	X X X X X X X	X X X X X
Aerodynamic Loading Level	Lieblein 23 Swan 78 Davis 60, 80 Heilmann 40, 41	X X	X X
Secondary Flows End-Wall Effects Tip Clearance	Lakshminarayana, Horlock 95, 96 Bardon, Moffatt 97 Smith 98	X X X	X X

1. UPSTREAM RELATIVE MACH NUMBER

In axial-flow compressors the Mach number level of the upstream relative flow may be either subsonic or supersonic. The influence of M_1 on the cascade flow field has been extensively studied in linear, annular and rotating blade cascades, with the primary objective of blade section loss optimization. Only a few data collections have focused on deviation/turning correlation.

In general, there is a minimal effect of relative upstream Mach number for $M_1 < M_{1,critical}$. This is shown in Refs. 23 and 77, with experimental support from rotor, stator and linear cascade data. Above the critical M_1 , correction equations are proposed in Refs. 78, 79 and 80, and correction curves derived principally from subsonic compressor data are given in Refs. 27 and 77. For choked cascade and supersonic upstream M_1 , correlations are rare, with most reported designs showing no direct correction procedure for M_1 .

2. REYNOLDS NUMBER

Turning/deviation corrections for Reynolds number level have been studied only in limited-objective experiments. Generally linear cascade correlations are reported as valid above a specified Re_c value, and the principal conclusions related to effects of Re_c on boundary layer transition, flow separation, and cascade loss coefficient.

3. FREE-STREAM TURBULENCE PARAMETERS

Compressor design/analysis systems do not usually account for turbulence parameters as independent variables. This is certainly due to the limited data reporting measured turbulence quantities in typical compressor configurations for locations other than the compressor inlet face. As is the case for Reynolds number, most linear cascade test documents have concentrated on the influence of turbulence parameters on boundary layer development and cascade loss coefficient.

4. INCIDENCE ANGLE

For two-dimensional linear cascade data, the change of deviation angle with incidence near the optimum or design incidence is very small unless the cascade aerodynamic loading is high. Near the optimum incidence, the correlated values of Ref. 23 may be used. As a general off-design performance prediction aid, these values are not acceptable.

5. AXIAL VELOCITY-DENSITY RATIO

Axial-velocity density ratio (AVDR), defined as

$$\Omega = \frac{(\rho v)_x}_{\text{trailing edge plane}} \frac{(\rho v)_x}{\text{leading edge plane}}$$

has for many years been recognized as an influential variable in linear cascade tests. However, lack of control of this independent variable has reduced the validity of numerous linear cascade data sets including some of those associated with the principal deviation/turning angle correlations.

Several of the experimental studies of AVDR influence have suggested that a correction equation of the form

$$\Delta\beta = \Delta\beta_{\Omega=1} + \left[\frac{d(\Delta\beta)}{d\Omega} \right]_{\Omega=1} (\Omega - 1.0)$$

is valid, with the derivative term determined by cascade geometry.

The difficulty of generalization of AVDR effects is due to several problems:

- 1) The AVDR effect in through-flow computation, as well as in linear cascade tests is a measure of the change in effective stream-tube area through the cascade row geometry. The rate of area variation through the cascade has an influence on both loss and turning.
- 2) The AVDR effect in higher Mach number cases is naturally related to the shock wave pattern existing in the blade row, and is therefore difficult to isolate for correlation.
- 3) The AVDR effect is completely interdependent and not separable from the general effect of cascade or row aerodynamic loading level.

6. CASCADE DIFFUSION FACTOR LEVEL

Turning/deviation characteristics of linear cascades have been demonstrated dependent on diffusion loading as measured by any of the recognized limit parameters. However, the level of diffusion has not been directly incorporated into turning/deviation angle prediction equations because the optimum incidence condition for all but a limited number of correlated cascade geometries was representative of low diffusion parameter levels. Lieblein (Ref. 23) made the observation that there was an effect of D on deviation in two-dimensional linear cascade results, and excluded from the NACA correlation all data for $D > 0.62$.

FLUID TURNING ANGLE ESTIMATION FOR THROUGH-FLOW CALCULATION METHODS USING COMPUTATION STATIONS WITHIN BLADE-TO-BLADE PASSAGE

Existing and future through-flow computation for axial-flow compressors requires initial estimation of the fraction of total cascade turning for each internal computation station. This estimation is significant in flow field determination. Most existing intrablade computation reported uses guessed approximations for turning rate. Some useful optical measurements in compressor rotors that may aid in the improvement of turning rate approximation have been generated in recent years (Refs. 58, 59, 99).

APPENDIX A

NATIONAL GAS TURBINE ESTABLISHMENT DEVIATION ANGLE CORRELATION¹

Base Equation

$$\delta = m\theta \sqrt{\frac{s}{c}} \quad (\text{Ref. 15})$$

at

$$i = i_{\text{opt}} \quad (\text{Ref. 15})$$

- δ deviation angle, angle between cascade exit average fluid angle and line tangent to blade section camber line at trailing edge, degrees
- m function of blade section stagger angle and camber line shape, Figure A-3.
- c blade section stagger angle, angle between chord line and axial direction, degrees
- θ blade section camber angle, angle between lines tangent to section camber line at leading and trailing edges, degrees
- s blade spacing, tangential distance between equivalent points on adjacent blade sections
- c chord length, length of straight line connecting points where camber line intersects leading and trailing edges
- i incidence angle, angle between cascade inlet average flow angle and line tangent to blade section camber line at leading edge, degrees

¹Symbols and notation defined in Appendix A correspond to original publication of correlation except for sign convention on stagger angle. See also Figures A-1 and A-2.

i_{opt} incidence angle predicted to give maximum lift/drag ratio for given cascade geometry, degrees
 α_1' blade section camber line angle at leading edge, measured from axial direction, degrees
 α_2' blade section camber line angle at trailing edge, measured from axial direction, degrees
 α_1 average fluid angle at cascade inlet, measured from axial direction, degrees
 α_2 average fluid angle at cascade exit, measured from axial direction, degrees
 ϵ fluid turning angle, degrees
 V_1 fluid velocity at cascade inlet
 V_2 fluid velocity at cascade exit

Base Airfoil Section Profiles

- C.1 (Ref. 11)
- C.2 (Ref. 11)
- C.4 (Ref. 22)

Base Camber Line Shapes

- Circular-arc (Ref. 11)
- Parabolic, $\frac{a}{c} = 0.40$ only (Ref. 11)

Base Cascade Geometry Limits

$$\frac{a}{c} \left\{ \begin{array}{l} 0.50 \text{ circular-arc camber line} \\ 0.40 \text{ parabolic camber line} \end{array} \right.$$

$$\frac{d}{c} \left\{ \begin{array}{l} 0.33 \text{ C.1 section} \\ 0.30 \text{ C.2 section} \\ 0.30 \text{ C.4 section} \end{array} \right.$$

$\frac{t}{c}$ Ref. 15 based on analysis and data for $t/c = 10\%$

$$\text{LER} \left\{ \begin{array}{l} 0.08t \text{ C.1 section} \\ 0.12t \text{ C.2 section} \\ 0.12t \text{ C.4 section} \end{array} \right.$$

$$\text{TER} \left\{ \begin{array}{l} 0.02t \text{ C.1 section} \\ 0.02t \text{ C.2 section} \\ 0.06t \text{ C.4 section} \end{array} \right.$$

ζ m defined for ζ from 0 to 60 deg

$\frac{s}{c}$ Ref. 15 based on data for $\frac{s}{c}$ from 0.5 to 1.5

θ Applicable camber limited by section loading

Base Aerodynamic Variable Range

- M_1 analysis-incompressible flow results used in Ref. 15 all were for low-speed plane cascade flow
- Re results used in Ref. 15 refer to effective Re of about 4×10^5 based on chord and exit velocity
- Ω $\Omega = 1.0$, two-dimensional flow assumed in analysis and experiments
- Turbulence data not available

Design/Analysis Application Examples

A. Modified Base Equation and Incidence

The NGTE rule has been used to predict deviation angle for a range of incidence levels when cascade diffusion loading is low. This is done on the assumption that deviation variation with incidence is not

large when profile losses are low.

Various investigators including Refs. 60 and 61 have given equations for m based on Fig. A-3.

Application of the NGTE rule to design has frequently included a capability to add an arbitrary angle correction (for examples, Refs. 62 and 63).

Ref. 49 applied a modified equation to design

$$\delta = \frac{(\epsilon - i) m_c \sqrt{\frac{s}{c}}}{1 - m_c \sqrt{\frac{s}{c}}}$$

with

$$m_c = 0.92 \left(\frac{a}{c} \right)^2 + 0.002 \alpha_2$$

Ref. 63 suggests the substitution of an equation for m_c of the form

$$m_{cm} = (0.219 + 0.0008916\gamma + 0.00002708\gamma^2) \times \left(\frac{2a}{c} \right)^{2.175 - 0.03552\gamma + 0.0001917\gamma^2}$$

The experimental support for this modified m is not clear, but the trends associated with its use are similar to those of other application modifications. It should be noted that the definition of the angle γ given in Ref. 63 is slightly different from that used in this report and in the NGTE correlation. This difference is not considered material.

B. Extended Blade Section and Cascade Geometry Limits

Airfoil Section Profiles and Camber Line Shapes

The NGTE rule has been used for NACA 65-series profiles on circular-arc camber lines (Ref. 61) and for double-circular arc and multiple-circular-arc (DCA and MCA) profiles (Refs. 49, 62, 63, 64). It has been applied to a polynomial camber line with a polynomial thickness distribution (Ref. 65).

Ref. 63 includes an NGTE rule option for the sections defined in that report.

Cascade Geometry Limits

$\frac{a}{c}$ Equations or curves for prediction of deviation for a/c values less than 0.4 and greater than 0.5 are given in Refs. 49, 62, 63, 64 and 65.

ζ m values extrapolated by equation to $\zeta > 60$ deg

Blade-to-Blade Surface Radius Change

The NGTE rule has been used for radius change and $\Omega = 1.0$ cases by substituting an equivalent circulation turning angle into an equation of the form (recommended notation)

$$\delta = \frac{\beta_1 - i - \beta_2 e}{\sqrt{\sigma} - 1}$$

This approach is used in Refs. 61, 62, 63 and 64. See Appendix E.

C. Extended Aerodynamic Variable Range

M_1 Rule used without M_1 correction for supersonic entrance flows in Refs. 49, 62, 63, 64 and 65.

R_e Correction suggested in Refs. 10, 11 and 12.

Ω See the method under radius change above and in Appendix E. This approach used in Refs. 61, 62, 63 and 64.

APPENDIX B

NACA/NASA DEVIATION ANGLE CORRELATION¹

Base Equation

$$\delta_{ref} = \delta_0 + \frac{m\sigma - 1}{\sigma b}\varphi \quad \text{see Figures B-5, B-6, B-7 and Ref. 23}$$

with

$$\delta_0 = (K_\delta)_{sh} (K_\delta)_t (\delta_0)_{10} \quad \text{see Figures B-3, B-4}$$

at

$$i = i_{ref} \quad (\text{Ref. 23})$$

δ_{ref} cascade exit average deviation angle measured from tangent to blade trailing edge camber line direction for cambered cascade, degrees

δ_0 deviation angle measured from camber (chord) line for zero camber cascade with same fluid inlet angle and solidity as the cambered cascade, degrees

$(\delta_0)_{10}$ value of δ_0 for cascade with NACA 65-series blade section airfoil profile and maximum section thickness 10% of chord length, degrees

$(K_\delta)_{sh}$ dimensionless correction factor to $(\delta_0)_{10}$ for effects of blade section profile not NACA 65-series

$(K_\delta)_t$ dimensionless correction factor to $(\delta_0)_{10}$ for effects of blade section maximum thickness not 10% of chord length

φ blade section camber angle, with equivalent circular arc camber angle used for NACA A₁₀ camber line shape, degrees

σ cascade solidity, ratio of blade section chord length to blade-to-blade spacing or pitch

$m_{\sigma=1}$ rate of change of deviation angle with camber angle for cascade with solidity of 1.0

b correction exponent accounting for variable influence of solidity on δ -slope associated with different fluid inlet angles

s blade spacing, tangential distance between equivalent points on adjacent blade sections

c chord length, length of straight line connecting points where camber line intersects leading and trailing edges

i incidence angle, angle between cascade inlet average flow angle and line tangent to blade section camber line at leading edge, degrees

i_{ref} reference minimum-loss incidence angle, degrees (Ref. 23)

K_1 blade section camber line angle at leading edge, measured from axial direction, degrees

K_2 blade section camber line angle at trailing edge, measured from axial direction, degrees

β_1 average fluid angle at cascade inlet, measured from axial direction, degrees

β_2 average fluid angle at cascade exit, measured from axial direction, degrees

$\Delta\beta$ fluid turning angle, degrees

v_1 fluid velocity at cascade inlet

v_2 fluid velocity at cascade exit

Base Airfoil Section Profiles

NACA 65-010 blower blade section (on NACA A₁₀ camber line only)

C-series airfoil section thickness distributions (on circular-arc camber line only)

Double circular arc airfoil sections

¹Symbols and notation defined in Appendix B correspond to original publication and correlation. See also Figures B-1 and B-2.

Base Camber Line Shapes

NACA A₁₀ ($a = 1.0$)
Circular Arc

Base Cascade Geometry Limits

$$\frac{a}{c} \left\{ \begin{array}{l} 0.50 \text{ NACA A}_{10} \\ 0.50 \text{ circular arc} \end{array} \right.$$

$$\frac{d}{c} \left\{ \begin{array}{l} 0.30-0.33 \text{ C-series} \\ 0.40 \text{ 65-010 blower blade section} \\ 0.50 \text{ double circular arc} \end{array} \right.$$

$$\frac{t}{c} \left\{ \begin{array}{l} (k_{\delta})t \text{ given in range 0 to 0.12} \end{array} \right.$$

$$\text{LER} \left\{ \begin{array}{l} 0.0067c \text{ 65-010 blower blade} \\ 0.08 \text{ to } 0.12t \text{ C-series} \end{array} \right.$$

$$\text{TER} \left\{ \begin{array}{l} 0.0015c \text{ 65-010 blower blade} \\ 0.02 \text{ to } 0.06t \text{ C-series} \end{array} \right.$$

γ (β_1 is correlation angle)

σ (δ_o)₁₀ given in range $\sigma = 0.4$ to 2.0

Applicable camber limited by section loading to $D < 0.62$ with 60 deg implied by $0 < c_{10} < 2.4$ in Fig. B-5

Base Aerodynamic Variable Range

M_1 very small effect of M_1 on deviation at i_{ref} was predicted up to limiting M_1 , where rapid increase in loss occurs

Re above 2.5×10^5 based on chord length and cascade inlet velocity

Ω data correlated for $\Omega \approx 1.0$ only

Turbulence data not available

Design/Analysis Application Examples

A. Modified Base Equation and Incidence

The NACA/NASA rule has been used for $i \neq i_{ref}$ with the equation (Ref. 23)

$$\delta = \delta_{ref} + (i - i_{ref}) \left(\frac{d\delta}{di} \right)_{ref}$$

Values of k_1 have been used in Figs. B-3 and B-7 to replace β_1 (Ref. 66).

Application of the NACA/NASA rule to design has frequently included a capability to add an arbitrary angle correction. Examples are in Refs. 63, 66 and 67.

B. Extended Blade Section and Cascade Geometry Limits

Airfoil Section Profiles and Camber Line Shapes

The NACA/NASA rule has been applied to exponential, polynomial and arbitrary camber line shapes with polynomial thickness distribution (Refs. 66, 68, 69 and 70).

Cascade Geometry Limits

$\frac{a}{c}$ equation is given for deviation with $\frac{a}{c}$ as a variable in Ref. 66

σ Ref. 71 suggests caution in application when σ is low and $\beta_1 > 60$ deg

Blade-To-Blade Surface Radius Change

Equivalent circulation turning angle (see Appendix E) is used in NACA/NASA deviation option in Ref. 63.

Ref. 72 suggests a solidity and thickness/chord ratio correction for average blade-to-blade stream surface slope in meridional projection.

C. Extended Aerodynamic Variable Range

- M_1 - correction suggested for M_1 above critical value in Refs. 60 and 67
- β - Ref. 71 suggests caution in application when $\beta_1 > 60$ deg
- Ω - see radius change above
- i - Ref. 23 suggests procedure for determining incidence correction

APPENDIX C

USSR FLUID TURNING ANGLE CORRELATION¹

Base Equation

$$\Delta\alpha_o = \left[\frac{(\Delta\alpha_o)_{\bar{x}_c}}{(\Delta\alpha_o)_{\bar{x}_c} = 0.4} \right] \left[\frac{(\Delta\alpha_o)_{\bar{c}}}{(\Delta\alpha_o)_{\bar{c}} = 10\%} \right] \left[\frac{K\varepsilon}{1000} + B \right]$$

$$K = (5 - 2t/b) \sqrt{v^2 - 1000 \frac{t}{b} + 100 (5.5 - 2.6 t/b)}$$

$$B = 8 \left(\frac{t}{b} \right)^2 - 17 \frac{t}{b} + 16$$

$$\frac{(\Delta\alpha_o)_{\bar{x}_c}}{(\Delta\alpha_o)_{\bar{x}_c} = 0.4} = 1 - 0.28 (\bar{x}_c - 0.40) \text{ for } \bar{x}_c = 0.3 \text{ to } 1.0$$

and

$$\frac{(\Delta\alpha_o)_{\bar{c}}}{(\Delta\alpha_o)_{\bar{c}} = 10\%} = 1 - 0.016 (10 - \bar{c}) \text{ for } \bar{c} = 1.25 \text{ to } 12.5\%$$

At Base Incidence

$$i_o = \alpha_1' - \sin^{-1} \frac{F_r}{t}$$

$\Delta\alpha_o$ fluid turning angle for cascade operation at base incidence i_o and low M_1

v blade section stagger angle, angle between chord line and tangential direction, degrees

ε blade section camber angle, angle between lines tangent to section camber line at leading and trailing edges, degrees

t blade spacing, tangential distance between equivalent points on adjacent blade section

b chord length, length of straight line connecting points where camber line intersects leading and trailing edges

i angle of incidence, angle between cascade inlet average flow angle and line tangent to blade section camber line at leading edge, degrees

i_o optimum incidence angle, degrees

α_1' blade section camber line angle at leading edge, measured from tangential direction, degrees

α_2' blade section camber line angle at trailing edge, measured from tangential direction, degrees

α_1 average fluid angle at cascade inlet, measured from tangential direction, degrees

¹Symbols and notation in Appendix C correspond to original publication. See also Figures C-1 and C-2.

- α_2 average fluid angle at cascade exit, measured from axial direction, degrees
 δ deviation angle, angle between cascade exit average fluid angle and line tangent to blade section camber line at trailing edge, degrees
 V_1 fluid velocity at cascade inlet
 V_2 fluid velocity at cascade exit
 F_T minimum flow passage width in blade-to-blade channel (throat) (Ref. 25)

Base Airfoil Section Profile

A-40 symmetric profile (Ref. 25)
(see x_c/b below)

Base Camber Line Shapes

- I145 parabolic used for camber angle ≤ 55 deg (Ref. 25)
K50 circular arc for all camber angles ≥ 55 deg (Ref. 25)

Base Cascade Geometry Limits

$$\frac{x_f}{b} \left\{ \begin{array}{l} 0.45 \text{ parabolic camber line} \\ 0.50 \text{ circular-arc camber line} \end{array} \right.$$

$$\frac{x_c}{b} \left\{ \begin{array}{l} 0.30 \text{ A-30} \\ 0.40 \text{ A-40} \\ 0.50 \text{ A-50} \\ 0.65 \text{ A-65} \\ 1.00 \text{ A-100} \end{array} \right. \quad (\text{Ref. 25 gives profile construction})$$

$$\frac{c}{b} \quad 0.0125 \text{ to } 0.125$$

$$\text{LER} \quad 0.055 c$$

$$\text{TER} \quad 0.05 c$$

$$\nu \quad 20 \text{ to } 110 \text{ deg}$$

$$\frac{b}{t} \quad 0.7 \text{ to } 2.5$$

$$\epsilon \quad 5 \text{ to } 85 \text{ deg}$$

} range of validity suggested in Ref. 26

Base Aerodynamic Variable Range¹

$$M_1 \quad 0.30 \text{ to } 0.92$$

Generalized curves are given for predicting change in $\Delta\alpha$ with M_1 in Ref. 25

$$\text{Re} \quad 2 \times 10^5 \text{ to } 8 \times 10^5 \text{ based on chord length and inlet velocity}$$

$$\Omega \quad 1.0 \text{ to } 1.15$$

Turbulence not reported

Design/Analysis Application Examples

Not available

¹Values given are ranges reported in Refs. 24-26.

APPENDIX D

COMPRESSOR BLADE SECTION PROFILES AND CAMBER LINE SHAPES

Table D-1 is a listing of some blade section profile geometries which have been adequately described and have been used in linear cascade experiments or in compressor blade row design. References are given which contain information on or instructions for layout or construction of each profile. In those cases where reasonably general correlation equations exist for aerodynamic performance, reference documents are also listed.

APPENDIX E

DERIVATION OF EQUIVALENT CIRCULATION FLUID TURNING ANGLE

The equivalent circulation fluid turning angle concept was developed to rationalize the use of correlations and parameters based on two-dimensional linear cascade experiments for the design and analysis of axial-flow compressor blade rows. In this context it accounts for the influence on effective cascade diffusion loading of changes in stream surface radius and meridional or axial velocity across the blade row.

An example velocity diagram for a rotating compressor cascade with $r_2 \neq r_1$ is shown in Figure E-1. The relative fluid turning angle indicated is

$$\Delta\beta = \beta_1 - \beta_2$$

and the circulation for the row is

$$\Gamma_{\text{row}} = r_2 v_{\theta,2} - r_1 v_{\theta,1}$$

If the flow through the rotor occurred with no change in radius but with the same total circulation, the equivalent exit tangential velocity would be

$$v_{\theta,2e} = \frac{r_2}{r_1} v_{\theta,2}$$

and

$$w_{\theta,2e} = u_{2e} - v_{\theta,2e} = u_1 - \frac{r_2}{r_1} v_{\theta,2}$$

The equivalent circulation velocity diagram is based on these exit tangential velocity components and

$$v_{m,2e} = v_{m,1}$$

The equivalent relative fluid angle at the rotor exit is

$$\beta_{2e} = \tan^{-1} \frac{u_1 - \frac{r_2}{r_1} v_{\theta,2}}{v_{m,1}}$$

and

$$\begin{aligned} \Delta\beta_e &= \beta_1 - \beta_{2e} \\ &= \beta_1 - \tan^{-1} \left\{ \frac{\frac{r_2 v_{m,2}}{r_1 v_{m,1}} \tan\beta_2 + \frac{u_1}{v_{m,1}} \left[1 - \left(\frac{r_2}{r_1} \right)^2 \right]}{1} \right\} \end{aligned} \quad (E-1)$$

For a stationary blade row

$$\Delta\beta_e = \beta_1 - \tan^{-1} \left[\frac{\frac{r_2 v_{m,2}}{r_1 v_{m,1}} \tan\beta_2}{1} \right] \quad (E-2)$$

In both the rotor and stator cases the equations for $\Delta\beta_e$ show that both $v_{m,2} < v_{m,1}$ and $r_2 < r_1$ cause an increased equivalent turning angle.

The equivalent circulation approach was suggested in 1957 by Lieblein (Ref. 76) as a means for extending the application of two-dimensional linear cascade diffusion loading parameters to compressor flow conditions. It also is similar to a method for correction of linear cascade turning angles for axial velocity changes used by Erwin and Emery (Ref. 28). The idea was further developed by Klaproth (Ref. 72) for diffusion parameters and was subsequently modified by Seyler and Smith (Ref. 62) and Wright (Ref. 61) to determine equivalent turning angles for deviation angle prediction. Equivalent circulation turning angles have been used for selection of compressor cascade geometries based on cascade plane projection (Ref. 62) and on the conical stream surface approximation (Ref. 63).

SYMBOLS AND NOTATION

The symbols and notation defined below are recommended for correlation of deviation/fluid turning angle data as described in the body of this report. Separate lists are given for existing correlation systems in the Appendices.

AVR	axial-velocity ratio across blade row, $v_{x,2}/v_{x,1}$
a	location of maximum camber point (see Fig. A-1)
a	acoustic velocity
a_0	acoustic velocity at local total temperature
b	maximum camber (see Fig. A-1)
b	exponent (see Appendix B)
c	chord length (see Fig. A-1)
D	cascade diffusion parameter
D_{eq}	cascade equivalent diffusion parameter
d	location of maximum blade section profile thickness (Fig. A-1)
i	incidence angle, angle between cascade entrance relative flow direction and line tangent to camber line at leading edge (see Fig. A-2)
i_{ss}	suction surface incidence angle, angle between cascade entrance flow direction and line tangent to suction surface where leading edge shape fairs into thickness distribution
l	arc length of camber line
M	Mach number, V/a
m_c	parameter in NGTE deviation angle correlation (see Appendix B)
m_{cm}	modified parameter in deviation angle correlation equation (see Appendix B)
Re_c	Reynolds number based on chord length, $Re_c = \rho_1 V_1 c / \mu_1$
r	radial coordinate
s	blade spacing, distance in tangential or circumferential direction between corresponding points on adjacent blades (see Fig. A-2)
t	maximum thickness of blade section profile (see Fig. A-1)
U	blade velocity
V	fluid velocity
W	fluid velocity measured relative to rotating blade row
X	coordinate parallel to chord line
x	axial coordinate direction
Y	coordinate perpendicular to chord line
y	tangential coordinate direction in linear cascade arrangement
z	spanwise coordinate in linear cascade arrangement
<u>Greek</u>	
β	fluid angle of relative flow measured from axial direction (see Fig. A-2)
γ	blade-chord angle or stagger angle, angle between blade section chord line and axial direction (see Fig. B-2)

γ	specific heat ratio
δ	deviation angle, angle between cascade exit relative flow direction and line tangent to camber line at trailing edge (see Fig. A-2)
θ	tangential or circumferential coordinate in compressor
κ	camber line angle, angle between line tangent to camber line and axial direction (see Fig. B-2)
ρ	fluid density
μ	dynamic molecular viscosity
σ	cascade solidity, c/s
ϕ	blade section camber angle (see Fig. A-2)
Ω	axial velocity-density ratio, $\rho_2 V_{x,2} / \rho_1 V_{x,1}$
ω	angular velocity of rotor

Subscripts

m	meridional component
o	zero-camber in NACA/NASA correlation; optimum in USSR correlation (see Appendix C)
ps	pressure surface
r	radial component
ref	reference minimum-loss
rel	measured relative to rotating blade row
ss	suction surface
x	axial component
θ	circumferential component
1	cascade entrance
2	cascade exit

REFERENCES

1. Föttner, Leonhard. "Ein Verfahren zum Bestimmen der Verlustbehafteten Transsonischen Schaufelgitterströmung bei vorgegebener Druckverteilung." *Forsch. Ing.-Wes.* 38(3):69-81. 1972.
2. Wilkinson, D. H. "Calculation of Blade-to-Blade Flow in a Turbomachine by Streamline Curvature." ARC Rep. and Memo. 3704. 1970.
3. Miller, Max J. and Serovy, George K. "Deviation Angle Estimation for Axial-Flow Compressors Using Inviscid Flow Solutions." *J. Eng. Power.* Trans. ASME, Series A. 97:163-172. 1975.
4. Delaney, Robert A. and Kavanagh, Patrick. "Transonic Flow Analysis in Axial-Flow Turbomachinery Cascades by a Time-Dependent Method of Characteristics." *J. Eng. Power.* Trans. ASME, Series A. 98:356-364. 1976.
5. Sanger, Nelson, L. "Two-Dimensional Analytical and Experimental Performance Comparison for a Compressor Stator Section with D-Factor of 0.47." NASA TM D-7425. 1973.
6. Hansen, E. C., Serovy, G. K. and Sockol, P. M. "Axial-Flow Compressor Turning Angle and Loss by Inviscid-Viscous Interaction Blade-to-Blade Computation." *J. Eng. Power.* Trans. ASME. 102:28-34. 1980.
7. Calvert, W. J. and Herbert, M. V. "An Inviscid-Viscous Interaction Method to Predict the Blade-to-Blade Performance of Axial Compressors." *Aeronautical Quarterly.* 31:173-196. 1980.
8. Costelow, J. P. "Review of Compressible Flow Theories for Airfoil Cascades." *J. Eng. Power.* Trans. ASME, Series A. 95:281-292. 1973.
9. Lichtfuss, H. J. and Starken, H. "Supersonic Cascade Flow." In: *Progress in Aerospace Science*, Vol. 15, pp. 37-149. New York Pergamon Press, Ltd. 1974.
10. Constant, H. "Performance of Cascades of Aerofoils." R.A.E. Note No. E.3696. A.R.C. 4155. 1939. (Unpublished)
11. Howell, A. R. "The Present Basis of Axial Flow Compressor Design. Part I. Cascade Theory and Performance." Aeronautical Research Council. Rep. and Memo. No. 2095. 1942.

12. Howell, A. R. "Fluid Dynamics of Axial Compressors." Proc. of the IME. 153:441-452. 1945.
13. Howell, A. R. "Note on the Theory of Arbitrary Aerofoils in Cascade." Philos. Mag., Series 7, 39:913-927. 1948.
14. Carter, A. D. S. and Hugheas, Hazel P. "A Theoretical Investigation into the Effect of Profile Shape on the Performance of Aerofoils in Cascade." ARC Rep. and Memo. 2384. 1950.
15. Carter, A. D. S. "The Low Speed Performance of Related Aerofoils in Cascades." ARC CP 29. 1950.
16. Weinig, F. Die Strömung um die Schaufeln von Turbomaschinen. Leipzig. J. A. Barth. 1935.
17. Schlichting, Hermann. "Problems and Results of Investigations on Cascade Flow." J. Aero. Sci. 21: 163-178. 1954.
18. Emery, James C., Herrig, L. Joseph, Erwin, John R. and Felix A. Richard. "Systematic Two-Dimensional Cascade Tests of NACA 65-Series Compressor Blades at Low Speeds." NACA Report 1368. 1958.
19. Herrig, L. Joseph, Emery, James C. and Erwin, John R. "Effect of Section Thickness and Trailing-Edge Radius on the Performance of NACA 65-Series Compressor Blades in Cascade at Low Speeds." NACA RM L51 J16. 1951.
20. Felix, A. Richard and Emery, James C. "A Comparison of Typical National Gas Turbine Establishment and NACA Axial-Flow Compressor Blade Sections in Cascade at Low Speed." NACA TN 3937. 1957.
21. Andrews, S. J. "Tests Related to the Effect of Profile Shape and Camber Line on Compressor Cascade Performance." ARC Rep. and Memo. 2743. 1955.
22. Howell, A. R. "A Note on the Compressor Base Aerofoils C.1, C.2, C.3, C.4, C.5, and Aerofoils Made Up of Circular Arcs." Power Jets, Ltd. Memo M. 1011. September 1944.
23. Lieblein, Seymour. "Experimental Flow in Two-Dimensional Cascades." In: "Aerodynamic Design of Axial Flow Compressors." Chapter VI, NASA SP-36. 1965.
24. Komarov, A. P. "Investigation of Flat Compressor Grids." FTD-MT-24-69-68. 26 April 1968. Translation of "Lopatochnyye Mashiny i Struynyye Apparaty." Sbornik Statey. Vypusk 2. Moscow. Izdatel'stvo Mashinostroyeniye. 1967. pp. 67-110. AD 682829.
25. Bumomovich, A. I. and Svyatogorov, A. A. "Aerodynamic Characteristics of Foil Compressor Cascades at High Subsonic Speed." FTD-MT-24-69-68. 26 April 1968. Translation of "Lopatochnyye Mashiny i Struynyye Apparaty." Sbornik Statey. Vypusk 2. Moscow. Izdatel'stvo Mashinostroyeniye. 1967. pp. 5-35. AD 682829.
26. Bumimovich, A. I. and Svyatogorov, A. A. "Generalization of Results of Investigation of Foil Compressor Cascades at Subsonic Speed." FTD-MT-24-69-68. 26 April 1968. Translation of "Lopatochnyye Mashiny i Struynyye Apparaty." Sbornik Statey. Vypusk 2. Moscow. Izdatel'stvo Mashinostroyeniye. 1967. pp. 36-66. AD 682829.
27. Miller, Max J. and Skönberg, Torbjorn. "Reference Incidence Angles in Constant Stagger Cascades." Iowa State University. ISU-ERI-Ames-99985. June 1971.
28. Erwin, John K. and Emery, James C. "Effect of Tunnel Configuration and Testing Technique on Cascade Performance." NACA Report 1016. 1950.
29. Mikolajczak, A. A., Morris, A. L. and Johnson, B. V. "Comparison of Performance of Supersonic Blading in Cascade and in Compressor Rotors." J. Eng. Power. Trans. ASME, Series A. 93:42-48. 1971.
30. Fleeter, Sanford, Holtman, Robert L., McClure, Robert B. and Sinnet, George T. "Experimental Investigation of a Supersonic Compressor Cascade." Aerospace Research Laboratories, ARL TR 75-0208. 1975.
31. Huffman, G. D. and Tramm, P. C. "Airfoil Design for High Tip Speed Compressors." J. Aircr. 11:682-689. 1974.
32. Emery, James C. "Low-Speed Cascade Investigation of Thin Low-Camber NACA 65-Series Blade Sections at High Inlet Angles." NACA RM L57E03. 1957.
33. Savage, Melvyn, Felix, A. Richard and Emery, James C. "High-Speed Cascade Tests of a Blade Section Designed for Typical Hub Conditions of High-Flow Transonic Rotors." NACA RM L55F07. 1955.
34. Emery, James C. "Low-Speed Cascade Investigation of Loaded Leading-Edge Compressor Blades." NACA TN 4178. 1957.
35. Erwin, John R., Savage, Melvyn and Emery, James C. "Two-Dimensional Low-Speed Cascade Investigation of NACA Compressor Blade Sections Having a Systematic Variation in Mean-Line Loading." NACA TN 3817. 1956.
36. Dunavant, James C., Emery, James C., Welch, Howard C. and Westphal, Willard R. "High-Speed Cascade Tests of the NACA 65-(12A₁₀) 10 and NACA 65-(12A₂I_{8b}) 10 Compressor Blade Sections." NACA RM L55I08. 1955.

37. Emery, James C. and Dunavant, James C. "Two-Dimensional Cascade Tests of NACA 65-(C₁₀A₁₀) 10 Blade Sections at Typical Compressor Hub Conditions for Speeds Up to Choking." NACA RM L57H05.
38. Dunavant, James C. and Emery, James C. "Two-Dimensional Cascade Investigation at Mach Numbers Up to 1.0 of NACA 65-Series Blade Sections at Conditions Typical of Compressor Tips." NACA RM L58A02. 1958.
39. Briggs, William B. "Effect of Mach Number on the Flow and Application of Compressibility Corrections in a Two-Dimensional Subsonic-Transonic Compressor Cascade Having Varied Porous-Wall Suction at the Blade Tips." NACA TN 2649. 1952.
40. Heilmann, W. "Experimentelle und Grenzschichttheoretische Untersuchungen an Ebenen Verzögerungsgittern bei Kompressibler Strömung, insbesondere bei Änderung des Axialen Strömdichteverhältnisses und der Zustromturbulenz." DLR FB 67-88. 1967.
41. Heilmann, W. "The Influence of Axial Velocity Density Ratio on Compressor Cascade Performance in Compressible Flow." In: "Boundary Layer Effects in Turbomachinery." AGARD-AG-164. 1972. Paper I-13.
42. Starken, H. "Untersuchung der Strömung in Ebenen Überschallverzögerungsgittern." DLR FB 71-99. 1971.
43. Starken, H., Breugelmans, F. A. E. and Schimming, P. "Investigation of the Axial Velocity Density Ratio in a High Turning Cascade." ASME Paper 75-GT-25. 1975.
44. Masek, Z. and Norbury, J. F. "Low-Speed Performance of a Compressor Cascade Designed for Prescribed Velocity Distribution and Tested with Variable Axial Velocity Ratio." In: "Heat and Fluid Flow in Steam and Gas Turbine Plant." IME Conference Publication 3, pp. 224-236. 1973.
45. Ilyas, M. and Norbury, J. F. "Effect of Axial Velocity Variation on the Subsonic Flow Through a Compressor Cascade." In: "Heat and Fluid Flow in Steam and Gas Turbine Plant." IME Conference Publication 3, pp. 276-287. 1973.
46. Ohounu, E. H. and Shaw, R. "Effect of Axial Velocity Variation on Deviation for Compressor Cascades." In: "Heat and Fluid Flow in Steam and Gas Turbine Plant." IME Conference Publication 3, pp. 110-114. 1973.
47. Stark, Udo and Starke, Jorg. "Theoretische und experimentelle Untersuchungen über die quasistationäre inkompressible Stromung durch vorgegebene ebene Verdichtergitter." Forsch. Ing. Wes. 40:172-186. 1974.
48. Sandercock, Donald M. Unpublished communications concerned with NASA Lewis Research Center fan and compressor data evaluation, 1975-1977.
49. Monsarrat, N. T., Keenan, M. J. and Tramm, P. C. "Single-Stage Evaluation of Highly-Loaded High-Mach Number Compressor Stages." Design Report. NASA CR-72562. 1969.
50. Sulam, D. H., Keenan, M. J. and Flynn, J. T. "Single-Stage Evaluation of Highly-Loaded High-Mach-Number Compressor Stages. II - Data and Performance Multiple-Circular-Arc Rotor." NASA CR-72694. 1970.
51. Keenan, M. J. and Monsarrat, N. T. "Experimental Evaluation of Transonic Stators." Preliminary Analysis and Design Report. NASA CR-54620. 1967.
52. Keenan, M. J. and Barcok, J. A. "Experimental Evaluation of Transonic Stators." Final Report. NASA CR-72298. 1969.
53. Harley, K. G. and Burdsall, E. A. "High-Loading Low-Speed Fan Study. Part 2: Data and Performance, Unslotted Blades and Vanes." NASA CR-72667. 1969.
54. Lewis, G. W., Jr. and Tysl, E. R. "Overall and Blade-Element Performance of a 1.20-Pressure-Ratio Fan Stage at Design Blade Setting Angle." NASA TM X-3101. 1974.
55. Osborne, W. M. and Steinke, R. J. "Performance of a 1.15 Pressure Ratio Axial-Flow Fan Stage with a Blade Tip Solidity of 0.5." NASA TM X-3052. 1974.
56. Kovich, G. and Steinke, R. J. "Performance of a 1.15 Pressure Ratio Axial-Flow Fan Stage with a Blade Tip Solidity of 0.65." NASA TM X-3341. 1976.
57. Moore, R. D. and Steinke, R. J. "Aerodynamic Performance of a 1.25 Pressure-Ratio Axial-Flow Fan Stage." NASA TM X-3083. 1974.
58. Urasek, Donald C., Gorrell, William T. and Cunnan, Walter S. "Performance of Two-Stage Fan Having Low-Aspect-Ratio, First-Stage Rotor Blading." NASA TP 1493 (AVRADCOM TR 79-49), 1979. (Test configuration for this AGARD study).
59. McDonald, P. W., Bolt, C. R., Dunker, R. J. and Weyer, H. B. "A Comparison Between Measured and Computed Flow Fields in a Transonic Compressor Rotor." ASME Paper 80-GT-7, 1980. (Test case configuration for this AGARD study).
60. Davis, W. R. "A Computer Program for the Analysis and Design of the Flow in Turbomachinery, Part B - Loss and Deviation Correlations." Ottawa. Carleton University. Division of Aerothermodynamics.

Report ME/A70-1. 1970.

61. Wright, I. C. "Blade Selection for a Modern Axial-Flow Compressor." In: NASA SP-304, Part 2, pp. 603-626. 1974.
62. Seyler, D. R., and Smith, L. H., Jr. "Single Stage Experimental Evaluation of High Mach Number Compressor Rotor Blading. Part I - Design of Rotor Blading." NASA CR-54581. 1967.
63. Crouse, James E. "Computer Program for Definition of Transonic Axial-Flow Compressor Blade Rows." NASA TN D-7345. 1974.
64. Ball, Calvin L., Janetzke, David C. and Reid, Lonnie. "Performance of 1380-Foot-Per-Second-Tip-Speed Axial-Flow Compressor Rotor with Blade Tip Solidity of 1.5." NASA TM X-2379. 1972.
65. Wennerstrom, A. J. and Hearsey, Richard M. "The Design of an Axial Compressor Stage for a Total Pressure Ratio of 3 to 1." U.S. Air Force Systems Command. Aerospace Research Laboratories, ARL 71-0061. 1971.
66. Hearsey, Richard M. "A Revised Computer Program for Compressor Design. Volume I: Theory, Descriptions and User's Instructions." U.S. Air Force Systems Command, ARL TR 75-0001, Volume I. 1975.
67. Novak, Richard A. "Flow Field and Performance Map Computation for Axial-Flow Compressors and Turbines." In: "Modern Prediction Methods for Turbomachine Performance." AGARD-LS-83. 1976.
68. Frost, G. R., Hearsey, R. M. and Wennerstrom, A. J. "A Computer Program for the Specification of Axial Compressor Airfoils." Aerospace Research Laboratories. ARL 72-0171. 1972.
69. Frost, G. R., and Wennerstrom, A. J. "The Design of Axial Compressor Airfoils Using Arbitrary Camber Lines." Aerospace Research Laboratories. ARL-73-0107. 1973.
70. Frost, G. R. "Modifications to ARL Computer Programs Used for Design of Axial Compressor Airfoils." Aerospace Research Laboratories. ARL 74-0060. 1974.
71. Lieblein, Seymour. "Incidence and Deviation-Angle Correlations for Compressor Cascades." J. Basic Eng., Trans. ASME, Series D. 82:575-587. 1960. (Discussions by L. H. Smith, Jr. and G. Sovran relate to β_1 , α limits).
72. Lieblein, Seymour. "Loss and Stall Analysis of Compressor Cascades." J. Basic Eng., Trans. ASME, Series D., 81:387-397. 1959. (Discussion by J. F. Klaproth relates to D_{eq} for annular cascades.)
73. Hearsey, Richard M. and Wennerstrom, Arthur J. "Axial Compressor Airfoils for Supersonic Mach Numbers." Aerospace Research Laboratories, ARL 70-0046. 1970.
74. Stanitz, John D. "Approximate Design Method for High-Solidity Blade Elements in Compressors and Turbines." NACA TA 2408. 1951.
75. Klaproth, John F., Jacklitch, John J., Jr. and Tysl, Edward R. "Design and Performance of a 1400-Foot-Per-Second-Tip-Speed Supersonic Compressor Rotor." NACA RM E55A27. 1955.
76. Todd, K. W. "Tests Related to the Effect of Profile Shape and Camber-Line on Compressor Cascade Performance." Aero. Res. Council, Rep. and Memo. No. 2743. 1955. (NGTE Rep. R. 60, Oct. 1949).
77. Robbins, William H., Jackson, Robert J. and Lieblein, Seymour. "Blade-Element Flow in Annular Cascades." In: "Aerodynamic Design of Axial Flow Compressors," Chapter VII, NASA SP-36, 1965.
78. Swan, W. C. "A Practical Engineering Solution of the Three-Dimensional Flow in Transonic Type Axial Flow Compressors." WADC Tech. Rep. 58-57. 1958.
79. Jansen, W. and Moffatt, W. C. "The Off-Design Analysis of Axial-Flow Compressors." J. Eng. Power, Trans. ASME. 89:453-462. 1967.
80. Davis, W. Roland and Millar, D. A. J. "Through Flow Calculations Based on Matrix Inversion: Loss Prediction." In: "Through-Flow Calculations in Axial Turbomachinery." AGARD-CP-195. 1976.
81. Horlock, J. H., Shaw, R., Pollard, D. and Lewkowicz, A. D. "Reynolds Number Effects in Cascades and Axial-Flow Compressors." J. Eng. Power, Trans. ASME. 86:236-242. 1964.
82. Hebbel, H. "Über den Einfluss der Machzahl und der Reynoldszahl auf die Aerodynamischen Beiwerte von Verdichter-Schaufelgittern bei verschiedener Turbulenz der Strömung." Forschung Ing.-Wesens, 33:1/1-150. 1967.
83. Roberts, William B. "The Effect of Reynolds Number and Laminar Separation on Axial Cascade Performance." J. Eng. Power, Trans. ASME. 97:261-274. 1975.
84. Hoheisel, Heinz and Klock, Reinhard. "Zwanzig Jahre Hochgeschwindigkeits-Gitterwindkanal des Instituts für Aerodynamik der DFVLR in Braunschweig." Zeit. Flugwiss. Weltraumforsch. 1:17-29. 1977.
85. Barsun, K. "Experimentelle Untersuchungen über den Einfluss der turbulenzgrades und eines Turbulenzfadens auf die kompressible Unterschallstromung durch ebene Verdichtergitter." DFL Rep. 68-34. Braunschweig. 1968.

86. Schlichting, H. and Das, A. "On the Influence of Turbulence Level on the Aerodynamic Losses of Axial Turbomachineries." In: "Flow Research on Blading." Amsterdam. Elsevier. pp. 243-274. 1970.
87. Klock, R. "Messung des Turbulenzgrades hinter einem ebenen Schaufelgitter sowie in einem dreistufigen Axialgebläse." DFL Bericht 68/32. Braunschweig. 1968.
88. Klock, R. "Einfluss des Turbulenzgrades auf die aerodynamischen Eigenarten von ebenen Verzogerungsgittern." Forschung Ing. Wes. 39:17-28. 1973.
89. Evans, B. J. "Effects of Free-Stream Turbulence on Blade Performance in a Compressor Cascade." Ph.D. Dissertation. Cambridge University. 1971.
90. Evans, R. L. "Turbulent Boundary Layers on Axial-Flow Compressor Blades." Ph.D. Dissertation. Cambridge University. 1973.
91. Evans, R. L. "Turbulence and Unsteadiness Measurements Downstream of a Moving Blade Row." J. Eng. Power, Trans. ASME. 97:131-139. 1975.
92. Gustafson, B. A. "Some Observations from Low-Speed Cascade Tests Concerning Side Wall Boundary Layer Suction." In: Secondary Flows in Turbomachineries. Paper 19 AGARD CP-214. 1977.
93. Starke, J. "The Effect of the Axial Velocity Density Ratio on the Aerodynamic Coefficients of Compressor Cascades." ASME Paper 80-GT-194. 1980.
94. Stark, U. and Hoheisel, H. "The Combined Effect of Axial Velocity Density Ratio and Aspect Ratio on Compressor Cascade Performance." ASME Paper 80-GT-138. 1980.
95. Lakshminarayana, B. "Methods of Predicting the Tip Clearance Effects in Axial-Flow Turbomachinery." ASME Paper 69-WA/GT-26. 1969.
96. Lakshminarayana, B. and Horlock, J. H. "Effect of Shear Flows on the Outlet Angle in Compressor Cascades - Methods of Prediction and Correlation with Experiments." J. Basic Engrg. Trans. ASME. 89:191-200. 1967.
97. Bardon, M. F., Moffatt, W. C. and Randall, J. L. "Secondary Flow Effects on Gas Exit Angles in Rectilinear Cascades." J. Eng. Power, Trans. ASME. 97:93-100. 1975.
98. Smith, Leroy H., Jr. "Casing Boundary Layers in Multistage Axial-Flow Compressors." In: "Flow Research on Blading." Amsterdam. Elsevier. pp. 275-304. 1970.
99. Strazisar, A. J. and Powell, J. A. "Laser Anemometer Measurements in a Transonic Axial Flow Compressor Rotor." In: "Measurement Methods in Rotating Components of Turbomachinery." ASME. pp. 165-176. 1980.

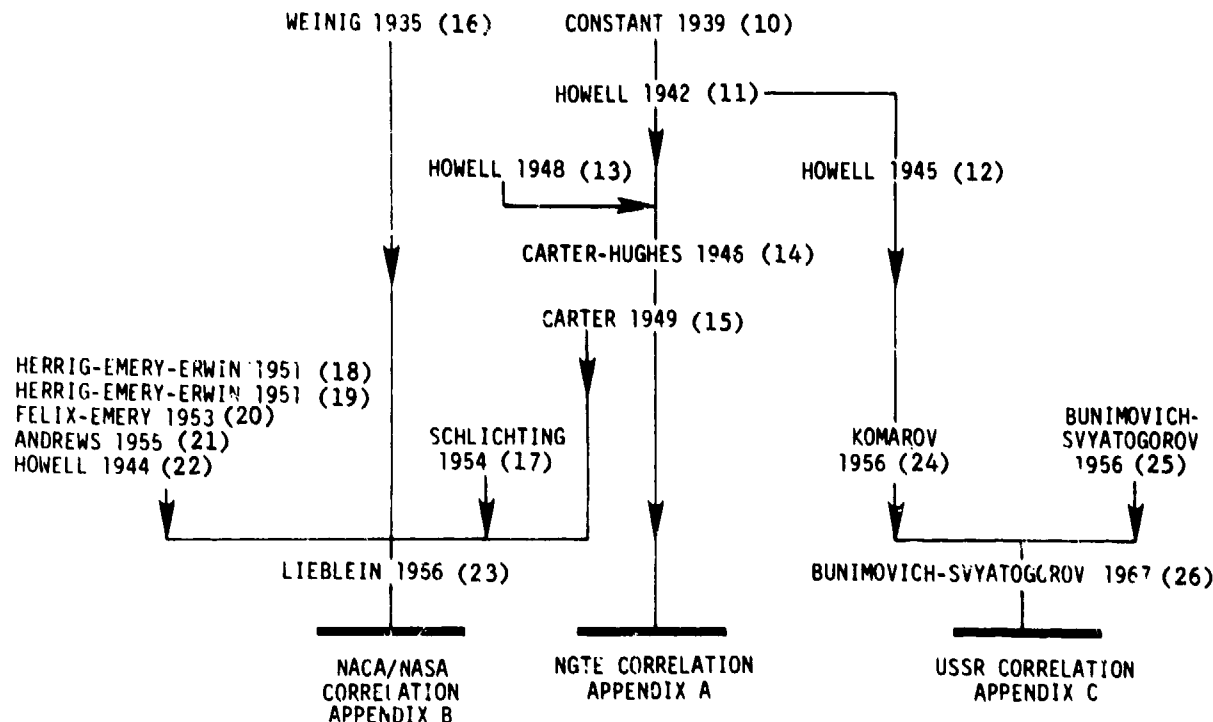
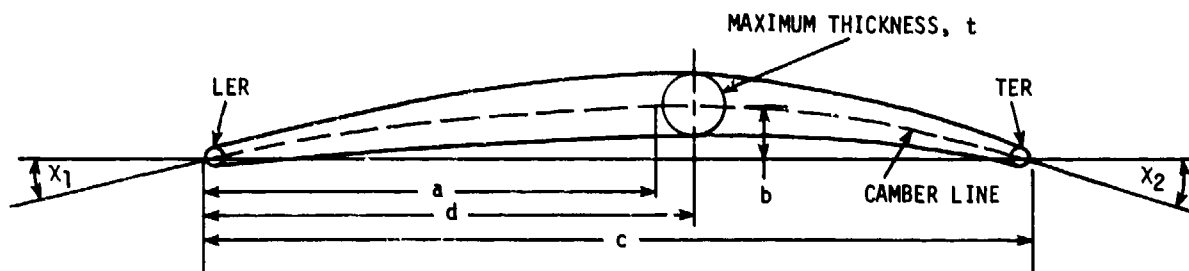


Fig.1 Pattern of development of deviation/fluid turning angle correlations.
Numbers in parentheses are reference numbers



- a = LOCATION OF MAXIMUM CAMBER
- b = COORDINATE OF MAXIMUM CAMBER
- c = CHORD LENGTH
- d = LOCATION OF MAXIMUM THICKNESS
- LER = LEADING EDGE RADIUS
- TER = TRAILING EDGE RADIUS
- x_1 = ANGLE BETWEEN LINE TANGENT TO BLADE SECTION CAMBER LINE AT LEADING EDGE AND CHORD LINE, DEGREES
- x_2 = ANGLE BETWEEN LINE TANGENT TO BLADE SECTION CAMBER LINE AT TRAILING EDGE AND CHORD LINE, DEGREES

Fig.A-1 NGTE blade section profile terminology (References 11 and 15)

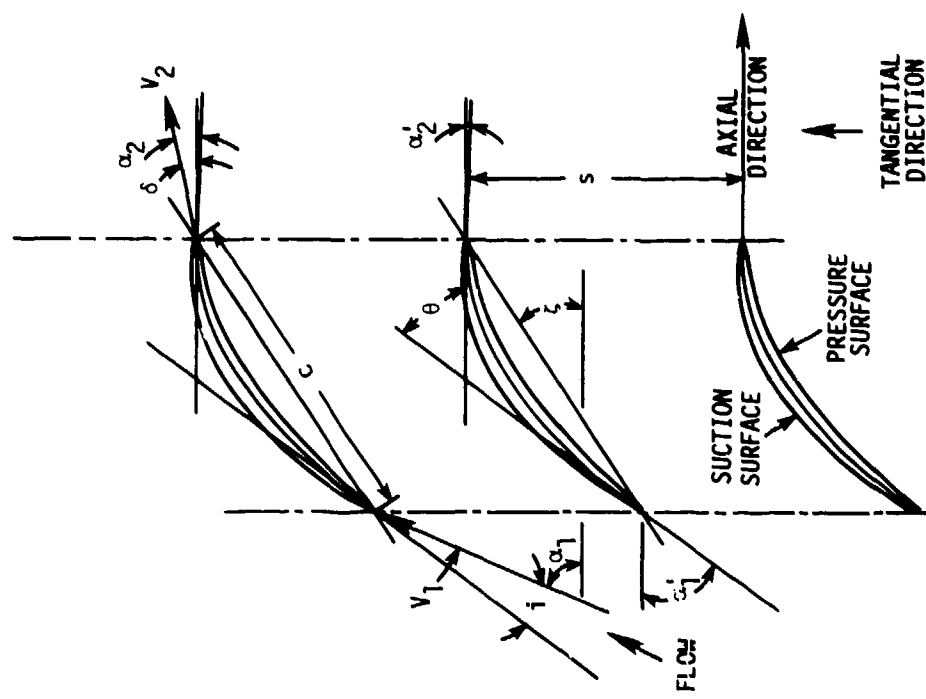
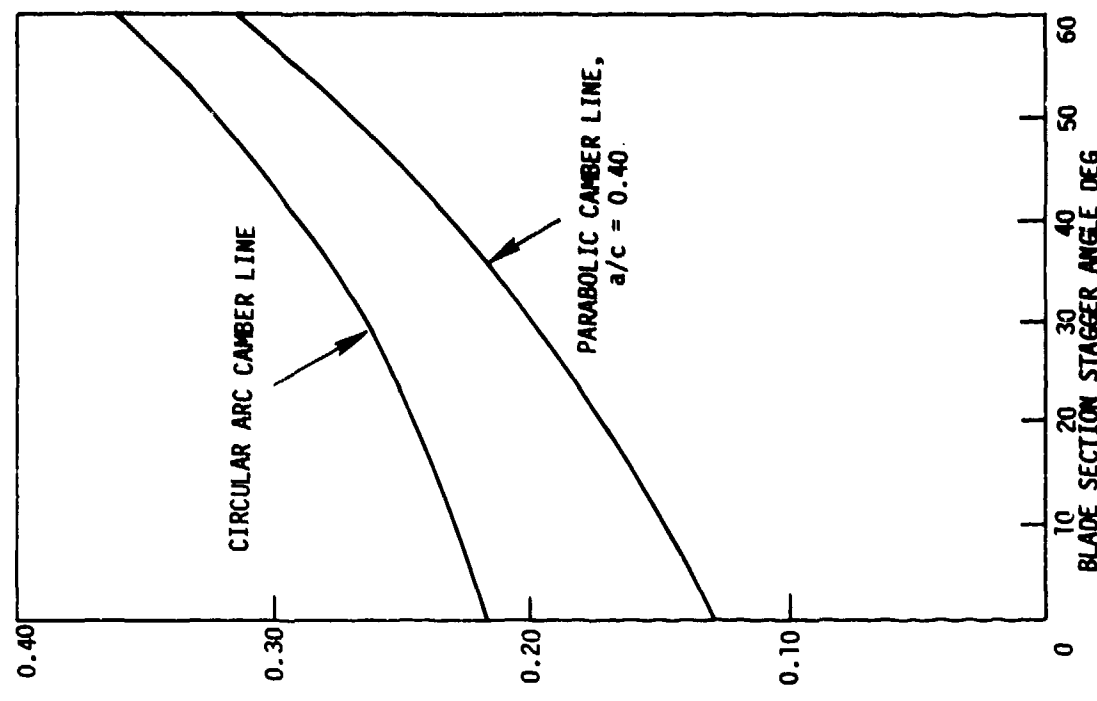


Fig.A-2 NGTE cascade terminology (References 11 and 15)

Fig.A-3 Coefficient m for NGTE deviation angle correction
(Ref.15)

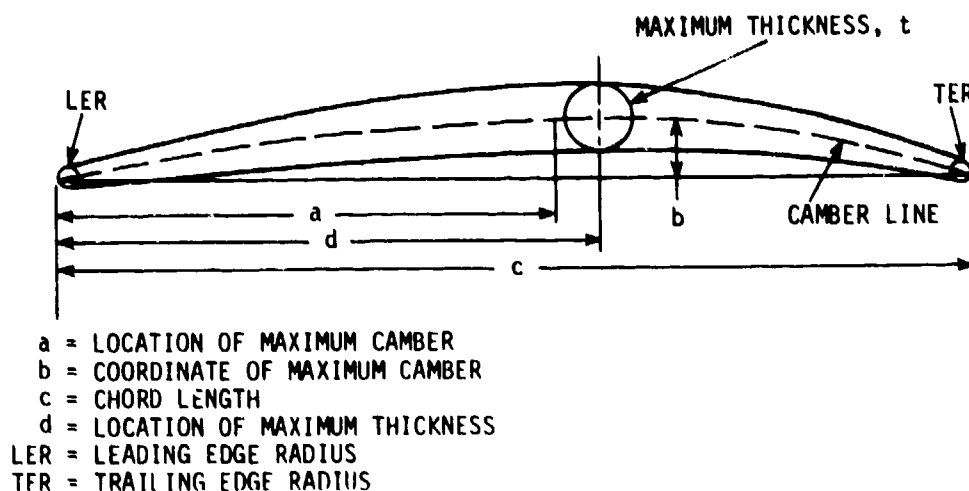
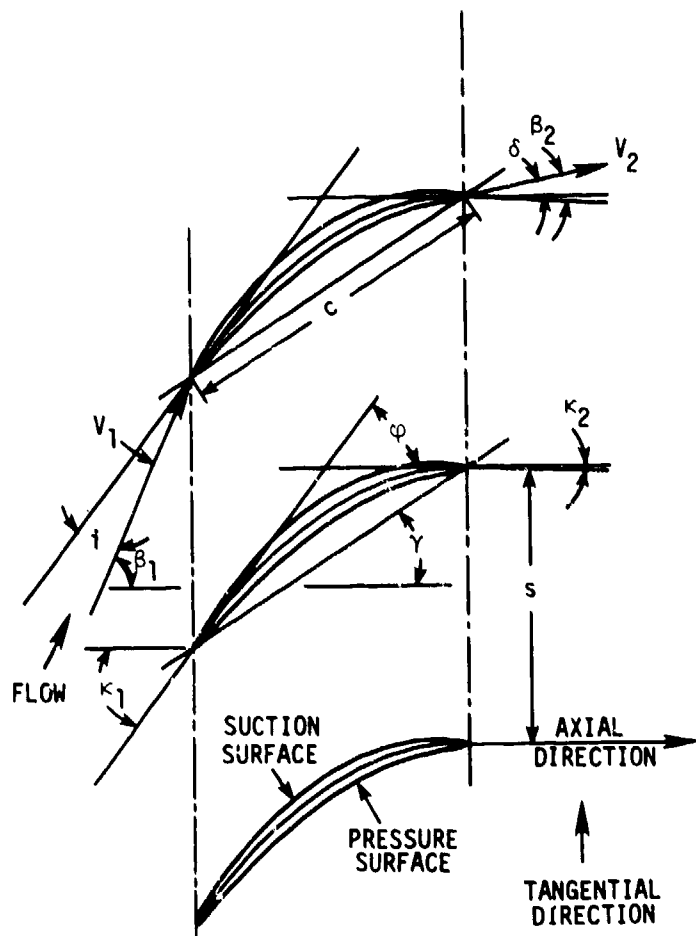


Fig.B-1 NACA/NASA blade section profile terminology



$$i = \beta_1 - k_1$$

$$\Delta\beta = \beta_1 - \beta_2$$

$$\delta = \beta_2 - k_2$$

$$\Delta\beta = \varphi + i - \delta$$

$$\varphi = k_1 - k_2$$

Fig.B-2 NACA/NASA cascade terminology

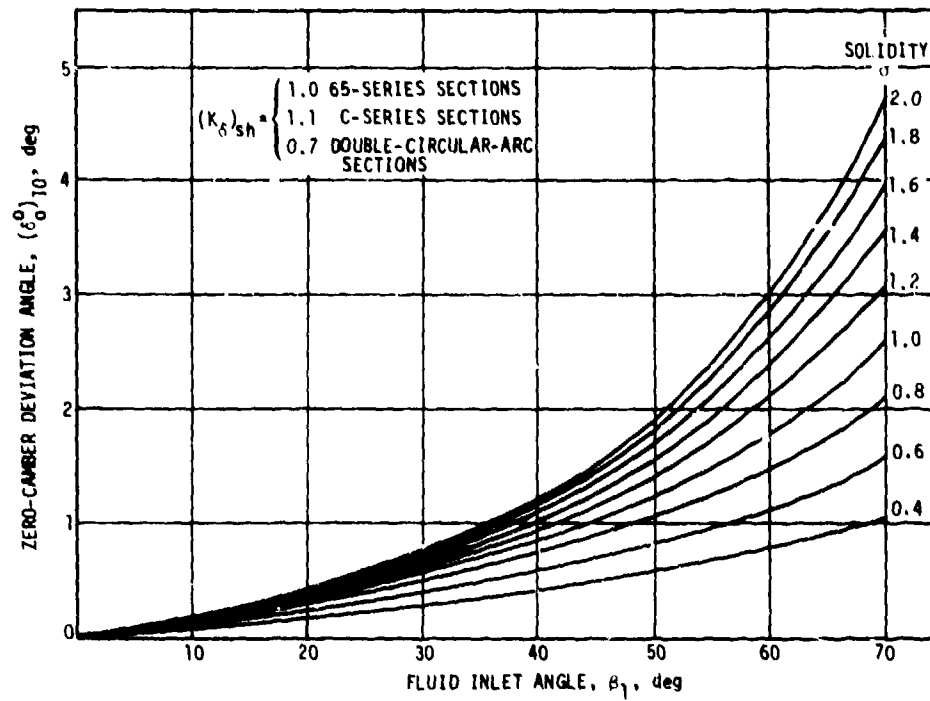


Fig.B-3 Zero-camber deviation angle at reference minimum-loss incidence angle deduced from low-speed-cascade data for 10-percent-thick NACA 65-series blades

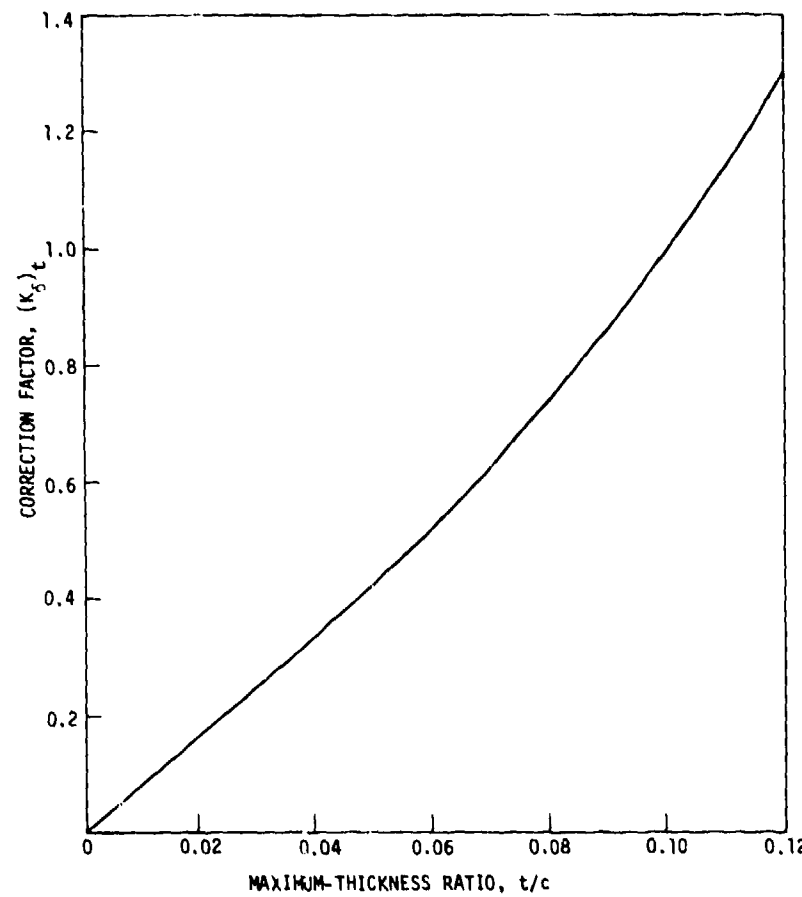


Fig.B-4 Maximum-thickness correction for zero-camber reference minimum-loss deviation angle

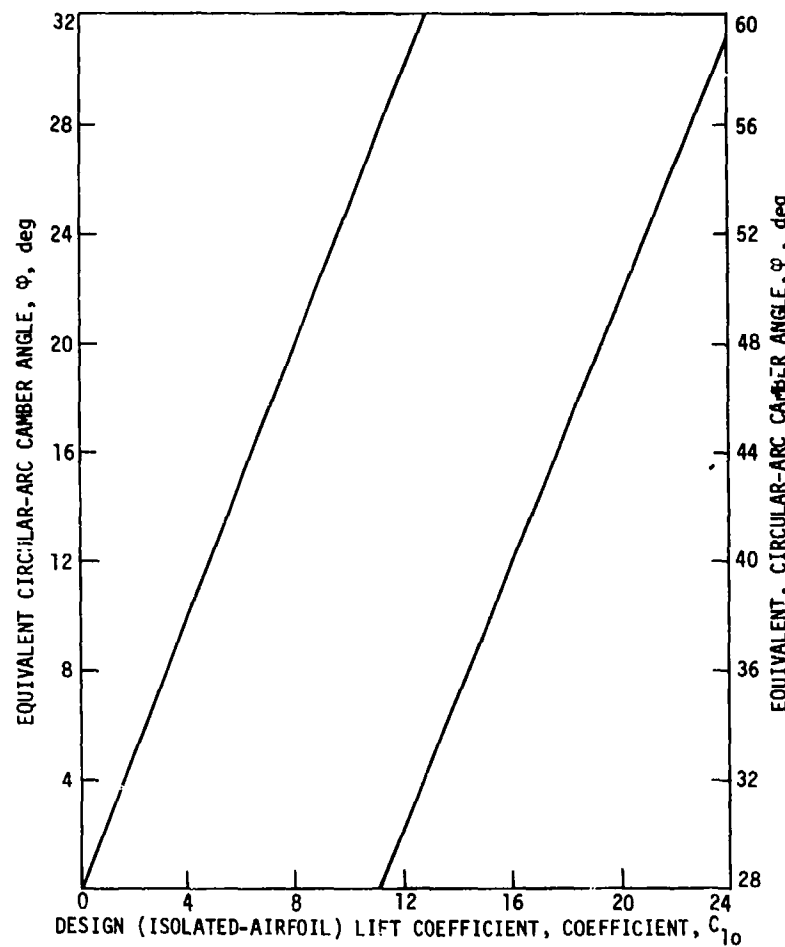


Fig. B-5 Equivalent camber angles for NACA A₁₀ camber line as equivalent circular arc
(see Reference 18 for camber line construction with $C_{10} \neq 10$)

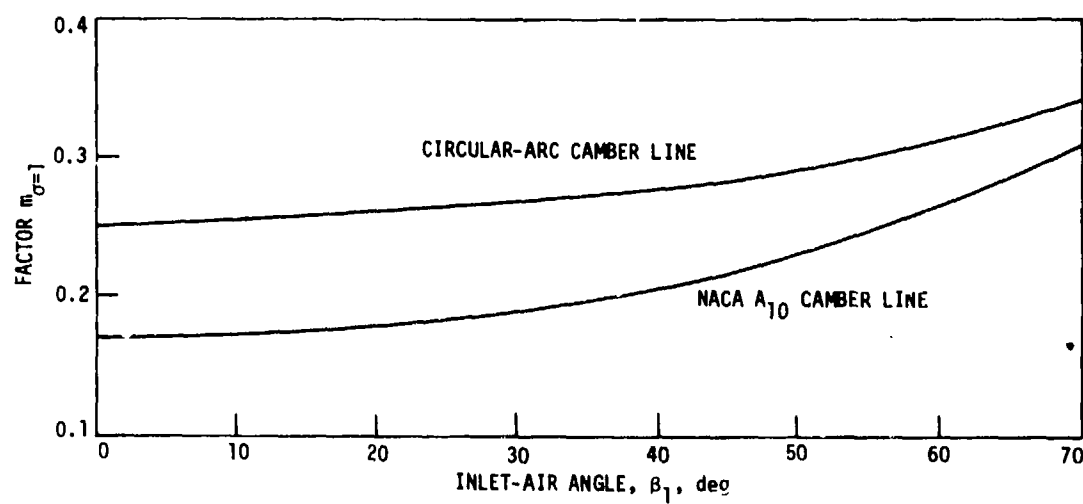


Fig. B-6 Factor $m_{\sigma=1}$ in deviation-angle rule

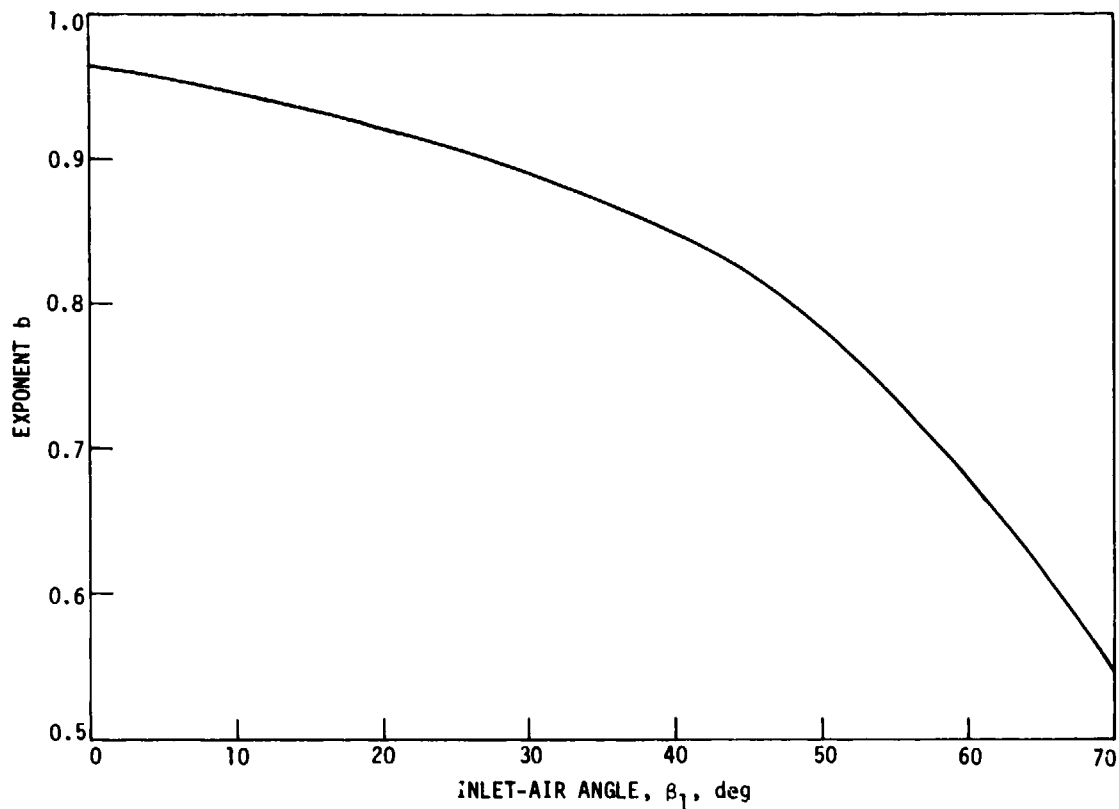


Fig.B-7 Value of solidity exponent b in deviation-angle rule deduced from data for 65-series sections on NACA A₁₀ camber line

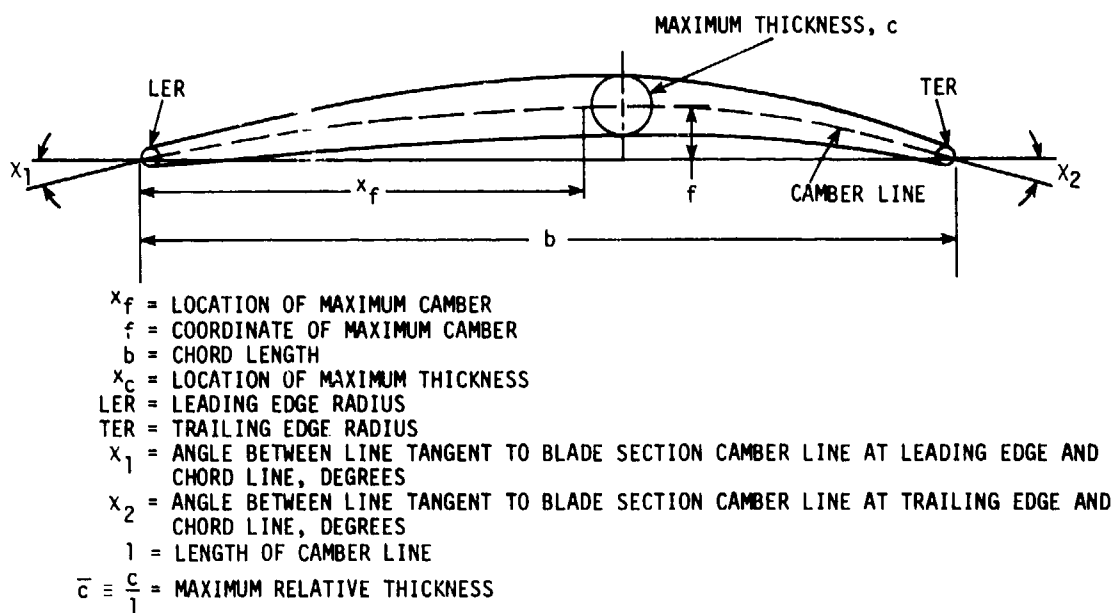
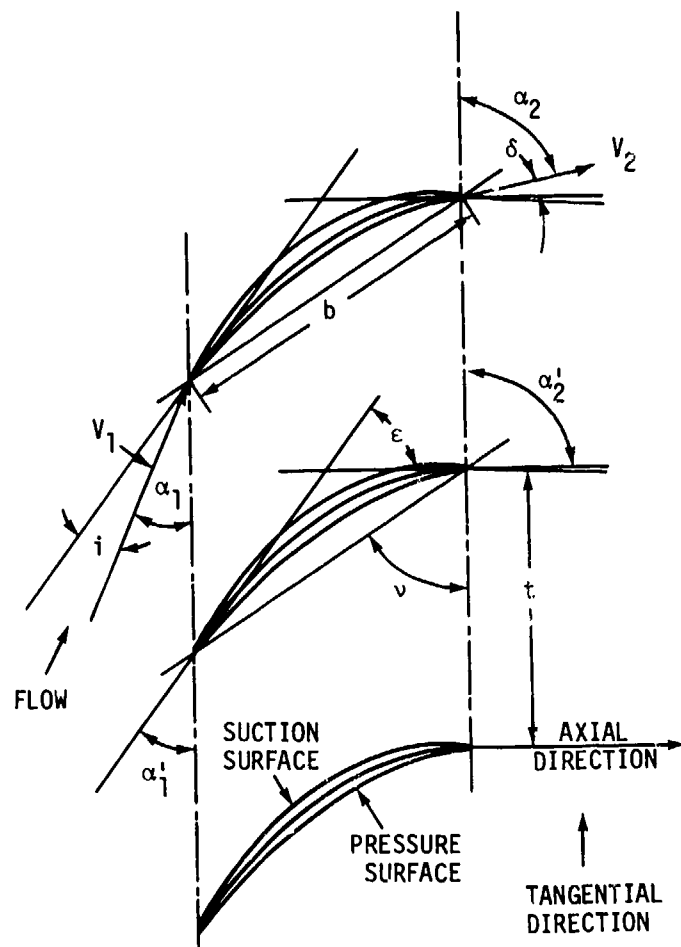


Fig.C-1 USSR blade section profile terminology (Ref.25)



$$\begin{aligned}
 i &= \alpha_1^* - \alpha_1 & \epsilon &= \alpha_2^* - \alpha_1^* \\
 \delta &= \alpha_2^* - \alpha_2 & \Delta\alpha &= \epsilon + i - \delta \\
 \Delta\alpha &= \alpha_2 - \alpha_1
 \end{aligned}$$

Fig.C-2 USSR cascade terminology (Ref.25)

TABLE D-1
Compressor Blade Section Profile Geometries

Camber Line	a/c	Typical Thickness Distribution	d/c	t/c	Construction References	Performance Correlation References
NACA a = 1.0	0.50	NACA 65-010 blower blade	0.40	variable from base 0.10	18	18,23,71,72
NACA combination	variable	NACA 65-010 blower blade	0.40	variable from base 0.10	35	
Circular arc	0.50	NACA 65-010 blower blade A - series	0.40	variable from base 0.40	61,18	61
		C - series	0.30-0.33	variable from base 0.10	25	25
		Double circular arc	0.50	variable	11,82	15
Parabolic					61	
NOTE	variable	C - series	0.30-0.33	variable from base 0.10	11,22	15
USSR	variable	A - series	variable from base 0.40	variable from base 0.10	25	26
Multiple circular arc						
Type A	variable	circular arc segments	variable	variable	62	—
Type B	variable	circular arc segments	variable	variable	51	—
Type C	variable	parabolic (quadratic equations)	variable	variable	31	—
Type D	variable	third-order polynomial	variable	variable	73,68,70	—
Exponential	variable	third-order polynomial	variable	variable	73,68,70	—
Polynomial	variable	third-order polynomial	variable	variable	73,68,70	—
dh/dl	variable	surface $dh/d(\text{surface})$ = constant	variable	variable	63	—
= constant						
SRL arbitrary	variable	third-order polynomial	variable	variable	69,70	—
NACA arbitrary	variable	variable	arbitrary	arbitrary	74,75	—

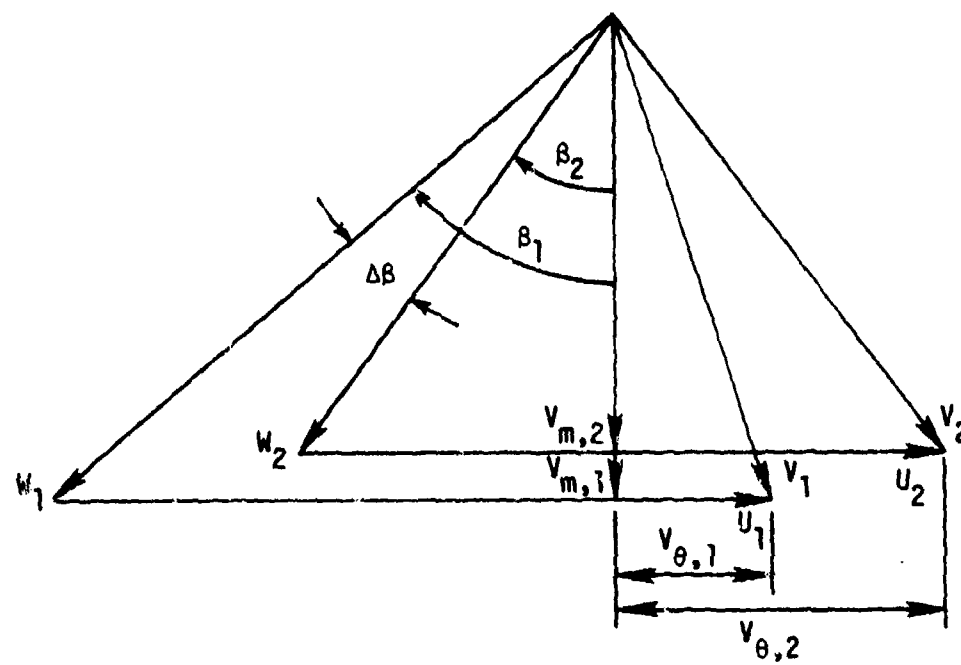


Fig.E-1 Rotating Cascade velocity diagram components

II.2.9 AXIAL COMPRESSOR STALL AND SURGE

INTRODUCTION

Although the evaluation of the so-called surge line of compressors was explicitly excluded from the original task of the Working Group due to the fact that it would constitute a full task in itself, it was requested at a later date that a short discussion on this subject be introduced in the review of the state of the art.

First, the name of stall line or surge line is improper and confusing. Stall refers either to a critical drop in performance or to some kind of steady or unsteady flow separation from walls or blade surge is characterized by large oscillations of mass flow rate. Neither are sufficient to define the so-called "surge" or "stall line", which in reality, is a line defined by couples of pressure ratio-mass flow values which limit, for each speed line, the region of safe operation of the compressor.

In the vicinity of this line, the flow changes from a stable generally axisymmetric configuration characterized by a large "sound flow region" and boundary layer type flows near walls and blade surfaces, to another stable configuration, with large low flow or zero flow zone which can be axisymmetric or not, steady or not. The change is made by passing through a transient (unstable) regime, characteristic of the compressor design and mode of operation, and determined by the axisymmetric original flow behaviour near its limit of existence.

Roughly, the second stable regimes can be described as follows when the rotational speed is increased : part-span or "small" rotating stall appearing in the front stages (without large modification of the overall characteristic), which, for smaller mass flow degenerate into "full span" or "large" rotating stall, affecting in a large way the characteristic of the stage concerned, and the overall compressor characteristic ; increasing speed one can then meet a "wall stall" or annular zone of low or zero flow covering a non negligible part of the span near the end walls, flutter generated by separation on blades, then again wall or blade steady stall, large rotating stall in the last stages and again flutter (in the transonic range). This would be typical of an advanced highly loaded jet engine type compressor. All the type of stall or aeroelastic effects are not necessary met for all compressors.

After that, there is a "system response" to change in flow nature, which depends on upstream and downstream volume, throttle characteristic, etc. One typical response is surge. The response can be affected by inlet distortions, as well as the form and nature of the second stable regime. The logical process to determine the Limit Line of "safe operation" should then be : evaluation of the unstable regime of the nature and characteristic of the "second stable regime" and of system response. This type of approach is now beginning to be applied.

Reference papers

An excellent paper, summarizing the present knowledge of the subject is about to be published by Greitzer(1). Important progress is being made in the determination of instability appearance and characterization. Ferrand (2) for instance has developed on an original idea by Fabri a general method to treat effect of distortion, the appearance of stall or surge, and is extending it to flutter appearance. A most remarkable series of studies have been led jointly at MIT and at the Whittle Laboratory by Greitzer, Cumpsty, Day et al (see (3, 4, 5) for the characterization -through reasoned correlations- of rotating stall, instabilities and especially system response. Their efficient approach is similar (but much improved) to that of Yershov (6) dating from 1960's whose work was unhappily unnoticed for a long time. Additional significant papers are those of Takata and Nagano (7) and Orner (8).

State of the art

References (2) to (8) open the way to the logical approach outlined above. They cover one-dimensional and quasi 3-D approaches, and work being done on 3-D approaches. The use of sound 1-D models has already aided in improved optimisation at the design stage, after having been either calibrated by a limited number of experiments, or validated by their use in parametric studies.

In general practice, however, the so-called "surge line" is either predicted from experience and extrapolation of previous data, or by methods which do not consider the change in flow regime, but when calibrated against experiments, give for particular forms of design the desired limit. Such methods are discussed in more detail in (1) , which also contains an extensive bibliography.

One such method consists in identifying the surge line through the use of a limit loading, expressed either by a pressure rise, or more often, through a limit diffusion factor or a conventional loss increase. This is done either on a one-dimensional basis (mean line approach) or in the scope of a through flow calculation method. It is implicitly assumed that all problems arise from blade separation. The more real justification is that such limit loadings are rough indicators of the stability limit, which has been shown (see (2) for instance) to strongly depend on the loss gradient in function of incidence or Mach number. Additionally, the criterion is local and applicable at most to a blade row characteristic. Thus additional criteria have to be defined to see when the whole compressor characteristic is affected (by stage stacking techniques, through flow calculation or otherwise). Such an approach cannot give rise to general correlations, but is quick, extremely useful and accurate enough when applied to forms of design for which they have been calibrated. The most satisfactory correlations are however proprietary.

Another method of the same type, but probably more general is to use, either with a mean line or a through flow calculation, a Mellor type method for pseudo-end wall boundary layer: when reducing mass flow, a sudden growth of the end-wall boundary layer is noticed, and can be taken as a limit for the stable regime (it is assumed that the limit of safe operation is due to annular stall) (Hirsch private communication).

CONCLUSION

The so-called "surge line" evaluation is an extremely complex area, which deserves in itself full attention. The intention here was only to define the problem.

In summary, the existing methods of prediction do not take the real physics of the flow into account, and cannot explain or consider or identify all the parameters of importance. They are however quick and useful for the range in which they have been calibrated, but are mostly not available in public literature.

A more generalized use of the pseudo-end wall boundary layer approach seems interesting.

Satisfactory solutions will come however only from the logical approach of instability detection, second flow regime and system response characterization, for which solid elements are now in hand but require further development.

LIST OF REFERENCES

- (1) Greitzer E.M. : Review-axial compressor stall phenomena.
J.Basic.Engr.,Trans. ASME ; 102 : 134 - 151.1980.
- (2) Ferrand P. and Chaupin J. : Theoretical study of flow instabilities and inlet distortions in axial compressors. ASME Preprint 81-GT-211.
- (3) Day I.J., Greitzer E.M. and Cumpsty N.A. : Prediction of compressor performance in rotating stall.
ASM J. Engr. Power Vol. 100 pp 1-14, Jan. 1978.
- (4) Greitzer E.M. : Surge and rotating stall in axial flow compressors.
Part I and II, ASME J. Engr. Power, Vol. 98, April 1976.
- (5) Cumpsty N.A. and Greitzer E.M. : A simple model for compressor stall cell propagation.
G.T. and PDL report 148, MIT, Feb. 1980.
- (6) Yershov V.N. : Unstable conditions of turbodynamic rotating stall.
Foreign Tech. Division Translation, Wright Patterson A.F.B., Aug. 1976.
- (7) Takata H. and Nogano S. : Non linear analysis of rotating stall.
ASME Transactions 72-GT-3, 1972.
- (8) Orner N. : Rotating stall in axial flow compressors.
Von Karman Institute lecture series "Unsteady flow in turbomachinery" (1979).

II.2.10 SUMMARY OF ANSWERS TO THE QUESTIONNAIRE

1. INTRODUCTION

To ascertain better the state of the art, a questionnaire bearing on particular points raised by the general survey paper of Hirsch (1) was prepared and distributed in industry and research groups, through the national representatives of the WG-18 questions, divided in 3 categories (compressor loss correlations, 12 questions - flow turning correlations, 3 questions - Secondary and Clearance effects, 3 questions) were asked. They are given in Appendix I. 14 answers were received from six countries, covering a typical cross section of aeronautical and non aeronautical industries, research establishments and university laboratories. (The list is given in Appendix II). Additional comments were received from N.G.T.E. and Rolls-Royce Aero Engine Div. (Bristol). Contributors are to be thanked most heartily, both for the time spent and for the extremely useful information provided, which has proven to be useful not only in assessing more accurately the state of the art but also in orienting the work on the WG and in shaping its conclusions.

A summary of the answers is presented below.

2. SUMMARY AND COMMENTS ON THE ANSWERS

The general impression conveyed by the answers is that the state of the art does not satisfy the users who have to complement the information provided by non-universal corrections. The shortcomings are particularly important when the correlations are not based on a sound understanding of the relevant physical phenomena. The need for a quick assessment of performance at both design and off-design remains essential, and does not ease the task of representing correctly the physics of the flow.

The general consensus appears to be that progress will be considerably helped by systematic use of numerical experiments from which to develop more soundly based correlations (for instance, blade to blade calculations for a better assessment of losses and turning) or by the inclusion of fast, integral numerical method of general application in the evaluation process. An example of the possibilities of the first type of approach is given in the paper of Koch and Smith (2), while the method derived from Mellor's concept of pseudo-end wall boundary layer (3) typifies the second one.

The answers also show that the use of through flow calculation for prediction of off-design performance is not fully generalized partly due to the lack of information in suitable form on loss and turning away from the design point.

More details are given below.

A. Compressor loss correlation

General remarks

The concept of diffusion factor and its correlation to losses is universally used at design point, introducing velocities and not angles, in its formulation. Its use for off-design prediction is not generalized and often questioned. Three questions implicitly arise : which of the many forms of diffusion factor (4) to use, which relation between D factor and momentum thickness applies at the TE, and relation between the latter and the loss coefficient.

For the first question, as suggested by one of the contributors, the interest lies in a form as general and simple as possible, but which gives a correct measure of W_{MAX}/W_{TE} , i.e. represents correctly the level of diffusion.

Note that all the expressions of diffusion factor have a common deficiency for off-design purpose : they neglect the pressure side effect which is important in the low incidence range.

The answers are favourable to the type of approach followed in (2) which, however, still need additional experimental cross-checks.

For the second question, as in (2), the effect of the flow and blading characteristic (Mach, Reynolds, incidence, etc.) should be better evaluated in terms of trailing edge momentum thickness. In actual practice either the value of diffusion factor is changed, while maintaining its relation with the losses or the D factor definition is kept and the evolution of momentum thickness with it, changed. Sometimes, both approaches are used simultaneously, and care should be taken to avoid accounting twice for the same effect.

The third question: several formulae express the loss coefficient in function of trailing edge thickness outlet angle and trailing edge momentum thickness, leading at high Mach number to differences in loss coefficient of the order of 100 %.

Data used for assessing the relation between D and losses, and thus for performance evaluation is for most responses, cascade data (straight or annular) corrected or not by compressor data, and applied mostly on conical surfaces. However, more and more the use of blade to blade calculation which can take into account real machine effects, such as streamtube area and radius change is used and/or advocated, either to derive correlations, as in (2) where it was used to calculate the diffusion factor expression, or to get directly the information.

Two remarks are in order : first, using compressor-corrected data (like a change of loss curve in function of radius) implies that all effects (area ratio, secondary flow and clearance effects, etc.) are implicitly incorporated and indistinguishable from each other. The validity of the correction is thus limited to similar designs, and in many cases is coherent only in a given through flow method structure as such a method is frequently used to reduce the compressor data. Second, the blade to blade method becomes cheaper and cheaper to use and more accurate, for all domains of operation. However, they are

still generally unable to deal, with very few exceptions, with the cases of separated flows, be it incidence or shock induced.

It seems possible to continue to use the diffusion factor concept in the transonic-supersonic range, and also at off-design but only by modifying the loss correlations.

Shortcomings

- The need for simple means of predicting both low and high Reynolds (and roughness) effects was emphasized. Hence, papers on the subject are included in the WG report.
- The information on Mach number effect is insufficient. There is a need for a simple "loss critical Mach number" evaluation, i.e. the inlet Mach number above which loss grows rapidly due to shock presence, but doubts are raised about obtaining a general single formulation. Blade to blade calculations are advocated again here. Shock losses models in use (1 or 2D) and evaluation of interaction losses are deemed insufficient, and valid mostly at design and for particular bladings. Cost of experimental cascade testing in time and money, for that range is deemed unpractical. Blade to blade calculation is advocated but the problem of separated flow remains.
- Effect of trailing edge thickness appears to be important for high performance multistage compressors, (blade row interference) and is not well understood.
- 3D effect and rotation effect must affect DF correlations but are not well ascertained.

B. Flow turning correlation

- There is a need for a Mach number correction to a Carter type formulation, above the critical one, and obviously for supersonic exit Mach number. Use should be made of the super-critical turbine experience.
- Except for very low Reynolds number, the influence of the latter is accepted to be small.
- The effect of axial velocity or axial velocity density ratio on turning is evaluated very differently from negligible to important, with an agreement of the fact that no good "out-house" correlations exist. The effect, which is both of the "potential" and "viscous" type -the latter at or near separation- could be assessed by blade to blade calculation.
- Opinions on the need for correction in function of incidence in the non-separated region are again very different from one response to another. For those who deem it necessary, the linear (NASA-type) approximation is not sufficient. This point although it may be not of first importance needs clarification.
- Some answers rightly indicate that the larger source of difference from the prediction of angle by the Carter-type correlation is to be sought in secondary flow and clearance effects which are generally not taken into account explicitly.

C. Secondary and clearance effects

Blockage evaluation is usually made by some sort of end-wall boundary layer calculation. Opinion on the evaluation of loss and turning correction due to secondary and clearance loss tends to a combined use of experimental correction and pseudo-end wall boundary layer approach, although the latter is seen to be the best way, once improved upon. Tip clearance effects are mostly taken into account by an efficiency correction only.

Three remarks are in order :

- As pointed out in the answers, in the present state of the art, blockage and deviation corrections cannot be chosen independently. They have the same effect on the accuracy of overall performance prediction by the through flow approach. The good results are, in some way, achieved by a "coherent compensation of errors" calibrated to get the right results. This indicates that the real physics of the phenomenon are not yet included in the loss and deviation subroutines, as shown often by the discrepancy between calculated and measured radial flow distribution.
- The Mellor-type of approach has the potential of accounting for not only global, but local secondary and clearance flow effects. These developments, especially that of Hirsch as reported elsewhere in the WG report and at Ecole Centrale de Lyon, constitute a major step in a correct flow modelling, allowing a proper separation of effects.
- Their main shortcoming might be in the angle correction evaluation, outside the pseudo-end wall boundary layer, where the effect of clearance and secondary flow is still felt.

Lakshminarayana's approach (5) has been applied successfully by one of the industrial participant, and is being further developed at Ecole Centrale de Lyon.

List of questions

A. COMPRESSOR LOSS CORRELATION

A.1. In subsonic flows well below the critical Mach number the flow losses (blade friction losses) at design are accepted to be a function of diffusion factor "DF" or equivalent diffusion factor "equ. DF". However, DF should be defined by using the velocity vectors instead of the flow angles, and a critical Mach number indicator should be included to identify the flow regime where losses increase strongly.

What is your experience ?

A.2. When designing a compressor blading do you use compressor data or cascade data or both ?

A.3. Are cascade data worthwhile for blade design on conical surface or is cascade projection necessary ?

A.4. What is the validity of DF expression of L.H. Smith (s. Hirsch paper) compared to the original Lieblein's formula ? Should DF be even more generalized for arbitrary blade shapes and cascade geometries ?

A.5. What are the effects of

- 3 D flow phenomena
- streamline curvature

- system's rotation (influence of streamline shift and boundary-layer centrifugation) on the diffusion factor concept ?

A.6. Influence of Re-number : It is recommended that a correlation for the critical Re-number indicating the presence of laminar separation bubbles should be developed as well as one for a Re-number indicating bursting of the separation bubbles. The continuous variation of losses in function of Re-number is considered to be of secondary importance. Another WG is planned to look at this point in more detail. However, comment on your basic experience.

A.7. What is the validity of diffusion factor (also equ.DF) at off-design ? Additional information to evaluate empirical constants must be obtained from existing tests or from calculations. The correlations should also be extended for small (5 to 10 % chord) separated zone.

A.8. Is trailing edge thickness accepted to be of secondary importance ?

A.9. In the transonic flow regime additional losses occur due to the appearance of shocks. Can the profile loss prediction any longer be based on diffusion factor?

A.10. What is the validity of 2D shock models for loss prediction in compressor blade rows at design and off-design ?

A.11. Is axial velocity density ratio to be considered for shock loss prediction besides its effect on the Mach number ahead of the shock ?

A.12. Is there an additional fraction of losses to be taken into account for shock-boundary-layer interaction and boundary-layer separation ?

B. FLOW TURNING CORRELATION

B.1. Current deviation angle prediction (based on solidity, thickness, camber, stagger angle and blade shape) covers primarily geometrical parameters and potential flow effects and is valid at design point. Should the methods be extended to account for roughness, Mach and Re-number ?

B.2. Influence of axial velocity density ratio and of viscosity (with and without separation) must be included. Can you give recommendations upon that ?

B.3. Is correction in function of incidence for the non-separated region important ? This can probably be answered by the people who make calculations of test cases by comparing results obtained with and without this correction.

C. SECONDARY AND CLEARANCE EFFECTS

C.1. Secondary flow corrections are important with respect to blockage and clearance effects. Are there valid blockage correlations available for all types of compressors incl. multistage machines? Please comment on Mellor's method of end wall boundary layer calculations.

C.2. Should the loss and turning correction be approached by correlation or by end-wall boundary layer computation or by both ?

C.3. How do you correct for the tip clearance effect ?

APPENDIX II

Organisations involved for the answers to the questionnaire :

1.	Nuovo Pignone,	It.
2.	NGTE	U.K.
3.	Rolls Royce, Bristol	U.K.
4.	Genova University	It.
5.	Centemeri	It.
6.	MTU	Ge.
7.	T.H. Darmstadt	Ge.
8.	GHH	Ge.
9.	BBC	Ch.
10.	Ecole Centrale de Lyon	Fr.
11.	NASA	USA
12.	Novack	USA
13.	Serovy	USA
14.	Detroit Diesel Allison	USA.

Comments were also received from NGTE and Rolls Royce, Great Britain.

CONCLUSION TO THE "REVIEW PAPERS" AND "ANSWERS TO QUESTIONNAIRE"

1. The concept of the basis for the correlation on losses and turning dates from the period 1953-1958 as well as the basic corresponding experimental information. Application to quite different types of tasks and of geometry has been made by extrapolation based on a very limited number of additional data. As a result the information is not always sufficiently based on a correct knowledge of the physical processes. The experimental data can also be questioned as all flow parameters were not always properly controlled. Especially, data at off-design is insufficient.
 2. The industry although using more and more sophisticated approaches - including fully 3D calculations - still has a strong need for a simple but physically-founded approach of the correlation type, and favors the use of the diffusion factor concept and of the Carter's type of approach for deviation rules -when applicable.
 3. It seems highly desirable, in the frame of the existing through flow approaches, to separate the main flow and end wall (including clearance) contributions to loss and deviation, the only sound alternative being a 3D approach, which is being developed but still too costly and has not enough good experimental data to back it up. The practice of correcting blade element correlations globally for "all other effects" lacks of generality as it is concealing in a recipe, several phenomena whose contribution is very much function of the compressor design.
 4. For pure blade loss, the concept of diffusion factor based on a boundary layer approach is sound in a wide range. Many forms of diffusion factor to exist, as well as several correlation between losses and diffusion factor. A form has to be found which expresses properly the W_{MAX}/W_2 ratio, for the widest possible range of flow conditions and blading geometries. The relation of the diffusion factor with the momentum thickness should incorporate the relevant variables. An approach of the type followed by Koch and Smith (2) which combines experiment and blade to blade calculations for its basis is promising, although further checks (some of which are carried in the scope of the WG activities) are needed.
 5. The principle and the bulk of the information on the deviation correlations date from 1945-1960. Even disregarding the secondary and clearance influence, they need up-dating, especially in function of loading, Mach number (especially above critical) and incidence.
 6. Information on the Re-number effect have been added. Robert's approach for the low Re range and Fottner and Schaffer's for the high Re number range are recommended.
 7. Existing global models for shock and shock-boundary layer interaction are insufficient, and applicable only to a limited number of geometries and flow conditions. Prediction methods for critical and choking Mach number are not general enough.
 8. It is expected that to remove the shortcomings mentioned above, extensive use of the blade to blade calculations (including boundary layer) backed by a few chosen validation experiments will be made. The main limitation of those methods is their present inability to predict performance in the separated regimes. An assessment of the value of the best existing method in their use in numerical, parametric experiments is needed, and is partly undertaken in the WG work.
 9. A limited amount of information on part-span damper losses has been reviewed and presented. Two approaches are given, the second model underestimating the losses by quite a large amount, the first one is essentially empirical. Data on geometries is insufficient to draw conclusions.
 10. Secondary flow and clearance effects should be evaluated by a Mellor type of approach, whose most developed versions have the potential to provide both global and local information, when coupled with a good through flow method. Angle correction outside the pseudo end-wall boundary layer needs to be taken into account. A method of the type described in (5) is suggested.
- Experimental correlations in this area do not properly account for the real flow phenomena and their improvement is not deemed useful. If a quick, global assessment is needed, the simplest one should be used (see conclusion of relevant paper).

LIST OF REFERENCES

- (1) Hirsch, Ch. : Axial compressor performance prediction survey of deviation and loss correlations. WG 12 - Survey paper.
- (2) Koch C.C. and Smith L.H. : Loss sources and magnitudes in axial flow compressors. ASME paper 75-WA-GT. 6.
- (3) De Ruyck J., Hirsch Ch. and Kool P. : Investigation on axial compressor end-wall boundary layer calculation. Preprint 1979 Int. Gas Turbine Congress and Exhibition. July 9-11, 1979. Technion, Israel.
- (4) Dunker R. and Weyer H.B. : Survey of diffusion factors and profile losses. Through flow calculation in axial turbomachines. WG 12 Report Chapter II.2.1.
- (5) Lakshminarayana B. : Method of predicting the tip clearance effects in axial flow turbomachinery. ASME Journal of Basic Engineering, Sept. 1970, pp 467-482.

II.3 PRESENTATION OF TEST CASES

Three test cases, representative of actual designs, were submitted for the Working Group; a single stage, a two stage and a four stage compressor.

The single stage compressor, developed and extensively tested at DFVLR was already used as test case for the PEP-47th Meeting (1). Classical as well as laser measurements inside the rotor are available. Appendix AII.3.1 presented by H. Weyer, contains the geometrical data as well as performance maps and some traverse obtained with conventional instrumentation. Appendix 3.1 gives also the coordinates of some blade sections at 45% span and the corresponding blade to blade velocity distribution at various inlet conditions, in cascade configuration and in the actual rotor.

The second stage compressor, submitted by NASA Lewis is fully documented in the literature (2), NASA TP 1493, August 1979, and is not introduced in this report at an appendix. The report includes measured as well as calculated data. It is to be noted that the measurements are performed with conventional instrumentation in the following way. Total pressures and temperatures and tangential flow angles are measured at stator outlets along circumferential traverses at fixed radii. The stagnation pressure and temperatures are mass averaged while the flow angle is arithmetically averaged. Moreover, a static pressure is measured in the middle of the passage.

All other variables at stator outlet and all variables rotor outlet are calculated along the design streamlines and for the design values of the end-wall blockage factors. In particular, the average total pressure at rotor outlet is taken equal to the value measured at stator exit outside the wake.

This two-stage fan has a low aspect ratio blading particularly in the first rotor, aspect ratio being equal to 1.56.

Several new design concepts are introduced in this rotor, such as elimination of the part-span damper blade maximum thickness is moved rearward, allowance for inlet tip boundary-layer by giving to the rotor a leading-edge end-wall bend. This resulted in a peak-efficiency of 0.846 at a pressure ratio of 2.47, even higher than the design value (2.4).

This test case is quite challenging with regard to performance prediction, especially at off-design as illustrated in the following chapter on the calculation results.

The four-stage compressor has been kindly presented by Brown Boveri & Cie./Sulzer and is typical of an industrial multistage configuration.

The geometrical data are presented in appendix AII.3.2 and the data include full performance maps as well as radial traverses of stagnation pressures and temperatures at the compressor outlet, for 6 operating points along the nominal speed lines. No information is available with regard to the accuracy of the measurements.

It is to be noted, that due to space limitations, only a summary of the geometrical data and of the results of the single stage compressor are published here. More extensive information is available, on request, from the Propulsion and Energetics Panel at AGARD headquarters.

List of References

- (1) AGARD-Conference Proceedings, CP 195, "Through Flow Calculations in Turbomachines".
- (2) D.C. URASEK, W.T. GORREL, W.S. CUNNAN; "Performance of Two-Stage Fan having Low-Aspect Ratio First-Stage Rotor Blading", NASA TP 1493, August 1979.

Appendix AII.3.1 Single-Stage Transonic Compressor and Equivalent Plane Cascade

Introduction

The WG 12 activities cover primarily turbomachinery off-design performance prediction, however include also blade-to-blade calculation on relevant test cases to get more information on those basic flow phenomena that affect flow losses and turning in blade rows.

One of the test cases selected is the DFVLP single-stage transonic compressor that has been tested in great detail with the results well documented (1, 2, 3). Particularly intrablade velocity data of the rotor are available from extensive flow studies with laser velocimetry. The data allow to compare blade-to-blade calculations to actual transonic compressor flow. Additionally to the rotor tests the rotor blade section at 45 % span was investigated in the DFVLR transonic cascade windtunnel (4, 5).

Single-Stage Transonic Compressor

The transonic compressor without inlet guide vanes was designed for a total pressure ratio of 1.51 at a mass flow rate of 17.3 kg/s and a tip speed of 425 m/s. The isentropic efficiency was estimated to be about 80.5 %. The rotor inlet diameter of 400 mm was prescribed by the DFVLR axial compressor test rig. The stage pressure ratio of 1.51 is predicted to occur at a temperature rise of 15.4 % of the inlet total value.

Fig.1 demonstrates the compressor annulus geometry. Hub and outer wall are shaped to adapt the flow path to the stage pressure rise, to achieve nearly constant axial velocity over the annulus height, and to balance rotor and stator diffusion factors properly. MCA-profiles were selected for the rotor blading from hub to tip. NACA-65 profiles with a circular arc camber line were used throughout the stator blade height as shown in Fig.2. 28 blades with a tip chord length of about 60 mm were selected for the rotor, 60 blades for the stator yielding usual blade solidities between 1.34 and 2.0 for the rotor and 1.5 to 2.4 for the stator. The maximum inlet Mach numbers to rotor and stator blading reach up to 1.37 and 0.76, respectively. The maximum diffusion factor is estimated to be 0.53 for the rotor and 0.48 for the stator. Further spanwise blade data including the axial location of blade leading and trailing edge are given in Fig.3 and 4.

Instrumentation and Test Results

The compressor has been investigated using both conventional and advanced measuring techniques. The instrumentation planes just upstream and downstream of the stage (Fig.1) were equipped with probe rakes or radial traversing probes to analyse the spanwise distribution of the total pressure and temperature, and of the flow direction. The compressor performance map - adiabatic efficiency and total pressure ratio versus mass flow - is shown in Fig.5.

The rotor flow field (ahead, within, and behind the blading) was studied in great detail using advanced laser velocimetry (6). These tests carried out at design (20 260 rpm) and off-design speeds yielded quite complete information on the span- and gapwise velocity profiles, on the 3-dimensional shock waves, on the flow separations, and on the blade wakes. Up to 15 circumferential measuring positions over one blade spacing were set in each measuring locus designated by circular symbols in Fig.6. The diagram demonstrates that measurements could be performed also in the vicinity of the hub and outer casing walls. The complete geometry of the rotor and stator as well as the velocity data given in tabular form for the rotor blade section at 45 span are available on request from AGARD-Headquarters.

Plane Cascade

The plane cascade equivalent to the 45 % rotor blade section was designed by projecting the rotor blade coordinates defined on stream-surfaces on an axis-parallel plane radially fixed by the blade stacking point. Thus, the cascade solidity corresponds to the rotor blade solidity at the stacking point. The 45 % blade section has been designed for an inlet Mach number of 1.09 assuming the upstream shock wave to be attached to the blade leading edge.

The primary cascade design data are:

Blade inlet angle ^{*)} :	55.1°
Blade outlet angle ^{*)} :	40.1°
Stagger angle ^{*)} :	48.5°
Chord length	: 90 mm
Solidity	: 1.61
Aspect ratio	: 1.88
Leading edge radius	: 0.4 % of chord length.

^{*)} angles related to axis.

Instrumentation and Test Procedure

As illustrated in Fig.7 wall static pressures were measured 63 % of chord ahead and 41 % behind the cascade to control inlet flow conditions and cascade flow periodicity. Downstream total pressure and air angle were measured versus blade pitch (mid-span) by probes positioned 47 % of chord behind the cascade, to determine the cascade performance characteristics. Detailed blade surface pressure measurements were carried out at the following cascade flow settings:

	1st run	2nd run	3rd run
Inlet Mach number	0.911	0.827	0.813
Inlet air angle ^{*)}	64.3	58.5	54.5
Outlet air angle ^{*)}	45.5	46.5	44.9
Axial velocity density ratio	1.249	1.098	1.06

^{*)} angles related to axis.

During the tests the axial velocity density ratio (AVDR) was not controlled but fixed by windtunnel side wall boundary-layer displacement.

Detailed geometric data particularly blade thickness distribution and test results are available on request from AGARD-Headquarters.

List of References

- (1) WEYER, H.B. Compressor Design and Experimental Results. AGARD-CP-195 (1976).
- (2) DUNKER, R., STRINNING, P., WEYER, H. Experimental Study of the Flow Field within a Transonic Axial Compressor Rotor by Laser Velocimetry and Comparison with Through-Flow Calculation. J. Eng. for Power, ASME Series A, Vol.100 (1978).
- (3) MC DONALD, P., BOLT, C., DUNKER, R., WEYER, H. A Comparison between Measured and Computed Flow Fields in a Transonic Compressor Rotor. ASME-Paper No. 80-GT-7 (1980).
- (4) STARKE, H., BREUGELMANS, F., SCHIMMING, P. Investigation of the Axial Velocity Density Ratio in a High Turning Cascade. ASME-Paper No. 75-GT-25 (1975).
- (5) SCHREIBER, H.A. Untersuchung des geraden Verdichtergitters LO30-4 bei schallnahen Zuströmmachzahlen. DFVLR-IB 352-79/10 (1979).
- (6) SCHODL, R. Laser-Two-Focus Velocimetry (L2F) for Use in Aero Engines. AGARD-LS-90 (1977).

Annulus Geometry

	Z	NABE (Hub)	GEHÄUSE (Shroud)		Z	NABE (Hub)	GEHÄUSE (Shroud)	
O-O	0	90,000	202,000	d-d	88	106,073	195,779	
	2	90,000	202,000		90	106,638	195,477	
	4	90,000	202,000		92	107,204	195,174	
	6	90,091	202,000		94	107,770	194,872	
	8	90,159	202,000		96	108,336	194,570	
	10	90,245	202,000		98	108,902	194,267	
	12	90,349	202,000		100	109,468	193,965	
	14	90,470	201,399		102	110,034	193,662	
	16	90,611	201,993		104	110,600	193,360	
	18	90,770	201,983		106	111,166	193,058	
	20	90,947	201,966		108	111,725	192,755	
	22	91,141	201,943		d-d	109,5	112,121	192,582
	24	91,354	201,914			110	112,253	192,451
	26	91,584	201,878			112	112,747	192,149
	28	91,833	201,834			114	113,210	191,354
	30	92,099	201,783			116	113,643	191,568
	32	92,382	201,723			118	114,046	191,293
	34	92,684	201,655			120	114,420	191,027
	36	93,003	201,578					
	38	93,339	201,492					
	40	93,693	201,395					
	42	94,065	201,289					
	44	94,453	201,172					
	46	94,859	201,044					
	48	95,283	200,904					
	50	95,723	200,753					
	52	96,181	200,590					
	54	96,655	200,413					
	56	97,147	200,224					
	58	97,655	200,021					
	60	98,180	199,804					
	62	98,723	199,574					
a	64	99,201	199,329					
b-n	64,5	99,423	199,513					
	66	99,349	199,068					
	68	100,415	198,792					
	70	100,980	198,500					
	72	101,545	198,198					
	74	102,112	197,896					
	76	102,678	197,593					
	78	103,244	197,290					
	80	103,810	196,988					
	82	104,376	196,686					
	84	104,941	196,383					
c-c	86	105,507	196,081					

Instrumentation

Z,mm	0,0	29,0	62,0	113,0	172,0

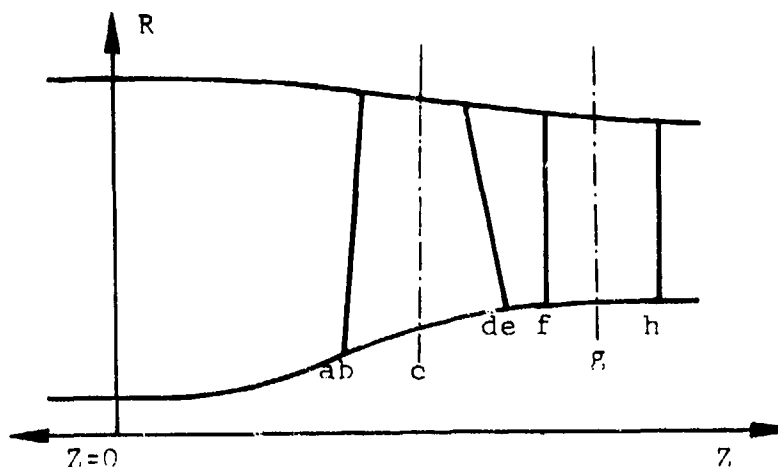


Fig.1 Annulus geometry DFVLR 1-stage transonic compressor

Stage No.	1	1
Blade Row	Rotor	Stator
Profile Type	MCA	NACA 65
Number of Blades	28	60

Fig.2 Profile type and number of blades - DFVLR 1-stage transonic compressor

Blade Row: Rotor

Radius, mm	Axial Location Z, mm	Leading Edge, mm	Trailing Edge, mm	Chord Length, mm	Solidity	Stagger Angle, deg.	Blade		max. Thickness % Chord	Leading Edge Radius % Chord
							Inlet Angle, deg.	Outlet Angle, deg.		
100	66,727	108,129	45,0704	2,0085	23,28	49,95	-12,92	9,527	0.6452	
110	66,972	107,587	46,6910	1,8916	29,56	50,75	-0,58	8,353	0.5706	
120	67,298	107,008	48,7313	1,8097	35,43	51,78	11,76	7,193	0.5019	
130	67,746	106,010	50,5970	1,7344	40,86	53,04	23,28	6,217	0.4465	
140	68,307	104,540	52,0685	1,6574	45,90	54,48	33,31	5,431	0.3995	
150	68,912	102,975	53,3947	1,5863	50,36	55,94	42,25	4,784	0.3619	
160	69,485	101,625	54,5956	1,5206	53,94	57,58	48,34	4,281	0.3335	
170	70,066	100,533	55,7175	1,4606	56,85	59,32	52,20	3,906	0.3100	
180	70,769	99,472	56,8111	1,4065	59,65	61,28	54,52	3,661	0.2883	
190	71,851	98,151	57,8678	1,3573	62,97	63,55	56,23	3,534	0.2713	
200	73,287	96,683	59,0365	1,3154	66,65	66,85	57,64	3,524	0.2504	

Angles in axial direction and with respect to compressor axis

Fig.3 Blade geometry (on blade sections parallel to axis) – DFVLR 1-stage transonic compressor

Blade Row: Stator

226

Radius, mm	Axial Location 7 Leading Edge, mm	Trailing Edge, mm	Chord Length, mm	Solidity	Stagger Angle, deg.	Blade Inlet Angle, deg.	Outlet Angle, deg.	max. Thickness % Chord	Leading Edge Radius % Chord
110	123,882	153,617	30,677	2,663	14,30	40,24	-12,59	8.0	0.44
120	123,881	153,219	30,175	2,401	13,59	39,03	-11,79		
130	123,864	152,874	29,768	2,187	13,03	34,15	-9,32		
140	123,825	152,644	29,534	2,014	12,70	32,24	-6,99		
150	123,846	152,526	29,380	1,870	12,59	31,75	-670		
160	123,829	152,474	29,328	1,750	12,45	31,75	-6,95		
170	123,818	152,452	29,349	1,649	12,74	32,62	-7,31		
180	123,864	152,530	29,457	1,563	13,38	34,79	-9,28		
190	123,934	152,907	29,822	1,499	13,78	42,02	-15,15	8.0	0.44

Angles in axial direction and with respect to compressor axis

Fig.4 Blade geometry (on blade sections parallel to axis) – DFVLR 1-stage transonic compressor

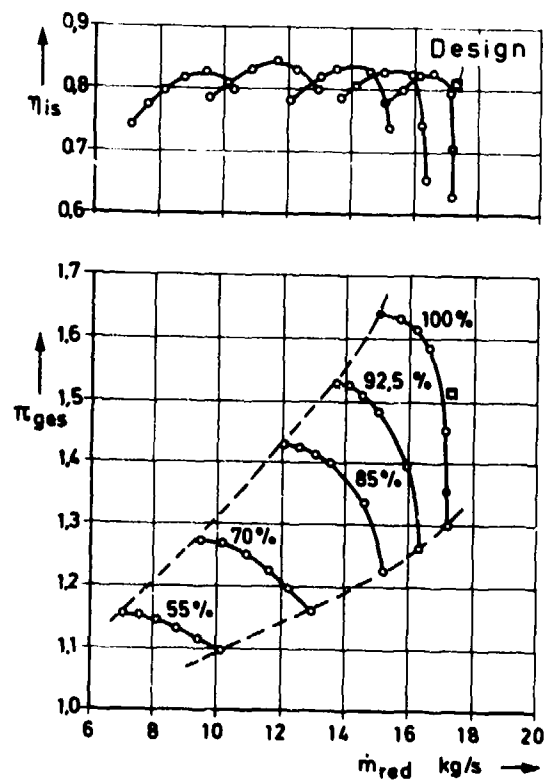


Fig.5 Performance map of single-stage transonic compressor

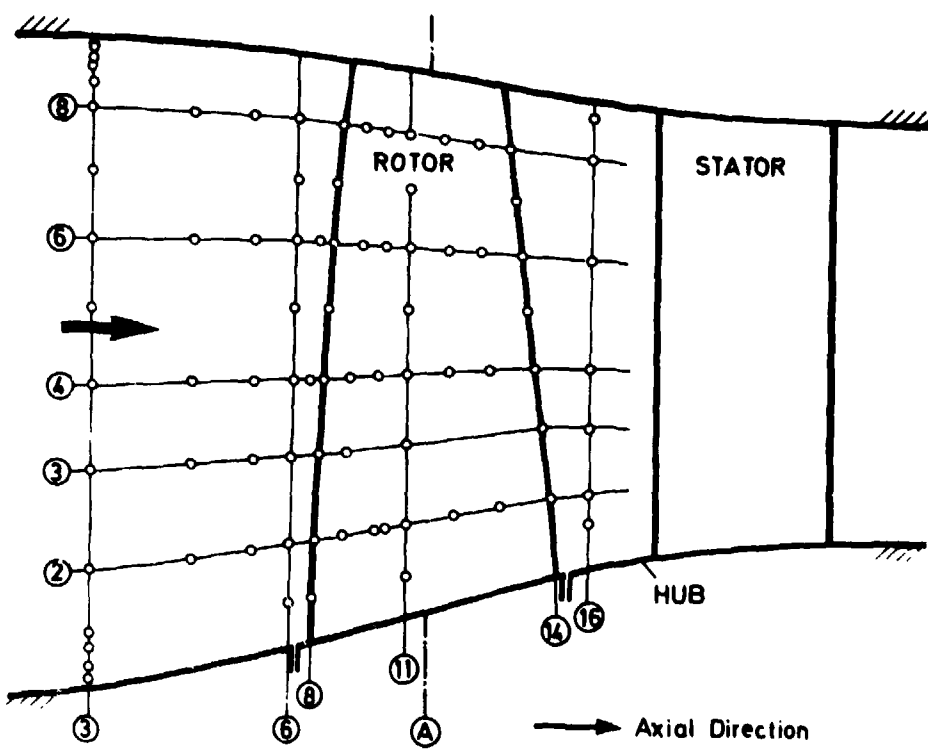


Fig.6 Stage annulus and laser velocimetry test locii

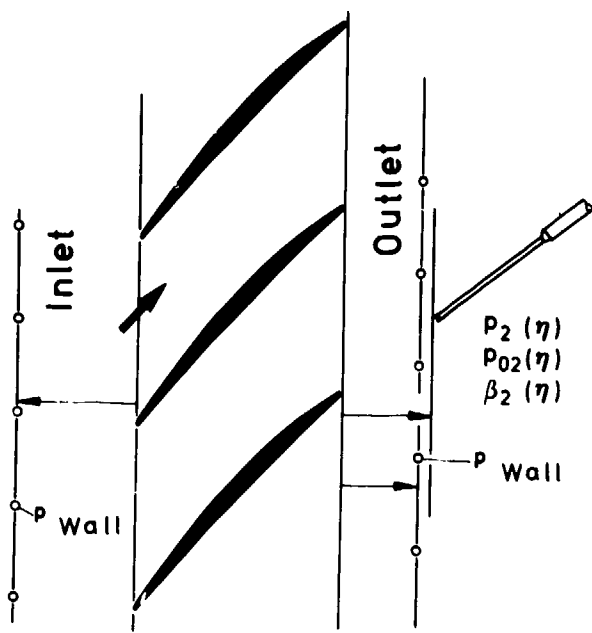


Fig. 7 Planar cascade installation and instrumentation

A.II.3.2. BBC/SULZER - 4-stage Transonic Compressor

Design speed 15000 rpm
 Inlet total pressure .975 bar
 Inlet total temperature 193.15° K
 Design pressure ratio 3.06

Test data available at following speeds (percent of design speed) 68.5 ; 90 ; 100 and 105 %.

The data were taken at the following inlet total pressures at reduced speed of :

68.5 %	$p_t = 0.94$ bar
90 %	$p_t = 0.60$ bar
100 %	$p_t = 0.57$ bar
105 %	$p_t = 0.48$ bar

The overall performance map and some traverses of stagnation pressure and temperature at compressor outlet are presented in Fig. 3.8. to 3.26.

Annulus Geometry

Z, mm	Hub	Tip
	R, mm	R, mm
-156.8	130.00	274.00
-125.0	130.00	
-87.5	130.00	
-34.1	134.26	
0.0	143.40	
36.8	152.93	
74.3	160.97	
101.0	165.57	
130.7	170.23	
165.6	175.71	
188.0	179.22	
211.1	182.85	
245.1	188.18	
266.0	191.46	
288.8	195.03	274.00
321.5	198.17	273.63
340.0	198.20	272.12
361.3		270.39
391.3		267.94
408.0		266.75
427.2		265.01
455.6		262.69
472.0		261.35
490.5		259.84
518.2		257.58
532.0		256.46
547.6		255.18
622.0	198.20	254.00

Instrumentation

Z, mm	792
-------	-----

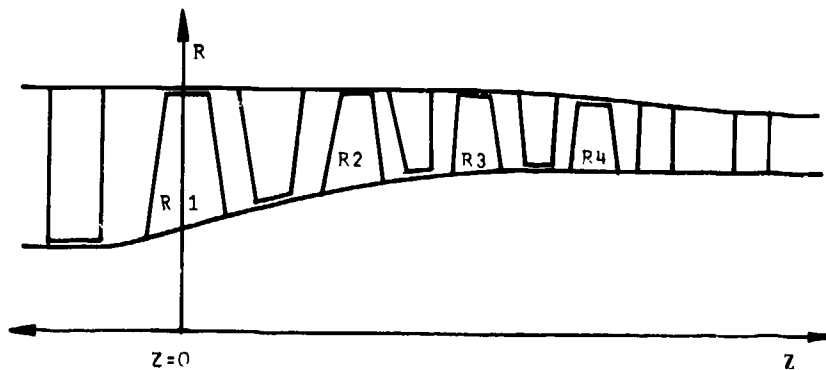


Fig. 3.8. : Annulus Geometry - BBC/SULZER 4-Stage Transonic Compressor

Stage No.	IGV	1	1	2	2
Blade Row	Stator	Rotor	Stator	Rotor	Stator
Profile Type	NACA	DCA	DCA	DCA	DCA
Number of Blade	18	17	28	27	34

Stage No.	3	3	4	4	OGV
Blade Row	Rotor	Stator	Rotor	Stator	Stator
Profile Type	DCA	DCA	DCA	DCA	DCA
Number of Blades	31	40	37	43	36

Fig. 3.9. : Profile Type and Number of Blades - BBC/SULZER 4-Stage Transonic Compressor -

Blade Row: Rotor Stage 1

Radius, mm	Axial Location z Leading Edge, mm	Trailing Edge, mm	Chord Length, mm	Solidity	Stagger Angle, deg.	Inlet Angle, deg.	Bleed Outlet Angle, deg.	max. Thickness to Chord	Leading Edge Radius % Chord
124.00	- 46.0	48.8	95.94	2.0934	10.46	32.00	-11.08	0.1160	0.5798
144.44	- 44.2	48.4	96.00	1.8357	19.77	37.07	2.48	0.0930	0.4653
183.82	- 39.1	43.8	102.12	1.5031	35.88	45.90	25.87	0.0564	0.2820
216.67	- 33.6	37.2	105.44	1.3171	47.75	52.58	42.92	0.0400	0.1999
245.86	- 29.2	30.8	108.48	1.1938	56.48	57.49	55.47	0.0360	0.1801
272.78	- 25.5	25.2	111.24	1.1034	62.99	60.79	65.19	0.0340	0.1699
284.00	- 24.1	23.0	112.40	1.0708	65.32	61.92	68.72	0.0335	0.1674

Angles in axial direction and with respect to compressor axis

Fig. 3.10: Blade Geometry (on blade sections parallel to axis)

Blade Row: Rotor Stage

Radius, mm	Axial Location Leading Edge, mm	Trailing Edge, mm	Chord Length, mm	Solidity	Stagger Angle, deg.	Blade Inlet Angle, deg.	Outlet Angle, deg.	max. Thickness to Chord	Leading Edge Radius Chord
165.08	156.8	222.6	70.00	1.8222	20.00	37.82	2.18	0.1018	0.5094
179.90	158.7	220.5		1.6721	28.01	41.05	14.94	0.0806	0.4029
207.30	162.3	216.0		1.4511	39.38	46.04	32.73	0.0533	0.2666
231.20	165.8	211.4		1.3011	49.53	52.05	47.02	0.0430	0.2149
252.90	168.7	207.8		1.1894	55.64	55.56	55.73	0.0400	0.2000
273.20	170.8	205.2		1.1010	60.60	58.78	62.42	0.0400	0.2000
284.00	171.6	204.0	70.00	1.0592	61.94	59.39	64.29	0.0400	0.2000

Angles in axial direction and with respect to compressor axis

Fig.3.11: Blade Geometry (on blade sections parallel to axis)
 - BBC/SULZER 4-Stage Transonic Compressor -

Blade Row: Rotor Stage 3

Radius, mm	Axial Location Z Leading Edge, mm	Trailing Edge, mm	Chord Length, mm	Solidity	Stagger Angle, deg.	Blade Inlet Angle, deg.	Outlet Angle, deg.	max. Thickness to Chord	Leading Edge Radius % Chord
188.20	313.2	369.5	60.00	1.5729	20.71	33.77	7.65	0.0945	0.4723
198.92	314.9	367.8		1.4882	28.51	40.00	17.02	0.0800	0.4000
218.28	318.2	364.4		1.3552	39.57	47.60	31.54	0.0600	0.3600
236.54	316.3	360.6		1.2515	48.91	53.56	44.26	0.0520	0.2600
254.24	324.0	357.2		1.1644	56.32	57.43	55.22	0.0500	0.2500
271.62	326.2	354.4		1.0899	61.81	59.52	64.10	0.0500	0.2500
283.00	327.3	353.0	60.00	1.0460	64.45	60.00	68.90	0.0500	0.2500

Angles in axial direction and with respect to compressor axis

Fig. 3.12: Blade Geometry (on blade sections parallel to axis)
 - BBC/SULZER 4-Stage Transonic Compressor -

Blade Row: Rotor Stage 4

Radius, mm	Axial Location Z Leading Edge, mm	Trailing Edge, mm	Chord Length, mm	Solidity	Stagger Angle, deg.	Blade Outlet Angle, deg.	max. Thickness to Chord	Leading Edge Radius	
								% Chord	0.5668
449.6	496.3	50.00	1.5645						
451.0	494.8		1.4802						0.4800
453.8	492.0		1.3489	3	3	3	3	3	0.3600
456.3	489.2		1.2448	Stagger	Stagger	Stagger	Stagger	Stagger	0.3120
458.6	486.4		1.1581	AS	AS	AS	AS	AS	0.3000
460.2	484.2		1.0840						0.3000
461.2	482.8	50.00	1.0404						0.3000

Angles in axial direction and with respect to compressor axis

Fig. 3-13: Blade Geometry On blade sections parallel to axis

= BBC/SUILLIEZER 4-Stage Transonic Compressor -

Blade Row: Stator Stage 1

Radius, mm	Axial Location Z Leading Edge, mm	Trailing Edge, mm	Chord Length, mm	Solidity	Stagger Angle, deg.	Blade Inlet Angle, deg.	Outlet deg.	max. Thickness to Chord	Leading Edge Radius & Chord
149.00	79.2	123.3	54.04	1.6162	36.24	39.58	32.90	0.0462	0.2309
165.38	77.9	124.7	57.16	1.5402	36.50	40.78	32.24	0.0515	0.2575
197.06	75.3	127.5	63.54	1.4369	36.53	43.73	30.13	0.0630	0.3151
224.56	73.3	129.3	69.36	1.3764	36.12	44.54	27.70	0.0725	0.3625
249.56	71.0	133.1	74.68	1.3335	35.54	45.99	25.09	0.0812	0.4060
273.10	69.2	135.8	79.84	1.3028	34.95	47.39	22.51	0.0900	0.4499
284.00	68.2	136.8	82.26	1.2908	34.73	48.13	21.33	0.0932	0.4661

Angles in axial direction and with respect to compressor axis

Fig.3.14: Blade Geometry (on blade sections parallel to axis)

Blade Row: Stator Stage

Radius, mm	Axial Location Z Leading Edge, mm	Trailing Edge, mm	Chord Length, mm	Solidity	Stagger Angle, deg.	Blade Inlet Angle, deg.	Outlet Angle, deg.	max. Thickness to Chord	Leading Edge Radius % Chord	
									%	Chord
177.70	249.2	283.8	43.28	1.3232	37.66	45.43	29.89	0.0450	0.2250	
191.40	248.0	285.3	45.88	1.2971	37.35	45.42	29.29	0.0515	0.2576	
214.30	246.2	287.3	49.92	1.2605	36.59	45.49	27.69	0.0621	0.3105	
235.16	244.6	288.8	53.42	1.2292	35.87	45.75	25.99	0.0719	0.3598	
254.66	243.2	290.4	56.88	1.2086	35.53	46.58	24.48	0.0810	0.4051	
273.14	241.8	292.0	59.88	1.1863	34.62	46.93	22.32	0.0897	0.4486	
284.00	240.8	293.0	61.64	1.1745	33.96	47.16	20.76	0.0950	0.4750	

Angles in axial direction and with respect to compressor axis

Fig. 3-15: Blade Geometry (on blade sections parallel to axis)

הנִזְמָן (וְכֹעַד) בְּרֵבָבָיו

Blade Row: Stator Stage 3

Radius, mm	Axial Location Z Leading Edge, mm	Trailing Edge, mm	Chord Length, mm	Solidity	Stagger Angle, deg.	Blade Inlet Angle, deg.	Outlet Angle, deg.	max. Thickness to Chord	Leading Edge Radius % Chord
188.00	392.7	424.8	39.80	1.3477	37.53	46.68	28.38	0.0440	0.2201
198.98	392.2	425.3	41.14	1.3162	37.44	47.93	26.96	0.0500	0.2499
216.08	391.7	426.4	43.24	1.2739	37.32	49.32	25.32	0.0600	0.3000
232.70	390.9	427.8	45.30	1.2393	37.18	50.85	23.51	0.0696	0.3479
249.34	390.4	429.2	47.34	1.2087	36.93	52.47	21.39	0.0795	0.3975
266.16	389.7	430.1	49.50	1.1840	36.80	54.45	19.16	0.0898	0.4489
280.00	388.9	430.8	51.26	1.1655	36.89	56.37	17.41	0.0973	0.4865

Angles in axial direction and with respect to compressor axis

Fig. 3.16: Blade Geometry (on blade sections parallel to axis)
 - BBC/SULZER 4-Stage Transonic Compressor -

Blade Row: Stator Stage 4

Radius, mm	Axial Location Z Leading Edge, mm	Trailing Edge, mm	Chord Length, mm	Solidity	Stagger Angle, deg.	Inlet deg.	Outlet deg.	Blade max. Thickness to Chord	Leading Edge Radius & Chord
177.89	519.5	545.3	32.16	1.3811					0.2201
188.87	519.0	545.8	33.24	1.3445					0.2500
205.97	518.5	546.7	34.94	1.2959	3	3	3	3	0.2999
222.59	517.9	547.8	36.61	1.2565	Stage 3	Stage 3	Stage 3	Stage 3	0.3480
239.23	517.6	548.8	38.26	1.2218	Stage 3	Stage 3	Stage 3	Stage 3	0.3975
256.05	517.1	549.7	40.00	1.1934					0.4490
269.89	516.7	550.2	41.42	1.1724					0.4865

Angles in axial direction and with respect to compressor axis

Fig. 3.17: Blade Geometry (on blade sections parallel to axis)

Blade Row: Inlet Guide Vane

Radius, mm	Axial Location Z Leading Edge, mm	Trailing Edge, mm	Chord Length, mm	Solidity	Stagger Angle, deg.	Inlet Angle, deg.	Blade Outlet Angle, deg.	max. Thickness to Chord	Leading Edge Radius % Chord
120.00	-157.0	-88.0	70.0	1.6711	13.70	30.82	-3.42	0.12	
130.54	-157.0	-88.0		1.5362	14.20	31.32	-2.92		
178.00	-157.1	-87.6		1.1266	16.80	33.92	-0.32		
214.68	-157.1	-87.2		0.9341	18.85	35.97	1.73		
245.86	-157.1	-86.9		0.8156	20.60	37.72	3.48		
273.52	-157.2	-86.7		0.7332	22.20	39.32	5.08		
280.00	-157.3	-86.6	70.0	0.7162	22.50	39.62	5.38	0.12	

Angles in axial direction and with respect to compressor axis

Fig. 3-18. Bladed sections parallel to axis.

DRC/SWITZERLAND STATEMENT ON CONSTITUTIONAL PARTIES

Blade Row: Outlet Guide Vane

Radius, mm	Axial Location Z Leading Edge, mm	Trailing Edge, mm	Chord Length, mm	Solidity	Stagger Angle, deg.	Inlet Angle, deg.	Blade Outlet Angle, deg.	max. Thickness to Chord	Leading Edge Radius % Chord
188.0	603.2	642.5	40.00	1.2191	14.30	34.35	- 5.75	0.09	0.4500
199.66	603.2	642.5		1.1479	13.22	34.33	- 7.89		
209.40	602.9	642.5		1.0945	12.34	34.44	- 9.76		
219.00	602.7	642.5		1.0465	11.39	34.55	-11.77		
228.58	602.5	642.6		1.0026	10.36	34.72	-14.00		
248.40	602.3	642.7		0.9226	8.06	35.76	-19.64		
260.00	602.2	642.8	40.00	0.8815	6.65	36.75	-23.45	0.09	C.4500

Angles in axial direction and with respect to compressor axis

Fig. 3.19: Blade Geometry (on blade sections parallel to axis)

אנו מודים לך על תרומותך לארץ ישראל וברוך הוא קוראתך לארץ ישראל

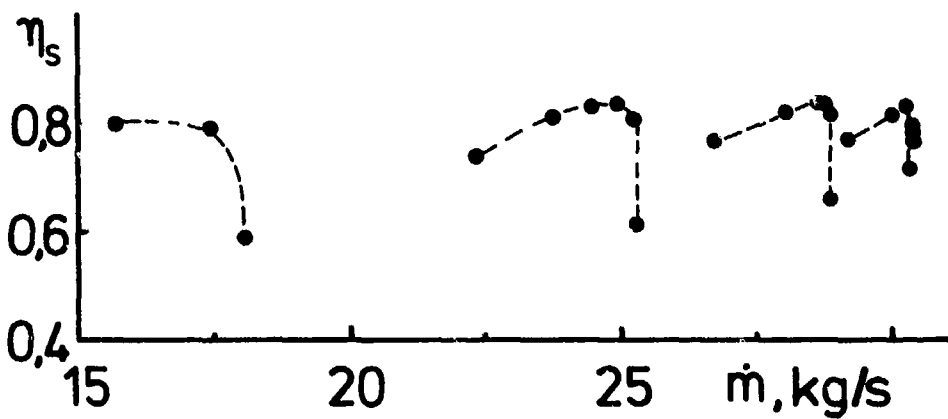
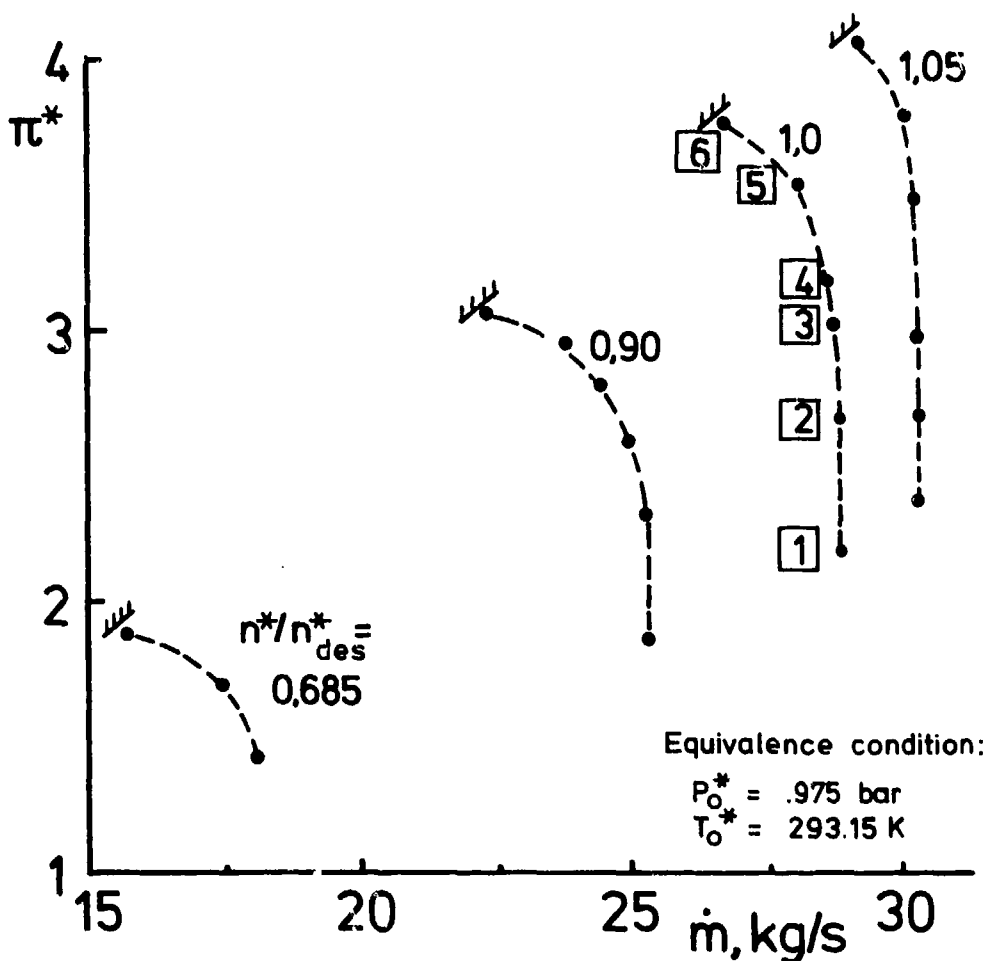


Fig. 3.20 : BBC/SULZER 4-Stage Transonic Compressor, Performance map

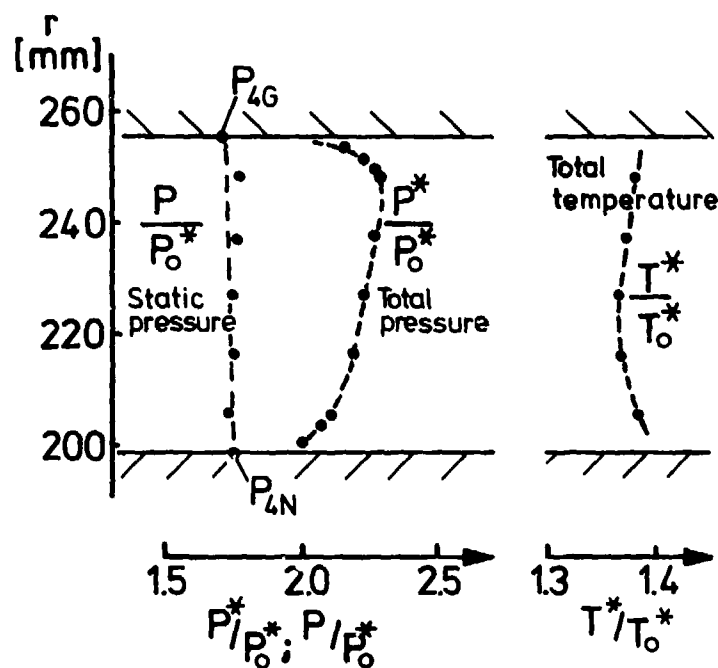


Fig. 3.21 : BBC/SULZER 4-Stage Transonic Compressor
Outlet Radial Distribution of Pressure and Temperature at a Pressure
Ratio of 2.12 (Point 1)

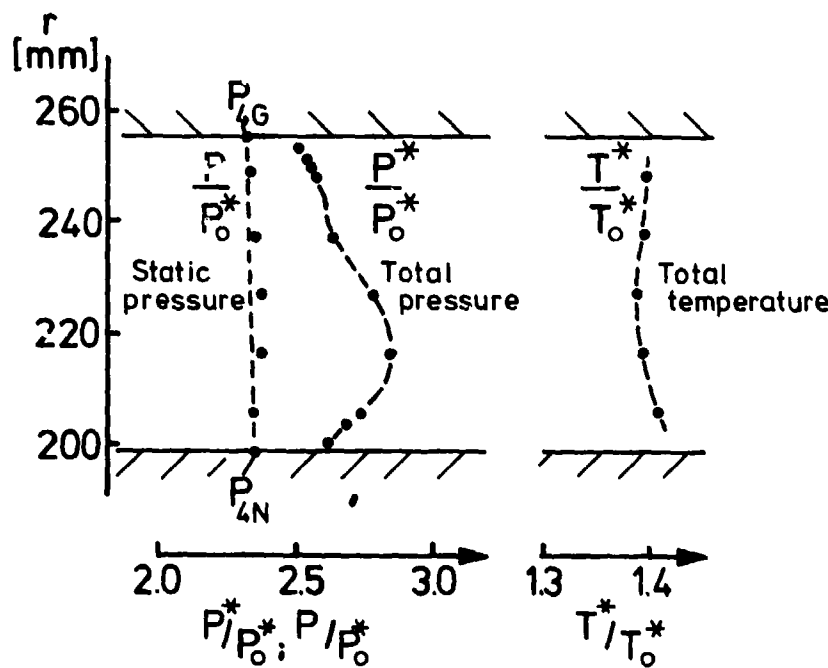


Fig. 3.22 : BBC/SULZER 4-Stage Transonic Compressor
Outlet Radial Distribution of Pressure and Temperature at a Pressure
Ratio of 2.68 (Point 2)

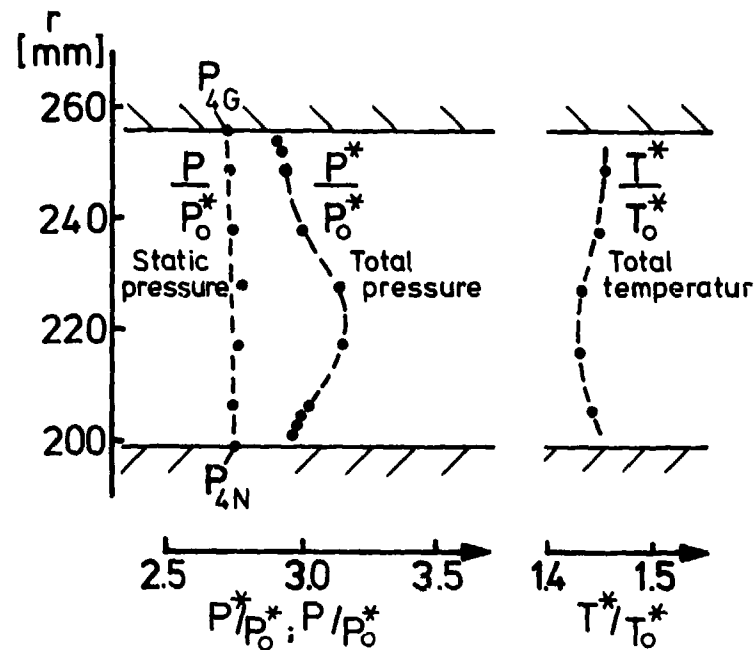


Fig. 3.23 : BBC/SULZER 4-Stage Transonic Compressor
Outlet Radial Distribution of Pressure and Temperature at a Pressure
Ratio of 3.02 (Point 3)

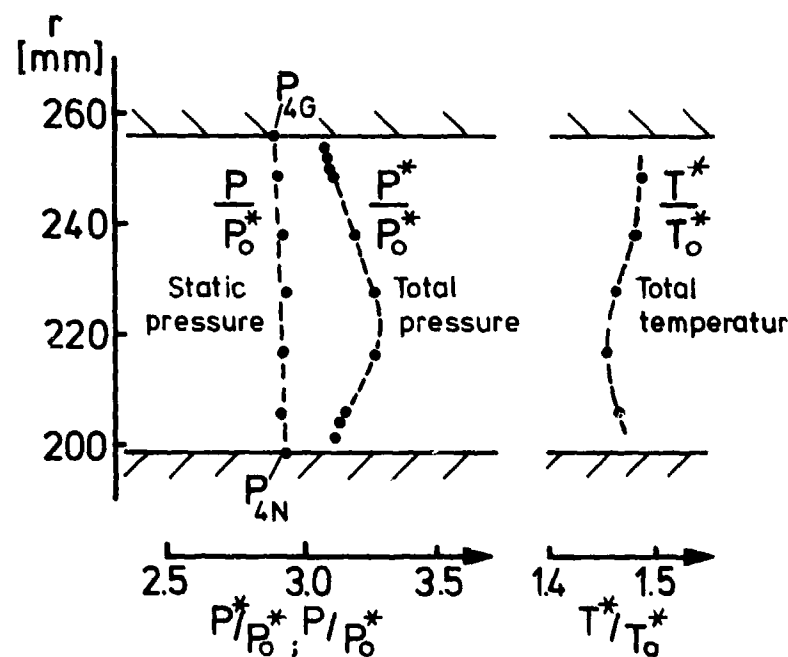


Fig. 3.24 : BBC/SULZER 4-Stage Transonic Compressor
Outlet Radial Distribution of Pressure and Temperature at a Pressure
Ratio of 3.19 (Point 4)

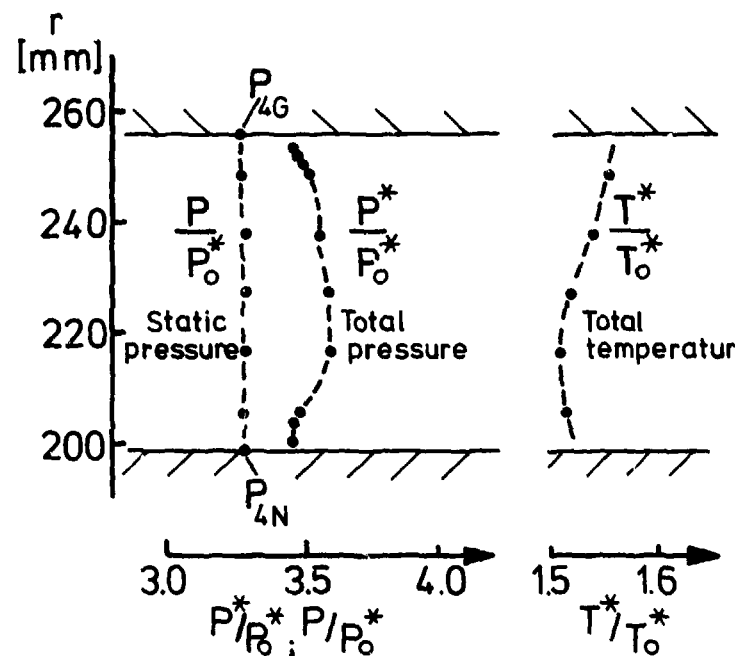


Fig. 3.25 : BBC/SULZER 4-Stage Transonic Compressor
Outlet Radial Distribution of Pressure and Temperature at a Pressure
Ratio of 3.54 (Point 5)

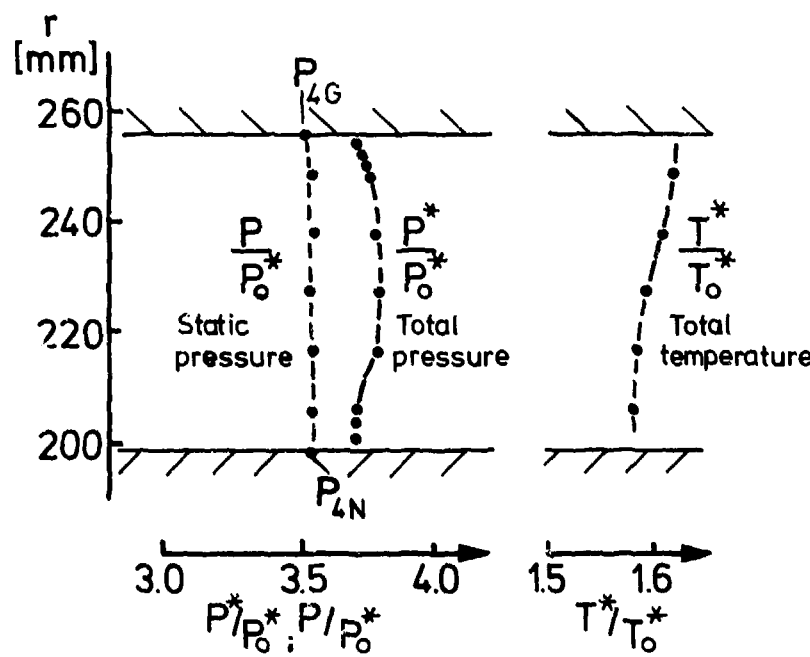


Fig. 3.26 : BBC/SULZER 4-Stage Transonic Compressor
Outlet Radial Distribution of Pressure and Temperature at a Pressure
Ratio of 3.78 (Point 6)

II.4. Results of Calculations

Two types of calculations were performed by various participants, each using his own method for through-flow calculations and blade-to-blade calculations. An important aspect of the Working Group's task was to demonstrate that the use of systematic blade-to-blade calculations could provide a support for the confirmation of an existing correlation or the development of a new one. It is indeed believed that the present development and state of the numerical tools available in order to compute complex flow structures, should be used more and more extensively in order to develop a deeper understanding of the flow mechanism of loss production and of turning.

The possibilities for blade-to-blade calculations, with inclusion of radius variation and stream-tube contraction and coupled to a boundary layer calculation could lead to serious improvements in the knowledge of the influence of these parameters, if some systematic series of such calculations were performed. That this is indeed a clear possibility is illustrated by Koch and Smith's correlation for design point, derived through systematic series of boundary layer calculations. Some limitations still exist however, due to the difficulties in the computation of separated flow regions. Due to time and cost limitation only a limited analysis was performed within the present work.

Since the central aerodynamic variable in loss correlations is the diffusion factor, blade-to-blade calculations were used on two blade sections in order to compare various existing formulas with the values obtained from the blade-to-blade flow distribution and from experimental data. This is discussed in the second part of this chapter.

The first part discusses results of through-flow calculations as obtained by the various participants who accepted to perform some calculations. Most of the calculations were done with the authors own correlation system and in several of these cases, complete informations could not be disclosed. Particular mention has to be made for the results provided by E. Benvenuti from Nuovo Pignone (Italy) who presented results (for the four stage compressor) with three different approaches, using the same code.

This is a very important aspect in the meaningful assessment of differences between correlations since their interaction with the through-flow computation method is strongly non-linear and can have a large influence on the results obtained. It is a well known fact that, even with the same correlation, different through-flow programs will lead to non-identical results on overall performance, see [1]. These aspects are also noticed by R. Novak in a communication to the Working Group. As R. Novak states :

" In using my program recently I uncovered some problems which, I believe, will be present with any of the currently used techniques. They also have bearing on the reliability of published cascade data, particularly for high Mach number cascades derived from running stage tests.

Most, if not all, off-design prediction schemes work with stations just at the L.E. and T.E. of blade rows. Streamline curvatures are iteratively computed from radii progressively established using these two stations. The blades, however, do have a finite thickness. If a station is included at a point near the maximum thickness locus, there can be a measurable difference in curvature computed at the L.E. and T.E. stations. The concave upward curvature which is generated by the thickness at this station raises the outer diameter through flow velocity, and lowers that at the inner diameter as compared with computations without the internal station.

My checks so far have indicated that a single station near the maximum thickness point traps the main effect, and that the intrablade blockage term is the most important. More than one intrablade station does not significantly add to the picture (in regard, most importantly, to the effect on L.E. and T.E. incidence and deviation computations); the introduction of other terms, such as blade lean entropy gradient, are of secondary importance.

The problem shows up most clearly for high-through-flow configurations where the velocity-squared coefficient on the curvature term becomes large.

I made some checks recently, using published data on a P&W 1600 ft/sec stage (NASA CR-72694). Using first, the measured rotor discharge pressures and temperatures, and no intrablade stations, I was able to duplicate the P&W vector diagrams. The incidence angle computed at the tip was, for example, seven degrees (this should have been a tip-off, since the tip relative Mach number was in the range of 1.6). A similar computation, using the same measured pressures and temperatures, but with an intrablade station with blockage, resulted in a tip incidence of three degrees. The tip incidence was lower and the hub incidence higher, as would be expected.

Since the blade was an MCA with small leading edge camber, and had a thin leading edge, the three degrees number is considerably more realistic than the seven degree.

The above has two immediate consequences in regard to compressor off-design prediction : for fan stages (high Mach number) and multistage inlet stages at least one intrablade station must be included; nearly everyone have reduced stage test data to effective incidence/loss/turning angle cascade data reduction program using just leading and trailing edge stations. To the extend that I am correct above, this says that all data must be re-investigated with intrablade stations."

Some caution is therefore needed in the discussion of the results of through flow calculation in order to be able to make distinction between the various influences on the overall results. In particular, the influence of the intrablade chordwise distribution of losses and angular momentum and the inclusion of blade wake blockage can be non-negligible on the overall pressure ratio prediction. Although very important, a detailed discussion of those points was considered outside the scope of the Working Group.

The second part of this chapter contains a discussion of the accuracy and degree of validity of diffusion factors and their relation to the loss coefficient.

Based on two test cases, NACA-65 blades and a DCA blade, of 18° camber, diffusion factors as calculated by the velocity ratio obtained from a blade-to-blade subsonic calculation are compared with the values obtained from various correlations and from experiments.

It appears, within the scope of the limited amount of calculations performed, that the potential flow calculations give an acceptable prediction of diffusion factors.

However, large discrepancies appear when the various loss relations are compared to the experimental data.

REFERENCE

- [1] W.R. DAVIS, D. MILLAR, "A Comparision of the Matrix and Streamline Curvature Methods of Axial Flow Turbomachinery Analysis from a User's Point of view", ASME Paper 74-WA/GT-4, November 1974

II.4.1. The Through Flow Calculations

Calculations of the three test cases were performed by various authors belonging to industrial or research organisations. Their contribution is particularly acknowledged and added a great deal to the progress of the work undertaken. We did benefit from contributions from NASA Lewis Center, Dr. Novak (G.E., USA), D. Bohm (KNU, Germany), Prof. Macchi (Italy), Dr. E. Benvenuti (Nuovo Pignone, Italy) and Ch. Hirach (Brussels, Belgium). These authors will be referred to respectively by the letters A, B, C, D, E and F.

Four Stage Transonic Compressor

Results for this test case were provided with several correlations of which we have limited knowledge in some of the cases.

The basic program and prediction system developed by R. Novak, based on [1] is used by E. Benvenuti and KNU. However, no information was provided for the values of the adjustable coefficients in this correlation.

No information is available on the correlations of the code used by NASA Lewis.

Fig. II.4.1.1. presents a comparison between the results obtained by A, B, E : the results of KNU (C) being practically identical to these of R. NOVAK (B). Dr Benvenuti's calculation contain some in-house modifications of the basic correlation (which is the one used by B). It is quite clear that non-negligible differences appear, but this information is to be considered as an indication of the considerable differences existing between different methods. The results of E in this figures are obtained with the correlation of Koch and Smith [9] for the design point and maintaining the original off-design contribution.

The Fig. II.4.1.2. to 5. present under graphical forms the differences between the correlations of Smith and Novak as obtained by E for the design point of this 4 stage compressor. It should be kept in mind that the curves indicated "Smith" contain also off-design contributions.

Clearly, the minimum losses, as predicted by Koch and Smith are higher than the minimum losses used by R. Novak for rotating blade rows. Also the way the various contribution, Mach number effects, tip losses (which are not included in Smith's approach where a correlation for the efficiency drop due to the end wall boundary layers is used) are accounted for is quite different. For stators, the Smith correlation gives appreciable lower values for the loss coefficients. Unfortunately, no experimental data are available to make a clear decision in favor of one of the other approach.

It is to be noted in particular, that Smith's correlation for the design minimum losses show a stronger Mach number influence and have a shock loss contribution which is lower than the one predicted by the model of Lewis and Hartman applied in Novak's correlation.

However, it is important to note that the final overall performance, predicted by the two methods, are very close, especially in view of the large differences in the detailed loss distributions as they are produced by the two sets of correlations. This raises the question of the level of accuracy which is required in the evaluation of losses and deviation, in order to predict an overall performance map, and of the definition of the most sensitive parameters. Is it the deviation (as in the case for turbines), or a loss gradient, or another property ?

The results obtained by E. Macchi (D) are derived with a program based on Vavra's [2] technique of solution for axisymmetric and steady flow in axial turbomachines; it solves the complete radial equilibrium equation - accounting for enthalpy and entropy gradients and streamline curvature effects - in a specified number of stations ahead of and after the blade rows. An orthogonal curvilinear system of coordinates having the meridional coordinates coincident with the generatrices of the flow stream surfaces is used in the solution. Iterative methods are used both for the numerical solution of radial equilibrium and continuity equation in single stations and for streamlines location and curvatures over the whole machine.

Incidence, deviation and losses produced by the blade rows at "reference" conditions are computed according to NASA rules [3] the only difference being the assumption that the streamline radial position has no influence on them (i.e., in making use of figs. 201, 202, 203 of [3], the curves given for 50 % of blade height are assumed to be valid for all streamlines).

Off-references deviations and losses are computed according to the correlations proposed by Creveling and Carmody [4] as a function of incidence angle and inlet relative Mach number. No AVDR influence on losses is considered; the simple Pollard & Gostelow [5] correlation is used for deviation. A modified version of the Mellor et al. [6] correlation is used; shock losses are accounted for also at high subsonic values of the velocity ahead of the blade row.

The original version of Mellor's theory on casing boundary layer described in [7] is incorporated in the computer program.

The Mellor equations are integrated across every blade row; this calculation is carried out every time the continuity equation is solved. The displacement thicknesses are

accounted for in locating streamlines, while all other pertinent boundary layer parameters yield the enthalpy and entropy increase caused by secondary losses.

The losses are then mass-averaged, i.e., uniformly distributed in the whole section. The following values of the four "arbitrary" coefficients in Mellor's theory are assumed, for both hub and tip of rotor and stator blades :

$$C_f = 0.003 \quad \epsilon = 0 \quad K = 0.65 \quad H = 1.4$$

The Reynolds number influence on C_f is accounted for by an exponential rule : Flow angle changes due to secondary effects are not considered.

The comparison of the computed overall performance with experiments is represented in Fig. II.1.6. While a good agreement is found at the design point, large differences are found at off-design, mainly at low flow rates. The differences of calculated and experimental flow rates for the same pressure ratio vary from about $\pm 1\%$ at choking, and at design point, up to as high as 10% near the surge line. As expected the differences are larger at speeds different from the design one.

A good agreement between calculations and experiments is found at nominal speed and at 90% , while about 5% error is obtained at low speed, where the calculation is optimistic.

The computed end-wall boundary layer thicknesses are represented in Fig. II.4.1.7. It can be seen that, as the design point, the predicted values are close to the suggested ones. For this reason, it was thought unnecessary to repeat the calculation with the suggested values of blockage and a large increase of the blockage factor (more than 20%) near surge can be observed.

Fig. II.4.8 to 10 show a comparative calculation by author E between three correlations : their own basic correlation, the Smith and Koch correlation for the design point with the original off-design calculation including Smith's EWBEL efficiency corrections, and a third approach including iteratively with the through glow, Hirsch and De Ruyck's EWBEL calculation method [8].

This result is particularly interesting in that it has been obtained with the same code and the same set of correlations with, in the third case, the inclusion of the end-wall boundary calculations. The trend of these results clearly supports an approach based on the end-wall boundary layer representation of secondary flow effects on overall performance.

The Two Stage Compressor

This test case has been calculated by NASA (author A). Author A ran their calculations with in-house correlations, of which the following elements have been communicated.

The total loss coefficient is the sum of a number of components. These include a profile loss, \bar{w} , plus a shock loss, \bar{w}_s , plus a secondary flow loss, \bar{w}_{sec} , plus a part span damper loss, \bar{w}_{psd} . The profile loss component, \bar{w}_f , currently is basically a function of D-factor but has corrections for axial-velocity ratio and incidence angle. The shock loss component, \bar{w}_s , basically uses the flow model developed in the reference "Shock Losses in Transonic Compressor Blade Rows" by Miller, Lewis and Hartmann (see ASME J. Eng. Power, July 1961). However the shock losses computed from the above model are reduced as a function of the inlet Mach number. The part span damper loss component, \bar{w}_{psd} , follows the flow model in the reference "Off-Design Correlations for Losses Due to Part-Span Dampers on Transonic Rotors" by Roberts, Crouse and Sandercock, NASA TP 1963, July 1980.

The deviation angle prediction method is basically an extension of Carter's Rule. Several of these extensions are noted in the paper for the AGARD WG-12 "Axial Compressor Performance Prediction Deviation/Turning Angle Correlations" by George K. Serovy. One extension makes the variable M a function of both setting angle and location of maximum camber as indicated by the equation on pg. 22. The second extension uses an equivalent circulation fluid turning angle as discussed in Appendix E. This accounts for the radius changes and the range of axial velocity ratio which occurs across the real compressor stages. Finally, the code increases the deviation angle an arbitrary amount when the D-factor is above a value near 0.7. For off-design operation the deviation angle prediction method also applies a correction which is a function of incidence angle and flow Mach number. It is also desired to add a correction term that accounts for the secondary flow effects. The results obtained for the overall performance are shown on Fig. II.4.11. The shifting of the design speed curve towards higher values than design has been attributed by the authors of the experiments to a locally uncambering (opening) of the blade leading edge in the tip region of close to 1.2° more than had been allowed for in the original, beam-analysis design. According to the authors, this off-design uncambering may have allowed the fan to overflow and explain also the reduced stall margin. Author A also produced the performance predictions separately for each blade row and stage (Figs. II.4.1.12 and 13). These results are a clear indication that even when overall performance is predicted in an acceptable way, blade row performance can be poor, and that global compensations of errors can occur.

This appears to be the case at part speed, where the correlations do not appear to be well adapted in this low Mach number region. Better results are obtained at design speed, as can be seen on Figs. II.4.1.14 and 15 showing the first stage radial distributions of the main variables.

Single Stage Compressor

This test case is extensively documented and has been calculated by Hirsch (author F). The correlations used by author E are based on Carter's rule for deviations, following the method of SP 36 for the design deviations and incidences. Corrections for Mach number and axial velocity ratio are introduced as well as off-design deviations, following the method outlined in [1] by Novak. The profile and shock losses are estimated following the approach by Koch and Smith [9] and an off-design contribution is calculated based on the estimation of incidence working ranges for stall and choking. A parabolic variation with incidence for off-design losses is then considered with respect to the corresponding range.

All secondary effects are taken into account by an end-wall boundary layer approach following [8] in an iterative calculation with the through-flow computation.

The predicted overall performance curve is shown in Fig. II.4.1.16 and radial transverses of total pressure (Fig. II.4.1.17), losses (Fig. II.4.1.18), axial Mach number (Fig. II.4.1.19) are shown at two mass flows for the design speed curve.

Although the overall performance curve is reasonably well predicted, clearly detailed flow distributions, although acceptable, are not as well predicted.

The full distributions of Mach number and flow angles (Figs. II.4.1.20 and 21) as obtained through the end-wall boundary layer interaction, show the prediction of the high skewing of the flow in the wall regions, and the boundary layer decrease of velocity. The influence of the EWBL is also to be seen on Fig. II.4.1.17, where the efficiency obtained only on basis of the profile losses is disclosed.

The predicted blockage factors compared with the experimental values, give the following result :

	<u>Exp.</u>	<u>Calc. (2 % blockage at inlet)</u>
Inlet rotor	2.55	1.82
Outlet rotor	4.10	3.95
Outlet stator	5.1	5.45

It appears clearly that the end-wall boundary layer calculation increases strongly the prediction capability of through-flow calculations.

REFERENCES

- [1] R.A. NOVAK, "Flow Field and Performance Map Computation for Axial-Flow Compressor and Turbines" in Modern Prediction Methods for Turbomachine Performance, AGARD-LS-83-1976
- [2] H.H. VAVRA, "Aero-Thermodynamics and Flow on Turbomachines", John Wiley & Sons, Inc. New York 1960
- [3] The members of the Staff of Lewis Research Center, Cleveland, Ohio, "Aerodynamic Design of Axial-Flow Compressors", NASA-SP-336, 1965
- [4] H.F. CREVELING, R.H. CARMODY, "Computer Program for Calculating Off-Design Performance of Multistage Axial-Flow Compressors", NASA CR
- [5] D. POLLARD, P. GOSTELOW, "Some Experiments at Low Speed on Compressor Cascades", J. Eng. Power, (1967), 427-436
- [6] G.R. MILLER, G.W. LEWIS, M.J. HARTMAN, "Shock Losses in Transonic Compressor Blade Rows", J. Eng. Power, July 1961, 235-242
- [7] G.L. MELLOR, "Secondary Flows in Turbomachines", Von Karman Institute for Fluid Dynamics Lecture Series", Jan. 1975
- [8] J. DE RUYCK, Ch. HIRSCH, "Investigations of an Axial Compressor End-Wall Boundary Layer Prediction Method", ASME Paper 80-GT-53 (1980)
- [9] C.C. KOCH, L.H. SMITH, "Loss Sources and Magnitudes in Axial Flow Compressors", Trans. ASME, J. Eng. for Power, July 1976, 411-424

+ Experimental points

Calculated points:

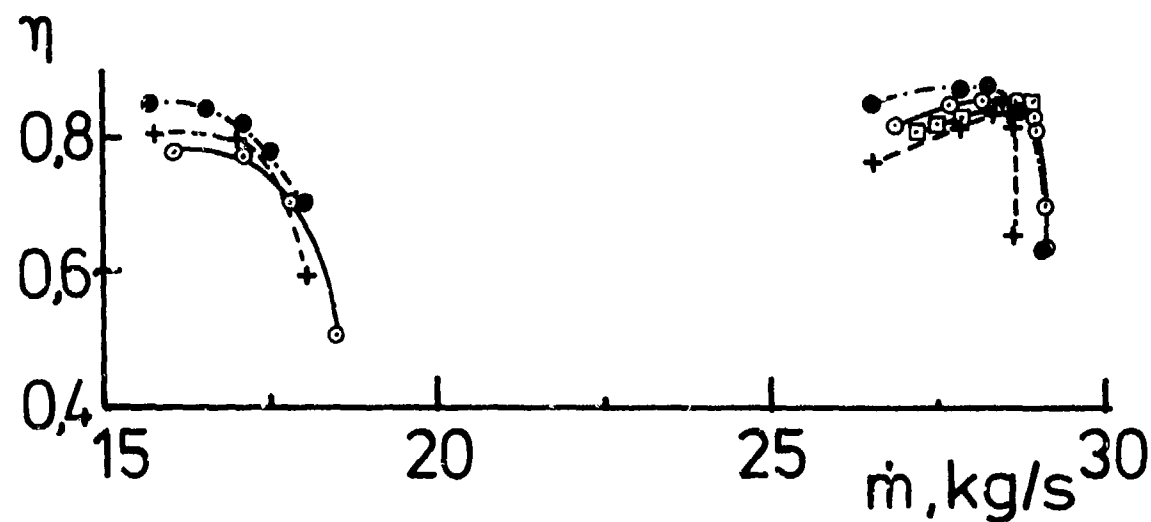
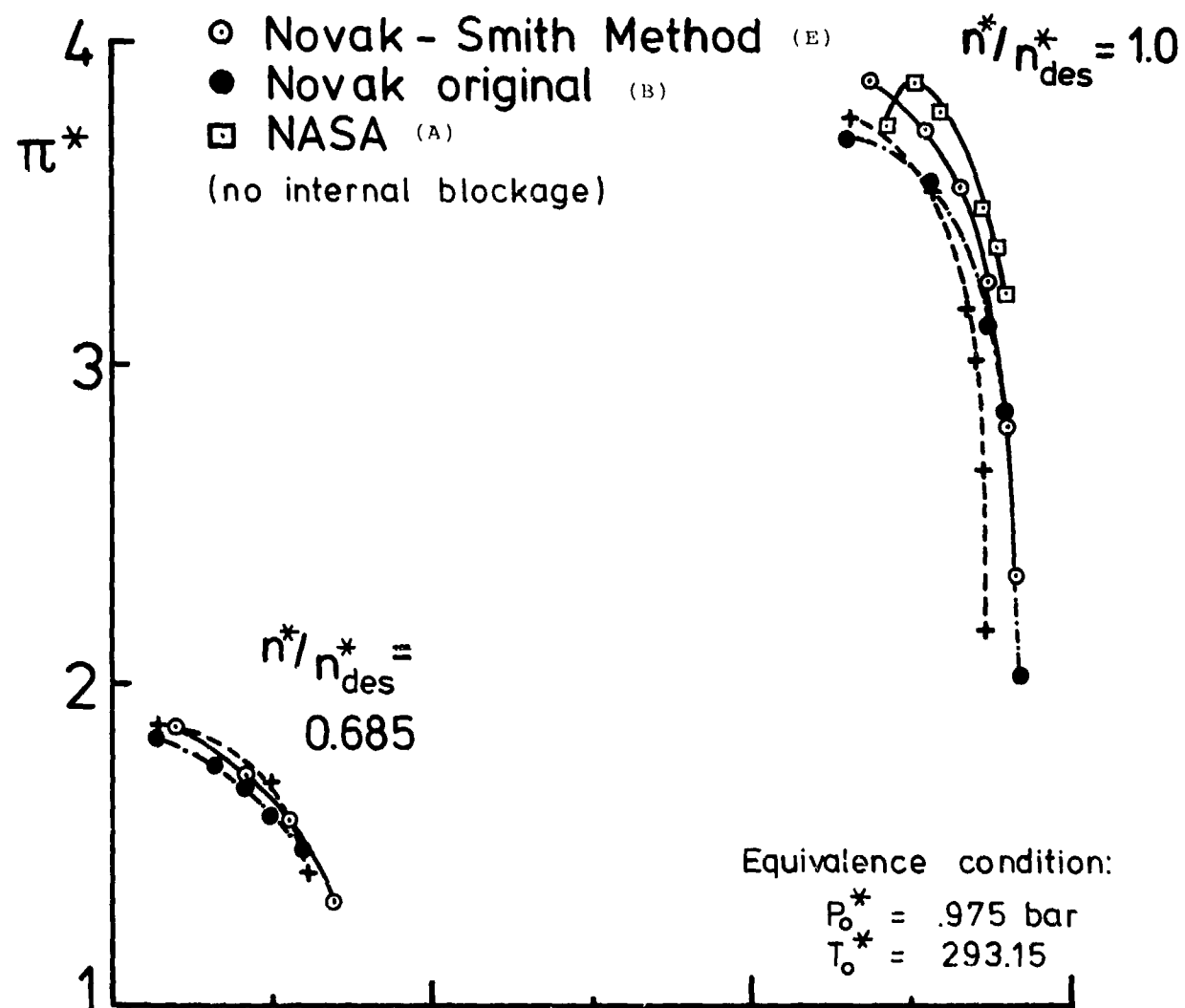


Fig. II.4.1.1 : Four Stage Transonic Compressor
Comparison of Calculated and Experimental Results, Authors A,B,E

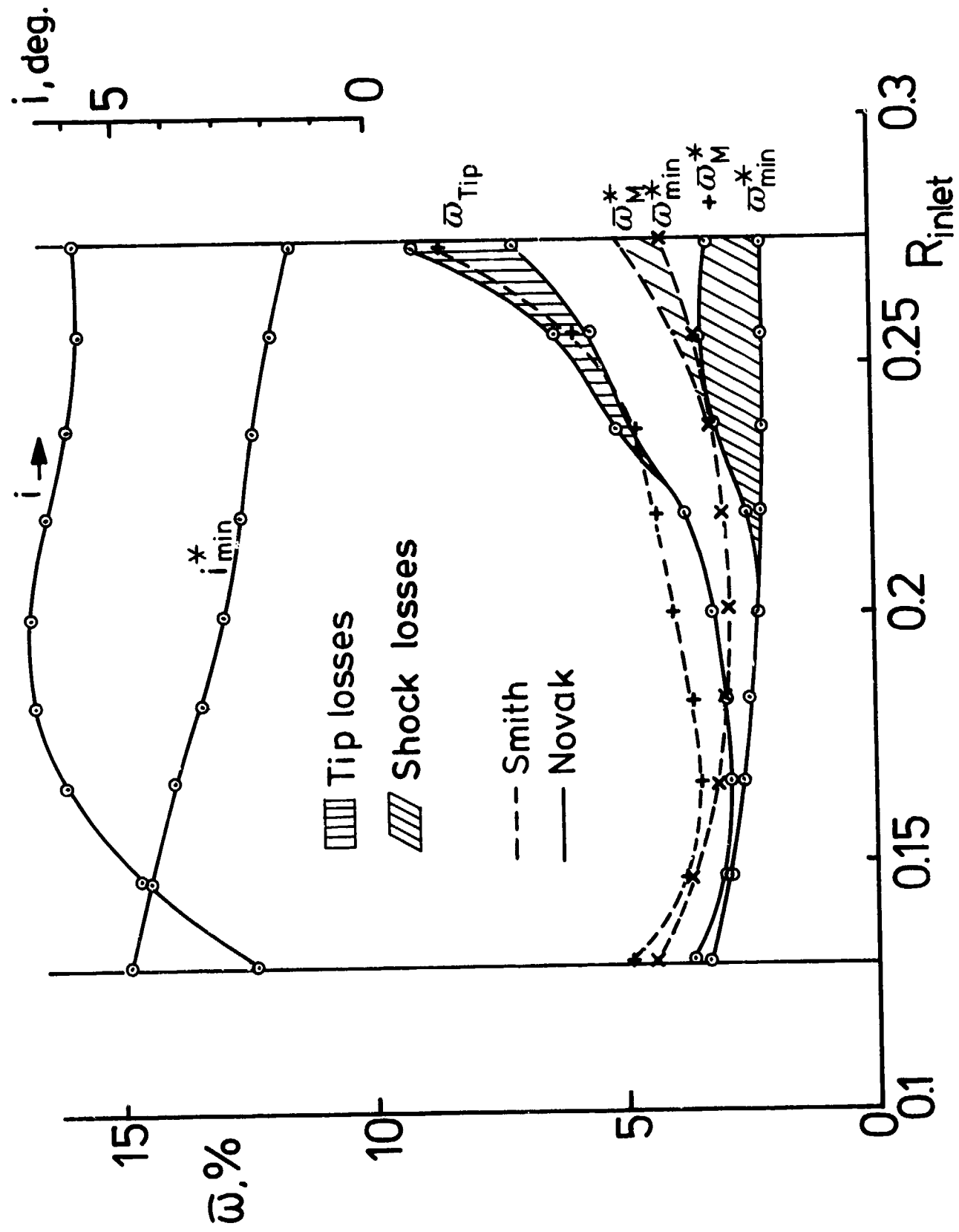


Fig. II.4.1.2 : Four Stage Transonic Compressor
Radial Distribution of Losses and Incidences for the Novak and
Smith Correlations - First Stage Rotor - Author E

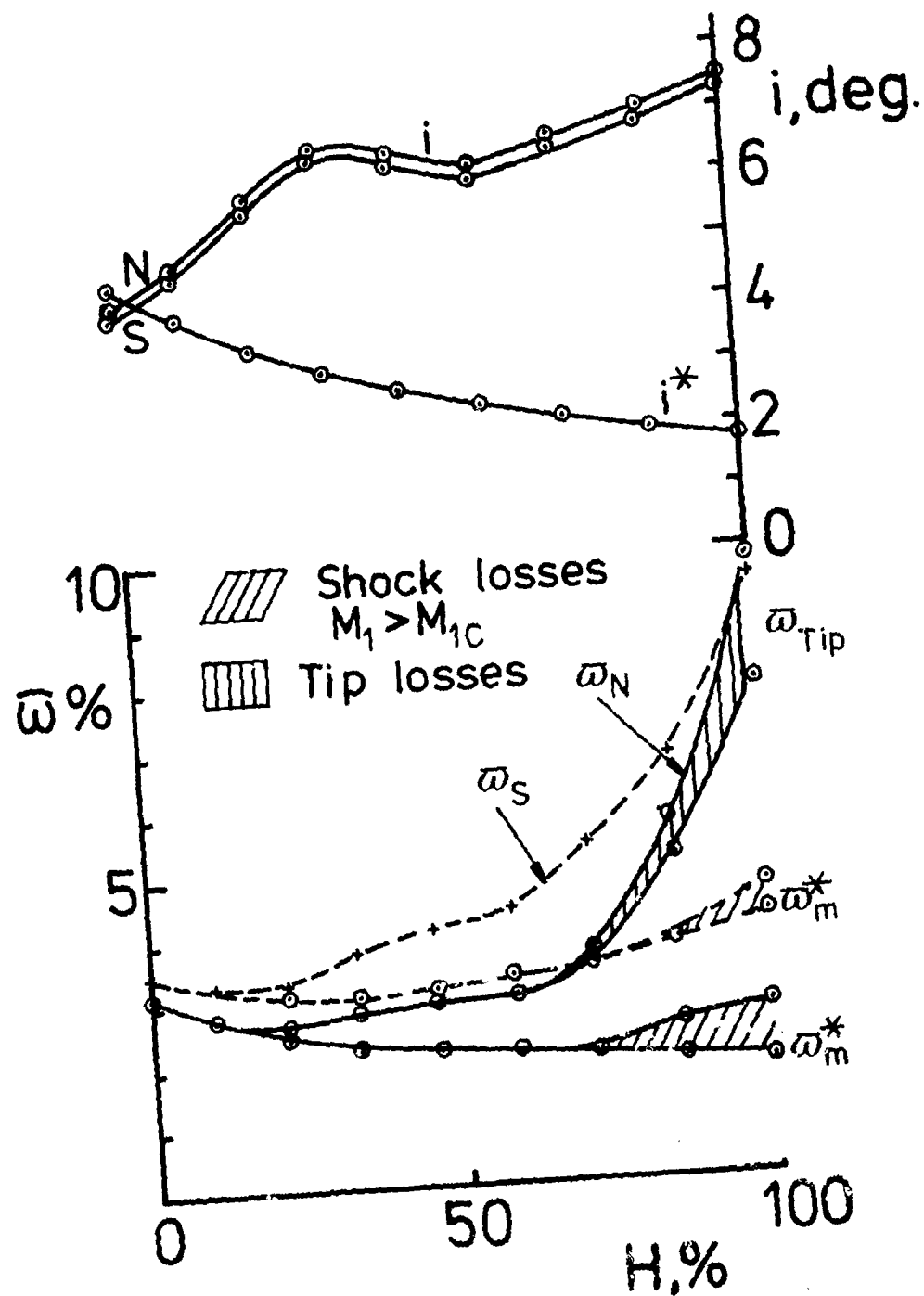


Fig. II.4.1.3 : Four Stage Transonic Compressor
Radial Distribution of Losses and Incidences for the Novak and
Smith Correlations - Second Stage Rotor - Author h

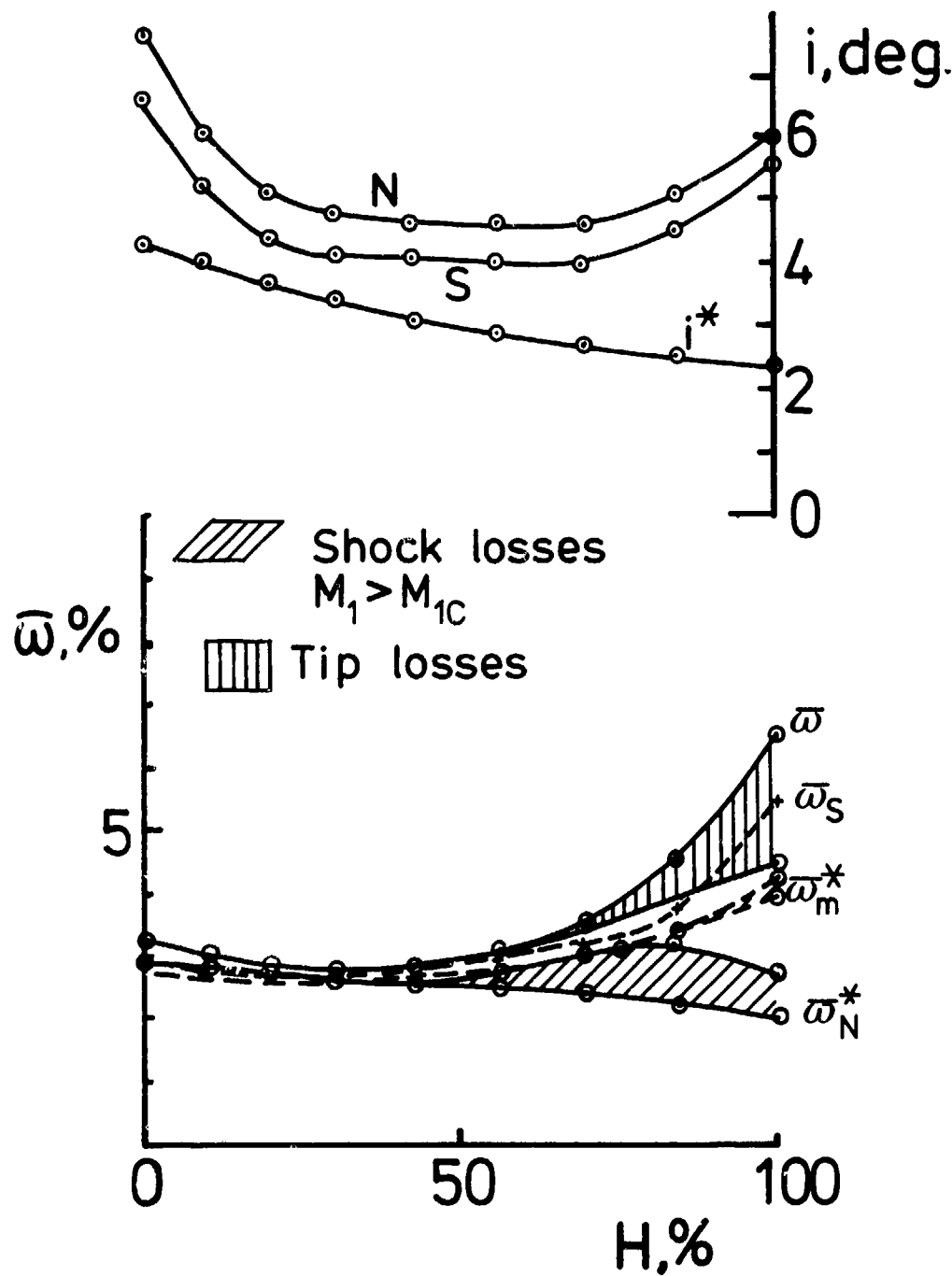


Fig. II.4.1.4 : Four Stage Transonic Compressor
Radial Distribution of Losses and Incidences for the Novak and
Smith Correlations - Third Stage Rotor - Author E

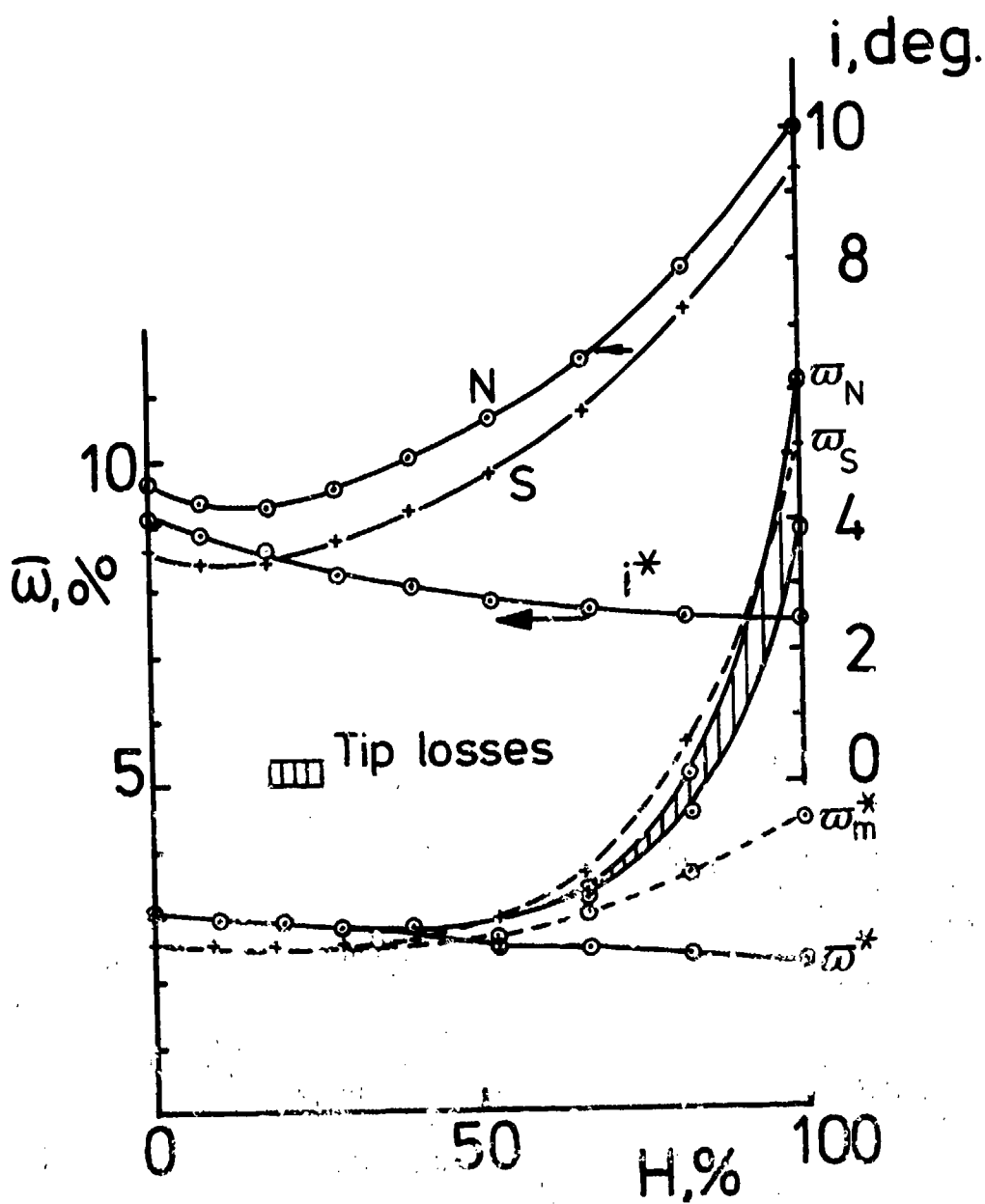


Fig. 11.1.4-5 : Four Stage Transonic Compressor
Radial Distribution of Losses and Incidences for the Novak and
Smith Correlations - Fourth Stage Rotor - Airflow: E

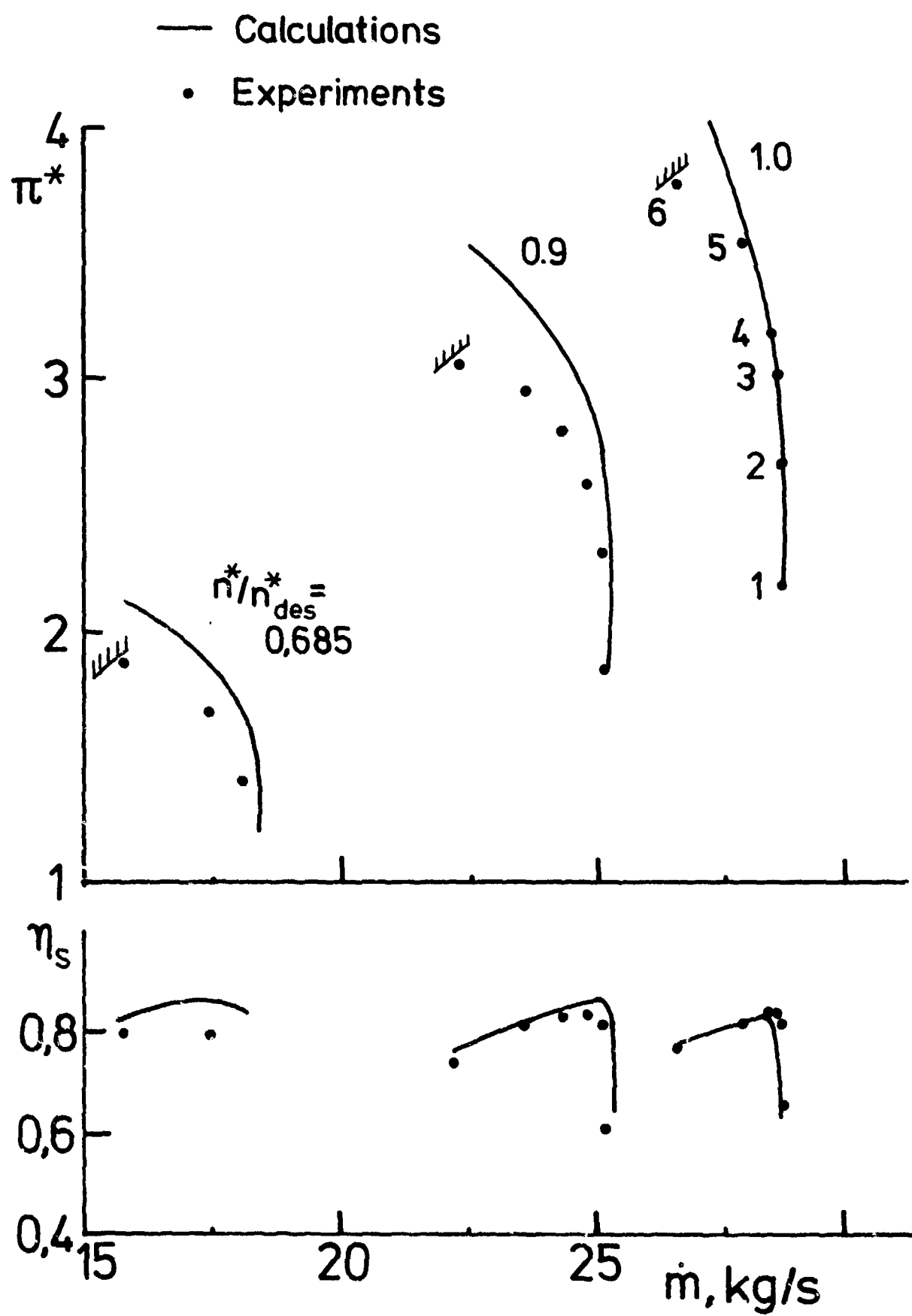


Fig. II.4.1.6 : Four Stage Transonic Compressor Performance Map Prediction - Author D

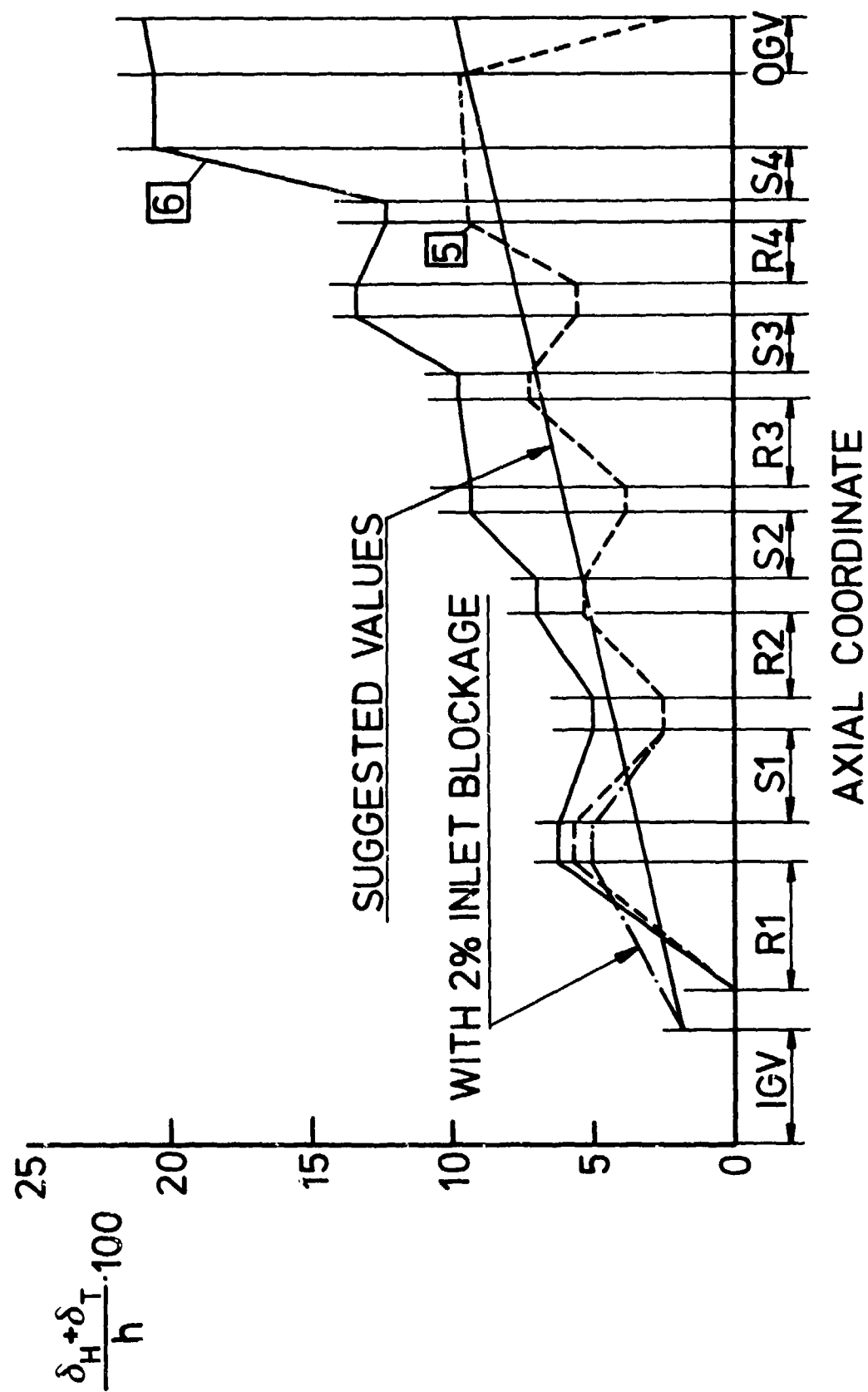


Fig. II.4.1.7 , Four Stage Transonic Compressor
End-Wall Boundary Layer Precision - Author D

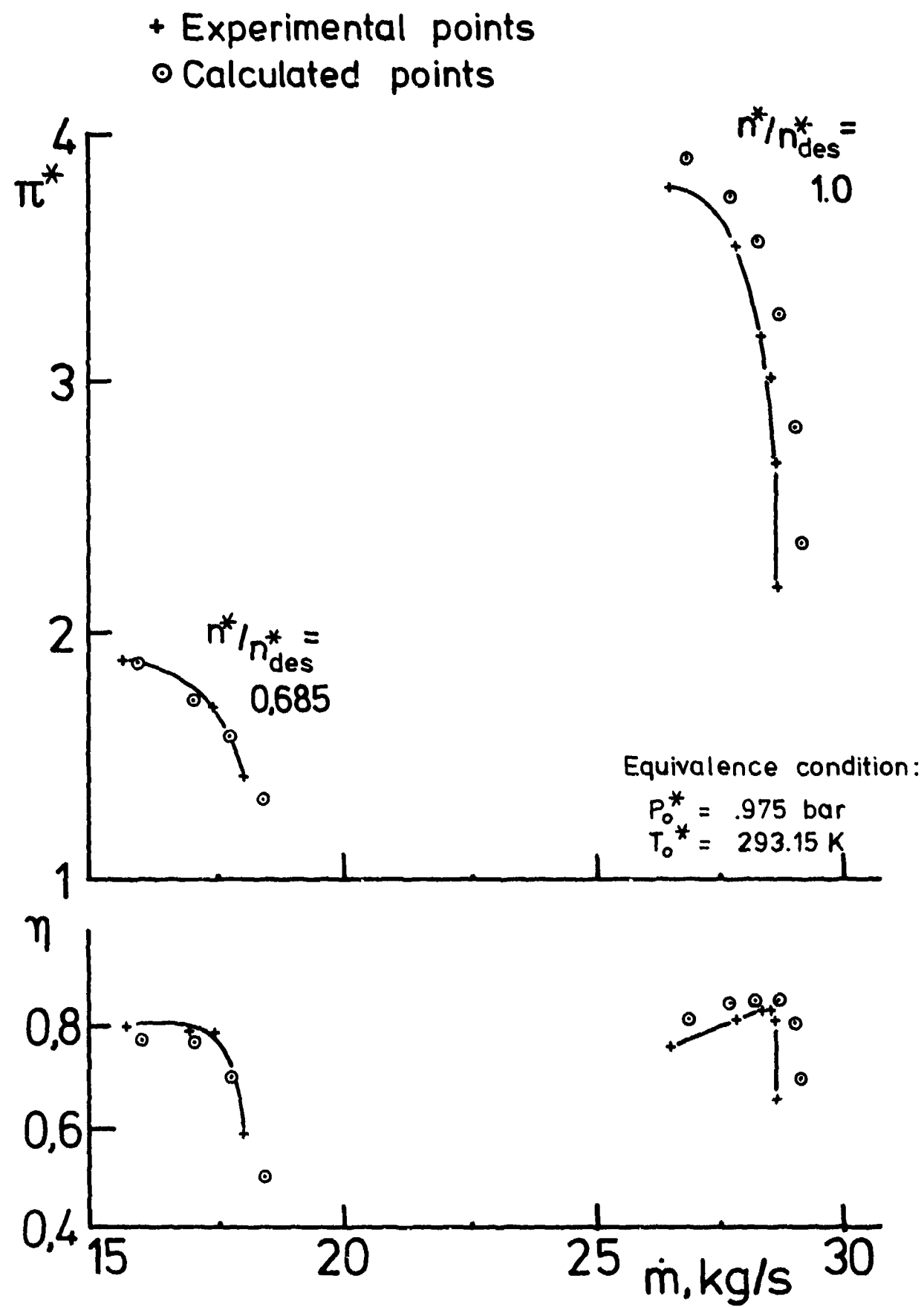


Fig. II.4.1.8 : Four Stage Transonic Compressor Performance Map Prediction - Original Correlation Set - Author E

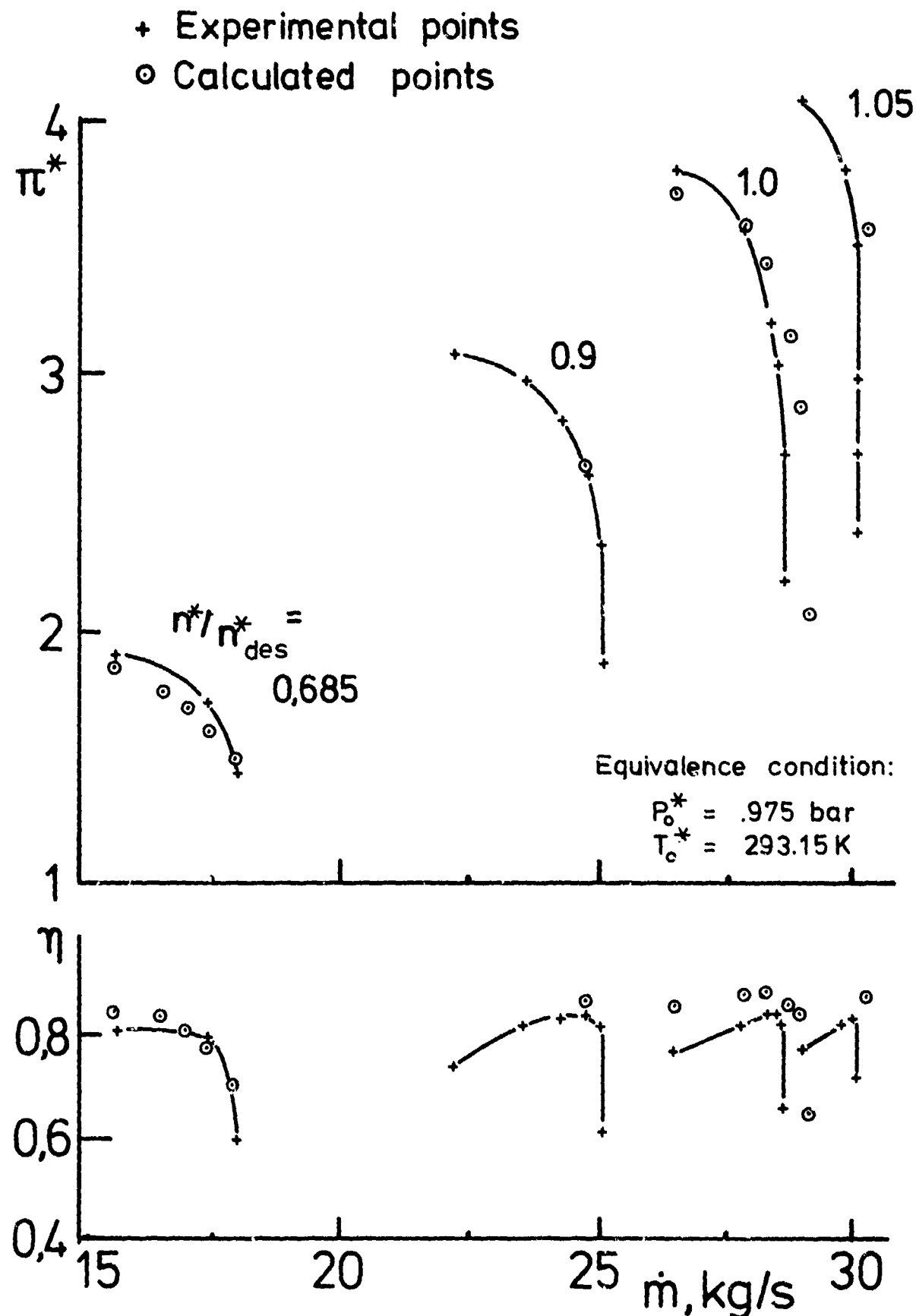


Fig. II.4.1.9 : Four Stage Transonic Compressor
Performance Map Prediction - Original Correlation and End-Wall
Boundary Layer Correlation of C.H. Smith - Author E

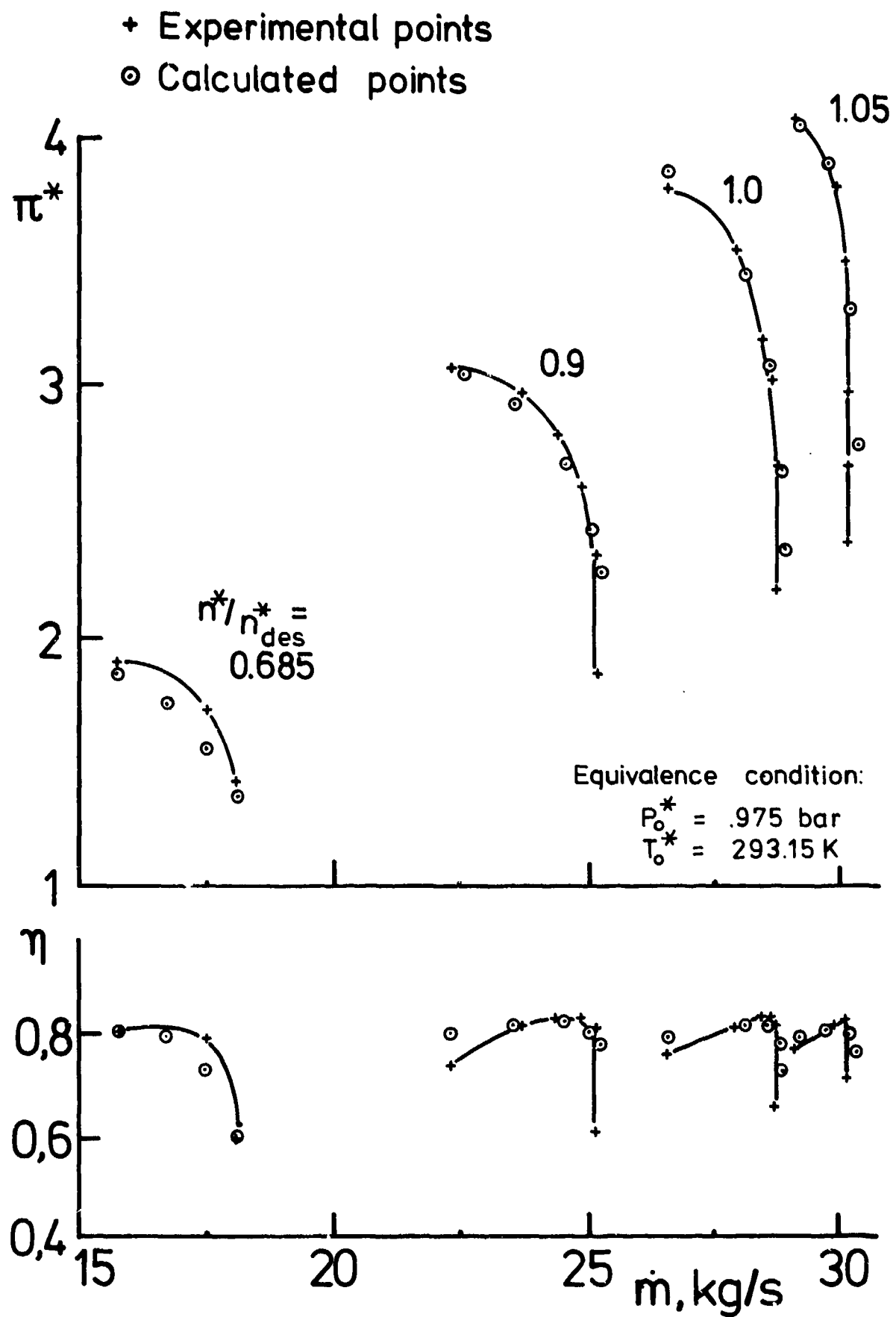


Fig. II.4.1.10 : Four Stage Transonic Compressor
Performance Map Prediction - Original Correlation with Hirsch's
End-Wall Boundary Layer method - Author E

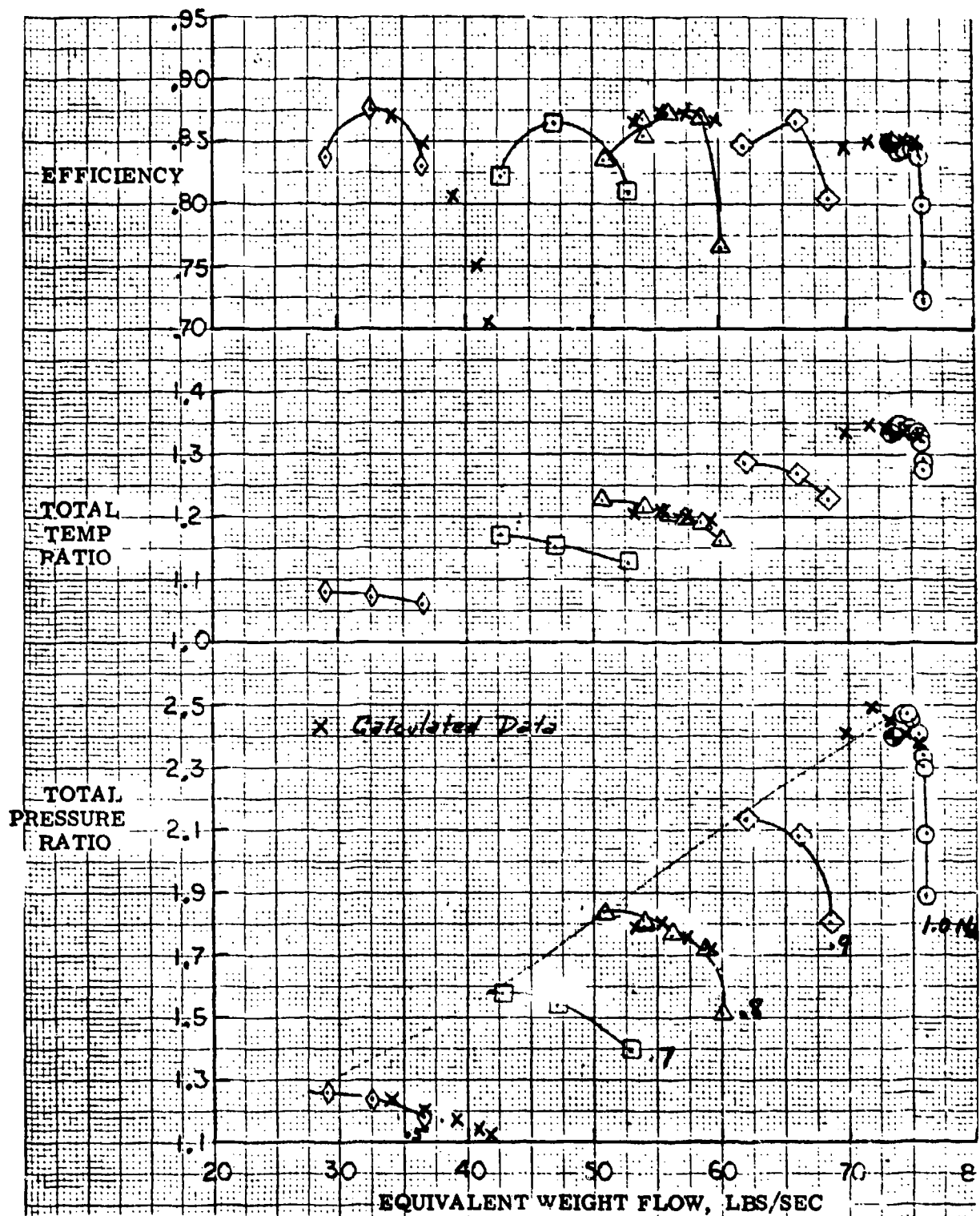


Fig. II.4.1.11 : Two Stage Compressor
Performance Map Prediction - Author A
Open Symbols are experimental data

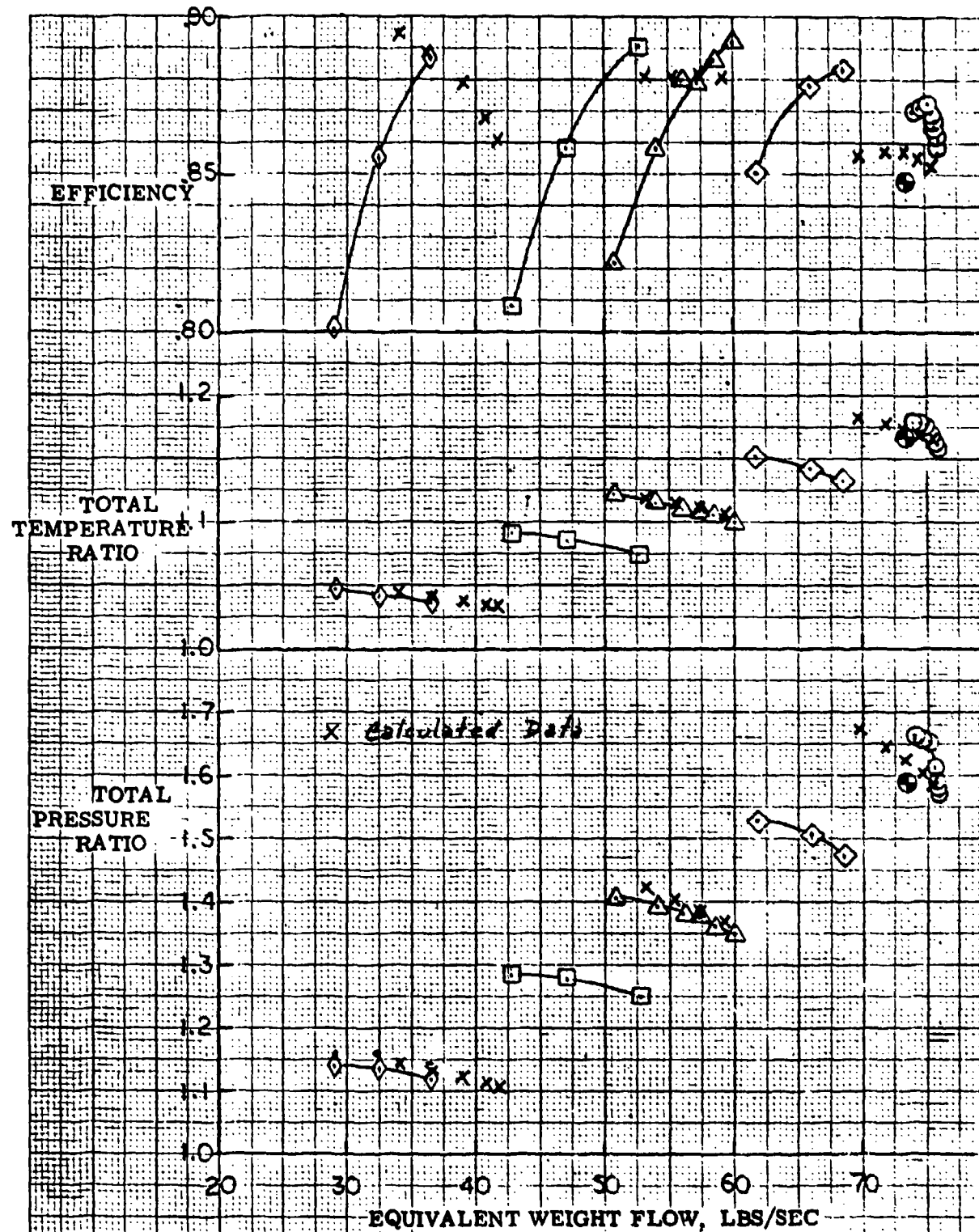


Fig. II.4.1.12 : Two Stage Compressor
Overall Performance Map of First Stage - Author A
Open symbols are experimental data

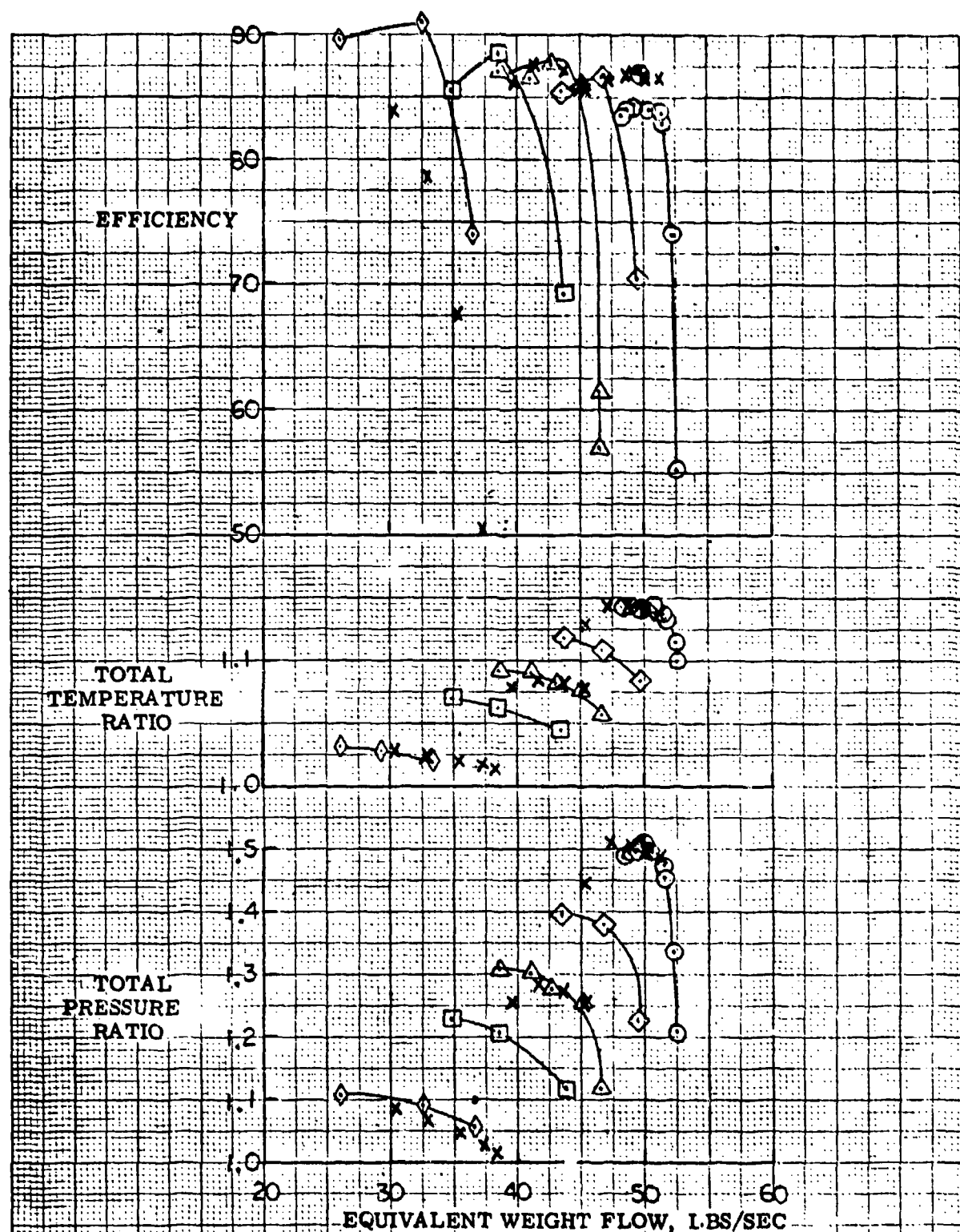


Fig. II.4.1.13 : Two Stage Compressor
Overall Performance Map of Second Stage - Author A
Open Symbols are Experimental data

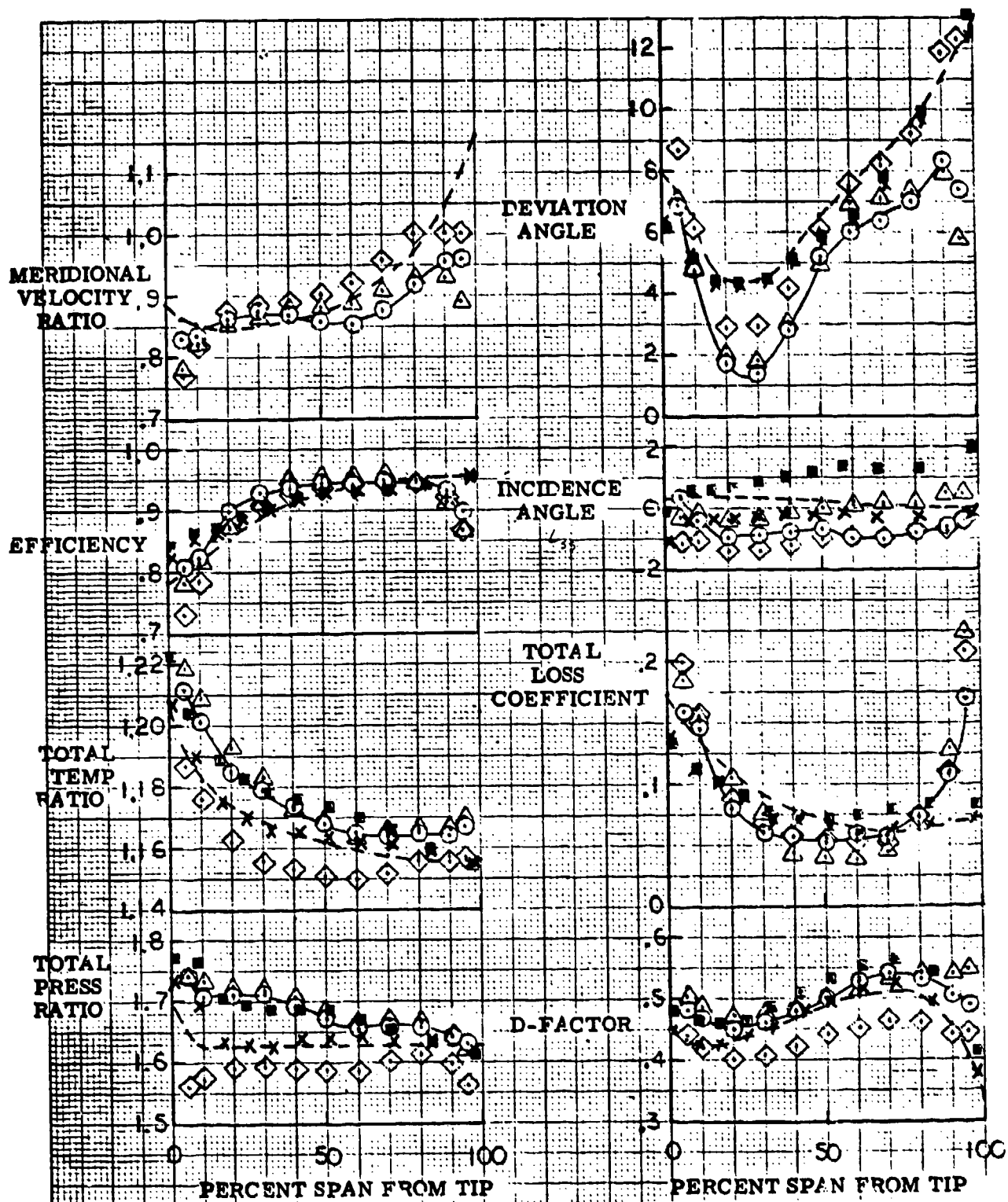


Fig. II.4.1.14 : Two Stage Compressor
Radial Distribution of First Stage Rotor - Author A
Open Symbols are Experimental Data

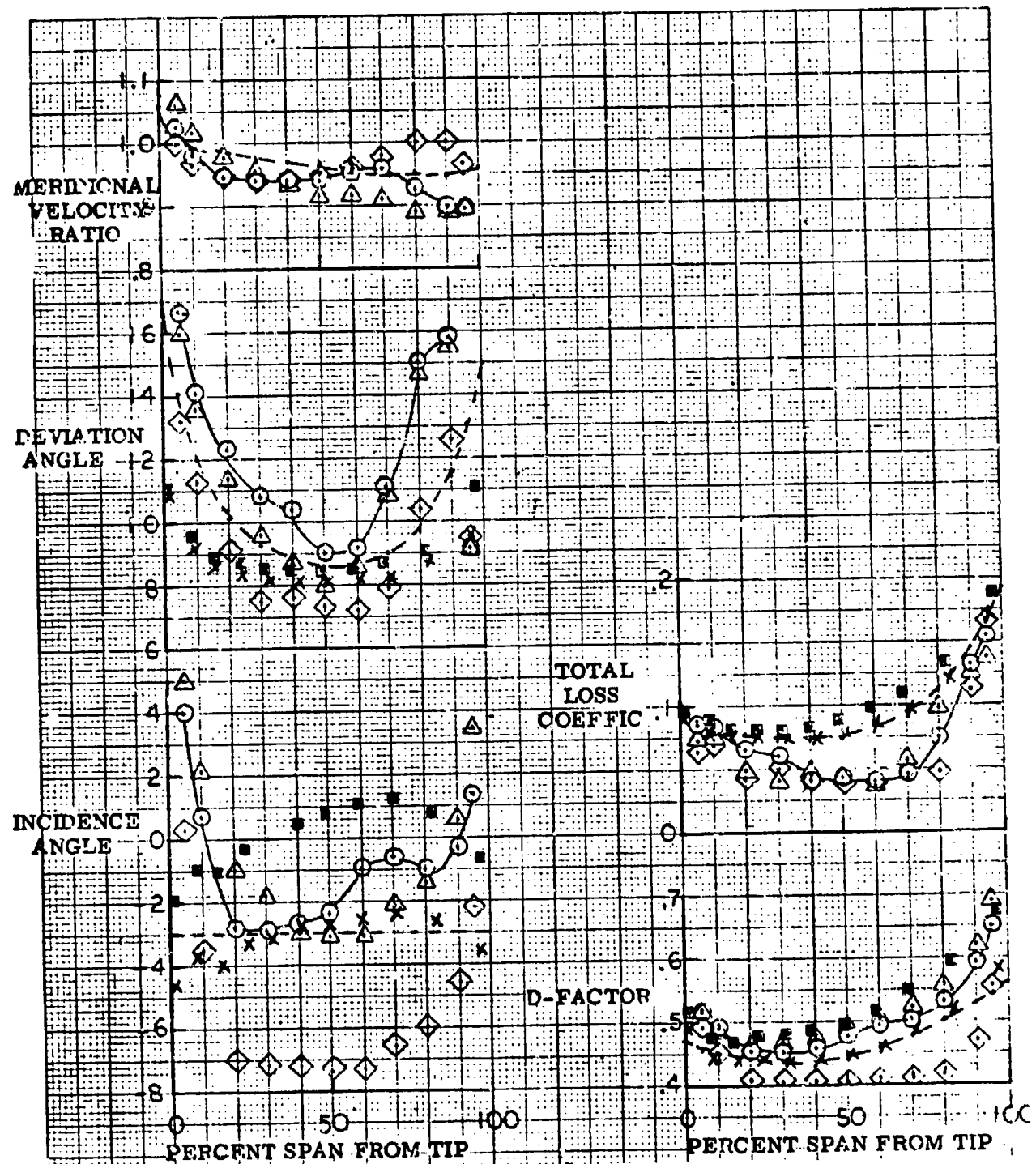


Fig. II.4.1.15 : Two Stage Compressor
Radial Distribution of First Stage Stator - Author A
Open Symbols are Experimental Data

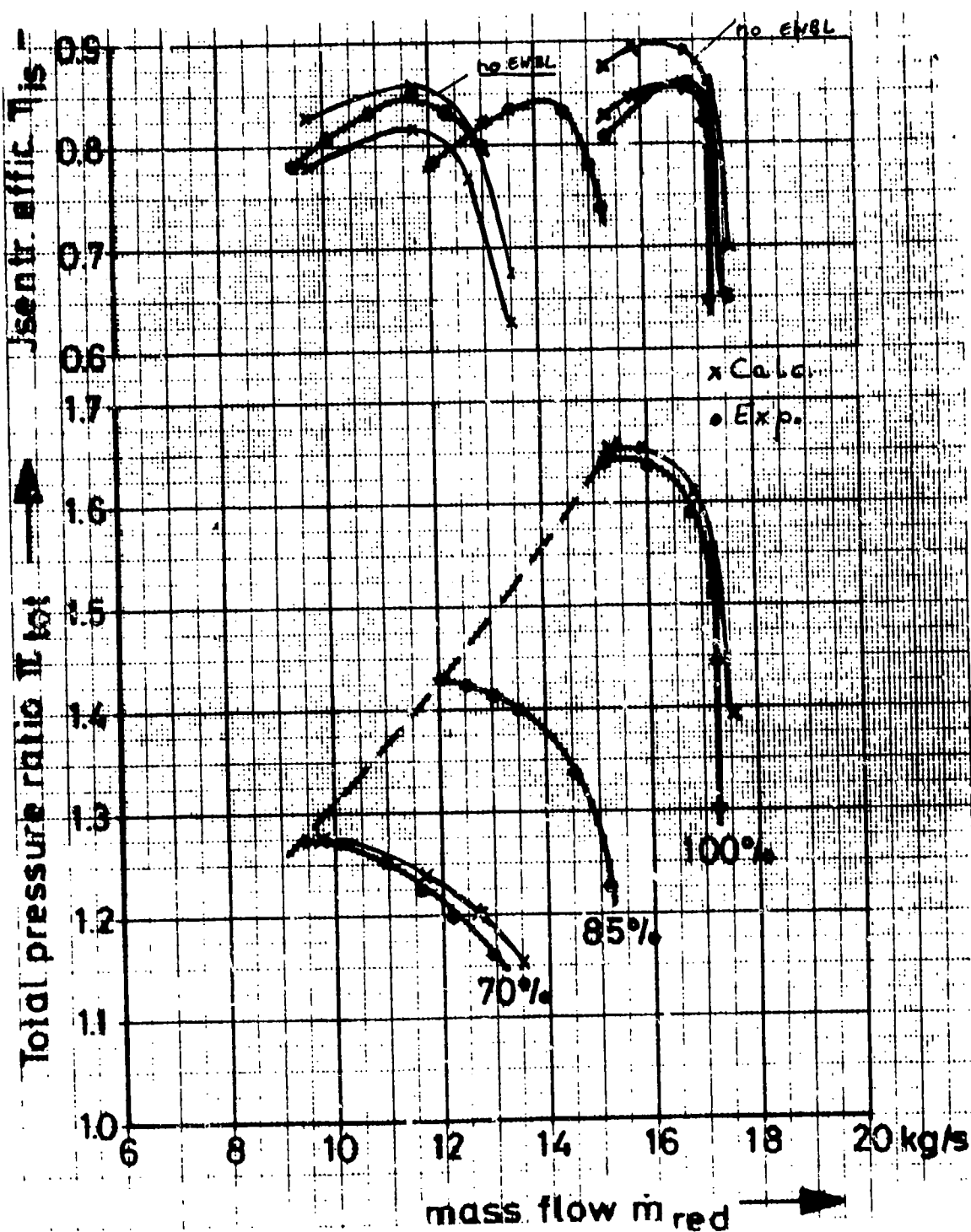


Fig. II.4.1.16 : Single Stage Compressor
Performance Map Prediction - Author F
Calculations with and without End-Wall Boundary Layer

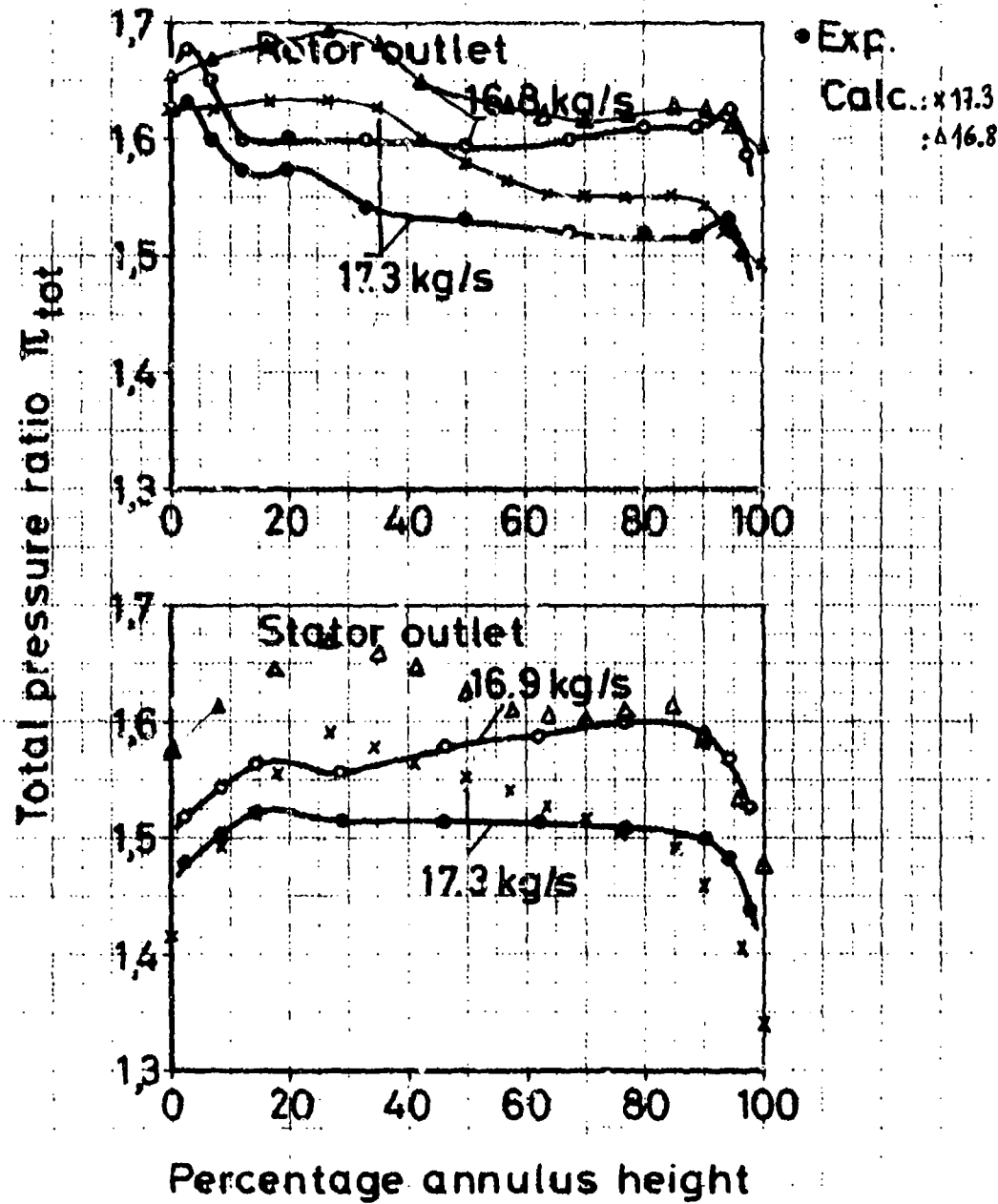


Fig. II.4.1.17 : Single Stage Compressor
Total Pressure Ratio Distribution - Author F

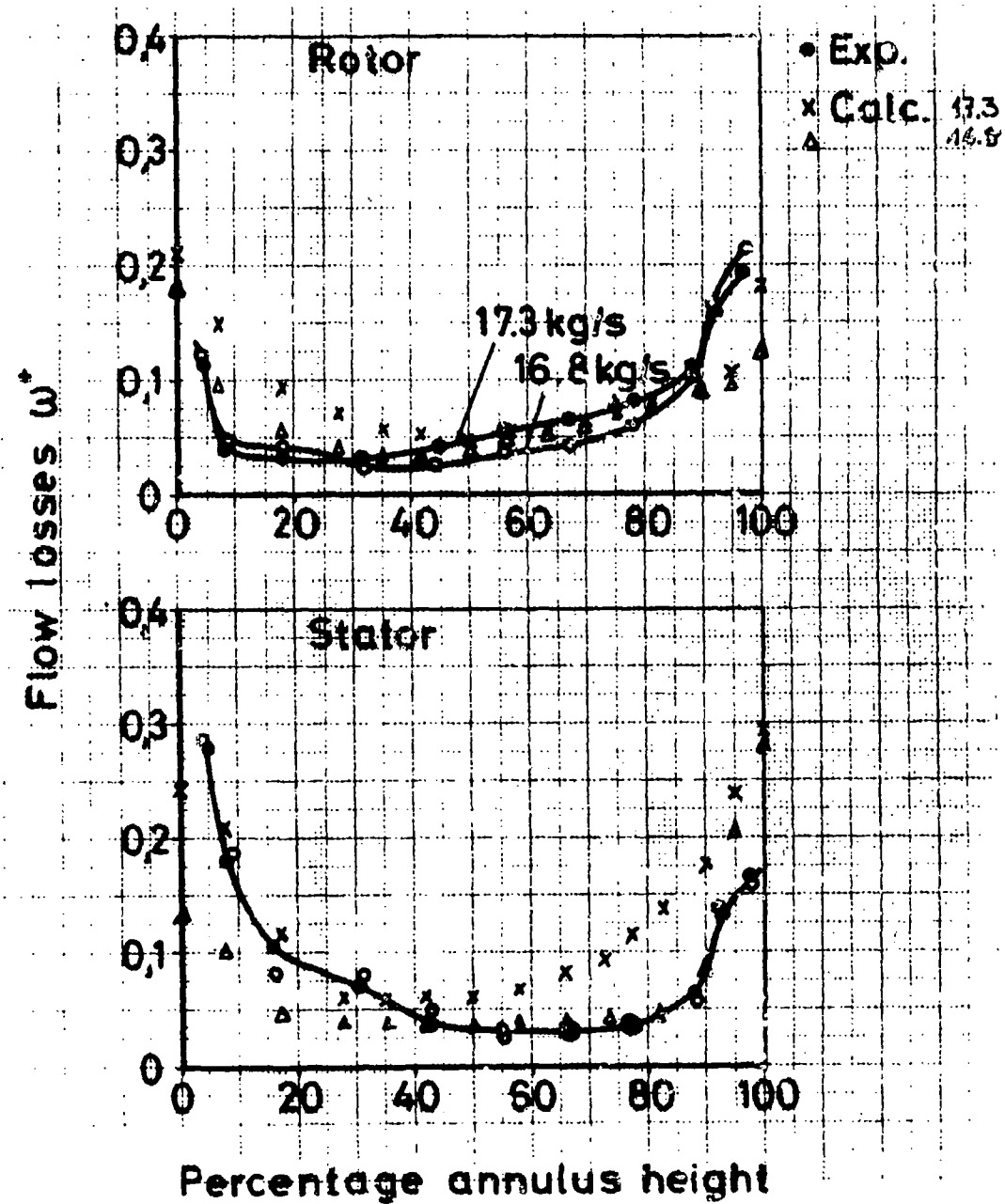


Fig. II.4.1.18 : Single Stage Compressor
Flow Losses Predictions - Author F

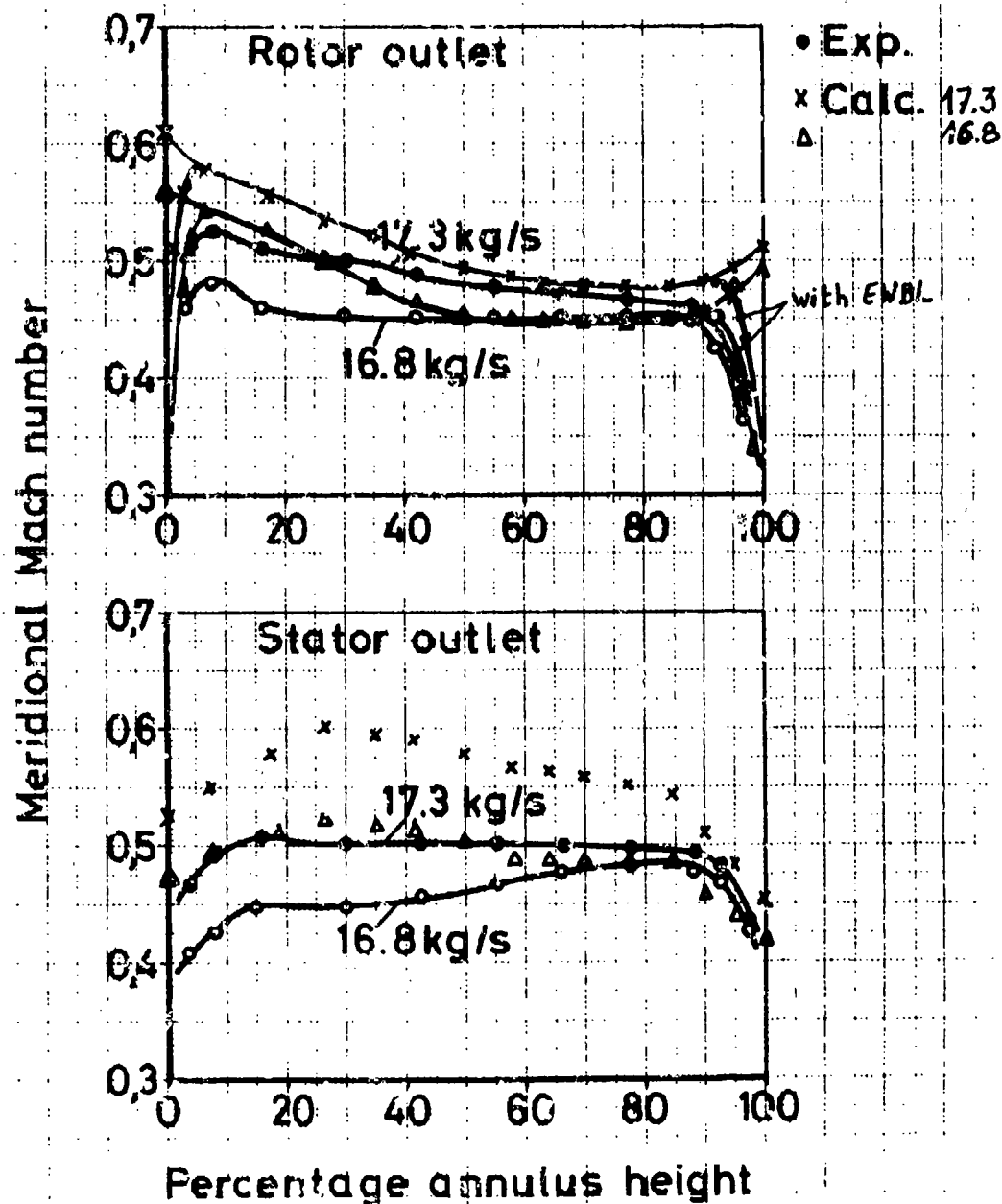


Fig. II.4.1.19 : Single Stage Compressor
Mach Number Prediction - Author F
Calculations with and without End-Wall Boundary Layers

II.4.2 EVALUATION OF PROFILE LOSS PREDICTIONS BASED ON DIFFUSION FACTORS

SUMMARY

A comparison between theoretically predicted and measured profile losses has been made, in order to evaluate the precision of the different prediction methods listed in reference 1.

These prediction methods are based on the relation between suction side diffusion and profile losses. The evaluation concerns as well the prediction of diffusion factor as predicted values of profile losses.

It is further shown that these correlations are not universally valid for all blade shapes and that some correlations perform as well at design as at off design if the suction side diffusion is correctly predicted.

II.4.2.1 introduction

Profile loss prediction methods are generally based on the following observations :
 a. wake momentum thickness at the trailing edge is mainly due to the flow deceleration along the blade suction side
 b. profile losses are functions of the blade wake and cascade geometry.

A first part of the loss predictions therefore consists of the definition of a diffusion factor as a measure of the suction side diffusion between V_{max} and V_2 . This diffusion factor is normally expressed in function of cascade geometry and inlet and outlet conditions.

A second part of these loss predictions consists of defining a relation between wake momentum thickness or profile losses and the diffusion factor.

The first correlations based on this principle were valid only for incompressible two dimensional flow at design incidence. Corrections for off design incidence and compressibility effects have been proposed.

This was done by changing the value of the diffusion factor, or by adding some extra loss terms.

The validity of this loss prediction has been evaluated by applying these correlations to two test cases and by comparing the theoretical predictions with experimental results.

Because of the limited number of test cases, no general conclusions can be obtained. However, this comparison allows to obtain some indications about the level of confidence one can have in these correlations, when applied to a typical design. They also illustrate the shortcomings of some correlations.

In order to evaluate both parts of this correlation, some calculations have been performed with a diffusion factor derived directly from V_{max}/V_2 obtained from potential flow calculations or from experiments.

II.4.2.2 Test_cases

The first test case concerns a cascade of NACA 65 (12A10) 10 blades with the following parameters :

$$\begin{aligned} \beta_1 &= 35^\circ \\ \sigma &= 1.25 \\ \alpha &= 14.1, 17.1, 20.1, 23.1 \end{aligned}$$

The experimental results at different inlet Mach numbers are shown in figures 29 to 32 of reference 2.

The second test case consists of 48° camber DCA blades with the following parameters :

$$\begin{aligned} \beta_1 &= 34.2, 38.5, 40.0, 42.0 \\ \sigma &= .614 \\ \gamma &= 13.58 \\ M_1 &= .6 \end{aligned}$$

The experimental results are published in reference 3.

II.4.2.3 Correlations

In order to avoid any confusion concerning the correlations used in this evaluation, we will shortly define the different calculations that have been performed. More details about these correlations are given in reference 1.

1. Lieblein's correlation based on equivalent diffusion factor

The definition of diffusion factors used here is valid only for incompressible flow

at design and off design angles of attack.

$$D_{eq} = \frac{\cos\beta_2}{\cos\beta_1} \left[1.12 + a(\alpha-\alpha^*)^{1.43} + .61 \frac{\cos\beta_1}{\sigma} (t_g\beta_1 - t_g\beta_2) \right]$$

The wake momentum thickness is obtained from a curve fitting of figure 11 of reference 4.

$$\begin{aligned} \frac{\theta_2}{c} = & .00497 + .011921 (D_{eq}-1.) - .078935 (D_{eq}-1.)^2 \\ & + .21399 (D_{eq}-1.)^3 - .20337 (D_{eq}-1.)^4 + .070112 (D_{eq}-1.)^5 \end{aligned} \quad (1)$$

The total pressure losses are calculated by following approximated equation :

$$\omega_2 = 2 \frac{\theta_2}{c} \frac{\sigma}{\cos\beta_2} \cdot \left(\frac{\cos\beta_1}{\cos\beta_2} \right)^2 \quad (2)$$

2. Lieblein's correlation based of V_{max}/V_1 obtained from potential flow calculations

$$D_{eq} = \frac{V_{max}}{2}$$

This diffusion factor accounts for variation as a function of angle of attack and compressibility effects. Combined with equations (1) and (2) it should give an indication of profile losses for compressible flow at design and off design.

The potential flow calculation is described in reference 5.

3. Lieblein's correlation based on V_{max}/V_1 obtained from experiments

$$D_{eq} = \frac{V_{max}}{V_2}$$

Combined with equations (1) and (2) one should again obtain the real losses for compressible flow at design and off design.

Calculations 2 and 3 are made in order to verify the idea that losses can be related to the suction side diffusion.

A comparison between the diffusion factor of calculation 1 with the one of calculations 2 and 3 also allows to investigate the precision, with which the V_{max}/V_2 is predicted.

4. Swan's correlation

Profile losses are first calculated for incompressible flow at design incidence in the same way as proposed by Lieblein ($i=i^*$). However, the relation between θ/c and D_{eq}^* is given as a function of radial position in rotor and stator (Hub to tip). In this comparison with cascade results, the loss correlation for a hub section is used and radial shift of streamlines has been neglected.

In order to account for off design operation and inlet Mach number, a correction term is added to the trailing edge momentum thickness.

It is important to notice here that at design incidence, a change of inlet Mach number has no influence on losses ($\frac{\theta}{c} = \frac{\theta^*}{c}$ if $D_{eq} = D_{eq}^*$).

5. Correlation of Jansen and Moffat

This correlation is based on the design diffusion factor for incompressible flow defined by

$$D^* = 1 - \frac{V_2}{V_1} + \frac{r_2 V_{\theta 2} - r_1 V_{\theta 1}}{(r_1 + r_2) V_1 \sigma}$$

In this comparison with cascade data a constant radius was used.

This correlation contains a correction of losses for inlet Mach number above the critical one and an increase of losses at off design.

6. Correlation of Fottner

This correlation contains an additional term in the definition of V_{max}/V_1 to account for blade thickness.

Inlet Mach number influence and correction for off design is the same as in previous correlation.

7. Strinining correlation

This correlation is valid only for design operation at different Mach numbers. The influence of inlet Mach number is introduced by modifying the diffusion factor.

The relation between losses and the modified diffusion factor is the same as the one used by Fottner for incompressible flow.

8. Smith's correlation

This correlation is valid only for design losses. The description given in reference 1, is incomplete and has been completed according to reference 7.

At design angle of attack V_{max}/V_2 is defined according to reference 1.

The trailing edge momentum thickness θ/c and shape factor HTE are a function of V_{max}/V_2 and Reynolds number. The value of Re used in this calculation is 10^6 . These values are further corrected in function of M_1 and V_{max}/V_2 . In this comparison, no correction is made for streamtube height.

Losses are calculated according to the mixing theory of reference 8.

9. Smith's correlation using V_{max}/V_2 from potential calculations

In order to use this correlation also for off design loss predictions, where V_{max}/V_2 is not predicted by the correlation, calculations have been performed with V_{max}/V_2 defined by potential calculations. The correlation is used only to define θ/c and HTE in function of V_{max}/V_2 .

10. Smith and Koch's correlation using V_{max}/V_2 experimental results

This calculation is similar to previous one but V_{max}/V_2 is defined from experiments. The value of this last calculation is in the verification of the relation between losses and V_{max}/V_2 .

II.4.2.4 Comparisons

Comparisons between correlations and experimental data are made on two levels, corresponding to the two parts of the loss correlation. In a first part the predicted values of V_{max}/V_1 are compared to the experimental ones. In a second part predicted losses are compared to the experimental ones.

The flow conditions corresponding to the different calculations are given in table 1. Tests numbers 001 to 016 concern the NACA cascade at different inlet Mach numbers and different angles of attack (Ref. 2). Test numbers 101 to 104 concern the DCA cascade at different inlet Mach numbers (Ref. 3).

Comparison of V_{max}/V_1

From all the correlations used in this comparison only those of Lieblein and Swan define a diffusion factor at off design, but for incompressible flow. For test cases numbers 001 to 008 and 013 to 016 a comparison of predicted and experimental V_{max}/V_1 is therefore limited to incompressible flows.

For compressible flow, only the results of the potential calculation can be compared to the experimental value. This is shown on figure 1 for test numbers 001 to 004. Calculated and experimental values of V_{max}/V_1 agree fairly well at different Mach numbers and the extrapolated values for $M=0$ are close to the value predicted by Lieblein.

Figure 2 shows the same comparison at design angle of attack (test Nos. 009 to 012). A comparison with the correlations of Smith & Koch, Jansen-Moffat, and Fottner are possible only for incompressible flow.

The correlation of Strinining allows calculation of V_{max}/V_1 for compressible flow at design conditions. However, this correlation underestimates the influence of compressibility on V_{max}/V_1 . The prediction of Jansen-Moffat and Fottner agree very well with Lieblein's prediction for incompressible flow.

Comparison of losses

Losses predicted by the different correlations are compared with experimental values of reference 2 on figures 3 to 7.

The conversion of C_w experimental to ω has been made according to reference 6.

Concerning the NACA blade cascade, most of the correlations predict losses which are higher than the experimental ones.

The losses predicted by Lieblein's correlation in combination with V_{max}/V_1 obtained from potential flow calculations or experimental results show good agreement.

Also Swan's correlation is very good for these blades especially at off design incidence. Close to design incidence and at higher inlet Mach numbers, the losses are underestimated.

This is due to the absence of a correction for compressibility when $D_{eq} = D^*$, as pointed out at the description of this correlation.

The correlations of Jansen-Moffat and Fottner predict losses which are much too high for the NACA blades at off design.

Smith and Koch's correlation also predict higher losses than the experimental ones and the use of V_{max}/V_2 , obtained from calculation or experiments does not show any improvement. However, one should keep in mind that in this correlation, losses are predicted at complete mixed-out conditions, and experimental values are measured one chord downstream of trailing edge.

For the cascade of DCA blades, test numbers 101 to 104, the situation is quite different. Most of the loss predictions are in a close band around the experimental values. Only the predictions of Jansen and Moffat are out of this range. However they are much closer to the values obtained in a real stator.

II.4.2.5 Conclusion

Previous comparisons indicate that the classical correlation of Lieblein's type are fairly good if one can estimate correctly the value of V_{max}/V_1 at off design and different values of the inlet Mach number. Using a value of V_{max}/V_1 obtained from potential calculations gives a correct trend for the variations at a correct level. Swan's correlation could be improved by introducing a better compressibility correction at design incidence.

The correlation of Fottner cannot be recommended for NACA blades but gives good results for DCA blades. The correlation of Jansen and Moffat indicates even higher losses for both cases.

Possible explanations could be that these correlations predict losses at complete mixed out conditions, where the experiments are the ones at one chord downstream of the cascade.

Furthermore, some correlations are based on experiments in rotors and stators, and could contain losses which are not present at the mid section of a cascade.

REFERENCES

1. DUNKER, R. & WEYER, H.B.: Axial compressor performance prediction. Survey on diffusion factors and profile losses.
Chapter II.2.1
2. EMERY, J.C. & DUNAVANT, J.C.: Two dimensional cascade tests of NACA 65 (12A10) 10 blade sections at typical compressor hub conditions for speeds up to choking.
NACA RM L57H05, 1959.
3. Transonic flows in turbomachinery.
VKI LS 59, 1973.
4. LIEBLEIN, S.: Loss and stall analysis of compressor cascades.
ASME J. Basic Engineering, September 1954, pp 387-400.
5. VAN DEN BRAEMBUSSCHE, R.: Calculations of compressible subsonic flow in cascades with varying blade height.
ASME J. Engineering for Power, Vol. 95, No. 4, 1973, pp 345-351.
6. LIEBLEIN, S.: Analysis of experimental low-speed loss and stall characteristics of two dimensional compression blade cascades.
NACA RM E57A28
7. KOCH, C.C. & SMITH, L.M.: Loss sources and magnitudes in axial flow compressors.
ASME Trans., J. Engineering for Power, Vol. 98, No. 3, 1976, pp 411-424.
8. SCHOLZ, N.: Aerodynamik der Schaufelgitter.
Translated and revised by A. Klein,
AGARDograph 220, 1977.

TEST NUMBER	β_2	α_1	M_1	β_2	σ
001	35°	20°1	.307	9°45	1.25
002			.509	9°34	
003			.706	9°19	
004			.747	9°16	
005	35°	17°1	.299	12°66	1.25
006			.511	12°63	
007			.696	12°62	
008			.762	12°62	
009	35°	14°1	.293	15°88	1.25
010			.507	15°91	
011			.679	16°00	
012			.742	16°05	
013	35°	23°1	.308	5°26	1.25
014			.500	5°09	
015			.618	9°89	
016			.750	10°50	
101	36°2	21.6	.6	-4°7	.614
102	38°5	23.9		-4°5	
103	40°0	25.4		-4°7	
104	42°0	27.4		-4°7	

$\alpha_1 = 20^\circ$

- LIEBLEIN'SWAN
- POT FLOW CALCULATION
- △ EXPERIMENTAL

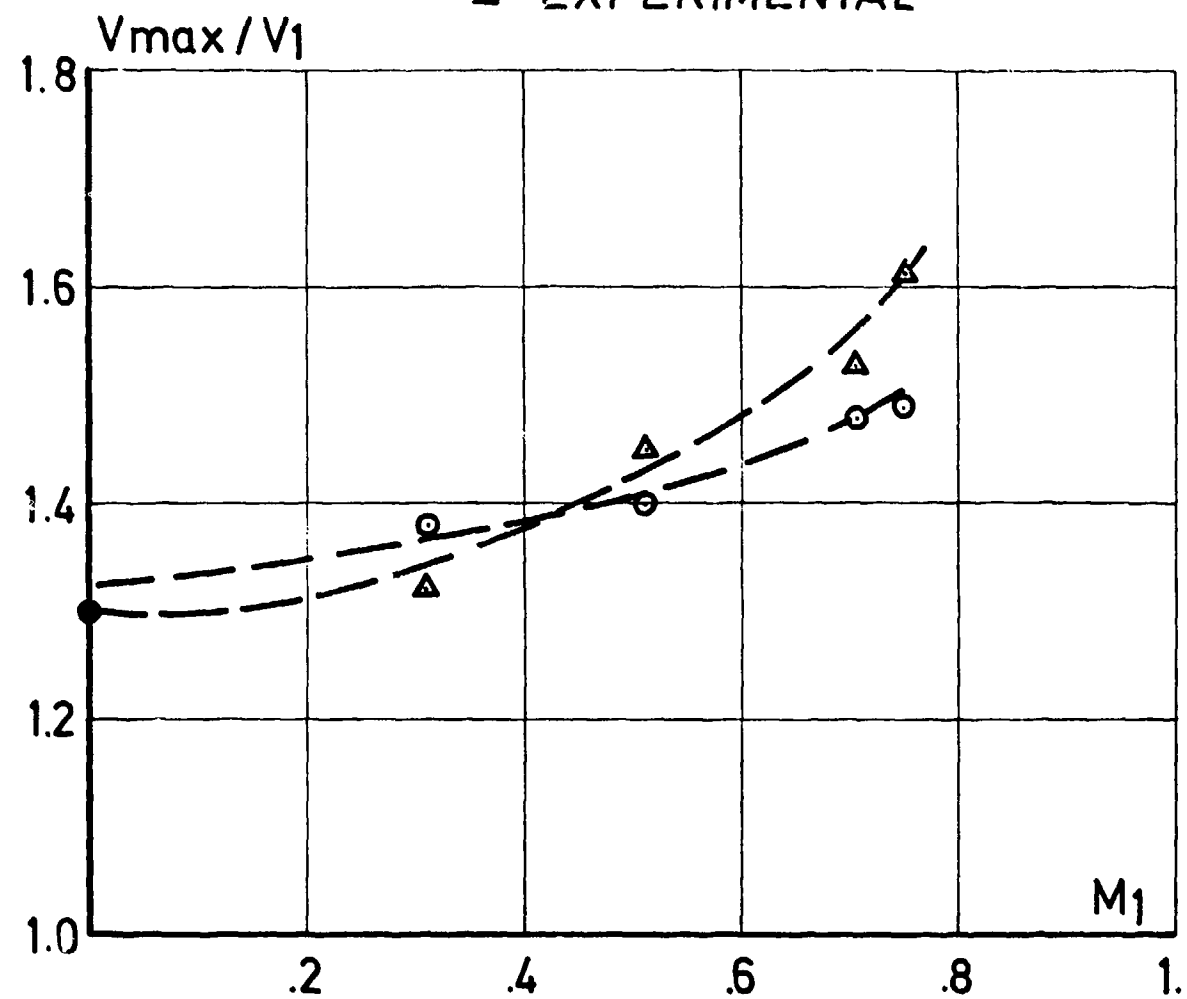


FIG. 1

● LIEBLEIN & SWAN ▽ STRINNING
○ POT FLOW CALC. □ JANSEN - MOFFAT
△ EXPERIMENTAL * FOTTNER

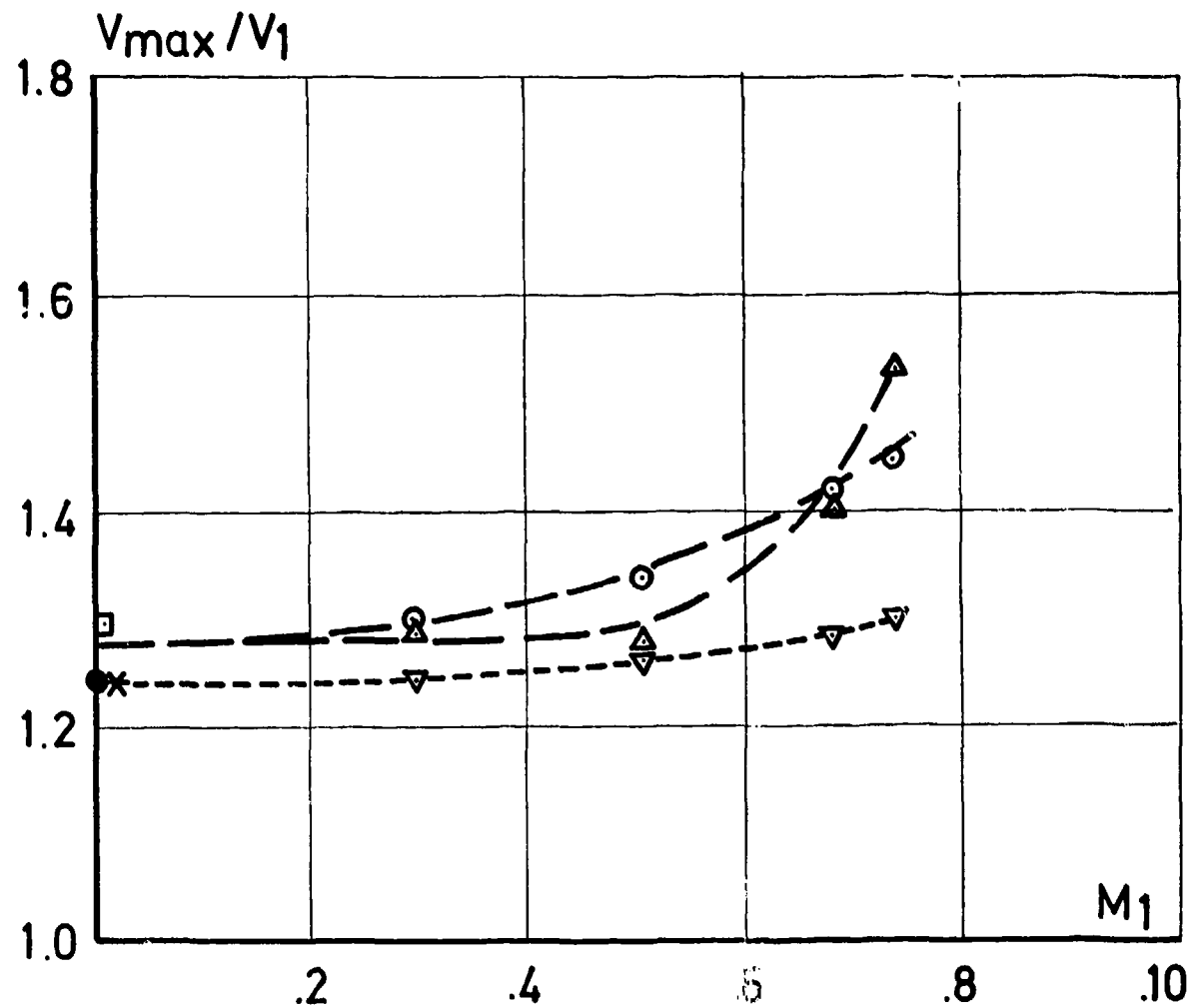


FIG. 2

001 - 004
 $\alpha_1 = 20^\circ 1$

- * EXPERIMENTS
- x LIEBLEIN INC.
- o LIEBLEIN V_{max}/V_1 from POT. CALC.
- Δ LIEBLEIN V_{max}/V_1 from EXP.
- ∇ SWAN
- \square JANSEN MOFFAT
- + FOTTNER
- \blacktriangle STRINNING
- \blacktriangledown SMITH & KOCH
- SMITH & KOCH V_{max}/V_1 from POT. CALC.
- SMITH & KOCH V_{max}/V_1 from EXP.

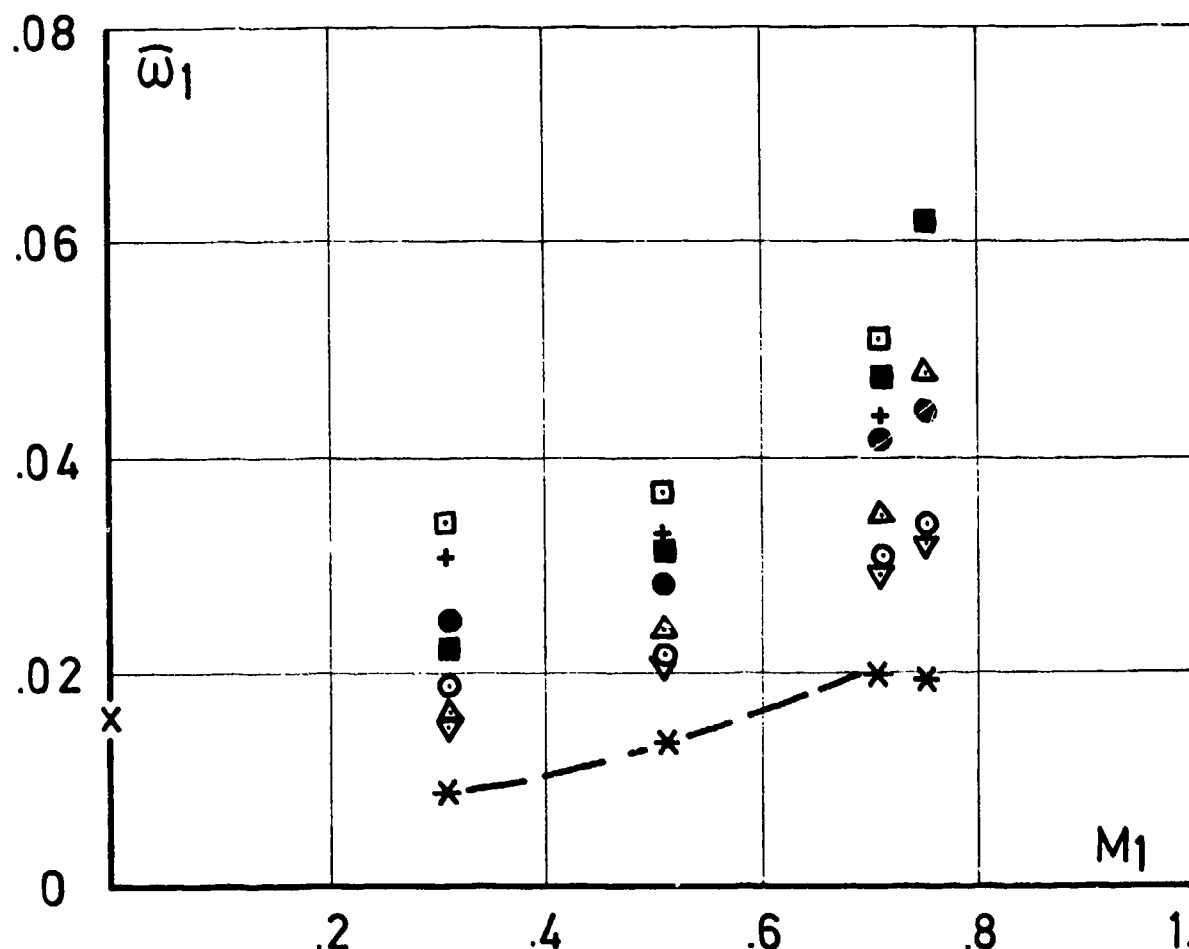


FIG. 3

005 - 008
 $\alpha_1 = 17^\circ 1$

- * EXPERIMENTS
- X LIEBLEIN INC.
- O LIEBLEIN V_{max}/V_1 from POT. CALC.
- A LIEBLEIN V_{max}/V_1 from EXP.
- V SWAN
- S JANSSEN MOFFAT
- + FOTTNER
- ▲ STRINNING
- ▼ SMITH & KOCH
- SMITH & KOCH V_{max}/V_1 from POT. CALC.
- SMITH & KOCH V_{max}/V_1 from EXP.

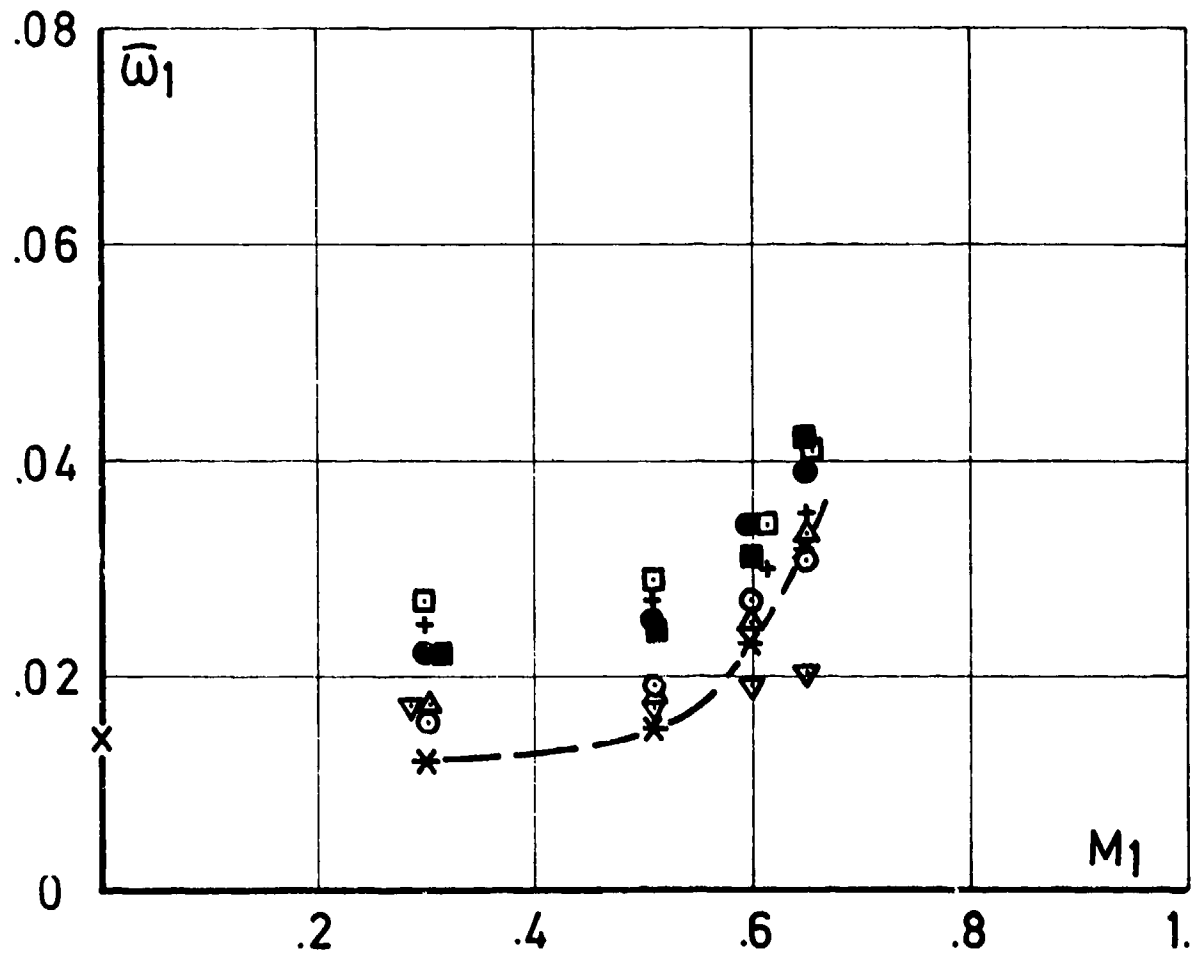


FIG. 4

009 - 012
 $\alpha_1 = 14^\circ 1$ DESIGN

- * EXPERIMENTS
- x LIEBLEIN INC.
- o LIEBLEIN V_{max}/V_1 from POT. CALC.
- Δ LIEBLEIN V_{max}/V_1 from EXP.
- ∇ SWAN
- \square JANSEN MOFFAT
- + FOTTNER
- \blacktriangle STRINNING
- \blacktriangledown SMITH & KOCH
- SMITH & KOCH V_{max}/V_1 from POT. CALC.
- SMITH & KOCH V_{max}/V_1 from EXP.

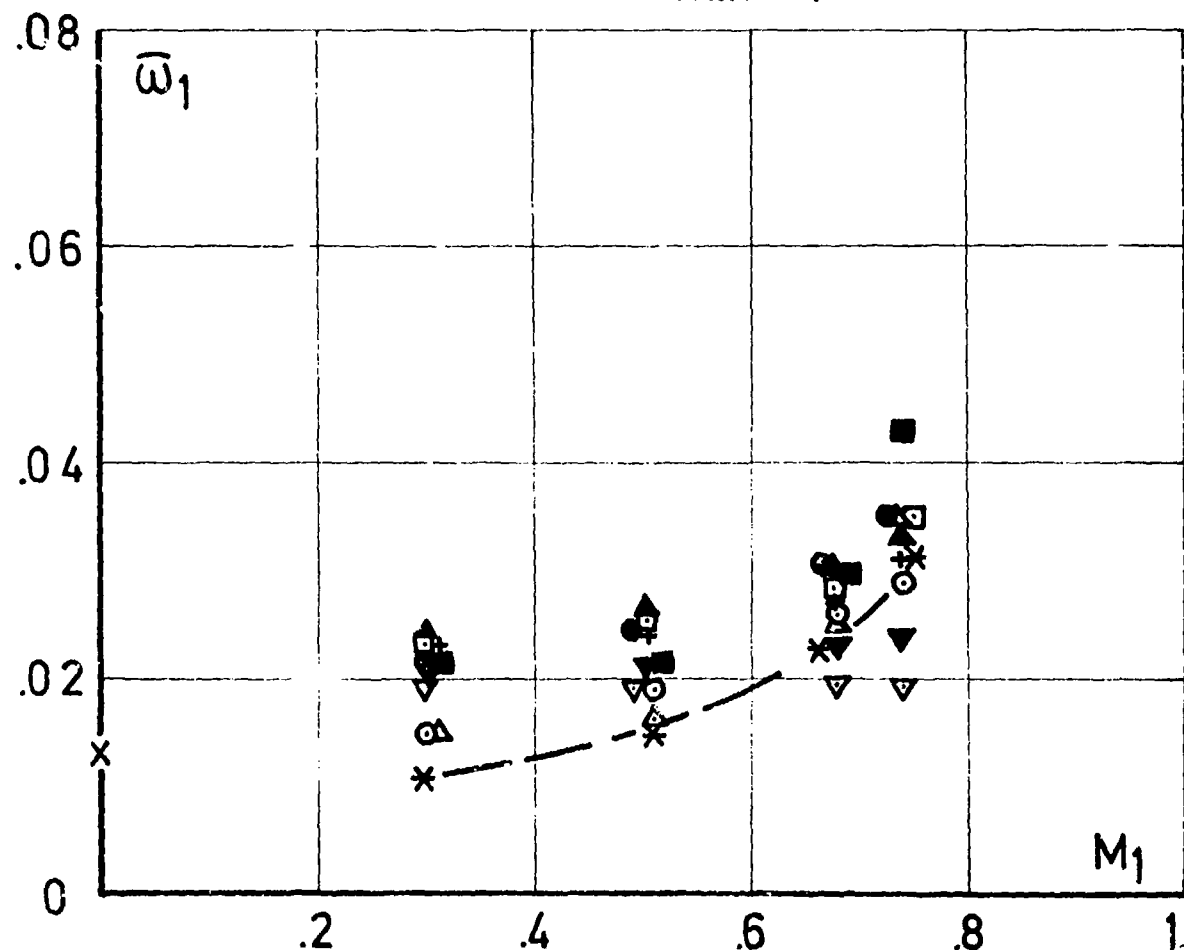


FIG. 5

013 - 016
 $\alpha_1 = 23^\circ 1$

- * EXPERIMENTS
- \times LIEBLEIN INC.
- \circ LIEBLEIN V_{max}/V_1 from POT. CALC.
- \triangle LIEBLEIN V_{max}/V_1 from EXP.
- ∇ SWAN
- \square JANSEN MOFFAT
- $+$ FOTTNER
- \blacktriangle STRINNING
- \blacktriangledown SMITH & KOCH
- \bullet SMITH & KOCH V_{max}/V_1 from POT. CALC.
- \blacksquare SMITH & KOCH V_{max}/V_1 from EXP.

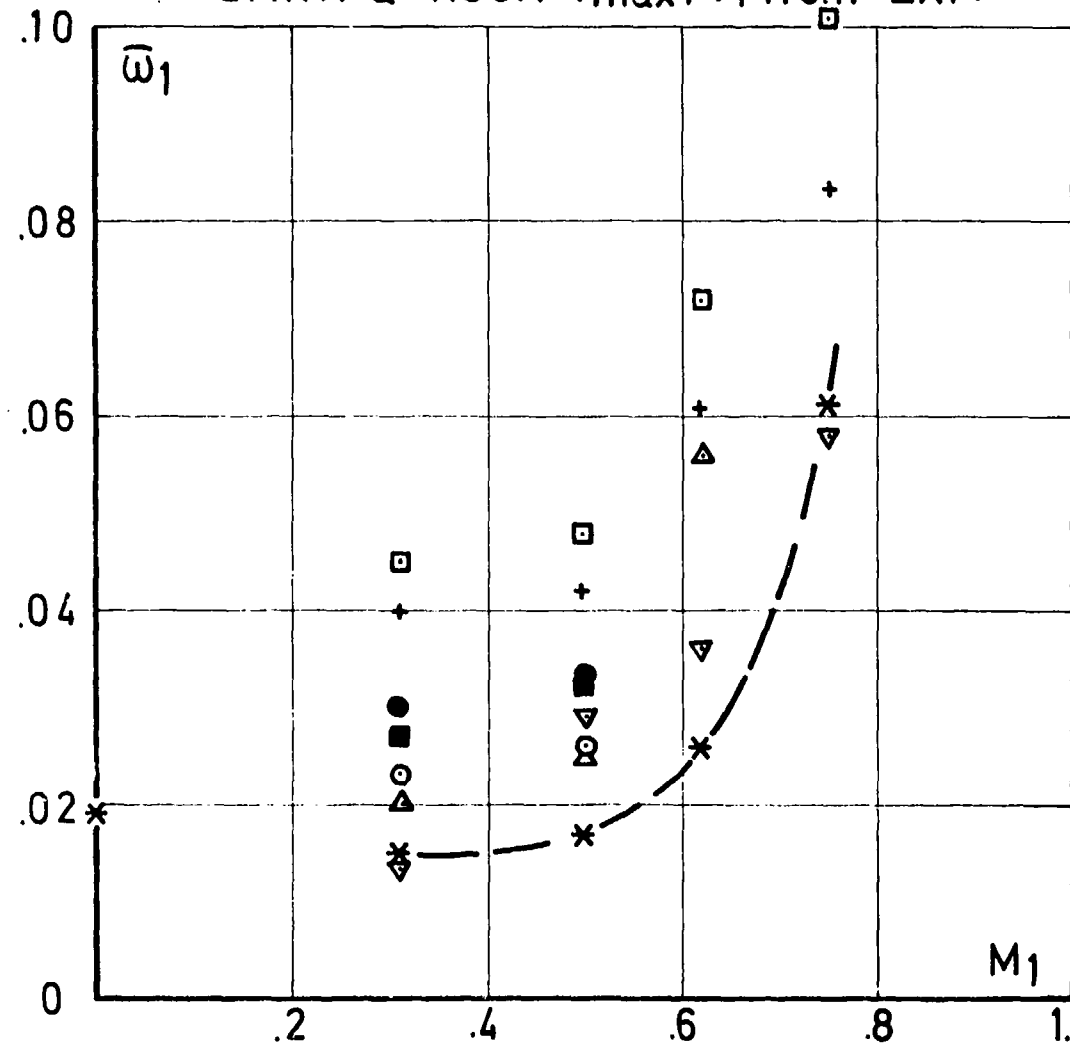


FIG. 6

101-104

- * CASCADE LOSSES $M_1 = .6$ AVR. = 1
- ⊕ STATOR LOSSES $M_1 = .65$
- ×
- LIEBLEIN INC.
- LIEBLEIN V_{max}/V_1 from POT. CALC.
- △ LIEBLEIN V_{max}/V_1 from EXP.
- ▽ SWAN
- JANSEN MOFFAT
- + FOTTNER
- ▲ STRINNING
- ▼ SMITH & KOCH
- SMITH & KOCH V_{max}/V_1 from POT. CALC.
- SMITH & KOCH V_{max}/V_1 from EXP.

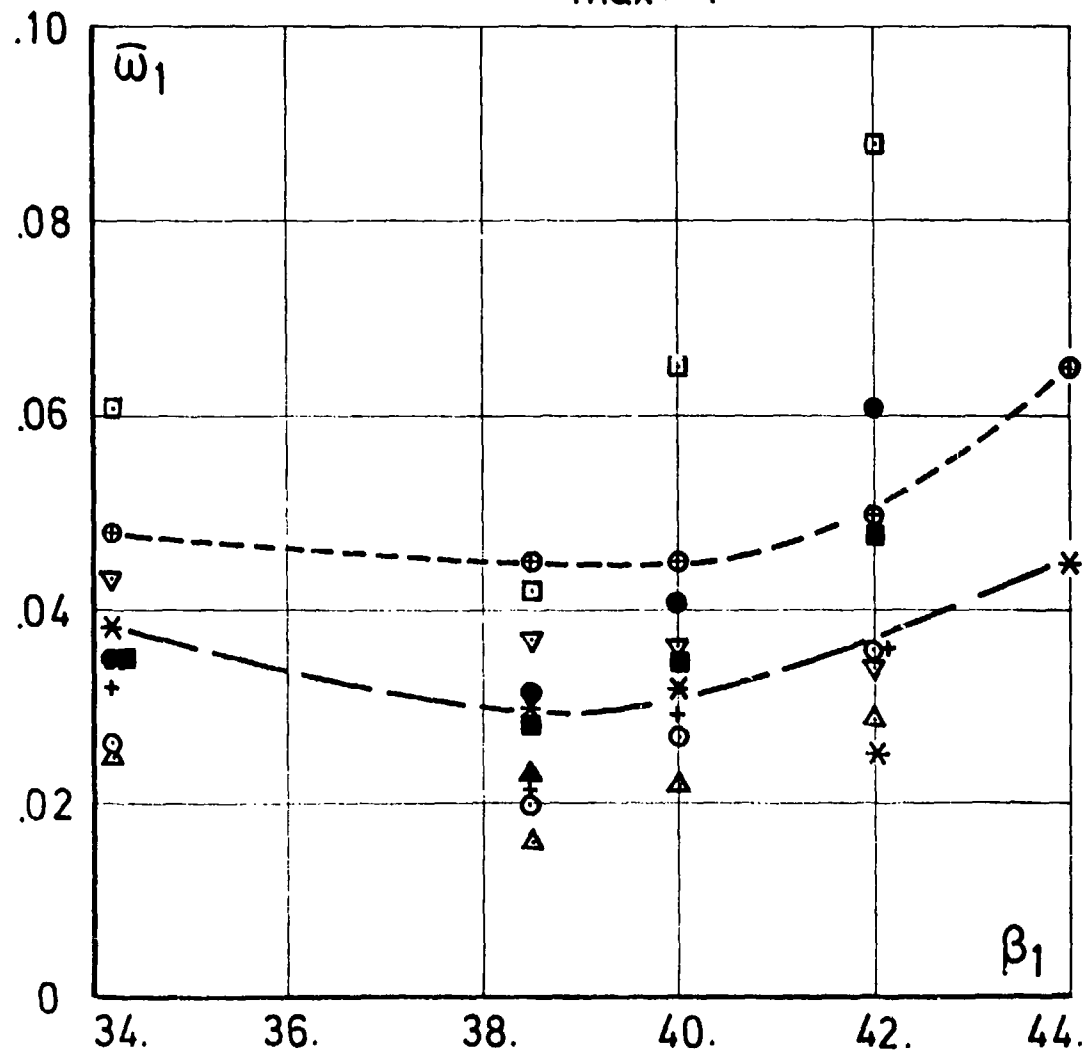


FIG. 7

II.5. Conclusions

Many aspects of axial compressor correlations have been reviewed by various members of the compressor Subgroup and are contained in chapter II, together with the answers to the questionnaire from industry and research organisations.

Obviously, many gaps are to be filled in order to achieve a satisfactory situation with regard to loss and turning correlations.

It is apparent however, that no set of correlations will ever be of general validity, since the philosophy behind it is to describe deviations and losses as functions of a very limited number of variables. The complexity of axial compressor flow phenomena, even without taking unsteady effects into account, is such that only trends can be defined without a description and a knowledge of the details of the flow behaviour. Therefore it is challenging to define a valid set of correlations of sufficient generality at design conditions. As it appeared also from the previous chapters, the degree of validity of existing correlations at off-design is still more limited.

Hence, the Compressor Subgroup members considered that progress could only come from an improvement in the basic physical understanding of the phenomena leading to the loss generation and to the flow deviation.

It is advocated that extensive use should be made of the present day tools, namely sophisticated experimental tools, in particular laser anemometry, and viscous flow calculation.

With regard to two dimensional phenomena, an extensive use should be made of the presently available blade-to-blade calculation methods, including boundary layer interaction in order to define general trends with regard to the influence of parameters (such as Mach number for instance) on losses and deviations. This approach, illustrated by the results of Koch & Smith at design conditions, is considered as particularly promising. A particular effort in this direction should be made, especially at off-design.

On the other hand, very little appears to be known about specific phenomena such as shock-boundary layer interactions. This is a typical instance where well selected and applied basic experiments should be encouraged in order to form a basis for a correlation approach.

More generally, a lack of valid multistage data has been noticed. It is of fundamental importance, if the transition is to be made from basic cascade data to real life situations, to dispose of a reliable set of data taken in multistage axial compressors, and especially of interstage and end-wall boundary layer data.

From the calculated test cases, it was clear that, even if overall performance could be predicted satisfactory (by adjustment of some free parameters) detailed flow distributions or (and) individual stage data are much more difficult to predict with confidence. This indicates that in many correlations, either the physical phenomena are not taken into account and an overall compensation of errors occurs, or different assumptions with regard to the loss mechanism lead to different contributions of the various loss sources - cfr chapter II.4. - leading to large differences in the predicted details of the flow behaviour, even if the overall performance is obtained correctly.

This observation illustrates the strong need for a very clear physical understanding of the basic phenomena, which cannot be stressed enough.

More specific conclusions, with regard to the content and the validity of various approaches to loss and turning correlations are summarized in the following remarks :

- . The level of accuracy required is sensibly higher for deviations than for losses. The influence on the predicted flow field of a small variation in outlet angle (one or two degrees) can be very important while a variation in loss level does not appear to be very significant below, roughly, 10 % variation.
- . The validity of the diffusion factor is generally accepted and several of the expressions to be found in the literature give a valid estimation, when compared with the values derived from blade-to-blade potential flow calculations.
- . Although a large scatter exists between the various predicted profile loss coefficients, most of them do have the right trends in function of Mach number or incidence. However, no correlation could be shown to behave significantly better than the others at off-design conditions.
- . Care should be taken to define a consistent set of relations between diffusion factor, trailing edge momentum thickness, and loss coefficient. Moreover, ambiguities can appear when comparisons are made with methods which take into account mixing losses in the through-flow calculation or in the loss definition. This consistency problem is of particular importance when combining various partial correlations from different sources.
- . The available information on Mach number effects, on shock-boundary layer interaction and shock induced separation is very limited. An important effort in this direction is strongly needed.
- . Secondary flow effects can be taken into account through correlations or through a more sophisticated and physically based approach of end-wall boundary layers. It is the Subgroup's opinion substantiated also by the results of the test calculations, that this latter approach should be developed and generalized, since it offers the possibi-

lity of a consistent description of secondary and clearance losses and deviations as generated by the end-wall layers. Moreover due to the coupling with a through-flow calculation, the important parameters of annulus blockage is predicted.

The correlation for deviations are generally very unsatisfactory. This is already the case at design conditions and hence, even more so at off-design, especially at high loading conditions.

There will always be a need for simple correlations, even with the increasing development of viscous flow calculations. The improvement can only be obtained from a coherent and systematic use of basic experiments together with 2D and 3D viscous calculations, in order to understand better the physical behaviour of the flow and to be able to derive the most meaningful parameters to be used in a correlation.

PART III
REVIEW OF CALCULATION METHODS

III.1. Axial-Flow Turbomachine Through-Flow Calculation Methods

INTRODUCTION

In this review a through-flow calculation method is considered to be a computational technique for prediction of fluid velocities and thermodynamic properties at designated locations in the internal flow path of a turbomachine. Defined in this way, a large part of the total spectrum of turbomachine flow field analysis methods is included. The objectives of this paper are to trace the development of several classes of through-flow calculation, to suggest the importance of understanding the assumptions underlying representative examples of each class, and to outline the principal problems in application of through-flow methods to current axial-flow compressors and turbines.

~~It should be understood that all of the analysis methods described have been developed as useful working tools over a period of about 30 years. This period roughly coincides with the period of rapid improvement of electronic digital computer systems. It will become evident that progress realized in analysis methods has come about through improved and more realistic modeling approximations in the equations describing the flow field combined with efficient numerical methods for solving the approximate equations. With the addition of ingenious methods for representation of those features of the experimentally observed flow field not adequately modeled by the equations, for example, flow detachment, clearance and corner flows, passage choking, shock waves, and density variations in the transonic and supersonic flow regimes, substantial gains have been made in practical resolution of a problem too complex for most human and computer memories to store, recall and assemble.~~

BASIS FOR THROUGH-FLOW CALCULATION METHODS

The overall structure of a turbomachine design system is exemplified by Figure 1. Necessarily, the initial phases of design involve "artistic" judgment based on experience and system technical requirements. The final phases include both extensive experimental verification and detailed prediction of critical flow field zones. The AGARD/PEP Working Group 12 study has been focused on the region of Figure 1 enclosed by a shaded boundary. Within this region, the lowest levels of elegance are represented by mean-line performance prediction methods and the highest by advanced computational procedures roughly corresponding to three-dimensional, steady relative flow.

In a mean-line performance prediction method for an axial-flow turbomachine, a single computation location, at the mean flow passage radius is specified at the entrance to and exit from each row of blades. In the more advanced methods, computation points may be specified at locations throughout the flow path, both in the axial spaces between rows and within the blade rows at arbitrary coordinate locations.

Characteristics of the Turbomachine Flow Field

The internal flow fields encountered in current turbomachines are viscous, compressible and unsteady. The flow passage geometry guarantees a thoroughly three-dimensional flow, and a significant fraction of the flow occurs in rotating passages.

As implied in the introduction, the situation is so complex that it is difficult to attain a comprehensive "mind's-eye" conception of the flow, a necessary prerequisite for development of a good engineering approximation. Some of the important phenomena influencing flow fields in modern axial-flow compressor blade rows are shown in Figure 2. These features have a significant effect on the overall flow field but they are not the only influential factors. What Figure 2 does not emphasize is that the phenomena shown take place in a strong through-flow or primary flow which is generally understandable in terms of the physical laws and corresponding equations of fluid dynamics. Many of the features of the flow field shown in Figure 2 might therefore be called secondary flows or secondary effects. This suggests the attractive, but not necessarily correct, possibility that such flows may be accounted for separately after determination of the primary flow field in a given case. How these flow features are included in individual through-flow calculation methods should be a central point in distinguishing between them.

Turbomachine flow fields occur in passages characterized by some unique geometric and kinematic features, which do not occur in other typical complex flows, either internal or external. These are shown in Figure 3, which also introduces the idea of looking at the flow field in a representative meridional, hub-to-tip section of a turbomachine.

An initial unique feature is the sequence of rotating and stationary internal flow passages. This introduces a recurring need to transfer frames of reference from inertial to non-inertial coordinates, considering relative flows in rotating rows and absolute flows in stationary blading. The effects of rotation on the flow within rotor blade rows should be considered.

A second unique feature existing in turbomachine flow fields is the transfer of energy in the flow process as work done on or by the fluid as it traverses the rotating elements.

A third unusual characteristic of turbomachine flows is the frequent close proximity of moving and stationary surfaces, clearly indicated in Figure 2. This complicates any attempts to evaluate the flow field using traditional boundary layer-main flow iterative methods.

Fluid Dynamics Supporting a Flow Model

The equations representing the physical laws controlling the flow field were clearly set forth with reference to turbomachine applications many years ago. Examples are found in work of Lorenz (1905), Bauersfeld (1905) and Stodola (1927). Because of the multiple forms and coordinate reference frames in which the equations are written in through-flow analyses, no attempt will be made to suggest a representative or recommended set in this review. The relevant physical laws and equation forms are listed in Table I.

It should again be noted that in development of flow models for the individual through-flow methods within the general classes described in the following sections, not all of the laws are necessarily used (satisfied), nor are all of the terms in the generalized equations representing each law used. It is of prime importance, but frequently very difficult, to determine what simplifications are made in each method.

Whether a specific through-flow method is based on the application of differential equation forms, integral equations or both, use is generally made of control surfaces which subdivide the flow passage by intersecting both the hub and tip (casing) boundaries. These control surfaces may be simple plane surfaces perpendicular to the rotational axis for some axial-flow compressors and turbines, or they may be conical or curved surfaces to conform to a leading or trailing edge trace in the meridional plane (see Figure 3), or to reach into some particular region of interest. The control surfaces may be, in particular through-flow methods, called computation surfaces, calculation stations, and channel solution surfaces. In this review the term control surface will be emphasized.

General Modeling Assumptions Used in Through-Flow Methods

A few assumptions are almost universally made in the through-flow calculation systems currently in use. The first of these is that the relative flow at the entrance and exit of each blade row is steady. Exceptions occur for some special analyses relating to non-uniform entrance flow (inlet distortion) and row interactions. The exceptions were considered outside the scope of the Working Group 12 effort.

The assumption of steady relative flow permits the definition of fluid particle paths by means of streamlines, stream surfaces and stream tubes. This simultaneously simplifies the through-flow problem and eliminates a feature of the real flow which is of unquestionable aerodynamic significance. Many through-flow procedures utilize the concept of S_1 and S_2 stream surfaces, generally attributed to Wu (1952a). S_1 surfaces are stream surfaces which cut the flow passage in the blade-to-blade direction as shown in Figure 4a. These surfaces are not surfaces of revolution but are a second kind of control surface which may be used to subdivide the total flow field into blade-to-blade stream tubes. S_2 surfaces are through-flow surfaces which intersect both the hub and casing as shown in Figure 4b. Notice that families of S_2 surfaces might be used as a third kind of control surface to divide the blade-to-blade flow into hub-to-shroud (casing) stream tubes.

A second nearly universal assumption in through-flow calculations, except for some cases concerned with cooled turbines, is that the flow is adiabatic so that no heat is transferred between fluid elements or across stream surfaces.

The terms axisymmetric flow and circumferential-average flow are frequently encountered in descriptions of assumed conditions in through-flow methods. The term axisymmetric flow is interpreted to mean that for any given set of axial and radial coordinate values in the flow field, no velocity component or fluid property varies in the circumferential direction. The term circumferential-average flow is usually used in reference to the flow on some designated S_2 surface (or approximation to an S_2 surface). It is taken to mean that the fluid velocity and properties at all coordinate points on that surface are correct circumferential averages of the values across the blade-to-blade passage at the corresponding radius and axial location. The significance of the two assumptions and the distinction between them is discussed by Wu (1952a), Smith (1966), Horlock and Marsh (1971) and Sehra (1979). One practical reason for either assumption is to permit or justify the subsequent modeling of S_1 surfaces as surfaces of revolution (axisymmetric S_1 surface approximations). This leads further to support of the use of linear cascade data in axial-flow turbomachine design, flow passage circumferential measurement surveys at constant radius, and the use of stream surface intersections with the meridional plane to show the nature of the hub-to-casing flow pattern.

A second reason for assuming the flow to be axisymmetric or for considering the flow on a particular approximation to an S_2 surface to be the circumferential average is that this allows one hub-to-shroud surface to be considered as representative. This obviously reduces the computational complexity of the through-flow analysis, along with the potential for predicting the true complexity of the flow.

CLASSIFICATION OF THROUGH-FLOW METHODS

The sequence of development of through-flow calculation systems is not easy to follow. There is evidence of numerous apparently independent efforts leading to remarkably similar approaches to the problem. In this section a brief review of the overall pattern of progression will be given. The emphasis is on the development of calculation systems primarily directed toward determination of the hub-to-shroud variations in the flow field. The elements involved in blade-to-blade flow field determination are contained in other contributions to the Working Group 12 report, and they are automatically included in those through-flow methods that are three-dimensional in character.

In studying through-flow calculation methods, it quickly becomes evident that some confusion may arise because of minor differences in the terminology used to classify individual methods into groups. In the following, six principal classes are used:

- (1) Mean-line method. For the flow passage under consideration, a mean line is defined. By one-dimensional calculations, heavily supported by empirical correlations of experimental data, fluid properties and velocities are estimated at specified locations on the mean line. These conditions are assumed representative of the passage at that location along the mean line.
- (2) Simple radial equilibrium method. A meridional flow passage is subdivided by a set of plane control surfaces perpendicular to the rotational axis. In each control surface the effects of any radial component of velocity are assumed negligible. The governing physical laws and empirical data are used to determine distribution of velocity and properties. This method is limited to assumed axisymmetric flows in axial turbomachines.
- (3) Streamline curvature method. This analysis method class is based on the direct determination, through iterative calculation, of the traces or projections of streamlines on a prescribed surface, for example on a meridional section of a turbomachine. An initial set of streamlines is assumed, and by successive iterative calculations, with each iteration improving the degree of satisfaction of the physical laws and empirical data correlations used in the flow model, a final set of streamlines is determined for a given flow rate, rotational speed, and entrance condition combination (see Figure 5). Velocities and fluid properties are predicted at locations on the streamlines corresponding to control surface intersections.
- (4) Finite-difference method. This analysis grouping is based on the initial definition of a system of grid points or nodes throughout the flow passage under study (see Figure 6). For the combination of physical laws and empirical information to be satisfied in the method, difference equations are written for each grid point. The equations are solved to determine the distributions of fluid properties and velocities at the nodal points. These distributions can be used to construct streamline patterns for the given passage operating condition.
- (5) Finite element method. The flow passage to be studied is subdivided by a network of lines into elements. Nodal points are located on the lines forming the boundary of each element. The physical laws and empirical input are formulated so that the fluid properties and velocities may be determined at each nodal point by iteration. Figure 7 shows an example set of elements.
- (6) Finite volume method. The flow passage is subdivided into a large number of small volume elements, fitted to the passage geometry as in Figure 8. The physical laws and empirical information governing the calculation are used to generate integral conservation equations for each small volume. The equations are solved, typically by an iterative time-marching process to reach a converged distribution of velocities and properties for the finite volume surfaces.

The vast majority of through-flow calculation methods may be placed within these classes.

SUMMARY OF THROUGH-FLOW CALCULATION DEVELOPMENT

This section will briefly describe the pattern of advancement leading toward current and projected through-flow calculation systems. The BIBLIOGRAPHY contains references to more extensive and detailed supporting documents.

The earliest through-flow calculation methods to be routinely used were mean-line analyses, and this class of methods continues to be developed and used for preliminary estimation of performance [e.g. Howell and Calvert (1978)]. The one-dimensional nature of mean-line analysis, with the necessary empiricism in estimation of the turning and loss characteristics of blade rows, eliminates the possibility for realistic flow field prediction.

Simple Radial Equilibrium Methods

As mentioned earlier, the differential equations of motion and the other relationships necessary for a through-flow field calculation were formulated in reference to a turbomachine problem during the early part of this century. However the first attempts to compute axial-flow turbomachine flow patterns used the simple-radial-equilibrium approximation. The idea of inviscid simple radial equilibrium was certainly understood in relation to the design point flow field before 1930 [Howell (1976)], and it was in common but not universal use for design by 1945. In design point application the equation was used without allowance for radial variation in blade row loss [Serovsky (1966), Voit (1953)]. The significance of the cumulative loss effect as measured by the radial gradient of entropy at a control surface was evaluated by Hatch, Giamattei and Jackson (1954), and later application to off-design flow field performance map prediction for compressors and pumps was based on non-isentropic simple radial equilibrium [Serovsky (1958), Serovsky, Kavanagh, Okiishi and Miller (1973)].

Streamline Curvature Methods

The influence on the hub-to-shroud flow patterns due to the terms in the radial component of the equation of motion representing streamline slope (due to radial velocity) and curvature (due to radial velocity change) was first described by Traupel (1942), and later by Wu and Wolfenstein (1950) and Hamric!, Ginsburg and Osborn (1950). Mechanisms for quantitative inclusion of the streamline shape effect in compressor and turbine design were reported by Smith, Traugott and Wislicenus (1953), Wright and Kovach (1953), and Hatch and Bernatowicz (1957). In design procedures used during this period there was little if any combined accounting for streamline shape and radial entropy gradient, although the possibility was mentioned by J. W. McBride in a discussion to the Smith et al. (1953) paper and by Giamattei

and Finger (1965). However, in performance prediction Swan (1958) included both streamline shape and loss distribution.

The term streamline curvature method became generally associated with this class of through-flow calculation following the work of Novak (1967) and Jansen and Moffatt (1967).

Although Wu (1952a) provided the basis for a hub-to-shroud flow field calculation including locations internal to blade rows and some design procedures tracing streamlines through blade rows were reported during the 1950s, performance prediction capability was first developed in about 1959 [Smith (1966)]. Smith also discussed the axisymmetric/circumferential-average flow question. Figure 5 shows a typical design point axial-flow compressor streamline set as computed by Smith's method.

Between 1960 and 1976 a substantial number of computer codes for axial-flow turbomachine flow field analysis were developed using streamline curvature methods. Most of these codes were based on assumption of axisymmetric, inviscid, adiabatic flow. Some of these codes permitted computation control surfaces internal to blade rows, but almost all depended on correlations of experimental linear and annular cascade results, including correlations of compressor and turbine test data for blade row turning and loss.

The assumption of inviscid flow in streamline curvature through-flow methods generally meant only that the local fluid shear stress effects were neglected by eliminating the corresponding terms in the momentum equations. However, the cumulative effect of fluid shear as measured by the entropy increase through a blade-to-blade stream tube was included through the hub-to-tip entropy variation.

Wu (1952a and 1980), Smith (1966), Horlock (1971), Wennerstrom (1974), and Bosman and Marsh (1974) have suggested similar mechanisms for removal of the inconsistency resulting from the local inviscid assumption by introducing correction terms to simulate the effect of fluid shearing stress in generation of irreversibility along fluid particle paths.

Finite Difference Methods

Finite difference methods for turbomachine through-flow analysis were first suggested and utilized between 1950 and 1960 [Wu (1950a, 1952a,b,c, and 1953)]. Figure 6 shows a grid point system used to predict a design point flow field by a finite difference method using relaxation solution techniques.

The term matrix through-flow method began to be commonly used to describe one group of finite difference methods following the work of Marsh (1968). Additional results from finite difference through-flow methods have been reported by Davis and Millar (1975 and 1976a), Biniaris (1975), Lindley et al. (1970) and Smith (1974).

Finite difference methods have demonstrated some advantages in calculations where internal blade row calculation locations are needed, and where three-dimensional effects are under study [Bosman and El-Shaarawi (1977)]. However the methods have not been as effectively developed for transonic flow cases as have some of the streamline curvature methods.

The finite difference methods developed up to about 1972 were of the inviscid type, and like the streamline curvature methods, included only the accumulated effects of viscous effects as an entropy distribution in the computed flow field. Loss correlations based on experiments were the basis for estimation of the entropy variation. More recent finite difference work [Bosman and Marsh (1974)] has included a mechanism for local viscous shear stress accounting.

Finite Element Methods

Finite element methods initially appeared as usable through-flow analysis techniques during the middle 1970s [Hirsch and Warzee (1974), Adler and Krimerman (1974)]. A key feature of the finite element method is its potential for development into a three-dimensional analysis system. Considerable progress has been made in this direction by Hirsch and Warzee (1979 and 1980).

The finite element mesh can be adapted readily to quite complex turbomachine geometries as shown in Figure 7. The same forms of correlation for turning and loss used in streamline curvature methods can and have been used in finite element analyses.

Finite Volume Methods

Along with the finite element methods, finite volume methods have a relatively short history. First proposed for blade-to-blade flow field analysis, recent investigations have focused on the hub-to-tip flow field, and on the strong potential for extension to an effective three-dimensional analysis method. Results have been reported by Denton and Singh (1979), Farn and Whirlow (1977), and Ivanov and Kimasov (1978).

The finite volume regions can, as in the case of the finite element mesh, be generated to conform to complex passage geometries. Figure 8 shows a three-dimensional example case.

Advanced Through-Flow Approaches

A number of additional through-flow analysis methods are in current use or under study. While the five classes of methods discussed above might be located in the LEVEL II category of Figure 1, all of the methods referenced in this section should be classified in Level III.

Dodge (1977) and Dodge and Lieber (1977 and 1978) have reported substantial use of a group of blade row flow field analyses programs. These techniques are useful in configuration development where detailed flow patterns not ordinarily available from Level II methods are needed internal to blade rows. Moore and Moore (1980a,b), Sovrano (1980) and Walitt (1980) have developed through-flow calculation systems for centrifugal compressor studies which appear to offer alternative capability in axial-flow turbomachine blade rows.

For unsteady through-flow calculations Erdos, Alzner and McNally (1977) have developed a time-dependent, inviscid computation system with capability in the transonic flow regime.

PROBLEM AREAS COMMON TO ALL THROUGH-FLOW METHODS

Aerodynamic Questions

Almost all of the through-flow calculation methods which have reached the status of routine use are in the Level II category of Figure 1. Except for a very limited number of finite element and finite volume methods, they are quasi-three-dimensional in character. This means that iteration occurs between two-dimensional hub-to-shroud computation and either two-dimensional blade-to-blade computation or correlations of experimental turning and loss data. The term two-dimensional as used here is not as restrictive as is ordinarily implied in, for example, linear cascade studies. In the two-dimensional through-flow case a blade-to-blade stream tube may change radius and vary in radial thickness. Variation in properties and velocity occur in the θ and x directions (Figures 4a and 4b), but the flow in each blade-to-blade stream tube is assumed to be independent of the flow in adjacent tubes. For this reason, the quasi-three-dimensional methods are not well adapted to accounting for passage three-dimensional aerodynamic flow features including flow separation, choking, shock waves, and end-wall, clearance and corner flows. Abundant evidence of the deficiencies in quasi-three-dimensional methods is available in reported work on non-axisymmetric streamline curvature and finite difference computation [e.g. Novak and Hearsey (1977)]. Some unusual strategies have been developed such as the introduction of an additional set of computational surfaces by Katsanis and McNally (1977) as shown in Figure 9. Although a considerable history now exists in the development of through-flow methods, it should be noted that flow models and equations remain controversial in some areas. This is recalled to attention by recently published work of Wu (1980) concerned with the modeling of the effects of shear stresses within blade rows.

For quasi-three-dimensional and three-dimensional methods in the Level II category of Figure 1, questions arise when fluid turning and loss data is used at blade row internal locations. These questions originate in both the scarcity of data and the mechanism for use of correlations.

Computational Questions

Reports on through-flow computation code development and application frequently do not provide adequate information concerning numerical methods and code organization. Because the solutions are iterative in character, the iterative strategy is important and methods used to improve stability at convergence significantly influence the cost and quality of results.

Table I. Equations for turbomachine through-flow calculation

PHYSICAL LAW	EQUATION FORM	EXAMPLE SOURCES
Conservation of linear momentum	Differential equations (3 components)	Wu and Wolfenstein (1950) Wu (1952a)
	Integral equation for fluid volume element	Denton and Singh (1979) Farn and Whirlow (1977)
Conservation of moment of momentum (Euler turbine equation)	Differential equation (1 component)	Wu (1952a)
	Integral equation - fluid volume element stream tube	Denton and Singh (1979) Wennerstrom (1974) Hearsey (1975)
Conservation of mass	Differential equation	Wu (1952a) Marsh (1976)
	Integral equation - fluid volume element	Denton and Singh (1979) Farn and Whirlow (1977)
	stream tube control surface	Wu and Wolfenstein (1950) Hearsey (1975)

Table I. Continued

PHYSICAL LAW	EQUATION FORM	EXAMPLE SOURCES
First law of thermodynamics	Differential equation	Wu (1952a)
	Integral equation - finite volume element	Denton and Singh (1979) Farn and Whirlow (1977)
	stream tube	Wu and Wolfenstein (1950) Hearsey (1975)
Second law of thermodynamics	Differential equation	Wu and Wolfenstein (1950) Wu (1980)

BIBLIOGRAPHY

- Adler, Dan. 1979. Status of centrifugal impeller internal aerodynamics: Experiments and calculations. U.S. Naval Postgraduate School. NPS67-79-004.
- Adler, Dan. 1980a. Status of centrifugal impeller internal aerodynamics. Part I: Inviscid flow prediction methods. *Journal of Engineering for Power, Transactions of the ASME* 102: 728-737.
- Adler, Dan. 1980b. Status of centrifugal impeller internal aerodynamics. Part II: Experiments and influence of viscosity. *Journal of Engineering for Power, Transactions of the ASME* 102: 738-746.
- Adler, D., and Y. Krimerman. 1974. The numerical calculation of the meridional flow field in turbomachines using the finite elements method. *Israel Journal Tech.* 12: 268-274.
- Adler, D., and Y. Krimerman. 1977. Calculation of the blade-to-blade compressible flow field in turbo impellers using the finite-element method. *Journal of Mechanical Engineering Science* 19: 108-112.
- Adler, D., and Y. Krimerman. 1980a. Comparison between the calculated subsonic inviscid three-dimensional flow in a centrifugal impeller and measurements. Pages 19-26 in *Performance prediction of centrifugal pumps and compressors*. New York. ASME.
- Adler, D., and Y. Krimerman. 1980b. On the relevance of inviscid subsonic flow calculations to real centrifugal impellers flow. *Journal of Fluids Engineering, Transactions of ASME* 102: 78-84.
- Araki, T. 1974. Three-dimensional flow through turbines. In *Heat and Fluid Flow in Steam and Gas Turbine Plant*, IME Conf. Proc. 3: 38-45. (Discussion J. D. Denton, pp. 290-292.)
- Balsa, T. F., and G. L. Mellor. 1975. The simulation of axial compressor performance using an annulus wall boundary layer theory. *Journal of Engineering for Power, Transactions of the ASME* 97: 305-318.
- Bauersfeld, W. 1905. *Zuschrift an die Redaktion. V.D.I. Zeitschrift.* 49: 2007-2008.
- Bauersfeld, W. 1922. Die Grundlagen zur Berechnung schnellaufender Kreiselräder. *V.D.I. Zeitschrift.* 66: 461-465, 514-517.
- Biniaris, S. 1975. The calculation of the quasi-three-dimensional flow in an axial gas turbine. *Journal of Engineering for Power, Transactions of the ASME* 97: 283-294.
- Bosman, C. 1973. The occurrence and removal of indeterminacy in flow calculations in turbomachinery. ARC Rep. and Memo. 3746.
- Bosman, C. 1980. An analysis of three-dimensional flow in a centrifugal impeller. *Journal of Engineering for Power, Transactions of the ASME* 102: 619-625.
- Bosman, C., and M. A. I. El-Shaarawi. 1977. Quasi-three-dimensional numerical solution of flow in turbomachines. *Journal of Fluids Engineering, Transactions of the ASME* 99: 132-140.
- Bosman, C., and J. Highton. 1979. A calculation procedure for three-dimensional, time-dependent, inviscid, compressible flow through turbomachine blades of any geometry. *Journal of Mechanical Engineering Science* 21: 39-49.
- Bosman, C., M. Hill, and L. Deshpande. 1974. The effect of damping factor on the behavior of flow calculations in turbomachines. ARC Rep. and Memo. 3766.
- Bosman, C., and H. Marsh. 1974. An improved method for calculating the flow in turbomachines, including a consistent loss model. *Journal of Mechanical Engineering Science* 16: 25-31.
- Bryans, A. C., and M. L. Miller. 1967. Computer program for design of multistage axial-flow compressors. NASA CR-54530.
- Burger, G. D., D. Lee, and D. W. Snow. 1979. Study of blade aspect ratio on a compressor front stage. Aerodynamic and Mechanical Design Report. NASA CR-159555.
- Calmon, J. 1969. L'Ecoulement d'un fluide compressible dans un étage de turbomachine. *Entropie*. No. 27, pp. 15-20, Mar-Juin. No. 28, pp. 38-44, Juillet-Aout. No. 29, pp. 19-27, Septembre-Octobre.
- Carter, Anthony F. 1976. A critical review of turbine flow calculation procedures. In *Through-flow calculations in axial turbomachinery*. AGARD-CP-195. Paper 9.
- Carter, A. F., and F. K. Lenherr. 1969. Analysis of geometry and design-point performance of axial-flow turbines using specified meridional velocity gradients. NASA CR-1456.
- Carter, A. F., M. Platt, and F. K. Lenherr. 1968. Analysis of geometry and design point performance of axial flow turbines. I - Development of the analysis method and the loss coefficient correlation. NASA-CR-1181.
- Caruthers, John E., and Theodore F. McKain. 1976. Through-flow calculations: Theory and practice in turbomachine design. In *Through-flow calculations in axial turbomachinery*. AGARD-CP-195. Paper 4.
- Celikovský, Karel. 1965. The solution of the direct problem of the viscous and compressible flow through an axial turbomachine under the axial-symmetry conditions. *Kandidátská Dízeracní Práce-VAAZ Brno*. (In CZECH).

- Celikovský, Karel. 1970. Model investigations of subsonic stages of an axial compressor (summary report). Zpráva VZLÚ, ARTI Report Z-14.
- Celikovský, Karel. 1974. Research into the axial-flow transonic compressor stages. Zpráva VZLÚ, ARTI Report Z-19.
- Cox, H. J. A. 1976. Through-flow calculation procedures for application to high speed large turbines. In Through-flow calculations in axial turbomachinery. AGARD-CP-195. Paper 7.
- Creveling, H. F., and R. H. Carmody. 1968a. Axial flow compressor design computer programs incorporating full radial equilibrium. Part I - Flow path and radial distribution of energy specified (Program II). NASA CR-54532.
- Creveling, H. F., and R. H. Carmody. 1968b. Axial flow compressor design computer programs incorporating full radial equilibrium. Part II - Radial distribution of total pressure and flow path or axial velocity ratio specified (Program III). NASA CR-54531.
- Creveling, H. F., and R. H. Carmody. 1968c. Compressor computer program for calculating off-design performance (Program IV). NASA CR-72427.
- Dallenbach, F. 1961. The aerodynamic design and performance of centrifugal and mixed-flow compressors. In Centrifugal compressors. SAE Tech. Progress Series, No. 3. pp. 2-30.
- Daneshyar, H. 1970. The off-design analysis of flow in axial compressors. Department of Engineering, University of Cambridge. CUED/A-Turbo/TR 19.
- Davis, W. R. 1968. A comparison of different forms of the quasi-three-dimensional radial equilibrium equation of turbomachines. Carleton University. Div. of Aerothermodynamics Report No. ME/A 68-1.
- Davis, W. R. 1970. A computer program for the analysis and design of the flow in turbomachinery. Part B - Loss and deviation correlations. Carleton University. Div. of Aerothermodynamics Report No. ME/A 70-1.
- Davis, W. R. 1971. A computer program for the analysis and design of turbomachinery--Revision. Carleton University. Div. of Aerothermodynamics Report No. ME/A 71-5.
- Davis, W. R. 1975. A general finite difference technique for the compressible flow in the meridional plane of centrifugal turbomachinery. ASME Paper 75-GT-121.
- Davis, W. R., and D. A. J. Millar. 1972. A discussion of the Marsh matrix technique applied to fluid flow problems. C.A.S.I. Trans. 5 (2): 64-70.
- Davis, W. R., and D. A. J. Millar. 1973. Axial flow compressor analysis using a matrix method--revision. Carleton University. Div. of Aerothermodynamics Report No. ME/A 73-1.
- Davis, W. R., and D. A. J. Millar. 1975. A comparison of the matrix and streamline curvature methods of axial flow turbomachinery analysis, from a user's point of view. Journal of Engineering for Power, Transactions of the ASME 97: 549-560.
- Davis, W. Roland, and D. A. J. Millar. 1976a. Through flow calculations based on matrix inversion: Loss prediction. In Through-flow calculations in axial turbomachinery. AGARD-CP-195. Paper 3.
- Davis, W. R., and D. A. J. Millar. 1976b. Axial flow compressor analysis using a streamline curvature method. Carleton University. Div. of Aerothermodynamics Report No. ME/A 76-3.
- Denton, John D. 1978. Throughflow calculations for transonic axial flow turbines. Journal of Engineering for Power, Transactions of the ASME 100: 212-218.
- Denton, J. D., and U. K. Singh. 1979. Time marching methods for turbomachinery flow calculations. von Karman Institute. Lecture Series, Application of numerical methods to flow calculations in turbomachines.
- DeRuyck, J., C. Hirsch, and P. Kool. 1979. An axial compressor end-wall boundary layer calculation method. Journal of Engineering for Power, Transactions of the ASME 101: 233-249.
- Deshpande, R. B. 1975. A new algorithm for the solution of turbomachinery flow problems. Journal of Fluids Engineering, Transactions of the ASME 97: 372-374.
- Dodge, Paul R. 1976. A non-orthogonal transonic relaxation method for cascade flows. ASME Paper 76-GT-63.
- Dodge, P. R. 1977. Numerical method for 2D and 3D viscous flows. AIAA Journal 15: 961-965.
- Dodge, P. R., and L. S. Lieber. 1977. A numerical method for the solution of the Navier-Stokes equations with separated flow. AIAA Paper 77-170.
- Dodge, P. R., and L. S. Lieber. 1978. 3-D flow analysis of compressor cascade with splitter vanes. AFAPL-TR-78-23.
- Dorfman, L. A. 1974. Chislennyye Metody v Gazodinamike Turbomashin (Numerical Methods in Gas Dynamic Turbomachines). Izd-vo Energiya, Lenigradskoye Otdeleniye.

- Doyle, M. D. C. 1971. Advanced through-flow analysis applied to a low speed axial flow compressor. *Intl. Jour. Mech. Engr. Sci.* 13: 833-842.
- Doyle, V. L., and C. C. Koch. 1970. Evaluation of range and distortion tolerance for high Mach number transonic fan stages, design report. NASA CR-72720.
- Dreyfus, L. A. 1946. A three-dimensional theory of turbine flow and its application to the design of wheel vanes for Francis and propeller turbines. *Acta Polytechnia, Mech. Engr. Series*, Vol. 1, No. 1.
- Duncombe, E. 1964. Aerodynamic design of axial flow turbines. In *Aerodynamics of turbines and compressors*. Princeton, Princeton Univ. Press. pp. 433-523.
- Dunker, R. J., P. E. Strinning, and H. B. Weyer. 1978. Experimental study of the flow field within a transonic axial compressor rotor by laser velocimetry and comparison with through-flow calculations. *Journal of Engineering for Power, Transactions of the ASME* 100: 279-286.
- Eckert, E., and G. K. Korbacher. 1947. The flow through axial turbine stages of large radial blade length. NACA TM-1118.
- Erdos, John I., and Edgar Alzner. 1977. Computation of unsteady transonic flows through rotating and stationary cascades. I - Method of analysis. NASA CR-2900.
- Erdos, John, Edgar Alzner, and Paul Kalben. 1977. Computation of steady and periodic two-dimensional non-linear transonic flows in fan and compressor stages. In *Transonic flow problems in turbomachinery*. Washington, D.C., Hemisphere Publ. Corp. pp. 95-111.
- Erdos, John, Edgar Alzner, Paul Kalben, William McNally, and Simon Slutsky. 1975. Time-dependent transonic flow solutions for axial turbomachinery. In *Aerodynamic analyses requiring advanced computers*. NASA SP-347, Part I. pp. 587-621.
- Erdos, J. I., E. Alzner, and W. McNally. 1977. Solution of periodic transonic flow through a fan stage. *AIAA Journal* 15: 1559-1568.
- Farn, C. L., and D. K. Whirlow. 1977. Application of time-dependent finite volume method to transonic flow in large turbines. In *Transonic flow problems in turbomachinery*. Washington, D.C., Hemisphere Publ. Corp. pp. 208-227.
- Flagg, E. E. 1967. Analytical procedure and computer program for determining the off-design performance of axial flow turbines. NASA CR-710.
- Frost, D. H. 1970. A streamline curvature through flow computer program for analyzing the flow through axial flow turbomachines. ARC Rep. and Memo. 3687.
- Fruehauf, Hans-Heiner. 1977. Applicability of axisymmetric analysis in predicting supersonic flow through annular cascades. *Journal of Engineering for Power, Transactions of the ASME* 99: 115-120.
- Giamati, G. C., Jr., and H. B. Finger. 1965. Design velocity distribution in meridional plane. In *Aerodynamic design of axial-flow compressors*. NASA SP-36. Chapter VIII.
- Glenny, D. E. 1974. An application of streamline curvature methods to the calculation of flow in a multistage axial compressor. Aerc. Res. Labs (Australia). Note ARL/M.E. 346.
- Glenny, D. E. 1975. Performance evaluation of a multistage axial compressor using a streamline curvature model. ASME Paper 75-WA/GT-10.
- Goulas, A. Flow in centrifugal compressor impellers--A theoretical and experimental study.
- Goulas, Apostoles, and Roger C. Baker. 1978. Through flow analysis of viscous and turbulent flows. Aero. Res. Council C.P. 1382.
- Goulas, A., and R. C. Baker. 1978. Through flow analysis of centrifugal compressors. ASME Paper 78-GT-110.
- Grahl, K. G. 1972. Prediction of compressor aerodynamic performance for multistage compressor. Report 29. Dynalysis of Princeton, Princeton, NJ.
- Grahl, Klaus G. 1972. Teillasbhrechnung für Axialverdichterstufen. *Zeit. Flugwiss.* 20: 42-51.
- Grahl, Klaus G. Über den Stand Der Kennfeldberechnung Mehrstufiger Axialverdichter. *Zeit. Flugwiss. Weltraumforsch.* 1: 29-41.
- Guiraud, J. P., and R. Kh. Zeytounian. 1971-2. Sur la structure des écoulements tourbillonnaires dans les turbomachines axiales. *La Rech. Aeron.* No. 1971-2, pp. 65-87.
- Guiraud, J. P., and R. Kh. Zeytounian. Analyse de l'écoulement l'entrée et la sortie d'une roue. *La Rech. Aeron.* No. 1971-5, pp. 237-256.
- Hajek, T., and S. Gopalakrishnan. 1980. Prediction of flow in centrifugal impellers. In *Performance prediction of centrifugal pumps and compressors*. New York. ASME pp. 27-31.
- Hamrick, Joseph T., Ambrose Ginsburg, and Walter M. Osborn. 1950. Method of analysis for compressible flow through mixed-flow centrifugal impellers of arbitrary design. NACA Report 1082.

- Hatch, J. E., and D. T. Bernatowicz. 1957. Aerodynamic design and overall performance of first spool of a 24-inch two-spool transonic compressor. NACA RM F56L07a.
- Hatch, J. E., G. C. Giamatyi, and R. J. Jackson. 1954. Application of radial-equilibrium condition to axial-flow turbomachinery design including consideration of change of entropy with radius downstream of blade row. NACA RM L54A20.
- Hearsey, R. A. 1975. A revised computer program for axial compressor design. Volume I: Theory, descriptions and user's instructions. ARL TR 75-0001, Volume I. 1975. Volume II: Program listing and program use example. ARL TR 75-0001, Volume II. 1975.
- Herzig, H. Z., and A. G. Hansen. 1965. Three-dimensional compressor flow theory and real flow effects. In Aerodynamic design of axial-flow compressors. NASA SP-36. Chapter XIV.
- Herzog, Josef. 1974. Calculation of flow distribution in large radius ratio stages of axial flow turbines and comparison of theory and experiment. In Fluid mechanics, acoustics, and design of turbomachinery. NASA SP-304, Part II, pp. 565-580.
- Hetherington, R. 1970. Computer calculations of the flow in axial compressors. In Internal aerodynamics (turbomachinery). London. IME. Paper 6, pp. 57-63.
- Hirsch, Ch. 1974. End-wall boundary layers in axial compressors. Journal of Engineering for Power, Transactions of the ASME 96: 413-426.
- Hirsch, Ch. 1976a. Unsteady contributions to steady radial equilibrium flow equations. In Unsteady phenomena in turbomachines. AGARD-CP-177, Paper 13.
- Hirsch, Ch. 1976b. Finite element method for through-flow calculations. In Through-flow calculations in axial turbomachinery. AGARD-CP-195. Paper 5.
- Hirsch, Ch. 1976c. Flow prediction in axial flow compressors including end wall boundary layers. ASME Paper 76-GT-72.
- Hirsch, Ch., Ch. Lacor, and G. Warzee. 1980. Three-dimensional inviscid calculations in centrifugal compressors. In Centrifugal compressors, flow phenomena and performance. AGARD-CP-282. Paper 7.
- Hirsch, Ch., and G. Warzee. 1974. A finite element method for flow calculations in turbomachines. Vrije Universiteit Brussel, Dienst Stromingsmechanica. Report VUB-STR-5.
- Hirsch, Ch., and G. Warzee. 1976. A finite element method for through-flow calculations in turbomachines. Journal of Fluids Engineering, Transactions of the ASME 98: 403-421.
- Hirsch, Ch., and G. Warzee. 1977. Blade-to-blade subsonic flow calculation with finite elements. Vrije Universiteit Brussel, Dienst Stromingsmechanica. Report VUB-STR-7.
- Hirsch, Ch., and G. Warzee. 1979. An integrated quasi-3D finite element calculation program for turbomachinery flows. Journal of Engineering for Power, Transactions of the ASME 101: 141-148.
- Hirsch, Ch., and G. Warzee. 1980. Quasi 3-D finite element computation of flows in centrifugal compressors. In Performance prediction of centrifugal pumps and compressors. New York. ASME. pp. 69-75.
- Holman, F. F., J. R. Kidwell, and T. C. Ware. 1976. Small axial compressor technology program. Volume I. NASA CR-134827.
- Holmquist, C. O., and W. D. Rannie. 1956. An approximate method of calculating three-dimensional compressible flow in axial turbomachines. Journal of Aeronautical Sciences 23: 543-556, 582.
- Horlock, J. H. 1971. On entropy production in adiabatic flow in turbomachines. Journal of Basic Engineering, Transactions of the ASME 93: 587-593.
- Horlock, J. H., and H. Marsh. 1971. Flow models for turbomachines. Journal of Mechanical Engineering Science 13: 358-368.
- Howell, A. R. 1976. Griffith's early ideas on turbomachinery aerodynamics. Aeronautical Journal 80: 521-529.
- Howell, A. R., and W. J. Calvert. 1978. A new stage stacking technique for axial-flow compressor performance prediction. Journal of Engineering for Power, Transactions of the ASME 100: 698-703.
- Ivanov, M. Ya., and Yu. I. Kimasov. 1978. Numerical solution of the problem of determining the average, axisymmetric flow of an ideal gas through turbomachine stages. Fluid Mechanics--Soviet Research 7: 4: 143-152. July-August.
- Jansen, W., and W. C. Moffatt. 1967. The off-design analysis of axial-flow compressors. Journal of Engineering for Power, Transactions of the ASME 89: 453-462.
- Jansen, W. 1970. A method for calculating the flow in a centrifugal impeller when energy gradients are present. In Internal aerodynamics (turbomachinery). London. IME. Paper 12, pp. 133-146.
- Japikse, David. 1976. Review--Progress in numerical turbomachinery analysis. Journal of Fluids Engineering, Transactions of the ASME 98: 592-606.

- Johnsen, I. A. 1952. Investigation of a 10-stage subsonic axial-flow research compressor. I - Aerodynamic design. NACA RM E52B18.
- Karlsson, T. 1953. On the influence of radial components of blade forces in axial turbomachines. M.E. Thesis. Cal. Inst. Tech.
- Katsanis, Theodore. 1964. Use of arbitrary quasi-orthogonals for calculating flow distribution in the meridional plane of a turbomachine. NASA TN D-2546.
- Katsanis, Theodore. 1965. Use of arbitrary quasi-orthogonals for calculating flow distribution on a blade-to-blade surface in a turbomachine. NASA TN D-2809.
- Katsanis, Theodore. 1966. Use of arbitrary quasi-orthogonals for calculating flow distribution in a turbomachine. Journal of Engineering for Power, Transactions of the ASME 88: 197-202.
- Katsanis, Theodore. 1967. A computer program for calculating velocities and streamlines for two-dimensional, incompressible flow in axial blade rows. NASA TN D-3762.
- Katsanis, Theodore. 1968. Computer program for calculating velocities and streamlines on a blade-to-blade stream surface of a turbomachine. NASA TN D-4525.
- Katsanis, Theodore. 1969. FORTRAN program for calculating transonic velocities on a blade-to-blade stream surface of a turbomachine. NASA TN D-5427.
- Katsanis, Theodore. 1971. FORTRAN program for quasi-three-dimensional calculation of surface velocities and choking flow for turbomachine blade rows. NASA TN D-6177.
- Katsanis, Theodore, and William D. McNally. 1969. Revised fortran program for calculating velocities and streamlines on a blade-to-blade stream surface of a turbomachine. NASA TM X-1764.
- Katsanis, Theodore, and William D. McNally. 1977. Revised fortran program for calculating velocities and streamlines on the hub-shroud midchannel stream surface of an axial-, radial-, or mixed-flow turbomachine or annular duct. I - User's Manual. NASA TN D-8430. II - Programmer's Manual. NASA TN D-8431.
- Khalil, I., W. Tabakoff, and A. Hamed. 1980. Viscous flow analysis in mixed flow rotors. Journal of Engineering for Power, Transactions of the ASME 102: 193-201.
- Kholshchevnikov, K. V. 1970. Teoriya i raschet aviationsionnykh lopatochnykh mashin (Theory and design of aircraft turbomachines). Moscow. Mashinostroyeniye Press.
- Kramer, James J., Norbert O. Stockman, and Ralph J. Bean. 1962. Non-viscous flow through a pure impeller on a blade-to-blade surface of revolution. NASA TN D-1108.
- Krimerman, Y., and D. Adler. 1978. The complete three-dimensional calculation of the compressible flow field in turbo impellers. Journal of Mechanical Engineering Science 20: 149-158.
- Kurmanov, B. I., G. L. Podvidz, and G. Yu Stepanov. 1977. Analysis of two-dimensional gas flow in turbomachinery cascades by means of integral relations. Fluid Dynamics. No. 4: 560-566. July-August.
- Lenherr, F. K., et al. The analysis of geometry and design point performance of axial-flow turbines using specified meridional velocity gradients. Part 2: Design examples. NASA CR-72585.
- Lieblein, Seymour. 1954. Review of high-performance axial-flow compressor blade element theory. NACA RM E53L22.
- Lindley, D., J. Westmoreland, and J. F. T. Whybrow. 1970. Some problems in the application of meridional flow programs to the design of large steam turbines. In Axial and radial turbomachinery. Proc. IME. 184, Part 3G (II): 38-48.
- Liu, H. C., T. C. Booth, and W. A. Tall. 1979. An application of 3-D viscous flow analysis to the design of a low-aspect-ratio turbine. ASME Paper 79-GT-53.
- Lorenz, H. 1905. Theorie und berechnung der volturbinen und krieselpumpen. V. D. I. Zeitschrift. 49: 41: 1670-1675.
- Luu, T. S., M. M. Abdelrahman, and Y. Ribaud. 1980. Transonic flow analysis in an impeller equipped with splitter blades. In Performance prediction of centrifugal pumps and compressors. New York, ASME pp. 47-60.
- McBride, Mark W. 1977. A streamline curvature method of analyzing axisymmetric axial, mixed and radial flow turbomachinery. Penn. State University, Applied Research Laboratory. TM 77-219.
- McBride, Mark W. 1979. The design and analysis of turbomachinery in an incompressible, steady flow using the streamline curvature method. Penn. State University, Applied Research Laboratory. TM 79-33.
- McDonald, P. W., C. R. Bolt, R. J. Dunker, and H. B. Wayer. 1980. A comparison between measured and computed flow fields in a transonic compressor rotor. ASME Paper 80-GT-7.
- Macchi, E. 1970. Computer program for prediction of axial flow turbine performance. U.S. Naval Post-graduate School. NPS-57Ma 70081a.

- Marsh, H. 1968. A digital computer program for the through-flow fluid mechanics in an arbitrary turbomachine using a matrix method. (NGTE Report R282. 1966.) ARC Rep. and Memo. 3509. 1968.
- Marsh, H. 1970. The through-flow analysis of axial flow compressors. In Advanced compressors. AGARD-LS-39-70. Paper 2.
- Marsh, H. 1972. The uniqueness of turbomachinery flow calculations using the streamline curvature and matrix through-flow methods. Journal of Mechanical Engineering Science 13: 376-379. 1971. Also Hearsey, R. M., and H. Marsh. Communication. Journal of Mechanical Engineering Science 14: 294-296. 1972.
- Marsh, H. 1976. Through-flow calculations in axial turbomachinery: A technical point of view. In Through-flow calculations in axial turbomachinery. AGARD-CP-195. Paper 2.
- Messenger, H. E., E. E. Kennedy. 1972. Two-stage fan. I - Aerodynamic and mechanical design. NASA CR-120859.
- Miller, M. L., and A. C. Bryans. 1967. Parametric study of advanced multistage axial-flow compressors. NASA CR-797.
- Monsarrat, N. T., M. J. Keenan, and P. C. Tramm. 1969. Design report. Single stage evaluation of highly-loaded high-Mach number compressor stages. NASA CR-72562.
- Moore, J., and J. G. Moore. 1980. Three-dimensional, viscous flow calculations for assessing the thermodynamic performance of centrifugal compressors--Study of the Eckardt compressor. In Centrifugal compressors, flow phenomena and performance. AGARD-CP-282. Paper 9.
- Moore, J., and J. G. Moore. 1980. Calculations of three-dimensional, viscous flow and wake development in a centrifugal impeller. In Performance prediction of centrifugal pumps and compressors. New York. ASME. pp. 61-67.
- Mukherjee, D. K. 1976. Design of turbine, using distributed or average losses; effect of blowing. In Through-flow calculations in axial turbomachinery. AGARD-CP-195. Paper 8.
- Ngo, Vinh-Hai, and D. A. J. Miller. 1973. The design and performance prediction of axial flow turbines. Carleton University Dept. of Mech. and Aeron. Engrg. Rep. No. ME 73-3.
- Novak, R. A. 1967. Streamline curvature computing procedures for fluid-flow problems. Journal of Engineering for Power, Transactions of the ASME 89: 478-490.
- Novak, Richard A. 1976. Flow field and performance map computation for axial-flow compressors and turbines. In Modern prediction methods for turbomachine performance. AGARD-LS-83. Paper 5.
- Novak, R. A., and R. M. Hearsey. 1977. A nearly three-dimensional intrablade computing system for turbomachinery. Journal of Fluids Engineering, Transactions of the ASME 99: 154-166.
- Oates, Gordon C. 1972. Actuator disk theory for incompressible highly rotating flows. Journal of Basic Engineering, Transactions of the ASME 94: 613-621.
- Oates, G. C., and C. J. Knight. 1973. Through-flow theory for turbomachines. AFAPL-TR-73-61.
- Oates, G. C., and G. F. Carey. 1974. A variational formulation of the compressible through-flow problem. AFAPL-TR-74-78.
- Oates, G. C., C. J. Knight, and G. F. Carey. 1976. A variational formulation of the compressible through-flow problem. Journal of Engineering for Power, Transactions of the ASME. 98: 1-8.
- Oldham, R. K. 1968. A computer program for predicting the performance of axial flow turbomachines by the streamline curvature model. NGTE NT717.
- Papailiou, Kyriacos D. 1971. Program for the design of an axial compressor stage based on the radial equilibrium equations. U.S. Naval Postgraduate School. NPS-57PY 71091A.
- Platt, M., and A. F. Carter. 1968. Analysis of geometry and design point performance of axial flow turbines. II - Computer Program. NASA CR-1187.
- Podvidz, G. L. 1971. Calculation of the quasi three-dimensional flow of a gas in the interblade channel of an axial turbine. Izv. Akad. Nauk SSSR, Mekh. Zhidk. i Gaza. No. 4: 92-101.
- Renaudin, A., and E. Somm. 1970. Quasi-three-dimensional flow in a multistage turbine--Calculation and experimental verification. In Flow research on blading. Amsterdam, Elsevier Publishing Company.
- Ribaut, M. 1968. Three-dimensional calculation of flow in turbomachines with the aid of singularities. Journal of Engineering for Power, Transactions of the ASME 90: 258-264.
- Ribaut, M., and R. Vainio. 1975. On the calculation of two-dimensional subsonic and shock-free transonic flow. Journal of Engineering for Power, Transactions of the ASME 97: 603-609.
- Ribaut, M. 1977. On the calculation of three-dimensional divergent and rotational flow in turbomachines. Journal of Fluids Engineering, Transactions of the ASME 99: 187-196.
- Richter, W. 1970. Discussion. In Internal aerodynamics (turbomachinery). London, IME. pp. 67-79.

- Ruden, P. 1944. Investigation of single stage axial fans. NACA TM 1062. (Trans. from *Luftfahrtforschung*, 14: 325-326, July 20, 1937 and 14: 468-473, Sept. 9, 1937).
- Sandercock, D. M., K. Kovach, and S. Lieblein. 1954. Experimental investigation of a five-stage axial-flow research compressor with transonic rotors in all stages. I - Compressor Design. NACA RM E54P24.
- Schilhansl, M. J. 1965. Three-dimensional theory of incompressible and inviscid flow through mixed flow turbomachines. *Journal of Engineering for Power, Transactions of the ASME* 87: 361-373.
- Schröder, H. J. 1972. Die Wirbelscheibenmethode in Anwendung auf die Auslegung Axialer Turbomaschinen. *VDI-Fortschr'tts-Bericht. Reihe 7. Nr. 28.*
- Schröder, H. J., and P. Schuster. 1972. Actuator disc flow calculated by relaxation. An approach to the analysis problem of turbomachinery. *ASME Paper 72-GT-26.*
- Schütz, J. 1971. Beitrag zur berechnung der strömung in stufen axialem thermischer turbomaschinen. Dissertation. TU Darmstadt.
- Sehra, Arun K. 1979. Boundary layer and wake modifications to compressor design systems: The effect of blade-to-blade flow variations on the mean flow field of a transonic rotor. *AFAPL-TR-79-2010.*
- Sehra, A. K., and J. L. Kerrebrock. 1979. The effect of blade-to-blade flow variations on the mean flow field of a transonic compressor. *AIAA Paper 79-1515.*
- Seippel, C. 1958. Three-dimensional flow in multistage turbines. *Brown Boveri Review.* 45: 99-107.
- Senoo, Y., and Y. Nakase. 1972. An analysis of flow through a mixed flow impeller. *Journal of Engineering for Power, Transactions of the ASME* 94: 43-50.
- Serovy, George K. 1958. A method for the prediction of the off-design performance of axial-flow compressors. Ph.D. Dissertation, Iowa State University, Ames, Iowa.
- Serovy, George K. 1966. Recent progress in aerodynamic design of axial-flow compressors in the United States. *Journal of Engineering for Power, Transactions of the ASME* 88: 251-261.
- Serovy, G. K. and E. W. Anderson. 1959. Method for predicting off-design performance of axial-flow compressor blade rows. *NASA TN D-110.*
- Serovy, G. K., and J. C. Lysen. 1963. Prediction of axial flow turbomachine performance by blade-element methods. *Journal of Engineering for Power, Transactions of the ASME* 85: 1-8.
- Serovy, George K., Patrick Kavanagh, Theodore H. Okiishi, and Max J. Miller. 1973. Prediction of overall and blade-element performance for axial-flow pump configuration. *NASA CR-2301.*
- Seyler, D. R., and L. H. Smith, Jr. 1967. Single stage experimental evaluation of high Mach number compressor rotor blading. Part I - Design of rotor blading. *NASA CR-54581.*
- Silvester, M. E., and R. Hetherington. 1966. Three dimensional compressible flow through axial flow turbomachines. *In Numerical analysis: An introduction.* New York. Academic Press.
- Sinnette, John T., Oscar W. Schey, and J. Austin King. 1943. Performance of NACA eight-stage axial-flow compressor designed on the basis of airfoil theory. *NACA Rep. 758.*
- Sirokin, Ya. A. 1961. Calculation of the axisymmetric, vortex flow, inviscid and compressible flow in axial-flow turbomachines. *Izv. Akad. Nauk SSR. Mekhanika i Mashinostroenie.* No. 2. pp. 78-80. March-April. (In Russian.)
- Sirokin, Ya. A. 1972a. Calculation of the twist of long blades in axial turbines and compressors with an electronic computer. *Energomashinostroenie.* 18: 4-7.
- Sirokin, Ya. A. 1972b. Aerodynamicheskiy raschet lopatok osevykh turbomashin. *Izd-vo Mashinostroyeniye. Moscow.*
- Smith, D. J. L. 1974. Computer solution of Wu's equations for compressible flow through turbomachines. *In Fluid mechanics, acoustics and design of turbomachinery.* NASA SP-304, Part I: 43-74.
- Smith, D. J. L., and J. F. Barnes. 1968. Calculation of fluid motion in axial flow turbomachines. *ASME Paper 68-GT-12.*
- Smith, D. J. L., and D. H. Frost. 1969-70. Calculation of the flow past turbomachine blades. *In Axial and radial turbomachinery.* Proc. IME. 184, Part 3G (II): 72-85.
- Smith, L. H., S. C. Traugott, and G. F. Wislicenus. 1953. A practical solution of a three-dimensional problem of axial flow turbomachinery. *Trans. ASME.* 75: 789-803.
- Smith, L. H., Jr. 1966. The radial-equilibrium equation of turbomachinery. *Journal of Engineering for Power, Transactions of the ASME* 88: 1-12. (Discussion in 88: 281-283. 1966.)
- Sovrano, R. 1980. Calcul de l'écoulement transsonique dans un compresseur centrifuge par une méthode pseudo-instantanée. *In Centrifugal compressors, flow phenomena and performance.* AGARD-CP-282. Paper 5.

- Spurr, A. 1976. Progress in the development of a time marching method for through flow calculations. CEGB MM/MECH/TG/9. ARC 36907.
- Stechkin, B. S., P. K. Kazandzhan, L. P. Alekseyev, A. N. Govorov, Yu. N. Nekhayev, and R. M. Fedorov. 1956. Teoriya reaktivnykh dvigateley (Theory of Jet Engines). State Press of the Defense Industry. Moscow.
- Steultz, W. G. 1980. Steam turbine blade path design considerations. In Steam turbines for large power outputs. von Karman Institute. Lecture Series.
- Stepanov, G. Yu. 1962. Gidrodinamika reshotoch turbomashin (Hydrodynamics of cascades of turbomachines). Moscow. Fizmatgiz.
- Stockman, Norbert O., and John L. Kramer. 1963. Method for design of pump impeller using a high-speed digital computer. NASA TN D-1562.
- Stodola, A. 1927. Steam and gas turbines, Volume II. New York. McGraw-Hill. pp. 990-997.
- Struve, E. 1943. Theoretical determination of axial fan performance. NACA TM 1042.
- Swan, W. C. 1958. A practical engineering solution of the three-dimensional flow in transonic type axial flow compressors. WADC Technical Report 58-57.
- Swan, W. C. 1961. A practical method of predicting transonic-compressor performance. Journal of Engineering for Power, Transactions of the ASME 83: 322-330.
- Thiaville, Jean-Marie. 1976. Modeles de calcul de l'ecoulement dans les turbomachines axiales. In Through-flow calculations in axial turbomachinery. AGARD-CP-195. Paper 1.
- Thompkins, William T., Jr., and David A. Oliver. 1976. Three-dimensional flow calculation for a transonic compressor rotor. In Through-flow calculations in axial turbomachinery. AGARD-CP-195. Paper 6.
- Topunov, A. M., and R. D. Iosifov. 1973. Classification of methods for solving the direct problem of calculating axisymmetric flow in turbomachines. Soviet Aeronautics. 16: 2, 116-121.
- Traupel, W. 1942. Neue allgemeine theorie der mehrstufigen axialen turbomaschinen. Zürich, Leeman.
- Traupel, W. 1977. Thermische turbomaschinen. Volume I. Third Edition. Berlin/Heidelberg/New York. Springer-Verlag.
- Vanco, M. R. 1972. Fortran program for calculating velocities in the meridional plane of a turbomachine. I - Centrifugal compressor. NASA TN D-6701.
- Vazsonyi, Andrew. 1945. On rotational gas flows. Quarterly Appl. Math. III: 1: 29-37.
- Vazsonyi, Andrew. 1948. On the aerodynamic design of axial flow compressors and turbines. Journal of Applied Mechanics 15: 1: 53-64.
- Veuillot, Jean-Pierre. 1977. Calculation of the quasi three-dimensional flow in a turbomachine blade row. Journal of Engineering for Power, Transactions of the ASME 99: 53-62.
- Voit, C. H. 1953. Investigation of a high-pressure-ratio eight-stage axial-flow research compressor with two transonic inlet stages. I - Aerodynamic Design. NACA RM E53I24.
- Walitt, Leonard. 1980. Numerical analysis of the three-dimensional viscous flow field in a centrifugal impeller. In Centrifugal compressors, flow phenomena and performance. AGARD-CP-282. Paper 6.
- Wasielewski, Eugene W. 1940. Design and preliminary tests of NACA axial-flow blower. NACA Memo. Rep. Dec. 18. 1940.
- Wennerstrom, A. J. 1965. Simplified design theory for highly loaded axial compressor rotors and experimental study of two transonic examples. Mitt. Institute für Thermische Turbomaschinen, No. 12. ETH, Zürich.
- Wennerstrom, Arthur J. 1974. On the treatment of body forces in the radial equilibrium equation of turbomachinery. In Traupel-Festschrift. Zürich. Juris-Verlag. pp. 351-367.
- Wiggins, J. O. 1963. A procedure for determining the off-design characteristics of multistage axial flow compressors. MS Thesis. University of Cincinnati.
- Wilkinson, D. H. 1969-1970. Stability, convergence and accuracy of two-dimensional streamline curvature methods using quasi-orthogonals. In Steady and unsteady flow. Proc. IME. 134, Part 3G (I): 108-119.
- Wilkinson, D. H. 1972. Calculation of blade-to-blade flow in a turbomachine by streamline curvature. ARC Rep. and Memo. 3704.
- Wright, Linwood C., and Karl Kovach. 1953. Design procedure and limited test results for a high solidity, 12-inch transonic impeller with axial discharge. NACA RM E53B09.
- Wright, L. C., and R. A. Novak. 1960. Aerodynamic design and development of the General Electric CJ805-23 Aft Fan Component. ASME Paper 60-WA-270.

- Wright, L. C., N. G. Vitale, T. Ware, and J. R. Erwin. 1973. High-tip speed, low-loading transonic fan stage. (Part I - Aerodynamic and Mechanical Design). NASA CR-121095.
- Wu, Chung-Hua. 1950a. A general through-flow theory of fluid flow with subsonic or supersonic velocity in turbomachines of arbitrary hub and casing shapes. NACA TN 2302.
- Wu, Chung-Hua. 1950b. Formulas and tables of coefficients for numerical differentiation with function values given at unequally spaced points and application to the solution of partial differential equations. NACA TN 2214.
- Wu, Chung-Hua. 1952a. A general theory of three-dimensional flow in subsonic and supersonic turbomachines of axial-, radial-, and mixed-flow types. NACA TN 2604.
- Wu, Chung-Hua. 1952b. Matrix and relaxation solutions that determine subsonic flow in an axial-flow gas turbine. NACA TN 2750.
- Wu, Chung-Hua. 1952c. A general theory of three-dimensional flow in subsonic and supersonic turbomachines of axial-, radial-, and mixed-flow types. Transactions of the ASME 74: 1363-1380.
- Wu, Chung-Hua. 1953. Subsonic flow of air through a single-stage and a seven-stage compressor. NACA TN 2961.
- Wu, Chung-Hua. 1976. Three-dimensional turbomachine flow equations expressed with respect to non-orthogonal curvilinear coordinates and methods of solution. In Third International Symposium on Air Breathing Engines. Munich. pp. 233-252.
- Wu, Chung-Hua, and Curtis A. Brown. 1951a. Method of analysis for compressible flow past arbitrary turbomachine blades on general surface of revolution. NACA TN 2407.
- Wu, Chung-Hua, and Curtis A. Brown. 1951b. A method of designing turbomachine blades with a desirable thickness distribution for compressible flow along an arbitrary stream filament of revolution. NACA TN 2455.
- Wu, Chung-Hua, and Curtis A. Brown. 1952. A theory of the direct and inverse problems of compressible flow past cascade of arbitrary airfoils. Journal of the Aeronautical Sciences 19: 183-196.
- Wu, Chung-Hua, Curtis A. Brown, and Eleanor L. Costilow. 1952. Analysis of flow in a subsonic mixed-flow impeller. NACA TN 2749.
- Wu, C-H., C. A. Brown, and V. D. Prian. 1952. An approximate method of determining the subsonic flow in an arbitrary stream filament of revolution cut by arbitrary turbomachine blades. NACA TN 2702.
- Wu, Chung-Hua, and Eleanor L. Costilow. 1951. A method of solving the direct and inverse problem of supersonic flow along arbitrary stream filament of revolution in turbomachines. NACA TN 2492.
- Wu, Chung-Hua, John T. Sinnott, Jr., and Robert E. Forrette. 1950. Theoretical effect of inlet hub-tip-radius ratio and design specific mass flow on design performance of axial-flow compressors. NACA TN 2068.
- Wu, Chung-Hua, and Lincoln Wolfenstein. 1950. Application of radial-equilibrium condition to axial-flow compressor and turbine design. NACA Report 955.
- Wu, Wen-Quan, Rong-Guo Zhu, and Cui-E Liu. 1980. Computational design of turbomachine blades. Jour. Aircraft 17: 319-325.
- Wu, Zhonghua (Chung-Hua). 1980. Fundamental aerothermodynamic equations for stationary and moving coordinate systems. Engineering Thermophysica in China. 1: 59-94. (Translation of paper first published in China in 1965).
- Wysong, R. R., T. C. Prince, D. T. Lenahan, et al. 1978. Turbine design system. AFAPL-TR-78-92.
- Zhukovskiy, M. I. 1967. Aerodinamicheskiy raschet potoka v osevikh turbomashinakh. (Aerodynamic Calculation of the Flow in Axial-Flow Turbomachinery). Leningrad. Izd-vo Mashinostroyeniye.
- Zhukovskiy, M. I., Ye. Ye. Karyakin, and O. I. Novikova. 1974. Application of the finite-difference method for solving the inverse problem of designing turbine blades. Fluid Mechanics - Soviet Research. 3: 6: 15-21. Nov.-Dec.

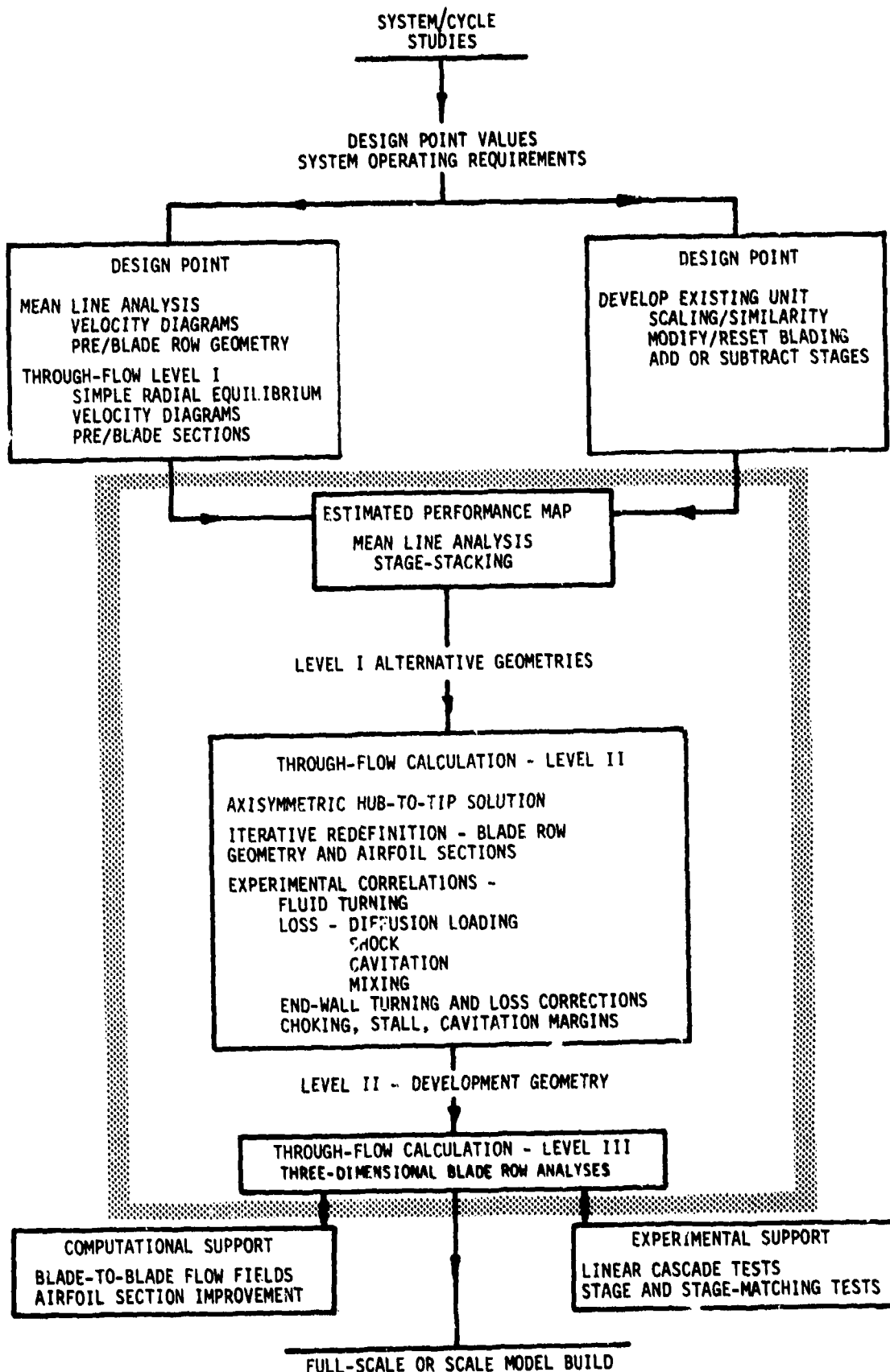


Figure 1. Typical structure of a design system for axial-flow turbomachines.

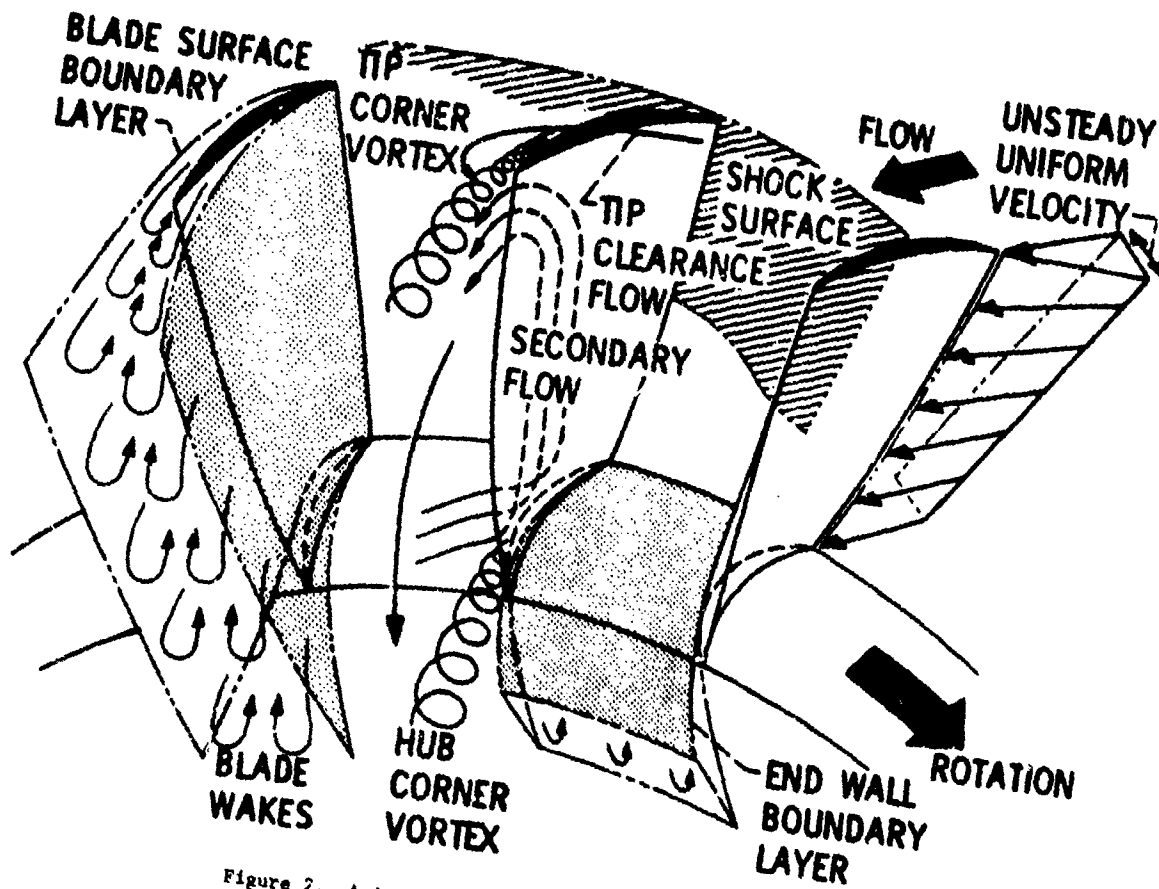


Figure 2. Axial-flow compressor rotor flow phenomena

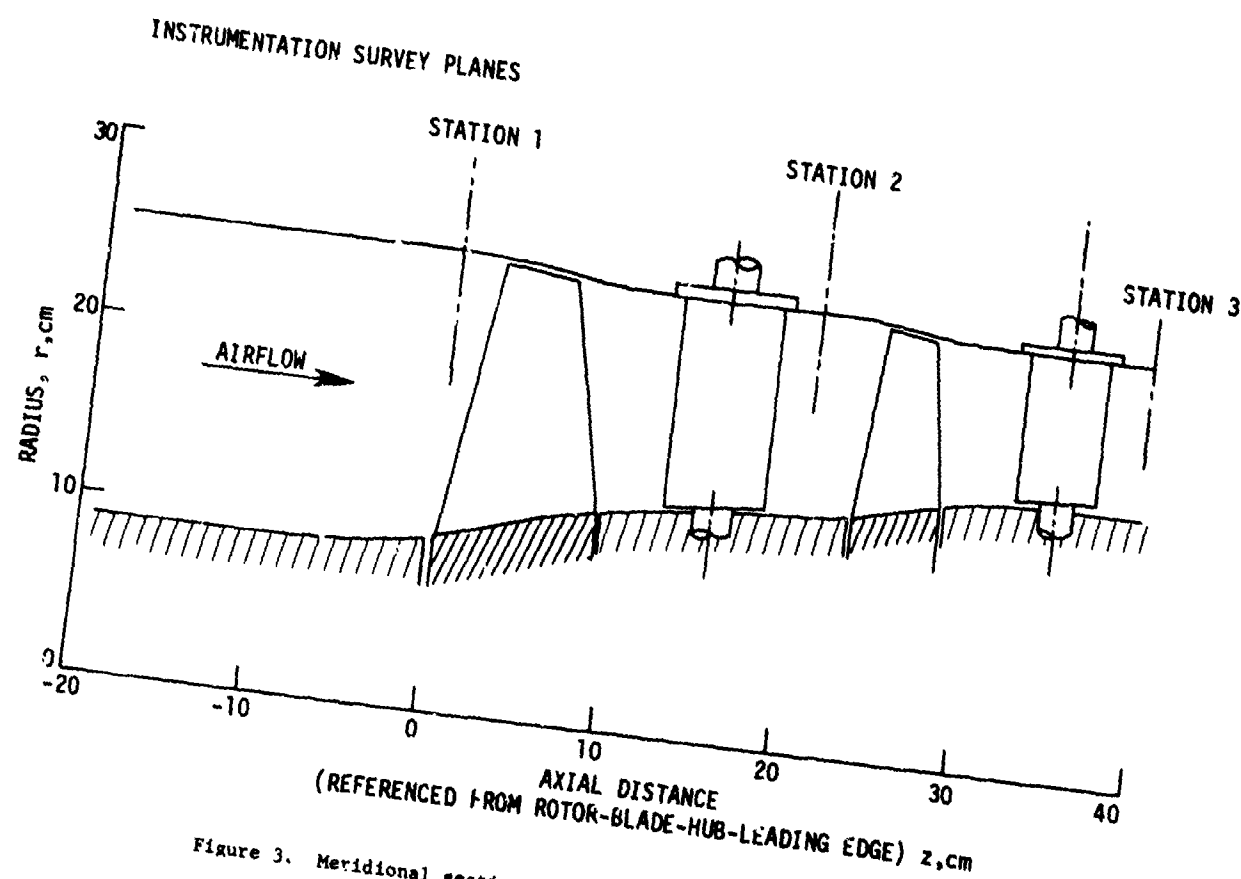


Figure 3. Meridional section of a two-stage axial-flow compressor

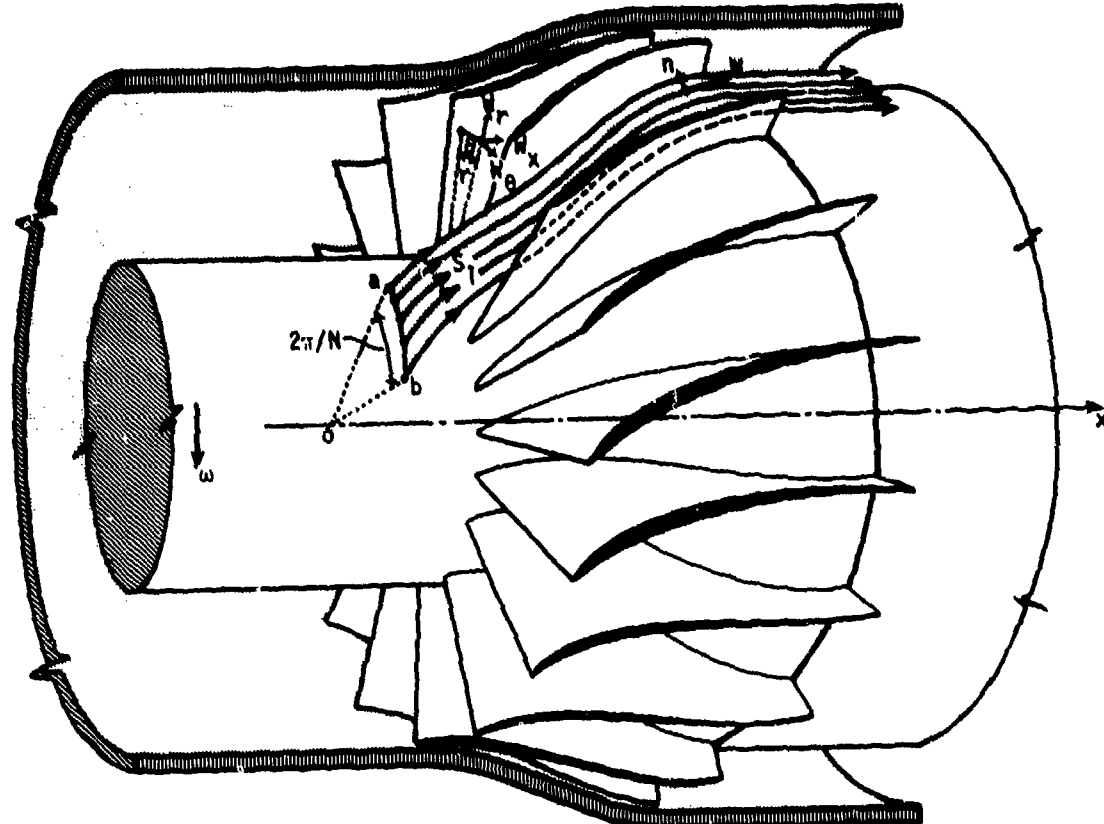


Figure 4a. S_1 blade-to-blade stream surface with related symbols and notation

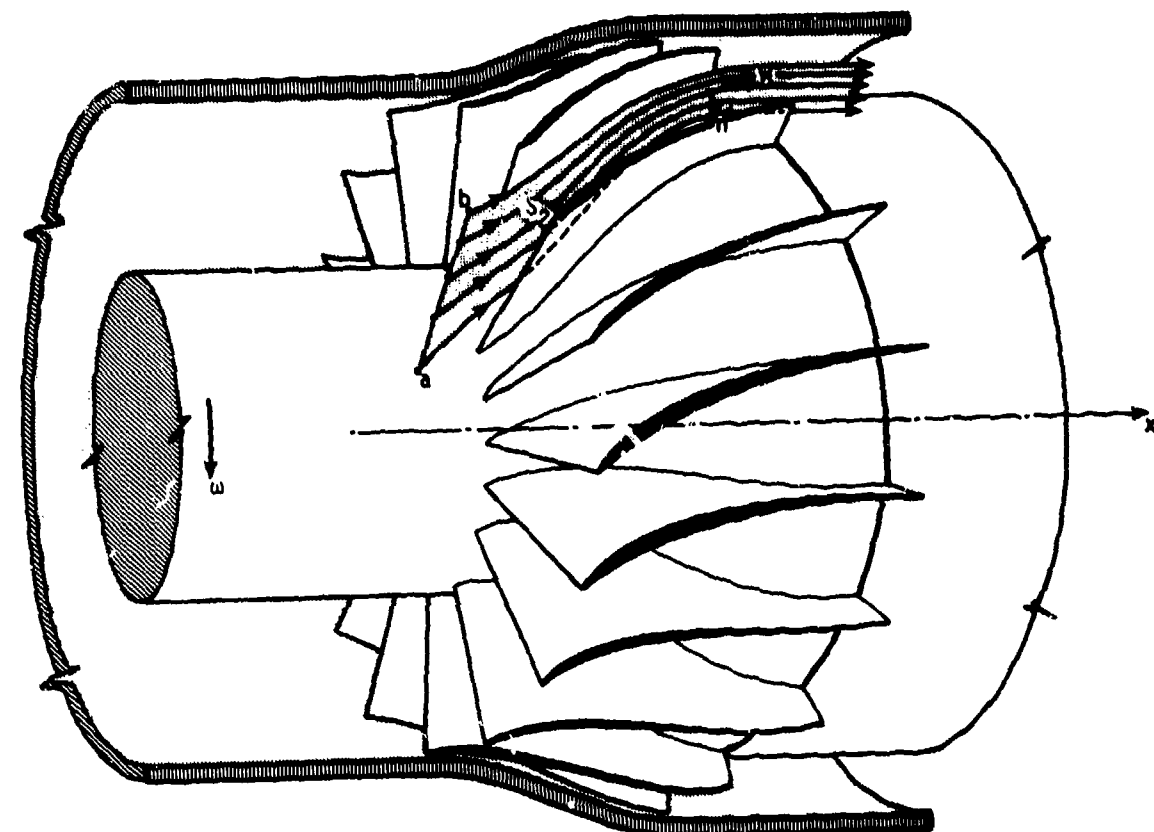


Figure 4b. S_2 hub-to-shroud stream surface with related symbols and notation

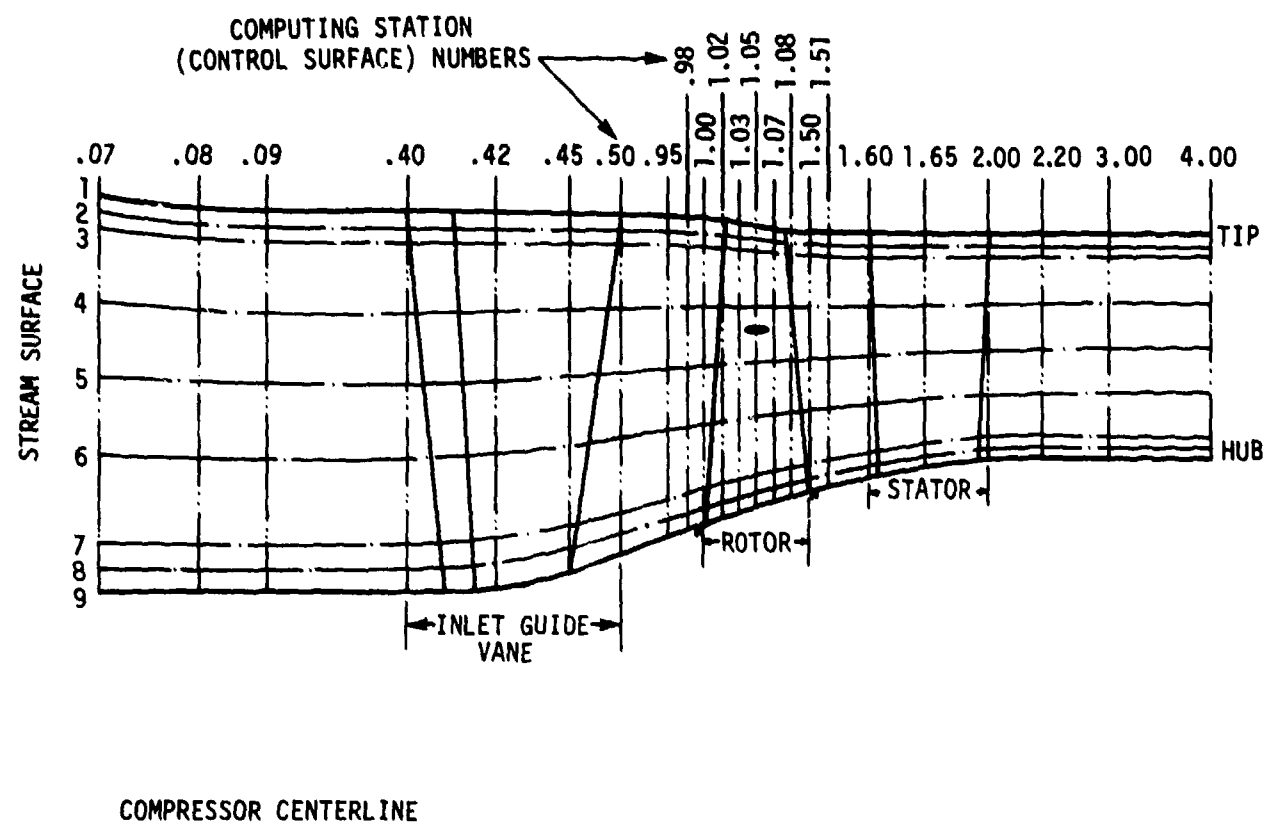


Figure 5. Intersection of stream surface approximations with meridional plane section of axial-flow compressor stage [from Doyle and Koch (1970)]

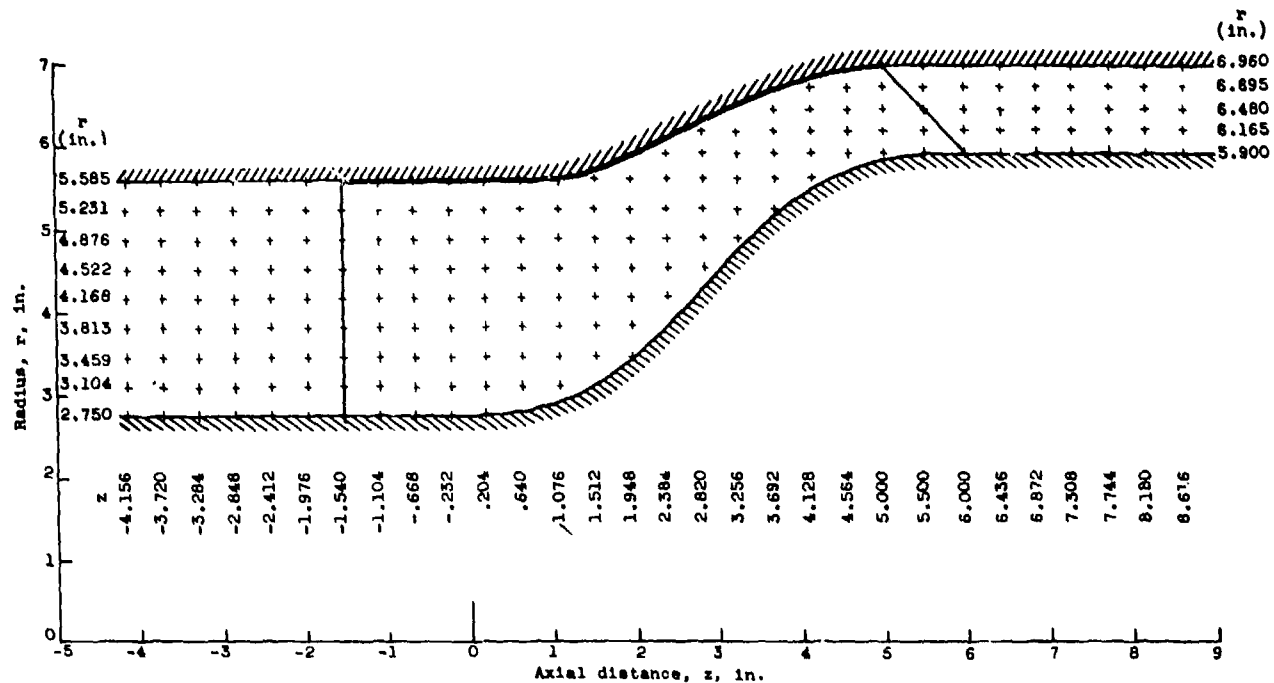


Figure 6. Calculation grid points for an axial-discharge, mixed-flow impeller [from Wu, Brown, Costilow (1952)].

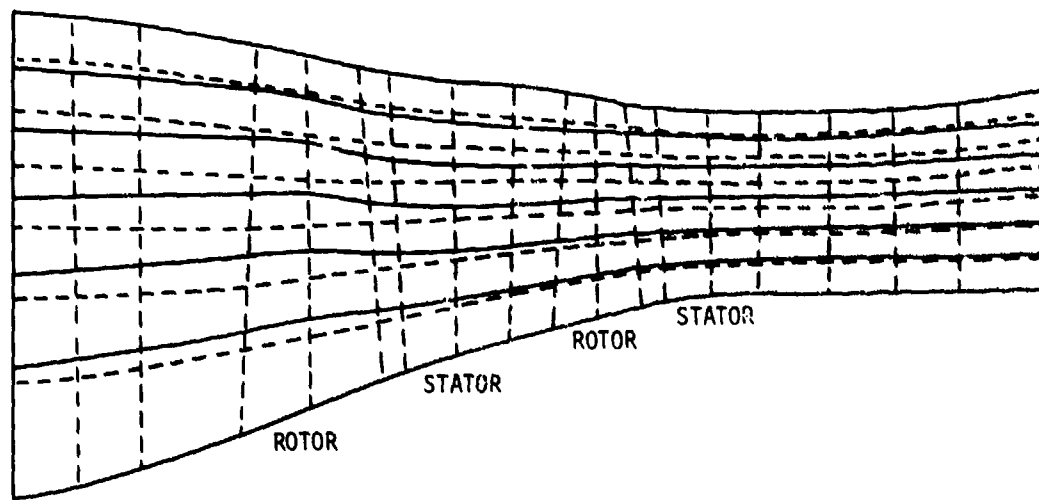


Figure 7. Two-stage fan geometry with element boundaries and calculated streamlines [from Hirsch and Warzee (1976)].

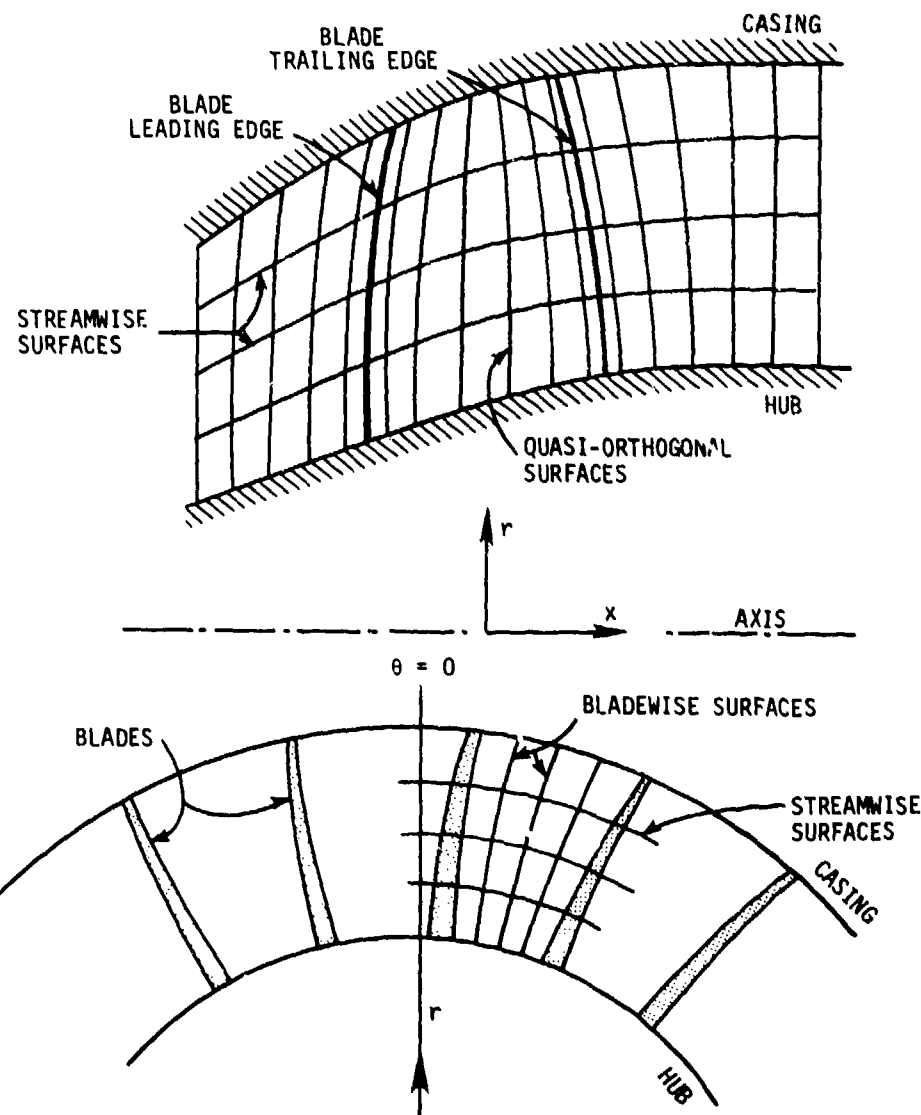


Figure 8. Construction of finite volume elements for a three-dimensional flow field computation [Denton and Singh (1979)].

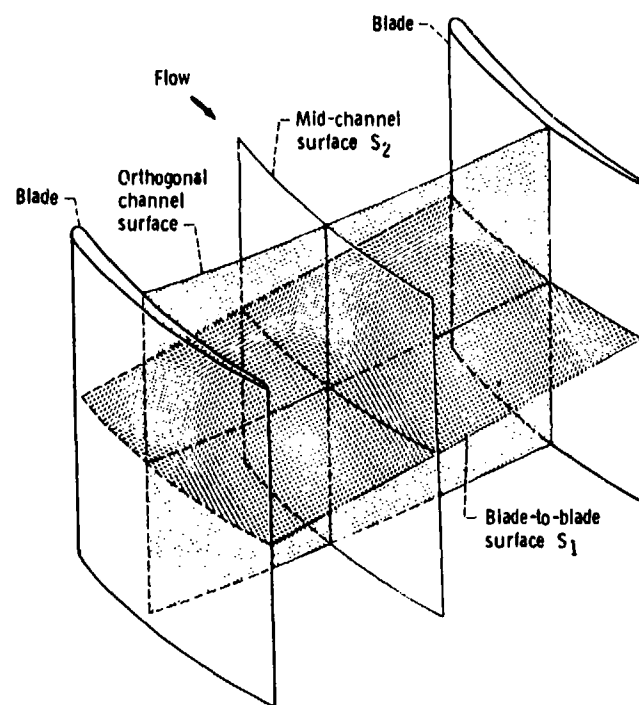


Figure 9. Channel control surface [Katsanis and McNally (1977)]

III.2 BLADE-TO-BLADE COMPUTATIONS AND BOUNDARY LAYER CORRECTIONS IN AXIAL COMPRESSORS AND TURBINES

III.2.1 Introduction

It is a common practice in industrial firms to evaluate the losses and deviations of compressor blade cascades by means of empirical correlation formulae derived from experimental results, and improved to a certain extent on the basis of compressor tests.

Due to the development of theoretical studies on cascades, we can now contemplate associating the calculations carried out in perfect fluids with boundary layer corrections, to allow for viscous effects on the suction and pressure surface. With such a method, a more efficient optimization of blade profiles, as well as higher machine performance can be achieved.

This is the reason why in this paper, we shall survey the existing methods, with particular emphasis on the association of calculations in perfect fluids and in viscous fluids.

In fact, the proposed method is an extension of Prandtl's boundary layer theory to the case of cascades. The general Navier-Stokes equations are solved here in a two-step process :

- within the flow, viscous effects are disregarded;
- near the wall, it is admitted that velocity and pressure gradients are imposed by the inviscid flow in the absence of a boundary layer separation.

Despite this dissociation, the interdependence of viscous and non-viscous effects is non negligible in a blade cascade channel. As a result the influence of viscosity cannot be determined "a posteriori" by means of a simple calculation in a perfect fluid. Therefore, it will be necessary to resort to iterations, to take the interaction effects into account.

As the methods described in the technical literature are numerous, such a survey will necessarily be incomplete, and will only address the main families of methods.

In Chapter II.2.2, we shall review the methods currently recommended for blade-to-blade calculations in the following configurations :

(i) Subsonic conditions :

the flow is subsonic in the whole field.

(ii) Supercritical conditions

the flow is quasi-subsonic to the whole field, with, at the utmost, supersonic pockets which do not extend from the upper surface of a blade to the lower surface of the next blade; in this case, the entropy variations associated with the passage through a possible shock wave can be disregarded.

(iii) Supersonic conditions :

the supersonic area of the flow occupies at least one full section of an interblade channel. In this area, recompression shock waves are more intense, and the corresponding entropy jump cannot be disregarded. As the methods described are to be applied only to existing cascades, we shall only review the direct, inviscid, blade-to-blade computation methods, and shall not be concerned with the inverse methods.

Chapter II.2.3 will be devoted to the description of boundary layer and wake computation methods. Obviously, these methods are still empirical to a great extent; however, they apply to more general flow patterns than those which can be solved by means of empirical loss correlations.

In the next chapter (Chapter II.2.4), the association methods are described, together with the reciprocal influence of calculations in perfect fluids and in viscous fluids.

A survey of methods to solve the Navier-Stokes equations is given in Chapter II.2.5.

III.2.2 Blade-to-blade flow calculations

There are essentially five categories of the blade-to-blade flow calculation methods; they differ by the numerical techniques used.

III.2.2.1 Singularity method

Singularity methods are based on the principle of the superimposition of potential flow solutions; the potential from which the flow is derived is considered as the sum of elementary potentials corresponding respectively to :

- the basic uniform flow;
- sources, sinks or vortices located in adequately selected points of the flow field.

The various singularity combinations proposed in the published literature are as follows :

- (1) Singularities located within the blade contour; this method applies essentially to low camber blades (1).
- (2) Singularities made up by vortices located on the blade contour (2). These methods lead generally to more accurate results than the previous ones. They were developed for flows in incompressible fluids, but can be extended to the case of subsonic flows of compressible fluids, by the addition of sources and sinks in the inter-blade channels, representing the compressibility effect (3), (4), (5).

With such methods, the precision of the inviscid solution on the trailing edge makes it possible to determine the direction of the flow issuing from the cascade, with the help of Kutta-Joukowski or an equivalent condition. This condition can be easily introduced in the computation program. In the case of moderate viscous effects, for instance in the case of turbine blades at the design point, the theoretical and experimental results obtained by this method correlate very well (Fig. 1). This method offers an additional advantage: due to its high degree of accuracy, it permits a fine analysis of high velocity gradient zones (in the vicinity of the leading edge, for instance) which is important in view of the prediction of boundary layer transition. Its major drawback lies in the fact that it is limited to the case of subsonic flows with shock-waves.

III.2.2.2 Methods based on the curvature of streamlines

Streamline curvature methods are quite commonly used. Their starting point is a family of pseudo streamlines deduced, by similarity, from the profile geometry. The transverse pressure gradients are connected to the curvature of these streamlines; a transverse velocity distribution is derived, and, by iteration on the continuity equation, the shape of the streamline is changed until a convergence of the process is reached (6), (7).

The main advantage of this method is the rapidity of the computation, also for subsonic compressible flows. For transonic flows, difficulties arise because of the discontinuity of the streamline curvature at the shocks and because of the ambiguity in the choice between a subsonic or supersonic solution. Another drawback lies in the lack of accuracy in areas of strong curvature (leading and trailing edges). As a result, local velocity peaks are smoothed out, which limits the capability in predicted boundary layer transition (Fig. 2).

III.2.2.3 Finite difference or volume methods

It is necessary to distinguish between methods where entropy is assumed to be constant, and methods where entropy variations are taken into account.

A - Stationary irrotational flows

(i) Relaxation methods using the stream function

The continuity equation allows definition of a stream function which combined with the condition of irrotationality provides a second order, non linear equation for compressible flow. This equation is generally discretized in an orthogonal grid, by means of a scheme suited for an elliptic type problem (subsonic flow).

The finite difference equation is solved by a relaxation technique (8), (9) or by a matrix technique (10).

This well proven type of method is relatively fast and shows good agreement with experiments (Fig. 3). A second advantage is the ease of extension of these methods to rotational flow on non cylindrical stream surfaces. The major drawback is the necessity to specify the outlet flow angle. This difficulty has been overcome at the cost of a more complex iterative calculation as discussed in Chapter 4. These methods are also limited to subsonic flows. Extensions to transonic flow, in combination with a streamline curvature technique have not been very successful (11).

(ii) Relaxation methods using the velocity potential

This type of method has first been developed to calculate transonic flow around isolated airfoils. However, the number of references about this method are too numerous to be all listed here.

The ambiguity between the subsonic and supersonic solution, when using a stream function has been avoided by the use of a potential function. However, this requires the assumption of irrotational flow. The continuity equation provides a non-linear, second order, partial derivation equation which is of the elliptic type in the subsonic field, and of the hyperbolic type in the supersonic field. Discontinuous solutions can be adopted for this equation; although they do not satisfy the Rankine Hugoniot relations for shock waves. The methods recommended in the published literature differ essentially by the discretization method adopted :

- it is possible to use mixed discretization schemes, that is centered meshes in the subsonic flow, and excentric meshes in the supersonic field (12), (13); (14); with this method, it is necessary to subject to a special treatment the points where discontinuities appear (shock waves), for the scheme to remain conservative.
- it is possible to put the scheme off center, systematically, by using a term of artificial viscosity; this type of method leads generally to a conservative scheme (15).

- an original method (16) consists in using a discretization method of the finite volume type

Numerical results obtained by this method are very satisfactory if the Mach number upstream of the shock is only slightly supersonic. However, the use of a potential function makes it difficult to control the mass flow through the flow channels (conservation problem) which puts a limitation to the prediction of choking. Furthermore, the use of a potential function does not allow to apply these methods to rotational flow on non cylindrical stream surfaces. A comparison of calculated and experimental results is shown in figure 4 for a compressor cascade for slightly transonic flow.

(iii) Pseudo non-stationary, isentropic method

The iterations of the relaxation method can be replaced by introducing in the equations time dependent derivatives which do not necessarily have a physical significance. The entropy is assumed to be constant in the whole field, even during transient periods, so that only the stationary asymptotic solution has a physical significance (17).

While this method, which requires a longer computation time, has a more extensive field of application than the previous methods, it is limited to the case of motions with only low intensity shock waves.

B - General solution to Euler equations under steady conditions

Until now, the problem raised by the mixed elliptic-hyperbolic nature of the Euler equations for steady transonic motion with intense shocks, could only be solved by non-steady type methods (18, 19). Here again, we find the characteristic (mentioned under A(iii)) of the steady flow considered as the asymptotic state of a non-steady motion.

Such methods offer the great advantage of being applicable to any transonic flow; however, they require very long computation times for the asymptotic condition to be achieved. As far as cascades are concerned, the computation time depends on rapidity with which disturbances get damped and disappear at the borders of the computation field. As the asymptotic solution is the only solution retained, the intermediate states do not need to have a physical significance, and the non-steady terms can be modified in order to accelerate the achievement of the final solution.

With these methods, shock waves are usually dealt with by means of a shock capturing method, with which they appear quite naturally, owing to the dissipative properties of the numerical schemes used (dissipative properties which are either natural or reinforced by an artificial viscosity term).

While this technique is simple, it is not accurate enough as regards the description of shocks; these do not appear as true discontinuities, but are somewhat spread out.

The use of a two-step calculation process (20), (21) offers the advantage of second order accuracy; however, the calculation time is doubled for each time step, which leads to very long computation times.

Owing to an improved computation method (22), a single step method, with a damping term whose intensity can be modified in the course of the computation, has been developed (23) : this method, which is definitely quicker, offers also a second order accuracy for the converged solution.

The computation time was further reduced using finite volumes, either for the isentropic scheme (22), or for the scheme which takes entropy variation into account (24). The latter method was even generalized to the cascades drawn on surfaces of revolution with an evolution of radius and a varying thickness of the stream tube.

A variant of this method (25) uses upwind differences for mass and momentum and downwind differences for pressure gradients. This procedure acts somewhat like a smoothing and together with the finite differentiation of the flow it tends to smear out high local gradients as seen in the leading edge region of figure 5.

This method is first order accurate and requires a large number of calculation points or else corrective terms to attain a sufficient degree of accuracy.

This method has also been extended to three dimensional flows (26).

III.2.2.4 Finite element method

Finite element methods are of increasing interest for computations using the stream function, as well as for those using the velocity potential.

This method is based on an approximation of dependent variables in the form of polynomials, and on an integral definition of the problem (27), (28).

The benefits expected from this technique are as follows :

- possibility of giving an optimum design to the grid of the plane, especially by using curvilinear meshes;
- automatic treatment of natural boundary conditions;
- preservation of symmetry in the discretization of differential operators;

On the other hand, we risk increasing the computation time due to the complexity of the meshes used and to the number of terms of the polynomials.

This method seems now to have reached an adequate level of efficiency for problems of the elliptic or parabolic type. Its application to transonic problems of the locally hyperbolic type requires further developments, although results have already been obtained in the case of transonic, irrotational flows (29), (Fig. 6).

III.2.2.5 Methods of characteristics

As supersonic flows lead to equations of the hyperbolic type, one can think about calculating the supersonic flow directly from the upstream boundary conditions. The field of dependence of each point is then defined by the characteristics issuing from it.

This very classical problem is described in numerous references (30) and the application to two dimensional or three dimensional blades is described in (31), (32) and (33).

The main difficulties encountered are as follows :

- the supersonic field must be perfectly well defined (fully supersonic flow), and upstream conditions (supersonic flow or sonic line) must be known;
- only oblique shock waves can be taken into account, since the flow is subsonic downstream of normal shocks; and the method is no longer applicable;
- the computation cannot be carried out unless the upstream boundary conditions are set. Thus, as regards turbine cascades, the sonic line has to be calculated first, for instance by a method of series development (34 to 37) : in this case, the subsonic portion of the flow is calculated by any method which can use the downstream boundary conditions as defined by the calculation of the sonic region.

For all these regions, the method of characteristics is only applicable to cascades with a well-defined minimum section, where the sonic line can be calculated in a sufficiently accurate manner.

In addition, the use of other computation methods suited to calculate the subsonic flow field increases markedly the complexity to the computation process.

III.2.3 Boundary layer calculations

The comparisons of the previous chapter between calculated and experimental results have mainly been made for turbine cascade because in this case, viscous effects are much less important than in compressor cascades.

However, in calculation of the flow in compressor cascades the influence of boundary layers can no longer be neglected.

The description of the many methods developed during the last decades for boundary layer calculation does not fall within the scope of this survey. We only shall classify them according to the assumptions on which they are based and the techniques they use.
(i) The oldest methods are the integral methods based on von Karman's integral equation (integral form of the equation of motion written along a streamline). In these methods, there are only two unknown quantities left (boundary layer thickness and shape factor), owing to the additional relations which provide the shape of the velocity profile, or to results obtained on similar boundary layers. Consequently, it is necessary to have a second (or auxiliary) equation, and the integral methods proposed differ mainly by the formulation of this equation. A first formulation consists in using the energy equation (38 to 42). A second formulation uses an equation based on the entrainment principle (43, 44, 45). The system of equations is then integrated along the wall streamline allowing calculation of the boundary layer parameters.

(ii) More recently, methods have been developed to solve the boundary layer equations by a finite difference technique (46, 47, 48) : In this approach, the discretization of partial derivative equations and the numerical technique to solve them constitute the difference between the methods proposed by various authors. Moreover, when the boundary layer is turbulent, an additional assumption is necessary to define the turbulent shear stresses, whose order of magnitude exceeds that of viscous stresses by one unit. With integral methods, it is sufficient to relate turbulent magnitudes, in particular through a mixing length (49, 50, 51).

The data necessary for this calculation, particularly velocity profiles, can be derived from similar solutions (52).

In finite difference methods, three different approaches can be used :

- a zero-equation model (use of mixing length resulting from previous calculations),
- a one-equation model, for instance the convection equation of one of the turbulent magnitudes (turbulent kinetic energy, Reynolds stress) (53).
- a two-equation model, using two convection equations, for instance the model (K, r) describing the evolution of the turbulent kinetic energy and that of the turbulent scale (54, 55, 56).

The last two models require long computation times, which limits their applicability for industrial calculations. They require also a large number of constants and parameters for which empirical models have to be established. On the other hand, they provide an improved description of the turbulence structure and are more generally applicable than integral methods. They are quite suited to the case of non equilibrium boundary layers -

for instance with a high pressure gradient - or to the case of blowing.

On the contrary, integral methods are applicable to boundary layers in equilibrium, where the evolution of external conditions is sufficiently progressive for turbulent stresses to adapt to the mean velocity profile. This can be further facilitated by using a delay in the calculation of local dissipation energy (40, 44), or by relating the latter to the shape of the velocity profile obtained during the previous calculation steps (57).

Excellent results have been obtained for the calculation of the boundary layer on flat plates. A few problems remain to be solved :

- the transition from laminar to turbulent boundary layer, or else its return to laminar, according to the evolution of external parameters, still requires complementary studies (58, 59)

- the streamline curvature and the Coriolis forces have an impact on the turbulent level. For the time being, this is not taken into account except by corrective terms which are functions of Richardson's or Rossby's number (60 to 63).

So far, we have considered only the case of boundary layers without separation. The calculation of separations by means of boundary layer methods raises essentially the following problems :

- validity of boundary layer theory assumptions,
- validity of Prandtl equations,
- validity of turbulence models.

The boundary layer theory is indeed at fault when a separation takes place, since it does not allow for the strong interaction with the external flow. It is possible to overcome this difficulty, together with the related numerical singularities, by associating the boundary layer computation with the external flow computation, and, especially by using the inverse methods described in III.2.4. This way, if the separation extends over a limited space, Prandtl theory continues to be applicable. However, the turbulence models which are currently used do not seem to provide an adequate representation of actual physical phenomena, and need to be improved.

Generalizing the boundary layer theory had led to the development of methods for calculating the evolution of wakes downstream of the blades (64 to 68).

In the case of tandem blades, it may be extremely useful to know the blockage of the inter-blade channel by the wake of the first blade, so that it may be taken into account for the calculation of the second blade (69). However, one is mainly interested in the downstream, stagnation pressure, velocity and flow angle conditions, and the detailed calculations of the wake can be replaced by a global calculation which eventually provides the exit angle and the losses.

III.2.4 Association of inviscid flow and viscous flow calculations in the boundary layer

The association of inviscid flow calculations with boundary layer calculations takes place at several levels :

- the mass flow deficit in the boundary layer, qualified by a displacement thickness, leads to a displacement of the walls by an equivalent quantity. As a result the distribution of velocities in the external flow is modified when this flow is confined within two relatively close walls. This effect is evidently considerable in the case of separated boundary layers.
- the direction of the exit flow is a function not only of the blade and cascade geometry, but also of the viscous effects on the trailing edge. The Kutta-Joukowski condition, or any equivalent condition takes these various conditions into account. However, the presence of the wake downstream of the blade and the shape of this wake exercise a considerable influence on the exit angle.
- The energy dissipation in the boundary layer and the wakes leads to pressure losses.
- In transonic and supersonic flows, the pressure jump of a shock wave creates a strong interaction with the boundary layer.

The resulting boundary layer thickness brings about a displacement of the shock wave and a modification of its intensity.

III.2.4.1 Evaluation of the exit angle

As mentioned above, the exit angle is defined by the cascade geometry and the viscous effects.

As long as the boundary layer remains thin along the trailing edge, it can be taken into consideration in a very simple way in the potential flow calculation, in particular by maintaining a stagnation point on the trailing edge itself (Kutta-Joukowski condition). However, it has been demonstrated (70) that a small displacement of this stagnation point is sufficient to induce a non negligible variation in the exit angle.

When the blade does not have a sharp trailing edge, the expression "trailing edge" hardly applies, and there is no real stagnation point, but an inert fluid area, located at the separation point of the boundary layer, almost at the point where the trailing edge curvature starts. Therefore, a more realistic criterion consists in imposing an equal

pressure on both sides of the blade, at the points where the trailing edge curvature starts (71).

This criterion yields good results in the case of turbine blades (72) and (73) but is less accurate in case of compressor blades, where the exit angle is predicted with an accuracy of $\pm 3^\circ$ only.

The difficulty we are faced with, results from the thickening of the boundary layer on the suction or pressure surface of compressor blades which often leads to a small separation zone.

An attempt to improve the equal pressure criterion through a correlation between the position of the corresponding points and the pressure increase between the highest overspeed point and the trailing edge (74), did not prove successful.

The only method which looks promising consists in allowing for the boundary layer separation in the inviscid flow (75) (Fig. 7) : Correct results were obtained, even for rather large separations near the trailing edge (76), as well as for operating modes with a laminar separation bubble (77). The singularity methods used in references 75 and 76 have also the advantage that they easily allow for a wake downstream of the blade.

In fact, the exit angle is influenced not only by the upper surface separation but also by the development of the wake downstream of the blades.

III.2.4.2 "Blockage" effects

The association of the perfect fluid with the viscous fluid is currently done for simple cases (cascades) in the following way : A first calculation in a perfect fluid, by a method suited to the test case, provides a velocity distribution which, through a boundary layer calculation, given an evolution of the displacement thickness. Two methods are generally used then to take into account the presence of the boundary layers. (1) Either one adds the boundary layer displacement thickness to the profile and, behind the trailing edge, one extends this blade further downstream in a way which, although it is somewhat arbitrary, is physically plausible (78). (2) Or one injects, at the blade wall, a mass flow which is a function of the evolution of the displacement thickness. Downstream of the trailing edge, one sucks back the mass flow injected along a sink line, with an arbitrary distribution (79, 80).

One starts a new calculation with a perfect fluid, either on the thickened blade or on the real blade, but with a wall mass condition, and so on, until the convergence is reached. It is to be noted that there are cases where this convergence is not ensured. The main problem consists in preventing the fictitious portion downstream of the trailing edge (thick segment or sink line) from contributing to the lift (81). If necessary, this condition may lead to adjusting either the shape of the segment added to the profile, or the sink distribution.

The influence of the wake is globally taken into account. For this purpose, one writes that the total enthalpy and the mass flow remain unchanged between the plane of the fictitious trailing edges and the infinite downstream. The calculation of the resulting exit angle (82, 83) must be combined with that of the losses. A more detailed calculation of the wake itself is given in reference 84.

These various calculation methods are relatively simple and yield good results, at least in the absence of a clean-cut separation resulting essentially from the interaction of the boundary layer and a high intensity shockwave, figure 8.

Specific methods have been developed to take this last phenomenon into account.

III.2.4.3 Shock-wave-boundary layer interaction

The shock-wave-boundary layer interaction can vary in intensity according to the value of the Mach number upstream of the shock, and to the pressure ratio. It may lead to a high amplitude separation, with a modification of the external flow (λ shock). To take this interaction into consideration, the inviscid flow calculation must be carried out in parallel with the boundary layer calculation.

The main methods currently recommended are the following :

- A - Global methods, or control volume methods which relate a boundary layer characteristic before and after the shock, to the overall shock intensity.
- B - Integral methods described previously have to be adapted to boundary layers with rapidly evolutive properties. Among these integral methods, direct methods have to be distinguished from inverse and semi-inverse methods.
- A direct boundary layer method has been used in (85) for modest shock strength. This was possible by using small integration steps and by limiting C_f to small but non zero values. The result shown in figure 9 shows a remarkable improvement in comparison to a pure inviscid calculation. A more sophisticated method (86) calculates the variation of boundary layer thickness and shape factor on the basis of an abrupt discontinuity in function of pressure ratio and shape factor of the upstream boundary.
- Inverse methods can overcome the difficulty generally encountered in integral methods due to the separation of the boundary layer induced by a high intensity shock : the singularity corresponding to the separation point can be eliminated in the inverse method. For this purpose, the pressure distribution at the external border of the boundary layer

must be chosen as the unknown quantity, and a longitudinal evolution of the friction coefficient or boundary layer displacement thickness must be set. Then, the pressure distribution in the external flow and the boundary layer characteristics are provided by the calculation (87 to 95). This procedure is not limited to shock induced separation, and has been successfully applied (Fig. 10) to calculation of the trailing edge separation zone in a compressor cascade (84).

- The methods, which take full account of inviscid and viscous flow interactions, make it possible to calculate boundary layers displacement thickness, as well as the external flow (96). This method is not only applicable to the shock wave-boundary layer interaction; it gives also good results in the case of an interaction with a laminar separation bubble, as well as for trailing edge separation, and for wakes. Initially used for supersonic flows, these methods are now being generalized to the case of subsonic or transonic flows, in association with either direct or inverse methods.

C - Different level methods compare the boundary layer to multiple layers fitted in each other, with different aerodynamic properties (the simplest case in a laminar sub-layer and a turbulent layer). In each layer, the flow is described by means of a system of partial differential equations which is obtained from the Navier-Stokes equations by retaining only the terms which are essential for the layer used. It is even possible to use, in some of these layers, the integral equations corresponding to the type of boundary layer which develops within them. In order that the solutions may be compatible with each other, adjusting conditions are written on the interfaces of the various layers (97 to 102).

III.2.5 Solution of the Navier-Stokes equations

The influence of viscosity on the flow has been calculated in the previous section by associating a boundary layer model with an inviscid calculation, and results in an interactive procedure.

However, the most rigorous way to solve this problem is by solving the complete Navier-Stokes equations. With this method, the external flow and the boundary layer are calculated simultaneously; thus, the close association between the two conditions is directly taken into account (103 to 106). Flow predictions for stationary blade rows are quite promising (Fig. 11).

For transonic flow, it is general practice to solve the instationary Navier-Stokes equations by a time step progression until complete convergence of the solution is attained (107 to 119).

The main difficulty with this method arises from the necessity of having a very fine grid in the area where the fluid viscosity plays a preponderant part, so that each term of the Navier-Stokes equation may be of the same order of magnitude. For numerical stability conditions this leads to very small time steps and long calculation durations. Therefore, the essential difference between the various numerical methods proposed results from the scheme retained, and the partial derivative equation discretization best suited to the problem.

The schemes currently retained vary from the fully explicit scheme to the fully implicit scheme, with every possible intermediate solution. The shortest calculation times have been obtained with mixed schemes.

Evidently, the modelling of turbulence poses additional problems, which are discussed above, and, here we find again the same three models (algebraic model, one-equation model and two-equation model), with their respective advantages and drawbacks.

III.2.6 Conclusions

The number of inviscid calculation methods, available today, is quite impressive, and they allow an accurate prediction of inviscid incompressible, subsonic compressible and transonic flow. Recent progress has also resulted in a remarkable decrease of required computational effort, which makes them even more attractive to industrial applications.

However, as these methods do not account for viscosity, the field of application is quite restricted, and good predictions can be obtained only for flow configurations where viscous effects can be neglected (f.g. turbines and low loaded compressor cascades).

A similar conclusion can be drawn about boundary layer methods, with a limitation on shock boundary layer interaction, where complete solutions still require a large amount of computational effort.

The combination of these two types of calculations has started quite recently, and a lot of progress can be expected in the near future. It is the opinion of the authors that the improvements which can be expected from a better combination of these two types of calculations will be more important than an improvement in the inviscid calculations.

Based on the present state of the art concerning shock boundary layer interaction calculations, it appears that integral or inverse methods are the best suited to industrial calculations.

However, in view of the considerable efforts currently made towards the development of the Navier-Stokes equation solution, it is more likely that, in the near future, this method will lead to more reasonable computation times and permit practical applications.

From now on, it can be recommended to use Navier-Stokes methods for flow analysis in limited fields such as the strong shock-boundary layer interaction field, and to associate them with simpler methods for other fields.

REFERENCES

1. SCHLICHTING, H.: Berechnung der reibungslosen inkompressiblen Strömung für ein vorgegebenes ebenes Schaufelgitter.
VKI Forschungsheft 447 - B/21, 1955.
2. MARTENSEN, E.: Berechnung der Druckverteilung an Gitter profilen in ebener Potentialströmung mit einer Fredholmschen Integralgleichung.
Archive for Rational Mechanics & Analysis, Vol. 3, N° 3, 1959.
3. IMBACH, H.: Die Berechnung der kompressiblen, reibungsfreien Unterschallströmung durch raumliche Gitter aus Schaufeln auch grosser Dicke und Wölbung.
ETH Zurich, Prom 3402, 1964.
4. VAN DEN BRAEMBUSSCHE, R.: Calculation of compressible subsonic flow in cascades with varying blade height.
ASME Trans., J. Engineering for Power, Vol. 95, No. 4, 1973, pp 345-351.
5. LUU, T.S.: Méthode d'équations intégrales en mécanique des fluides,
Computing Methods in Applied Sciences and Engineering,
R. Glowinski & J.L. Lyons Eds., Lecture Notes in Economic and Mathematical System,
Vol. 134, Springer, 1976, pp 359-373.
6. WILKINSON, D.M.: Stability, convergence and accuracy of two dimensional streamline curvature methods using quasi orthogonals.
Thermodynamics and Fluid Mechanics Convention 1970,
Inst. Mech. Engrs., London, Vol. II.
7. BINDON, J.R.: Stability and convergence of streamline curvature flow analysis procedures.
Int. J. for Numerical Methods in Engineering, Vol. 7, 1973, pp 69-83.
8. KATSANIS, T.: Computer program for calculating velocities and streamlines on a blade to blade streamsurface of turbomachines.
NASA TN D 4525, April 1968.
9. FENAIN, M.: Méthodes de relaxation pour la résolution d'équations elliptiques dans les domaines de frontières quelconques. Applications au calcul d'écoulements subcritiques.
J. de Mécanique Appliquée, Vol. 1, 1977, pp 27-67.
10. CALVERT, W.J. & SMITH, D.J.L.: A digital computer program for the subsonic flow past turbomachine blades using a matrix method.
ARC R&M 3838, 1976.
11. KATSANIS, T.: Fortran program for calculating transonic velocities on a blade to blade streamsurface of a turbomachine.
NASA TN D 5427, 1969.
12. DODGE, P.: A transonic relaxation method for cascade flow systems,
in Transonic Flows in Turbomachinery,
VKI LS 59, May 1975.
13. LUU, T.S. & COULMY, G.: Calcul de l'écoulement transsonique avec choc à travers une grille d'aubes.
ATMA 1975.
14. RAE, W.J. & HORNICJ, G.F.: A rectangular coordinate method for calculating non linear transonic potential flowfields in compressor cascades.
AIAA Paper 78-248, 1978.
15. IVES, D.C. & LIUTERMOZA, J.F.: Second order accurate calculations of transonic flow over turbomachinery cascades.
AIAA Paper 78-1149, 1978.
16. CASPAR, J.R.: HOBBS, D.E. & DAVIS, R.L.: The calculation of two dimensional compressible potential flow in cascades using finite area techniques.
AIAA Paper 79-007, 1979.
17. VEUILLOT, J.P. & VIVIAND, H.: A pseudo unsteady method for the computation of transonic potential flows.
AIAA Paper 78-1150, 1978.
18. MAGNUS, R. & YOSHIHARA, H.: Steady inviscid transonic flow over planar airfoils - A search for simplified procedure.
NACA CR 2186, 1972.

19. MAGNUS, R. & YOSHIHARA, H.: Inviscid transonic flow over airfoils.
AIAA J., Vol. 8, No. 2, 1970, pp 2157-2162.
20. GOPALAKRISHNAN, S.: Fundamentals of time marching methods,
in Transonic Flows in Turbomachinery,
VKI LS 59, 1973.
21. VIVIAND, H. & VEUILLOT, J.P.: Méthodes pseudo-instationnaires pour le calcul
d'écoulements transsoniques.
ONERA Publication No. 1978-4
22. McDONALD, P.: The computation of transonic flow through two dimensional
gas turbine cascades.
ASME P 71 G 89, 1971.
23. COUSTON, M.: McDONALD, P. & SMOLDEREN, J.J.: The damping surface technique for time
dependent solutions to fluid mechanic problems.
VKI TN 109, March 1975.
24. COUSTON, M.: Méthode de calcul de l'écoulement inter-aube pseudo-tridimensionnel
VKI ULB Ph.D. Thesis, September 1976.
25. DENTON, J.D.: Extension of the finite area time marching method for three
dimensions,
in Transonic Flows in Axial Turbomachinery,
VKI LS 84, February 1976.
26. DENTON, J.D. & SINGH, U.K.; Time marching methods for turbomachinery flow
calculations,
in Application of Numerical Methods to Flow Calculations in Turbomachines,
VKI LS 1979-7, April 1979.
27. KRIMERMAN, Y. & ADLER, D.: Calculation of the blade to blade compressible flow
field in turbo impellers using the finite element method.
Fac. Mech. Eng. Technion, Israel Inst. of Technology, Haifa, 1976.
28. MORICE, Ph.: Une méthode numérique basée sur les principes variationnels pour des
écoulements avec frontières libres.
ONERA TP 1978-40.
29. HIRSCH, Ch.: Transonic flow calculations in blade rows with an optimal control -
Finite element formulation.
Bat-Sheva Seminar on Finite Element for Non-elliptic Problems.
Tel-Aviv Univ., July 1977.
30. SHAPIRO, A.: The dynamics and thermodynamics of compressible fluid flow.
The Ronald Press Company, New York, 1953.
31. LAWACZECK, O.: Verfahren zur Ermittlung der Auströmgrößen transsonischer
Turbinenränder.
AVA Göttingen Bericht 68 A 62.
32. FRUEHAUF, H.M.: A method of characteristic for three dimensional steady supersonic
flow in rotating and stationary annular cascades.
ESRO TT-44, July 1975.
33. MARTINON, J.: Use of the characteristics method for the prediction of the three
dimensional flow field in high transonic compressors.
ASME Paper 79 GT 34, 1979.
34. MEYER, T.M.: Forschungsheft 62, 1908.
35. HILL, I.M.: Transonic flow in two dimensional and axially symmetric nozzles.
ARC 23,347, 1961.
36. MOORE, A.W.: The transonic flow in the throat region of a two dimensional nozzle
with walls of arbitrary smooth profile.
ARC R&M 3481, 1965.
37. DECUYPERE, R.: Berekening van de bidimensionale, wrijvingsloze, schok-golfvrije
stroming doorheen subkritische, kritische en superkritische turbineschoepenrijen.
Beauw van een bidimensionale transsonische stoomtunnel.
VKI-RUG Ph.D. Thesis, August 1973.
38. LEFOLL, J.: A theory of representation of the properties of boundary layers on
a plane.
Proc. Seminar on Advanced Problems in Turbomachinery,
VKI LS 1, March 1965.
39. PAPAILLIOU, K.: Blade optimization based on boundary layer concept.
VKI CN 60, March 1967.

40. NASH, J.F. & MCUNALD, A.G.: A calculation method for the incompressible turbulent boundary layer, including the effect of upstream history on the turbulent shear stress.
ARC 29,088, NPL Aero R 1234, 1967.
41. KUHN, G.D. & NIELSEN, J.N.: Prediction of turbulent separated boundary layers.
AIAA Paper 73-663, 1973.
42. FLAMERTY, R.J.: A method for estimating turbulent boundary layers and heat transfer in arbitrary pressure gradient
United Aircraft Research Labs., Rep. UAR-G-51, August 1968.
43. HEAD, M.R.: Entrainment in a turbulent boundary layer.
ARC R&M 3152, 1960.
44. GREEN, J.E.; WEEKS, D.J. & BROOMAN, J.W.F.: Prediction of turbulent boundary layers and wakes in compressible flow by a lag-entrainment method.
RAE TR 72231, January 1973.
45. MICHEL, R.; QUEMARD, C. & COUSTEIX, J.: Méthode pratique de prévision des couches limites turbulentes bi et tridimensionnelles.
La Recherche Aérospatiale, No. 1972-1, pp 1-14.
46. BRADSHAW, P. & FERRISS, D.H.: Calculation of boundary layer development using the turbulent energy equation : compressible flow on adiabatic walls.
J. Fluid Mechanics, Vol. 46, Part 1, 1971, pp 83-110.
47. PATANKAR, S.V. & SPALDING, D.B.: Heat and mass transfer in boundary layers.
Intertext Books, London (2nd edition), 1967.
48. KELLER, H.B.: Numerical methods in boundary layer theory.
Annual Review of Fluid Mechanics, Vol. 10, 1978, pp 417-433.
49. DE LA CHEVALERIE, A.: Application d'une méthode intégrale au calcul d'interaction onde de choc-couche limite turbulente en écoulement faiblement supersonique.
Ph.D. Université de Poitiers CEAT-ENSMA.
50. SHANG, J.S.; HANRAY, W.L. & WOYER, D.: Numerical analysis of eddy viscosity models in supersonic turbulent.
AIAA Paper 73-164, 1973.
51. HORSTMAN, C.C.: Turbulence model for non equilibrium adverse pressure gradient flows.
AIAA J., Vol. 15, No. 2, February 1977, pp 131-132.
52. MICHEL, R.; QUEMARD, C. & DURANT, R.: Application d'un schéma de longueur de mélange à l'étude des couches limites turbulentes d'équilibre.
ONERA NT 154, 1969.
53. RUBESIN, M.W.: Numerical turbulence modelling.
in Computational Fluid Dynamics,
AGARD LS 86, 1976.
54. CHAMBERS, T.L., & WILCOX, D.C.: Critical examination of two equation closure models.
AIAA Paper 76-352, July 1976.
55. COAKLEY, T.J. & VIEGAS, J.R.: Turbulence modelling of shock separated boundary layers flow.
Turbulent Shear Flow Conference, Penn. State, 1977.
56. MICHARD, P. & DUTOYA, D.: Calcul des coefficients d'échanges sur les aubes de turbines à haute température.
La Recherche Aérospatiale 1978-3, pp 133-137.
57. HUO, S.: Optimization based on the boundary layers concept for compressible decelerating flows.
VKI TN 111, June 1975.
58. MORKOVIN, M.V.: Technical evaluation report of the Fluid Dynamics Panel Symposium on Laminar Turbulent Transition.
AGARD AR 122, 1978.
59. Proceedings of AGARD Fluid Dynamics Panel Symposium on Laminar Turbulent Transition.
AGARD GP 224.
60. SO, R.M.C. & MELLOR, G.L.: An experimental investigation of turbulent boundary layers along curved surfaces.
NASA CR 1940, 1972.

61. TETERVIN, N.: An exploratory theoretical investigation of the effect on longitudinal surface curvature on the turbulent boundary layer.
NOL TR 69-22, February 1969
62. BRADSHAW, P.: Effects of streamline curvature on turbulent flow.
AGARDograph 169, 1973.
63. COUSTEIX, J. & HOUDEVILLE, R.: Méthode intégrale de calcul d'une couche limite turbulente sur une paroi courbée longitudinalement.
La Recherche Aérospatiale 1977-1, pp 1-13.
64. TOWNSEND, A.A.: The structure of turbulent shear flow.
Cambridge University Press, 1956.
65. HILL, P.G.; SCHAUB, U.W. & SENOO, Y.: Turbulent wakes in pressure gradients.
ASME Trans., J. Applied Mechanics, 1963, pp 518-624.
66. SOLIGNAC, J.L.: Calcul du sillage turbulent bidimensionnel en aval d'un obstacle mince.
CANCAM 73; also ONERA TP 1253, 1973.
67. QUEMARD, C. & J.P. ARCHAMBAUD, J.P.: Méthode intégrale de calcul d'un sillage avec gradient de pression longitudinale.
CERT-DERAT Fiche technique No. 1/76.
68. HODGE, J.G.; STONE, A.L. & ILLER, T.E.: Numerical solution for airfoils near stable in optimized boundary-fitted curvilinear coordinate.
AIAA J., Vol. 17, No. 5, 1979, pp 458-464.
69. LOUDET, C.L.: Contribution théorique et expérimentale de l'étude des grilles d'aubes en tandem à forte déflexion et à forte charge.
IVK-ULB Ph.D. Thesis, April, 1971.
70. MILLER, M.J.: Estimation of deviation angle for axial-flow compressor blade sections using inviscid-flow solutions.
NASA TN D 7549, 1974.
71. WILKINSON, D.: A numerical solution of the analysis and design problems for the flow past one or more aerofoils or cascades.
ARC R&M 3545, 1967.
72. VAN DEN BRAEMBUSSCHE, R.: Calculation of compressible subsonic flow in cascades with varying blade height.
ASME Paper 73-GT-59, 1973.
73. DODGE, P.: The use of a finite difference technique to predict cascade stator and rotor deviation angles and optimum angles of attack.
ASME Paper 73-GT-10, 1973.
74. MILLER, M.J. & SEROVY, G.K.: Deviation angle estimation for axial flow compressors using inviscid flow solutions.
ASME Paper 74-GT-74, 1974.
75. GELLER, W.: Berechnung der Druckverteilung an Gitterprofilen in ebener inkompres-sibler Strömung mit Grenzschichtablösung in Bereich der Profilenden.
DLR FB 72-62, 1972.
76. GOUJON-DUBOIS, A. & VAN DEN BRAEMBUSSCHE, R.: Calcul d'un écoulement incompressible décollé dans une grille d'aubes.
U-VKI 1972-72.
77. GEROPP, D. & GRASHOF, J.: Berechnung von Strömungen mit ablosenblasen bei grossen Reynoldszahlen.
DLR FB 76-52, 1976.
78. MEAUZE, G.: Comparaison calcul-expérience de l'écoulement transsonique bidimension-nel dans une grille d'aubes à forte déviation.
La Recherche Aérospatiale 1978-4, pp 175-180.
79. HANSEN, E.C.; SEROVY, G.K. & SOCKUL, P.M.: Axial flow compressor turning angle and loss by inviscid-viscous interaction blade-to-blade computation.
J. Engrg. for Power, Trans. ASME, Vol. 102, 1980, pp 28-34.
80. DECONINCK, H. & HIRSCH, C.H.: A finite element method solving the full potential equation with boundary layer interaction in transonic cascade flow.
AIAA Paper 79-0312, 1979.
81. GOSTELOW, J.P.; LEWKOWICZ, A.K & SHALAAN, M.R.A.: Viscosity effects on the two dimensional flow in cascades.
ARC CP 872, 1965.

82. SCHOLZ, N.: Aerodynamics of cascades.
AGARDograph 220, 1977.
83. TRAUPEL, W.: Thermische Turbomaschinen.
Springer Verlag, 1968.
84. CALVERT, W.J. & HERBERT, M.V.: An inviscid-viscous interaction method to predict the blade to blade performance of axial compressors.
NGTE M 80012
85. SINGH, U.K.: Computation of transonic flows in cascade with shock boundary layer interaction,
in Shock-Boundary Layer Interaction in Turbomachines,
VKI LS 1980-8.
86. PANARAS, A.: Calculation of a boundary layer interacting with a normal shock by discontinuity analysis.
VKI TN 121, 1976.
87. DELERY, J.; CHATTOT, J.J. & LE BALLEUR, J.C. Interaction visqueuse avec décollement transsonique.
ONERA TP 1975-15.
88. THIEDE, P.G.: Ein inverses Integralverfahren zur Berechnung abgelöster turbulenter Grenzschichten.
DLR FB 1977-16, pp 245-255.
89. LE BALLEUR, J.C.: Couplage visqueux - non visqueux : méthode numérique et applications aux écoulements bidimensionnels transsoniques et supersoniques.
La Recherche Aérospatiale 1978-2.
90. LA BALLEUR, J.C.: Couplage visqueux - non visqueux : analyse du problème incluant décollements et ondes de chocs.
La Recherche Aérospatiale 1977-6.
91. KLINEBERG, J.M. & STEGER, J.L.: Calculation of separated flow at subsonic and transonic speeds.
3rd Int. Conf. Num. Methods in Fluid Dynamics. Springer 1973.
92. LEES, L. & REEVES, B.L.: Supersonic separated and reattaching laminar flows.
AIAA J., Vol. 2, No. 11, 1964, pp 1907-1920.
93. NIELSEN, J.M.; LYNES, L.L. & GOODWING, F.K.: Calculation of laminar separation with free interaction by the method of integral relations.
AFFDL-TR 65-107, June 1965.
94. CARRIERE, P.; SIRIEIX, M. & DELERY J.: Méthodes de calcul des écoulements turbulents décollés en supersonique.
Progress in Aerospace Science., Vol. 16, No. 4 1975, pp 385-429.
95. GEORGEFF, M.P.: Momentum integral method for viscous inviscid interactions with arbitrary wall cooling.
AIAA J., Vol. 12, No. 10, 1974, pp 1393-1400.
96. LE BALLEUR, J.C.: Calculs couplés visqueux - non visqueux incluent décollements et ondes de choc en écoulement bidimensionnel
in Three Dimensional and Unsteady Separation at High Reynolds Numbers.
AGARD LS 94, 1978.
97. TU, K.M. & WEINBAUM, S.: A nonasymptotic triple deck model for supersonic boundary layer interaction.
AIAA J., Vol. 14, No. 6, June 1976, pp 767-775.
98. LIOU, M.S.: Asymptotic analysis of interaction between a normal shock wave and a turbulent boundary layer in transonic flow.
Ph.D. Thesis, University of Michigan, 1978.
99. BRIALLIANT, H.M. & ADAMSON, T.C.: Shockwave boundary layer interactions in laminar transonic flow.
AIAA J., Vol. 12, No. 3, March 1974, pp 323-329
100. STEWARISON, K.: Multistructured boundary layers on flat plates and related bodies.
Advances in Applied Mechanics, Vol. 14, 1974 pp 145-239.
101. PANARAS, A.G.: Normal shock boundary layer interaction in transonic speed in the presence of a streamwise pressure gradient.
VKI-ULB Ph.D. Thesis, May 1976.
102. INGER, G.R. & MASON, W.H.: Analytical theory of transonic normal shock - turbulent boundary layer interactions.
AIAA J., Vol. 14, No. 9, September 1976, pp 1266-1272.

103. DOUGE, P.R.: A numerical method for two and three dimensional viscous flows.
AIAA Paper 76-425, 1976.
104. McDONALD, H.: Computational aspects of viscous flows,
in Application of Numerical Methods to Flow Calculations in Turbomachinery
VKI LS 1979-7.
105. MOORE, J. & MOORE, J.G.: A calculation procedure for three dimensional viscous
compressible duct flow. Parts I & II.
ASME Trans., J. Fluids Engineering Vol. 101, No. 4; 1979, pp 415-428.
106. WALLIT, L.: Numerical analysis of the three dimensional viscous flow field in a
centrifugal impeller.
AGARD CP 282, 1980.
107. MacCORMACK, R.W.: Numerical solution of the interaction of a shock wave with a
laminar boundary layer.
Lecture Notes in Physics. Vol. 8, Springer-Verlag, 1970.
108. MATEER, G.: BROSH, A. & VIEGAS, J.R.: A normal shock wave turbulent boundary
layer interaction at transonic speeds.
AIAA Paper 76-161, 1976.
109. HJENS, R.W. & MacCORMACK, R.W.: Numerical solutions of supersonic and hypersonic
laminar flow over a three dimensional compression corner.
AIAA Paper 77-4694, 1977.
110. BEAM, R.M. & WARMING, R.F.: An implicit factored scheme for the compressible
Navier-Stokes equations.
AIAA Paper 77-645, 1977.
111. WAGNER, B. & SHMIDT, W.: Theoretical investigation of real gas effects in cryogenic
wind tunnels.
AIAA Paper 77-669, 1977.
112. SHANG, J.S.: Implicit-explicit method for solving the Navier-Stokes equation.
AIAA Paper 77-646; AIAA J., Vol. 16, No. 5, 1978, pp 496-502.
113. SHANG, J.S. & HANKEY, W.L.: Supersonic turbulent separated flows utilizing
the Navier-Stokes equations,
in Flow Separation, AGARD CP 168, 1975.
114. BALLHAUS, W.F.: Some recent progress in transonic flow computation,
in Computational Fluid Dynamics,
VKI LS 87, March 1976.
115. MacCORMACK, R.W.: An efficient explicit implicit characteristic method for solving
the compressible Navier-Stokes equations.
SIAM-AMS, New York, April 1977.
116. LI, C.P.: A mixed explicit implicit splitting method for the compressible Navier-
Stokes equation.
Lecture Notes in Physics, Vol. 59, Springer Verlag 1976 pp 285-292
117. VIVIAND, H.: Traitements des problèmes d'interaction fluide parfait, fluide
visqueux en écoulement bidimensionnel compressible à partir des équations de
Navier-Stokes,
in Three Dimensional and Unsteady Separation at High Reynolds Numbers,
AGARD LS 94, 1978.
118. PEYRET, P. & VIVIAND, H.: Computation of viscous compressible flows based on the
Navier-Stokes equations.
AGARDograph 212, September 1975.
119. HALLANDERS, H. & VIVIAND, H.: The numerical treatment of compressible high Reynolds
number flows,
in Computational Fluid Dynamics.
VKI LS 1979-7; also ONERA TP 1979-22.

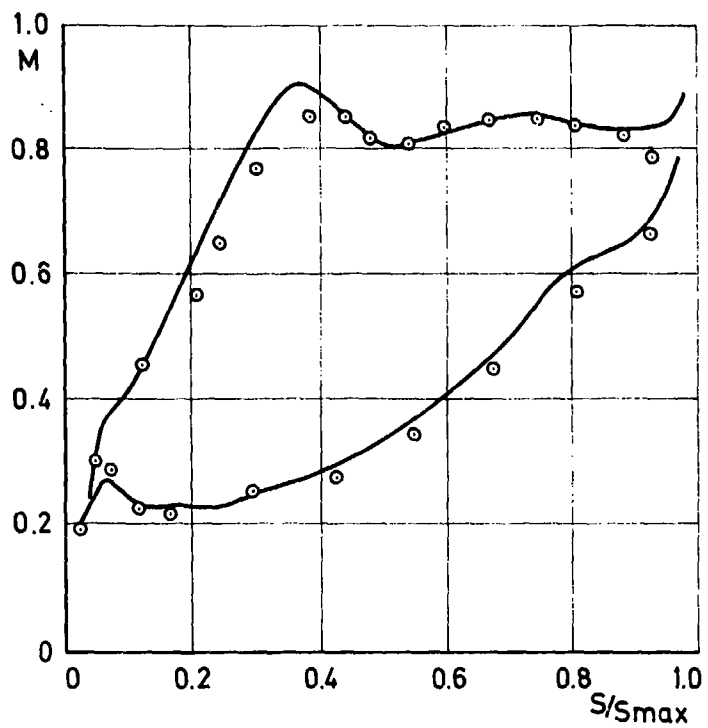


FIG. 1 - NASA TN D-3751 STATOR MEAN SECTION

 $M_1 = .23$

○ EXPERIMENTAL

— CALCULATED REF (4)

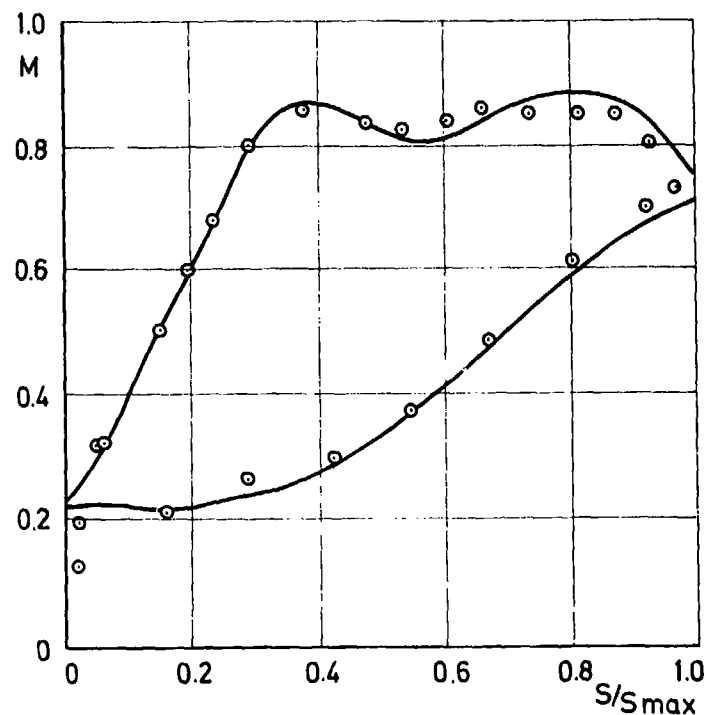


FIG. 2 - NASA TN D-3751 STATOR MEAN SECTION

 $M_1 = .231$

○ EXPERIMENTAL

— CALCULATED REF (6)

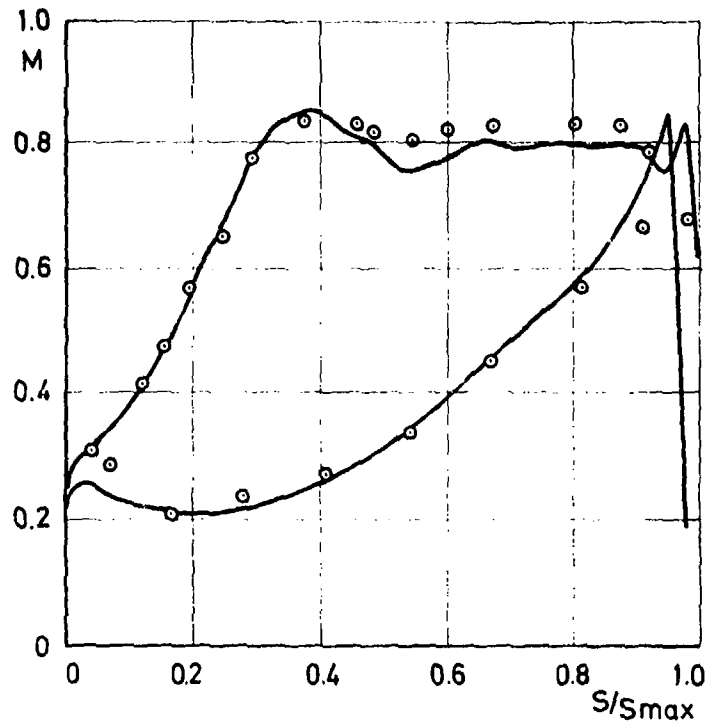


FIG. 3 - NASA TN D-3751 STATOR MEAN SECTION
 $M_1 = .23$
 ○ EXPERIMENTAL
 — CALCULATED REF (10)

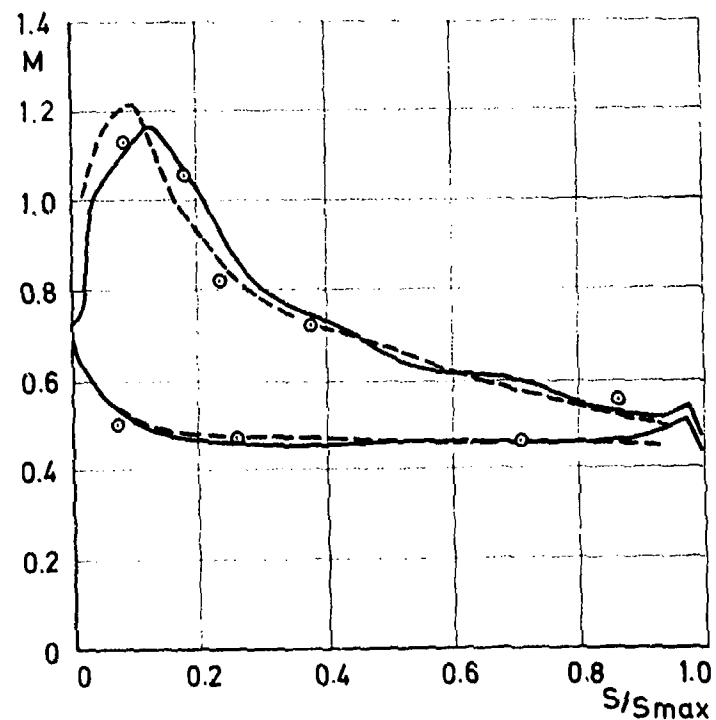


FIG. 4 - TRANSONIC STATOR
 $M_1 = .82$
 ○ EXPERIMENTAL
 - - - RELAXATION METHOD
 — TIME MARCHING METHOD REF (24)

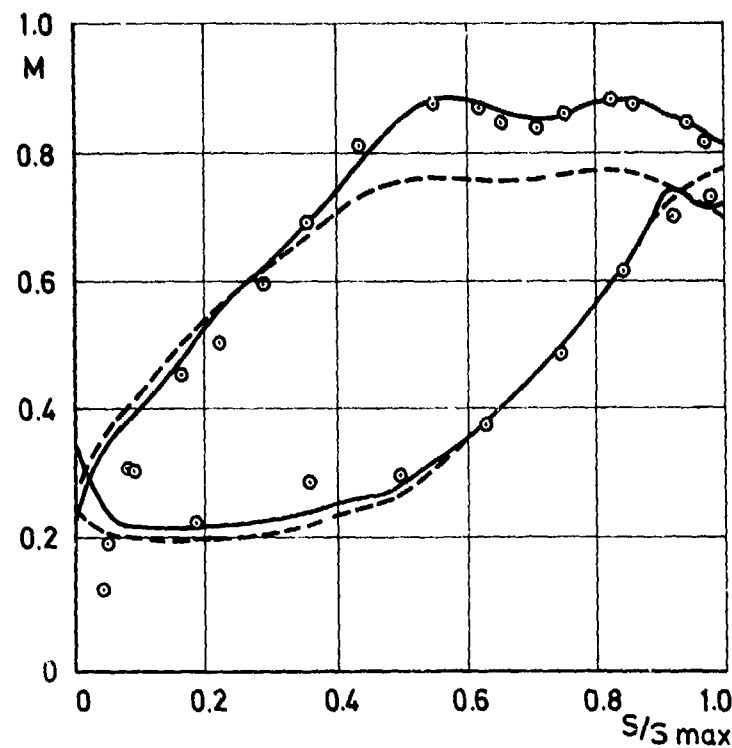


FIG.5 - NASA NOZZLE BLADE
 ○ EXPERIMENTAL
 --- SOLUTION WITHOUT CORRECTION
 — STANDARD SOLUTION REF (25)

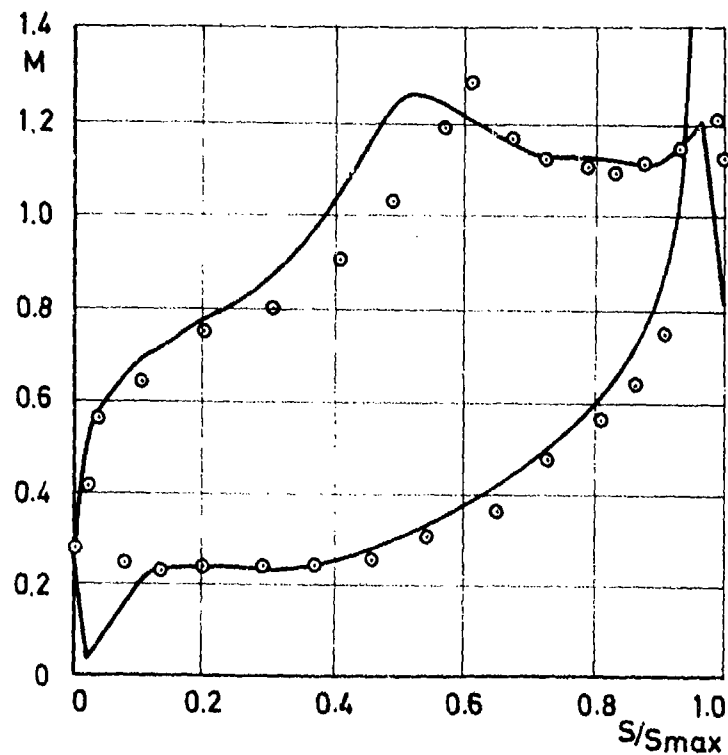


FIG. 6 - VKI LS 59 TURBINE BLADE
 ○ EXPERIMENTAL
 — CALCULATED REF (29)

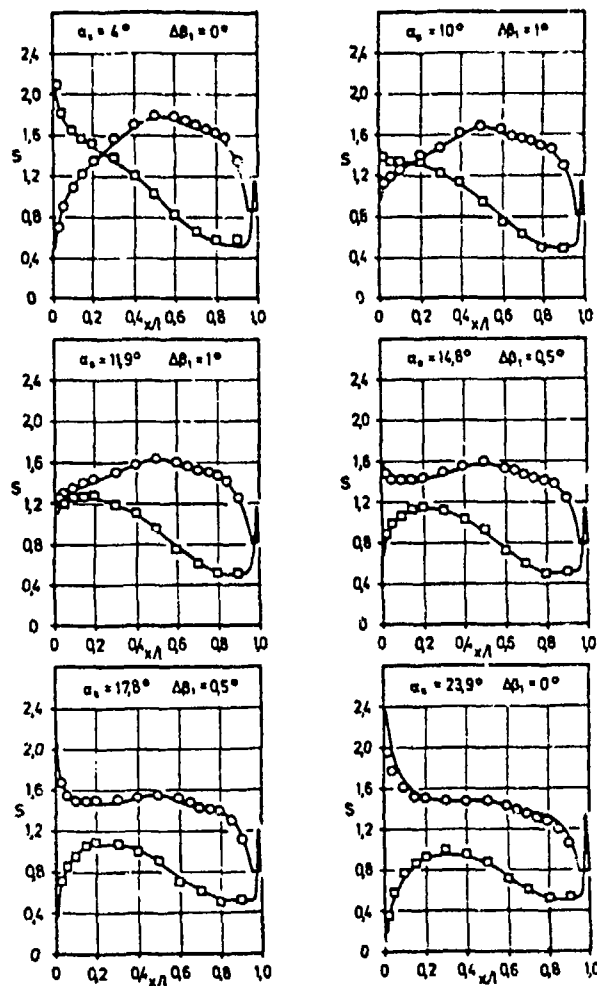


FIG. 7 - COMPARISON OF MEASURED AND CALCULATED
PRESSURE DISTRIBUTIONS.

○ MEASUREMENT (UPPER SURFACE)
 □ MEASUREMENT (LOWER SURFACE)
 — CALCULATION

ref. (75)

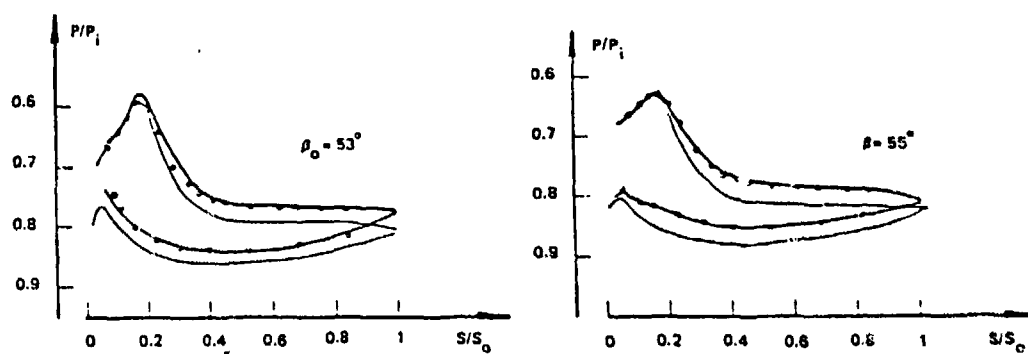


FIG. 8 - EXPERIMENTAL PRESSURE DISTRIBUTIONS OVER
A BLADE AT MID-SPAN(103).

○ EXPERIMENT
 — COMPUTATION WITH THICKENING.
 - - - COMPUTATION WITHOUT THICKENING

ref. (78)

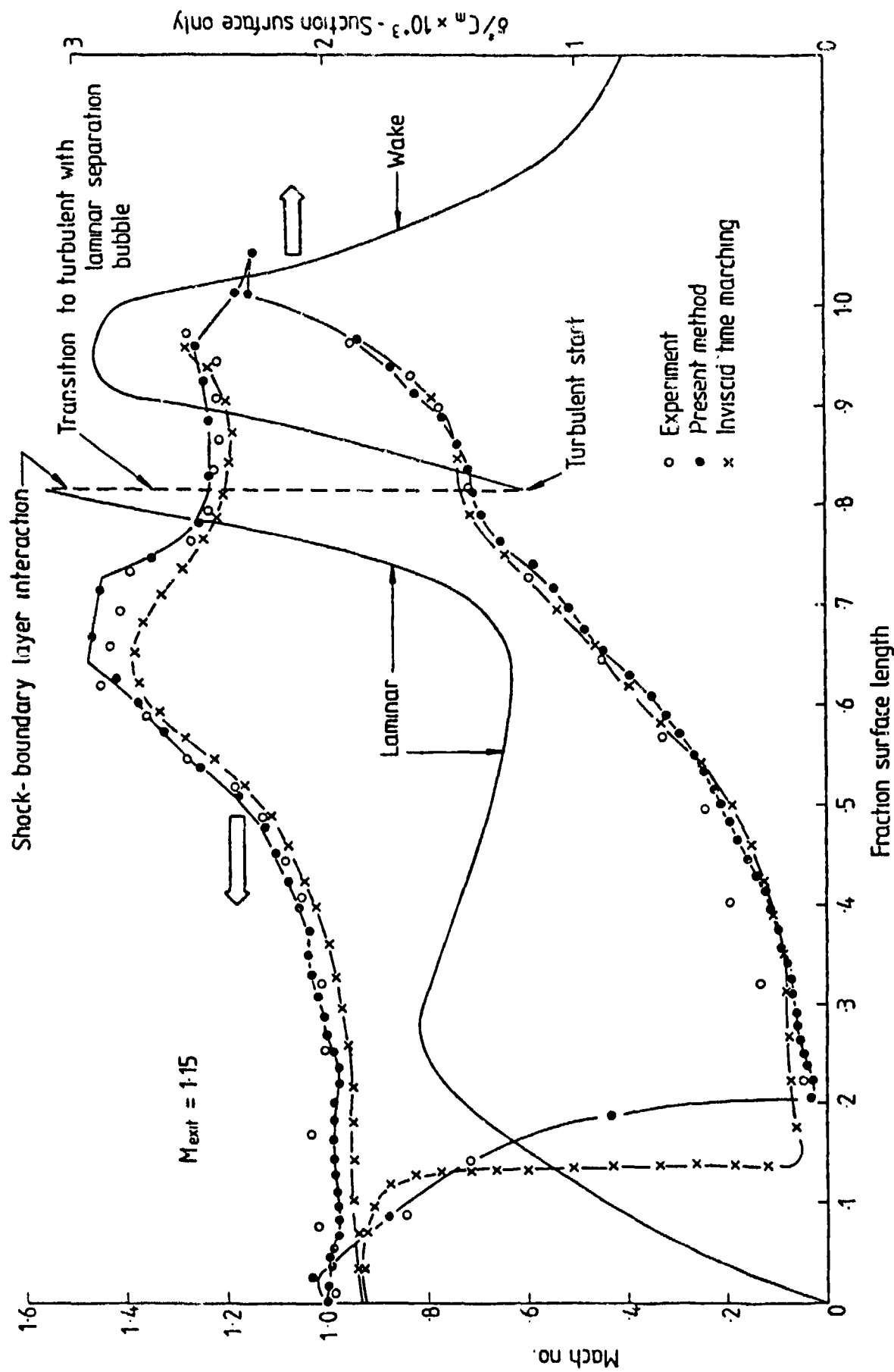


FIG. 9 - ROLLS ROYCE NOZZLE SECTION RA ref. (85)

V1 CASCADE : $M_1 = 0.8$: $\alpha_1 = 54.5^\circ$

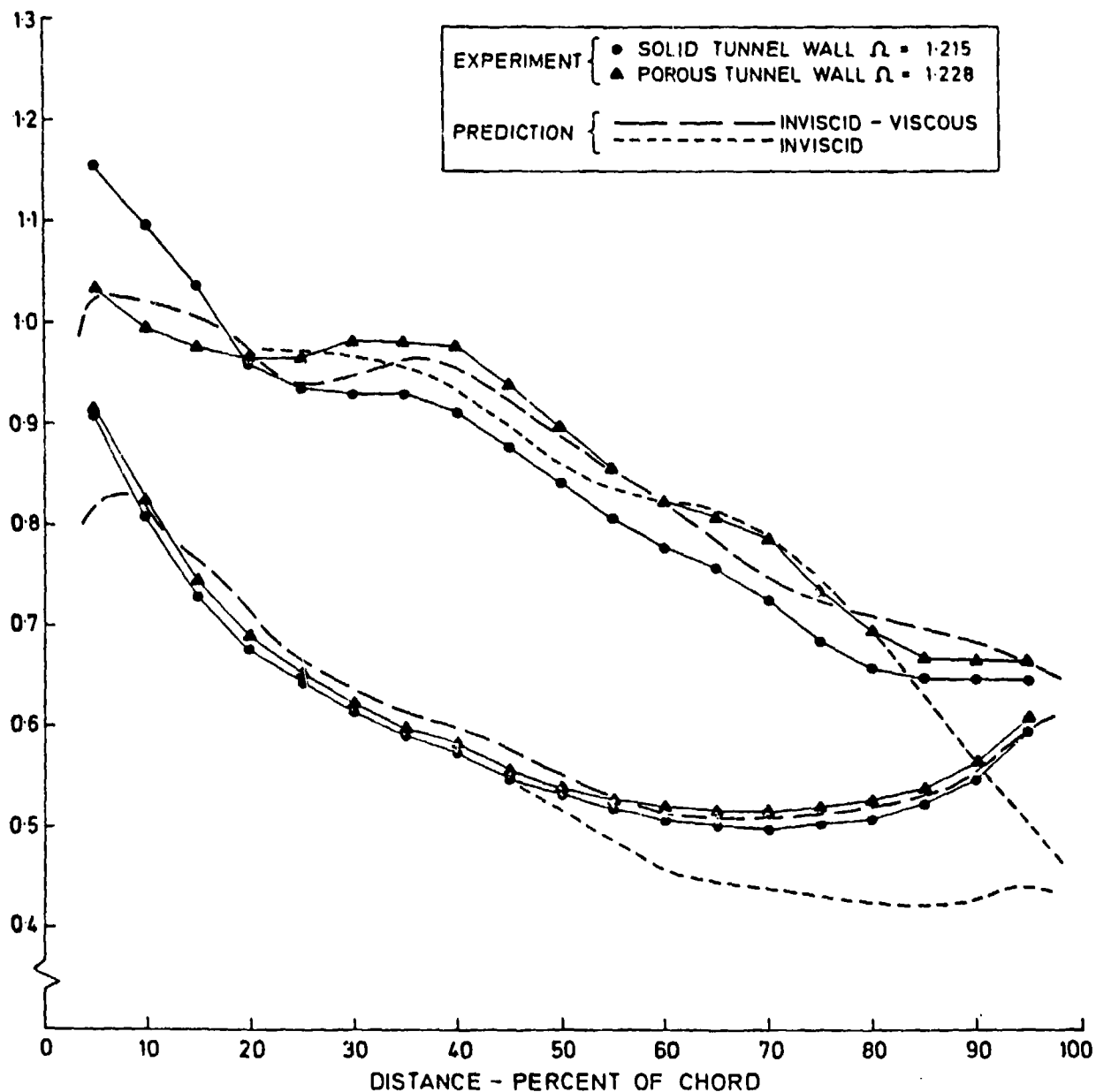
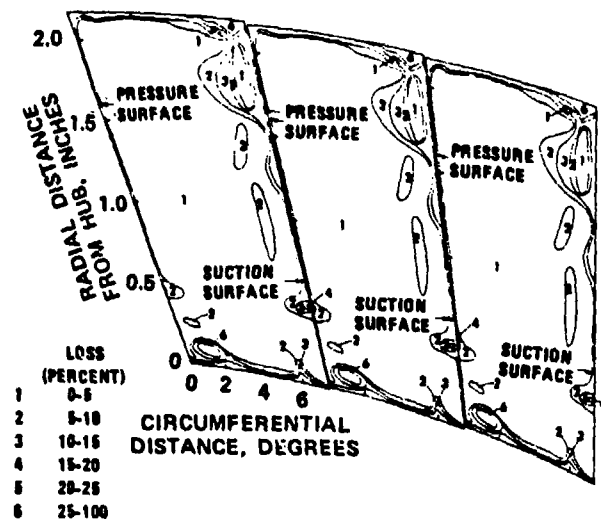


FIG.10-MACH NUMBER DISTRIBUTION FOR
V1 CASCADE ref (84)



Third iteration contours of constant loss for NACA TN 2871 turbine stator.

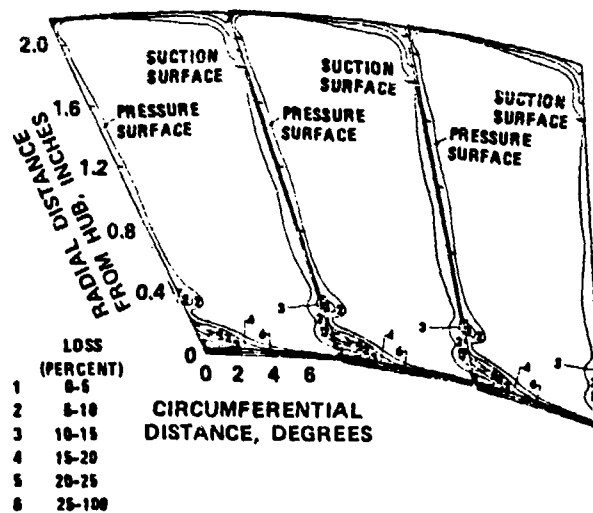


Fig. 11 Measured contours of constant loss for NACA TN 2871 turbine stator.
Ref (103)

PART IV
GENERAL CONCLUSIONS AND RECOMMENDATIONS

Part IV - General Conclusions and Recommendations

Faced with the task of comparing the overall performance and detailed flow predictions with experimental data, it appears that the outcome of this exercise is dependent on the accuracy and consistency of three components : the available experimental data, the through-flow calculation method and finally the loss and turning correlations.

Although the main task of the Working Group was to investigate the reliability of existing loss and turning correlations at design and off-design conditions, it could not be separated from the two other components as soon as comparisons with experimental results were to go beyond simple cascade data.

The first observation was the lack of reliable and publicly available data especially for multistage compressors. Although some data can be found showing overall performance, there is a strong need for detailed flow field data in multistage machines, representative of present day technology.

Moreover great care should be given to the accuracy of the data recording and more particularly to the data reduction programs. Generally, experimentalists deduce detailed flow data from a reduced set of measurements taken behind the stators. The determination of the losses and deviations behind the rotors for instance are obtained from the data reduction code based on some assumptions with regard to the streamline shape (usually the design shape) and eventually on some model for the loss and turning distributions within the blade rows. The data reduced in this way are subject to an uncertainty and make any comparison with calculated data, especially at off-design, doubtful. Hence, we suggest the most extreme attention to this problem and advice to establish comparisons of data reduced from the measurements in an unambiguous and objective way.

The second problem is concerned with the interaction between a particular through-flow method and a set of loss and turning correlations. For the same system of correlations, it is well known that different results can be obtained with different through-flow programs. This is not connected to the numerical aspects of the methods (although, due to the strong non-linearity of the equations, the particular iterative procedure used could have an influence on the overall converged results), but to the various assumptions which enter in each program. The need and the influence on the calculated data of internal stations in streamline curvature methods has been stressed by Novak and already reported in Chapter II.4. This has also a strong influence on reduced experimental data and adds to the caution to be kept in mind as mentioned above.

With additional internal stations in through-flow calculations, assumptions have to be made with regard to the law of variation, with chordwise distance, of losses and deviations. Presently, there is no systematic analysis available of how the profile losses (connected to the streamwise variation of blade boundary layer thickness) and the streamwise variation of angular momentum, behave under various conditions of incidence, Mach number and blade profile geometry. Informations about the angular momentum could easily be obtained from two dimensional inviscid blade-to-blade calculations and the rate of increase of the profile losses could be obtained from a boundary layer calculation. This is a typical example of how some general trend could be obtained from systematic blade-to-blade calculations and correlated in order to be used in through-flow calculations. It is our experience that the assumptions on the law of variation of these two variables inside the blade row can have strong effects on the predicted results. For instance, going from a linear to a parabolic variation of angular momentum in function of axial distance inside the blade rows, can lead in some cases to variations of the order of 10 % on the predicted overall pressure ratio.

Another parameter influencing strongly the results of through-flow calculations is the inclusion of the tangential blockage due to the blade boundary layers inside the blade row and to the wakes at blade trailing edge which have to be added to the blade blockage. Besides the effect on the calculated data, this introduces an additional interaction between the kinematic flow parameters, such as the blockage, with the loss correlations, since the wake blockage is proportional to the profile loss coefficient.

A parameter of fundamental importance is the end-wall blockage which, even calculated with an end-wall boundary layer theory of the type described in Section II.2.3., adds a strong non-linear interaction between the kinematics and the loss and turning correlation.

It was the Working Group's opinion that these sources of ambiguity should be kept in mind when it comes to assess the influence of the chosen set of correlations on the predicted flow and overall performance data.

However, both Subgroups - Turbine and Compressor - came to the observation that with the present level of experimental accuracy, the existing methods of through-flow were compatible with the level of accuracy of the correlations, especially with regard to the overall performance prediction. In both fields, detailed flow predictions such as spanwise flow angle of loss distribution at a given blade row outlet are however far from being satisfactory for compressors as well as for turbines. This is true even if the overall performance is satisfactorily predicted.

The level of accuracy needed for performance prediction is not equivalent for the losses and the deviations. It appeared clearly that, in the turbine field as well as in the compressor field, the required accuracy for deviations is appreciably higher than for losses. Indeed, one or two degrees on deviation angle have a considerable influence on

the predicted flow behaviour and on the machine performance. On the other hand, the predicted flow behaviour is less sensitive to small variations in the loss coefficient.

Present day designs are faced with two complementary requirements : the need for rapid, reliable and simple correlations in order to optimize stage design and, on the other hand, the need for more accurate detailed flow predictions in the advanced stage of the design and conception work.

These requirements are indeed complementary, since the way to the improvement of simple correlations lies in the better understanding of the basic physical phenomena. It was the Working Group's consensus that this could be achieved by a systematic use of two- and three-dimensional blade-to-blade calculations in order to derive simple and sound physical correlations. This implies the development and use of 2D and 3D viscous flow calculations and, on the other hand, the definition of basic experiments.

Hence, in addition to the specific observations to be found in the conclusions of the Parts I and II of this report, the following recommendations came forward out of the activity of the Working Group :

- . An important effort should be made to obtain good and reliable multistage compressor and turbine data.
- . A deep physical understanding is needed with regard to the various loss sources and their particular generation mechanism. Basic experiments allowing one to separate and understand the various contributions should be considered.
- . Care should be taken to define a consistent set of relations within the correlations in order to avoid the duplication of effects and influence of parameters.
- . A particular effort is required with regard to secondary flow deviations and end-wall boundary layer effects. When possible, in axial compressors and high aspect ratio turbines, end-wall boundary calculations, coupled interactively with the through-flow calculations, should be used.
- . Notwithstanding the continuous development of three dimensional viscous flow calculation and the increase of computing power of the digital computers, it is not likely that through-flow calculations in multistage machines will be replaced by full viscous calculations in the near future. Therefore the need for good correlations will continue to be of great importance.

WORKING GROUP 12

MEMBERSHIPPEP MEMBERS

<u>BELGIUM</u>	<u>FRANCE</u>	<u>GERMANY</u>	<u>TURKEY</u>	<u>U.K.</u>	<u>U.S.</u>
M. le Professeur Ch. HIRSCH Vrije Universiteit Brussel Dienst Stromingsmechanica Pleinlaan 2 1050 Brussel	M. le Professeur J. CHAUVIN Université d'Aix Marseille II Directeur du Laboratoire Associé LA 03 Institut de Mécanique des Fluides 1 rue Honnorat 13003 Marseille	Professor Dr-Ing. G. WINTERFELD Institut für Antriebstechnik DFVLR Postfach 90 60 58 5000 Köln 90	Professor Dr. A. UÇER Middle East Technical University O D T Ü Makina Muh. Bölümü Ankara	Dr. J. DUNHAM National Gas Turbine Establishment Pyestock Farnborough, Hants GU14 OLS	Mr. J. ACURIO Director, Propulsion Laboratory US Army Research and Technology Laboratories (AVRADCOM) 21000 Brookpark Road Cleveland, Ohio 44135

NON-PANEL MEMBERS

<u>BELGIUM</u>	M. le Professeur R. VAN DEN BRAEMBUSSCHE Von Karman Institute for Fluid Dynamics 72 Chausseé de Waterloo 1640 Rhode Saint Genèse
<u>FRANCE</u>	M. le Professeur K. SIEVERDING Von Karman Institute for Fluid Dynamics 72 Chausseé de Waterloo 1640 Rhode Saint Genèse
	M. G. MEAUZE Chef de Groupe de Recherches Office National d'Etudes et de Recherches Aérospatiales 29 Avenue de la Division Leclerc 92320 Châtillon sous Bagneux

MEMBERSHIP (Ct-1)GERMANY

Professor Dr.-Ing. L. FOTTNER
 WE 12 Strömungsmaschinen
 Hochschule der Bundeswehr
 Werner-Heisenberg Weg 39
 8014 Neubiberg

Dr.-Ing. H.B. WEYER
 Institut für Antriebstechnik
 DFVLR
 Postfach 90 60 58
 5000 Köln 90

ITALY

Dott. Ing. E. BENVENUTI
 Responsabile Sezione Fluidodinamica
 dell'Ufficio Studi e Ricerche
 Soc. Nuovo Pignone
 Via Matteucci 2
 50100 Firenze

Professor E. MACCHI
 Istituto di Macchine
 Politecnico di Milano
 Piazza Leonardo da Vinci 32
 20133 Milano

U.K.

Dr. J.D. DENTON
 Science Research Council
 Whittle Laboratory
 University Engineering Department
 Madingley Road
 Cambridge CB3 OEL

U.S.

Dr. R.A. NOVAK
 Aircraft Engine Group MS A24048
 1000 Western Avenue
 Lynn, Massachusetts 01910

Dr. A.M. PFEFFER
 Pratt & Whitney Aircraft
 Engineering Building 2 C
 400 Main Street
 East Hartford, Connecticut 06108

Dr. D.M. SANDERCOCK
 NASA Lewis Research Center
 21000 Brookpark Road
 Cleveland, Ohio 44135

Professor G. SEROVY
 207 Mechanical Engineering Building
 Iowa State University
 Ames, Iowa 50011

OBSERVERSITALY

Mr. G. DORIA
 ANSALDO
 Via Pacinotti 20
 Genoa-Sampierdareva 16151

Ing. B. INNOCENTI
 Soc. Nuovo Pignone
 Via Matteucci 2
 50100 Firenze

Dr. P. ZUNINO
 ANSALDO
 Via Pacinotti 20
 Genoa-Sampierdareva 16151

THROUGH FLOW CALCULATIONS IN AXIAL TURBOMACHINESEditors

Ch. HIRSCH
J.D. DENTON

LIST OF CONTRIBUTORS

Name	Address	Chapters
VAN DEN BRAEMBUSSCHT, Prof. R.	Von Karman Institute for Fluid Dynamics 72 Chaussée de Waterloo 1640 Rhode Saint Genèse, Belgium	II.4.2 III.2
CHAUVIN, Prof. J.	Université d'Aix Marseille II Directeur du Laboratoire Associé LA 03 Institut de Mécanique des Fluides 1 rue Honnorat 13003 Marseille, France	II.2.4 II.2.9 II.2.10
DENTON, Dr. J.D.	Science Research Council Whittle Laboratory University Engineering Department Madinfly Road Cambridge CB3 OEL, UK	Notation Part I I.1 I.4 I.5 A.J
DUNKER, Dipl-Ing. R.	Institut für Antriebstechnik DFVLR Postfach 90 60 58 5000 Köln 90, Germany	II.2.1
FOTTNER, Prof. Dr-Ing. L.	WE 12 Strömungsmaschinen Hochschule der Bundeswehr Werner-Heisenberg Weg 39 8014 Neubiberg, Germany	II.2.2 II.2.6
HIRSCH, Prof. Ch.	Vrije Universiteit Brussel Dienst Stromingsmechanica Pleinlaan 2 1050 Brussel, Belgium	Gen. Introduction II.1 II.2 II.2.3 II.3 A.II.3.2 II.4 II.4.1 II.5 IV
MACCHI, Prof. E.	Istituto di Macchine Politecnico di Milano Piazza Leonardo da Vinci 32 20133 Milano, Italy	A.I
McDONALD, Mr. P.W.	Pratt & Whitney Aircraft Group Commercial Products Division 400 Main Street East Hartford, Connecticut 06108, US	I.3
MEAUZE, M. G.	ONERA Chef de Groupe de Recherches 29 Avenue de la Division Leclerc 92320 Châtillon sous Bagneux, France	III.2
NOVAK, Dr. R.A.	Aircraft Engine Group MS A24048 1000 Western Avenue Lynn, Massachusetts 02139, US	II.2.7
ROBERTS, Mr. W.B.	FAR 1543 Vernal Avenue Fremont, California 94538, US	II.2.5 II.2.7

LIST OF CONTRIBUTORS (Ctd)

Name	Address	Chapters
de RUYCK, Mr.	Vrije Universiteit Brussel Dienst Stromingsmechanica Pleinlaan 2 1050 Brussel, Belgium	II.2.3
SCHÄFFLER, Dipl.-Ing. A.	Motoren und Turbinen Union Dachauerstrasse 665 8000 München 80, Germany	II.2.6
SIEVERDING, Prof. K.	Von Karman Institute for Fluid Dynamics 72 Chaussee de Waterloo 1640 Rhode Saint Genèse, Belgium	I.2
SEROVY, Prof. G.	207 Mechanical Engineering Bldg Iowa State University Ames, Iowa 50011, US	II.2.8 III.1
UÇER, Prof. Dr. A	Middle East Technical University O D T Ü Makina Muh. Bölümü Ankara, Turkey	A.I
WEYER, Dr.-Ing. H.B.	Institut für Antriebstechnik DFVLR Postfach 90 60 58 5000 Köln 90	II.2.1 II.3 A.II.3.1
ZUNINO, Dr. P.	ANSALDO Societe Generale Elettromecanica Via Pacinotti 20 Genoa-Sampierdareva 16151, Italy	A.I

LIST OF CONTRIBUTIONS

<u>Chapter</u>	<u>Author</u>	<u>Chapter</u>	<u>Author</u>
Gen. Introduction	HIRSCH	II.2.6	SCHÄFFLER FOTTNER
Notation Part I	DENTON	II.2.7	ROBERTS NOVAK
I.1	DENTON	II.2.8	SEROVY
I.2	SIEVERDING	II.2.9	CHAUVIN
I.3	MCDONALD	II.2.10	CHAUVIN
I.4	DENTON	II.3.	HIRSCH WEYER
I.5	DENTON	A.II.3.1	WEYER
A.I	DENTON MACCHI UCER ZUNINO	A.II.3.2	HIRSCH
II	HIRSCH	II.4	HIRSCH
II.1	HIRSCH	II.4.1	HIRSCH
II.2	HIRSCH	II.4.2	VAN DEN BRAEMBUSSCHE
II.2.1	DUNKER WEYER	II.5.	HIRSCH
II.2.2	FOTTNER	III.1	SEROVY
II.2.3	HIRSCH de RUYCK	III.2	MEAUZE VAN DEN BRAEMBUSSCHE
II.2.4	CHAUVIN	IV	HIRSCH
II.2.5	ROBERTS		

REPORT DOCUMENTATION PAGE			
1. Recipient's Reference	2. Originator's Reference	3. Further Reference	4. Security Classification of Document
	AGARD-AR-175	ISBN 92-835-1400-9	UNCLASSIFIED
5. Originator	Advisory Group for Aerospace Research and Development North Atlantic Treaty Organization 7 rue Ancelle, 92200 Neuilly sur Seine, France		
6. Title	PROPULSION AND ENERGETICS PANEL WORKING GROUP 12 on THROUGH FLOW CALCULATIONS IN AXIAL TURBOMACHINES		
7. Presented at			
8. Author(s)/Editor(s)	Edited by Ch.Hirsch and J.D.Denton		9. Date October 1981
10. Author's/Editor's Address	See Flyleaf		11. Pages 342
12. Distribution Statement	This document is distributed in accordance with AGARD policies and regulations, which are outlined on the Outside Back Covers of all AGARD publications.		
13. Keywords/Descriptors	Axial turbines Axial compressors	Through flow calculations Performance estimation	
14. Abstract	<p>In 1977, the Propulsion and Energetics Panel of AGARD had set up its Working Group 12 on 'Through Flow Calculations in Turbomachines' after having found in the 47th (B) Meeting that the prediction of off-design performances, especially for axial flow compressors, was not fully satisfactory.</p> <p>The objectives were to review the existing information on blade performance and wall effect prediction, and to extend this information by systematic application of numerical methods to representative geometries.</p> <p>In its performance period Working Group 12 had confined to axial turbomachines only and split into a Turbine Sub-Group and a Compressor Sub-Group. In the Turbine Sub-Group five correlations were reviewed and evaluated against the test cases. Each correlation had its strengths and weaknesses and room for further improvements.</p> <p>The Compressor Sub-Group report begins with a comprehensive survey of the various loss and deviation mechanisms. For comparison of the prediction methods to the test cases five authors have used their own correlations, while the sixth employed a single code in conjunction with three correlations for the four stage compressor. The results of the evaluation are similar to those of the Turbine Sub-Group, but the spanwise parameter distribution is often poorly predicted.</p> <p>This Advisory Report was prepared at the request of the Propulsion and Energetics Panel of AGARD.</p>		

<p>AGARD Advisory Report No.175 Advisory Group for Aerospace Research and Development, NATO PROPELLSION AND ENERGETICS PANEL WORKING GROUP 12 ON THROUGH FLOW CALCULATIONS IN AXIAL TURBOMACHINES Edited by Ch.Hirsch and J.D.Denton Published October 1981 342 pages</p>	<p>AGARD-AR-175 Axial turbines Axial compressors Through flow calculations Performance estimation</p>	<p>AGARD Advisory Report No.175 Advisory Group for Aerospace Research and Development, NATO PROPELLSION AND ENERGETICS PANEL WORKING GROUP 12 ON THROUGH FLOW CALCULATIONS IN AXIAL TURBOMACHINES Edited by Ch.Hirsch and J.D.Denton Published October 1981 342 pages</p> <p>In 1977, the Propulsion and Energetics Panel of AGARD had set up its Working Group 12 on 'Through Flow Calculations in Turbomachines' after having found in the 47th (B) Meeting that the prediction of off-design performances, especially for axial flow compressors, was not fully satisfactory.</p>	<p>P.T.O.</p>	<p>AGARD-AR-175 Axial turbines Axial compressors Through flow calculations Performance estimation</p> <p>In 1977, the Propulsion and Energetics Panel of AGARD had set up its Working Group 12 on 'Through Flow Calculations in Turbomachines' after having found in the 47th (B) Meeting that the prediction of off-design performances, especially for axial flow compressors, was not fully satisfactory.</p>
<p>AGARD Advisory Report No.175 Advisory Group for Aerospace Research and Development, NATO PROPELLSION AND ENERGETICS PANEL WORKING GROUP 12 ON THROUGH FLOW CALCULATIONS IN AXIAL TURBOMACHINES Edited by Ch.Hirsch and J.D.Denton Published October 1981 342 pages</p>	<p>AGARD-AR-175 Axial turbines Axial compressors Through flow calculations Performance estimation</p>	<p>AGARD Advisory Report No.175 Advisory Group for Aerospace Research and Development, NATO PROPELLSION AND ENERGETICS PANEL WORKING GROUP 12 ON THROUGH FLOW CALCULATIONS IN AXIAL TURBOMACHINES Edited by Ch.Hirsch and J.D.Denton Published October 1981 342 pages</p> <p>In 1977, the Propulsion and Energetics Panel of AGARD had set up its Working Group 12 on 'Through Flow Calculations in Turbomachines' after having found in the 47th (B) Meeting that the prediction of off-design performances, especially for axial flow compressors, was not fully satisfactory.</p>	<p>P.T.O.</p>	<p>AGARD-AR-175 Axial turbines Axial compressors Through flow calculations Performance estimation</p> <p>In 1977, the Propulsion and Energetics Panel of AGARD had set up its Working Group 12 on 'Through Flow Calculations in Turbomachines' after having found in the 47th (B) Meeting that the prediction of off-design performances, especially for axial flow compressors, was not fully satisfactory.</p>

The objectives were to review the existing information on blade performance and wall effect prediction, and to extend this information by systematic application of numerical methods to representative geometries.

In its performance period Working Group 12 had confined to axial turbomachines only and split into a Turbine Sub-Group and a Compressor Sub-Group. In the Turbine Sub-Group five correlations were reviewed and evaluated against the test cases. Each correlation had its strengths and weaknesses and room for further improvements.

The Compressor Sub-Group report begins with a comprehensive survey of the various loss and deviation mechanisms. For comparison of the prediction methods to the test cases five authors have used their own correlations, while the sixth employed a single code in conjunction with three correlations for the four stage compressor. The results of the evaluation are similar to those of the Turbine Sub-Group, but the spanwise parameter distribution is often poorly predicted.

This Advisory Report was prepared at the request of the Propulsion and Energetics Panel of AGARD.

ISBN 92-835-1400-9

The objectives were to review the existing information on blade performance and wall effect prediction, and to extend this information by systematic application of numerical methods to representative geometries.

In its performance period Working Group 12 had confined to axial turbomachines only and split into a Turbine Sub-Group and a Compressor Sub-Group. In the Turbine Sub-Group five correlations were reviewed and evaluated against the test cases. Each correlation had its strengths and weaknesses and room for further improvements.

The Compressor Sub-Group report begins with a comprehensive survey of the various loss and deviation mechanisms. For comparison of the prediction methods to the test cases five authors have used their own correlations, while the sixth employed a single code in conjunction with three correlations for the four stage compressor. The results of the evaluation are similar to those of the Turbine Sub-Group, but the spanwise parameter distribution is often poorly predicted.

This Advisory Report was prepared at the request of the Propulsion and Energetics Panel of AGARD.

ISBN 92-835-1400-9

The objectives were to review the existing information on blade performance and wall effect prediction, and to extend this information by systematic application of numerical methods to representative geometries.

In its performance period Working Group 12 had confined to axial turbomachines only and split into a Turbine Sub-Group and a Compressor Sub-Group. In the Turbine Sub-Group five correlations were reviewed and evaluated against the test cases. Each correlation had its strengths and weaknesses and room for further improvements.

The Compressor Sub-Group report begins with a comprehensive survey of the various loss and deviation mechanisms. For comparison of the prediction methods to the test cases five authors have used their own correlations, while the sixth employed a single code in conjunction with three correlations for the four stage compressor. The results of the evaluation are similar to those of the Turbine Sub-Group, but the spanwise parameter distribution is often poorly predicted.

This Advisory Report was prepared at the request of the Propulsion and Energetics Panel of AGARD.

ISBN 92-835-1400-9

The objectives were to review the existing information on blade performance and wall effect prediction, and to extend this information by systematic application of numerical methods to representative geometries.

In its performance period Working Group 12 had confined to axial turbomachines only and split into a Turbine Sub-Group and a Compressor Sub-Group. In the Turbine Sub-Group five correlations were reviewed and evaluated against the test cases. Each correlation had its strengths and weaknesses and room for further improvements.

The Compressor Sub-Group report begins with a comprehensive survey of the various loss and deviation mechanisms. For comparison of the prediction methods to the test cases five authors have used their own correlations, while the sixth employed a single code in conjunction with three correlations for the four stage compressor. The results of the evaluation are similar to those of the Turbine Sub-Group, but the spanwise parameter distribution is often poorly predicted.

This Advisory Report was prepared at the request of the Propulsion and Energetics Panel of AGARD.

ISBN 92-835-1400-9

B134

AGARD
NATO OTAN
7 RUE ANCELLE · 92200 NEUILLY-SUR-SEINE
FRANCE
Telephone 745.08.10 · Telex 610176

**DISTRIBUTION OF UNCLASSIFIED
AGARD PUBLICATIONS**

AGARD does NOT hold stocks of AGARD publications at the above address for general distribution. Initial distribution of AGARD publications is made to AGARD Member Nations through the following National Distribution Centres. Further copies are sometimes available from these Centres, but if not may be purchased in Microfiche or Photocopy form from the Purchase Agencies listed below.

NATIONAL DISTRIBUTION CENTRES

BELGIUM

Coordonnateur AGARD – VSL
Etat-Major de la Force Aérienne
Quartier Reine Elisabeth
Rue d'Evere, 1140 Bruxelles

CANADA

Defence Science Information Services
Department of National Defence
Ottawa, Ontario K1A OK2

DENMARK

Danish Defence Research Board
Østerbrogades Kaserne
Copenhagen Ø

FRANCE

O.N.E.R.A. (Direction)
29 Avenue de la Division Leclerc
92320 Châtillon sous Bagneux

GERMANY

Fachinformationszentrum Energie,
Physik, Mathematik GmbH
Kernforschungszentrum
D-7514 Eggenstein-Leopoldshafen 2

GREECE

Hellenic Air Force General Staff
Research and Development Directorate
Holargos, Athens

ICELAND

Director of Aviation
c/o Flugrad
Reykjavik

UNITED STATES

National Aeronautics and Space Administration (NASA)
Langley Field, Virginia 23365
Attn: Report Distribution and Storage Unit

THE UNITED STATES NATIONAL DISTRIBUTION CENTRE (NASA) DOES NOT HOLD STOCKS OF AGARD PUBLICATIONS, AND APPLICATIONS FOR COPIES SHOULD BE MADE DIRECT TO THE NATIONAL TECHNICAL INFORMATION SERVICE (NTIS) AT THE ADDRESS BELOW.

PURCHASE AGENCIES

Microfiche or Photocopy

National Technical
Information Service (NTIS)
5285 Port Royal Road
Springfield
Virginia 22161, USA

Microfiche

Space Documentation Service
European Space Agency
10, rue Mario Nikis
75015 Paris, France

Microfiche

Technology Reports
Centre (DTI)
Station Square House
St. Mary Cray
Orpington, Kent BR5 3RF
England

Requests for microfiche or photocopies of AGARD documents should include the AGARD serial number, title, author or editor, and publication date. Requests to NTIS should include the NASA accession report number. Full bibliographical references and abstracts of AGARD publications are given in the following journals:

Scientific and Technical Aerospace Reports (STAR)
published by NASA Scientific and Technical
Information Facility
Post Office Box 8757
Baltimore/Washington International Airport
Maryland 21240; USA

Government Reports Announcements (GRA)
published by the National Technical
Information Services, Springfield
Virginia 22161, USA



Printed by Technical Editing and Reproduction Ltd
Harford House, 7-9 Charlotte St, London W1P 1HD

ISBN 92-835-1400-9